

PENETRATION OF ORGANIC AND INORGANIC IONIC  
TRACERS INTO THE SKIN FOLLOWING  
IONTOPHORESIS: A COMPARATIVE STUDY 'IN VIVO'

Mohamed Akram Almotabagani

A Thesis Submitted for the Degree of PhD  
at the  
University of St Andrews



1989

Full metadata for this item is available in  
St Andrews Research Repository  
at:

<http://research-repository.st-andrews.ac.uk/>

Please use this identifier to cite or link to this item:

<http://hdl.handle.net/10023/13827>

This item is protected by original copyright

Penetration of organic and inorganic ionic tracers  
into the skin following iontophoresis:  
a comparative study *in vivo*.

A thesis submitted to the University of St Andrews  
for the degree of Doctor of Philosophy.

by

Mohamed Akram ALMOTABAGANI

Department of Biology and  
Preclinical Medicine,  
University of St Andrews

June, 1988





Th A810

## Abstract

Ionic materials in solution do not penetrate the skin following local (topical) application. Such a low permeability can, however, be altered by iontophoresis. Utilization of transmission and scanning electron microscopy and cryostat techniques has made it possible to demonstrate the penetration and site of deposition of ionic tracers in the skin of the rat. It has been found that the penetration of cationic dyes and metal cations is facilitated by positive iontophoresis while the penetration of anionic dyes is facilitated by negative iontophoresis. The extent of penetration is determined by the current density, the concentration of the tracer in the vehicle, the physico-chemical properties of the tracers and the type of vehicle used. The removal of surface lipid is regarded as insignificant in terms of enhancing the penetration of tracers by iontophoresis.

It has been found that the penetration of ionic tracers into the skin is preferentially transfollicular. However, the penetration of electron-dense tracers into the stratum corneum of the epidermis and the follicular infundibula is preferentially intercellular, while that into the sebaceous glands is transcellular.

It is considered that the whole of the stratum corneum of the epidermis is the major barrier to cutaneous penetration by electrolytes. In addition, a barrier function is suggested for sebum situated in the follicular infundibula.

## CONTENTS

### VOLUME 1

#### Chapter 1 Introduction

1.1	Structure and function of skin	1
1.2	Methods for studying skin penetration	14
1.3	Location of the barrier	20
1.4	Properties of the stratum corneum	25
1.5	Routes of penetration across the skin	34
1.6	Factors affecting the permeability of skin	37
1.7	Iontophoresis	53
1.8	Aims of the present study	65

#### Chapter 2 Materials and Methods

2.1	Instrumentation	67
2.2	Materials used for penetration trials	79
2.3	Animals	84
2.4	Anaesthesia	84
2.5	Hair clipping	85
2.6	Control experiments	86
2.7	Iontophoresis	86
2.8	Intradermal injections	88
2.9	Pre-excision	88
2.10	Excision of the treated skin	88
2.11	Preparation of the excised skin for cryostat sectioning	89
2.12	General histological techniques	92
2.13	Special histological techniques	93
2.14	Preparation of excised skin for transmission electron microscopy	96
2.15	Preparation of excised skin for X-ray analysis	109

Chapter 3	Results	
3.1	Cationic dyes	115
3.2	Anionic dyes	162
3.3	Neutral dyes	172
3.4	Compound dyes	174

## Volume 2

### Continuation of Chapter 3 (Results)

3.5	Lanthanum	177
3.6	Silver	221
3.7	Ruthenium Red	250

## Volume 3

### Continuation of Chapter 3 (Results)

3.8	Copper	266
3.9	Iron	283
3.10	Iodine	293
3.11	Tissue changes	295

## Chapter 4 Discussion

4.1	Initial observations	304
4.2	Justification of methods used and significance of results	306
4.3	Evaluation of extent of penetration	313
4.4	Efficacy of iontophoresis	314
4.5	Variation in penetration caused by the specification of the apparatus	316
4.6	Penetration through treated and untreated skin	319
4.7	Effect of variation in current density on skin penetration	321
4.8	Polarity effect	324
4.9	The effect of concentration on skin penetration by iontophoresis	332

4.10	The effect of aprotic solvents on skin penetration by iontophoresis	341
4.11	The effect of detergents on skin penetration by iontophoresis	344
4.12	Effect of organic solvents on skin penetration by iontophoresis	349
4.13	Physico-chemical factors influencing skin penetration by iontophoresis	354
4.14	Tracer-tissue interaction	366
4.15	Mode of action of iontophoresis	370
4.16	The location and nature of the cutaneous barrier	376
4.17	Routes of entry	396
4.18	Advantages and disadvantages of iontophoresis	411
4.19	Suggestion for future investigations	413
	Conclusions	415
	References	417
	Appendices	
	Corrigendum	

CERTIFICATE

I hereby certify that the candidate has fulfilled the conditions of the Resolution and Regulations appropriate to the Degree of Ph. D.

Signature of Supervisor ..... Date *29th June 1988*

ACADEMIC RECORD

I was admitted to the Faculty of Science of the University of St Andrews under Ordinance General No 12 in October, 1983 and as a candidate for the degree of Ph. D. in October, 1984.

Signed

Date 29. 6. 1988.

In submitting this thesis to the University of St Andrews, I wish access to it to be subject to the following conditions:

for a period of 18 months from the date of submission, the thesis shall be with-held from use.

I understand, however, that the title and abstract of the thesis will be published during this period of restricted access; and that after the expiry of this period the thesis will be made available for use in accordance with the regulations of the University Library for the time being in force, subject to any copyright in the work not being affected thereby, and a copy of the work may be made and supplied to any *bona fide* library or research worker.



## ACKNOWLEDGEMENTS

It is my pleasant duty to thank Dr. David Jackson for his supervision, help and encouragement throughout this study.

I also thank the members of staff whose comments and advice have been appreciated. I must also thank Mr R. J. Stuart for technical assistance and Mrs A. Aiton for preparation of the manuscript.

I am extremely grateful to my friend K. S. Ben Yamin for his financial support.

I wish to acknowledge the long-suffering support of my family who sacrificed many years of companionship so that this work could be possible.

I owe apology to my wife, Effat, and my children, Hossain and Samerah, for lack of attendance during the preparation of this thesis.

I dedicate this work to my mother, Fawziah.

Finally I should like to thank Dr. D. McEwan Jenkinson, currently working at the Moredun Research Institute, Gilmerton Road, Edinburgh, for making available to me the apparatus used for the iontophoresis studies.

**VOLUME**

**1**

CHAPTER 1  
*INTRODUCTION*

## CONTENTS

	Page	
<b>1.1</b>	<b>Structure and function of skin</b>	<b>1</b>
1.1.1	The epidermis	2
1.1.1.1	Stratum germinativum	
1.1.1.2	Stratum spinosum	
1.1.1.3	Stratum granulosum	
1.1.1.4	Stratum lucidum	
1.1.1.5	Stratum corneum	
1.1.2	The epidermal-dermal junction	8
1.1.3	The dermis	9
1.1.3.1	The papillary layer	
1.1.3.2	The reticular layer	
1.1.4	The hypodermis	10
1.1.5	The hair follicle	10
1.1.6	The skin as a protective organ	13
<b>1.2</b>	<b>Methods for studying skin penetration</b>	<b>14</b>
1.2.1	<i>In vitro</i> methods	14
1.2.2	<i>In vivo</i> methods	15
1.2.2.1	Detection in body fluids and tissues	
1.2.2.2	Elicitation of biologic responses	
1.2.2.3	Loss of material from the surface	
1.2.2.4	Stripping techniques	
1.2.2.5	Histological studies	
<b>1.3</b>	<b>Location of the barrier</b>	<b>20</b>
1.3.1	The surface film	21
1.3.2	The barrier layer	22
1.3.3	Diffusion below the barrier layer	25
<b>1.4</b>	<b>Properties of the stratum corneum</b>	<b>25</b>
1.4.1	Contents of corneal cells	27
1.4.2	Plasma membranes of corneal cells	30
1.4.3	The intercellular region	31

1.4.4	Routes of penetration across the stratum corneum	34
<b>1.5</b>	<b>Routes of penetration across the skin</b>	<b>34</b>
<b>1.6</b>	<b>Factors affecting the permeability of skin</b>	<b>37</b>
1.6.1	Skin condition	37
1.6.2	Age of the skin	38
1.6.3	Species variations	39
1.6.4	Racial variations	39
1.6.5	Sex variation	40
1.6.6	Repeated application	40
1.6.7	Seasonal variations	40
1.6.8	Regional variations	40
1.6.9	Blood flow	41
1.6.10	Hydration	42
1.6.11	Concentration of penetrant	43
1.6.12	Vehicles and solubility characteristics of penetrants	46
1.6.13	Treatment of skin with aprotic solvents, organic solvents and surfactants	48
<b>1.7</b>	<b>Iontophoresis</b>	<b>53</b>
1.7.1	Definition and synonyms	53
1.7.2	Historical review	54
1.7.3	Significance and importance of iontophoresis	55
1.7.4	Basic aspects	58
1.7.4.1	Electrophysics	
	(i) Electric current	
	(ii) Current strength and current density	
	(iii) Resistance	
	(iv) Electromotive force	
	(v) Typical features of the apparatus	
1.7.4.2	Electrochemistry	
1.7.5	Mode of application	63
1.7.6	Conditions for iontophoresis	63

1.7.7	Distribution of the current	64
1.8	<b>Aims of the present study</b>	<b>65</b>

## 1.1 Structure and function of skin

The skin is a multi-layered structure which forms the boundary between the interior of the body and the external environment, and serves as a communicating agent between them. It is a highly specialized organ with remarkable and diverse functions. It helps to maintain internal homeostasis by thermoregulatory secretory activity, forms a self-repairing barrier against physical and chemical assault, provides an important route for the transmission of information about the external environment, and retains, in the layer immediately subjacent, a major store of energy. With the skin as an effective barrier, the interior of the body containing the delicate living cells, tissue and organs remains remarkably undisturbed during wide fluctuations in the external, often unfriendly, environmental conditions. These functions of the skin are made possible by a complex structure. It is, therefore, appropriate to begin by describing the structure of the skin. A large number of publications are available describing the morphological features of mammalian skin at the light and electron microscope levels (Stoughton, 1959; Serri and Montagna, 1961; Ebling, 1964, 1970a, 1970b, 1979, 1986; Zelickson, 1967; Champion, 1970; Gillman, 1970; Rook, 1970; Sims, 1970a, 1970b; Breathnach, 1971; Jarrett, 1973, 1977; Montagna and Parakkal, 1974; Ackerman, 1975; Ebling and Rook, 1975a, 1975b; Hashimoto and Shibasaki, 1976; Millington and Wilkinson, 1983; Odland, 1983).

Despite variation in thickness, colour and presence of hairs and glands, which reflects different functional demand, all types of mammalian skin have the same basic structure. The skin, or integument, consists of an external cellular envelope called the

epidermis and beneath this is a layer of a dense fibroelastic connective tissue called the dermis. These two parts of the skin meet at the epidermal-dermal junction. Immediately deep to the skin is a layer of loose connective tissue, the hypodermis.

Embryologically, the epidermis arises from ectoderm and the dermis from mesoderm, and the former gives rise to the skin appendages, namely hair follicles, sebaceous glands and apocrine and eccrine sweat glands.

There are two main types of skin, thick and thin. Thick or glabrous skin is characterized by a thick epidermis, lack of hair follicles and sebaceous glands, and the presence of ridges and grooves arranged in spiral and concentric patterns on the surface. A typical example of this type of skin is that which is found on the human palm and sole. Thin skin, on the other hand, is characterized by a relatively thin epidermis, the presence of hair follicles and sebaceous glands, and the absence of the highly organized superficial ridges and grooves. The hair-containing skin of mammals is of the thin skin type.

### 1.1.1 The epidermis

The epidermis is classified as a stratified squamous keratinizing epithelium. It is a highly organized system in which cells in the deepest layer divide, migrate, differentiate, and eventually are shed at the surface. The stages of this transformation process characterise the four main layers into which the epidermis, for descriptive purpose, is divided. Proceeding from within to the surface, these are the stratum germinativum (basale), the stratum



spinosum, the stratum granulosum and the stratum corneum. An additional layer, the stratum lucidum, has been described between the stratum granulosum and stratum corneum but it is not prominent in all skin types. Identification of cells in these strata is based on their cytological appearance and anatomical position.

#### 1.1.1.1 Stratum germinativum (basale)

This is the deepest region in the epidermis and consists of a single layer of mainly columnar cells resting on a basal lamina, and which are arranged with their long axes at right angles to the epidermal-dermal junction. The prominent elongated nuclei occupy the major part of the cells and stain well with basophilic stains. Each basal cell is connected to its neighbouring cells and to the cells above it by intercellular bridges which are similar to those in the overlying stratum, but they are less conspicuous because of the proximity of the cells. These intercellular bridges contain desmosomes. The basal portion of the cell membrane facing the basal lamina is extremely irregular and contains many hemidesmosomes. The cytoplasm of basal cells contains fine tonofilaments which are loosely aggregated into bundles (tonofibrils), and are orientated mainly in a vertical direction. Some of these tonofibrils have one of their ends connected to the attachment plaques of desmosomes and hemidesmosomes. Basal cells are regarded as being the proliferative cells of the epidermis; they are responsible, via mitosis, for the continued generation of "keratinocytes" in the upper layers of the epidermis. Thus the basal layer contains cells that are capable of proliferation in addition to cells that, having completed their last scheduled division, are present as post-mitotic, maturing cells awaiting their turn to migrate suprabasally (Hume, 1985). Lavker and Sun (1982) have identified two

structurally distinct populations of basal keratinocytes, termed serrated and non-serrated cells, and suggested that the non-serrated cells represent a stem cell population and serrated cells help anchor the epidermis to the dermis beneath.

#### 1.1.1.2 Stratum spinosum

This stratum is located above the stratum basale, and it consists of several layers of polyhedral cells. Each keratinocyte in this zone contains prominent intercellular bridges ('spines' or 'prickles') extending to similar processes in adjacent cells, making contact via numerous desmosomes. These spines give the layer its name. The cytoplasm contains oval or rounded nuclei with prominent nucleoli, and numerous aggregations of tonofilaments extending across the cell in many directions especially terminating at desmosomes. Another cytoplasmic feature is the appearance of small membrane-bound oval or rod-shaped bodies which have been assigned various names including Odland bodies and membrane-coating granules.

#### 1.1.1.3 Stratum granulosum

As the cells of the stratum spinosum are displaced towards the surface, they gradually become flattened, elongated and lie parallel to the surface. The most characteristic feature of the granular cell is the presence of irregularly shaped non-membrane bound keratohyalin granules, which increase in number and size as the overlying stratum is approached. The nuclei of granular cells exhibit signs of degeneration, or may be completely disintegrated in some cells. The intercellular bridges seen in the subjacent stratum spinosum are lost. The cytoplasmic membrane-coating granules are discharged into the

intercellular spaces. Tonofilaments abound and are closely associated with the keratohyalin granules.

Membrane-coating granules (MCGs): these granules have been given a variety of descriptive names such as small dense granules (Selby, 1957), membrane-coating granules (Matoltsy and Parakkal, 1965), keratinosomes (Weinstock and Wilgiam, 1970), cementosomes (Hashimoto, 1971) and lamellar bodies (Elias and Friend, 1975). The origin of membrane-coating granules has not been definitely established. They have been interpreted as attenuated mitochondria (Selby, 1957; Odland, 1960); whilst others have noted them in close association with the Golgi apparatus (Matoltsy and Parakkal, 1965; Martinez and Peters, 1971).

The life cycle of these granules is well documented by a number of sources (Matoltsy and Parrakal, 1965; Hashimoto, 1971; Hayward and Hackemann, 1973; Lavker, 1976). They first appear in the keratinocytes of the stratum spinosum. They may be seen as round, ovoid or pear-shaped bodies. The average length of the individual granule is about  $0.4 \mu$  and the width varies between  $0.04$  and  $0.16 \mu$ . The individual granule is bound by a trilaminar membrane,  $60-70 \text{ \AA}$  thick, consisting of a lighter leaflet sandwiched between two dense leaflets. Within the granule a regularly repeating lamellar pattern is present. This lamellar pattern of contents is brought about by the presence of alternating dense and lighter lamellae. There are two types of dense lamellae, thick ( $20 \text{ \AA}$  wide) and thinner ( $10 \text{ \AA}$ ). Intervening between the alternating thick and thin dense lamellae are lighter lamellae ( $20 \text{ \AA}$ ). Figure 1A is a schematic representation of a membrane-coating granule. As the spinous cells continue to move

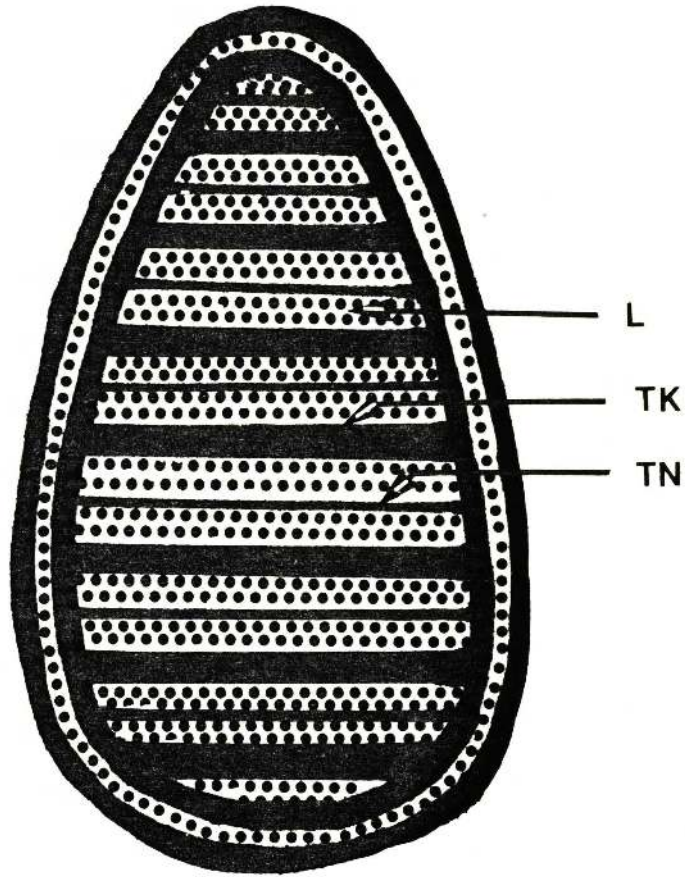


Fig. 1A. Schematic representation of a membrane-coating granule. The granule is bounded by a trilaminar membrane. The lamellar pattern consists of alternating thick (TK) and thin (TN) dense lamellae with lighter lamellae (L) intervening between them (after Martinez and Peters, 1971).

superficially and differentiate into granular cells, keratohyalin granules are formed within their cytoplasm. As keratohyalin granules increase in size, membrane-coating granules tend to migrate towards the plasma membrane nearest to the epithelial surface. Subsequently they become apposed to the inner cytoplasmic surface of the plasma membrane of the granular cell and are discharged into the intercellular spaces. The newly discharged granules are similar in appearance and dimensions to intracellular granules. However, during subsequent migration and transformation of granular cells into cornified cells, the intercellular membrane-coating granules undergo definite alterations in ultrastructure and composition. Firstly, at the granular-cornified cell layer interface and between the first and second layers of cornified cells, the individual intercellular granules coalesce into broad lamellae. Secondly, the initially secreted granules contain polar lipids and little neutral lipids, whereas the broad lamellae are neutral lipid-rich (Elias *et al.*, 1977).

With regard to chemical composition, membrane-coating granules have been reported to contain polysaccharides (Motoltsy and Parakkal, 1965; Hayward and Hackermann, 1973), hydrolytic enzymes (Weinstock and Wilgram, 1970), and lipids (Breathnach and Wylie, 1966; Hashimoto, 1971; Elias *et al.*, 1977).

Because membrane-coating granules contain a variety of materials, they may be important for several functions, including corneal intercellular adhesion (Hashimoto, 1971), the extracellular breakdown of cell to cell contacts responsible for the dyshesion of cornified cells and also the intracellular nuclear breakdown (Allen and Potten,

1975; Grayson *et al.*, 1985), the modification of corneal cell membranes (Matoltsy and Parakkal, 1965; Matoltsy, 1966), and forming a permeability barrier (Squire, 1973; Elias and Friend, 1975, Elias *et al.*, 1979; Hayward, 1983; Bowser and White, 1985).

Woo-Sam (1978) identified two structurally different types of membrane-coating granules, one which was oval or rounded and structureless, which could represent the cementosome (Hashimoto, 1971) and the other with the typical lamellar structure, which could contain hydrolytic enzymes (Weinstock and Wilgram, 1970). It has been reported (Woo-Sam, 1978) that there is a significant decrease of about 40% in the number of MCGs during comedo formation when compared to controls.

#### 1.1.1.4 Stratum lucidum

This layer is prominent in thick skin (for example human palm and sole) where it is represented by a poorly staining hyalin band, consisting of one or two layers of extremely flattened cells sandwiched between the stratum granulosum and the stratum corneum.

#### 1.1.1.5 Stratum corneum

This is the outermost layer of the epidermis, and is the final product of epidermal differentiation. As the cells enter this layer, all common intracellular organelles are lost, and the cells now contain densely packed keratin filaments embedded in an amorphous matrix. The keratin is of a low sulfur ('soft') type which does not make the skin hard. The spaces between the flattened keratinized cells contain materials derived from or modified by the contents of membrane-coating granules which are discharged at a lower level. The plasma membranes

of "corneocytes" are thicker than elsewhere in the epidermis. As the cells move up towards the surface of the stratum corneum, there is a reduction of intercellular cohesion (King *et al.*, 1979) with ultimate dyshesion and sloughing of the cells.

### 1.1.2 The epidermal-dermal junction

The epidermal-dermal junctional zone is anatomically quite complex consisting of four component areas: (1) the basal cell plasma membrane with its hemidesmosomal attachment devices; (2) an electron-lucent area, the lamina lucida; (3) the basal lamina; (4) the sub-basal lamina fibrous components composed of anchoring fibrils, single collagen fibres and bundles of fibrils resembling microfibrils. Briggaman and Wheeler (1975) and Marks *et al.*, (1975) described this junction in great detail. The plasma membrane of basal cells is approximately 7 to 9 nm. thick and is composed of three asymmetrical layers: a thick internal leaflet which abuts the cytoplasm, an intermediate more electron-lucent zone, and a relatively thin external leaflet. An electron-opaque thickening, the attachment plaque, is present on the cytoplasmic face of the internal leaflet of the plasma membrane.

The lamina lucida is an electron-lucent zone which separates the plasma membrane from the basal lamina. In the region of hemidesmosomes, fine anchoring filaments traverse the lamina lucida perpendicularly from the outer leaflet of the plasma membrane through the sub-basal dense plaque into the basal lamina.

### 1.1.3 The dermis

The dermis (cutis or corium) consists of networks of collagen, elastin and reticulin fibres embedded in a semi-gel matrix called the ground substance which is composed mainly of mucopolysaccharides. In addition, the dermis contains different types of connective tissue cells such as fibroblasts, mast cells and macrophages. The dermis is traversed by blood vessels, nerves and lymph vessels, and into it penetrate the epidermal appendages. The dermis is divided, for histological descriptive purposes, into a superficial epidermis-associated stroma called the papillary layer (pars or stratum papillaris) and a deeper tough fibrous layer that has mostly a mechanical supporting role called the reticular layer (pars or stratum reticularis).

#### 1.1.3.1 The papillary layer

This relatively thin layer is folded into papillae which interdigitate with the downward extensions of the epidermis (the rete ridges), and thus it bears the negative imprint of the undersurface of the epidermis. It contains fine collagen fibres intermeshed with some elastic fibres. It is richly vascularized in the form of the superficial arterial and venous plexuses and the capillary loops rising from them. The anatomical position of these capillaries reflects their biological function and that is to provide nutrition for the avascular epidermis, and to serve as heat regulators. The papillary layer is relatively rich in cells most of which are fibroblasts and macrophages.

#### 1.1.3.2 The reticular layer



This relatively thick region is the main fibrous bed of the dermis. It is classified as a dense irregular connective tissue that consists of a network of thick, collagen fibres interspersed with elastin fibres. This characterizes the mechanical properties of the skin as its ability of withstanding stretch forces. Embedded in the vicinity of this layer are the epidermal appendages, blood and lymph vessels, and nerves. Smooth muscles (arrectores pilorum) associated with hair follicles are also present. The deeper aspect of the reticular layer merges with the underlying subcutaneous layer.

#### 1.1.4 The hypodermis

Also called the subcutaneous layer, adipose layer, panniculus adiposus or superficial fascia. It is classified as a loose connective tissue, and it is located immediately beneath the dermis. It contains varying numbers of fat cells (adipocytes) depending on the region of the body and the state of nutrition. For example, in the human abdomen this layer may be 10 cm. thick whereas the skin of the eyelids, penis and scrotum is devoid of fat. The superficial region of the hypodermis may contain the lower parts of hair follicles and sweat glands. A flat sheet of striated muscle, the panniculus carnosus, when present separates the hypodermis from the interior of the body. The hypodermis allows for movement of the skin in relation to underlying structures. Generally, the hypodermis is not considered a part of the skin, but it is functionally nevertheless quite important in connecting the dermis to underlying structures, and furthermore it carries the major blood vessels and nerves to the skin.

#### 1.1.5 The hair follicle

This exclusively mammalian structure comprises a pocket of epithelium which is derived from and remains continuous with the surface epidermis, and extends into the dermis. Each follicle is set at an angle to the skin surface. The follicle, together with the sebaceous gland that grows from its side, form what is known as a pilosebaceous unit. The activity of any hair follicle is cyclic. The main stages of the hair follicle cycle are anagen which is the period of active growth, catagen, which is a transitional period of active regression and telogen, which is the period of rest. A detailed description of the changes which take place in a hair follicle during its cyclic activity has been reported by Rook (1970), Montagna and Parakkal (1974), Johnson (1977) and Spearman (1977).

It is a common practice to describe the structure of a hair follicle in its anagen stage. The hair follicle is composed of three major portions: the hair, the inner and the outer root sheaths. At its lower pole the follicle shows an onion-shaped expansion known as the hair bulb. A small connective tissue structure, the dermal papilla, protrudes into the centre of the bulb. An imaginary line drawn across the widest diameter of the dermal papilla divides the bulb into two regions. The part below this critical level consists mostly of undifferentiated matrix cells and in general most of the mitotic activity is located here, although some mitotic activity may occur in the upper part of the bulb. The growth and differentiation of matrix cells give rise to all the cells of the hair shaft and the inner root sheath. The outer root sheath, on the other hand, represents a downward extension of the epidermis.

The outer root sheath extends from the orifice or surface opening of the hair follicle downward to the sides of the hair bulb. The outer root sheath can be divided into three segments: upper, middle and lower.

The upper segment extends from the orifice of the follicle down to the opening of the sebaceous duct, forming the walls of the pilary canal. In this segment, the outer root sheath is similar in structure to that of the surface epidermis and the cells are arranged into basal, spinous, granular and cornified layers. Thus this segment of the outer root sheath may be termed the intrafollicular epidermis. It has also been termed the infundibulum which is divided into two smaller anatomical units: the superficial fifth of the infundibulum, that is the epidermal part is called the acro-infundibulum, whereas the larger four-fifths dermal part is called the infra-infundibulum. The fully keratinized cells of the infundibulum are sloughed off into the pilary canal.

The middle segment of the sheath extends from the opening of the sebaceous duct down to the neck of the bulb. Here the outer root sheath is many layers thick; cells at the periphery are tall columnar and oriented perpendicularly to the long axis of the follicle. Those on the inner surface are flattened and lie parallel to the long axis of the follicle.

In the lower segment, which surrounds the bulb, the outer root sheath consists of only one or two layers of cells.

### 1.1.6 The skin as a protective organ

The prime function of skin is to interpose a barrier between the internal environment and external events. This barrier limits egress of physiologic fluids and limits ingress of noxious or undesirable substances.

**Percutaneous penetration:** This event can be defined as the passage of substances from the outside into the skin and through the skin into the blood stream. With regard to the epidermis, this penetration involves a series of individual transport processes occurring in sequence. First, substances must come into contact with the skin surface where a lipid film is present, they must diffuse through the stratum corneum, desorb and diffuse through the viable epidermis, penetrate the epidermal-dermal boundary, diffuse through the papillary dermis to reach the papillary capillaries, and diffuse through these plexuses to enter the circulating blood. There are six distinct events in this sequence, and theoretically each penetrant substance may encounter different barriers in accordance with its own physico-chemical properties and its interaction with the skin as it traverses it. However, it is generally accepted that the barrier to percutaneous penetration resides almost entirely in the stratum corneum, and the evidence for this is discussed below (page 22).

**Loss of physiologic fluids:** As well as being a barrier to the percutaneous entry of materials, the skin also regulates the loss of body fluids. The classic and vital barrier property of skin is that which limits the rate of transfer of water outwards, indeed, the rate of transepidermal water loss is a convenient parameter for expressing

barrier function. It is this barrier which provides all mammals with the capacity to maintain an internal fluid balance in a dry external environment.

## 1.2 Methods for studying skin penetration

Stoughton (1964), Idson (1975), Ayres and Hooper (1978), Anjo *et al.* (1980) and Polano (1984) have reviewed the methods used for studying skin penetration. These methods can generally be divided into two major groups, namely *in vitro* and *in vivo* methods. The former involves excised skin usually in diffusion chambers whilst the latter employs the skin of the living animal or human subject *in situ*.

For the same penetrant and same skin type, the results obtained with the *in vivo* and *in vitro* methods show close and good correlation (Ainsworth, 1960; Marzulli *et al.*, 1965; Tregear, 1966; Bronaugh and Franz, 1986). This is due largely to the fact that the fully keratinized, metabolically inactive stratum corneum is the major barrier layer.

### 1.2.1 *In vitro* methods

These involve, firstly, the placement of excised whole skin (Marzulli, 1962), epidermis (Marzulli, 1962; Scheuplein, 1965) or isolated stratum corneum (Bowser and White, 1985) into some type of diffusion chamber. The diffusion chamber is a simple device consisting of two compartments separated by the selected excised membrane. In the donor compartment the penetrant is applied to the skin surface. The acceptor compartment contains some type of fluid bath, usually

isotonic solution, into which diffusion takes place. The collecting fluid in the acceptor compartment may flow continuously, stirred by a magnetic device or may remain static. With this technique it is possible to quantitate penetration rates. If a radioactive agent is used as the penetrant, counts of radioactivity may be applied and penetration can be expressed in terms of quantity per unit area per unit time (Stoughton, 1964; Idson, 1975). Alternatively, many chemical agents may be used as penetrants and penetration is detected by one of the techniques of physico-chemical analysis which include, for example, spectrophotometric test (Blank *et al.*, 1964) and chemical detection (Smith *et al.*, 1961). Scheuplein and Blank (1971) developed mathematical equations in relation to *in vitro* studies of skin penetration. Different designs for the diffusion chamber are available, and the *in vitro* method has been employed by a large number of investigators (Blank and Gould, 1959; Ainsworth, 1960; Marzulli, 1962; Scheuplein, 1965; Bronaugh *et al.*, 1982; Bronaugh and Franz, 1986).

Another form of *in vitro* study involves the incubation of freshly excised skin samples in a tracer-containing solution, and thereafter determining the localization of the tracer by histological techniques (Hayward, 1983; Squier and Edie, 1983; Squier, 1984). This method provides a means by which the relationship between permeability and structure at a specific anatomical site can be investigated.

### 1.2.2 *In vivo* methods

Penetration *in vivo* can be studied by various techniques of analysis of the presence of a test material following exposure to the skin.

These techniques may include detection in body fluids and tissues, elicitation of biologic responses, loss of material from the surface, stripping techniques, and histological studies.

#### 1.2.2.1 Detection in body fluids and tissues

The locally applied agent may be recovered in body fluids or in a body organ and may be detected by a number of ways which include specific colour reactions, chromatographic separation and identification, fluorescence and radioactivity (Stoughton, 1964). For example, Laug *et al.* (1944) investigated the penetration of mercury from the skin surface by determining mercury concentration in the kidney and liver. Analysis of urine samples however is the method most commonly used in studying percutaneous absorption. Malkinson and Ferguson (1955) investigated the penetration of hydrocortisone -4-C<sup>14</sup> incorporated into an ointment base by detection of radioactivity in urine samples. Pinson (1952) studied water exchange through the skin by using tritium as a tracer of hydrogen in water and analysing urine specimens. Tas and Feige (1958) carried out studies on the penetration of radioiodide (I<sup>131</sup>) by detection of radioactivity in the thyroid gland and urine. Rogers *et al.* (1978) investigated the penetration of methyl alcohol through the skin by means of gas liquid chromatography of urine specimens. Reifenrath *et al.*, (1984) studied the penetration of radiolabelled compounds by the recovery of radioactivity in the excreta (urine, faeces and carcass).

#### 1.2.2.2 Elicitation of biologic responses

This method involves the use of agents that are pharmacologically active and thus capable of producing certain biological responses. With this technique it is possible to demonstrate whether or not a

biologically active substance can penetrate into the skin and, if it does penetrate, to determine the time required for the reaction to develop. This method has been applied by Stoughton *et al.* (1960) who studied penetration through the skin of nicotinic acid and seven closely related derivatives by observing the biological reaction vasodilatation. In studying allergic skin reactions Abramson (1938) demonstrated the penetration of histamine and allergens by weal formation. More recently, Hornqvist *et al.* (1984) investigated the penetration into the skin of various drugs by the development of skin reactions such as blanching, piloerection and erythema.

#### 1.2.2.3 Loss of material from the surface

As with *in vitro* methods, this involves the application of radioactive substances to the surface of the skin and observing the residual activity at the site of application. Loss of radioactivity counts determines penetration, and thus this method is also called the disappearance technique. It has been employed by Malkinson (1958) in investigating the penetration of  $C^{14}$  labelled steroids (hydrocortisone, cortisone and testosterone) under varying conditions through the skin of human subjects. Skog and Wahlberg (1964) also used disappearance measurements to investigate the penetration of radioactive metal compounds through the skin of guinea pigs.

#### 1.2.2.4 Stripping techniques

Penetration *in vivo* can also be studied by application of radio-labelled materials to the skin which is subsequently stripped at intervals. Measurements of radioactivity in the stripped stratum corneum indicates the amount of penetration into this layer (Polano, 1984).



#### 1.2.2.5 Histological studies

Histological demonstration of a test material following application to the skin can yield valuable information not only about penetration *per se*, but also about the specific site of deposition and route of penetration. The histological observations can be carried out either directly or by means of chemical reactions, autoradiography or autofluorescence.

##### (i) Direct examination

By this method no special histochemical test is necessary to demonstrate the penetrant in skin sections. This is equivalent to saying direct observation of penetrant in tissue sections is possible. This method is limited to dyes and materials which by nature are electron-dense. For example, Mackee *et al.* (1945) investigated the penetration into the skin of locally applied dyes by direct examination of frozen sections. Squire and Rooney (1976) applied solutions of lanthanum salts to the surface of keratinized and non-keratinized oral epithelia, and lanthanum penetration was studied by direct observation of the location of electron-dense material in ultrathin sections.

Some investigators have injected solutions of electron-dense materials into the skin of living animals in order to investigate the relationship between permeability and structure (Wolff and Honigsmann, 1971; Elias and Friend, 1975; Squier and Rooney, 1976; Hayward, 1983). Direct observation of electron-dense deposits by the electron microscope has also been used to study abnormality in barrier function (Elias and Brown, 1978).

### (ii) Chemical reactions

This method differs from the direct examination method in that a specific chemical reaction is required to show the location of the applied test material; without such a reaction the applied material cannot be observed histologically. This method is, therefore, applied to substances that yield precipitable coloured end-products in a specific chemical reaction, or substances that can be made electron-dense by chemically reacting with specific reagents. Mackee *et al.* (1945) used Perl's reaction to reveal the localization of iron in tissue sections sometimes following local application of ferric compounds. Pereyra (1945) demonstrated copper in tissue sections by Mallory's haematoxylin technique when solutions of copper salt had previously been introduced into the skin. Ferguson and Silver (1947) demonstrated the penetration of chlorine into the skin from two chlorine-liberating ointments by the use of an O-tolidine-citric acid reagent on frozen sections. Squire (1973) investigated, by the electron microscope, the permeability of keratinized and non-keratinized oral epithelia to horseradish peroxidase (HRP). The localization of HRP in ultrathin sections was determined by incubation of specimens, during processing, in a Tris-maleate buffered solution containing diamino-benzidine and hydrogen peroxide.

### (iii) Autoradiography

This is one of the well established techniques in skin penetration studies, and it involves the application of a radioactive material to the intact skin and subsequently determining its location in tissue sections. For example, Witten *et al.* (1951, 1953) and Fleischmajor and Witten (1955) employed autoradiography to investigate routes and degree of penetration of thorium X through intact human skin. Since

the use of radioactive materials for penetration studies *in vivo* is often accompanied by restrictions, this method has also been applied to *in vitro* studies. For example, Blank and Gould (1959) used a radioactive surfactant (sodium laurate) to investigate its penetration through isolated human abdominal skin, and the position of the radioactive chemical was determined by autoradiography from frozen cryostat sections. Scott and Kalz (1956) utilized autoradiography in studying the site of deposition of topically applied  $C^{14}$ -hydrocortisone. Ayres and Hooper (1978) investigated the penetration of cortisol from different ointments into intact porcine skin by measurements of radioactivity in skin sections as well as by autoradiography.

#### (iv) Autofluorescence

Another technique employed in skin penetration studies is autofluorescence. Montagna (1954) investigated the penetration of locally applied vitamin A through the skin of the guinea pig. The localization and thus penetration of vitamin A was studied by its brilliant fluorescence in unfixed frozen sections examined under near-ultraviolet light filtered to transmit rays at  $3600 \text{ \AA}^0$ .

### 1.3 Location of the barrier

Any skin component which interposes itself in the pathway of a skin penetrant so as to retard or prevent percutaneous penetration, or to regulate loss of body fluids, can be thought of as a barrier. Crouse (1965) indicated that it is improper to speak of a barrier as if to imply a static and constant anatomical membrane responsible for limitation of passage of all substances in either direction, that is,

from within to the outside and vice versa. Instead it is proper to speak of a barrier function which is best defined for each material and in each direction as a rate of transfer of a given material. Many arguments as to the location of the barrier are related to different experimental substances and conditions, and often measuring passage in different directions.

### 1.3.1 The surface film

The first skin component which a penetrant substance encounters when applied to the skin is a thin film of emulsified materials located on the top of the skin surface. This film is mainly composed of sebum, but in addition it contains lipids of epidermal origin (Wheatley, 1963) and sweat. It has been considered, but not definitely proved, that sweat glands contribute lipid to the surface film (Nicolaidis, 1963). The relative quantities of each of these constituents is dependent upon the relative proportions of the contributing sources. The thickness of this film has been estimated to vary between 0.4 and 4.0  $\mu$  (Tregear, 1966). The role of this film in the barrier function of skin has caused some controversy. Certain experiments (Calvery *et al.*, 1946; Onken and Moyer, 1963) have shown that removal of lipids facilitates penetration, whilst replacement of the extract restores the barrier property. Others believe that the effect of this film on penetration is probably very slight. It has been mentioned that the surface film does not form a functionally complete layer over the skin, hence it offers little resistance to a penetrating species (Tregear, 1966). Laug *et al.* (1947) studied penetration of mercury from ointments, and found that washing the skin with soap and water prior to ointment application had no effect. Removal of surface film

is not followed by free movement of water through the skin (Winsor and Burch, 1944), or by increased penetration of anionic surfactants (Blank and Gould, 1961) or cationic surfactants (Blank *et al.*, 1964).

### 1.3.2 The barrier layer

Rein (1924, 1925, 1926) conducted a series of electrophysiological studies on skin and theorized about a specialized barrier region between the acid stratum corneum and the mildly alkaline Malpighian layer, and characterized this region (the stratum lucidum) as an electric double layer which was responsible for the virtual impermeability of the skin, especially to ions. But since the stratum lucidum cannot be seen with sufficient clarity in all skin types, Rein (1929) proposed that a "transitional" layer between cornified and non-cornified epidermis should be regarded as the site of the barrier, without specifying as to whether this was the stratum granulosum, the stratum lucidum, or even included the infrabasal horny layer. Rothman (1943) indicated that the horny layer cannot be regarded as a membrane in the electrophysiological sense, because it represents a rather rough network of horny lamella with large holes in it, and therefore is easily permeable for ions as well as for larger molecules. Mackee *et al.* (1945) noted that certain dyes appeared to come to a sudden halt in the stratum lucidum, and postulated the lucidum barrier both for ions and uncharged molecules. Calvery *et al.* (1946) regarded the stratum lucidum as the least impermeable of the various layers of the epidermis.

The water permeability experiments on isolated skin, epidermis and stratum corneum of Burch and Winsor (1944, 1946) and Berenson and

Burch (1951) showed that the stratum corneum has a similar permeability as whole skin and thus removed all reasonable doubt that the horny layer was indeed the permeability barrier. The technique of Pinkus (1951), whereby successive layers of the stratum corneum are removed by repeated strippings with adhesive cellophane tape, appeared to offer a way to relocate the barrier zone within the stratum corneum. This was employed by Blank (1953) who found that as the cornified epithelium is removed the rate of diffusion of water remained practically unchanged until the base of the stratum corneum is reached, when there was an abrupt increase in the diffusion rate. He concluded that the major barrier in the skin is not the entire cornified epithelium but is in the lower part of the stratum corneum. Szakall (1955) claimed to have isolated the barrier from the lower stratum corneum on adhesive tape as a coherent sheet of corneal cells and this coherent portion has been named the stratum corneum conjunctum, and the loose surface cells that strip individually as the stratum corneum disjunctum.

The stripping technique has not been limited to water, but other materials have also been employed to investigate barrier property. For example, Blank and Gould (1961) used six sodium alkyl sulphates and four sodium alkyl benzene sulphonates to investigate penetration from different vehicles and showed that none of these synthetic anionic surfactants penetrated normal excised human skin whereas penetration occurred following mechanical removal of the lower layers of the stratum corneum. This led the investigators to suggest that the rate-limiting barrier is in the stratum corneum conjunctum.

Kligman (1964) disputed the differentiation of the corneum into disjunctum and conjunctum, and maintained that the conjunctum is not an anatomical entity nor the real skin barrier but simply a modest portion of the stratum corneum.

Another approach in determining the site of the barrier within the stratum corneum has come from studies that show the location of a particular compound within the stratum corneum some time after compound application. The results are summarized by Kligman (1964), Malkinson (1964), and Tregear (1966). The largest amount is found in the outer corneal layers with decreasing, sometimes undetectable, amounts in the lower corneal layers. Malkinson (1964) maintains this infers a barrier in the lower stratum corneum while Kligman (1964) maintains it is a reflection of the concentration gradient in a uniformly permeable stratum.

Thus, what is not in dispute is that the epidermal barrier is located in the stratum corneum. Further supporting evidence has been provided by the observed decrease in permeability with regeneration of the stratum corneum after stripping experiments (Malkinson, 1958; Monash and Blank, 1958; Marzulli, 1962; Matoltsy *et al.*, 1962; Kumatsu and Suzuki, 1982). What remains in dispute, however, is whether the barrier is provided by the bulk of the stratum corneum (Kligman, 1964; Idson, 1975; Scheuplein and Bronaugh, 1983), or whether it is located only in the lower portion of the stratum corneum (Ainsworth, 1960; Marzulli, 1962; Grice *et al.*, 1975; Blake *et al.*, 1981; Bowser and White, 1985). The latter authors (Bowser and White), incidentally, introduced the term "stratum compactum" to describe the lowest region of the stratum corneum.

### 1.3.3 Diffusion below the barrier layer

Once a substance passes through the superficial barrier there is apparently no significant hindrance to further penetration of the remaining epidermal layers into the papillary dermis, following which there is ready entry into the circulation via the capillaries.

For a few substances, however, there has been a claim for a second barrier situated at the epidermal-dermal junction (Ferguson and Silver, 1947). These authors found that when two chlorine-liberating ointments were applied to the skin of rabbits and guinea pigs, the chlorine penetrated the various epidermal strata (corneum, granulosum and germinativum) but no deeper than the epidermal-dermal interface. Another example of this barrier action, demonstrable with autoradiographs, is the almost complete arrest at the epidermal-dermal junction of certain electrolytes once the superficial barrier is passed (Witten *et al.*, 1951, 1953).

Available data indicate that once a substance passes through the epidermis and into the dermis, its further passage into the capillaries is virtually assured. For example, radioactive lewisite, which appears to be fixed almost exclusively in the epidermis and in hair follicles, can still be demonstrated in blood vessels (Axelrod and Hamilton, 1947).

### 1.4 Properties of the stratum corneum

The cells of the stratum corneum (the corneocytes) are keratin-filled, metabolically inactive squamous hexagonal plates that lie parallel to



the skin surface. These cells do not overlay each other in a random manner, but are stacked in ordered columns of cells (MacKenzie, 1969, 1970; Christophers, 1971; Allen and Potten, 1974). At their lateral edges, cells in adjacent columns interdigitate to form horizontal laminae, and the lateral digitations are usually aligned vertically throughout the thickness of the stratum corneum. A schematic representation of such an arrangement is shown in Figure 1B. It has been suggested that this highly ordered arrangement of cells in the stratum corneum may, at least in part, be responsible for minimizing cutaneous permeability (Menton and Elsen, 1971).

The thickness of the stratum corneum varies widely between regions of the body and between species. For example, in man estimates of the corneum's thickness give values of 8.2, 9.4, 10.9 and 12.9  $\mu$  for the abdomen, back, thigh and flexor forearm respectively (Scheuplein, 1978). Corneum thickness appears to vary proportionately with the number of cell layers. On average about 19 cells, each 0.55  $\mu$  thick, give the corneum an overall thickness of 10.4  $\mu$  (Holbrook and Odland, 1974). Brody (1973) gave the average length and height of the corneocyte as 32.8  $\mu$  and 2.7  $\mu$  respectively. The corneum's thickness also varies with sex. For example, in the rat the thickness of the stratum corneum of the back and abdomen in the male is 34.7 and 13.8  $\mu$ , while that of the female is 18.2 and 13.7  $\mu$  respectively (Bronaugh *et al.*, 1983). Variation in the permeability of different skin sites has been attributed to variations in stratum corneum thickness (Holbrook and Odland, 1974; Frosch *et al.*, 1980; Bronaugh *et al.*, 1983).

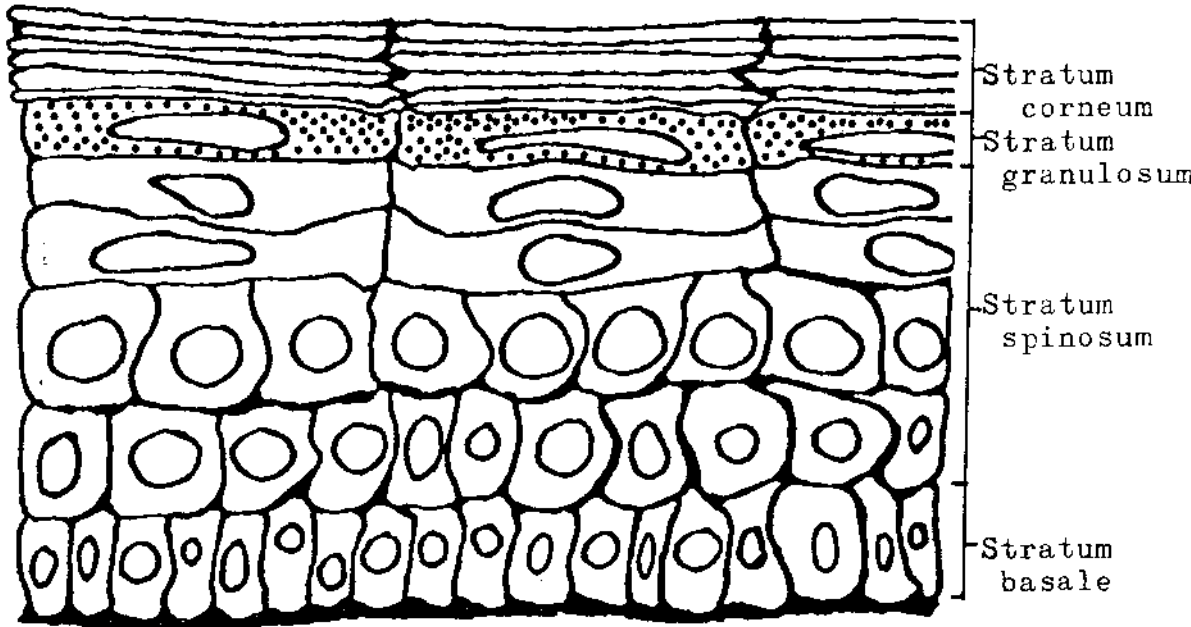


Figure 1B. Schematic representation of the epidermis. The corneal cells (corneocytes) are stacked in orderly columns. This orderly pattern is evident within 2 to 3 subcorneal cell layers ( Christophers, 1971).

#### 1.4.1 Contents of corneal cells

The prime biochemical product of the epidermis is a mixture of proteins called keratin. The ultrastructural studies of Brody (1959, 1960, 1964) demonstrated that the cytoplasmic mass of the cells of the stratum corneum consists of a compact arrangement of bundles of lightly stained filaments distributed in a more darkly stained matrix, and this arrangement has been termed the "keratin pattern". The filament bundles show a wavy or twisted course, and traverse the cells in different directions. The ultrastructural and chemical characterization of keratin, and in particular cortical wool cells, has received a lot of attention (Mercer, 1962; Lundgren and Ward, 1963; Rogers, 1964; Zelickson, 1967; Lee and Baden, 1975; Baden *et al.*, 1976). The results of these studies are consistent with a highly ordered filament-matrix pattern, and indicate that this pattern is formed by two components. The first is a fibrous protein ( $\alpha$ -keratin) which forms the keratin filaments; it has a low sulphur content which explains its low uptake of osmium stain. The other component is an amorphous globular protein of a high sulphur content which is believed to form the matrix surrounding the  $\alpha$ -keratin filaments. The filaments appear to be made up of still finer protofilaments about 200 Å in diameter, and each of these consists of two or three helically coiled polypeptide chains (Fraser *et al.*, 1965; Fraser, 1969).

Under normal *in situ* conditions the stratum corneum is always partially hydrated. A gradient in water concentration exists through the tissue corresponding to an average water concentration of 0.9 g/g dry tissue (Scheuplein and Morgan, 1967; Scheuplein and Black, 1971). The water content of the stratum corneum is of great importance in

maintaining flexibility, and the experiments by Blank (1952) have shown that water is the only plasticizer of dry corneum. Bulgin and Vinson (1967) used differential thermal analysis and illustrated that there are three types of water in the stratum corneum as judged by the observed endothermic peaks at 103<sup>o</sup>, 114<sup>o</sup> and 135<sup>o</sup> C. The 103<sup>o</sup> peak may be described as the elimination of free water and the 114<sup>o</sup> and 135<sup>o</sup> peaks as the elimination of "bound" water. Another investigation (Hanson and Yellin, 1972) has confirmed the existence of three types of water: (1) primary water of hydration, which is a tightly bound water absorbed at polar sites of the protein, for example, carbonyl or amine groups, and present at all levels of hydration. (2) secondary water of hydration which is a less tightly bound water probably representing that bound by hydrogen-bonds to the primary water of hydration. (3) water with weak interactions with the corneum's protein which is more like bulk liquid water than the first two. Figure 1C is a schematic representation of water in the stratum corneum. Scheuplein and Blank (1971) indicated that the mobility of water molecules *per se* within hydrated keratin is crucial to the permeability of water-soluble substances because they are very probably dissolved within this water. The effect of hydration on skin permeability is mentioned elsewhere (page 42).

Blank (1953) showed that very little change occurred in either the water binding capacity in a humid atmosphere or in the weight of human callus when it was extracted with water or polar solvents. However, there was a significant decrease in both the weight and the water binding capacity when the callus was extracted with water after the solvent treatment. The loss in weight is due to the extraction of water-soluble substances, and these have been investigated by a number

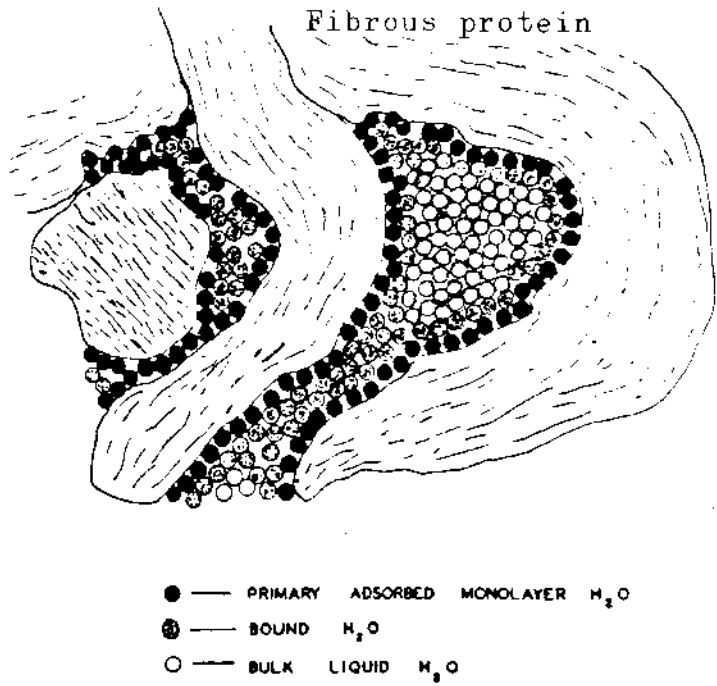


Fig. 1C. Diagrammatic representation of water in the stratum corneum (from Scheuplein, 1965).

of workers (Bolliger and Gross, 1954; Laden, 1965; Middleton, 1968). These substances consist of a mixture of amino acids, organic acids, urea and inorganic ions, and have been held responsible for the water binding capacity of corneum. Jacobi (1959) has used the term "natural moisturizing factor" to describe them. They are hygroscopic in nature, and it appears that sodium lactate (Fox *et al.*, 1962) and the sodium salts of 2-pyrrolidone-5-carboxylic acid (Laden and Spitzer, 1967) are the most hygroscopic components of this natural mixture.

The finding that the water-soluble substances of the stratum corneum can only be extracted by water after a solvent extraction suggests that lipid material is protecting them from dissolution in water, and that this lipid covering allows the passage of water but not the water-soluble substances themselves (Middleton, 1968). There is, however, a difference of opinion with regard to the location of the lipid system. Swanbeck (1959a, 1959b) and Swanbeck and Thyreson (1962) indicated that the lipid is located intracellularly and that it might form a coating around the individual keratin fibres. Brody (1960) however revealed, by ultrastructural studies of horny layers, the existence of a strongly electron-dense, osmiophilic substance between the keratin filaments which could be lipid. X-ray diffraction studies by Goldsmith and Baden (1970) revealed the presence of a uniquely oriented lipid in the intracellular matrix, the long axis of the lipid molecules being perpendicular to the axis of the keratin filaments. On the other hand, Middleton (1968) believed that the lipid is located in the plasma membrane of individual corneal cells, and not in the cytoplasmic matrix.

With regard to barrier function many workers believe that the barrier to diffusion is provided by the cytoplasmic content of the corneal cells (Marzulli, 1962; Tregear, 1962, 1966; Christophers, 1971; Scheuplein and Blank, 1971).

#### 1.4.2 Plasma membranes of corneal cells

The plasma membranes of basal, spinous and granular cells are trilaminar structures 60-70  $\text{\AA}$  thick. After granular cells discharge their membrane-coating granules and become horny cells, the plasma membranes undergo certain modifications. Matoltsy and Parakkal (1965, 1967) and Farbman (1966) indicated that the plasma membrane of keratinizing cells "thickens" during their ascent to the stratum corneum. Brody (1969) described the plasma membranes of horny cells as consisting of an outer triple-layered plasma membrane proper, which corresponds in thickness, ultrastructure and opacity with the plasma membranes of non-cornified cells, and an inner 100 to 120  $\text{\AA}$  thick "broad zone". This forms a continuous layer along the entire intracytoplasmic face of the inner leaflet of the plasma membrane and consists of two less opaque layers separated by a more opaque layer. Martinez and Peters (1971) indicated that the peripheral dense layer (broad zone) is continuous with the attachment plaques of desmosomes and appears to be fused to the inner leaflet of the plasma membrane. Fukuyama and Epstein (1969) suggested that the dense peripheral cytoplasmic band may result from the migration of cyst(e)ine-containing proteins to the cell periphery. The outer leaflet of the horny cell membrane is also modified by materials derived from the contents of membrane-coating granules expelled into the intercellular spaces, and these appear to fuse with the outer leaflets of the cell

membranes, thus forming an external coat. Other experiments have confirmed that there is no true thickening of the plasma membrane proper but a deposition of material on its inner and outer surfaces (Breathnach *et al.*, 1973). Studies of the structural and chemical properties of the horny cell envelopes indicate that this cell constituent has the highest degree of stabilization amongst the components of the horny cell (Matoltsy, 1961; Kligman, 1964). Whether all of these characteristics and modifications reflect in any way a significant decrease in cell membrane permeability remains to be elucidated. Nonetheless, Kligman (1964) indicated that the plasma membrane of corneal cells is able to act as an efficient permeability barrier. Matoltsy (1961) mentioned that it seemed appropriate to consider, in addition to cytoplasmic matrix, the envelope of the horny cell as part of the protective system.

#### 1.4.3 The intercellular region

Anatomically, the intercellular regions, or spaces, are of significance to skin penetration studies since they constitute a potential diffusion pathway through the stratum corneum which bypasses the keratinized corneal cells. On histological examination the intercellular space may contain intercellular substance, the intercellular components of desmosomes, or it may appear to be electron-optically empty.

Tregear (1966) reported that the intercellular space is  $400 \text{ \AA}$  in width, and that the total intercellular path length ( $250 \text{ \mu m}$ ) is longer than the thickness of the stratum corneum ( $50 \text{ \mu m}$ ) because of the extensive interdigitation of the corneal cells. Brody (1966) reported



that the intercellular space varies in width from 300 Å to 20,600 Å. This variation is not restricted to any particular sub-layer of the corneum and variations in electron microscopy technique do not appear to affect the measured width of the intercellular space. Scheuplein and Blank (1971) indicated that the volume of the intercellular spaces may be as large as 5% of the total volume in normal stratum corneum, but decrease to approximately 1% in fully hydrated corneum.

The histological custom of examining skin sections after fixation, dehydration, embedding and staining tends to perpetuate the erroneous notion that the intercellular spaces of the stratum corneum are wide and empty. In fact these spaces are normally filled (Brody, 1966) and the bulk of the corneum, with the exception of the few desquamating cells, is mechanically coherent (Scheuplein, 1978). The material occupying the intercellular spaces, that is the intercellular substance, originates at least in part from the discharge of membrane-coating granules from the interior of cells in the granular layer into the intercellular spaces (page 5).

Although the composition of lipids extracted from the stratum corneum varies in different species (Gray and White, 1978; Elias, 1981), it is generally accepted that the stratum corneum contains a large amount of neutral lipid (free sterols, sterol esters, free fatty acids and triglycerides), a lesser amount of glycosphingolipids (glucosylceramide) and cholesterol sulphate, and very little phospholipid (Gray and Yardley, 1975; Elias *et al.*, 1979; Elias, 1981).

Despite the view that the corneum's lipids are located intracellularly and surround keratin filaments (Swanbeck and Thyresson, 1962; Goldsmith and Baden, 1970), more recent morphological and biochemical studies suggest that the lipid system is located mainly in the intercellular spaces, and that it is derived from the excreted contents of membrane-coating granules (Matoltsy, 1976; Elias *et al.*, 1979; Elias, 1981).

The intercellular substance is believed to play a role in regulating the epidermal permeability. It has been shown that the intercellular substance prevents the inward and outward access to the stratum corneum of water-soluble, intercellular, electron-dense tracers such as lanthanum (Elias and Friend, 1975; Squier and Rooney, 1976; Elias *et al.*, 1977; Hayward, 1983; Squier and Edie, 1983) and horseradish peroxidase (Squire, 1973; Squire and Hall, 1985). Further support for a barrier function provided by the corneal intercellular substance has come from studies employing phospholipase C to digest the intercellular substance following which penetration of electron-dense tracers into the spaces between fully keratinized cells is observed (Hashimoto, 1971; Squire, 1984). Furthermore, essential fatty acid deficient rodents have been shown to have an abnormal barrier function, manifested by increased transepidermal water loss and by the ability of lanthanum to penetrate into the intercellular spaces of the stratum corneum. These changes are believed to be due to a decreased elaboration and deposition of the corneum's intercellular lipids (Elias and Brown, 1978).

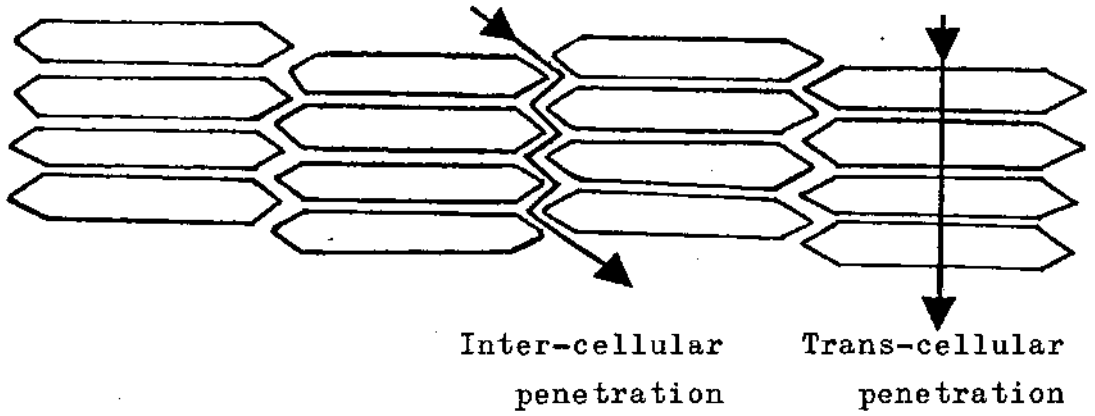
#### 1.4.4 Routes of penetration across the stratum corneum

Penetration of substances across the stratum corneum may be transcellular, that is through the cells and the bulk tissue, or intercellular, that is between the corneal cells. Figure 1D is a schematic representation of such penetrations. Available data conflict in terms of the relative importance of these two pathways. Some investigators believe that penetration across the stratum corneum is transcellular in that it has generally been held that water and water-soluble substances traverse the corneum by adhering to intracellular keratin filaments, whilst lipid-soluble substances traverse via lipid-rich interfilamentous matrix regions (Crouse, 1965; Blank, 1969; Goldsmith and Baden, 1970; Scheuplein and Blank, 1971; Baden *et al.*, 1976). Moreover, as a consequence of the rapid flux of molecules across the stratum corneum, the intercellular spaces have been dismissed as an important pathway of entry because their volume is insufficient to explain the observed rapid flux (Blank, 1969; Scheuplein and Blank, 1971). On the other hand, Elias and Friend, (1975), Elias and Brown, (1978), Nemanic and Elias, (1980) and Elias (1981) have provided morphological, histochemical and biochemical information indicating that the intercellular region of the stratum corneum is an important factor in both regulating the epidermal permeability and in providing an important route of penetration across the corneum.

#### 1.5 Routes of penetration across the skin

Three possible anatomical routes of penetration through the normal (or undamaged) intact skin are available:

Fig. 1D. Schematic representation of the routes of penetration through the stratum corneum.



(1) the bulk of the stratum corneum of the surface epidermis. Penetration through this route is termed transepidermal.

(2) the pilosebaceous units (hair follicles and their associated sebaceous glands). Penetration through this route is termed transfollicular.

(3) the ducts and coils of eccrine sweat glands. Penetration through this route is termed transudoriferous. Since hair follicles and sweat glands are appendages of the surface epidermis, penetration through these two structures is termed transappendageal.

Available data conflict in terms of the relative importance of these pathways. Some favour the epidermal appendages as the principal route of entry, while others favour the surface epidermis as the principal pathway of penetration. Rather interestingly, there is substantial confirmed data in the literature which seems to support both views. A few examples now follow.

Mackee *et al.* (1945) showed preferential penetration for dyes via the follicles by a histological study which examined skin 5 to 60 minutes after compound application. The results of Abramson and Alley (1937) and Cronin and Stoughton (1962) were consistent with mainly follicular penetration, as were the results of Shelley and Milton (1949) who demonstrated perifollicular weals within minutes of histamine application. Further support for transfollicular penetration came from the study of Montagna (1954) who found that vitamin A in four different vehicles (chloroform, alcohol, linoleic acid and oleic acid) penetrated intact skin of the guinea pig by way of the pilosebaceous

canals and the sebaceous glands. Evidence for transudoriferous penetration was provided by Abramson and Gorin (1940) and Abramson and Engle (1942) who demonstrated the rapid penetration of charged dyes through the sweat ducts under a potential gradient, with no comparable transport through the surface epidermis.

Other investigators have questioned the importance of the epidermal appendages in the penetration of materials, and favour the surface epidermis as the major route of entry. Radioactive tracer studies with tri-n-butyl phosphate showed that the hair follicles of pig skin are no more penetrable than the epidermis (Tregear, 1961). Wahlberg (1968) concluded that the ionic compound sodium chromate passes through the surface stratum corneum faster than through hair follicles or sweat ducts. Ainsworth (1960) indicated that the rate of absorption of tributyl phosphate into the skin was nearly the same whether the hair follicles were involved or not. Flesch *et al.* (1951) showed that the sweat "pore pattern" observed by Abramson and Gorin (1940) following dye penetration was readily erased by the scraping-off of the horny layer with a scalpel, and that penetration of the dye into the duct could not be demonstrated histologically. Scott and Kalz (1956) showed that C<sup>14</sup>-hydrocortisone penetrated the skin mainly via a transepidermal route, and that no substantial penetration occurred through follicular structures. Scott (1957) demonstrated that the penetration of radioactive sulphur through normal human skin was exclusively through the surface epidermis, and that no preferential absorption through hair follicles or other appendageal orifices was noted. The *in vitro* studies of Treherne (1956), Tregear (1960), Blank (1964) and Scheuplein (1965) are all measurements of

steady state fluxes and are in agreement with bulk diffusion through the unbroken stratum corneum.

Scheuplein (1967) and Scheuplein and Blank (1971) were able to reinterpret many of these apparently conflicting results and reached the conclusion that appendageal diffusion predominates in the initial stages of penetration, the so-called transient diffusion which occurs shortly after the application of a substance to the surface of the skin, whereas after the surface stratum corneum becomes saturated with the penetrant and the steady state diffusion is established, the dominant diffusion mode is no longer transappendageal but occurs through the stratum corneum. In other words it is transepidermal diffusion.

## **1.6 Factors affecting the permeability of the skin**

### **1.6.1 Skin condition**

Damaged skin is more permeable than undamaged skin regardless of the nature of the injury, viz stripping, scarification, prolonged hydration, prolonged treatment with surfactants, disease, etc. For example, if the skin is damaged by alkali, by lipid solvents, or by stripping with tape the impermeability of the skin to cationic (Blank *et al.*, 1964) and anionic (Blank and Gould, 1961) detergents decreases greatly. Frosch *et al.* (1980) demonstrated that the wealing reaction produced by exposure of skin to dimethyl sulphoxide (DMSO) is significantly intensified following scarification of the skin, or stripping of the stratum corneum with scotch tape. By means of radioactive counts, Scott (1957) showed that diseased human skin

(seborrhoeic dermatitis, acne vulgaris, psoriasis) is more permeable than normal skin. Loeffler and Thomas (1951) demonstrated the very rapid penetration of radiostrontium  $\text{Sr}^{89}$  through mechanically damaged (abraded and lacerated) skin of rats, and that the penetration rate is reduced and returned to its normal level when the skin is healed. Epidermis damaged by ultraviolet light irradiation, topical application of vitamin A acid or acetic acid is more permeable to topically applied hydrocortisone than undamaged epidermis (Solomon and Lowe, 1979). Similarly, Scott and Kalz (1956) reported that skin subjected to ultraviolet and Grenz irradiation is more permeable than non-irradiated skin, whilst Freeman *et al.* (1950) reported that skin damaged by heat burn is more permeable to phenol than undamaged skin.

#### 1.6.2 Age of the skin

Little detailed study has been carried out to determine the relationship between age and skin permeability. It appears that ageing has little effect on the permeability of the skin, with a single exception being preterm infants, in whom the stratum corneum is not completely formed, and where permeability is measurably larger (Nachman and Esterly, 1971). Hunt (1966) observed that the impermeability of rat skin to 5% aqueous triethyl phosphate appears during the later stages of foetal development and the first few days after birth and continues to rise thereafter until the epidermis appears histologically mature, that is, when the stratum corneum is fully developed. In fully developed skin, Kligman (1979) showed that the ability of the stratum corneum to prevent water loss did not decline with age.



### 1.6.3 Species variations

Humans and experimental animals exhibit large differences in skin permeability. Previous studies have shown that the skin of densely-haired animals (mice, rats, rabbits and guinea pigs) tends to be highly permeable, while the permeability properties of the skin of the pig are more comparable to that of man (Tregear, 1964; Marzulli *et al.*, 1969). Reifenrath *et al.* (1984) showed that weanling pig skin is a good model for permeability for human skin. Although the rank order of the permeability of skin of various species varies with the penetrant, Tregear (1966) listed the general order of species skin permeability as :-

rabbit > rat > guinea pig > pig > man.

Rats are convenient and frequently used laboratory animals for dermal toxicity evaluation. Previous permeability studies indicate that for some compounds (nandrolone and alkyl oestrenol) rat skin can be a reasonable model for human skin (Foreman *et al.*, 1983).

### 1.6.4 Racial variations

Frosch *et al.* (1980) illustrated that the skin of white subjects responded well to dimethyl sulphoxide-wealing formation whereas a lesser response was observed in black subjects. Furthermore this difference was statistically significant and was related to the previous findings of Weigand and Gaylor (1974) who indicated that there is a greater number of cell layers in the stratum corneum of blacks than in caucasian stratum corneum.

### 1.6.5 Sex variation

Variation in sex may result in variation in permeability. For example, Bronaugh *et al.* (1983) reported that, in the rat, female back skin was twice as permeable as male back skin, and was attributable to the thickness of the stratum corneum.

### 1.6.6 Repeated application

Kaidbey *et al.* (1975) reported that repeated exposure of normal skin to retinoic acid resulted in a reduction of the thickness of the stratum corneum accompanied by an increase in the permeability of the horny layer to dimethyl sulphoxide and histamine.

### 1.6.7 Seasonal variations

Frosch *et al.* (1980) reported that intense wealing responses could be produced by exposure of intact skin to dimethyl sulphoxide during the cold winter season (November to February). In contrast, when the same subjects were tested again during the hot summer season (June to August) much smaller weals were obtained, and this difference was shown to be statistically significant.

### 1.6.8 Regional variations

The permeability of the skin varies in different sites. Smith *et al.* (1961) showed that, in man, the scrotal skin is more permeable to topically applied anaesthetic, salicylic acid and hydrogen sulphide gas than abdominal skin, and that water vapour loss is also greater

through the scrotal skin than the abdominal skin. Feldmann and Maibach (1967) applied  $C^{14}$  cortisone to human skin and found the scrotal skin to be most permeable, followed by the skin of the forehead, scalp and axilla, back, and the palm and sole. Frosch *et al.* (1980) investigated the intensity of the wealing response at different sites of the human body consequent to exposure to dimethyl sulphoxide, and found the forehead to be the most reactive and the ventral aspect of the wrist to be the least reactive. They presented the rank of order of decreasing reactivity as:-

forehead > upper back > anticubital fossa > mid-ventral forearm > lower leg > ventral wrist.

In other species, it has been shown that the abdominal skin of the male rat is more permeable than back skin (Bronaugh *et al.*, 1983). A regional difference in permeation has also been observed in the monkey (Wester *et al.*, 1980). The variation of permeability at different skin sites has been attributed to the anatomical variation of the stratum corneum thickness (Holbrook and Odland, 1974; Bronaugh *et al.*, 1983) or to regional differences in the lipid content of the corneum (Elias *et al.*, 1981). The lower permeability of hyperkeratonic and lichenified skin compared to normal skin was also attributed to the thickness of the stratum corneum (Scott and Kalz, 1956).

#### 1.6.9 Blood flow

Malkinson (1964) indicated that the faster the rate of removal of a topically applied substance by the dermal vasculature, the greater became the concentration gradient between the skin surface and the deeper tissue, thereby promoting passage inwards. Since diffusion through the stratum corneum is usually the rate-limiting factor in

percutaneous penetration, Tregear (1966) indicated that cutaneous circulation should have little effect on penetration rate, unless blood flow was drastically reduced. Frosch *et al.* (1980) produced hypothermia by application of ice cubes to the skin of human subjects, and found that in these areas the wealing reaction produced by exposure of the skin surface to dimethyl sulphoxide was decreased when compared to control areas. Pinson (1952) found that a reduction in blood flow through the superficial skin capillaries, caused by cooling the skin, resulted in retardation of the penetration of the radioactive tracer tritium.

#### 1.6.10 Hydration

Water plays an important role in skin permeability as the endogenous plasticizer of the stratum corneum (Blank, 1952) and as a common vehicle. Under normal conditions the stratum corneum is always partially hydrated, and the average water concentration in the stratum corneum *in vivo* has been estimated at approximately 0.9 g/g dry tissue (Scheuplein and Blank, 1971). The water permeability of skin has been studied extensively (Burch and Winsor, 1944; Berenson and Burch, 1951; Blank, 1952, 1953, 1965; Onken and Moyer, 1963; Scheuplein, 1966; Matoltsy *et al.*, 1968).

A number of studies have demonstrated that there is increased penetration as a result of increased hydration of the stratum corneum. The excess water causing the increased hydration can originate from two sources: (1) from within the skin, for example, as a result of occlusion, or (2) from outside the skin, for example, as a result of exposure of intact or isolated skin to a moist external environment.

The following are a few selected examples which demonstrate the effect of hydration on skin permeability.

Cronin and Stoughton (1962) demonstrated increased rates of penetration of nicotinic acid *in vivo* by direct wetting of the skin. Malkinson (1964) demonstrated an increase in the percutaneous absorption of salicylic acid as a result of hydration. Scheuplein *et al.* (1969) were able to obtain up to a 20-fold enhancement in the rate of cortisone permeation *in vitro* by exposing the dry stratum corneum to water vapour. The use of occlusive dressings to promote the penetration of topically applied materials is an effective exploration of the enhanced penetration produced by hydration (McKenzie, 1962; McKenzie and Stoughton, 1962; Vickers, 1963). Here the reduction of water loss and the subsequent increase of water concentration in the stratum corneum enhance the inward penetration. It is relevant to note that prolonged hydration increases susceptibility to irritation as a result of increased penetration. For example, workers afflicted with cement dermatitis are usually those who handle the wet cement/sand mixture, and not those handling the dry powder (Possick, 1969). Although hydration increases the permeability of the stratum corneum, the fully hydrated corneum remains one of the most impermeable of all biological tissues (Scheuplein and Blank, 1971).

#### 1.6.11 Concentration of penetrant

The percutaneous penetration of a substance is some function of its concentration in the vehicle as presented to the surface of the skin. It is generally accepted that penetration through the fully keratinized, metabolically inactive stratum corneum is via passive

diffusion (Blank, 1969). The similarity between penetration data of *in vivo* and *in vitro* experiments (Ainsworth, 1960; Bronaugh and Franz, 1986) supports this view. Thus, the effect of concentration as a factor controlling penetration can be examined by reference to Fick's general law of diffusion which, in essence, states that substances move across a membrane from a region of higher to a region of lower concentration (that is, passive diffusion) in direct proportion to the difference in concentration on the two sides of the membrane. This is commonly written as:

$$J_s = K_p \cdot \Delta C_s \quad \dots \quad \dots \quad \text{equation (1)}$$

where  $J_s$  is the flux across the membrane, that is, the amount of material (micromoles) that penetrates a unit area of skin ( $1 \text{ cm}^2$ ) in unit time (1 hr),  $K_p$  is the permeability constant and  $\Delta C_s$  is the difference in concentration between the two sides of the membrane.

There are many examples which demonstrate the adherence to Fick's law of transport across the skin, that is, increased penetration as result of an increase in concentration of the penetrant in the presenting vehicle (Treherne, 1956; Blank, 1964; Tregear, 1966; Maibach and Feldmann, 1969).

Blank (1969) indicated that the flux is more accurately related to the difference in concentration in the top and bottom layers of the stratum corneum rather than to the difference in concentration in the solutions on the two sides of the membrane. It has also been shown the flux of penetrant substances is inversely proportional to the thickness of the stratum corneum (Blank, 1953). Thus, Fick's general

law is now expanded to:

$$J_s = \frac{D_m}{\delta} \Delta C_s \quad \dots \dots \text{equation (2)}$$

where  $\delta$  is the thickness of the stratum corneum and  $D_m$  is the diffusion constant (Blank, 1969). From this it is seen that the flux is proportional to the "concentration gradient" across the stratum corneum, that is the difference in concentration divided by the thickness of the corneum  $\left(\frac{\Delta C_s}{\delta}\right)$ .

In a study of the penetration of low molecular weight alcohols, Blank (1964) prepared pentanol in olive oil to various concentrations up to 5M, and found that initially the flux is nearly a straight-line function of concentration for weak solutions, that is, increase in concentration results in an increase in penetration. As the concentration is increased above 1M, the flux does not continue to rise but levels off and finally decreases as the concentration is further increased. Consistent with this are the results of Skog and Wahlberg (1964) who studied the penetration of radioactive metal compounds by the disappearance technique. They found a definite increase in penetration with increasing concentration up to a particular value, which seemed to be characteristic of each substance, and that further increase in concentration resulted in a gradual decrease of penetration. From the above it emerges that the linear relationship between penetration and concentration holds accurately for relatively low concentrations, whereas if the concentration is increased sufficiently the linear relationship breaks down. This has been attributed to an interaction between the penetrant and the skin

or to a change in the chemical activity of the penetrant in the applied vehicle (Higuchi, 1960; Blank and Scheuplein, 1964).

#### 1.6.12 Vehicles and solubility characteristics of penetrants

A vehicle may be defined as the substance in which the test material is prepared. General types of vehicles include ointments, aqueous and organic solvents. Physical and chemical interactions between the vehicle, the incorporated test material and the skin itself may result in either enhancement, hindrance or even prevention of penetration. Although Scott and Kalz (1956) failed to reveal any major difference in the penetration of  $C^{14}$  hydrocortisone when this was prepared in four different ointment bases, a number of studies are available which indicate that a particular test material penetrates the skin better from one vehicle than another. Some examples follow. In a study of mercury penetration, Laug *et al.* (1944) reported that: (1) poor penetration was noted from lanolin, mineral oil and petroleum vehicles, whereas good penetration was noted from lard and corn oil. (2) a paste of propylene glycol and calmel gave outstanding penetration in contrast to a paste of water and calmel which gave the poorest penetration. (3) a 50-50 mixture of lanolin and lard gave penetration better than from either alone. Using an autofluorescence technique, Montagna (1954) found that vitamin A penetrated skin most rapidly when it was dissolved in chloroform, whereas penetration was slow from lineolic acid, oleic acid and viscous petrolatum paste. Using petrolatum, water and ethylene glycol as vehicles, Bronaugh and Franz (1986) demonstrated that caffeine penetrated skin most readily from the petrolatum vehicle, whilst the greatest testosterone penetration was from water. Ayres and Hooper (1978) showed that the



penetration of cortisol into intact skin from Alphaderm was better than from Calmurid HC, Efcortelan or Topisone vehicles. Yankell (1969) has listed other examples.

Some investigators related skin penetration rates of substances to their relative solubilities in the vehicle (water) and in lipid solvents. Treherne (1956) studied the permeability of a variety of compounds, including glucose, urea, glycerol, thiourea, methanol, ethanol and ethyl iodide, and found that those with an ether:water partition coefficient nearest to 1 were most readily absorbed, that is, maximum permeability was observed for those which had about equal ether - and water - solubility. Stoughton *et al.* (1960) investigated the percutaneous absorption of nicotinic acid and seven derivatives and found a good correlation between the relative solubility in water and ether of a compound and its rate of penetration. Other workers focused their attention on the competitive affinities of the vehicle and the stratum corneum for the penetrating substance as being a major factor controlling penetration. The view that the relative solubility of the penetrant in the stratum corneum and the presenting vehicle (the partition coefficient) is a major penetration-controlling factor has been discussed and confirmed (Blank, 1964, 1969; Blank and Scheuplein, 1964; Scheuplein and Blank, 1971; Bronaugh and Franz, 1986). Thus an additional factor may now be added to equation (2) (page 45) in order to make it yet more meaningful, namely:-

$$J_s = \frac{K_m D_m}{\delta} \Delta C_s \quad \dots \dots \text{equation (3)}$$

where  $K_m$  is the partition coefficient.

From the above it is clear that penetration (or flux) is proportional to the stratum corneum-vehicle partition coefficient, and that this applies to all vehicles, assuming the vehicle itself does no damage to the tissue (Scheuplein and Bronaugh, 1983). In a biophysical examination of the subject of percutaneous penetration, Scheuplein and Bronaugh (1983) indicated that penetration can increase either by an increase in the solubility of the solute in the tissue or by a decrease in the solubility of the solute in the vehicle. Thus, depending on the vehicle used, a lipophilic solute may penetrate faster, slower, or at the same rate as a comparable water-soluble substance. As an illustration of this Scheuplein and Blank (1971) exemplified water, isopropyl palmitate and olive oil as vehicles and a homologous series of alcohols as solutes.

#### 1.6.13 Treatment of skin with aprotic solvents, organic solvents and surfactants

There are many substances which, when applied to the skin, can alter its permeability properties. Of major interest are those substances which have a mild effect or even a reversible effect on the tissue, as it might be possible with these substances to temporarily alter the properties of the skin to the advantage of the investigator. Therefore, excluded from consideration are strongly corrosive chemicals which severely, or even permanently, damage the skin.

##### Aprotic solvents:

These solvents have been widely proposed as penetration accelerants or enhancers. Dimethyl sulphoxide (DMSO), dimethyl acetamide (DMAC), and dimethyl formamide (DMFA) are examples of this class of solvents.

DMSO has been the subject of extensive investigation in particular. It is a dipolar aprotic solvent, it differs from water or alcohol in its tendency to accept rather than donate protons, it is miscible with water and organic solvents, and it is capable of bringing into solution a large number of organic and inorganic substances including metal salts (Scheuplein and Bronaugh, 1983).

As a penetrant, DMSO passes rapidly through the skin following topical application (Allenby *et al.*, 1969a). As a vehicle or enhancer, DMSO has been found to accelerate the penetration through the skin of numerous substances applied *in vivo* (Stoughton and Fritsch, 1964; Kligman, 1965a, 1965b; Baker, 1968) and *in vitro* (Stoughton and Fritsch, 1964; Elfbaum and Laden, 1968a, 1968b, 1968c; Malkinson, 1958).

The effect of DMSO in enhancing penetration is dependent upon its concentration. It is effective in increasing skin penetration when used in solvent concentrations in excess of 50-70% (Allenby *et al.*, 1969b, Scheuplein and Ross, 1970).

The mechanism of action of DMSO is not yet fully understood, but it is clear that its potentiating effect is not due to a carrier mechanism (Elfbaum and Laden, 1968b) or to more favourable partitioning of the solute (Scheuplein and Ross, 1970). The enhanced penetration of ions as a result of DMSO action has been attributed to lipid extraction or protein denaturation (Elfbaum and Laden, 1968b). DMSO is extremely hygroscopic and miscible with water in all proportions (MacGregor, 1967). It is capable of swelling and unfolding several proteins and the swelling of wool fibres by DMSO has been demonstrated (Bradbury

and Chapman, 1964; Abbott *et al.*, 1968). Scheuplein and Ross (1970) and Scheuplein and Blank (1971) proposed that DMSO displaces "bound water" from the stratum corneum and substitutes for it a looser, less associated solvent-protein structure.

The action of DMSO is largely reversible, that is, the original low permeability of the skin is, to a large extent, restored when the DMSO is removed (Kligman, 1965b; Baker, 1968; Allenby *et al.*, 1969a). However, Scheuplein and Ross (1970) reported that permanent damage to skin may result from exposure to pure (100%) DMSO for a prolonged period (6 hrs).

#### Surfactants:

Surfactants are routinely and widely applied to the skin either as soaps or detergents, or as emulsifying agents in drug and cosmetic formulations (Scheuplein and Bronaugh, 1983). Scheuplein (1978) indicated that soaps and detergents are perhaps the most damaging of all substances applied routinely to the skin. Unlike other substances such as organic solvents and dimethyl sulphoxide, which have to be applied in high concentrations in order to damage the skin, anionic and cationic surfactants are deleterious even in very dilute solution (Dugard and Scheuplein, 1973). Therefore, it seems reasonable to assume that if a potential irritant is placed on the skin surface, penetration as far as the viable epidermis is necessary for it to exert its irritant effect (Bettley, 1963). Indeed, there is evidence that anionic and cationic surfactants do penetrate through the skin (Blank and Gould, 1959; Bettley, 1963; Blank *et al.*, 1964), with anionics penetrating best followed by cationics and nonionics (Bettley, 1963; Wahlberg, 1968).

Among the three classes of surfactants (anionic, cationic, and nonionic), the anionics appear to exert the most marked effect on skin permeability. For example, it has been observed that nickel salts compounded with anionic surfactants cause eczema, but nickel salts combined with nonionic or cationic surfactants do not (Vinson and Choman, 1960). Furthermore, irritation and histological damage observed in mouse skin with ionic surfactants, cannot be produced with similar concentrations of Tween 80, a nonionic surfactant (Lansdown and Grasso, 1972). The ability of anionic surfactants to promote absorption was confirmed by the observation that 1% potassium palmitate markedly increases the permeability of skin to water and to salicylate anion (Bettley, 1961, 1963). Of all anionic substances, the laurate ion has received the greatest attention in permeability studies. Sodium lauryl sulphate was found to increase the permeability of skin to water (Scheuplein and Ross, 1970; Prottey *et al.*, 1976). Frosch *et al.* (1980) reported that exposure of skin to 0.25% sodium lauryl sulphate rendered the skin more permeable to dimethyl sulphoxide when compared to controls. Pereyra (1945) reported that the incorporation of sodium lauryl sulphate with copper salts in solutions markedly increased the extent of penetration of copper ions into the skin by iontophoresis.

The effect of surfactants on cutaneous permeability is reported to be reversible, that is, the permeability of the tissue, for example to water (Bettley and Donoghue, 1960), returns to normal when the surfactants are removed. It is also reported that topical application of lineolic acid restores to normal the abnormally high rate of transepidermal water loss in skin treated with sodium laurate (Prottey *et al.*, 1976).

The accelerant action of surfactants may be attributed to their interactions with the proteins of the stratum corneum. They are considered to bind strongly with the keratin filaments which undergo an  $\alpha$  to  $\beta$  conformational change accompanied by uncoiling of the filaments. This induces tissue swelling and an alteration in the corneum's water binding capacity which also reduces the diffusional resistance of the skin and thus permits a greater permeability (Scheuplein and Ross, 1970; Scheuplein and Blank, 1971). The effect of surfactants on tissue structure appears to be concentration-dependent. When applied at low concentrations, the above changes are observed and the original dimensions of the tissue are restored after the surfactant is removed, but at sufficiently high concentrations over prolonged periods dissolution of keratin occurs (Scheuplein and Ross, 1970).

#### Organic solvents:

When organic solvents, like methanol, acetone, ether, hexane and chloroform, come into contact with the skin, they dissolve and remove surface lipids and lipids (free and/or combined) from the stratum corneum (Blank and Gould, 1961). Pretreatment with solvents so alters the cornified epithelium that subsequent hydration removes relatively large amounts of a strongly hydrophilic material which is not normally removed with water alone (Blank, 1953). When the stratum corneum is immersed in organic solvents for 30 minutes the gross appearance of the tissue is unchanged, the mechanical strength is not greatly altered, and no detectable change in the birefringence of the keratin filaments is observed (Scheuplein and Ross, 1970). However, delipidization, resulting from prolonged treatment with organic solvents, produces a fairly porous non-selective membrane (Scheuplein,

1978), that is, it markedly alters the permeability of the skin. Blank *et al.* (1964) reported that little, if any, of the cationic detergent benzalkonium chloride penetrated normal skin whereas the impermeability of the skin decreased following treatment with lipid solvents (over 65 hours). Similarly, Blank and Gould (1961) demonstrated that none of the six sodium alkyl sulphates (octyl, decyl, dodecyl, tetradecyl, hexadecyl, and octadecyl) and the four sodium alkyl benzene sulphonates (P-decyl, P-dodecyl, P-1-methyl dodecyl and P-1-methyl hexadecyl) penetrated normal excised human skin in measurable or detectable amounts, whereas penetration occurred after the skin had been treated with organic solvents. Further evidence of increased permeability as a result of treatment with organic solvents has come from the study of Scheuplein and Ross (1970) who showed that pretreatment of the stratum corneum with ethanol, acetone, ether, or a mixture of chloroform and methanol (2C:1M) greatly increased the permeability of the membrane to water. They also observed that each solvent changed the membrane permeability to a different degree with chloroform-methanol mixture having by far the greatest effect.

## **1.7 Iontophoresis**

### **1.7.1 Definition and synonyms**

The term iontophoresis is applied to the process of introducing ions into the tissues of the body by means of a direct (unidirectional uninterrupted) galvanic current. This process has been given a variety of other names including medical ionization, electrotherapy,

ionic medication, electrophoresis, ion transfer, ionization, iontotherapy and galvanotherapy.

### 1.7.2 Historical review

The introduction and use of electric current in the medical field is by no means a recent discovery. Probably the earliest work available on this subject is contained in a publication entitled *Tractatus De Magnete*, published in the year 1600 by one Dr Gilbert who was physician-in-ordinary to Queen Elizabeth (cited in Cross, 1925). One of the early textbooks available on the subject of the use of electricity in medicine is that of Guilleminot (1906). This author listed the names of some investigators who experimented with iontophoresis between the years 1833 and 1904. There is, however, no textbook that has included the names of workers on the subject of electrotherapy to the extent of Stillwell (1983), who spent 20 years collecting articles published in different languages and from different libraries in different parts of the world. This author has listed the names of more than 923 investigators who experimented with electrotherapy, most of which date back to the 1700's and the 1800's.

It was not until the turn of this century that iontophoresis was recognised as a valuable addition to the medication armament. The credit is due to some classic experiments carried out by Leduc in 1900 (cited in Guilleminot, 1906; Fleming, 1943; Pereyra, 1945). It is worthwhile to mention some of these experiments. Two rabbits received iontophoretic treatment, the electrodes being applied to the flanks which had been shaved previously. In the first rabbit, the positive electrode was saturated with a solution of strychnine sulphate and the



negative electrode was saturated with saline solution. In the second rabbit, the positive electrode was saturated with the saline solution, and the negative electrode with a solution of potassium cyanide. A current of 60 to 100 milliamperes was passed for a period of up to 20 seconds, following which the first rabbit died of strychnine intoxication and the second rabbit died of hydrocyanic poisoning. If the current was passed in the reverse direction, so that the strychnine cation was introduced from the negative electrode and the cyanide anion from the positive electrode, neither animal was affected in the slightest degree.

### 1.7.3 Significance and importance of iontophoresis

Since its introduction, iontophoresis has been used as a therapeutic tool. It has been tried in the treatment of almost every accessible surface tissue in the body, notably in the eyes, nose, ears, mouth, genital areas and skin. It is appropriate to review some of the clinical aspects of the use of iontophoresis since this throws some light on the significance and importance of this technique.

In ophthalmology, Erlanger (1939) described the treatment of acute and chronic infections of the eye by iontophoresis using zinc, calcium and adrenaline. Erlanger (1936) also discussed the treatment by iontophoresis of many eye diseases, including catarrhal ulcers of the cornea, inflammation of the everted eyelid, *ulcers serpens corneae*, keratitis disciformis and many others. He concluded that iontophoresis was of great therapeutic value in most of the common diseases of the eye and, when used in the uncommon and rare diseases, sometimes produced astonishing and very impressive therapeutic

results. Fleming (1943) used iontophoresis in the treatment of bilateral gonococcal conjunctivitis with calcium-adrenalin-silver nitrate, double acute conjunctivitis with calcium-adrenalin-prontosil, supra-orbital hepatic eruption with acetylcholine-calcium, and many other conditions including deep infections such as scieritis, iridocyclitis and retro-bulbar neuritis. He concluded that one could rely with confidence on iontophoresis to bring about very considerable betterment, if not a cure.

In otology, rhinology and laryngology, Friel (1919) described the treatment of acute and chronic inflammation of the middle ear and nasal sinuses using zinc iontophoresis. Smit (1936) and Hollender and Fabricant (1938) also employed iontophoresis in the treatment of different forms of rhinitis and investigated tissue changes during treatment.

In dentistry, Deuschle (1943) outlined methods for managing dental and alveolar infections using aluminium sulphate iontophoresis.

In gynaecology, Craig and Kraff (1943) treated many cases of acute pelvic inflammation masses of tubal origin by iontophoresis of acetyl- $\beta$ -methylcholine, and reported that iontophoresis was a valuable therapeutic tool. Jacoby and Derbrucke (1942) reported the use of iontophoresis in the treatment of vaginal disorders.

Interestingly, iontophoresis has also been employed in neurology. Ehrenwald (1942) reported the use of iontophoresis in the treatment of various conditions such as migraine, habitual headaches, essential

hypertension and cerebral sclerosis, as well as inflammatory cases such as chorea and post-infective encephalitis.

Iontophoresis has received greater attention and wider use in dermatology. It has been employed widely in the study of allergic skin reactions such as wheal formation with histamine and allergens (Abramson and Alley 1937; Abramson, 1938; Abramson and Gorin, 1939). More recently, Hornqvist *et al.* (1984) studied skin reactions (blanching, piloerection and erythema) by iontophoresis of a variety of drugs including phenylephrine hydrochloride, isoprenaline chloride, clonidine hydrochloride and propranolol hydrochloride.

Jersild and Plesner (1940) reported the treatment of epidermophytia on the extremities with copper iontophoresis. Knox (1943) also treated fungus infections on the feet by copper iontophoresis. Shaffer and Zackheim (1947) employed potassium iodide iontophoresis in the treatment of sporotrichosis following which the infected area showed complete healing. Furthermore, they indicated that treatment with iontophoresis could prove to be of value in cases in which the disease did not respond to oral iodides, or in which symptoms of intolerance to large oral doses of iodides developed. Kramer (1937) applied iontophoresis of acetyl- $\beta$ -methylcholine chloride in the treatment of peripheral vascular diseases and concluded that such a procedure gave relief in many cases by improving peripheral circulatory function. Martin *et al.* (1937) also administered acetyl- $\beta$ -methylcholine chloride by iontophoresis in the treatment of infectious and metabolic forms of arthritis, and reported that many patients were helped, some becoming symptom-free. Hill *et al.* (1977) used iontophoresis of adenine arabinoside monophosphate (Ara-AMP) in treating lesions of

herpes simplex viruses. There have been several reports on the successful treatment of hyperhidrosis of the palms and soles with iontophoresis (Grice *et al.*, 1972; Shrivastava and Singh, 1977; Midtgaard, 1986). Midtgaard (1986) found iontophoresis to be so effective in the treatment of axillary hyperhidrosis that he recommended it in preference to surgical excision of the sweat gland. In other species, iontophoresis has also been employed with successful results in the treatment of demodex infestation of the dog and ringworm infections of cattle (McEwan Jenkinson *et al.*, 1974).

All the examples cited above are included to emphasize the importance of iontophoresis as a valuable therapeutic tool. It is by no means a complete list, for Stillwell (1983) has listed more than 50 conditions involving different parts of the human body in which success has been claimed by using such a technique. The striking clinical results mentioned above have brought about renewed interest in iontophoresis as an experimental tool, particularly for investigating penetration through normal (non-diseased) skin.

#### 1.7.4 Basic aspects

In order to understand the processes by which ions can be introduced into and through the skin by a galvanic current, it is necessary first of all to spend a short time reviewing the elementary principles of physics employed in the design of an iontophoresis apparatus, as well as chemical aspects concerning the behaviour of ions when subjected to an electric current.

#### 1.7.4.1 Electrophysics

(i) Electric current: A stream of loose electrons passing along a conductor is called a current of electricity. To establish or maintain an electric current it is necessary that there be a source of energy generating an electric charge, and that there be an unbroken conducting material maintained between the higher and lower level of electrons. The path of the current from the generating source through the various conductors (including the experimental subject) back to the generating source is called an electric circuit. As the electric current flows, the circuit is said to be "closed". If an interruption or a break occurs in the circuit it is said to be "open" and the current ceases to flow. This has led to the employment of switches which can be closed (turned on) in order to start the current, and opened (turned off) so as to discontinue the current.

Two forms of current are employed in every-day commercial life, the direct and the alternating. In the case of the direct current, which is used for iontophoresis, the flow of electrons continues unchanged in the same direction, while in the case of alternating current the direction of flow changes periodically.

The ampere measures the rate of flow of electricity and serves as the unit of current. For commercial or industrial purposes a current flow of several hundred amperes may be used. For electro-medical work a much lower rate of flow is required; therefore only  $10^{-3}$  ampere (the milliamperere) is employed as a measuring unit.

(ii) Current strength and current density:

The words "strong" and "weak", when applied to electric currents, refer to the quantity of electricity that is passing. If the quantity is large the current is strong, and vice versa.

The density of a current refers to the quantity of electricity in relation to the surface area over which it is passing. It is determined by the area of the electrodes or, more precisely, by the area of contact of the electrodes with the skin, and by the strength of the current and the duration of flow. The density of a current is inversely proportional to the surface area. A current of the same strength has a higher density where it enters (or leaves) the body by way of an electrode of small area than where it enters (or leaves) by way of an electrode of large area. The current density is, however, directly proportional to the value of the current amperage and the time of flow; the stronger the current and/or the longer the time of flow, then the higher the current density.

(iii) Resistance: A rheostat or resistor makes use of the constructive ability of certain conductors or combinations of alloys, placed in the path of the current, to regulate the amperage. There is usually a very negligible flow of current when the full resistance is in the circuit and as the resistance is gradually decreased the current flow correspondingly increases. The unit of resistance is the ohm.

A resistor of the type most generally used in electro-medical apparatus consists of a single layer of resistance wire wound in a straight or a circular form and so arranged that a sliding contact

cuts in or out as much of the coil as is necessary to give the required current. If a number of resistors are used, then they are connected in series so that the total resistance is the sum of the individual resistances.

(iv) Electromotive force: The pressure or push which moves electrons from a terminal with an excess of electrons (high potential) towards a terminal with a deficiency of electrons and an excess of protons (low potential) is known as the electromotive force (EMF). This potential difference and so EMF which causes the flow of current, can be produced by a variety of techniques including electromagnetic induction in dynamos, friction, and chemical action in cells (for example, dry batteries). The unit of EMF is the volt. The most popular source of current for iontophoresis is the dry battery.

(v) Typical features of the apparatus: The apparatus for iontophoresis purposes usually consists of:-

- (1) a source of current (dry batteries).
- (2) a switch by which the current is turned on or off.
- (3) a milliammeter showing the intensity of the current (mA).
- (4) a resistor, or a group of resistors, which regulate(s) the strength of the current as needed.
- (5) terminals for the insertion of conducting cords which lead the current from and to the apparatus. The signs positive (+) and negative (-) are marked on the terminals to designate the direction of the flow of the current. Electrons always flow from the negative to the positive terminal while the current flows in the opposite direction.

All these typical and basic parts are connected in series and usually contained within a box or cabinet. All switches, knobs and terminals are mounted on insulating material such as hard rubber or porcelain.

According to the type of apparatus, there may be other controls such as a pilot light, which lights up as the current starts to flow, and a timing device by which the current flow can be set for a selected period of time at the end of which the current is automatically cut off. Different designs of apparatus have been described for iontophoresis by Clayton (1952), Suzuki, (1956), Watkins, (1962) and Liventsev (1964).

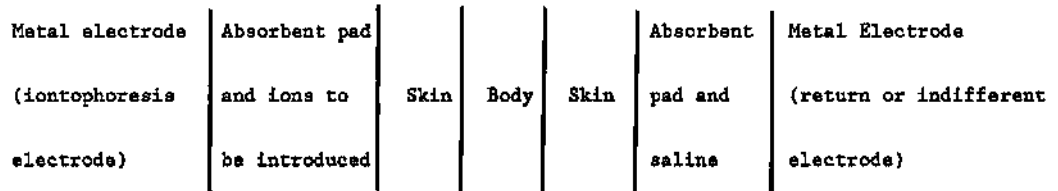
#### 1.7.4.2 Electrochemistry

When a current is passed through a solution containing free ions, that is through a solution of an electrolyte, a definite and orderly movement commences. Ions that carry a positive charge (cations) move towards the negative electrode (cathode) according to the basic law of attraction and repulsion, whereas those having a negative charge (anions) travel towards the positive electrode (anode). This phenomenon is used for introducing therapeutic or experimental ions into the skin. Thus, in theory, ions can be introduced into the skin according to the sign of the charge which they assume when dissociated in solution. From the positive electrode the ions of metals, as well as particles of complex substances which are positively charged in solutions, are introduced into the skin. From the negative electrode, the ions of acid radicals as well as particles of complex substances which are negatively charged in solutions are introduced into the skin.



### 1.7.5 Mode of application

At least two publications (Abramson and Gorin, 1939; McEwan Jenkinson *et al.*, 1974) describe the way in which electrodes are used for iontophoresis treatment. The human subject or the experimental animal is placed in the galvanic circuit as indicated below:-



### 1.7.6 Conditions for iontophoresis

According to Hill *et al.* (1977) the conditions necessary for iontophoretic treatment are as follows.

- (1) The drug must be charged or modified to carry a charge.
- (2) The drug is applied under an electrode of the same charge (iontophoresis electrode)
- (3) A return electrode opposite in charge to the drug is placed at an indifferent site of the body.
- (4) The current is allowed to flow below the level of pain threshold for an appropriate amount of time.
- (5) The condition to be treated must be at a superficial location.
- (6) The electrical current assures penetration of the drug into the surface tissue.

### 1.7.7 Distribution of the current

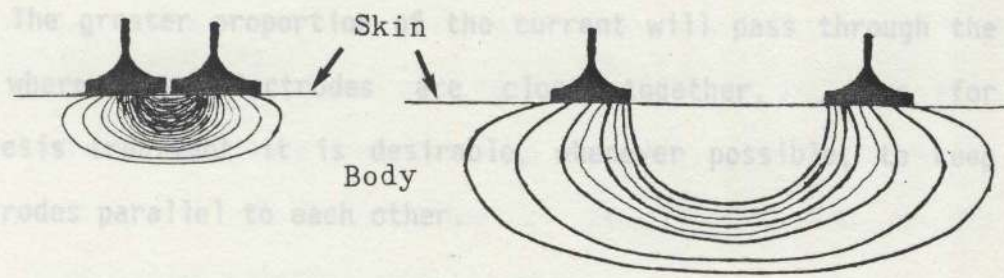
The relationship of the electrodes to each other is of practical importance in the distribution of electric current in the body (Browne, 1931; Cumberbatch, 1933; Dyson, 1936; Cross, 1936). If both electrodes are placed on the same side of a particular region, the flow of current is mainly by curves which spread out from one pole, dip down into the deeper parts and converge again to the other. The density of the current will be greater under the electrodes, less in the superficial parts, and almost negligible in the deeper parts. If the electrodes are placed further apart, more of the current will flow through the deeper parts than in the case when they are placed closer together. Figures 1E and 1F are diagrammatic representations of lines of flow of current when the electrodes are placed on the same side.

If both electrodes are placed on opposite aspects of a particular region of the body, the current will flow not only along the short direct paths between the electrodes, but also along divergent paths in outlying regions. This is represented schematically in Figure 1G. In this case the current density attains its maximum level in the tissues immediately under the electrodes; it diminishes rapidly as the tissues midway between the electrodes are approached, and still more rapidly in the outlying tissues. In other words, the current is more concentrated at the areas of entry and exit, and it is weakly diffused all through the tissues of the body. If one electrode is made smaller than the other, the current density will be greater over the area onto which the smaller electrode is applied. This follows as the same amount of current is passing through both electrodes but is spread over a larger area in one place and is more concentrated on a smaller

Diagrammatic representation of lines of flow of current when the electrodes are placed on the same side of the body

Fig. 1E

Fig. 1F



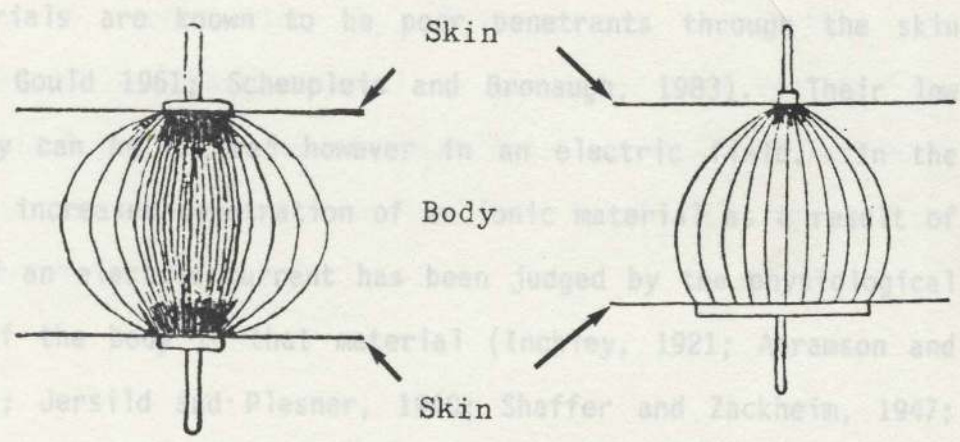
1.8 Aims of the present study

Although the application of iontophoresis in dermatology has been accepted (report of the Council on Pharmacy and Chemistry and the Council on Physical Therapy, 1941) and has been employed in the treatment

Diagrammatic representation of lines of flow of current when the electrodes are placed on the opposite side of the body

Fig. 1G

Fig. 1H



of ionic materials are known to be poor skin penetrants through the skin (Blank and Gould 1961; Scheuple and Brons 1983). Their low permeability can, however, in an electric field. In the literature, iontophoresis of ionic materials is one of the methods of the flow of an ionic material has been judged by the clinical responses of the material (Inoué, 1921; Stanton and Alley, 1937; Jersild and Plesner, 1947; Shaffer and Zackheim, 1947; Grice et al., 1972; Shrivastava and Singh, 1977), or by direct

When one electrode is made of a large surface and the other of a small surface, the former is said to be the indifferent (return) electrode and the latter the iontophoresis (active) electrode (Fig. 1H)

area in the other. For this reason, the electrode used for introducing ionic materials into the body is usually made smaller than the other electrode in most types of iontophoresis apparatus (Fig. 1H). If the electrodes are placed on opposite sides but are not parallel to each other, the distribution of the current will be uneven. The greater proportion of the current will pass through the tissues where the electrodes are close together. Thus for iontophoresis treatment it is desirable, whenever possible, to keep the electrodes parallel to each other.

### 1.8 Aims of the present study

Although the application of iontophoresis in dermatology has been accepted (report of the Council on Pharmacy and Chemistry and the Council on Physical Therapy, 1941) and has been employed in the treatment of many skin disorders (Knox, 1943; Jenkinson *et al.*, 1974; Midtgaard, 1986), iontophoresis is mentioned only briefly in some dermatology textbooks, for example, Rothman (1954) and Rook *et al.* (1975). One possible reason for this is the lack of comprehensive experimental data on the subject.

Ionic materials are known to be poor penetrants through the skin (Blank and Gould 1961; Scheuplein and Bronaugh, 1983). Their low permeability can be altered however in an electric field. In the literature, increased penetration of an ionic material as a result of the flow of an electric current has been judged by the physiological responses of the body to that material (Inchley, 1921; Abramson and Alley, 1937; Jersild and Plesner, 1940; Shaffer and Zackheim, 1947; Grice *et al.*, 1972; Shrivastava and Singh, 1977), or by direct

observation of a coloured test material on the intact skin surface (Abramson and Gorin, 1940; Abramson and Engle, 1942). In contrast, relatively little work (Pereyra, 1945; Fleischmajor and Witten, 1955) has been carried out using histological methods to demonstrate penetration and localization of materials in skin sections following iontophoresis. The reported favourable and sometimes excellent therapeutic results (see above and page 55) clearly indicate that previous observers were more interested in the clinical effects rather than in an analysis of the fundamental factors involved in the electrically propelled material into the skin.

In view of this situation, the present study has been undertaken to:

- (1) evaluate the site(s) responsible for the low permeability of skin by ionic materials.
- (2) investigate the efficacy of iontophoresis in driving organic and inorganic ions into and through the skin and to determine within what limits the galvanic current facilitates penetration from the surface into and through the skin and the underlying tissues.
- (3) observe the preferential route of entry into the skin by ionic materials.
- (4) investigate the effect of a number of components which may influence skin penetration by iontophoresis, including the concentration of the test material in the presenting vehicle, the physico-chemical properties of the test material, the combination of detergents and accelerants with the test material in solution, and the use of different vehicles.

CHAPTER 2  
MATERIALS  
AND  
METHODS

<b>2.3</b>	<b>Animals</b>	<b>84</b>
<b>2.4</b>	<b>Anaesthesia</b>	<b>84</b>
<b>2.5</b>	<b>Hair clipping</b>	<b>85</b>
<b>2.6</b>	<b>Control experiments</b>	<b>86</b>
<b>2.7</b>	<b>Iontophoresis</b>	<b>86</b>
2.7.1	Polarity selection	87
<b>2.8</b>	<b>Intradermal injections</b>	<b>88</b>
<b>2.9</b>	<b>Pre-excision</b>	<b>88</b>
<b>2.10</b>	<b>Excision of the treated skin</b>	<b>88</b>
<b>2.11</b>	<b>Preparation of the excised skin for cryostat sectioning</b>	<b>89</b>
2.11.1	Trimming	89
2.11.2	Specimen selection	89
2.11.3	Freezing the specimens	90
2.11.4	Cryostat sectioning	91
2.11.5	Examination of frozen sections	91
2.11.6	Selection of results	92
2.11.7	Photography	92
<b>2.12</b>	<b>General histological techniques</b>	<b>92</b>
2.12.1	Haematoxylin and eosin	92
2.12.2	Tartrazine	93
<b>2.13</b>	<b>Special histological techniques</b>	<b>93</b>
2.13.1	Haematoxylin method for copper and iron	94
2.13.2	Rubeanic acid technique for copper	94
2.13.3	Prussian blue method for iron	96

2.14	<b>Preparation of excised skin for transmission electron microscopy</b>	96
2.14.1	Theoretical aspects	96
2.14.2	Preparation of reagents	98
2.14.2.1	Initial solution	
2.14.2.2	Buffer solution	
2.14.2.3	Primary fixative	
2.14.2.4	Secondary fixative	
2.14.2.5	Embedding reagents	
2.14.2.6	Resin/Epoxypropane mixture	
2.14.2.7	Dehydrating mixture	
2.14.3	<b>Electron microscopy procedures</b>	101
2.14.3.1	Specimen preparation and primary fixation	
2.14.3.2	First rinsing	
2.14.3.3	Secondary fixation	
2.14.3.4	Second rinsing	
2.14.3.5	Dehydration	
2.14.3.6	Pre-infiltration	
2.14.3.7	Infiltration	
2.14.3.8	Embedding and polymerization	
2.14.3.9	Sectioning with the ultramicrotome	
	(a) Preparation of glass knives	
	(b) Block trimming	
	(c) Semi-thin sections	
	Staining of semi-thin sections	
	(d) Ultra-thin sections	
	Selection of ultra-thin sections	
	Staining of ultra-thin sections	
2.14.3.10	Examination of the sections	
2.14.3.11	Development of TEM negatives	
2.15	<b>Preparation of excised skin for X-ray analysis</b>	109
2.15.1	Chemical method	110
2.15.1.1	Resin-embedded specimens	
2.15.1.2	Critical point drying	
	(a) Theoretical aspects	
	(b) Procedures	
	Dry fracture	
	Freeze fracture	
2.15.2	Physical methods	113
2.15.3	Coating	113
2.15.4	Stub mounting	113



## 2.1 Instrumentation

### 2.1.1 Iontophoresis apparatus \*

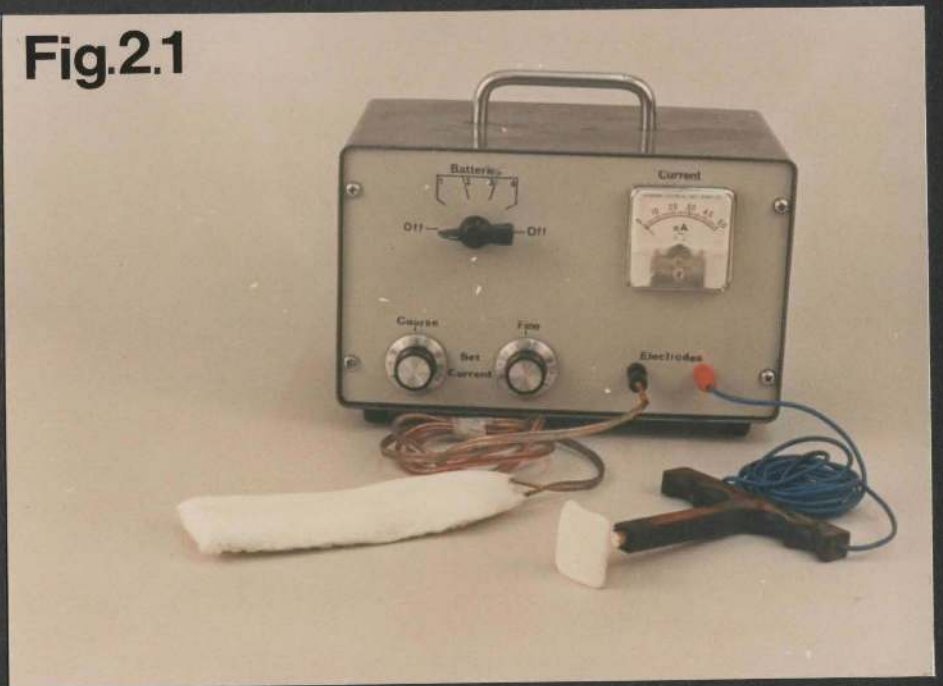
The apparatus used is compact and portable (fig. 2.1) and consists of a simple electrical circuit (fig. 2.2). The circuit contains four batteries (nine volts each), two variable resistors of ten and one kilo-ohms for a coarse and fine control of the current, and a milliammeter with a scale starting from zero up to fifty milliamperes. All these components are connected in series and contained within a metal cabinet. Figure 2.3 is a diagram of the circuit.

Two electrodes, an iontophoresis electrode (X) and indifferent electrode (Y), are inserted into the circuit at the terminals of the apparatus. The iontophoresis electrode is made of a square flat copper plate with a surface area of approximately 12.25 square centimetres. The plate is traversed by a number of pores to allow free passage of any gases during iontophoresis (fig. 2.4b). This electrode is mounted on an insulated wooden handle for ease of application (fig. 2.4a). The indifferent electrode is made from a flexible sheet of aluminium foil approximately 15 centimetres long and 7 centimetres wide (fig. 2.5).

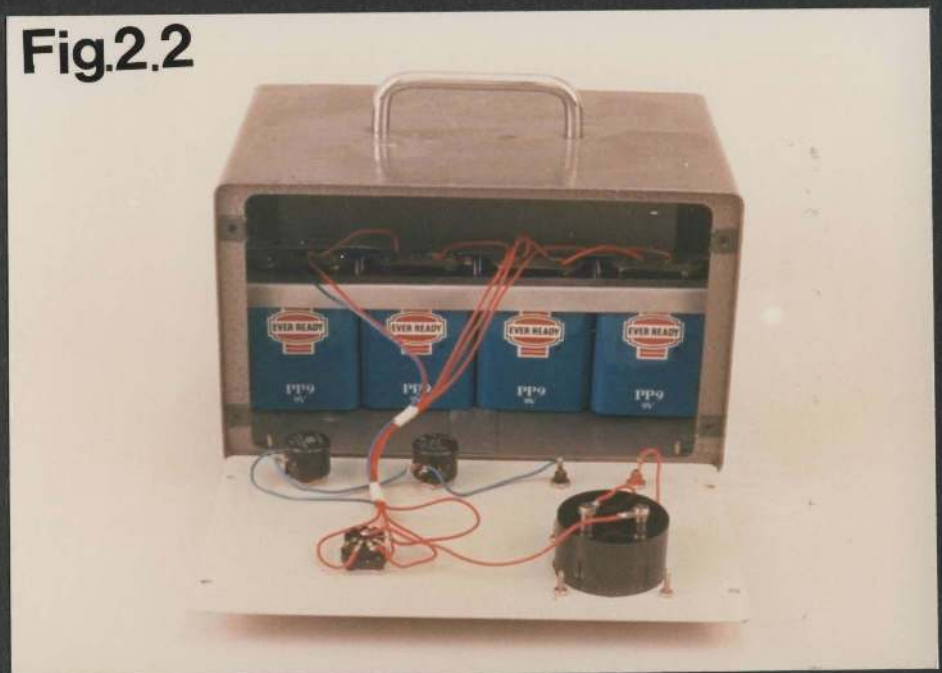
Each electrode is connected to the apparatus via a conducting lead. The lead is soldered on to the indifferent electrode, whereas it is attached to the iontophoresis electrode by a special clip sealed inside the insulated handle. The leads are made of flexible

\* This apparatus is not available commercially. It was assembled at the Hannah Research Institute, Ayr, for use in that establishment.

**Fig.2.1**



**Fig.2.2**



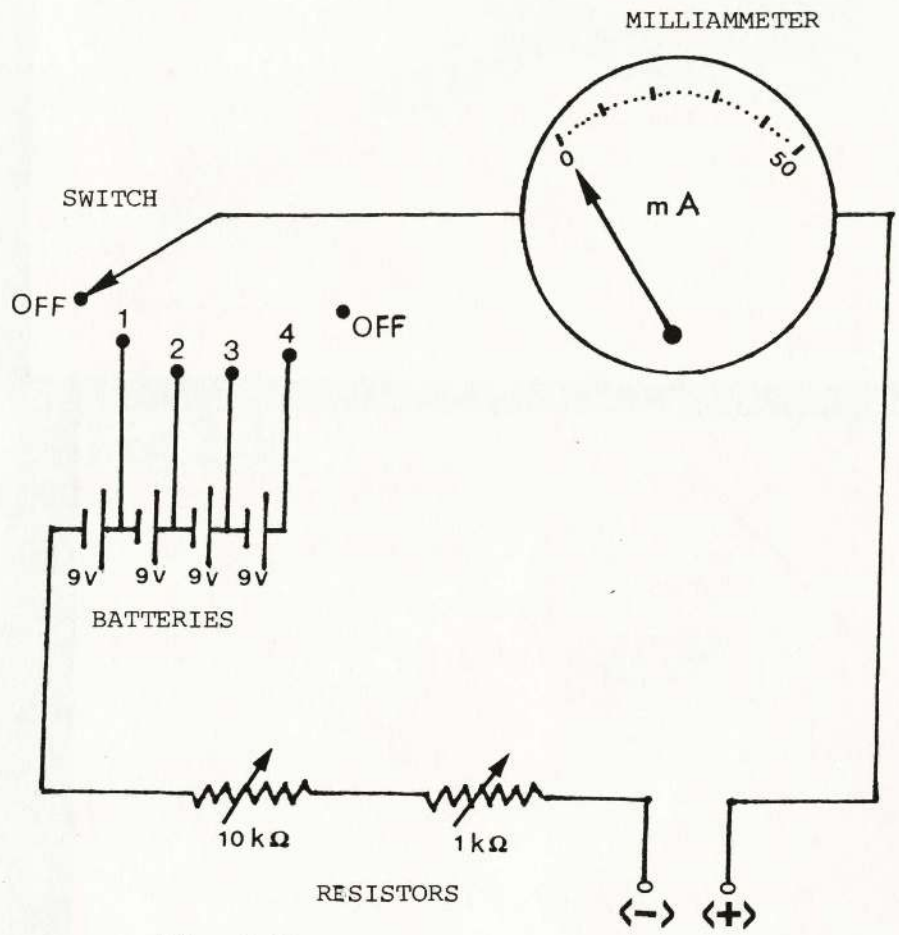


Fig. 2.3

Schematic diagram of the circuit of the iontophoresis apparatus.

**Fig.2.4a**



**Fig.2.4b**



**Fig.2.5**



(stranded) wire with rubber insulation, and are plugged into the apparatus via insertion clips.

#### 2.1.1.1 Electrode dressing

##### (a) Theoretical aspects

The application of the metal electrodes directly on to the surface of the skin is not advisable as the products of electrolysis forming and accumulating on the surface of the skin during iontophoresis may have a caustic effect. Furthermore, a direct contact between the metal electrodes and the skin may cause iontophoretic burns resulting from excessive generation of heat in the skin due to the passage of the current.

To prevent the above, the surface of the skin is separated from the electrodes by absorbent pads. In addition, the pads function as a reservoir, that is, they absorb the test solution and release it to the surface of the skin, thus ensuring the presence of excess solution on the surface.

##### (b) Application of absorbent pads

The surface of the iontophoresis electrode was covered by a pair of folded medical tissues (Kleenex, Kimberly-Clark) enclosed in a sheath of absorbent material (General purpose cleansing tissues, Smith and Nephew, Southalls Ltd), all of which were wrapped around the iontophoresis electrode and secured in position by a piece of thread (fig. 2.4a). Care was taken to ensure that the absorbent pads were free from folds and creases, hence ensuring a uniform distribution of current over the surface of the skin.



The indifferent electrode was covered by a thin pad of cotton wool enclosed in cotton gauze. This covering was also made as uniform as possible (fig. 2.5).

#### 2.1.1.2 Care of the apparatus

Apparatus in good working order is essential for iontophoretic studies. Contaminated electrodes result in a poor conduction of current. Therefore, prior to each experiment, care was taken to ensure that both electrodes were contamination free. This was achieved by polishing the surfaces of the electrodes with a fine sand paper. The absorbent pads covering the electrodes were replaced with new ones prior to each experiment. The insulated handle itself was cleaned by inserting into it as far as possible, a clean piece of cloth and then drawing the cloth out. This was performed shortly after each experiment. Finally, the batteries were checked regularly to ensure that they were in good working condition. This was done by connecting each battery in turn to a small light bulb.

#### 2.1.2 Transmission electron microscope (TEM)

The electron microscope column consists of a metal tube in which are aligned from above down an electron gun, a number of lenses, a viewing screen and a photographic plate. Figure 2.6a is a diagram of a transmission electron microscope.

The source of the beam is the electron gun. This consists of a tungsten filament enclosed in a metal casing called the cathode shield, and an anode plate. Both the cathode shield and the anode plate have centrally positioned apertures and these are aligned so

that they lie on a common axis running through the tip of the filament. The filament emits electrons when a heating current is sent through it. A potential difference between the cathode and the anode accelerates the electrons down the column.

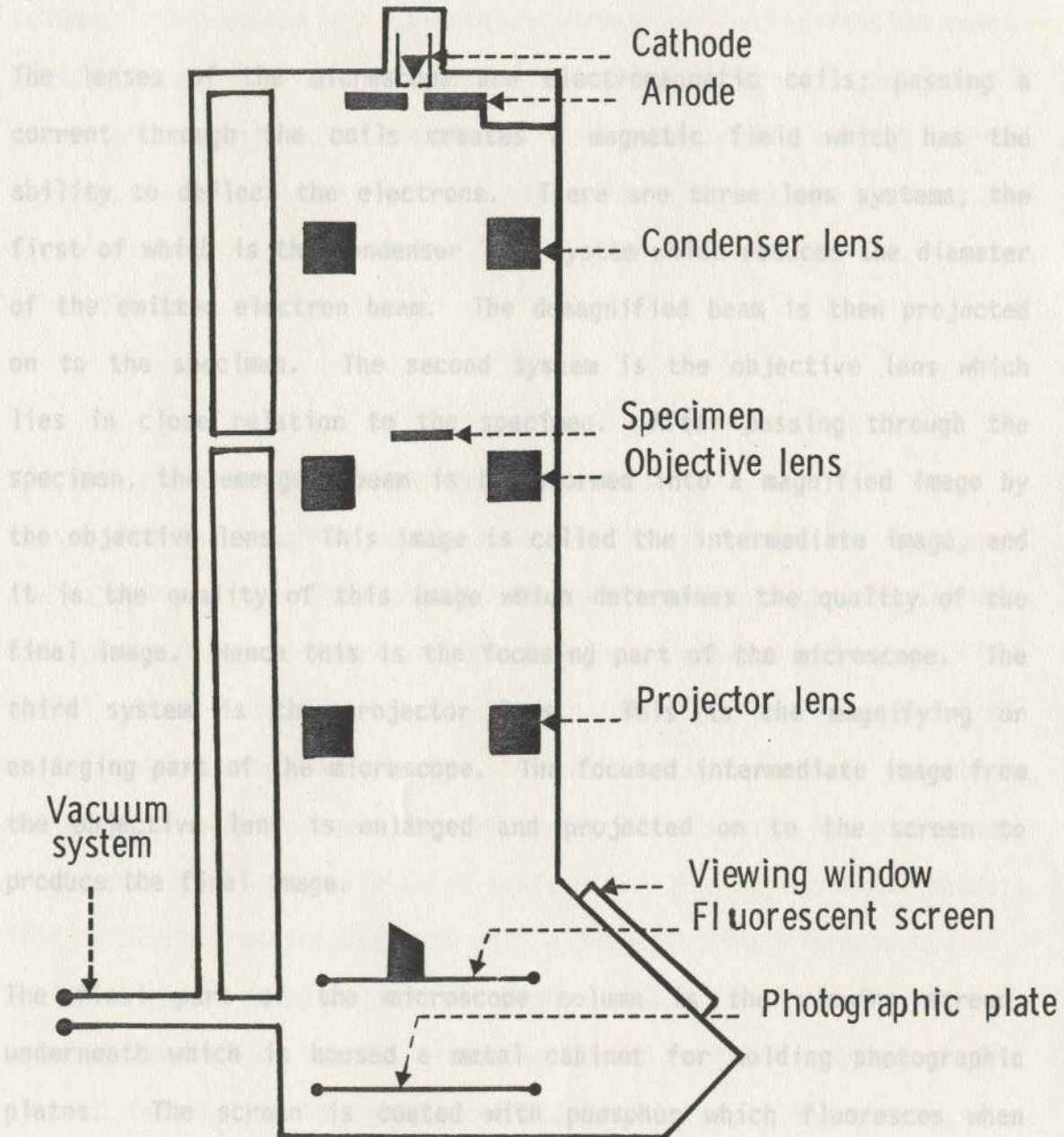


Figure 2.6 a . A diagram of the transmission electron microscope.

that they lie on a common axis running through the tip of the filament. The filament emits electrons when a heating current is sent through it. A potential difference between the cathode and the anode accelerates the electrons down the column.

The lenses of the microscope are electromagnetic coils; passing a current through the coils creates a magnetic field which has the ability to deflect the electrons. There are three lens systems, the first of which is the condenser lens system which reduces the diameter of the emitted electron beam. The demagnified beam is then projected on to the specimen. The second system is the objective lens which lies in close relation to the specimen. After passing through the specimen, the emergent beam is transformed into a magnified image by the objective lens. This image is called the intermediate image, and it is the quality of this image which determines the quality of the final image. Hence this is the focusing part of the microscope. The third system is the projector lens. This is the magnifying or enlarging part of the microscope. The focused intermediate image from the objective lens is enlarged and projected on to the screen to produce the final image.

The final part of the microscope column is the viewing screen, underneath which is housed a metal cabinet for holding photographic plates. The screen is coated with phosphor which fluoresces when bombarded with electrons thus making the image visible. Fine changes in focus are not easily observed with the unaided eye and consequently accurate focusing is carried out by viewing the final image produced on the screen with a binocular microscope. A record of the final image is made by temporarily replacing the screen with a photographic



plate which is coated with an electron-sensitive photographic emulsion. The electron microscope column is maintained under vacuum to minimize interference of the electron beam by extraneous particles such as gas molecules, and so allow the electrons to pass down the column. The vacuum is achieved by rotary and oil diffusion pumps. During operation of the microscope, the pumps generate a considerable amount of heat which is reduced by circulating water through special cooling channels. The transmission electron microscope used in the present study was a Carl Zeiss EM 9S-2 operating at 60KV and a vacuum of  $5 \times 10^{-4}$  Torr.

#### 2.1.2.1 Electron beam - specimen interaction

In the TEM the electron beam passes through extremely thin specimens. The majority of the incident electrons will pass straight through each specimen. Other electrons in the beam can interact either with the nuclei of the specimen (atoms) or with the electrons surrounding the nuclei. If an incident electron interacts with a nucleus, it will be deflected through an angle, but will not suffer energy loss; this type of interaction is called elastic scattering. If, on the other hand, a fast incident electron collides with a slow orbiting electron around a nucleus, their energies will be shared which produces a change in velocity as well as in the direction of the incident electron. This type of interaction is called inelastic scattering. Figure 2.6b is a diagrammatic representation of the major events in an electron beam-specimen interaction in the TEM.

2.1.2.2 Image formation

Image formation consists of the removal of electrons from the beam mainly by the process of inelastic scattering, since there are far more electrons in a specimen than there are in a hole. The emergent beam is deficient in electrons in areas in the specimen of high mass-density. These "holes" in the emergent beam are imaged by the microscope as dark areas in the final image. In contrast, few electrons are scattered from more electron transparent areas of low mass-density. Therefore these low mass-density areas appear bright in the final image. In other words, the final image is a density map of the specimen.

2.1.3 Scanning electron microscopy

The SEM may be used to investigate the surface topography, luminescence, surface conductivity, and the surface potential distribution of solid specimens. Such information is typically on a video and is derived from the electron microscope. The electron scanning the surface in a square raster type of image.

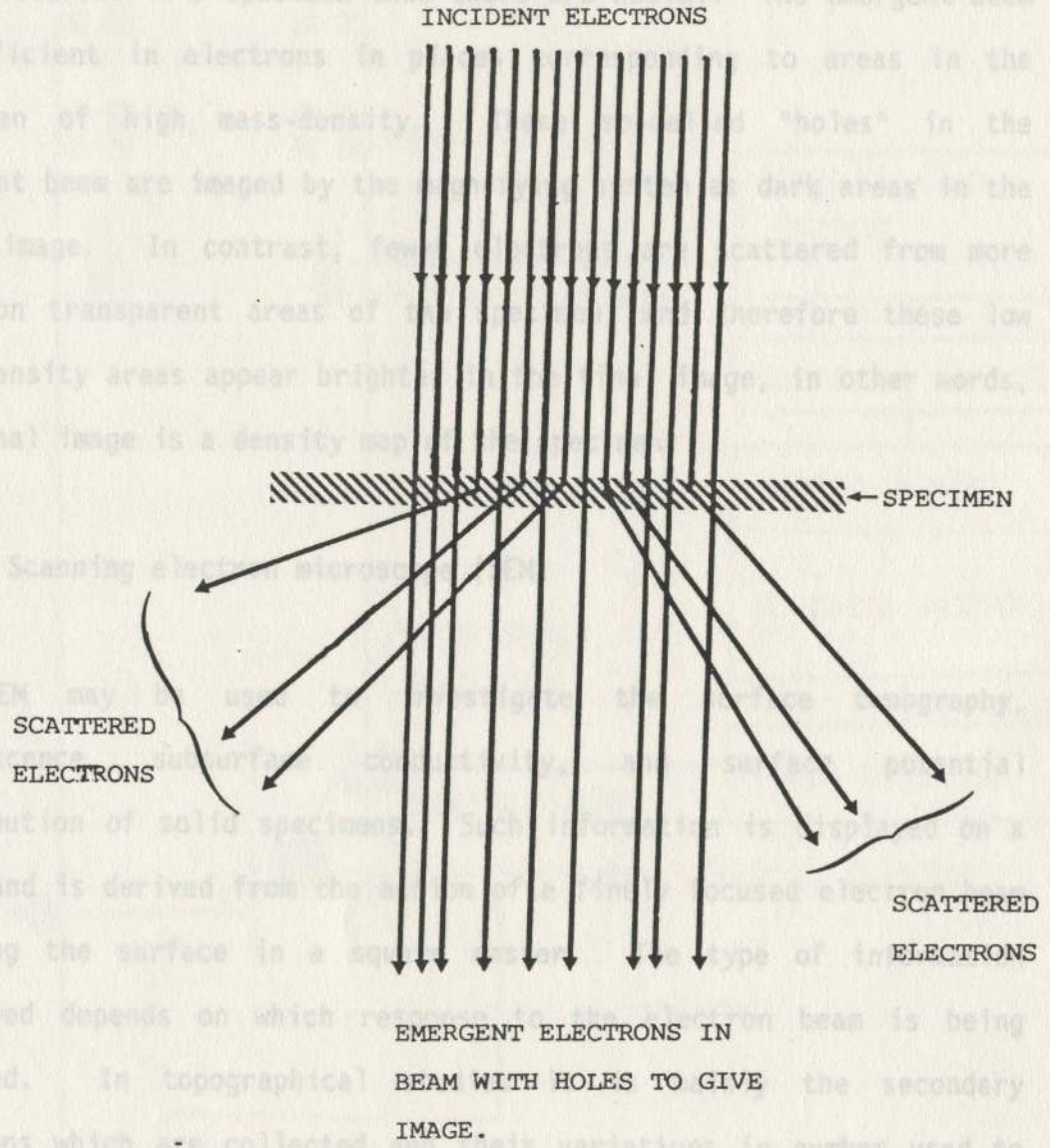


Fig.2.6b  
ELECTRON BEAM-SPECIMEN INTERACTION IN THE T.E.M.

SEM. The production and control of a beam of electrons is the same in the SEM as it is in the TEM. The source of the electrons is a hot tungsten filament, the cathode. A potential difference between the cathode and the anode accelerates the electrons and thus produces a beam. The beam is focused by means of electromagnetic condenser

### 2.1.2.2 Image formation

Image formation consists of the removal of electrons from the beam mainly by the process of inelastic scattering, since there are far more electrons in a specimen than there are nuclei. The emergent beam is deficient in electrons in places corresponding to areas in the specimen of high mass-density. These so-called "holes" in the emergent beam are imaged by the magnifying system as dark areas in the final image. In contrast, fewer electrons are scattered from more electron transparent areas of the specimen, and therefore these low mass-density areas appear brighter in the final image, in other words, the final image is a density map of the specimen.

### 2.1.3 Scanning electron microscope (SEM)

The SEM may be used to investigate the surface topography, luminescence, subsurface conductivity, and surface potential distribution of solid specimens. Such information is displayed on a video and is derived from the action of a finely focused electron beam scanning the surface in a square raster. The type of information displayed depends on which response to the electron beam is being detected. In topographical studies it is mainly the secondary electrons which are collected and their variations in number used to modulate the display video. Figure 2.7a is a schematic representation of the electronics involved in topographical investigations in the SEM. The production and control of a beam of electrons is the same in the SEM as it is in the TEM. The source of the electrons is a hot tungsten filament, the cathode. A potential difference between the cathode and the anode accelerates the electrons and thus produces a beam. The beam is focused by means of electromagnetic condenser

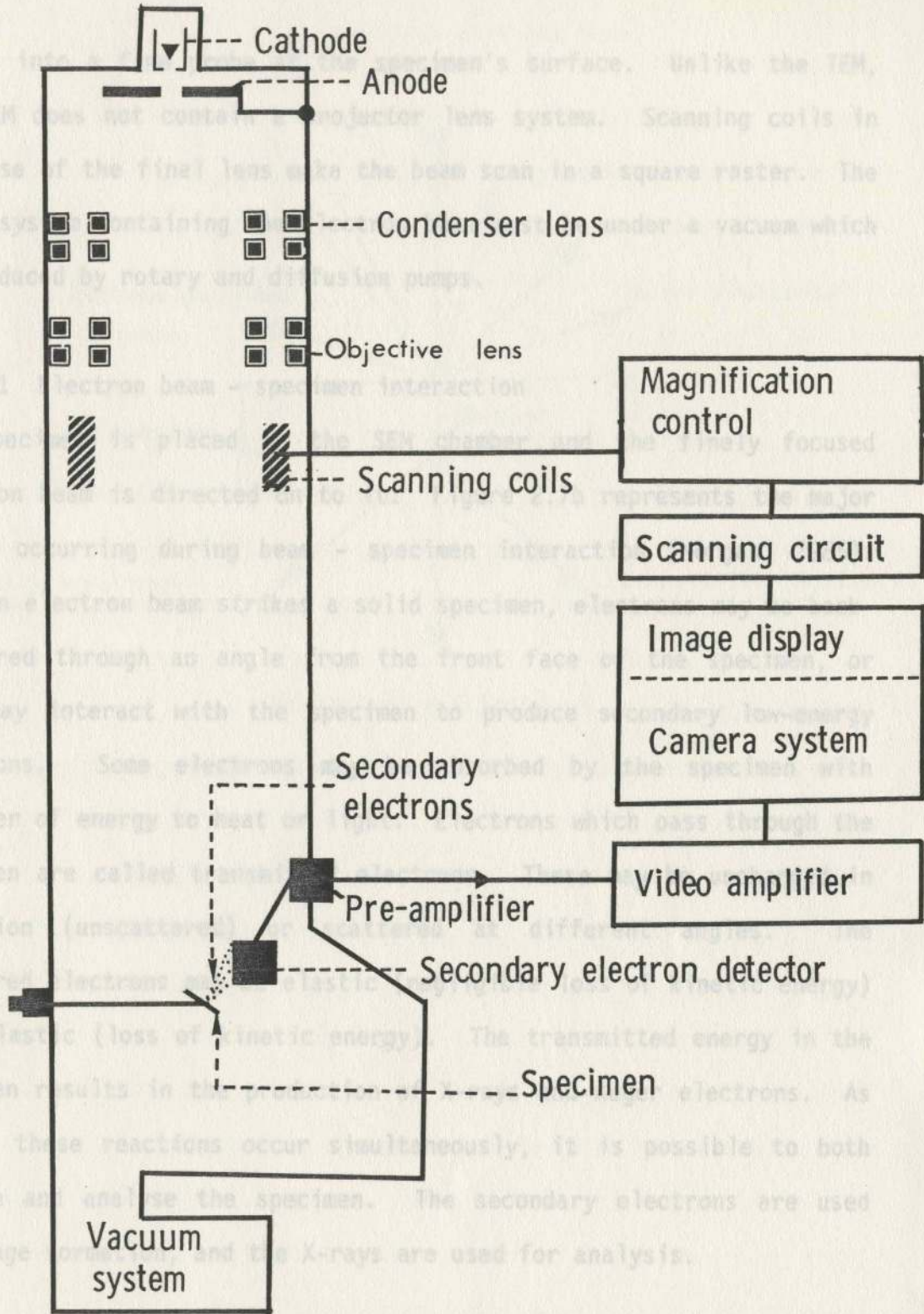


Fig. 2.7a . A diagram of the scanning electron microscope.

2.1.3.2 Image formation

Secondary electrons are produced by the interaction of the incident beam with the weakly bound conduction electrons in the specimen. These secondary electrons are collected by a secondary electron detector mounted in the SEM sample chamber. They pass through a scintillator

lenses into a fine probe at the specimen's surface. Unlike the TEM, the SEM does not contain a projector lens system. Scanning coils in the base of the final lens make the beam scan in a square raster. The whole system containing the electron beam must be under a vacuum which is produced by rotary and diffusion pumps.

#### 2.1.3.1 Electron beam - specimen interaction

The specimen is placed in the SEM chamber and the finely focused electron beam is directed on to it. Figure 2.7b represents the major events occurring during beam - specimen interaction (Morgan, 1985). When an electron beam strikes a solid specimen, electrons may be back-scattered through an angle from the front face of the specimen, or they may interact with the specimen to produce secondary low-energy electrons. Some electrons may be absorbed by the specimen with transfer of energy to heat or light. Electrons which pass through the specimen are called transmitted electrons. These may be unchanged in direction (unscattered) or scattered at different angles. The scattered electrons may be elastic (negligible loss of kinetic energy) or inelastic (loss of kinetic energy). The transmitted energy in the specimen results in the production of X-rays and Auger electrons. As all of these reactions occur simultaneously, it is possible to both observe and analyse the specimen. The secondary electrons are used for image formation, and the X-rays are used for analysis.

#### 2.1.3.2 Image formation

Secondary electrons are produced by interaction of the incident beam with the weakly bound conduction electrons in the specimen. These secondary electrons are collected by a secondary electron detector mounted in the SEM sample chamber. They pass through a scintillator

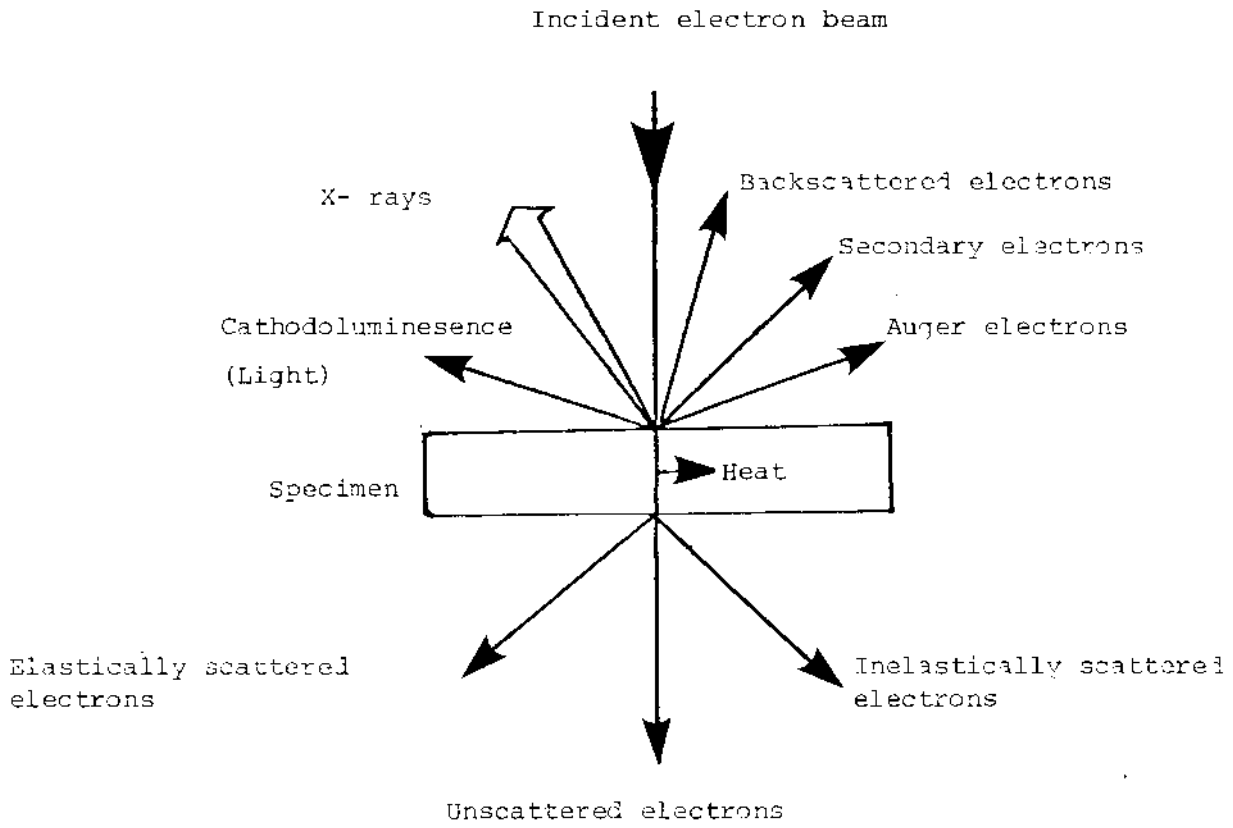


Fig.2.7b. ELECTRON BEAM-SPECIMEN INTERACTION IN S.E.M.



which produces photons, a photomultiplier which magnifies the photons signals, and an amplifier which produces electrical signals. These pass into a video amplifier connected to the display of a cathode ray tube. Thus from one spot on the specimen, a spot is produced on the display screen. The beam of electrons is scanned across the specimen by means of scanning coils, synchronised with deflection coils of the display amplifier, in an X and Y axis in a rectangular set of lines. The signal from the detector varies from each point traversed on the specimen, and this variation appears as a variation in intensity of the spot also traversing on the display screen at the same time. A picture is therefore built up from all these spots of varying brightness. The image is digital, that is formed from points, and not analogue as in the TEM. The SEM image is either displayed on the screen as mentioned above or photographed with an attached camera system.

#### 2.1.3.3 X-ray production

When the high velocity electron beam strikes the specimen, it interacts with inner-shell electrons of the atoms contained in the specimen, which results in the removal of bound electrons from their normal positions. Each atom is now unstable with a vacancy in the inner shell. The resting state is restored when the vacancy is filled by an electron dropping from a higher orbital within the same atom, the excess energy being emitted as an X-ray photon. If the original vacancy is created in the innermost (K) shell, the resultant X-rays are called K X-rays. However since the transition to fill the vacancy can occur from either the L or M shells, and since these shells are at different energies, the K X-rays are sub-divided into  $K \alpha$  (transition from L shell) and  $K \beta$  (transition from M shell) X-rays respectively.

Since the K shell is itself divided into sub-shells of different energies, the K X-rays can be further divided into  $K_{\alpha 1}$ ,  $K_{\alpha 2}$ ,  $K_{\beta 1}$ , etc, depending on the transition energy differences. Similarly, if an electron is ejected from the L shell, the resultant X-rays are called  $L_{\alpha}$  and  $L_{\beta}$  indicating transition from M and N shells respectively, and so on. As before, these can be further divided into  $L_{\alpha 1}$ ,  $L_{\alpha 2}$ ,  $L_{\beta 1}$ , etc. Figure 2.7c is a schematic representation of the major events involved in the production of X-rays, where n = nucleus of an atom (modified from Morgan, 1985).

#### 2.1.3.4 X-ray detection

Two methods are available to analyse emitted X-rays; these are known as energy-dispersive and wavelength-dispersive methods.

##### (a) Energy-dispersive method

This method utilises the principle that the potential energy difference between the orbitals involved in electron transition is characteristic of the element (table of characteristic x-ray transitions of the elements used in the present study is shown in Appendix CI). Therefore, by measuring the energy of the emitted X-rays with a suitable instrument, analysis of the atoms and hence the element(s) present in the specimen may be made. Figure 2.8a represents the general arrangement of instrumentation used in this method. The X-rays which are generated by electron beam - specimen interaction enter a scintillation semiconductor detector made of silicon and lithium. Within the detector, each x-ray photon is absorbed and its energy is used to raise electrons to the conduction band. The electrons are then collected by an applied voltage and the detector is ready within a fraction of a microsecond for the next X-ray to enter into it. The electron charge from each X-ray is



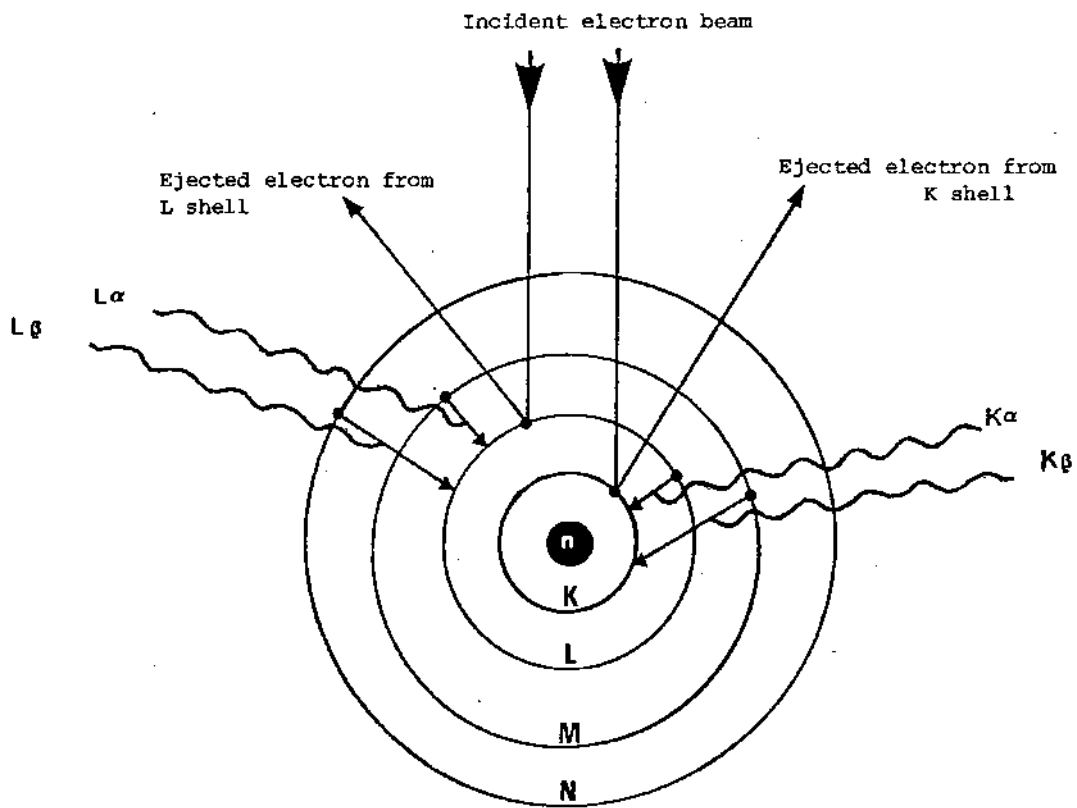


Fig. 2.7c. X-RAY PRODUCTION.

accumulated in and converted to a small voltage pulse by a field-effect transistor/pre-amplifier which is closely connected to the detector. The pulses are amplified in the pulse-processor (amplifier), each pulse having a magnitude linearly proportional to the energy of the X-ray that produced it. The height of each voltage pulse is measured by allowing it to charge up a capacitor and measuring the time required for it to discharge on a high-frequency clock, that is, the voltage pulses are digitised in an analogue/digital convertor. The number of pulses is entered and stored in the memory of a multichannel analyser, so that a complete X-ray spectrum is built up with X-ray energy on the horizontal axis and the number of photons counted per energy-interval on the vertical axis. The location of peaks in the spectrum thus identifies their energy and hence the element(s) from which the X-rays originate.

In the present study, spectra obtained with this method of analysis will be referred to as EDXS, that is energy-dispersive X-ray spectra. The spectra were produced by a scanning electron microscope Jeol JSM-35 CF equipped with an EDX system.

#### (b) Wavelength-dispersive method (WDX)

The basic principle of this method is that identification of elements can be made by measuring the wavelength of X-ray photons which are characteristic of the elements (table of characteristic X-ray emission wavelength of some elements (ruthenium and chlorine) is shown in Appendix CII). Figure 2.8b represents the general arrangement of instrumentation applicable to this method. X-rays, like all photons, can be thought of as having a wave-form as well as a particle behaviour. Under electron bombardment, the various elements in the

Fig.2.8 a .

ELECTRONICS IN ENERGY-DISPERSIVE SYSTEM.

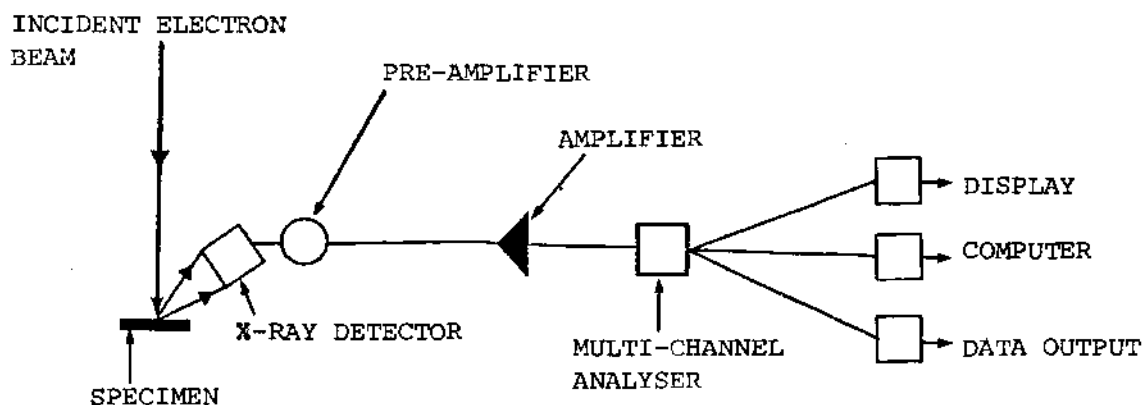
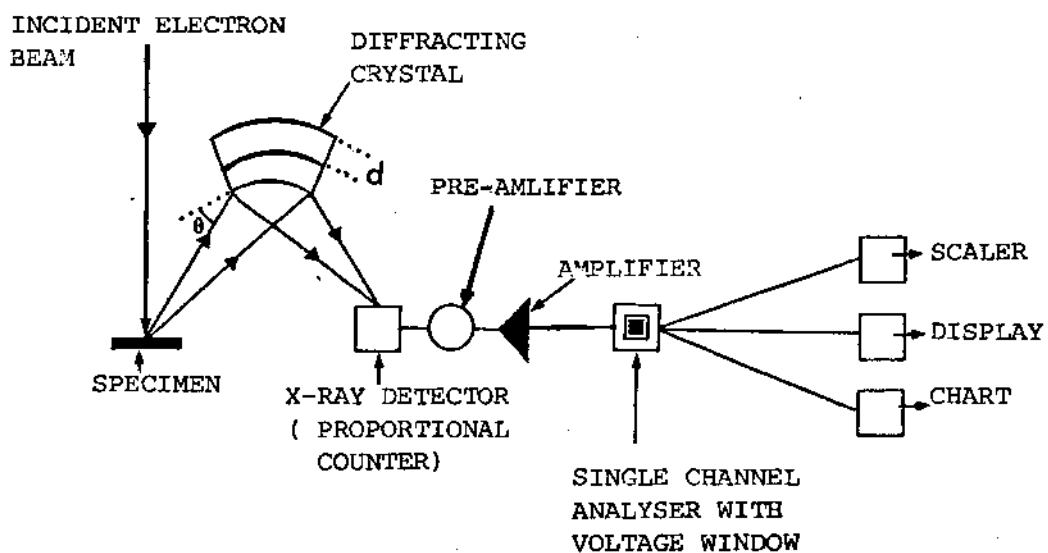


Fig. 2.8 b.

ELECTRONICS IN WAVELENGTH-DISPERSIVE SYSTEM



specimen emit X-rays. Only a narrow cone of these X-rays will be reflected by a finite curved crystal. The fraction of the X-ray beam which is reflected obeys a basic principle, that is only one particular wavelength is strongly reflected at a certain angle to the exclusion of all others. This is described in an equation form by Bragg (cited by Morgan, 1985),

$n\lambda = 2d \sin \theta$  [where (n) is an integer (1,2,3 ... etc); ( $\lambda$ ) is the wavelength; (d) is the interplanar lattice spacing and ( $\theta$ ) is the angle of incidence (and of reflection) of the X-rays arriving at the crystal].

Thus, for a crystal of known lattice spacing (PET type crystal is used) and for a selected angle of incidence (Appendix CII), the wavelength of the diffracted X-rays entering the detector can be calculated. In practice, the crystal is rotated through a range of angles until a peak, that is maximum intensity, is reached in the detector at which point the conditions of Bragg's law are met and the wavelength of the X-ray detected can be identified. After being selectively diffracted by the crystal, the X-rays of a particular wavelength pass through a detector (proportional counter). In the detector electrical pulses are produced. These pulses accumulate and are converted to voltage signals by a field-effect transistor/pre-amplifier. The signals are delivered to an amplifier and then pass to a single channel analyser which selectively allows a particular signal to pass to a scaler. The scaler counts the number of X-rays passing from the single channel analyser in a given time interval. A chart recorder can plot these signals and a record of the peaks of intensity occurring at specific wavelengths is obtained, and hence the identification of the presence or absence of an element in the specimen.

In the present study, spectra obtained with this method of analysis will be referred to as WDXS, that is, wavelength-dispersive X-ray spectra. The spectra were produced by a scanning electron microscope Jeol superprobe 733 equipped with a WDX system.

(c) Comparison between EDX and WDX systems

Each of these methods has its advantages and disadvantages. The EDX system has the advantage of simultaneous processing of a specimen to show the peaks from all the elements present in the analysed sample in a single run. The data collection time is relatively short, being approximately ten minutes per run. Its major disadvantage is that occasionally a peak-overlap occurs, in which a peak from one element overlaps partially or completely another peak from a different element. In contrast, the WDX system has the advantage of producing very sharp peaks, that is, it eliminates overlapping of peaks from different elements. However, there are two limitations in the use of the WDX system. Firstly, it is only able to detect a single band of X-rays, that is a single element, during a single run, and secondly, it is time consuming in that its data collection time is approximately twenty-five minutes per single run.

(d) Selection of method used for X-ray analysis

No single method provides a total characterisation of the analysed specimen. The use of either the EDX or the WDX system for analysis is a matter of choice. In the present study, X-ray analysis was carried out to verify the presence (or absence) of exogenous inorganic materials introduced to the skin. For the major part of the present study, the EDX system was selected as the method of analysis on account of its shorter data collection time and ease of operation.

However, when a peak-overlap occurred in the EDX spectrum, the WDX system was used as an alternative method of analysis.

## **2.2 Materials used for penetration trials**

The materials (tracers) used for penetration trials are classified according to their physico-chemical natures into two major groups, namely organic and inorganic materials.

### **2.2.1 Organic materials**

Dyes have been used as representatives of this group of compounds since no histological tests are required to demonstrate their location in the skin, that is, the colours of the dyes are sufficiently characteristic in themselves. According to their physico-chemical nature, organic dyes may be classified into four groups: basic, acidic, non-ionic, and compound dyes.

#### **2.2.1.1 Basic (cationic) dyes**

Basic dyes, by definition, are those which ionize to carry a positive charge. They are accordingly attracted to negatively-charged (basophilic) tissue loci. The basic dyes used were methylene blue, toluidine blue, pyronin Y, aniline blue alcohol-soluble and chrysoidin Y.

#### **2.2.1.2 Acid (anionic) dyes**

Acid dyes, by definition, are those which ionize to carry a negative charge, or the balance of the charge on the dye-ion is negative. They

are accordingly attracted to positively-charged (acidophilic) tissue loci. The ionic dyes used were eosins, aniline blue water-soluble, picric acid, alizarin red S and trypan blue.

#### 2.2.1.3 Non-ionic (lipid-soluble) dyes

These are characterised by an absence of strongly polar groups which ensures solubility of these dyes in lipids and organic solvents. The dyes are so soluble in liquid lipids that they pass rapidly from the organic solvent into the cellular lipid droplets (Dixon, 1970). Hence, they are generally used to demonstrate lipids in tissue. Sudan Black B was used as an example of lipid soluble dyes.

#### 2.2.1.4 Compound (amphoteric) dyes

These may be defined as cationic-anionic dyes. Jenner's stain was selected as an example of this class of dyes. This stain is a methylene blue eosinate and is obtained as the precipitate formed on neutralising unoxidised methylene blue with eosin Y. Gurr (1960) states that although it is a neutral dye the eosin portion of its molecule still acts as an acid dye, whilst the methylene blue portion behaves as a basic dye. The stain used was of Gurr microscopy materials type and supplied by BDH Chemicals Ltd.

#### 2.2.1.5 Dye selection

The selection of each dye for the penetration trials was based on one (or more) of the following factors:

- (a) Chemical nature, that is, whether the dye was basic, acidic, non-ionic, or compound.
- (b) Solubility in water and/or alcohol. The solubilities of the dyes used for the penetration studies are quoted from Gurr (1960), since

the temperature at which the solubility values are given ( $15^{\circ}$  C) was very close to that of the laboratory ( $17^{\circ}$  C).

(c) Molecular weight.

(d) Availability and documentation following previous investigations.

The physico-chemical properties of the dyes are presented in Appendix A. They are derived from Gurr (1960, 1971), Lillie (1969), The Merck Index (1976) and Weast and Astle (1980).

#### 2.2.1.6 Preparation of dye solutions

The dyes were prepared in water and/or alcohol by dissolving a given weight in grams of each dye in 100 mls of solvent, unless indicated otherwise. The concentration therefore is given in the form of a percentage. The concentration of each dye in solution was selected so that it was below its solubility value, thus ensuring complete dissolution in the solvent.

#### 2.2.2 Inorganic materials

As with organic materials histological demonstration, that is localisation of inorganic materials introduced to the skin by local application (controls) or iontophoresis, appears to be the most appropriate method for investigating the penetration through the skin. A number of inorganic materials have been used as tracers to investigate the preferential route(s) of penetration and the influence of iontophoresis on such penetration.

Inorganic materials can be divided into two groups, namely metal cations and non-metal anions.



### 2.2.2.1 Selection of materials

The metal cations used were lanthanum, silver, ruthenium red, copper and iron. Lanthanum and silver have been used for some time as tracers in electron microscopy due to their property of being electron-dense (Revel and Karnovsky, 1967; Smith and Stuart, 1971; Shaklai and Tavassoli, 1982). An additional material which may be observed in ultrathin sections in the electron microscope is ruthenium red (Luft, 1971). Therefore, by using these tracers and noting their localisation in ultrathin sections of the skin, a study of their preferential route(s) of penetration may be carried out at the electron microscopy level without employing histochemical techniques. On the other hand, numerous chemical techniques are available for the localisation of other metals in tissues. These histochemical techniques depend on the ability of metals to form coloured compounds with special reagents. Copper and iron were selected as additional tracers as satisfactory and simple methods exist for their demonstrations (p 93). Thus a study of the preferential route(s) of penetration at the light microscope level may be carried out.

In order to confirm the histological findings, an alternative method of localising metals in the skin was used namely X-ray analysis.

Inorganic anions are difficult to localise successfully by histological methods in tissue sections. In the event, iodide ions were used as a representative of inorganic anions and their location in the skin was determined by X-ray analysis.

All the above mentioned materials are reasonably cheap to purchase.

The physico-chemical properties of the inorganic materials used are detailed in Appendix B. The data shown are derived from Merck (1976) and Weast and Astle (1980), unless otherwise indicated.

#### 2.2.2.2 Preparation of solutions

The solutions were prepared by dissolving a given weight in grams of each test material (tracer) in 100 mls of solvent (Vehicle). Hence the concentration is given in the form of a percentage.

#### 2.2.3 Other materials involved in the penetration studies

##### 2.2.3.1 Accelerants (Dimethyl sulphoxide)

Dimethyl sulphoxide (DMSO) is a colourless, highly polar liquid miscible in all proportions with water and alcohol. It can solvate many organic and inorganic compounds. Its molecular formula is  $\text{CH}_3\text{SOCH}_3$ , it has a molecular weight of 78.13, and is supplied by BDH Chemicals Ltd.

##### 2.2.3.2 Detergents

(a) Sodium lauryl sulphate (SLS) is also called sodium dodecyl sulphate (SDS). It is an anionic detergent supplied as a white powder. Its molecular formula is  $\text{C}_{12}\text{H}_{25}\text{OSO}_3\text{Na}$ , and it has a molecular weight of 288.38. The type used in the present study is especially purified for chemical work by Fisons Scientific Apparatus, Loughborough, Leicestershire, England.

(b) Tween 20 is also called polyoxyethylene (20) sorbitan monolaurate. A non-ionic detergent supplied as an orange-yellow viscose liquid, with a molecular weight of 1227.54. It is soluble in

water and in alcohol. The detergent used in the present study is supplied by Sigma Chemical Co., USA.

### 2.3 Animals

Male Wistar albino rats were used throughout the major part of the present study. They were selected in preference to other conventional laboratory animals in accordance with the shape and dimensions of the iontophoresis electrode. The weight of the rats varied from 240 to 300 grams, and their ages from 8 to 11 weeks.

The animals were obtained from, and bred at, the Animal House, Bute Medical Buildings, University of St Andrews. They were kept in a daily 12 hours light and 12 hours darkness cycle and at 20° C throughout the year. They were fed on rat and mouse number 1 modified maintenance diet (product number 801155W, Special Diet Services, BP Nutrition, England). This is a high quality diet designed to maintain rats and mice in good health over long periods of time. Water was supplied *ad libitum*.

### 2.4 Anaesthesia

The use of anaesthesia was not only to prevent the animals feeling pain but also to ease manipulation during experimental procedures. Initially, each rat was anaesthetised in ether vapour in a glass jar. The ether, (diethyl ether) used was a general purpose reagent type supplied by BDH Chemical Ltd. Paper hand towels were used to prevent

contact between the liquid ether and the surface of the skin, whilst the level of anaesthesia was judged by deep unconsciousness and muscular relaxation. Hair was removed using clippers following this initial anaesthesia. Thereafter, each rat was kept anaesthetised by placing near its nasal and oral orifices cotton wool to which ether had been applied.

At the end of each experiment, that is following the removal of a skin sample, the animal was sacrificed either by excess ether inhalation or by cervical dislocation.

## **2.5 Hair clipping**

The hair was carefully and lightly clipped as short as possible by using electric clippers (Aesculap favorita II, Aesculap-Werke AG, W Germany). Care was taken not to damage the superficial layers of the skin during clipping. For control experiments, the hair was clipped from the abdominal skin only. For iontophoresis, the hair was clipped from the abdominal (ventral) and dorsal surfaces to achieve good electrical contact.

Throughout the present study, care was taken to ensure that the treatments were applied to areas of undamaged skin.

## 2.6 Control experiments (local applications)

The animal was placed in its experimental position (dorsum downwards), and the selected test solution applied evenly and in excess over the surface of the shaved area of the rat's abdomen. This was achieved by gentle and regular swabbing using a fine, soft painting brush impregnated with the test solution. This area was covered with the iontophoresis electrode, which was also saturated with the test solution, but without turning on the current. Following the procedures just described, each test solution was left in contact with the surface of the skin for a standard time of application of fifteen minutes.

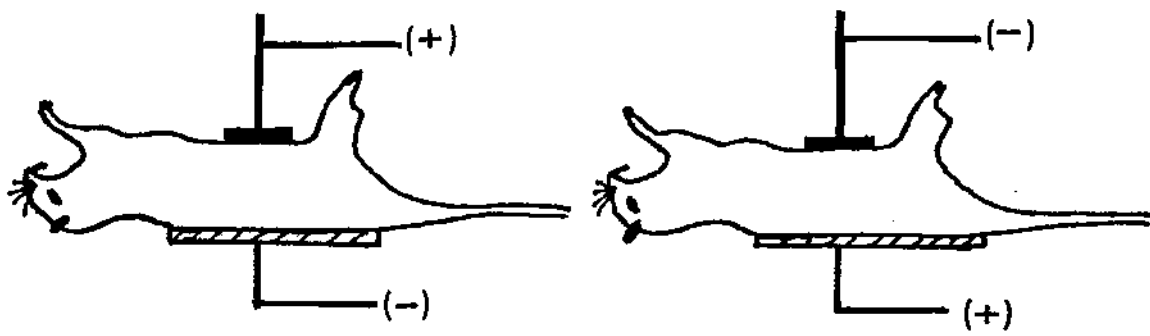
## 2.7 Iontophoresis

With the animal positioned dorsum downwards, the indifferent electrode was impregnated with physiological saline and placed carefully against the dorsal skin, with its long axis parallel to that of the rat. The selected test solution was first applied locally on to the surface of the abdominal skin as in the control experiments. Care was taken to ensure that the surface area of the shaved abdominal skin exceeded that of the iontophoresis electrode. The iontophoresis electrode, which was saturated with the same test solution, was next applied on to the shaved area. It was held in position by hand, care being taken to keep the hand as steady as possible during iontophoresis. The two electrodes were placed parallel to each other and parallel to the ventral (abdominal) and dorsal surfaces of the animal to ensure a uniform passage and distribution of the current traversing the treated

area. The conducting leads of both electrodes were connected to the appropriate terminals of the apparatus (see below). With the resistances at maximum, the voltage was first raised in nine volt steps to either 27 or 36 volts. The current was allowed to flow for a selected time, during which continuous wetting of the electrodes with the appropriate solutions was necessary to prevent the electrodes from drying out. At the end of the selected duration of treatment, the current was gradually decreased to zero to avoid a sudden change of current which results in the animal experiencing an electric shock. The apparatus was then switched off and the iontophoresis electrode removed from the animal.

#### 2.7.1 Polarity selection

Ions, whether anions or cations, are introduced from the iontophoresis electrode. If the iontophoresis electrode is connected to the positive pole of the apparatus (to become the anode) and the indifferent electrode is connected to the negative pole (to become the cathode), this arrangement is referred to as positive iontophoresis. If, on the other hand, the polarity is reversed, that is the iontophoresis electrode is connected to the negative pole (to become the cathode) and the indifferent electrode is connected to the positive pole (to become the anode), this arrangement is referred to as negative iontophoresis. Unless indicated otherwise, cations (positively charged ions) are introduced into the skin using positive iontophoresis, whereas anions (negatively charged ions) are introduced using negative iontophoresis. Figure 2.9 is a diagrammatic representation of such arrangements.



POSITIVE IONTOPHORESIS

NEGATIVE IONTOPHORESIS

Fig. 2.9. A diagram of polarity selection.

## **2.8 Intradermal injections**

These injections were carried out by inserting a needle obliquely into the skin for some 5 millimeters and injecting 0.1 ml portions. Specimens were removed 15 minutes later.

## **2.9 Pre-excision**

Following both local application and iontophoresis, excess test solution on the abdominal surface was removed by gentle and regular wiping with clean pieces of cotton wool lightly soaked with physiological saline. This prevented excess solution being carried into the skin during excision. No appreciable damage was observed in the intact, treated skin following iontophoresis at lower values of current and shorter times of application. However, at higher current densities, although no inflammation or skin irritation was observed, the treated area had a harder surface than the neighbouring areas. This phenomenon was used as a guide to distinguish the treated area from the neighbouring skin, especially when a colourless test solution was used for an iontophoresis study.

## **2.10 Excision of the treated skin**

Excision was performed with a clean pair of scissors. Great care was taken to keep the lines of incision well outside and distant from the edges of the treated area to minimise transfer of the test solution during excision of the skin. The skin was excised to the depth of the



subcutaneous layer or superficial fascia. No blood was allowed to flow over the surface of the treated area during this procedure.

## **2.11 Preparation of excised skin for cryostat sectioning**

### **2.11.1 Trimming**

The excised skin was placed on a clean, dry surface with the epidermal side facing upwards. A plastic petri dish was used for this purpose since it was shown to be not too hard or too brittle for trimming. Using new clean razor blades, the skin was diced into thin longitudinal strips. Remnants of hair were used as a guide for the direction of the cuts. Except on a few occasions, unwanted skin surrounding the treated area was discarded at this stage. The selected strips were further cut up, without appreciable pressure, into smaller blocks using new clean razor blades. Each skin block measured approximately 1 cm in length, 0.5 cm in width and 0.5cm in depth.

### **2.11.2 Specimen selection**

In each experiment, specimens were chosen from the central, middle and peripheral areas of the treated skin, following both local application and iontophoresis. On a few occasions, following iontophoresis, specimens were also taken from that area of skin just outside the treated area for comparative investigations.

### 2.11.3 Freezing the specimens

A cork disc moistened with water, approximately 1.5 cm in diameter, was frozen on to the cryostat chuck by means of carbon dioxide snow (The Distillers Company (CO<sub>2</sub>) Ltd, Coleshill) from a bench freezer (Slee and Co Ltd, London). A small amount of tissue-tek OCT compound (embedding medium for frozen tissue specimens, Miles Scientific, USA) was also frozen with carbon dioxide on to the cork disc. The surface of the frozen OCT compound was trimmed horizontally using a razor blade. This provided a platform on which the skin specimen was mounted, and in addition it provided a continuum with the tissue that would not damage the cryostat blade as the last sections were cut. Without fixation, the skin specimens were placed onto the OCT platform, a single specimen per cryostat chuck. Each specimen was orientated in such a way that once placed in the cryostat, conventional sagittal sections would be obtained, that is, the edge of the cryostat blade passed along the longitudinal axis of the hair follicles and perpendicular to the surface of the skin. Remnants of hair were used as a guide for this orientation. The addition of the OCT compound around the skin specimen and continuous freezing with carbon dioxide secured the specimen in position and provided support for the specimen during sectioning. Every effort was made to ensure that these procedures were performed as carefully but as rapidly as possible to minimise changes in the specimens due to autolytic processes.

#### 2.11.4 Cryostat sectioning

The cryostat chuck (holding the specimen) was placed in position in the cryostat in such a way that sectioning started at the subcutaneous layer, followed by the dermis, the epidermis, and finally the skin surface. Sectioning the specimens in this way minimised carriage of materials (if any) from the upper layers as a contaminant of the deeper layers of the skin. During sectioning the cryostat was kept at  $-20^{\circ}$  C. Serial sectioning was carried out on each skin specimen until no further tissue was observed. The thickness of the sections varied from 15 to 20  $\mu$ . At this thickness, sections are relatively easy to produce. The cryostat blade was normally cleaned after each section to avoid displacement of material from the blade to the following section. The sections were transferred directly on to clean, dry glass slides, examined with an optical microscope (Laborlux II, Leitz, Germany) to check orientation and degree of penetration, and left to dry. It was necessary to re-freeze each specimen at regular intervals as the "block-face" became soft and sections disintegrated.

#### 2.11.5 Examination of frozen sections

The first and last few sections obtained from each skin specimen were discarded as displacement of unrecovered test material can occur from the surface (and upper layers) into the deeper layers of the skin when trimming with a razor blade. In addition, examination of the lateral edges of each section was neglected. That is, careful examination was made of the central region of each section and hence the central region of each skin specimen.

### 2.11.6 Selection of results

When the location and distribution of a selected test material appeared to be consistent in the serial sections obtained from a single specimen, and consistent with those obtained from different specimens of the same experiment, this was considered to be the initial result of that particular experiment. On average, each experiment was repeated at least three times. Furthermore, when the location and distribution of a test material appeared to be consistent in specimens obtained from a particular experiment and consistent with those obtained from its repetition, this was considered to be the final result of that particular set of experiments.

### 2.11.7 Photography

Photographs were taken of representative sections selected from the final result of each set of experiments using a Zeiss optic microscope shortly after mounting.

## 2.12 General histological techniques

### 2.12.1 Haematoxylin and eosin

- (1) Frozen sections were stained in Mayer's haemalum for 10 minutes. The method of preparation of the staining solution is described elsewhere (Cook, 1974).
- (2) Rinsed in running tap water for 1 minute.
- (3) Stained in 0.5% eosin for 15 seconds.

- (4) Rinsed in running tap water for 3 minutes.
- (5) Dehydrated in ascending grades of alcohol, cleared in xylol and mounted in DePeX.

#### 2.12.2 Tartrazine

Tartrazine is an acid dye of the hydroxy-pyrazol group. In the solid state it is present as a yellowish-orange powder which dissolves in water to give a clear golden solution. Tartrazine stains connective tissue selectively, hence it is used to indicate the extent of the dermis and the hypodermis in the unfixed, unstained frozen sections.

- (1) Frozen sections were stained in 0.125% aqueous tartrazine (Microscopical stain, George T Gurr Ltd, England) for 2 or 3 seconds.
- (2) Rinsed in running tap water for 2 minutes.
- (3) Allowed to dry in air, or dehydrated in ascending grades of alcohol and cleared in xylol. All sections were mounted thereafter in DePeX, unless indicated otherwise.

#### 2.13 Special histological techniques

Three techniques were used to demonstrate various elements in tissue sections. These were firstly, a haematoxylin method for copper and iron, secondly, a rubeanic acid method for copper and, thirdly, a prussian blue method for iron. These methods were applied to dry cryostat sections, unless indicated otherwise.

### 2.13.1 Haematoxylin method for copper and iron

Mallory (1938), and Mallory and Parker (1939) described a method for demonstrating copper and iron in tissue sections using freshly prepared haematoxylin solution. The basis of this method is the ability of unripened haematoxylin to form blue-black "lakes" with these metals.

Preparation of staining solution:

0.4 grams of haematoxylin (Standard stain, BDH Chemicals Ltd, England) were dissolved in 30 mls of absolute alcohol. 400 mls of freshly prepared distilled water were added gradually with continuous mixing.

Procedure:

- (1) The sections were stained in the haematoxylin solution for 1 hour.
- (2) Rinsed in several changes of distilled water for 1 hour.
- (3) Dehydrated in ascending grades of alcohol, cleared in xylene, and mounted in DePex.

Result:

Blue-black "lakes" indicate location of copper and iron.

### 2.13.2 Rubeanic acid technique for copper (Pearse, 1972; Cook, 1974).

The basis of this method is that rubeanic acid (dithiooxamide) forms a coloured compound with copper. Bancroft and Stevens (1977) believed this to be due to the formation of an inner complex salt of the di-imido form of rubeanic acid (copper rubeanate).

#### Preparation of staining solution:

Rubeanic acid (dithiooxamide, Sigma Chemicals Co., USA) was dissolved in 70% ethanol to a concentration of 0.1% (W/V) respectively.

#### Procedure:

- (1) Thin slices (approximately 5 mm thick) of freshly excised skin were immersed in the rubeanic acid solution for 10 min.
- (2) 200 mg of sodium acetate (analytical reagent, BDH Chemicals Ltd, England) were added to each 100 mls of the above solution, and the specimens left in it for 36 hours.
- (3) They were then washed briefly in 70% ethanol and left in this solution for 75 min.
- (4) The 70% ethanol was replaced with absolute ethanol in which the specimen was left for 24 hours.
- (5) Subsequently, the specimens were cleared in chloroform and embedded in paraffin wax. Chloroform was used as a transitional agent as it is miscible with both the dehydrating agent (alcohol) and the embedding medium (paraffin wax).
- (6) 8  $\mu$  sections were cut on a microtome (Leitz, Wetzlar), mounted on microscope slides, dewaxed with xylene and mounted in DePeX. Alternatively, the sections were taken to water through xylene and descending grades of alcohol, stained with 0.125% aqueous tartrazine (10 sec), rinsed in water, dehydrated in ascending grades of alcohol, cleared in xylene and mounted in DePeX.

#### Result:

Black deposits (copper rubeanate) indicate location of copper in the sections.

### 2.13.3 Perl's Prussian blue method for iron (Cook, 1974)

In this method, a mixture of hydrochloric acid and potassium ferrocyanide is used. The basis of the method is that hydrochloric acid liberates protein-bound iron, allowing the potassium ferrocyanide to combine specifically with the liberated ferric iron to form ferric ferrocyanide (Prussian blue).

Procedure:

- (1) Sections were exposed to a fresh mixture of equal parts of 2% aqueous potassium ferrocyanide (laboratory reagent, BDH Chemicals Ltd, England) and 2% hydrochloric acid (v/v in distilled water) for 45 min.
- (2) Washed in distilled water.
- (3) Counterstained with 1% aqueous neutral red (product number n-2880, Sigma Chemical Co., USA) for 3 min.
- (4) Washed in water, dehydrated in ascending grades of alcohol, cleared in xylene and mounted in DePeX.

Result:

Prussian blue indicates location of iron.

## 2.14 Preparation of excised skin for transmission electron microscopy

### 2.14.1 Theoretical aspects

The method used to prepare the excised skin for examination with the electron microscope can be summarised as follows:

primary fixation and rinsing; secondary fixation and rinsing; dehydration; infiltration; embedding and polymerization; trimming, sectioning and mounting; section staining.



The aim of fixation is to preserve the structural details of a tissue with minimum alteration from the living state, and to protect them against disruption during subsequent treatments. The fixatives most commonly used are aldehydes and osmium tetroxide. Aldehyde fixatives are effective in cross-linking proteins and thus extraction of the cytoplasmic matrix is minimized. Osmium tetroxide fixes tissue by reacting with the double bonds in lipids which leads to cross-linking of adjacent molecules. In addition, osmium itself, which is a heavy metal, imparts density to the tissue it fixes. A double fixation by an aldehyde and osmium tetroxide is usually employed in order to stabilize the maximum number of different types of molecules and hence tissue structures.

Many factors influence the quality of fixation. These include the size of the tissue block, pH, temperature, concentration of the fixative, and the duration of fixation. Fixatives are made up in buffer solutions so that some of these factors can be controlled. The most commonly used buffers are cacodylate, veronal acetate and phosphate. The quality of fixation is dependant primarily upon the rate of penetration of the fixatives into the tissue blocks which is, in turn, dependant upon the size of the blocks. In general, the smaller the tissue blocks the higher the rate of penetration and the better the fixation. The pH of the fixative must remain close to the pH of the tissue because a change in the tissue pH, caused by the fixative, is bound to alter the structure of the tissue. Consequently, the fixatives are buffered in the range of pH 7.2 to 7.4 as the average pH values of most animal tissues is pH 7.4. Fixation is carried out at a low temperature as this reduces postmortem changes and keeps extraction of tissues to a minimum. The concentration of

the fixatives also affects the quality of fixation. Osmium tetroxide is usually used as a 1% solution whilst aldehyde fixatives vary between 2% and 4%. The duration of fixation should be short enough to prevent undue extraction of materials from the tissue, but long enough to allow complete penetration of the fixative into the sample in order to stabilize tissue components. The general principle of fixation and the techniques used in electron microscopy have been described in detail by Palade (1952), Bahr (1954), Watson (1958), Luft (1961), Reynolds (1963), Pearse (1964), Hayat (1970) and Meek (1980).

#### 2.14.2 Preparation of reagents

##### 2.14.2.1 Initial solution - 0.2M sodium cacodylate buffer (pH 7.3)

2.14 grams of sodium cacodylate (general purpose reagent, BDH Chemicals Ltd, England) were dissolved in 50 mls of distilled water, and the pH of the solution adjusted to 7.3 with N HCl. The pH was measured using a glass electrode digital pH meter (model 7065, Electronic Instruments Ltd, Kent).

##### 2.14.2.2 Buffer solution - 0.08M sodium cacodylate buffer (pH 7.3)

40 mls of the initial solution were diluted to 100 mls with distilled water, the pH being adjusted to 7.3 if necessary. The buffer solution was placed in the refrigerator at 4<sup>0</sup> C for storage, and was used within two to three days after preparation.

##### 2.14.2.3 Primary fixative - 4% paraformaldehyde/5% gluteraldehyde in 0.08M sodium cacodylate buffer, pH 7.3

1 gram of paraformaldehyde (laboratory reagent, BDH Chemicals Ltd, England) was dissolved in 9 mls of distilled water at 60<sup>0</sup> C using a

magnetic stirrer regulator hotplate (Gallenkamp, England). 1 to 3 drops of N NaOH were added to clear the solution which was then allowed to cool. 5 mls of 25% gluteraldehyde solution (electron microscopy materials, BDH Chemicals Ltd, England) were added to the paraformaldehyde solution. Finally, the remaining 10 mls of the initial solution and 1 ml of distilled water were added to give a total volume of 25 mls of primary fixative, and the pH was adjusted to 7.3. The primary fixative was placed in the refrigerator for storage.

#### 2.14.2.4 Secondary fixative - 1% osmium tetroxide in 0.08M sodium cacodylate buffer, pH 7.3

Osmium tetroxide (general purpose reagent, BDH Chemicals Ltd, England) is supplied in sealed ampoules each containing 0.1 grams. All traces of label and glue were removed from the ampoule using tap water. The ampoule was cracked open and placed in a suitable vial to which 10 mls of the buffer solution were added. The vial was capped and left to rotate for 1 hour on a rotary apparatus (Spiramix 5, Danley, England) to dissolve the osmium tetroxide crystals. The vial was then placed in a securely-capped plastic container and left in the refrigerator for storage.

#### 2.14.2.5 Embedding reagents

The embedding resins have two chemically reactive groups spaced along the length of the backbone chain, these being hydroxyl groups and epoxy end-groups. The hydroxyl groups are capable of reacting with acid anhydrides to form cross-bridges between the resin molecules. The acid anhydride is called the hardener. The hardener dodeceny succinic anhydride (DDSA) is used. On the other hand, the epoxy end-groups readily attach themselves to groups containing reactive

hydrogen atoms, notably amines. Therefore, the addition of an amine-containing agent to the resin will cause the resin molecules to join up end-to-end, forming long-chain polymers. The end-to-end linking agent is called the accelerator. The accelerator N-benzyl, N-N-dimethylamine (BDMA) is used. If the hardener (DDSA) is used alone, the final resin will be too hard for sectioning most tissues. Therefore, the addition of a "plasticizer" to the mixture makes the blocks relatively elastic but still hard enough for sectioning. Di-butyl-phthalate is the plasticizer used.

#### Preparation:

Mixture (A) - 10 grams of araldite resin (CY 212, Agar Aids, Essex) were mixed by rotation with 10 grams of DDSA (Agar Aids, Essex) for 1.5 hours.

Mixture (B) - 1.5 grams of BDMA (Agar Aids, Essex) and 2 drops of Di-butyl-phthalate were mixed as above.

Embedding resin [(AB) mixture] - 0.375 grams of mixture (B) were added to 15 grams of mixture (A) and mixed by rotation for 1.5 hours.

#### 2.14.2.6 Resin/Epoxypropane mixture

The remaining 5 grams of (A), 0.125 grams of (B) and 5 mls of epoxypropane were mixed in a vial.

#### 2.14.2.7 Dehydrating agent (Ethanol)

A series of solutions of distilled water and absolute ethanol of increasing ethanol concentration were prepared by mixing the two in appropriate volumes to give 50%, 75% and 96% ethanol.

### 2.14.3 Electron microscopy procedures

#### 2.14.3.1 Specimen preparation and primary fixation

Following excision of the treated area, the skin was immersed immediately in the primary fixative in a clean plastic petri dish, with the epidermal side facing upwards. The skin was then cut into thin strips using new, clean razor blades. The strips were cut in turn into smaller pieces under a dissecting microscope (Meoptan DM23, Praha, Czechoslovakia). Each piece was cuboidal in shape with a side measuring approximately 0.5 to 1 mm. Specimens were chosen from central, middle and peripheral sites of the treated area. The selected specimens were then transferred by means of a pipette to a vial containing fresh primary fixative and left to fix on a rotatory apparatus for 2.5 hours.

#### 2.14.3.2 First rinsing

The primary fixative must be removed since aldehyde combines with and reduces osmium tetroxide resulting in unwanted precipitation within the specimens. Consequently, the primary fixative was poured out of the vial, and any remainder carefully removed from the vial with a finely drawn pipette. The specimens were washed thereafter by rotation with three changes of the buffer solution, 10 minutes each, to remove excess aldehyde in the specimens.

#### 2.14.3.3 Secondary fixation

The final buffer wash was poured off and replaced with the secondary fixative ( $O_5O_4$ ). The specimens were left to post-fix for 1.5 hours.

#### 2.14.3.4 Second rinsing

It is desirable to remove excess osmium tetroxide before dehydration since it is reduced by alcohol to insoluble osmium dioxide. Consequently, the secondary fixative was carefully pipetted out of the vial and the skin specimens were then rinsed by rotation with three changes of the buffer solution, 10 minutes each, to remove excess secondary fixative.

#### 2.14.3.5 Dehydration

The aim of dehydration is to remove all the free water from the fixed and rinsed specimens and to replace it with a suitable organic solvent. The removal of the free water is essential if the specimens are to be embedded in a water-insoluble resin. To minimize any damage to the tissue resulting from changes in solvent concentration, dehydration takes place through a gradual series of solvents. As a result, the last buffer wash was poured off, any remainder pipetted out, and 50% ethanol was then added to the vial and left in contact with the specimens on the rotatory mixer for 15 minutes. In turn it was replaced by 75% ethanol for a further 15 minutes, followed by a third rinse in 96% ethanol for another 15 minutes. This was then discarded and the specimens were rinsed with three changes of absolute ethanol (dried especially by standing over anhydrous copper II sulphate), each rinse being for 15 minutes.

#### 2.14.3.6 Pre-infiltration

Since ethanol is immiscible with the embedding medium, a "transitional agent" which is miscible with both the alcohol and the resin must replace the alcohol in the specimens prior to infiltration. The

transitional agent used is 1,2-epoxypropane (also called propylene oxide).

The final rinse of absolute ethanol was poured off as usual and replaced with equal parts of absolute ethanol/epoxypropane prepared by mixing the two in equal volumes. This was followed by three changes of epoxypropane, all 15 minutes each.

#### 2.14.3.7 Infiltration

The aim of infiltration is to impregnate the specimens with the embedding resin with the aid of the transitional agent. The first step of this process is the introduction of a mixture of epoxypropane and the embedding resin. Epoxypropane itself is extremely volatile and has a low viscosity, so it penetrates the specimen very rapidly, carrying with it the resin. Thereafter it evaporates leaving the resin behind.

In order to facilitate the above, the final change of epoxypropane was discarded, substituted by an (AB)/epoxypropane mixture and left for 16 hours with the lid of the vial loose to allow evaporation of the epoxypropane. In turn, the (AB)/epoxypropane mixture was discarded, replaced by approximately 5 grams of (AB) mixture and left for 7 hours, once again with the lid of the vial loose to allow evaporation of excess epoxypropane.

#### 2.14.3.8 Embedding and polymerization

The skin specimens were next transferred to plastic embedding moulds containing the remainder of the (AB) mixture. The specimens were placed at regular intervals with the surface of the skin facing

upwards. This was carried out under a binocular microscope. The embedding moulds were then placed in an incubator at 60° C and left for 48 hours to polymerise the resin.

#### 2.14.3.9 Sectioning with the ultramicrotome

(a) Preparation of glass knives: A bar of glass was positioned securely into a plastic frame marker and scored transversely using a diamond wheel cutter. Pressure was then applied with specially curved pliers to break the glass bar at the score and thereby produce a square. The glass square was then positioned in another plastic frame marker and scored diagonally, and broken as before to produce two triangular knives. Usually one of these knives had a straight and sharp edge of high quality and was used for sectioning. Assessment of the quality of the knife edge was carried out by examining it under a binocular microscope. A short length of adhesive tape was wrapped around the knife from one side to the other and excess tape cut off with a razor blade. The gap between the bottom of the tape and the sloping back face of the knife was then sealed with UHU glue.

(b) Block trimming: The original resin block was cut into smaller blocks, each containing a single skin specimen, by using a jeweller's saw with fine teeth. A single block was then clamped firmly into the ultramicrotome and excess embedding medium trimmed away by cutting horizontally across the top of the block until the tissue was exposed. This was carried out with a new, clean, single-edged razor blade under a stereo binocular microscope (Carl Zeiss, W Germany). Four additional cuts were then made in a vertical direction to produce a truncated pyramid in which the horizontal top becomes a trapezium. The trapezium was next trimmed horizontally with a new, degreased razor blade to obtain a smoother shiny surface, this being the block face



from which sections were produced. The sides of the block face were also trimmed with the new razor blade until they were sharp and smooth.

(c) Semithin sections: The ultramicrotome chuck was clamped firmly in the ultramicrotome stage (OMU2, Richert, Austria). A glass knife, filled with filtered distilled water up to its cutting edge was also clamped firmly in the ultramicrotome. Geometrical adjustments were necessary to ensure that the horizontal lower and upper sides of the block face were parallel to the cutting edge of the knife and that all were present in the same vertical plane of sectioning.  $0.5 \mu$  sections were cut and picked up by using an eyelash mounted on a small wooden stick. They were then transferred to a drop of water on a clean microscope slide to which they adhered firmly following drying on a hot plate. These sections were stained for examination with the light microscope to give a general idea of the orientation of the tissue and to enable areas of interest in the block face to be pinpointed and hence trimmed further.

Staining of semi-thin sections:

(i) Preparation of the staining solution: Toluidine blue stains resin-embedded tissue if used at a high alkaline pH and with the application of heat. Consequently, 0.5 grams of sodium tetraborate (di-sodium tetraborate (borax), laboratory reagent, BDH) and 0.25 grams of toluidine blue (Gurr, George T Gurr Ltd, England) were dissolved by heat in 100 mls of distilled water. The solution was filtered, left to cool and stored in a dropping bottle.

(ii) Staining procedure: Sections were stained by covering them with a few drops of the staining solution and then heating the slide on a hotplate until the dye began to "steam". Excess dye was washed off

with distilled water, the sections were allowed to dry and then mounted in DePeX.

(d) Ultrathin sections: When an area for fine structural examination was selected from the semithin sections, the block face was retrimmed by cutting vertically with a new, degreased razor blade under a binocular microscope. A new glass knife was adjusted to the correct geometrical position relative to the block face and filled with filtered distilled water up to its cutting edge. The automatic drive motor of the ultramicrotome was started and ultrathin sections were obtained. These sections adhere at their horizontal sides forming unbroken straight ribbons.

Selection of ultrathin sections: Flattening of the ultrathin sections is a necessary step since the sections are compressed as they are cut. This was achieved by holding a sealed glass tube dipped in chloroform just above the sections. As the chloroform evaporated, the vapour produced expansion of the sections. The white light from the ultramicrotome becomes reflected at two levels, that is from the upper surface of the sections and from the surface of the water beneath the sections. The difference in optical path length between the two gives rise to interference, and hence makes the sections appear coloured. Ultrathin sections with silver or silver-gold interference (approximately 60 to 100 nm thick) were mounted on formvar coated copper grids. The grids were coated with formvar to provide additional support for the sections during examination with the transmission electron microscope.

Staining of ultrathin sections:

The aim of staining ultrathin sections is to increase the existing differential electron scattering power (contrast) of the tissue constituents by reacting them with solutions of heavy metals. The

most commonly used heavy metals for section staining are lead and uranium due to their great affinity for many tissue structures.

Preparation of staining solutions:

(1) 2% uranyl acetate solution: 0.1 grams of uranyl acetate (Analar analytical reagent, BDH, England) were dissolved by rotation for 30 minutes in 5 mls of 50% alcohol. Since uranyl acetate is photometrically active, that is, on exposure to light a cloudy precipitate is formed, this solution was prepared in a black glass vial and staining with it was performed in the dark under a cardboard box.

(2) 0.4% lead citrate solution: 0.04 grams of lead citrate (laboratory reagent, BDH, England) were dissolved in 10 mls of 0.1 N NaOH carbonate free (analar reagent, BDH, England).

Staining procedure:

(1) The grids were immersed, sections upwards, in a black glass petri dish containing the uranyl acetate solution. The lid of the petri dish was added and the staining dish covered with a cardboard box for approximately 20 minutes.

(2) The grids were rinsed by dipping them into a filtered distilled water bath for about 5 seconds.

(3) Excess water on the grids was removed by touching them with a filter paper and the grids were floated, sections downwards, on the surface of the lead citrate solution in a petri dish for 5 minutes. Breathing near the staining dish was avoided since lead can react with atmospheric carbon dioxide resulting in the formation of lead carbonate as a contaminant on the surface of the sections. This also explains why the lead citrate was dissolved in carbonate-free sodium hydroxide.

(4) The grids were next rinsed in 0.1 N NaOH (carbonate-free), and excess NaOH was quickly removed with a clean filter paper.

(5) Finally, the grids were rinsed in a water bath containing freshly filtered distilled water and placed, sections upwards, on a clean filter paper and left to dry.

#### 2.14.3.10 Examination of the sections

The ultrathin sections were examined, with or without staining, and photographed in a Zeiss EM9S transmission electron microscope (TEM), operating at 60 KV. The magnification of each exposure was recorded.

#### 2.14.3.11 Development of TEM negatives

The following procedures were carried out in a dark room equipped with a safelight (Wratten series, Kodak Ltd, England) on to which a red filter has been mounted. Once removed from the electron microscope, the negatives were placed in a rack and immersed in developer (Kodak D19, Kodak Ltd, England) for 3 minutes at 20<sup>0</sup> C. The negatives were then rinsed in a bath containing running tap water and placed in fixer (Kodafix, Kodak Ltd, England) for another 3 minutes. Following fixation, the negatives were given a good wash for approximately 15 minutes in running tap water and placed in an incubator to dry.

Printing of TEM negatives:

(i) Preparation of chemicals:

**Developer:** The concentrated developer (Ilford Ilfospeed multigrade paper developer, Ilford Ltd, England) was diluted with water in a ratio of 1:9 (v/v) and warmed to 20<sup>0</sup> C.

**Fixer:** The concentrated fixer solution (Kodafix, Kodak Ltd, England) was diluted with water to a ratio of 1:3 (v/v).

(ii) Procedures: The following procedures were carried out in a dark room with a safelight on to which a yellow filter has been mounted. Each negative was placed in an enlarger (DA900, Durst, Italy) and focused on to a masking frame (D243, Durst, Italy). A sheet of photographic paper (Ilfospeed multigrade II, Ilford, England) was secured in position in the masking frame. The negative was then exposed on to the photographic paper and the magnification on the enlarger was recorded. The photographic paper was then placed in developer for 1.5 minutes, during which the dish containing the developer was rocked gently backwards and forwards to ensure even development of the print. A control test was carried out to select the most suitable time of exposure. Once developed, excess developer on the print was drained off and the print was immersed in a stop bath (1% acetic acid in distilled water) for 30 seconds to stop development. The print was then rinsed in a water bath to remove excess acetic acid and immersed in the fixer solution for 5 minutes. Subsequently the print was rinsed in running tap water for 3 minutes and left to dry. The final magnification of each photograph was recorded by multiplying the initial magnification obtained with the transmission electron microscope by the magnification noted on the enlarger.

### **2.15 Preparation of excised skin for X-ray analysis**

Several detailed accounts are available describing the methods used to prepare specimens for X-ray analysis (Chandler, 1977; Erasmus, 1978; Hayat, 1980; Goldstein *et al.*, 1981; Morgan, 1985).

A scanning electron microscope (Jeol JSM 35CF) equipped with an X-ray microanalyzer (Link System Ltd) was used throughout the present investigation. The scanning electron microscope (SEM) gives morphological information, whereas the X-ray microanalyzer gives analytical information about each specimen. The aim of using the SEM X-ray microanalyzer was to determine whether a particular element used for iontophoresis was present in the analysed specimen (qualitative analysis) and, furthermore, to determine its approximate site of deposition within the specimen.

Figure 2.10 summarizes the different methods which were used to prepare the excised skin specimens for analysis. These methods were restricted by the tissue-processing and data-analysis equipment available, and fell into two main classes, namely, chemical and physical.

#### 2.15.1 Chemical methods

These include resin-embedded specimens and critical point dried specimens. The critical point dried specimens were prepared by dry fracture and freeze fracture methods.

##### 2.15.1.1 Resin-embedded specimens

Similar procedures to those described already for transmission electron microscopy were used. These can be briefly summarized as follows:

- (1) The excised specimens were fixed in primary (aldehyde) fixative.
- (2) Rinsed in three changes of buffer.
- (3) Post-fixed in secondary (osmium) fixative.

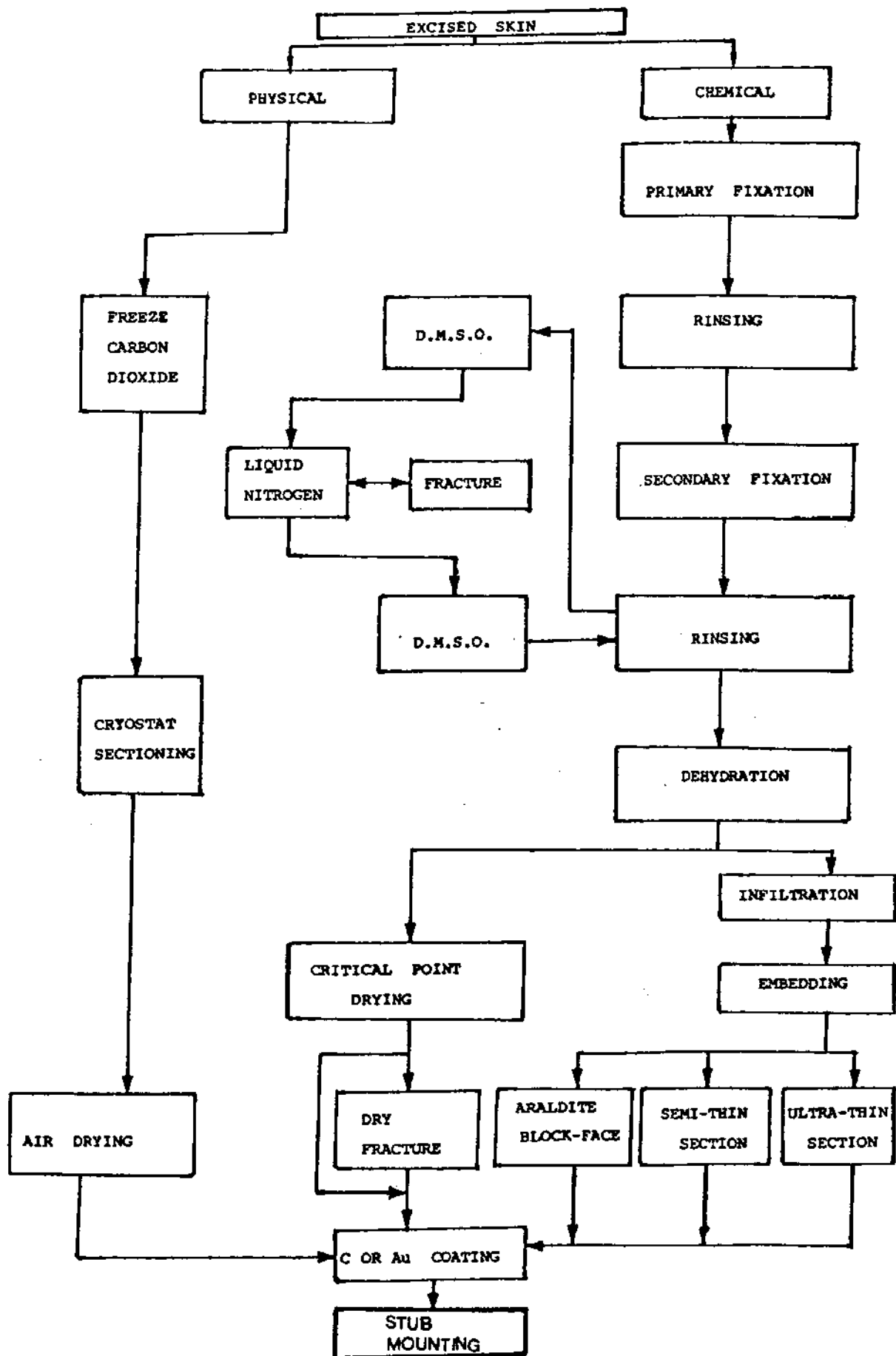


Fig. 2.10. Methods used to prepare skin specimens for x-ray analysis.

- (4) Rinsed in three changes of buffer.
- (5) Dehydrated in increasing concentrations of alcohol.
- (6) Embedded in resin and sectioned on an ultramicrotome.

X-ray microanalysis was carried out on ultrathin sections (approximately 600-900 nm) mounted on copper grids, on semithin sections (0.5 to 1  $\mu$ ) mounted on glass slides and on the araldite block-face following ultrathin sectioning. Only the semithin sections and the resin block-face however gave good results in terms of detection of elements of interest during subsequent analysis. The ultrathin sections proved unsuitable as they were damaged immediately when exposed to the electron beam.

#### 2.15.1.2 Critical point drying (CPD)

(a) Theoretical aspects: Air drying of soft specimens can cause deformation and the collapse of structures due to surface tension effects. The rationale behind CPD is that the two-phase stage (vapour and liquid) of volatile liquids disappears at a certain temperature and pressure, the so-called critical point. At the critical point, the two phases are in equilibrium, the phase boundary disappears and there is therefore no surface tension. Carbon dioxide is commonly used to dry specimens in this way and has a critical temperature of 31<sup>o</sup> C and a critical pressure of 1,073 psi.

The practical aspects of the method involve passing the tissue from the dehydrating fluid into liquid CO<sub>2</sub> in a pressurised container and then warming up to just over 31<sup>o</sup> C. This causes the liquid CO<sub>2</sub> to change state to a gas at the above-mentioned pressure. The gas is then released from the container and the dry specimens are removed.



The specimens dry without any surface tension effects and thus damage is minimised.

(b) Procedures:

Dry fracture:

(1) The excised skin specimens were fixed, rinsed, post-fixed, rinsed and dehydrated according to the method described previously (page 101).

(2) Following dehydration, the specimens underwent critical point drying and some of them were then dry fractured. This was achieved by making a small cut in each specimen, the two edges of which were held by fine forceps and then pulled apart, thus allowing the interior of the specimen to be exposed for examination and X-ray analysis. The other specimens were analysed without dry fracture.

Freeze fracture:

(1) The excised skin specimens were fixed, rinsed, post-fixed and rinsed according to the method described previously (page 101).

(2) Following the second rinsing in the buffer, the specimens were placed in 25% dimethyl sulphoxide (DMSO) for 10 minutes. During electron microscopy, DMSO is used as a cryoprotectant which minimizes ice crystal damage produced in the specimens during freezing.

(3) The specimens were then placed in 50% DMSO for 10 minutes.

(4) Next, the specimens were frozen in liquid nitrogen to convert them to brittle solid masses. The solid specimens were then fractured under liquid nitrogen, hopefully along a surface of structural continuity, but frequently at some random point, using a blunt scalpel. This allowed the internal surface of each specimen to be exposed for examination and analysis.

(5) The fractured specimens were placed in 50% DMSO for 5 minutes.

(6) They were rinsed finally in three changes of buffer, dehydrated in increasing concentrations of alcohol and critical point dried. The critical point drying method produced a good three-dimensional image but was unsatisfactory in terms of detection of elements of interest during subsequent X-ray analysis.

#### 2.15.2 Physical methods

The excised skin was frozen and sectioned with the cryostat according to the method described previously (page 89). Thick sections (approximately 15  $\mu$ ) were then used for X-ray analysis of the elements of interest.

#### 2.15.3 Coating

All the tissue destined for analysis was coated before examination in the SEM with a thin film of conducting material in order to increase the electrical conductivity of the tissue, and hence to reduce damage due to heating and the build up of a local charge resulting from bombardment with the electron beam. The most commonly used conducting materials were carbon and gold which were chosen so that they would not interfere with the analysis. A thin film was deposited by evaporation *in vacuo* on to each sample to be analyzed using a Speedivac coating unit (Edwards High Vacuum Ltd, England).

#### 2.15.4 Stub mounting

The glass slides bearing the semithin and cryostat sections were mounted on SEM stubs using a conducting aluminium tape, whereas the

araldite blocks and critical point dried specimens were mounted on stubs using a quick drying carbon (Aquadag, EM Scope Laboratories Ltd, England). Following mounting, the stubs were placed in the SEM for examination and analysis.

CHAPTER 3  
*RESULTS*

## CONTENTS

	Figure	Page
<b>3.1 Cationic dyes</b>		115
3.1.1 Methylene blue		115
3.1.1.1 Effect of current intensity and duration of application	1-19	115
3.1.1.2 Regional variations	20-25	133
3.1.1.3 Effect of reversing the current	26-27	138
3.1.1.4 Effect of negative iontophoresis	28	140
3.1.1.5 Effect of absorbent pad thickness	29	141
3.1.1.6 State of iontophoresis electrode	30	142
3.1.1.7 Effect of concentration of dye	31-38	143
3.1.1.8 Effect of vehicle	39-43	150
3.1.2 Toluidine blue	44-46	156
3.1.3 Pyronin Y	47-48	159
3.1.4 Aniline blue alcohol-soluble	49-50	160
3.1.5 Chrysoidin Y	51-52	161
<b>3.2 Anionic dyes</b>		162
3.2.1 Eosins	53-60	162
3.2.2 Aniline blue water-soluble	61-63	167
3.2.3 Picric acid	64-65	169
3.2.4 Alizarin red S	66-67	170
3.2.5 Trypan blue	68-69	171
<b>3.3 Neutral dyes</b>		172
Sudan black B	70-72	172
<b>3.4 Compound dyes</b>		174
Jenner's stain	73-75	174
<b>3.5 Lanthanum</b>		177
3.5.1 Intradermal injection	76	179
3.5.2 Incubation method	77	188
3.5.3 Effect of concentration	78-80	194

3.5.4	Effect of removal of surface lipid	81	205
3.5.5	Effect of vehicle		208
3.5.5.1	Accelerants	82	208
3.5.5.2	Detergents	83	211
3.5.5.3	Organic solvents	84-85	214
<b>3.6</b>	<b>Silver</b>		221
3.6.1	Intradermal injection	86	222
3.6.2	Effect of concentration	87-92	227
3.6.3	Effect of vehicle		245
	Accelerants	93	245
3.6.4	Effect of removal of surface lipids	94	248
<b>3.7</b>	<b>Ruthenium red</b>	95-97	250
<b>3.8</b>	<b>Copper</b>		266
3.8.1	Intradermal injection	98	267
3.8.2	Effect of current intensity	99-102	269
3.8.3	Effect of concentration	103-108	273
3.8.4	Effect of vehicle		279
3.8.4.1	Accelerants	109-110	279
3.8.4.2	Detergents	111-112	281
<b>3.9</b>	<b>Iron</b>		283
3.9.1	Intradermal injection	113	284
3.9.2	Effect of concentration	114-117	286
3.9.3	Effect of vehicle		290
3.9.3.1	Accelerants	118-119	290
3.9.3.2	Alcohols	120-121	291
<b>3.10</b>	<b>Iodine</b>		293
<b>3.11</b>	<b>Tissue changes</b>		295
3.11.1	Untreated skin	122-123	297

3.11.2	The skin following local applications	124	300
3.11.3	The skin following iontophoresis		301
3.11.3.1	Positive iontophoresis	125	301
3.11.3.2	Negative iontophoresis	126	302

### 3.1 Cationic dyes

#### 3.1.1 Methylene blue

Methylene blue has been shown by previous investigators (Abramson and Engel, 1942; McEwan Jenkinson *et al.*, 1974) to penetrate the skin under the influence of an electric current. In the present study, a number of preparations of methylene blue have been used to investigate the effects of concentration, current intensity and duration of application on their penetration through the skin following local application (control) and iontophoresis.

##### 3.1.1.1 Effect of current intensity and duration of application

The following experiments were carried out to investigate the effect of changing the current intensity and duration of application on the penetration of methylene blue from the surface into the skin when the dye was introduced from the same vehicle (distilled water) at a fixed concentration (2% W/V). The dye solution was applied either locally (control) or introduced iontophoretically according to the following Table :-



Figure	Current Intensity (Milliamperes)	Duration of application (Minutes)
1 (a - d)	0 (Control)	15
2 (a and b)	5	5
3	5	10
4 (a and b)	5	15
5	10	5
6	10	10
7 (a and b)	10	15
8 (a and b)	15	5
9 (a and b)	15	10
10	15	15
11	20	5
12	20	10
13	20	15
14	25	5
15	25	10
16	25	15
17	30	5
18	30	10
19	30	15

## Figures 1a - 1d

Local application (control) of a 2% aqueous methylene blue solution for 15 minutes.

## Figure 1a: A typical cryostat section (x 40)

The penetration of methylene blue through the skin following local application is minimal. The dye is visible in the superficial part of the skin only, especially in those areas surrounding the orifices of the hair follicles, and in the uppermost parts of the follicular canal epidermis (FCE) which extend from the surface to the level of the sebaceous glands (SG).

## Figure 1b: A similar cryostat section to that shown above stained with tartrazine (x 40)

The location and distribution of methylene blue are similar to those described above. In addition, this section shows the extent of the dermis (D) and the upper part of the hypodermis (H), both of which are stained with tartrazine (yellow) but not with methylene blue.

Although the upper parts of the ostia of the hair follicles (HF) are filled with the cationic dye, methylene blue does not extend any deeper into the follicles or into the sebaceous glands (SG). The hair follicles and their associated sebaceous glands are characterized by the lack of the tartrazine stain.

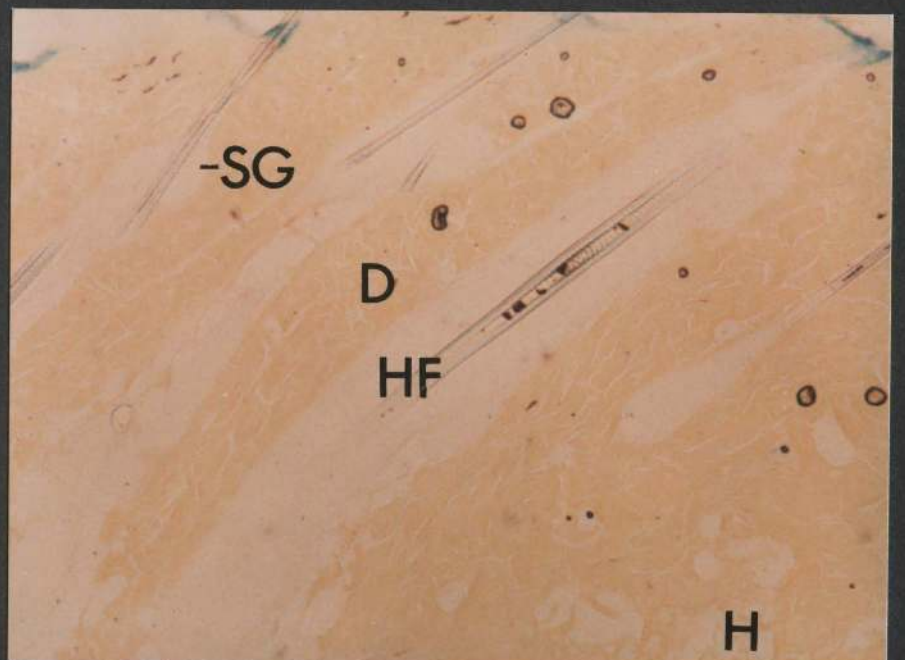


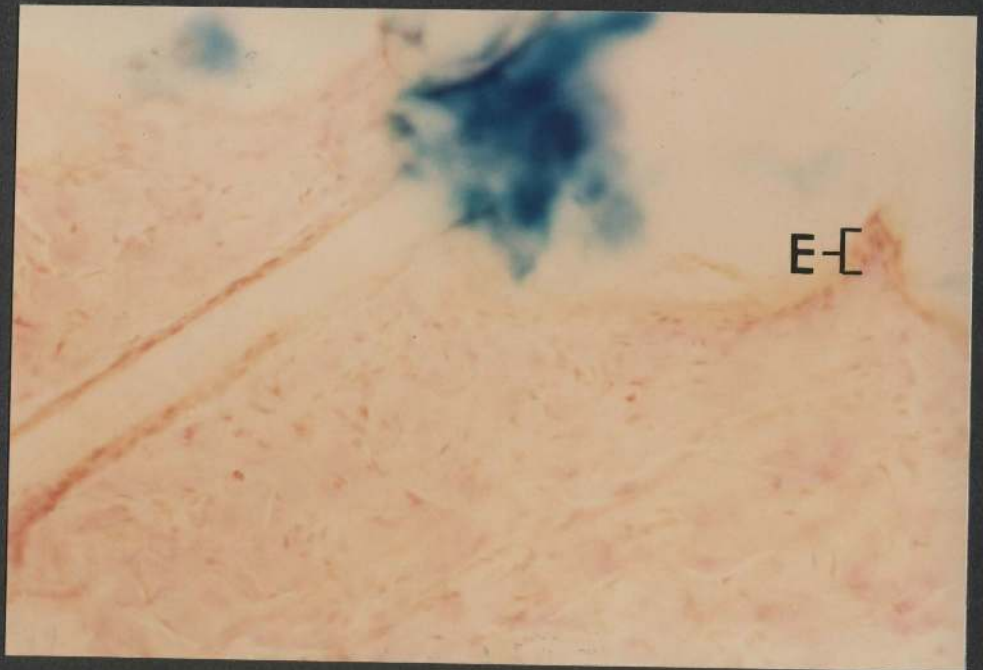
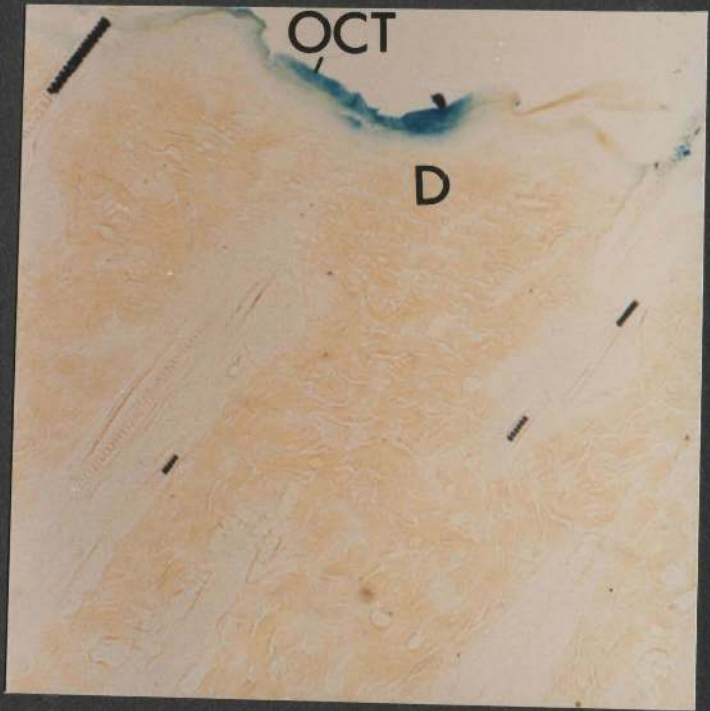
Figure 1c: A cryostat section stained with tartrazine (x 80)

At this magnification, a remnant of the embedding medium (OCT compound) is visible on the surface of the skin. There is a colour-free zone situated between the superficial part of the skin stained with methylene blue and the superficial dermal areas (D) stained with tartrazine.

Figure 1d: A cryostat section stained with haematoxylin and eosin (x 100)

It is apparent that the methylene blue, which has persisted and is visible in this section, is confined to the surface of the epidermis (E), including the surface squames and, in addition, forms a coating around the hair shaft just above the surface of the skin.

It appears that, by comparing Figures 1c and 1d, the colour-free zone seen in Figure 1c consists of the entire epidermis, excluding the most superficial squames.



## Figures 2a and 2b

Positive iontophoresis of a 2% aqueous methylene blue solution at 5 milliamperes for 5 minutes

Figure 2a: A cryostat section (x 40)

The tracer, methylene blue, is visible in parts of the epidermis (E), some follicular canal epidermis (FCE), and occasionally in the dermis immediately adjacent to these structures.

Figure 2b: A cryostat section similar to that shown in Figure 2a but stained also with tartrazine (x 40)

The staining of the epidermis (E) along the surface is not continuous and is interrupted by colour-free segments of varying extent. Some follicular canal epidermis (FCE) is stained with methylene blue whereas other areas are unstained. Sebaceous glands (SG) are also devoid of tracer.



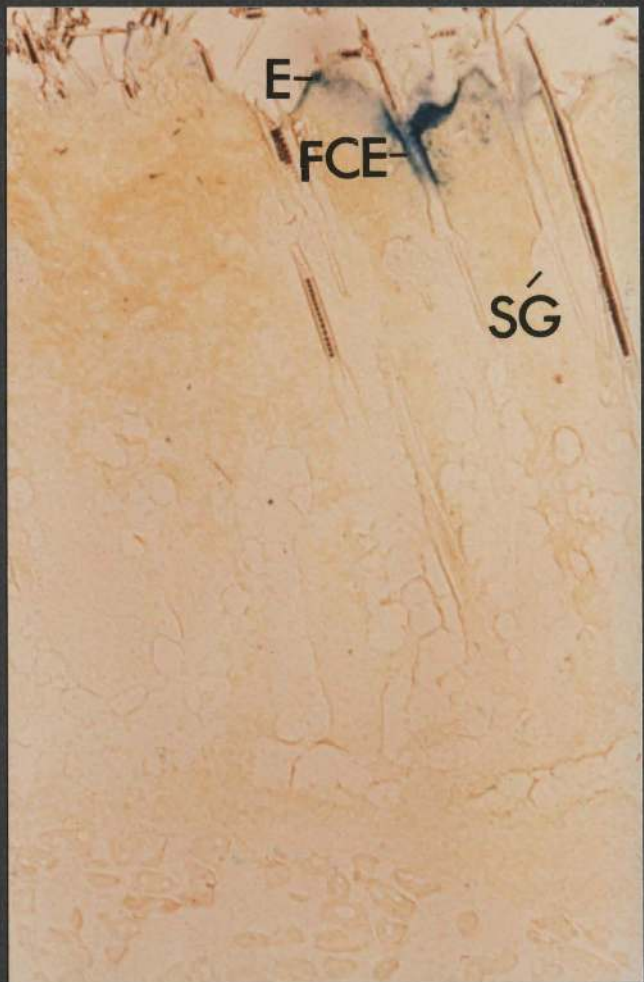


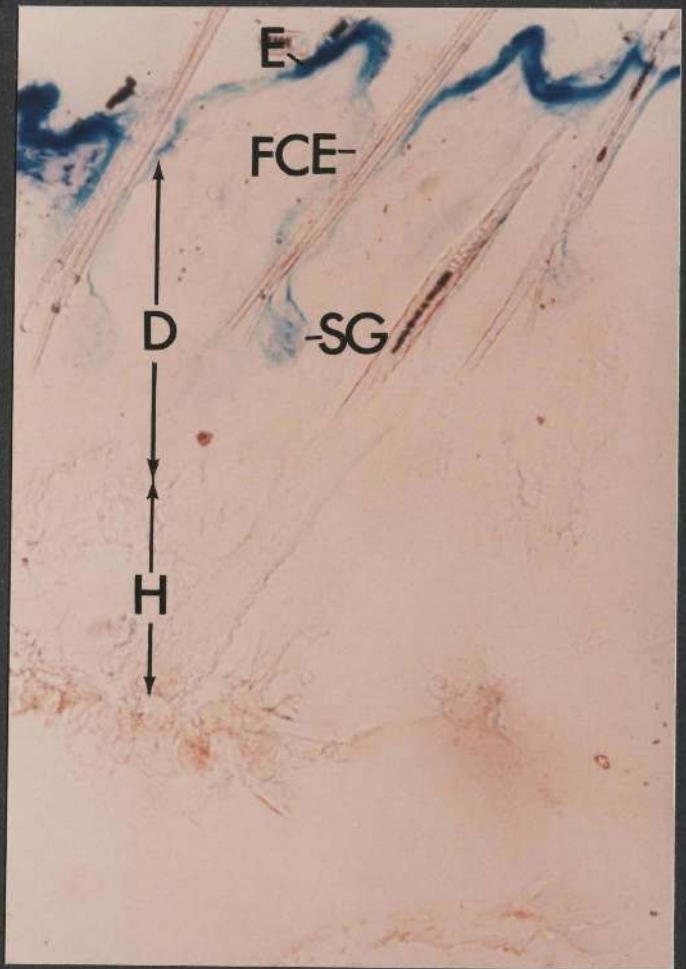
## Figure 3

Positive iontophoresis of a 2% aqueous methylene blue solution at 5 milliamperes for 10 minutes

A cryostat section (x 40)

Methylene blue is visible in the epidermis (E), follicular canal epidermis (FCE) and in some sebaceous glands (SG). Very little or no staining is observed in the bulk of the dermis (D), except for that part immediately beneath the epidermis and adjacent to the upper part of the follicular canal epidermis. The extent of the hypodermis (H) is shown.





Figures 4a and 4b

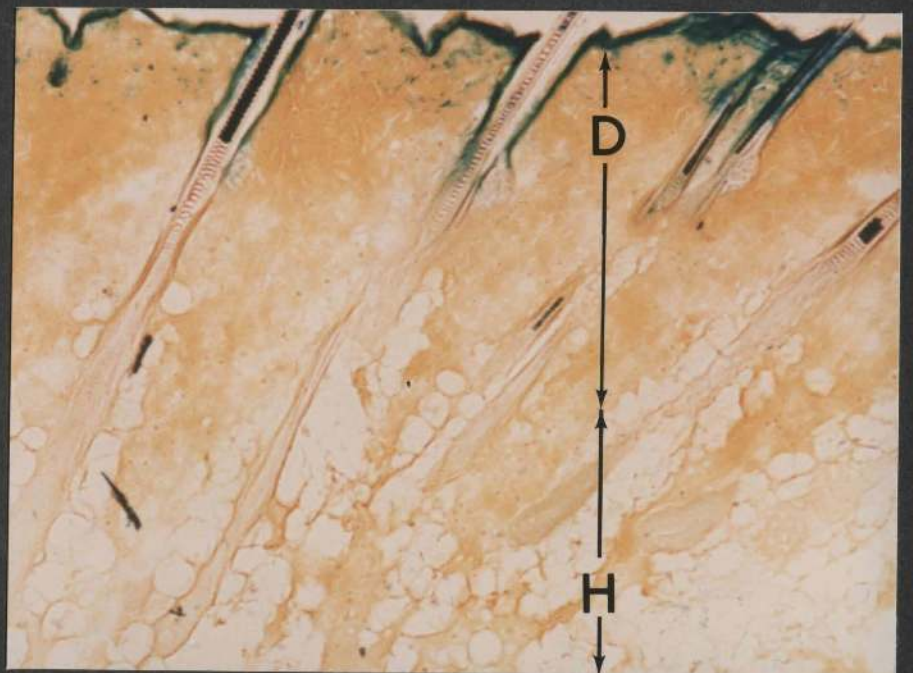
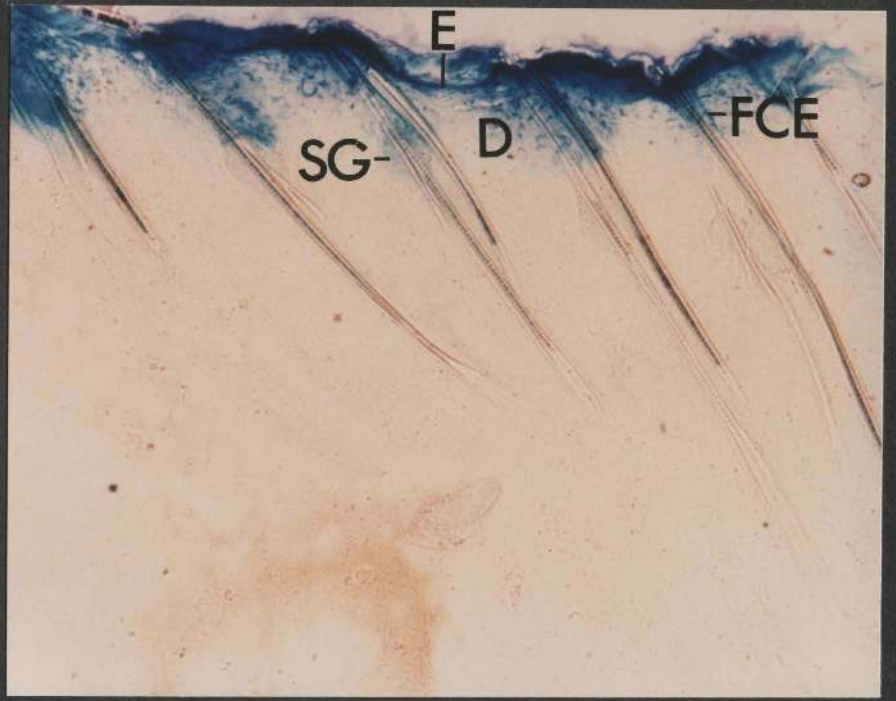
Positive iontophoresis of a 2% aqueous methylene blue solution at 5 milliamperes for 15 minutes

Figure 4a: A cryostat section (x 40)

The cationic blue tracer has stained the epidermis (E), follicular canal epidermis (FCE), and some sebaceous glands (SG). Dermal (D) regions adjacent to the follicular canal epidermis are also stained, whereas interfollicular regions of the dermis at the same level remain relatively unstained.

Figure 4b: A cryostat section stained with tartrazine to show the extent of the dermis (D) and hypodermis (H) (x 40)

It is evident that penetration through the upper part of the dermis is deeper in areas containing hair follicles.



## Figure 5

Positive iontophoresis of a 2% aqueous methylene blue solution at 10 milliamperes for 5 minutes

A cryostat section (x 80)

Methylene blue is visible in the epidermis (E), follicular canal epidermis (FCE), and in some sebaceous glands (SG). Occasionally, dermal regions (D) just below the epidermis also contain tracer. However, the connective tissue surrounding and between the sebaceous glands is not stained.

The extent of the penetration is similar in this case to that obtained when the dye solution is introduced using a current of 5 milliamperes for a period of 10 minutes (Figure 3).

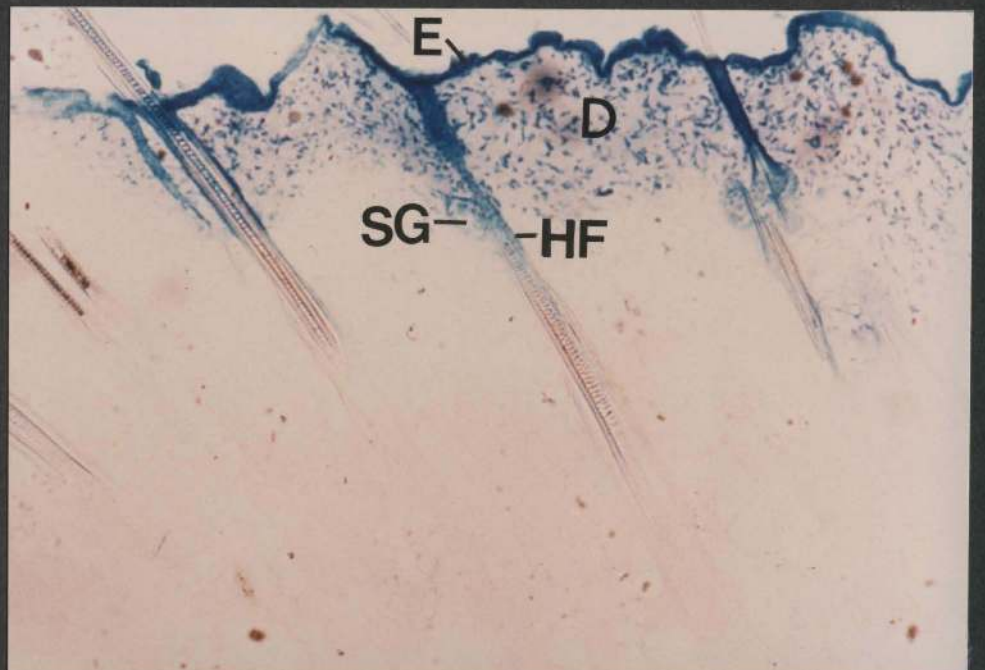
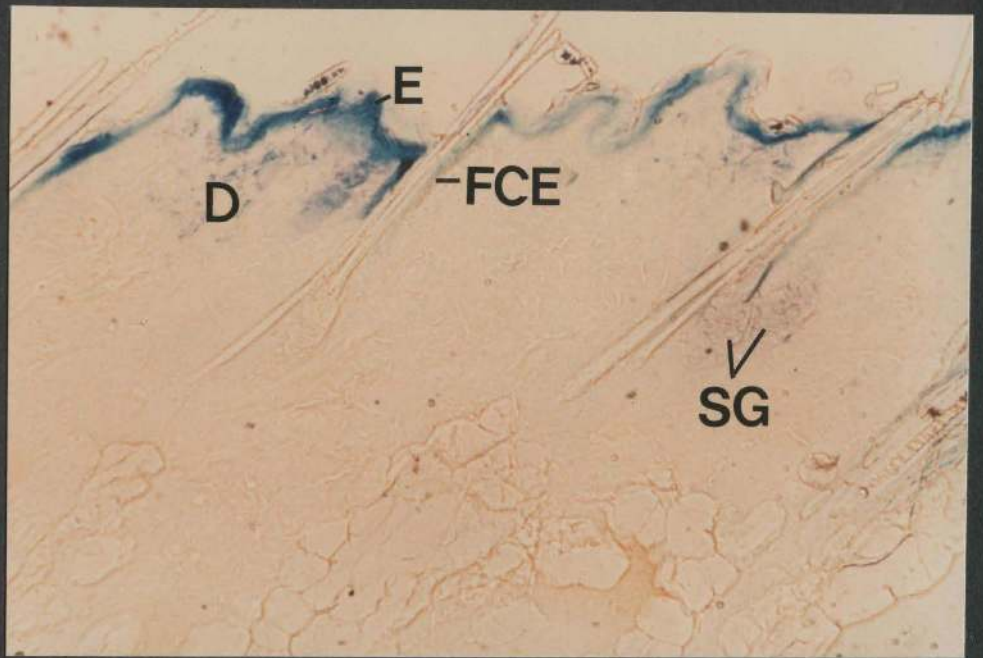
## Figure 6

Positive iontophoresis of a 2% aqueous methylene blue solution at 10 milliamperes for 10 minutes.

A cryostat section (x 40)

This shows that methylene blue has stained the epidermis (E), many sebaceous glands (SG), and hair follicles (HF) approximately down to the level of the bases of the glands. Dermal (D) areas at and above the level of the sebaceous glands and in close relation to the hair follicles are also stained, whereas the colouration is less obvious in dermal regions between the follicles. Occasionally pale segments are present in the epidermis.





## Figures 7a and 7b

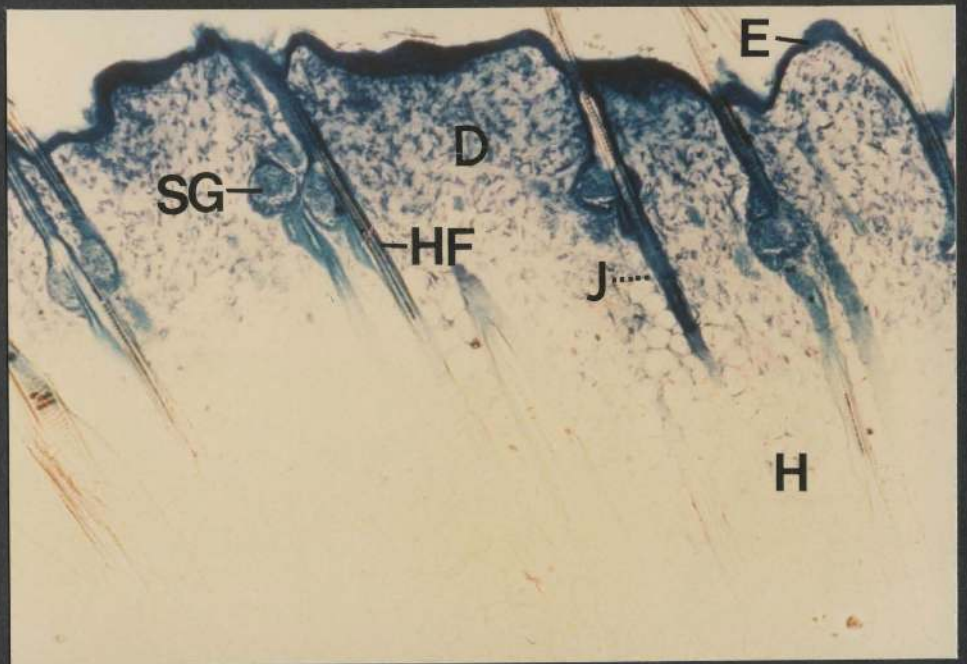
Positive iontophoresis of a 2% aqueous methylene blue solution at 10 milliamperes for 15 minutes

Figure 7a: A cryostat section (x 40)

Methylene blue is visible in the epidermis (E), sebaceous glands (SG), hair follicles (HF) down to a short distance below the level (J) at which the dermis merges with the hypodermis, most of the dermis (D), and in the superficial parts of the hypodermis (H).

Figure 7b: A cryostat section similar to that shown above but also stained with tartrazine (x 40)

The location and distribution of methylene blue is similar to that described in Figure 7a. In addition, this section shows that although the superficial parts of the panniculus adiposus (H) surrounding the hair follicles are stained with methylene blue, the deeper interfollicular regions of the dermis (D) are less intensely stained or remain unstained.





## Figures 8a and 8b

Positive iontophoresis of a 2% aqueous methylene blue solution at 15 milliamperes for 5 minutes

## Figure 8a: A cryostat section (x 16)

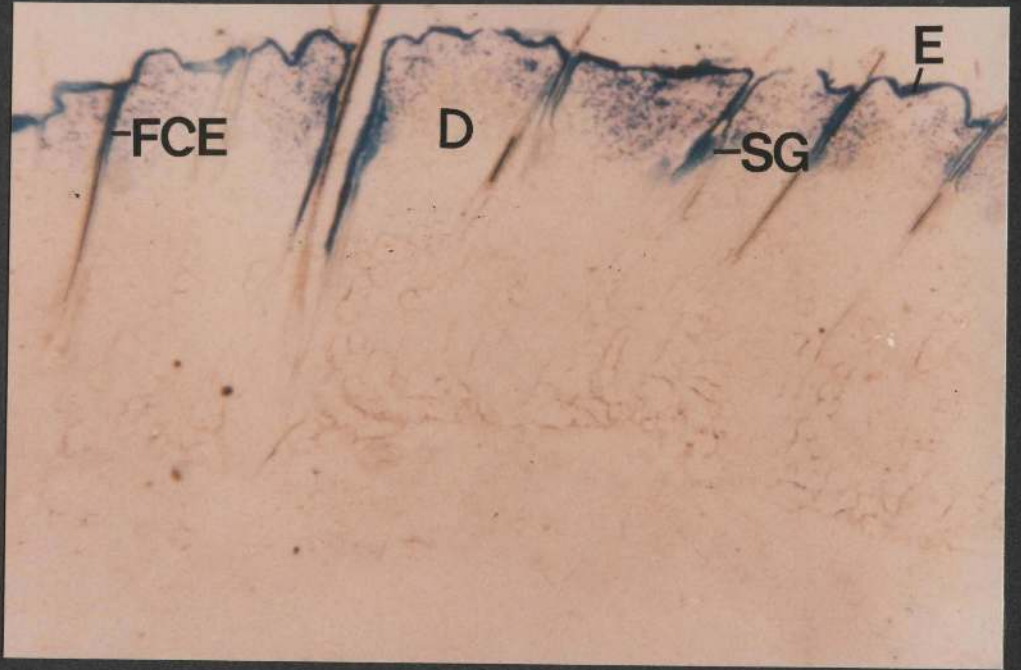
It is apparent that methylene blue has stained the epidermis (E), the follicular canal epidermis (FCE), and the sebaceous glands (SG). Dermal (D) regions just outside the follicular canal epidermis and sebaceous glands are stained intensely, whereas dermal regions located at the same level but between the follicles are less intensely stained.

## Figure 8b: A tartrazine-stained cryostat section (x 40)

In addition to the features described in Figure 8a, this section shows that the staining intensity of the epidermis (E) is not uniform along its surface but is characterized by alternating dark and pale segments of varying extent. Usually the darker segments are those parts of the epidermis surrounding and immediately adjacent to the orifices of the hair follicles. It is also apparent that penetration of dye through the dermis (D) is deeper in areas containing hair follicles.

The location and distribution of methylene blue in this case resemble closely that seen when the same dye solution is introduced at 5 milliamperes for 15 minutes (Figure 4).





## Figures 9a and 9b

Positive iontophoresis of a 2% aqueous methylene blue solution at 15 milliamperes for 10 minutes

Figure 9a: A cryostat section (x 40)

The blue tracer is visible in the epidermis (E), the hair follicles (HF) down to the level (J) at which the dermis merges with the hypodermis, the sebaceous glands (SG), and most of the dermis (D). Frequently, penetration of the dye extends into the most superficial regions of the hypodermis (H) immediately adjacent to the hair follicles.

Figure 9b: A cryostat section similar to that shown above but stained additionally with tartrazine to show the extent of the dermis and the hypodermis (x 40)

The location and distribution of methylene blue is similar to that in Figure 9a. In addition, this section shows that although the superficial regions of the hypodermis (H) surrounding the hair follicles are stained, the deeper interfollicular regions of the dermis (D) which interface with the superficial areas of the hypodermis are devoid of methylene blue.

The extent of the penetration of the blue cationic dye shown above is similar to that seen when the same dye solution is introduced iontophoretically at 10 milliamperes for 15 minutes (Figure 7).

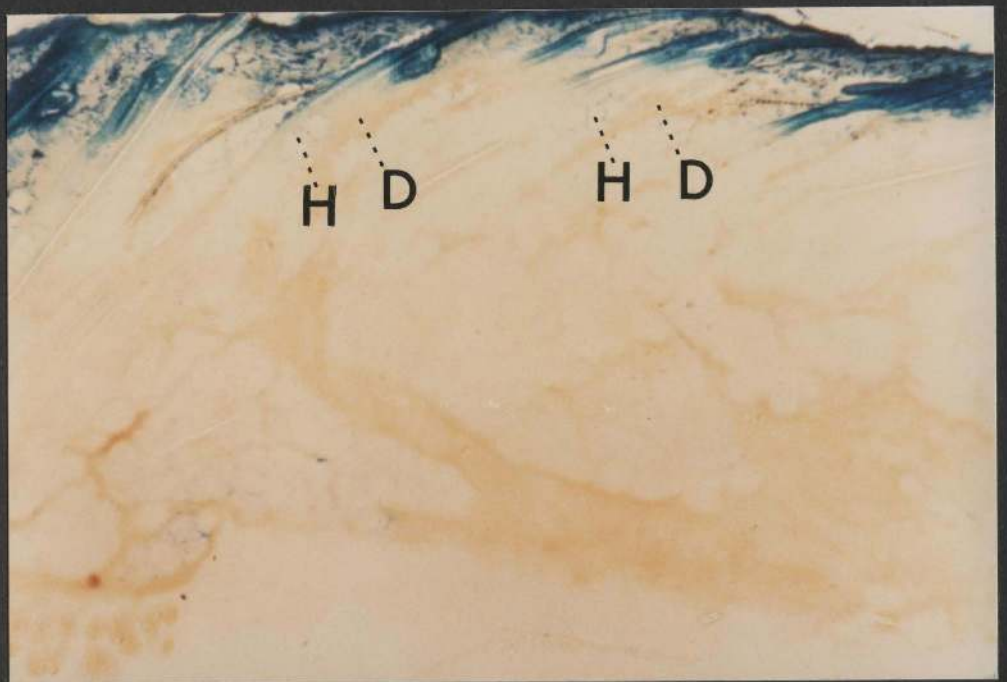
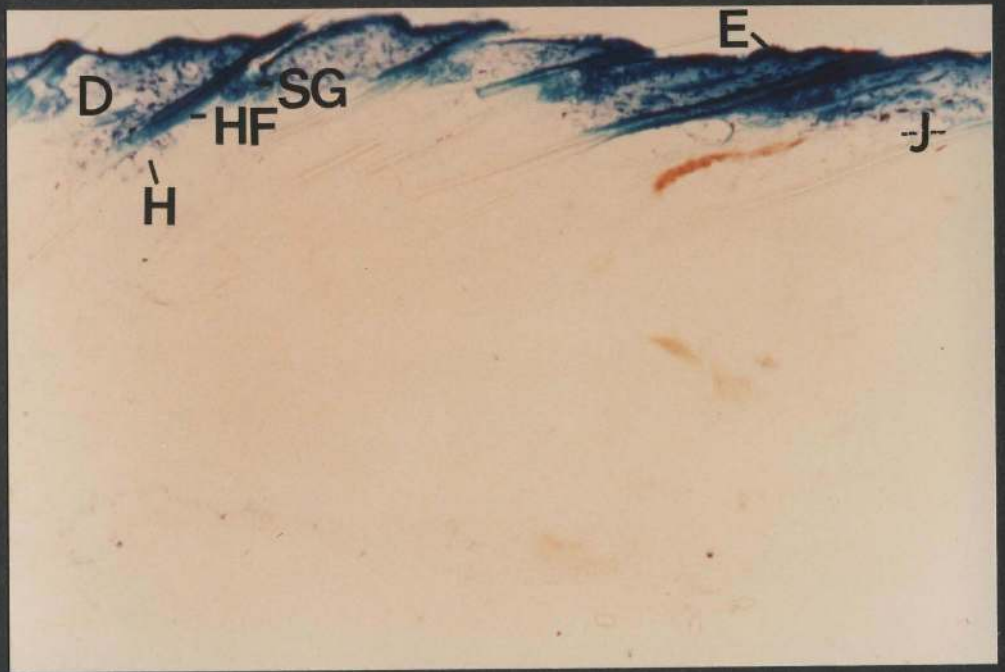


## Figure 10

Positive iontophoresis of a 2% aqueous methylene blue solution at 15 milliamperes for 15 minutes

A cryostat section (x 40)

The dye has stained the epidermis (E), the hair follicles (HF) down to a short distance below the level (J) at which the dermis interlaces with the hypodermis, sebaceous glands (SG), the dermis (D), and the most superficial part of the hypodermis (H). The panniculus adiposus adjacent to the deeper parts of the follicular walls does not contain methylene blue.



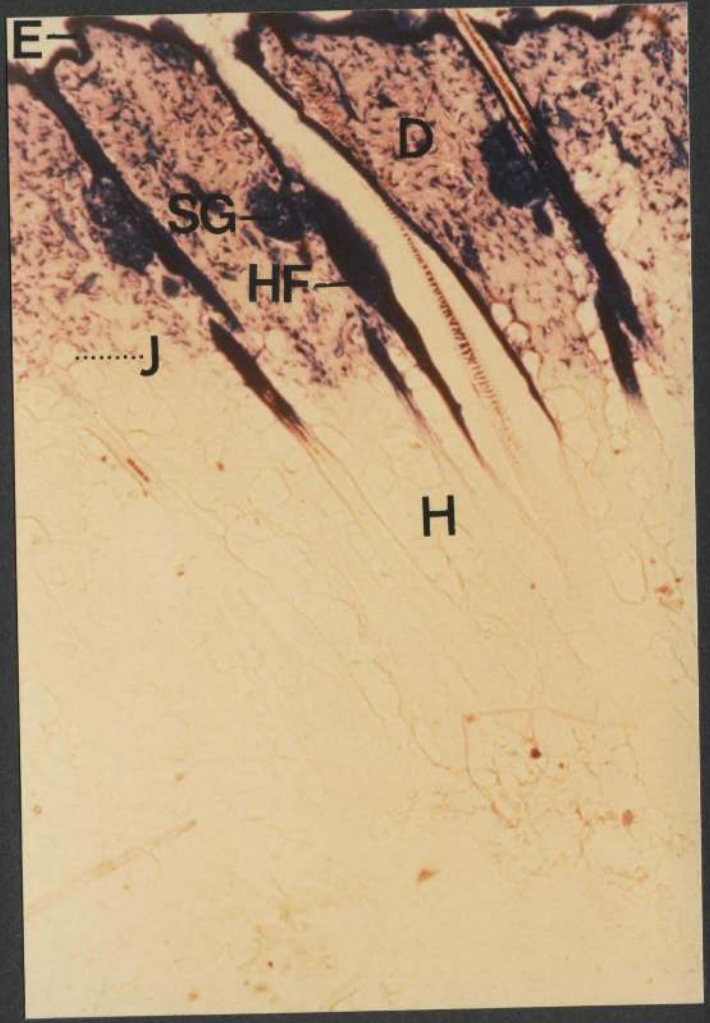


## Figure 11

Positive iontophoresis of a 2% aqueous methylene blue solution at 20 milliamperes for 5 minutes

A cryostat section (x 40)

Methylene blue is seen in the sebaceous glands (SG) and the hair follicles (HF) down to the level of the bases of the glands. The dermis (D) is stained adjacent to the upper parts of the hair follicles, in contrast to interfollicular areas of the dermis which remain relatively unstained. The intensity of staining of the surface epidermis (E) is not uniform but characterized by alternating dark and pale segments of varying sizes. The dark segments often included hair follicles. The location and distribution of the dye in this case resemble closely that seen when the same dye solution is introduced at 10 milliamperes for 10 minutes (Figure 6).

## Figure 12

Positive iontophoresis of a 2% aqueous methylene blue solution at 20 milliamperes for 10 minutes

A cryostat section (x 40)

Methylene blue has stained the epidermis (E), the hair follicles (HF) down to the level (J) between the dermis and the hypodermis, sebaceous glands (SG), the dermis (D) and the superficial part of the hypodermis (H).

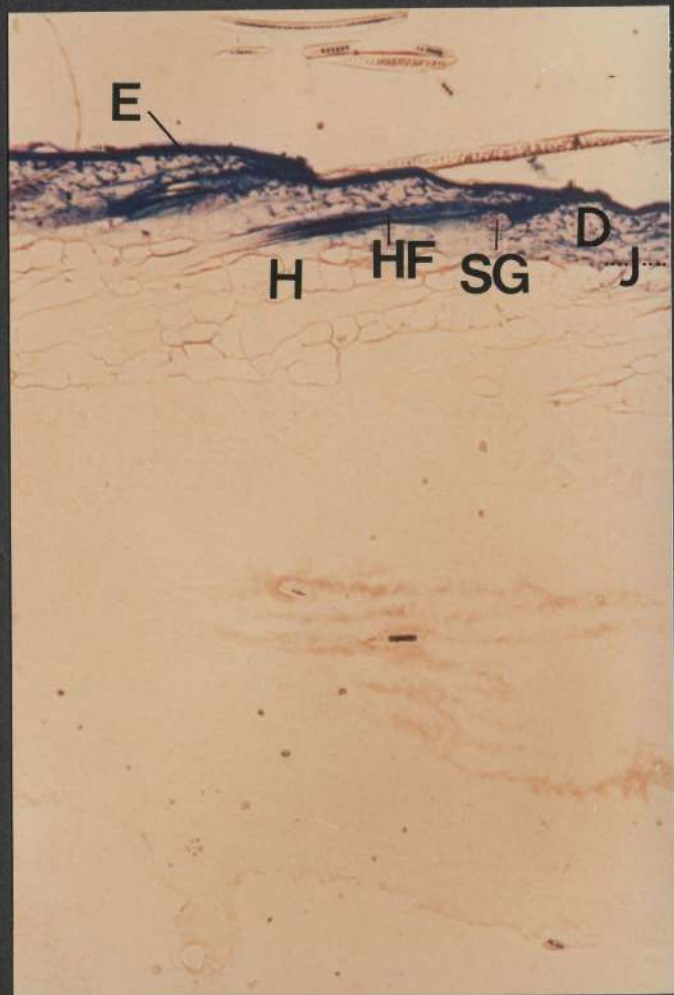
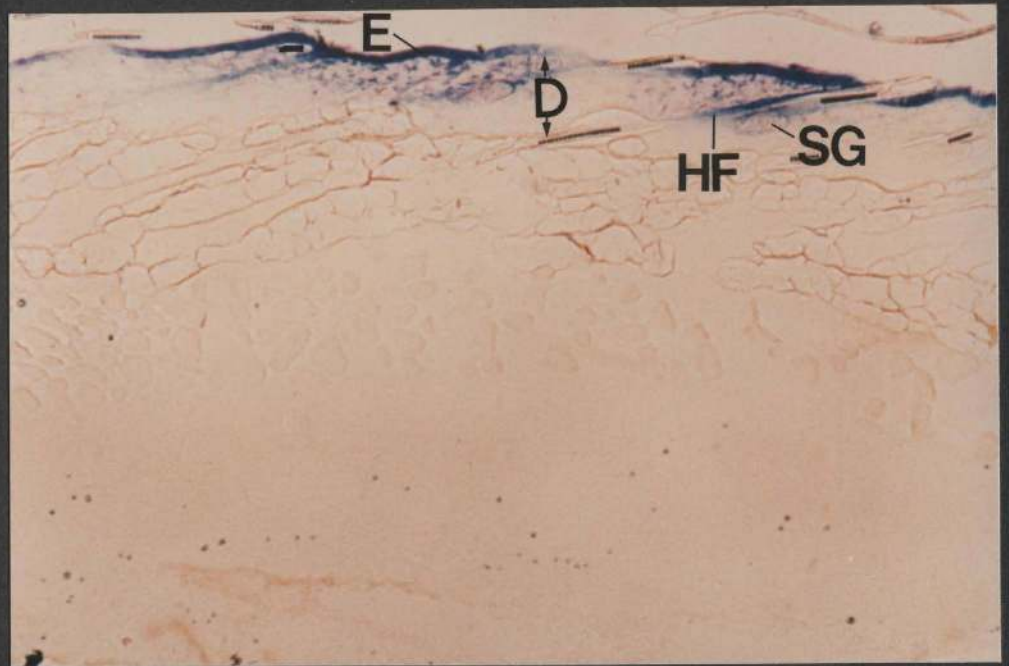


## Figure 13

Positive iontophoresis of a 2% aqueous methylene blue solution at 20 milliamperes for 15 minutes

A cryostat section (x 40)

Methylene blue is visible in the epidermis (E), the sebaceous glands (SG), the dermis (D), and in the superficial part of the hypodermis (H). In addition, a great majority of the hair follicles (HF) showed uptake of the dye down to a short distance above the follicular bulb (B), although occasionally some bulbs were only lightly tinted. (J) represents the approximate level at which the dermis merges with the hypodermis.



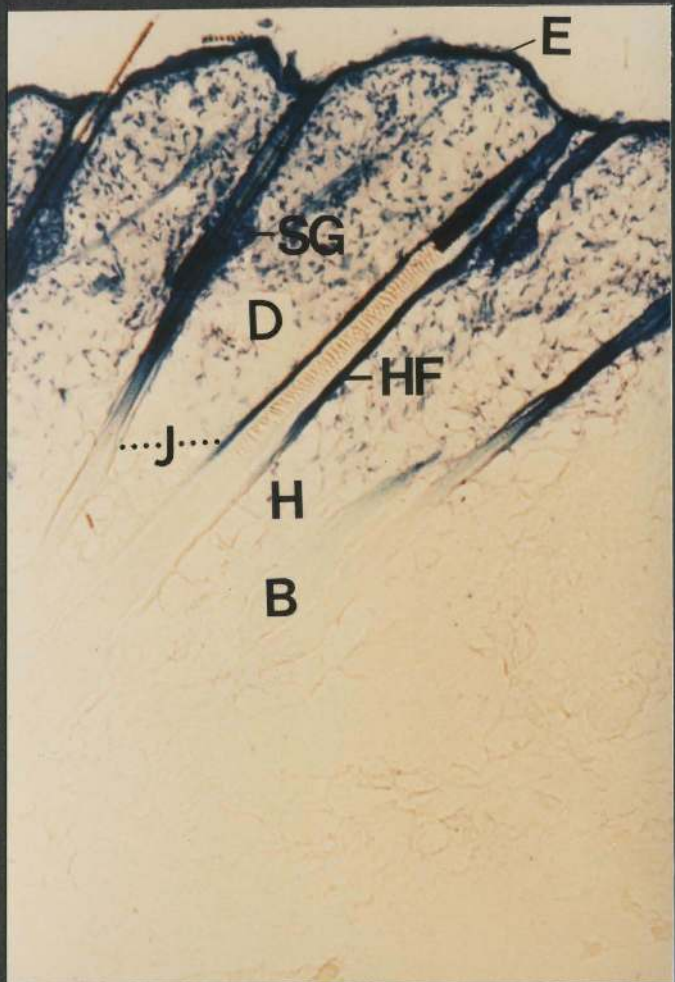


## Figure 14

Positive iontophoresis of a 2% aqueous methylene blue solution at 25 milliamperes for 5 minutes

A cryostat section (x 40)

This shows that methylene blue has stained the epidermis (E), the sebaceous glands (SG), the hair follicles (HF) down to or slightly below the level of the bases of the sebaceous glands, and the dermal areas surrounding the follicular canal epidermis. (D) represents the extent of the whole dermis. Furthermore, the dermal areas adjacent to the sebaceous glands are also stained, whereas the areas present at the same level but situated between the glands are preponderantly less intensely stained or remain unstained.

## Figure 15

Positive iontophoresis of a 2% aqueous methylene blue solution at 25 milliamperes for 10 minutes

A cryostat section (x 40)

The methylene blue has stained the epidermis (E), the hair follicles (HF) to a point just below the level (J) where the dermis merges with the hypodermis, the sebaceous glands (SG), the dermis (D) and the most superficial part of the hypodermis (H). It appears therefore, that the dye has penetrated along the hair follicles to a slightly deeper level than that seen in the hypodermis.



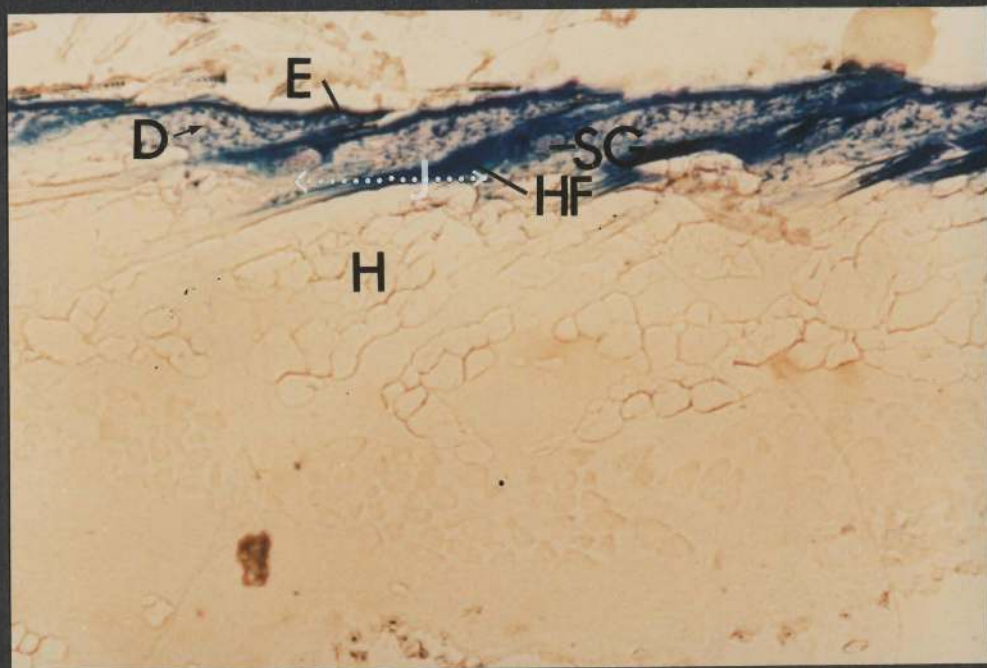
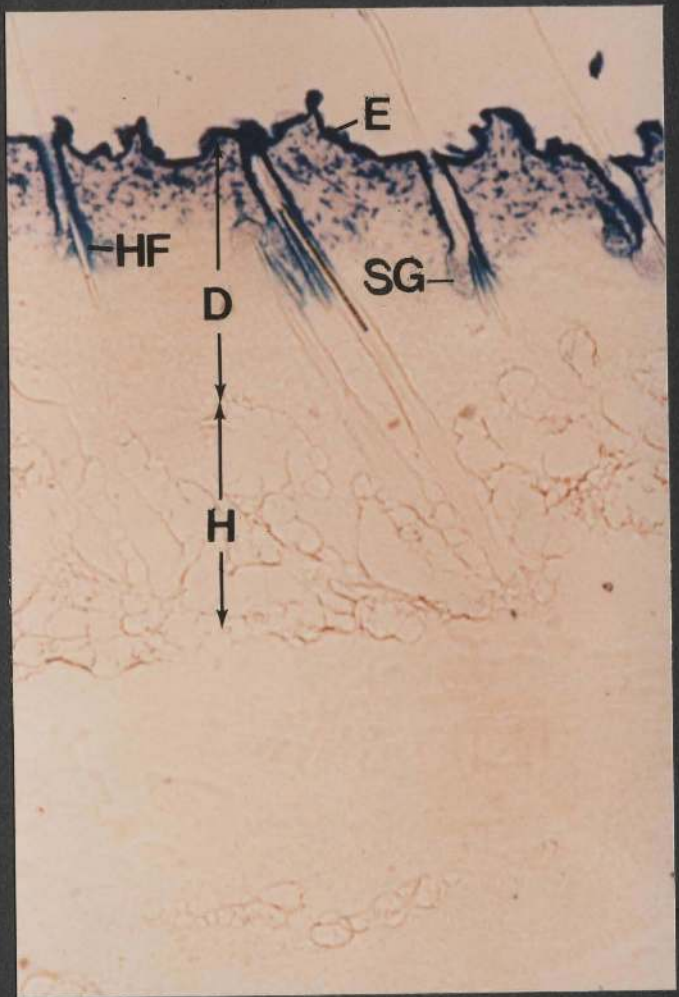
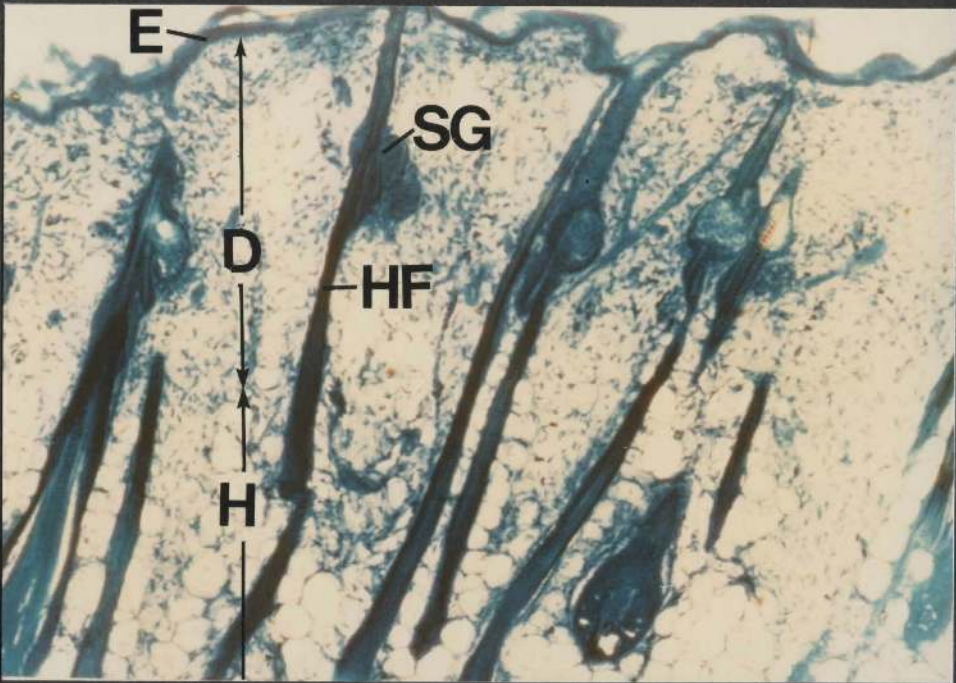


Figure 16

Positive iontophoresis of a 2% aqueous methylene blue solution at 25 milliamperes for 15 minutes

A cryostat section (x 40)

The penetration of methylene blue through the skin and the subcutaneous tissue is complete, that is, the dye has stained the epidermis (E), the hair follicles (HF), the sebaceous glands (SG), the dermis (D), and the hypodermis (H).





## Figure 17

Positive iontophoresis of a 2% aqueous methylene blue solution at 30 milliamperes for 5 minutes

A cryostat section (x 40)

The dye is visible in the epidermis (E), the hair follicles (HF) down to the level between the dermis and the hypodermis, the sebaceous glands (SG), and in most of the dermis (D). The extent of the penetration is similar in this case to that obtained when the dye solution is introduced using a current of 10 milliamperes for a period of 15 minutes (Figures 7a and 7b), or a current of 15 milliamperes over a period of 10 minutes (Figures 9a and 9b).

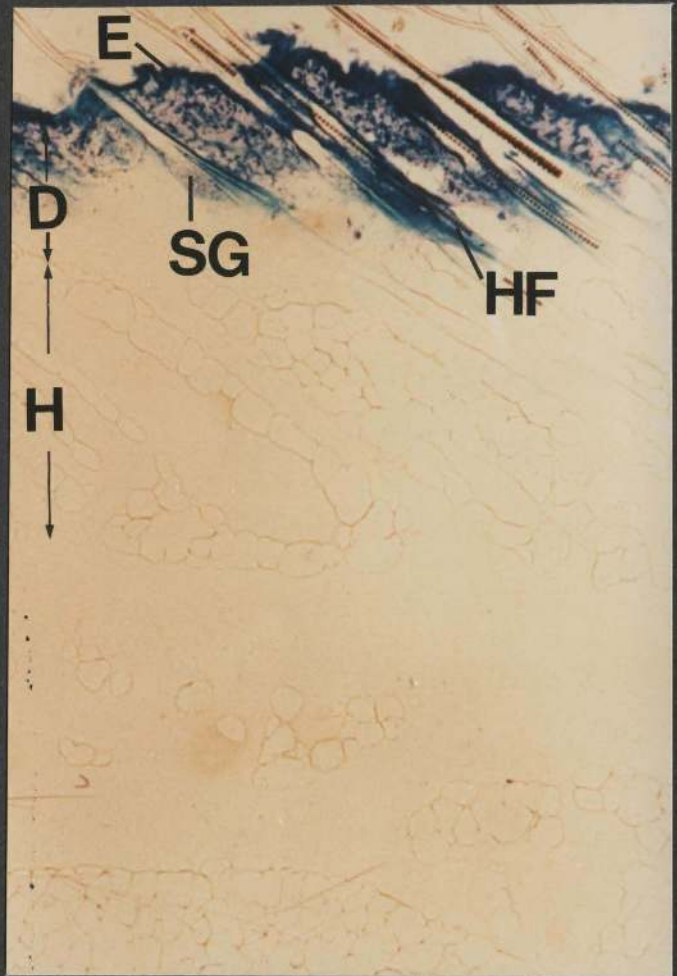


## Figure 18

Positive iontophoresis of a 2% aqueous methylene blue solution at 30 milliamperes for 10 minutes

A cryostat section (x 40)

It is apparent that methylene blue has stained the epidermis (E), the sebaceous glands (SG), the dermis (D), and the superficial parts of the hypodermis (H). The penetration of the dye is complete in hair follicles (HF) whose bulbs are embedded in the upper parts of the hypodermis, whereas follicular bulbs (HB) embedded in deeper areas of the hypodermis are not stained. The location and distribution of the dye is similar in this case to that seen when the same dye solution is introduced at 20 milliamperes for 15 minutes (Figure 13).

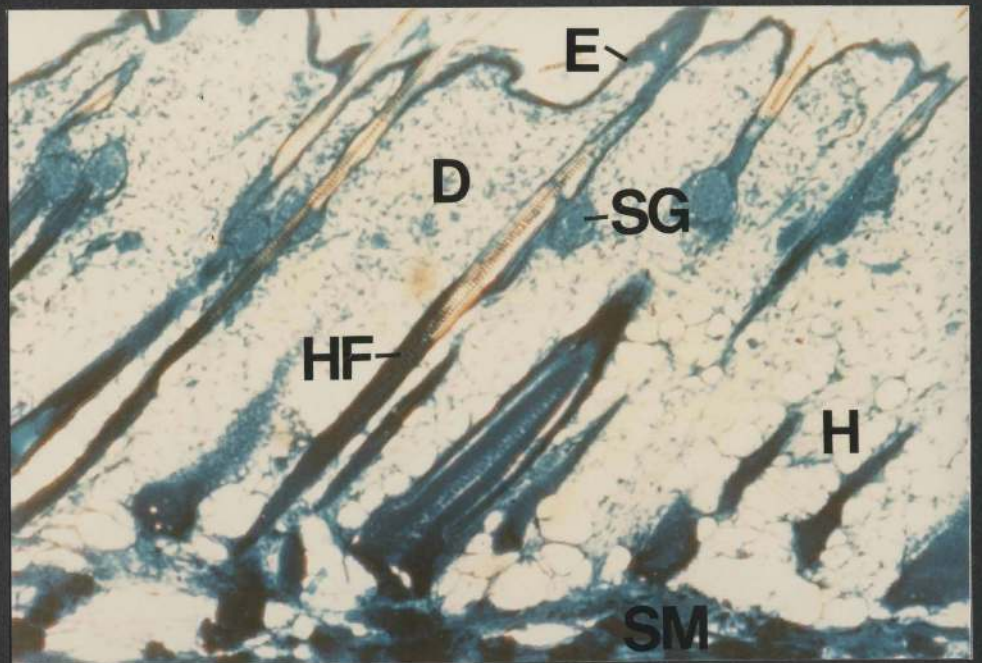
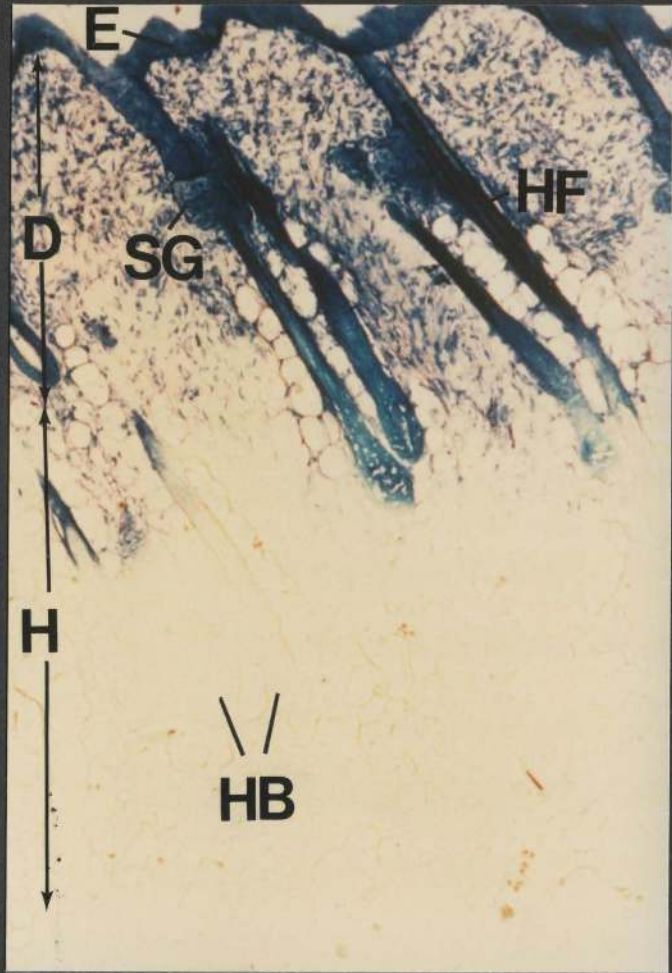
## Figure 19

Positive iontophoresis of a 2% aqueous methylene blue solution at 30 milliamperes for 15 minutes

A cryostat section (x 40)

At this current intensity and duration of application, methylene blue has penetrated the skin completely, staining the epidermis (E), the hair follicles (HF), the sebaceous glands (SG), and the dermis (D). Furthermore, having penetrated beneath the skin, methylene blue has also stained the panniculus adiposus (H) and the underlying striated muscle (SM). There is a uniform distribution of colour throughout the section.

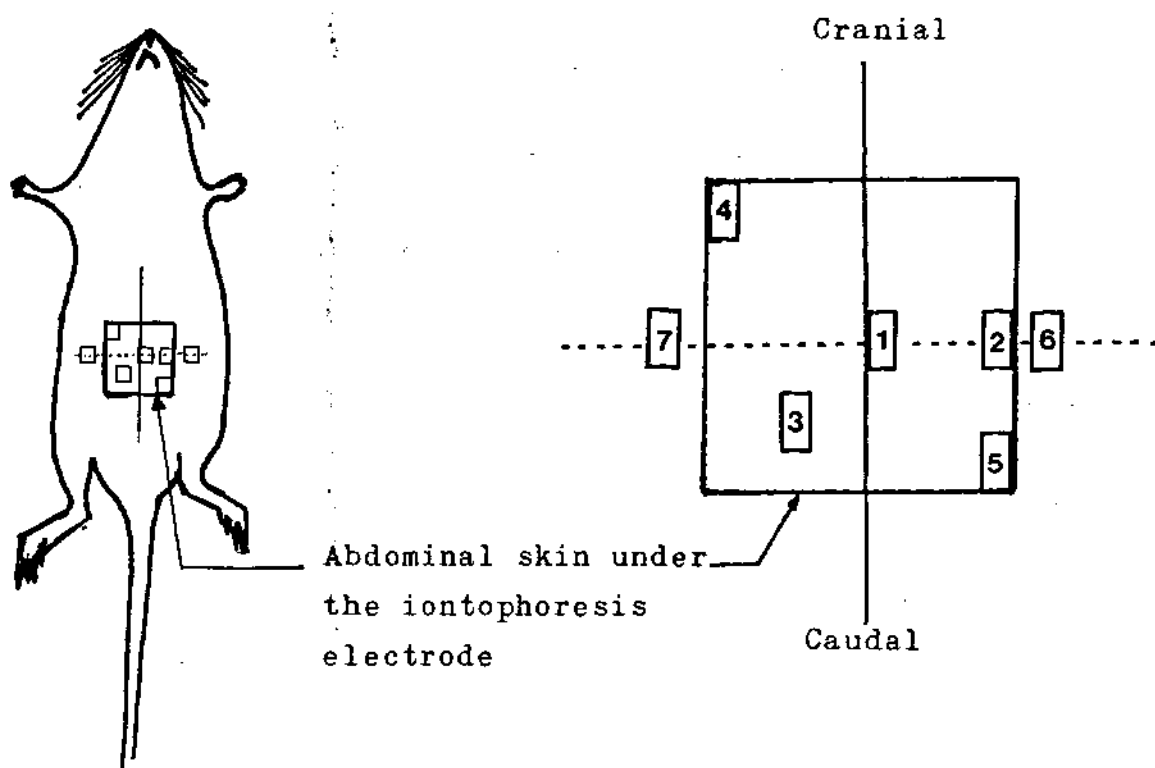




### 3.1.1.2 Regional variations

In order to evaluate the extent of penetration of methylene blue into and through the treated area, specimens were selected from the centre, the edges and the corners of the area under the iontophoresis electrode. Figures 20 to 24 are sections taken from such sites. For comparison, additional specimens were selected from areas just outside the treated skin (Figure 25). These are indicated in the diagram below.

Diagram 3.1 Sites of the selected specimens



## Figures 20 - 24

Positive iontophoresis of a 2% aqueous methylene blue solution at 25 milliamperes for 10 minutes

## Figure 20

A cryostat section of abdominal skin just to the right of the midline and at the centre of the treated area, that is, area 1 in diagram 3.1 (x 40)

Methylene blue has stained the epidermis (E), the sebaceous glands (SG), the dermis (D), the superficial part of the hypodermis (H), and the hair follicles (HF) down to a short distance below the level (J) at which the dermis interlaces with the hypodermis.

## Figure 21

A cryostat section of a specimen selected near to the edge of the treated area and lateral to that shown in Figure 20, that is, area 2 in diagram 3.1 (x 40)

The location and distribution of methylene blue in the epidermis (E), hair follicles (HF), sebaceous glands (SG), the dermis (D), and the hypodermis (H) are similar to those described in Figure 20.



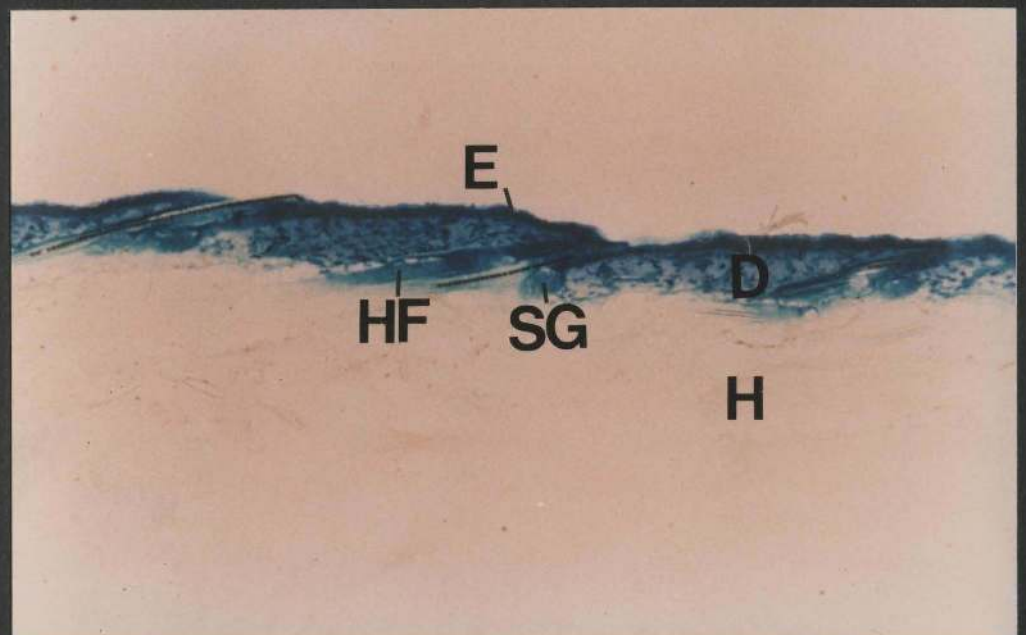
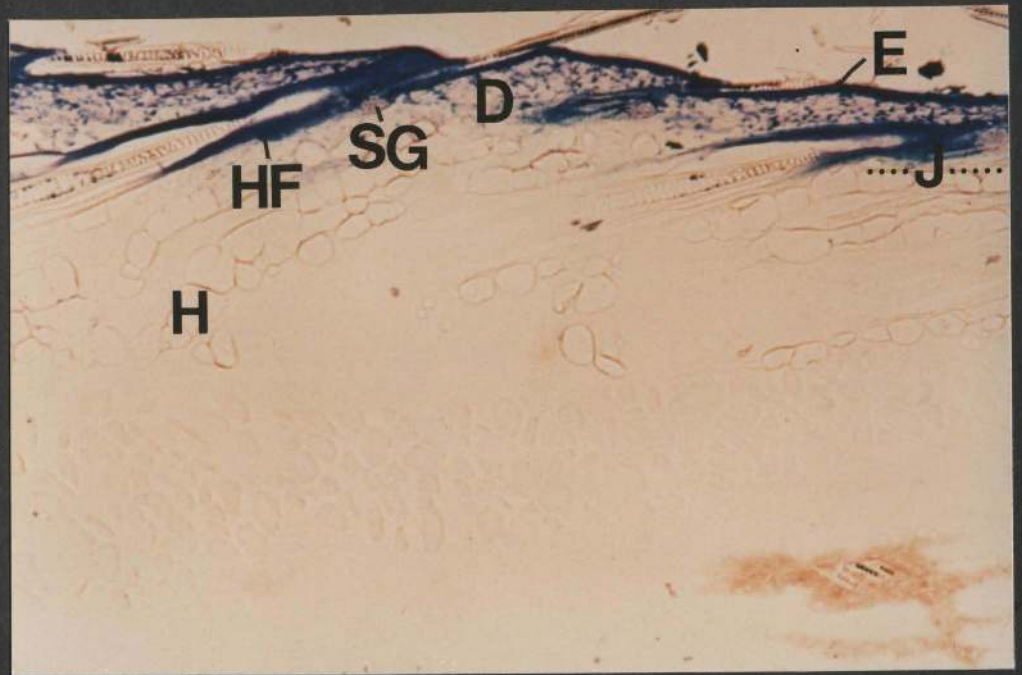


## Figure 22

A cryostat section from the centre of the lower left quadrant of the treated area, that is, area 3 in diagram 3.1 (x 40). The extent of penetration of methylene blue through the epidermis (E), the hair follicles (HF), the sebaceous glands (SG), the dermis (D) and the hypodermis (H) is similar in this case to that described in Figure 20.

## Figure 23

A cryostat section from the corner of the treated area lying cranially and to the left of the midline (area 4 in diagram 3.1) (x 40). The location and distribution of methylene blue in the epidermis (E), the hair follicles (HF), the sebaceous glands (SG), the dermis (D) and the hypodermis (H) are similar once again to those described in Figure 20.

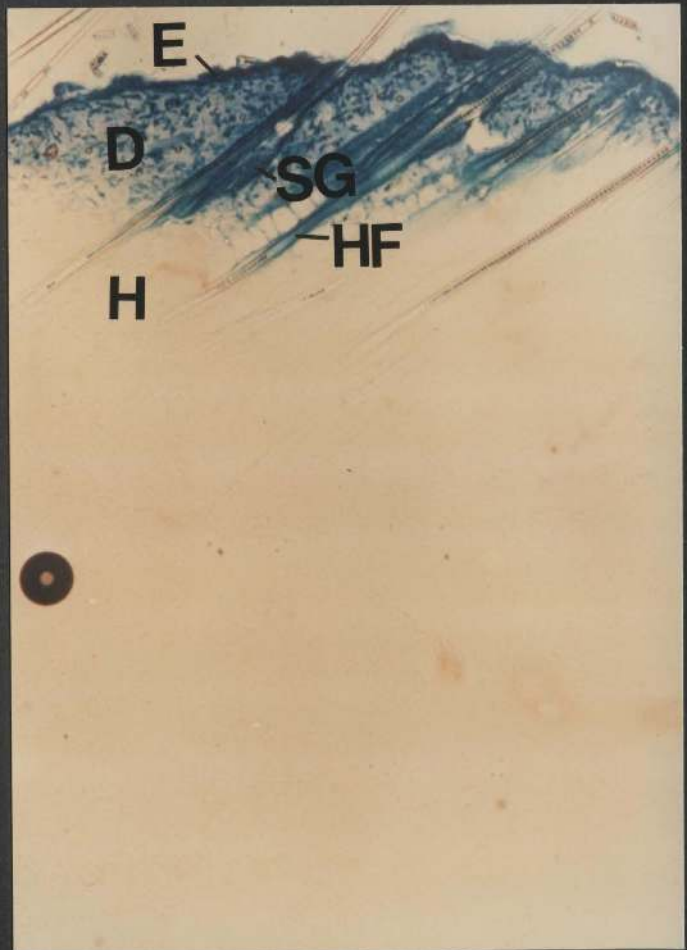
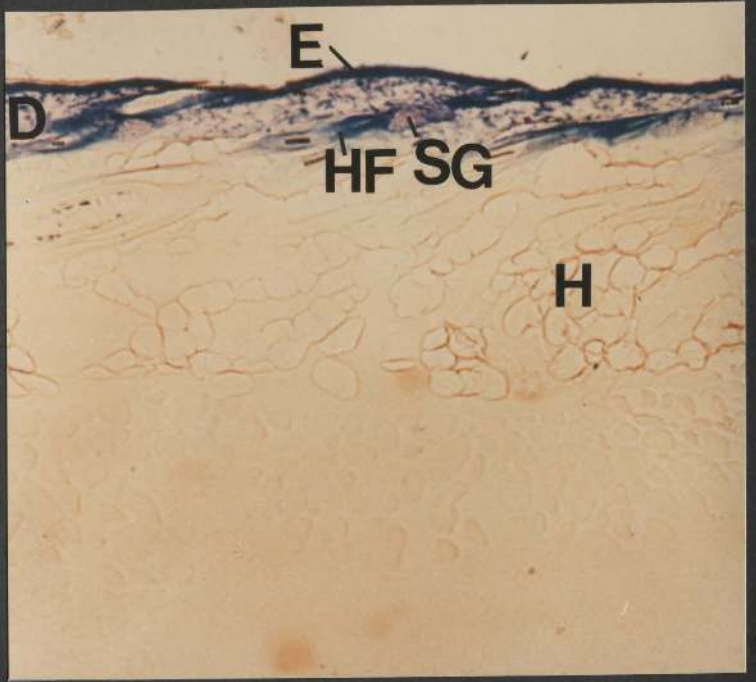


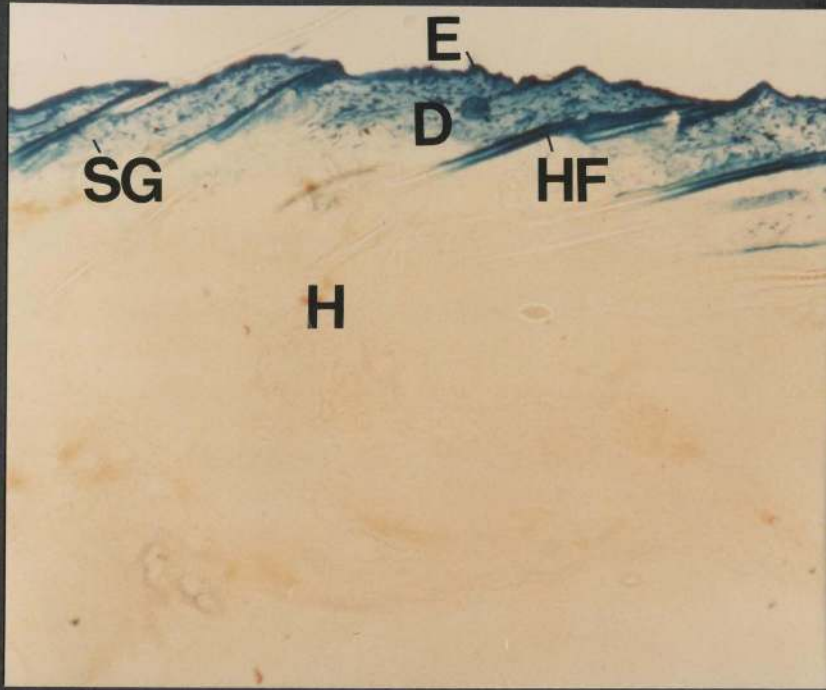
## Figure 24

A cryostat section from the corner of the treated area lying diagonally opposite to that shown in Figure 23, that is, area 5 in diagram 3.1 (x 40)

The location and distribution of the dye in the epidermis (E), the hair follicles (HF), the sebaceous glands (SG), the dermis (D) and the hypodermis (H) are similar once again to those described in Figure 20.

From Figures 20 to 24 it appears that the penetration of methylene blue is as deep and intense at the edges and corners of the treated area as it is in the centre.







## Figures 25a and 25b

These sections are taken from skin situated just outside the area under the iontophoresis electrode (areas 6 and 7 in diagram 3.1).

## Figure 25a: A cryostat section (x 40)

The penetration of methylene blue into such skin is minimal. The dye is visible in the superficial part of the skin only, especially in those areas surrounding the orifices of the hair follicles (HF), but it does not extend any deeper into the follicles or into the sebaceous glands (SG). In addition, this section shows the dermis (D) and the hypodermis (H), both of which are not stained.

## Figure 25b: A similar cryostat section to that shown above stained with haematoxylin and eosin (x 100)

It is apparent that methylene blue, which has persisted and is visible, in this section, is confined to the surface of the epidermis (E).

The results shown in Figures 25a and 25b are very similar to those shown in Figures 1a to 1d.



### 3.1.1.3 Effect of reversing the current

The following experiments were undertaken to investigate the effect of alternating the current, by reversing the polarity of the electrodes at regular intervals, on the penetration of a 2% aqueous methylene blue solution into the skin. The results are presented in Figures 26 and 27.

(A) In this set of experiments, the methylene blue solution was introduced by positive iontophoresis at 15 mA for 5 minutes. The apparatus was switched off and the polarity was reversed. The dye solution was then subjected to negative iontophoresis also at 15 mA for 5 minutes. This was followed by a second positive iontophoresis and finally a second negative iontophoresis using a current intensity of 15 mA over a duration of 5 minutes in both.

#### Figure 26

A cryostat section (x 40)

Methylene blue is visible in the epidermis (E), sebaceous glands (SG), hair follicles (HF) down to the level where the dermis (D) and the hypodermis (H) merge with each other, and in most of the dermis.

There is no significant difference between the extent of penetration of the dye solution in this case and that seen when the same dye solution is subjected to continuous positive iontophoresis using a current of 10 mA for 15 minutes (Figure 7) or using a current of 15 mA for 10 minutes (Figure 9).



(B) In this set of experiments a 2% aqueous methylene blue solution was applied to the surface of the skin with positive iontophoresis using a current intensity of 15 mA for 5 minutes, followed by negative iontophoresis with the same current intensity and duration of application.

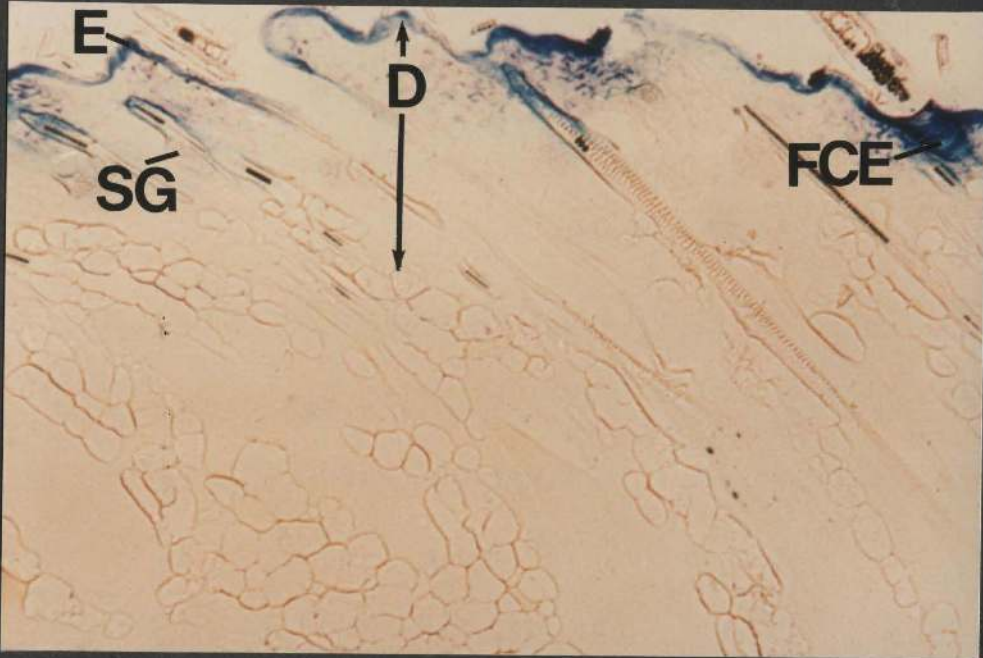
#### Figure 27

A cryostat section (x 40)

The cationic blue tracer is visible in the epidermis (E), follicular canal epidermis (FCE), and in some sebaceous glands (SG). Dermal (D) regions adjacent to the follicular canal epidermis are also stained, whereas interfollicular regions of the dermis at the same level remain relatively unstained.

It appears that, the location and distribution of methylene blue in this case are similar to those seen when the same dye solution is applied to the skin surface with continuous positive iontophoresis using a current of 15 mA for 5 minutes (Figure 8) or using a current of 5 mA for 15 minutes (Figure 4).





#### 3.1.1.4 Effect of negative iontophoresis

This group of experiments was carried out to investigate the efficacy of negative iontophoresis in facilitating the penetration of methylene blue into the skin.

Figures 28a and 28b show the results of negative iontophoresis of a 2% aqueous methylene blue solution at 30 milliamperes for 15 minutes.

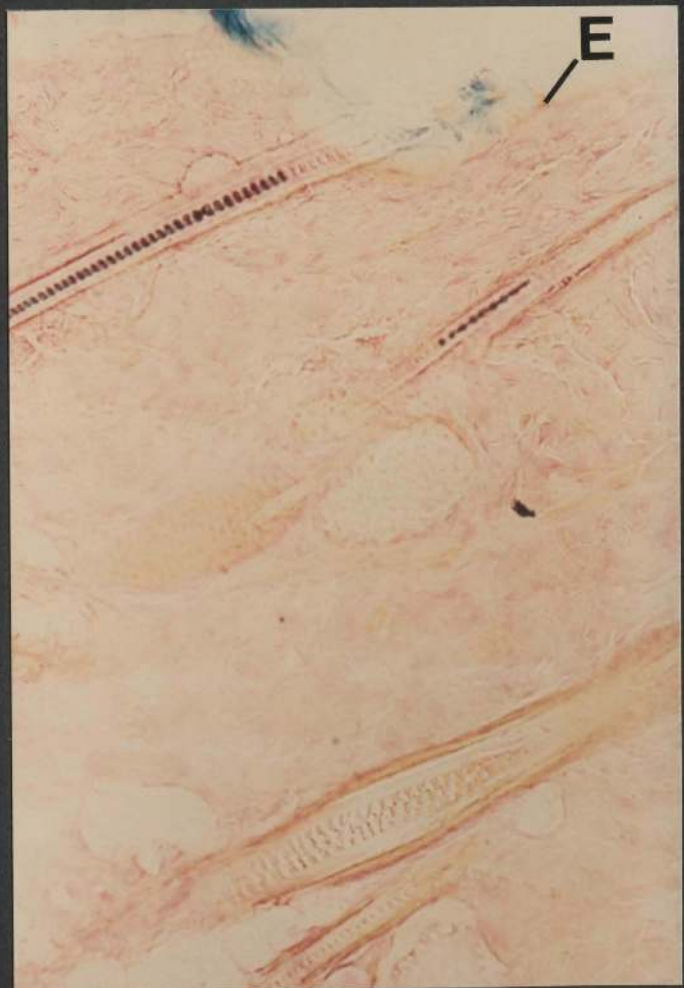
Figure 28a: A cryostat section (x 32)

The penetration of methylene blue through the skin is negligible. The dye is visible in the superficial part of the skin, but does not extend deeper into the hair follicles (HF), sebaceous glands (SG), the dermis (D) or the hypodermis (H).

Figure 28b: A cryostat section stained with haematoxylin and eosin (x 80)

It is apparent that the tracer is confined mainly to the surface of the epidermis (E), including the surface squames.

The results shown above do not differ significantly from those seen when the dye solution is applied to the surface of the skin for a duration of 15 minutes without the flow of a current (Figures 1a-1d).

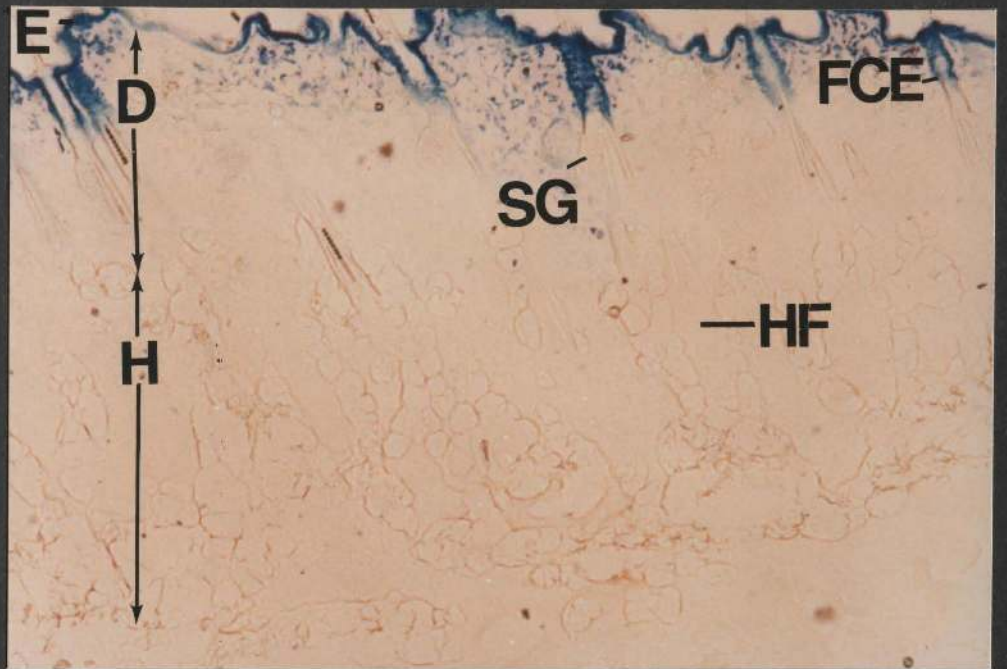




### 3.1.1.5 Effect of absorbent pad thickness

The following experiments were carried out to investigate the effect of increasing the thickness of the absorbent pad of the iontophoresis electrode on the penetration of methylene blue into the skin. Instead of the standard dressing (3 mm thick, p68), the iontophoresis electrode was covered by a thick pad of cotton wool sheathed in cotton gauze (12 mm thick).

Figure 29 is a cryostat section (x 40) and illustrates the result of positive iontophoresis of a 2% aqueous methylene blue solution at 30 milliamperes for 15 minutes. It is apparent that some parts of the epidermis (E) are stained intensely whereas other parts are less intensely stained. Only a few sebaceous glands (SG) are stained. Although the follicular canal epidermis (FCE) is stained, the dye does not extend deeper into the hair follicles (HF). The penetration is deep in some dermal areas (D), whereas in other dermal areas the penetration is minimal. The subcutaneous tissue (H) is devoid of the stain. Consequently the penetration of the tracer into and through the skin is irregular. It is clear therefore, that when applied to the skin using the same current intensity and duration of treatment, the extent of the penetration of methylene blue into the skin is significantly reduced by thickening the absorbent pad of the iontophoresis electrode, when compared to that obtained with the standard dressing (Figure 19).



### 3.1.1.6 Condition of iontophoresis electrode

The following experiment was undertaken to investigate the effect of the condition of the iontophoresis electrode in the penetration of methylene blue into the skin.

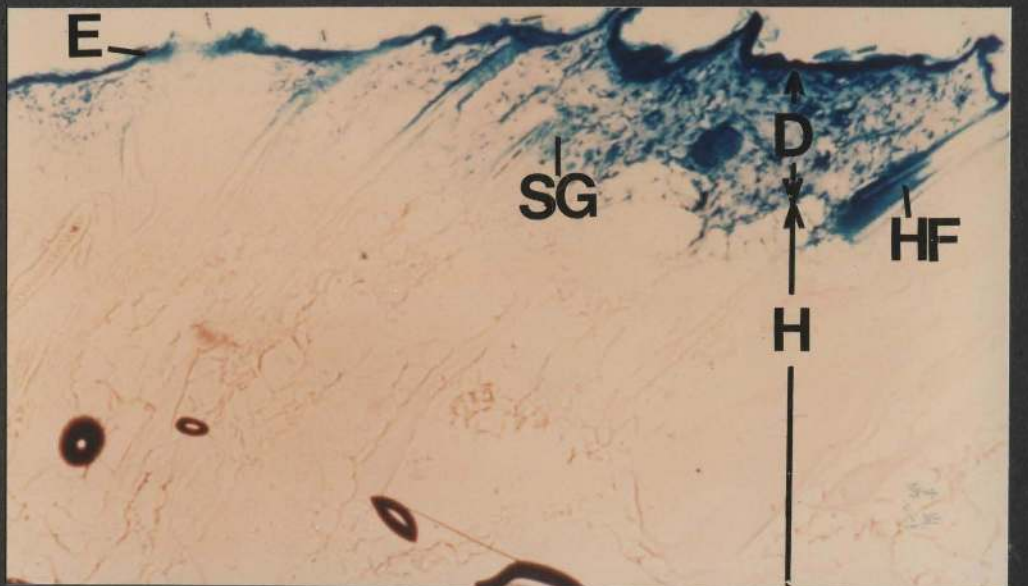
Figure 30a: In this photograph, the iontophoresis electrode was allowed to dry without cleaning and polishing after a number of iontophoresis experiments. It should be compared with the appearance shown after cleaning (Figure 2.4b, page 67).

A clean standard dressing was applied onto a contaminated iontophoresis electrode. Positive iontophoresis of a 2% aqueous methylene blue solution was carried out using a current intensity of 30 mA for 15 minutes.

Figure 30b: A cryostat section stained with 1% aqueous eosin for approximately 2 seconds (x 40)

In the right half of the field, methylene blue is visible in the epidermis (E), the full extent of the dermis (D), the superficial parts of the hypodermis (H), and in the hair follicles (HF) down to the level between the dermis and the hypodermis. In the left half of the field, however, the blue dye is visible only in the epidermis, sebaceous glands (SG), hair follicles down to a short distance below the level of these glands, and in the dermal regions surrounding the upper parts of the follicles.

By using a contaminated electrode, it becomes apparent that the penetration of methylene blue into and through the skin is not uniform, and that the extent of penetration is significantly reduced when compared to that obtained with a clean electrode (Figure 19).



### 3.1.1.7 Effect of concentration of dye

The following experiments were designed to investigate the effect of changing the concentration of the dye on its penetration into the skin. Methylene blue was prepared in distilled water to a concentration of 1% and 3%. These solutions were applied locally (controls) or introduced by positive iontophoresis according to the following Table :-

% concentration	Current (milliamperes)	Duration (minutes)	Figure
1	0	15	31 (a and b)
	10	10	32
	15	15	33 (a and b)
	30	15	34
3	0	15	35
	10	10	36
	15	15	37
	30	15	38

## Figure 31a and 31b

Local application (control) of a 1% aqueous methylene blue solution for 15 minutes.

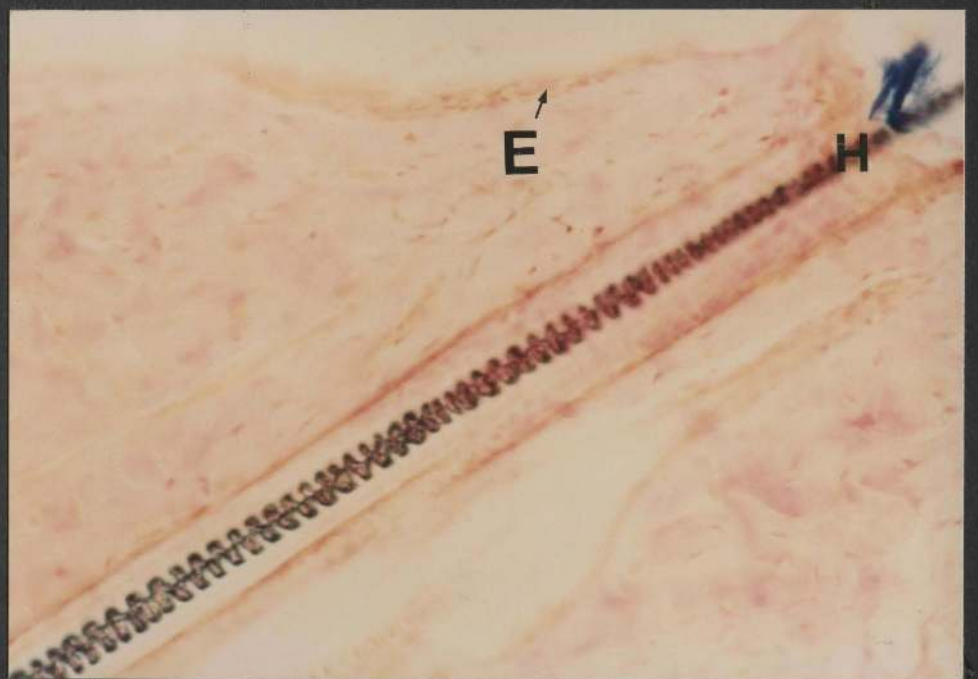
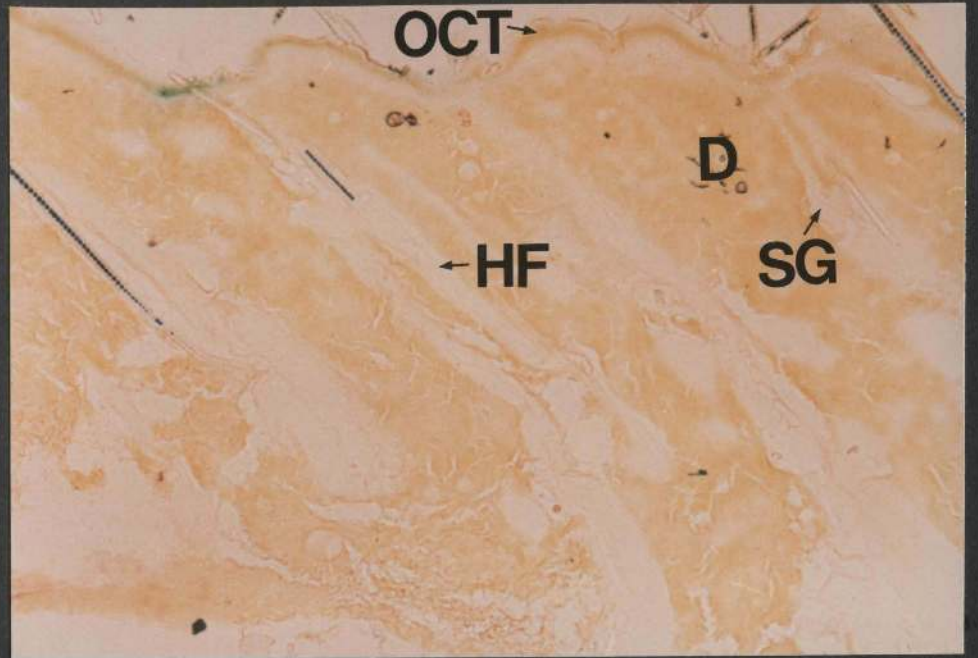
Figure 31a: A cryostat section stained with tartrazine (x 40) Although the upper parts of the ostia of the hair follicles (HF) are stained with methylene blue, the tracer does not extend any deeper into the follicles nor into the sebaceous glands (SG). There is a continuous unstained zone lying between the remnant of the embedding medium (OCT compound) and the superficial part of the dermis (D), both of which are stained with tartrazine.

Figure 31b: A cryostat section stained with haematoxylin and eosin (x 120)

The blue tracer forms a coating around the hair shaft (H) just above the surface of the skin. By comparison, it appears that the colour-free zone seen in Figure 31a consists largely of the epidermis (E).

The results shown in Figures 31a and 31b are very similar to those seen when a 2% solution of the dye is applied locally in the same vehicle and for the same duration of time (Figures 1a - 1d).





## Figure 32

Positive iontophoresis of a 1% aqueous methylene blue solution at 10 milliamperes for 10 minutes.

A cryostat section (x 40)

Methylene blue is visible in the epidermis (E), many sebaceous glands (SG), and in the hair follicles (HF) down to or slightly above the level of the sebaceous glands. Dermal areas (D) at and above the sebaceous glands and in close relationship to the hair follicles are also stained with methylene blue, whereas the colouration is less obvious in dermal areas between the follicles.



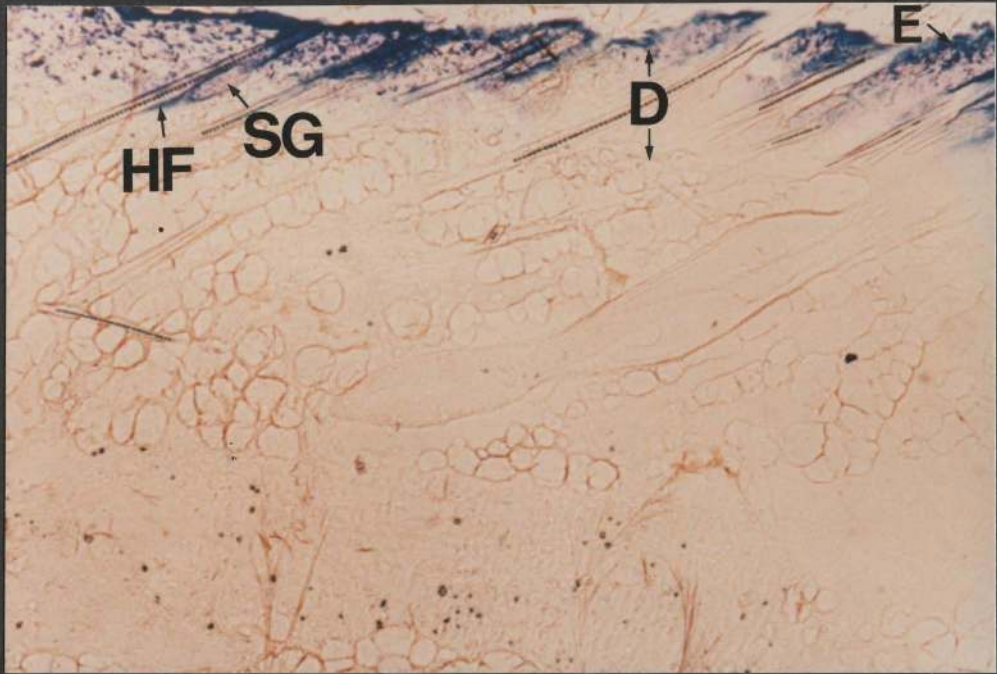


## Figure 33a and 33b

Positive iontophoresis of a 1% aqueous methylene blue solution at 15 milliamperes for 15 minutes

Figure 33a: A cryostat section (x 80)

Methylene blue is visible in the epidermis (E), the sebaceous glands (SG), most of the dermis (D), and in the hair follicles down to a short distance below the level at which the dermis merges with the hypodermis (H). Frequently, penetration of the dye extends into the superficial regions of the hypodermis immediately adjacent to the hair follicles.

Figure 33b: A cryostat section similar to that shown above but stained with tartrazine to show the extent of the dermis and the hypodermis (x 80)

The location and distribution of methylene blue is similar to that in Figure 33a. In addition, this section shows that although the superficial areas of the hypodermis (H) surrounding the hair follicles (HF) are stained, the deep interfollicular regions of the dermis (D) are devoid of methylene blue.

The extent of the penetration of the dye shown above is similar to that seen when a 2% aqueous methylene blue solution is introduced using the same intensity of current but over a period of 10 minutes only (Figures 9a and 9b).

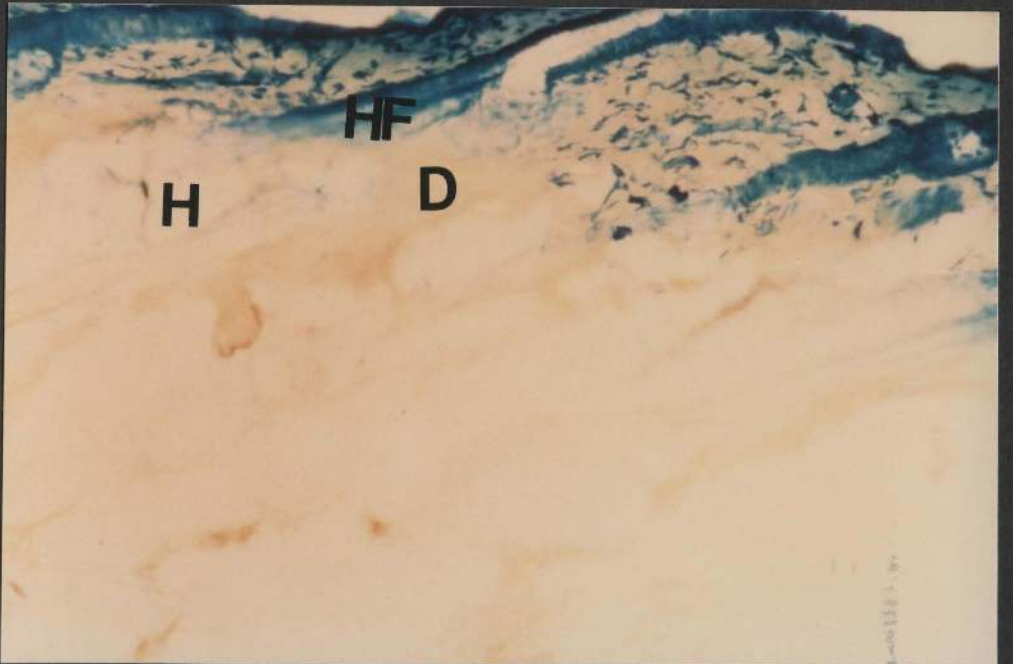
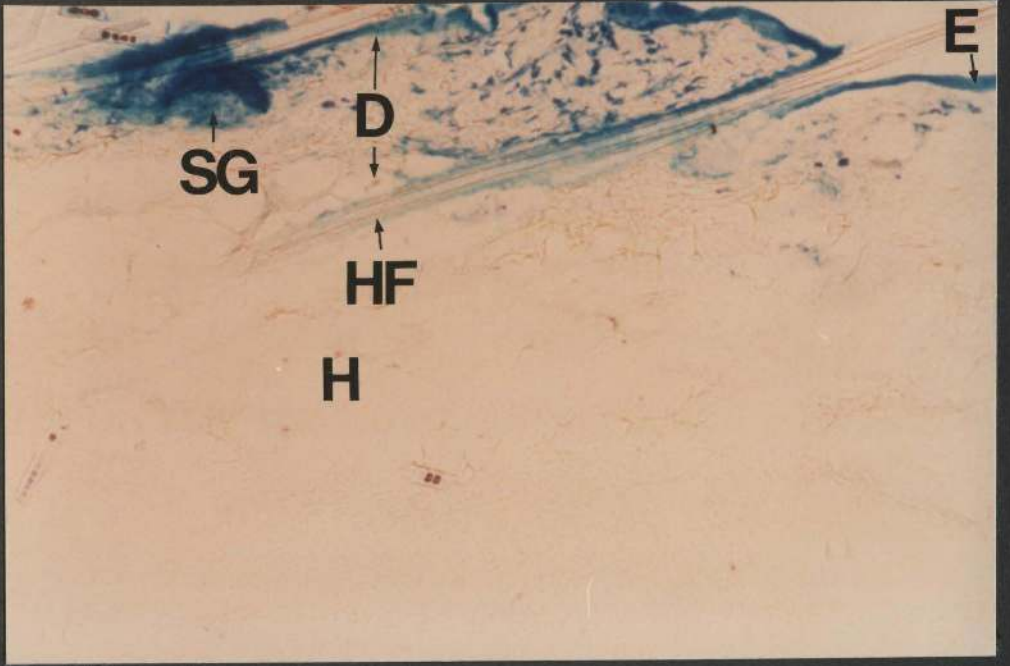


Figure 34

Positive iontophoresis of a 1% aqueous methylene blue solution at 30 milliamperes for 15 minutes

A cryostat section (x 40)

The penetration of methylene blue through the skin and the underlying tissues is complete, that is, the dye has stained the epidermis (E), the hair follicles (HF), the sebaceous glands (SG), the dermis (D), the hypodermis (H) and the striated muscle (SM).

The extent of penetration in this case is similar to that observed when the dye is introduced with the same experimental protocol but using a 2% solution (Figure 19). However, the intensity of staining in this case appears to be slightly less than that in Figure 19.



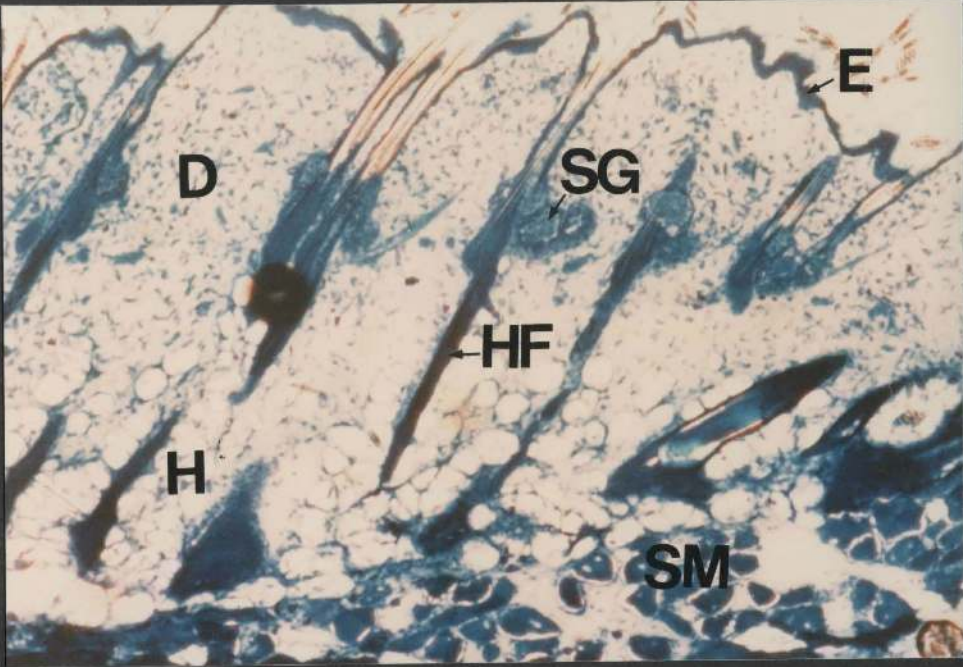


## Figure 35

Local application (control) of a 3% aqueous methylene blue solution for 15 minutes

A cryostat section stained with tartrazine (x 80)

The penetration of methylene blue through the skin is minimal. The dye is visible in the superficial part of the skin only, but does not extend into the epidermis (E), the hair follicles (HF), the sebaceous glands (SG), or into the dermis (D).

The extent of penetration is similar in this case to that obtained with local application of 1% (Figures 31a and 31b) and 2% (Figures 1a - 1d) solutions.

## Figure 36

Positive iontophoresis of a 3% aqueous methylene blue solution at 10 milliamperes for 10 minutes

A cryostat section (x 40)

It is apparent that methylene blue has stained the epidermis (E), the follicular canal epidermis (FCE) and the sebaceous glands (SG). Dermal regions (D) close to the follicular canal epidermis and sebaceous glands are stained intensely, whereas dermal regions located at the same level but between the follicles are less intensely stained.

The extent of penetration in this case resembles closely that seen when a 2% aqueous dye solution is introduced at 15 mA for 5 minutes (Figures 8a and 8b).



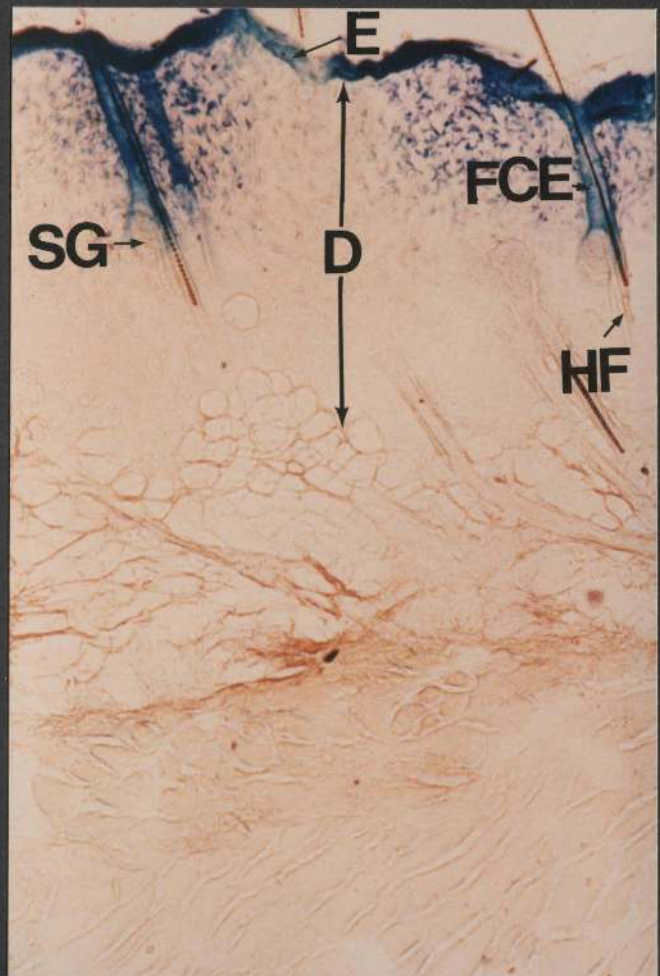


## Figure 37

Positive iontophoresis of a 3% aqueous methylene blue solution at 15 milliamperes for 15 minutes

A cryostat section (x 80)

The blue tracer is visible in the epidermis (E), the hair follicles (HF) down to the level (J) where the dermis (D) interlaces with the hypodermis (H), and in most of the dermis. The most superficial regions of the hypodermis immediately adjacent to the hair follicles are frequently stained.

The location and distribution of methylene blue is similar in this case to that obtained when a 2% aqueous dye solution is introduced by iontophoresis using the same current intensity but for a duration of 10 minutes (Figures 9a and 9b).

## Figure 38

Positive iontophoresis of a 3% aqueous methylene blue solution at 30 milliamperes for 15 minutes

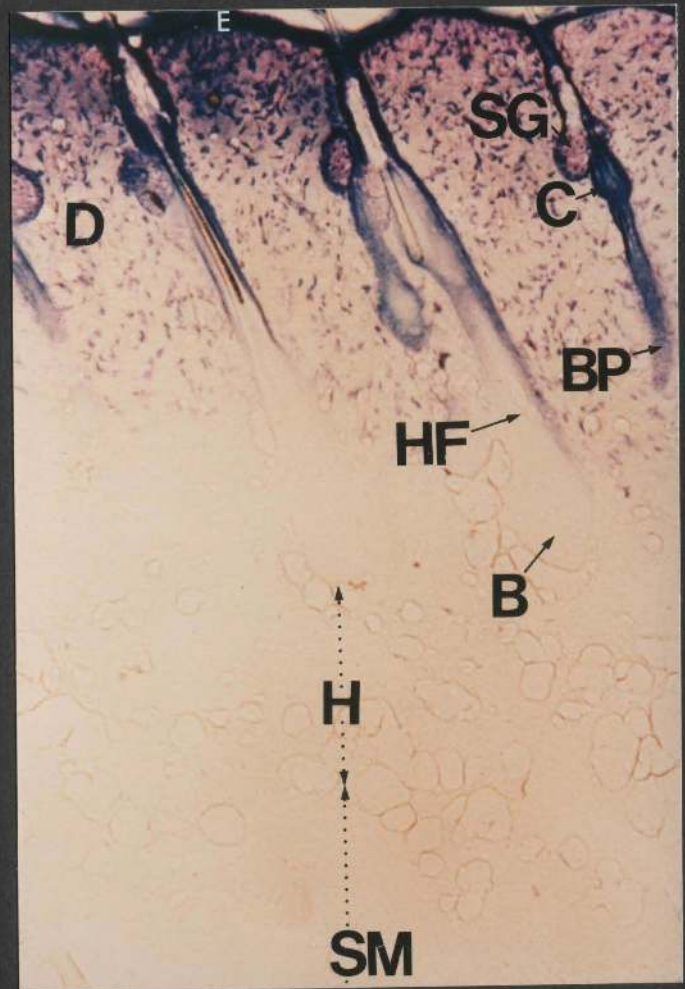
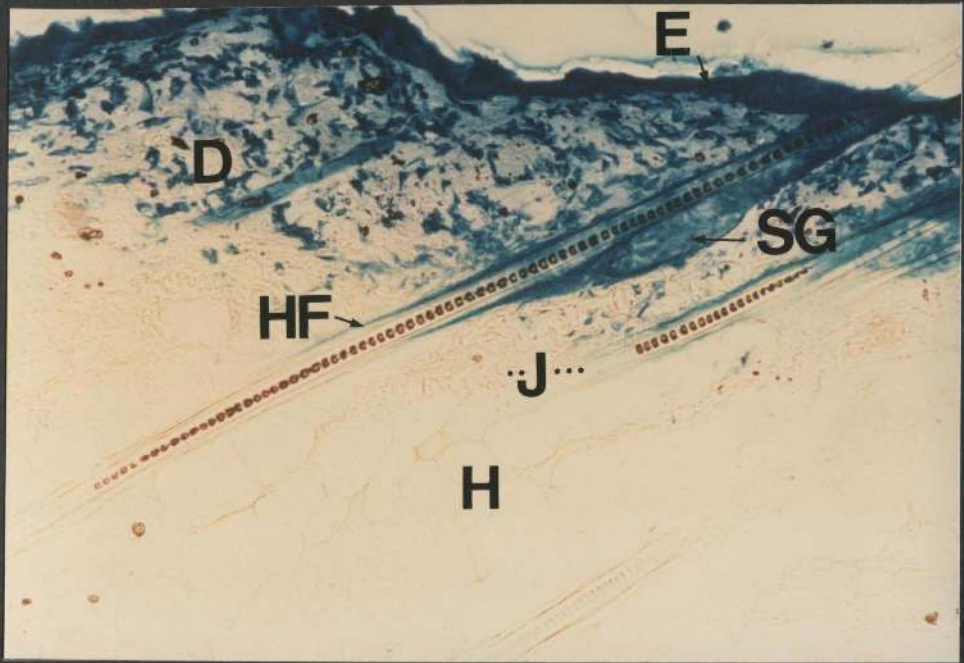
A cryostat section (x 40)

Methylene blue has stained the epidermis (E), the sebaceous glands (SG) and the dermis (D). The penetration of the dye has ceased just above the bulb (B) in active (anagen) follicles (HF), whereas the penetration is complete in resting (catagen) follicles which are characterized by the presence of club (C) and basal plate (BP).

Skin structures located at and above the level of the bases of the sebaceous glands are stained more intensely than those located below this level. No staining is visible in the hypodermis (H).

It appears that methylene blue does not extend as deeply into the hypodermis or into the striated muscle (M) from a 3% solution as it does from a 2% solution (Figure 19).





### 3.1.1.8 Effect of vehicle

The following sets of experiments were carried out to investigate the effect of changing the vehicle on the penetration of methylene blue into the skin.

The dye was prepared in absolute ethanol to a concentration of 2%. This was either applied locally (control) or introduced by iontophoresis as outlined in the following Table:

Current (milliamperes)	Duration (minutes)	Figure
0	15	39 (a - c)
5	5	40
10	10	41 (a and b)
15	15	42 (a and b)
30	15	43

## Figure 39 a - c

Local application (control) of 2% (W/V) methylene blue in absolute ethanol for 15 minutes

Figure 39a: A cryostat section (x 80)

A remnant of the embedding medium (OCT compound) stained with methylene blue is visible on the surface of the skin. The tracer is also visible in parts of the epidermis (E), especially those adjacent to the hair follicles, and in the follicular canal epidermis (FCE). No penetration is evident in the sebaceous glands (SG) or in the dermis (D).

Figure 39b: A cryostat section similar to that shown in Figure 39a but stained with tartrazine (x 80)

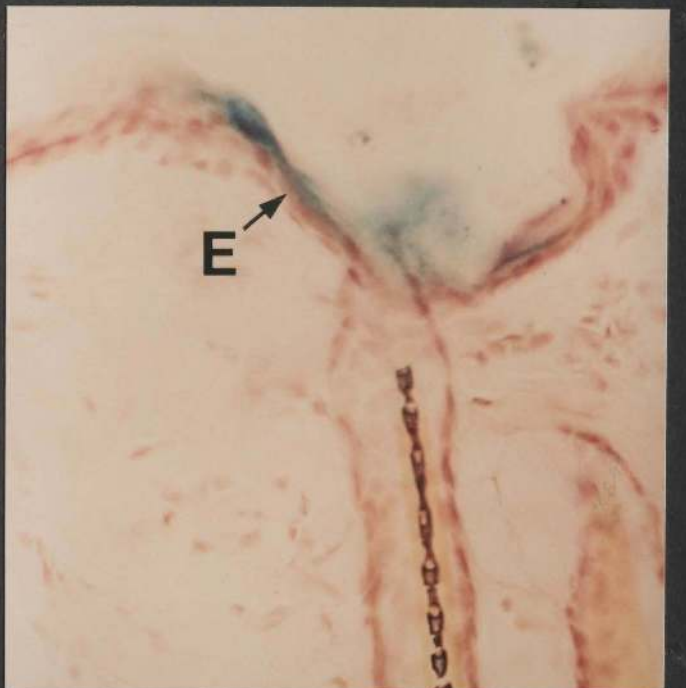
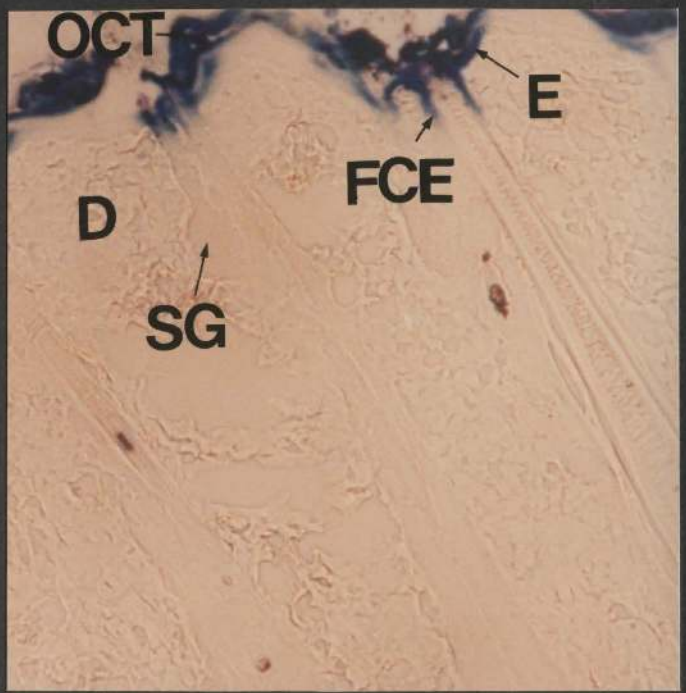
In addition to the features described in Figure 39a, this section shows that the staining intensity of the epidermis (E) is not uniform along its surface but is characterized by alternating dark and pale segments of varying extent.

Figure 39c: A cryostat section stained with haematoxylin and eosin (x 100)

At this magnification, methylene blue is only visible in the viable epidermis adjacent to the orifices of the hair follicles.

The extent of penetration in this case does not differ significantly from that seen when a 2% aqueous methylene blue solution is applied to the skin by iontophoresis using a current of 5 mA for 5 minutes (Figure 2a and 2b).





## Figure 40

Positive iontophoresis of 2% (W/V) methylene blue in absolute ethanol at 5 milliamperes for 5 minutes

A cryostat section (x 40)

The cationic blue tracer has stained the epidermis (E), some sebaceous glands (SG) and the hair follicles (HF) down to or slightly below the level of those glands. Dermal regions (D) adjacent to the upper parts of the hair follicles and surrounding the sebaceous glands are also stained, whereas interfollicular regions of the dermis remain relatively unstained.

The extent of penetration in this case resembles closely that seen when a 2% aqueous methylene blue solution is applied to the skin with iontophoresis using a current of 15 mA over a duration of 5 minutes (Figures 8a and 8b).

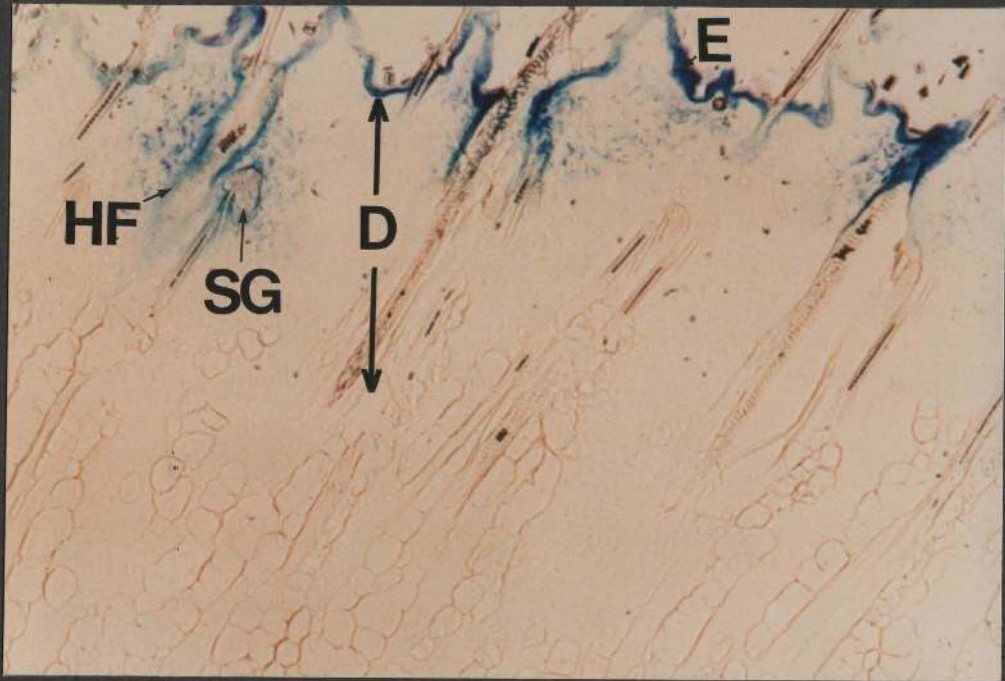


## Figure 41a and 41b

Positive iontophoresis of 2% (W/V) methylene blue in absolute ethanol at 10 milliamperes for 10 minutes

Figure 41a: A cryostat section (x 80)

Methylene blue is visible in the epidermis (E), the hair follicles (HF) down to the upper part of the hypodermis (H), the sebaceous glands (SG), and in most of the dermis (D).

Figure 41b: A cryostat section similar to that shown above but stained with tartrazine (x 80)

The location and distribution of methylene blue is similar to that described in Figure 41a. In addition, this section shows that although the superficial regions of the hypodermis (H) surrounding the hair follicles are stained, the deeper interfollicular regions of the dermis (D) which interlace with the superficial areas of the hypodermis are only occasionally stained.

The extent of penetration of methylene blue shown above is similar to that seen when a 2% aqueous solution of the tracer is introduced iontophoretically at 15 mA for 10 minutes (Figures 9a and 9b).



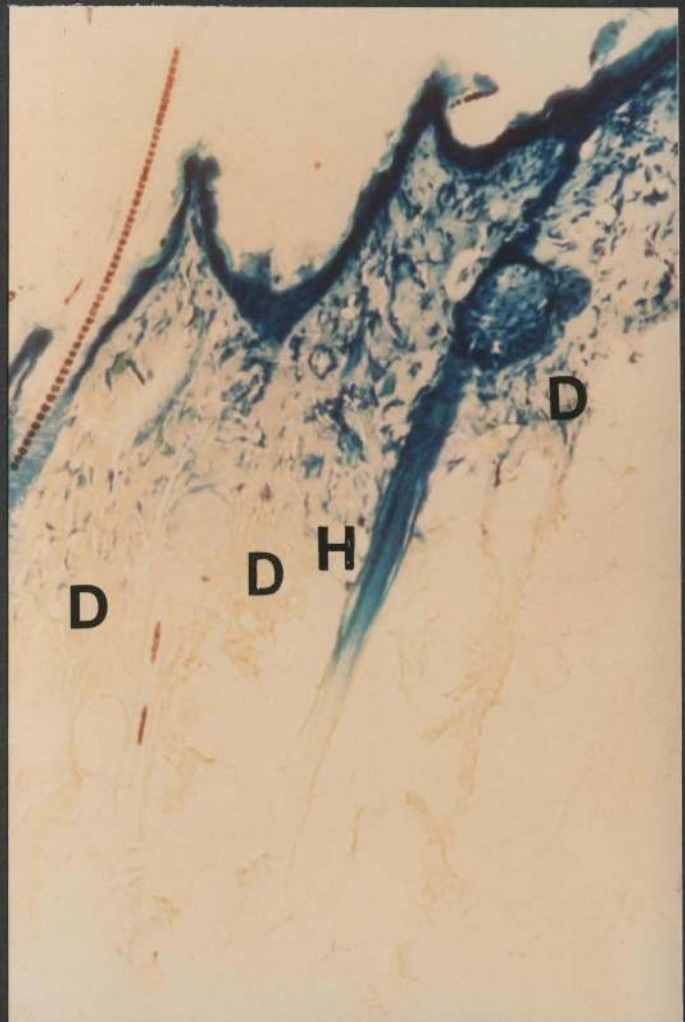
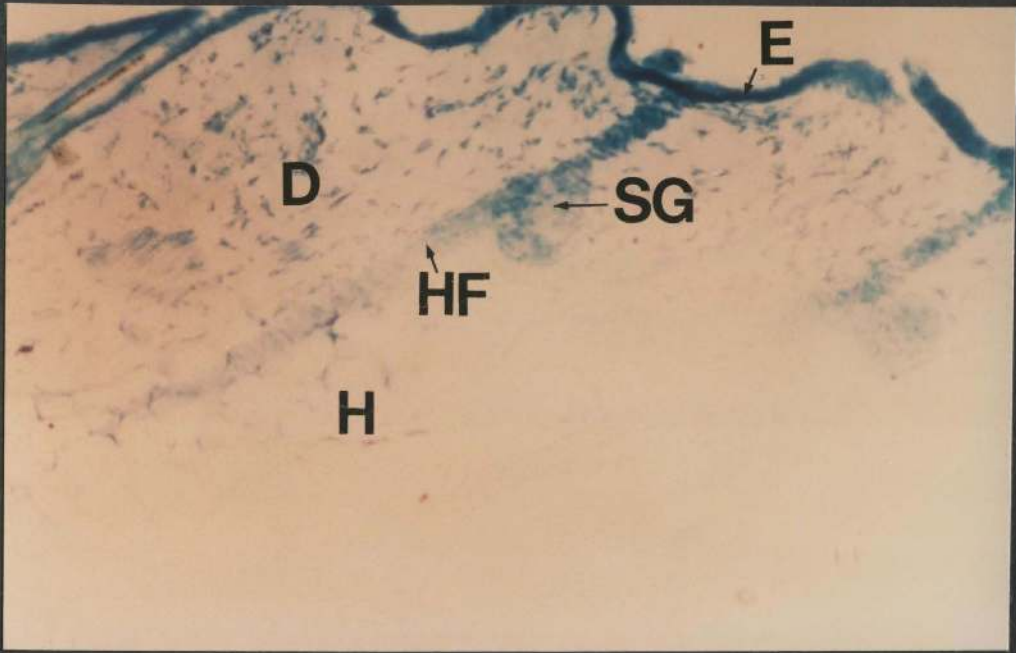




Figure 42a and 42b

Positive iontophoresis of 2% (W/V) methylene blue in absolute ethanol at 15 milliamperes for 15 minutes

Figure 42a: A cryostat section (x 40)

It is apparent that methylene blue has stained the epidermis (E), the hair follicles (HF), the sebaceous glands (SG), the dermis (D), and the superficial part of the hypodermis (H).

Figure 42b: A cryostat section similar to that shown above but stained with haematoxylin and eosin to show the extent of the dermis and the hypodermis (x 40)

It appears that, by comparing this figure with that shown in 42a, the colouration of the dermis is more intense in areas containing the hair follicles.

The location and distribution of methylene blue is similar in this case to that obtained when the dye is introduced at the same concentration but from an aqueous vehicle at a current of 30 milliamperes over a period of 10 minutes (Figure 18).

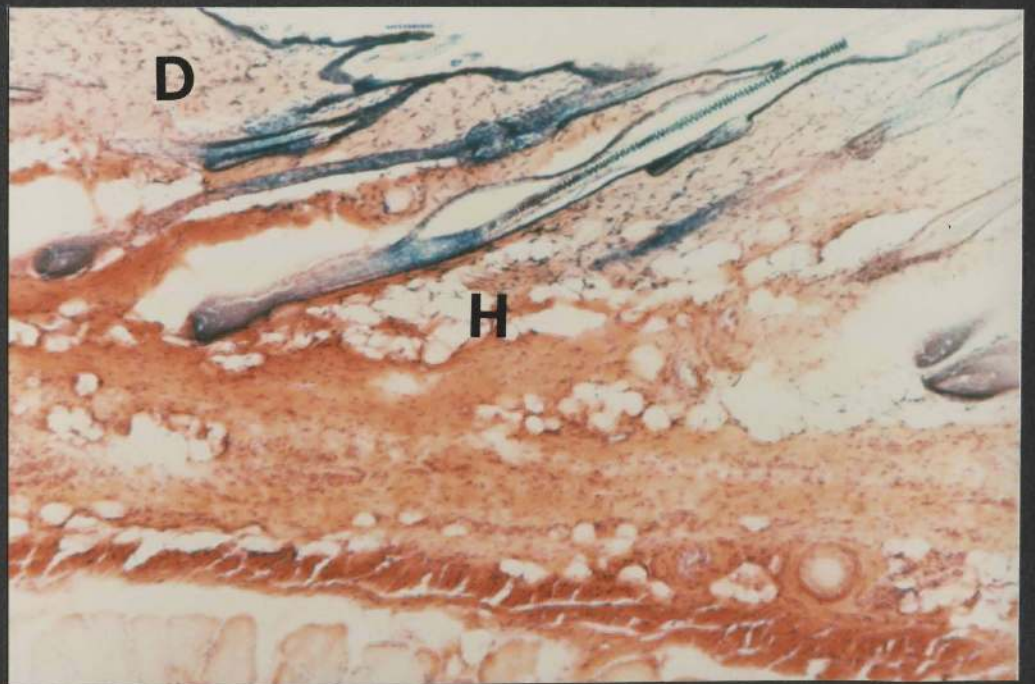
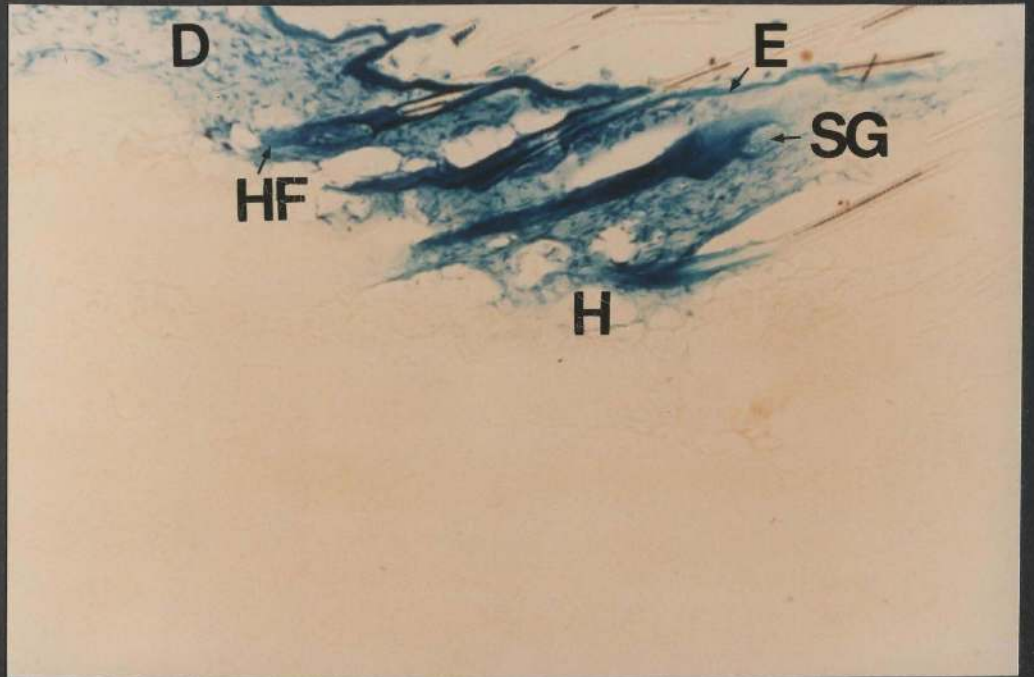


## Figure 43

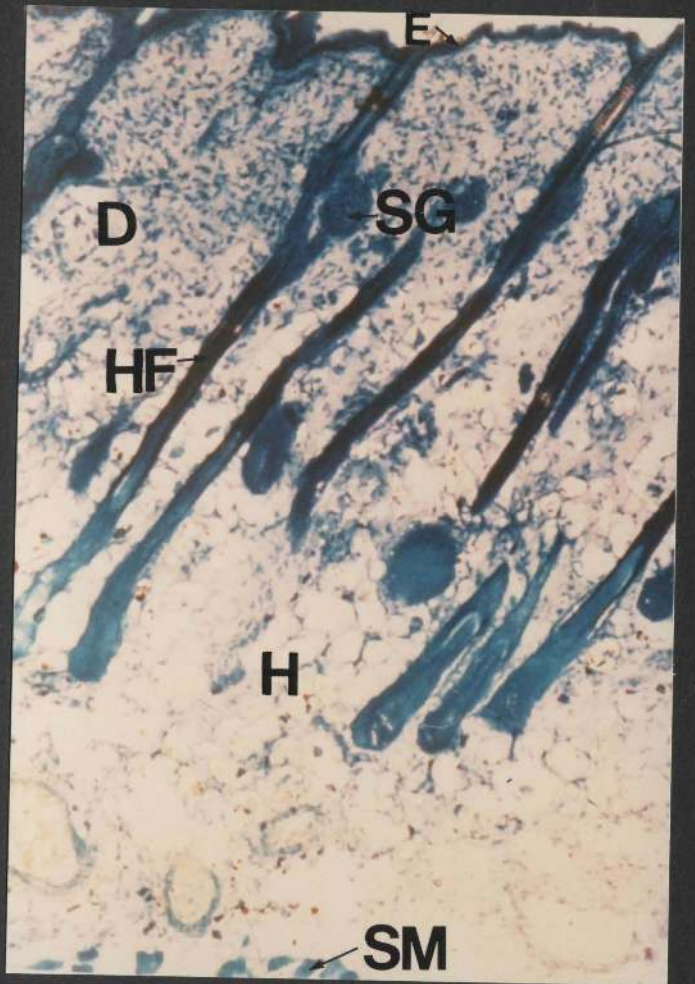
Positive iontophoresis of 2% (W/V) methylene blue in absolute ethanol at 30 milliamperes for 15 minutes

A cryostat section (x 40)

The penetration of the tracer through the skin and the underlying tissues is complete. The dye has stained the epidermis (E), the hair follicles (HF), the sebaceous glands (SG), the dermis (D), the hypodermis (H) and the striated muscle (SM).

Although the extent of penetration of methylene blue closely resembles that obtained when the dye is introduced from an aqueous vehicle with the same iontophoresis (Figure 19), the intensity of staining obtained with the alcoholic vehicle is greater than that seen with the aqueous vehicle.





### 3.1.2 Toluidine blue

The following experiments were carried out to investigate the efficacy of iontophoresis in introducing the basic dye, toluidine blue into and through the skin.

This dye was selected for penetration trials because firstly it is of the same chemical group (thiazine series) and has approximately similar molecular and cationic weights as methylene blue, and secondly because it is soluble in both water and absolute alcohol, although its solubility values differ from those of methylene blue.

Toluidine blue was prepared in distilled water to a concentration of 2% and applied to the surface of the skin with or without positive iontophoresis according to the following Table :-

Current (milliamperes)	Duration (minutes)	Figure
0	15	44 (a and b)
5	15	45
30	15	46

Figure 44a and 44b

Local application (control) of a 2% aqueous toluidine blue solution for 15 minutes

Figure 44a: A cryostat section (x 16)

The penetration of toluidine blue through the skin following local application is minimal. The dye is visible in the superficial part of the skin only.

Figure 44b: A similar cryostat section to that shown above but stained with tartrazine (x 16)

It is apparent that toluidine blue, which has persisted and is visible in this section, is confined to the surface of the epidermis (E). Toluidine blue does not extend into the deeper epidermal layers (arrow), the hair follicles (HF), the sebaceous glands (SG), or into the dermis (D).



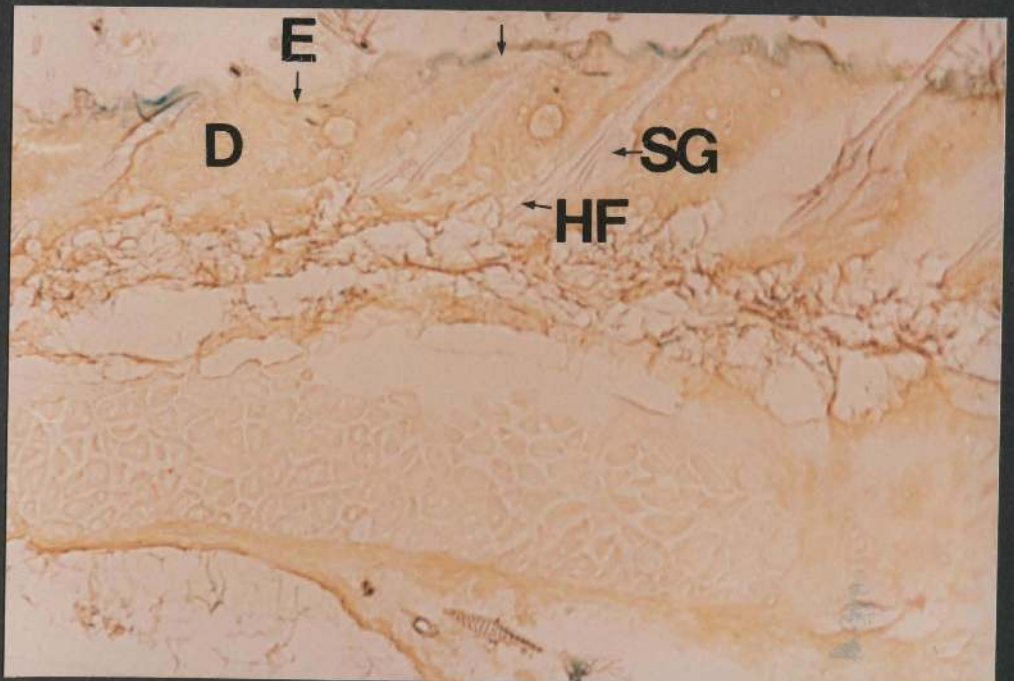
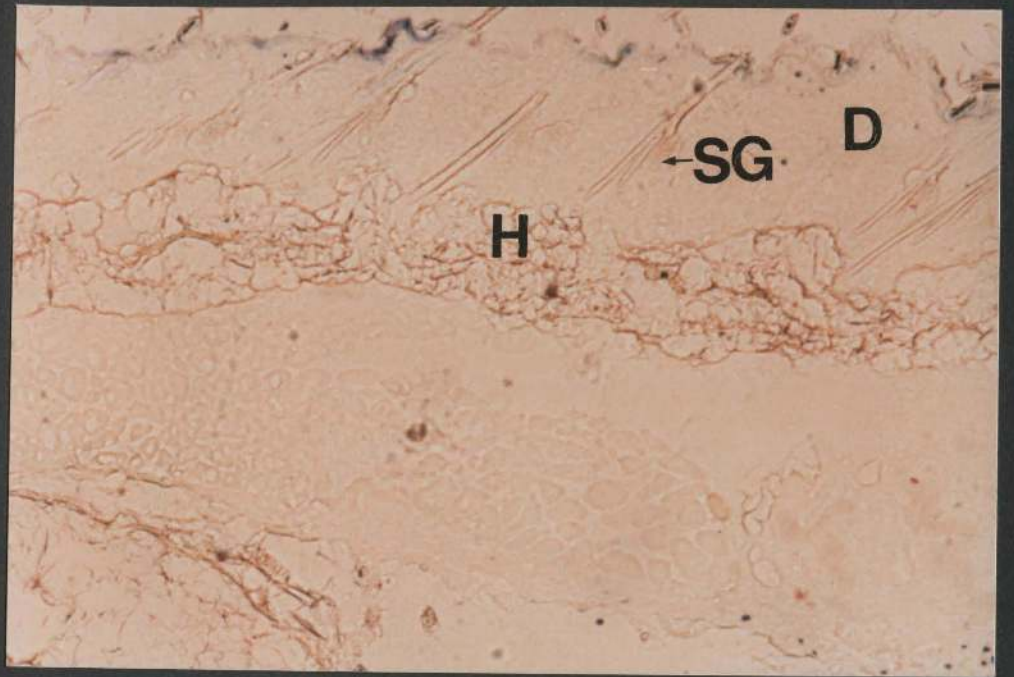


Figure 45

Positive iontophoresis of a 2% aqueous toluidine blue solution at 5 milliamperes for 15 minutes

A cryostat section (x 32)

The tracer is visible in the epidermis (E), some sebaceous glands (SG), the hair follicles (HF) down to or slightly below the level of these glands, and in some dermal areas (D) at and above these glands.

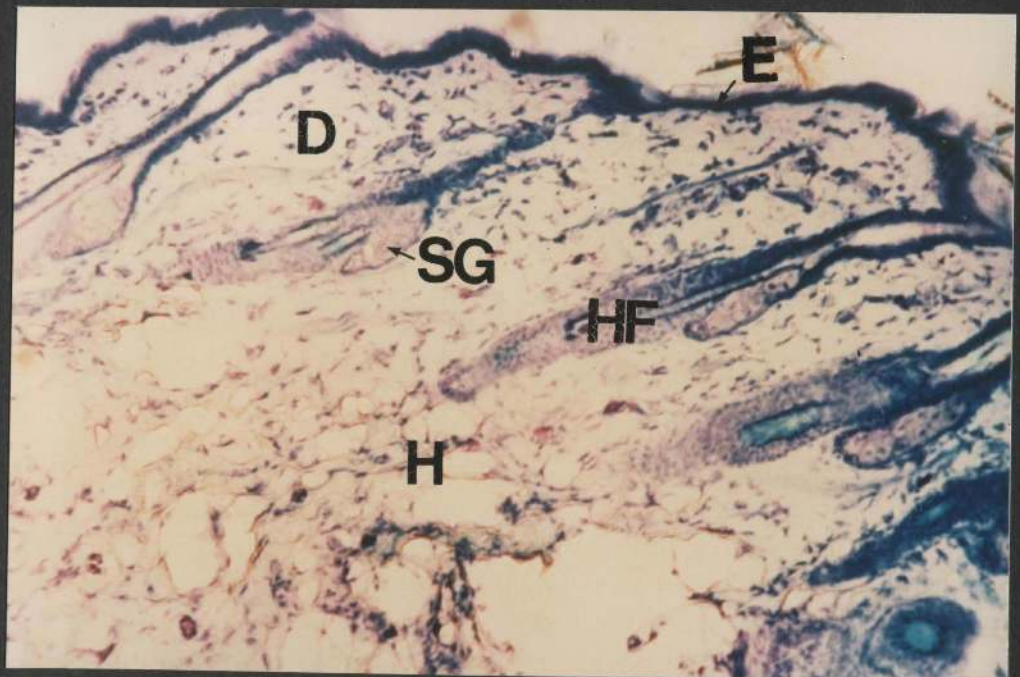
Figure 46

Positive iontophoresis of a 2% aqueous toluidine blue solution at 30 milliamperes for 15 minutes

A cryostat section (x 80)

The penetration of toluidine blue through the skin and the subcutaneous tissue is complete, that is, the dye has stained the epidermis (E), the hair follicles (HF), the sebaceous glands (SG), the dermis (D) and the hypodermis (H).





### 3.1.3 Pyronin Y

This red basic dye was selected for penetration studies because it has a relatively high solubility in water (10%) and a low solubility in alcohol (0.5%).

It has a molecular and a cationic weight similar to those of methylene blue and toluidine blue; however, unlike these dyes, pyronin Y is a member of the xanthene series.

Pyronin Y was prepared in distilled water to a concentration of 2% and applied locally (control) or introduced iontophoretically as described in Figures 47 and 48.

#### Figure 47

Local application (control) of a 2% aqueous pyronin Y solution for 15 minutes

A cryostat section stained with tartrazine (x 80)

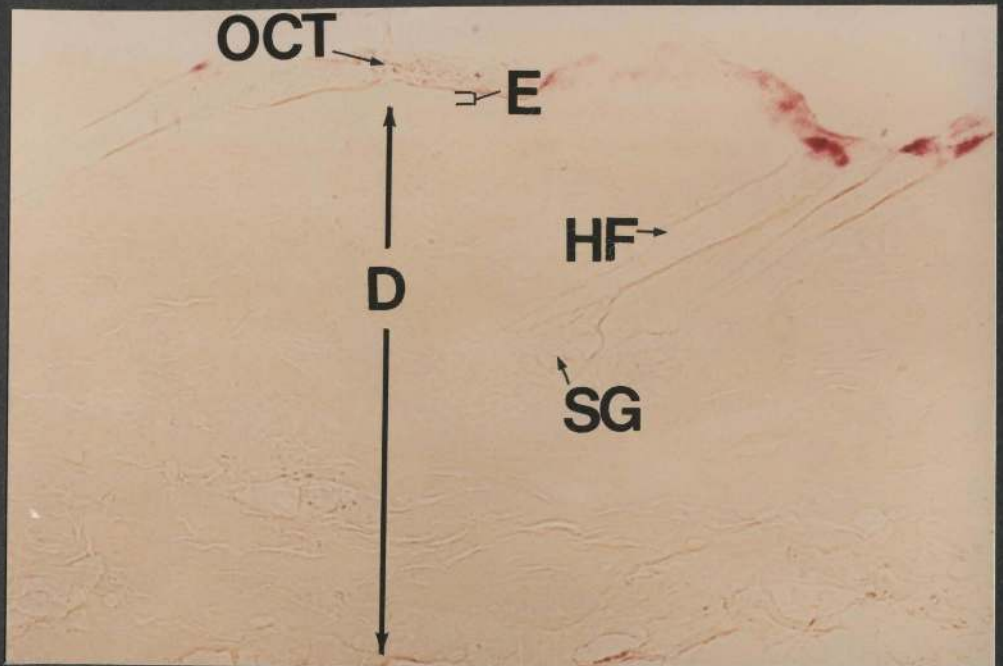
The penetration of pyronin Y through the skin is minimal, that is, the dye is confined to the surface of the skin where a remnant of the embedding medium (OCT compound) is present. In addition, the tracer forms a coating around the hair shafts just above the surface of the skin. No penetration is evident in the epidermis (E), the hair follicles (HF), the sebaceous glands (SG), or in the dermis (D).

#### Figure 48

Positive iontophoresis of a 2% aqueous pyronin Y solution at 30 milliamperes for 15 minutes

A cryostat section (x 80)

Pyronin Y has stained the epidermis (E), the follicular canal epidermis (FCE), and occasionally the upper parts of the sebaceous glands (SG). Dermal (D) regions adjacent to the follicular canal epidermis are also stained, whereas interfollicular regions of the dermis located at the same level remain relatively unstained.





### 3.1.4 Aniline blue alcohol-soluble (solvent blue 3)

This dye was selected because of its solubility in absolute alcohol (1.5%) and insolubility in water.

The dye was prepared in absolute ethanol to a concentration of 1% and applied locally (Figure 49) or introduced by iontophoresis (Figure 50).

#### Figure 49

Local application of 1% (W/V) aniline blue alcohol-soluble in absolute ethanol for 15 minutes

A cryostat section stained with tartrazine (x 100)

The dye is visible on the surface of the skin. No penetration is seen into the epidermis (E), the hair follicles (HF), the sebaceous glands (SG) or in the dermis (D).

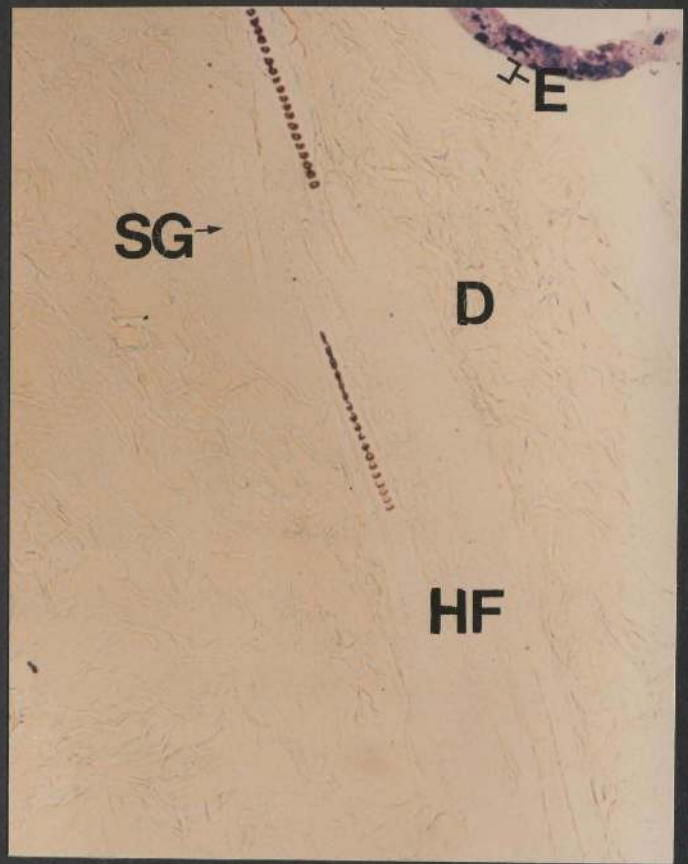
#### Figure 50

Positive iontophoresis of a 1% (W/V) aniline blue alcohol-soluble in absolute ethanol at 30 milliamperes for 15 minutes

A cryostat section stained with tartrazine (x 100)

Apart from its localization in the upper parts of the follicular canal epidermis (FCE), the extent of penetration of the tracer through the epidermis (E), the sebaceous glands (SG) and the dermis (D), is similar to that described above in Figure 49.

It is clear therefore, that the penetration of aniline blue alcohol-soluble through the skin following iontophoresis is minimal.



### 3.1.5 Chrysoidin Y

The following experiments were undertaken to study the influence of iontophoresis on the penetration of chrysoidin Y into the skin. This dye has a good solubility both in water (5.5%) and in absolute alcohol (4.75%). However, unlike methylene blue, chrysoidin Y is a member of the mono-azo group and, in addition, it has lower molecular and cationic weights than those of methylene blue.

Chrysoidin Y was prepared in distilled water to a concentration of 2% and applied locally (Figure 51) or introduced by iontophoresis (Figure 52).

#### Figure 51

Local application (control) of a 2% aqueous chrysoidin Y solution for 15 minutes

A cryostat section stained with 0.1% aqueous eosin for approximately 2-3 seconds (x 32)

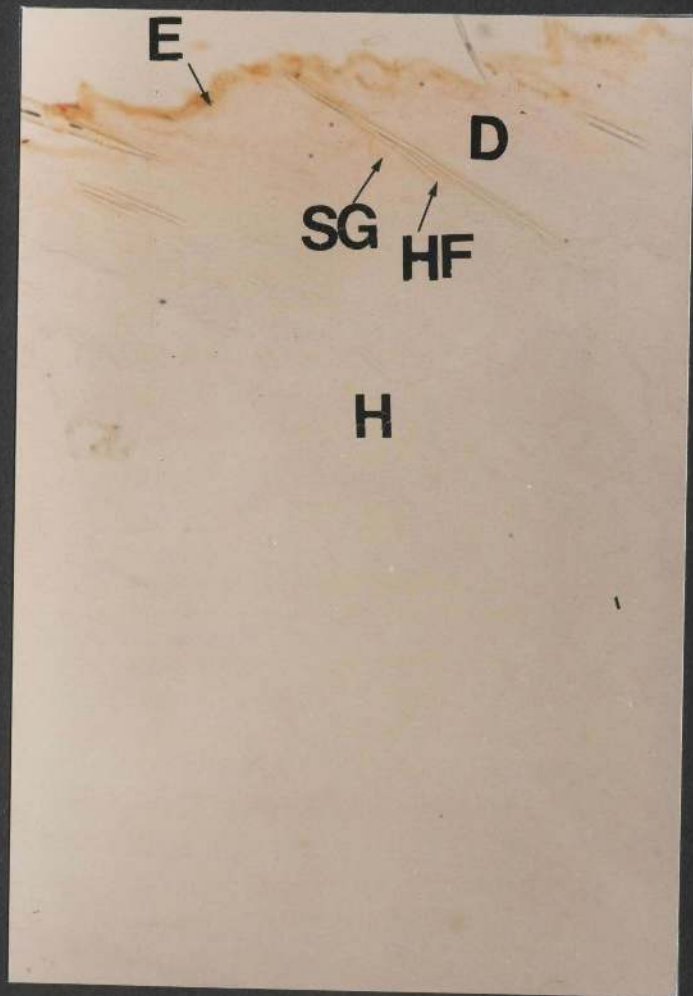
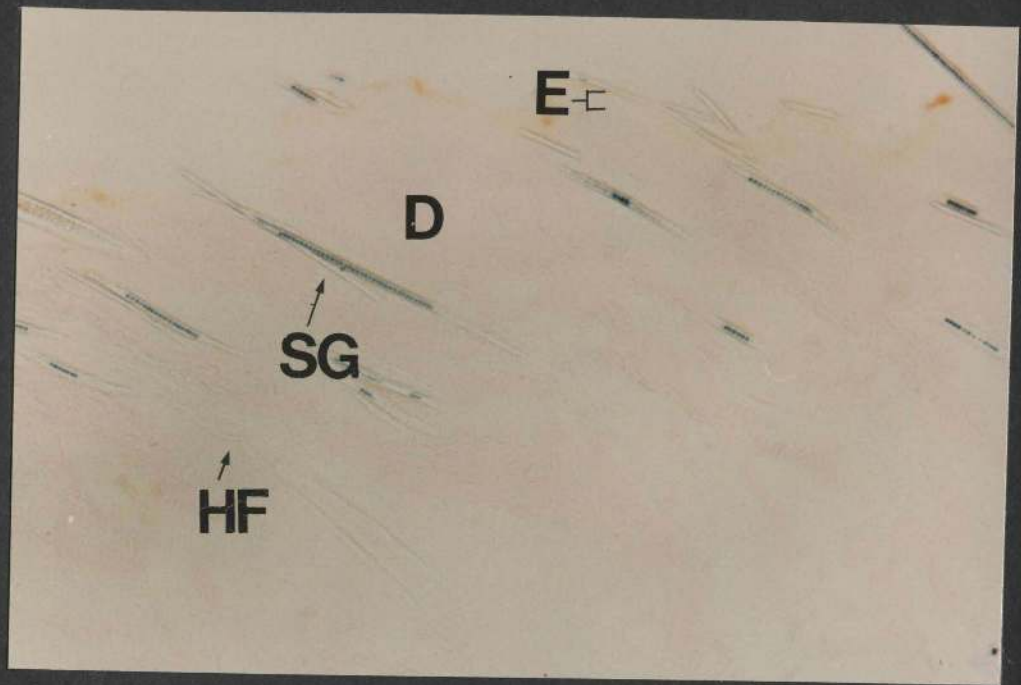
The penetration of chrysoidin Y following local application is negligible, that is, a light yellow stain is only visible in the superficial part of the skin. No penetration is evident in the epidermis (E), the hair follicles (HF), the sebaceous glands (SG) or in the dermis (D).

#### Figure 52

Positive iontophoresis of a 2% aqueous chrysoidin Y solution for 15 minutes

A cryostat section stained as above (x 32)

The penetration of chrysoidin Y into the skin is facilitated by iontophoresis. The dye is visible in the epidermis (E), the hair follicles (HF), the sebaceous glands (SG), and in the dermis (D). The tracer is less obvious in the hypodermis (H).



### 3.2 Anionic Dyes

#### 3.2.1 Eosins

Different types of eosins were prepared in different vehicles according to their chemical nature. Eosin water-soluble was prepared in distilled water to a concentration of 4%. Eosin alcohol soluble was prepared in absolute ethanol to a concentration of 0.5%. Eosin water-and alcohol-soluble was prepared in both distilled water and in absolute alcohol to a concentration of 1% in each vehicle.

Each of these solutions was applied locally (control) or introduced by negative iontophoresis according to the following Table :-

Test solution	Current (milliamperes)	Duration (minutes)	Figure
Eosin water-soluble	0	15	53
	30	15	54
Eosin alcohol-soluble	0	15	55
	30	15	56
Eosin water- and alcohol-soluble in distilled water	0	15	57
	30	15	58
Eosin water- and alcohol-soluble in absolute ethanol	0	15	59
	30	15	60

Using the procedures described above, not only was the effect of iontophoresis on the penetration of these anionic dyes studied, but also the influence of the solubility characteristic and the type of vehicle in which the dyes had been dissolved.



## Figure 53

Local application (control) of 4% (W/V) eosin water-soluble in distilled water for 15 minutes.

A cryostat section stained with tartrazine (x 80)

Eosin has formed a red layer along the surface of the skin where a remnant of the embedding medium may be seen. The epidermis (E) is seen as a colour-free band.

No penetration is evident in the hair follicles (HF), sebaceous glands (SG) or in the dermis (D).

## Figure 54

Negative iontophoresis of 4% (W/V) eosin water-soluble in distilled water at 30 milliamperes for 15 minutes

A cryostat section stained with tartrazine (x 80)

Eosin is visible in the surface of the skin. Although many segments of the epidermis (E) are stained with eosin, the tracer does not extend into the hair follicles (HF), the sebaceous glands (SG) or into the dermis (D).

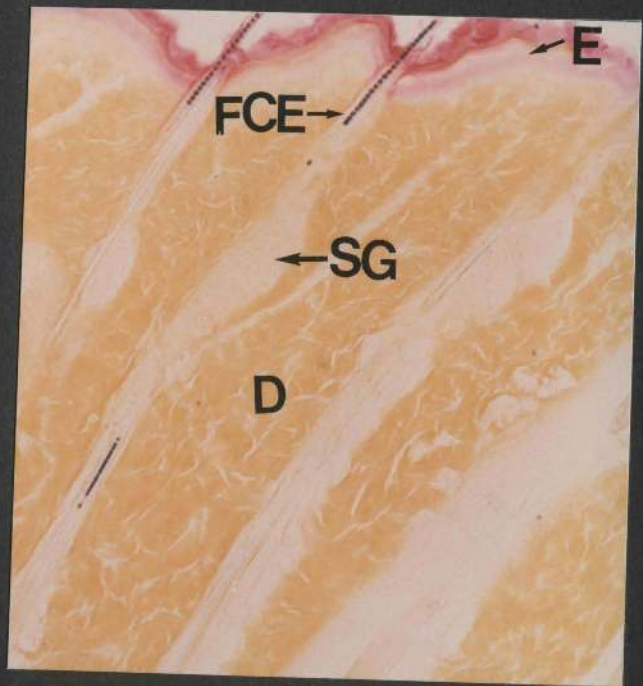


## Figure 55

Local application (control) of 0.5% (W/V) eosin alcohol-soluble in absolute ethanol for 15 minutes

A cryostat section stained with tartrazine (x 80)

The red tracer is visible on the surface of the skin and in the upper parts of the follicular canal epidermis (FCE). The epidermis (E), the sebaceous glands (SG), the hair follicles (HF) and the dermis (D) are devoid of the tracer.

## Figure 56

Negative iontophoresis of 0.5% (W/V) eosin alcohol-soluble in absolute ethanol at 30 milliamperes for 15 minutes

A tartrazine-stained cryostat section (x 80)

Many segments of the epidermis (E) are stained with eosin. Although the tracer is visible in the upper parts of the follicular canal epidermis (FCE), it does not extend any deeper into the hair follicles, the sebaceous glands (SG) or into the dermis (D).

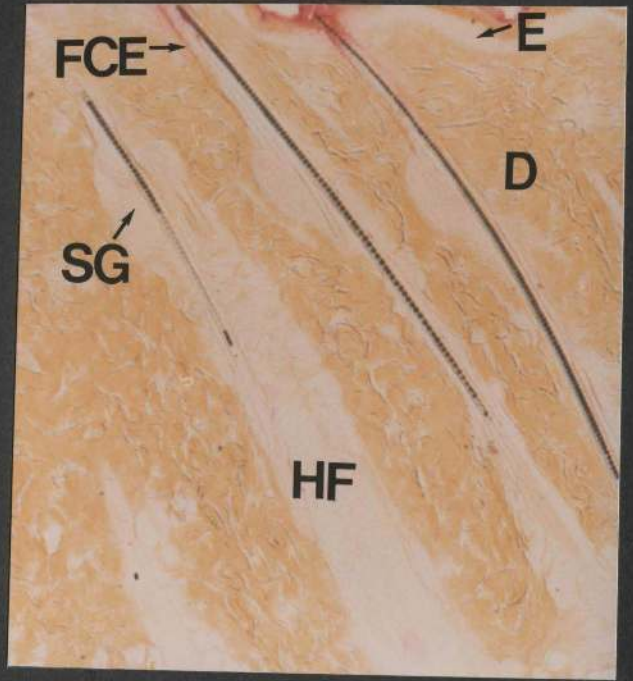


## Figure 57

Local application (control) of 1% (W/V) eosin water- and alcohol-soluble in distilled water for 15 minutes

A cryostat section stained with tartrazine (x 80)

Eosin is visible on the surface of the skin and in the upper parts of the follicular canal epidermis (FCE). No penetration is evident in the epidermis (E), the lower parts of the follicular canal epidermis, the sebaceous glands (SG), or in the dermis (D).

## Figure 58

Negative iontophoresis of 1% (W/V) eosin water- and alcohol-soluble in distilled water at 30 milliamperes for 15 minutes

A cryostat section stained with tartrazine (x 80)

The red tracer has stained those parts of the epidermis (E) immediately adjacent to the orifices of the hair follicles, whereas the interfollicular epidermis remains relatively unstained. Although the tracer is also visible in the hair follicles (HF), very little or no staining is seen in the sebaceous glands (SG) and the dermis (D).



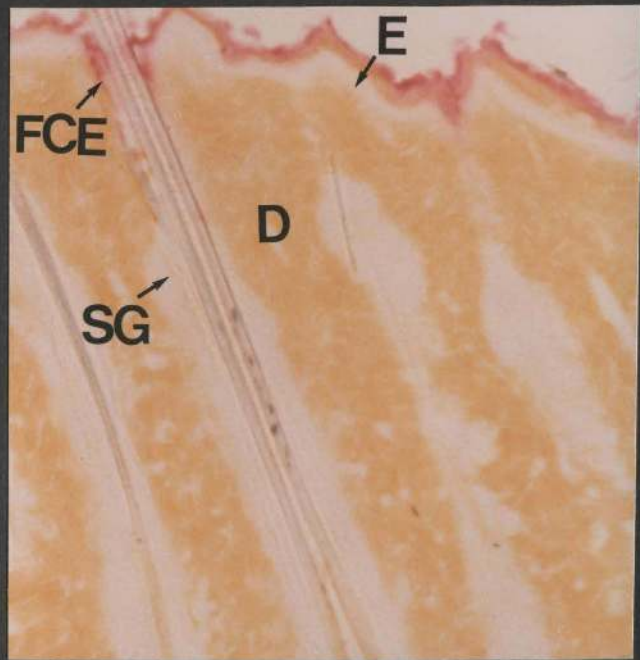


Figure 59

Local application (control) of 1% (W/V) eosin water- and alcohol-soluble in absolute ethanol for 15 minutes

A cryostat section (x 80)

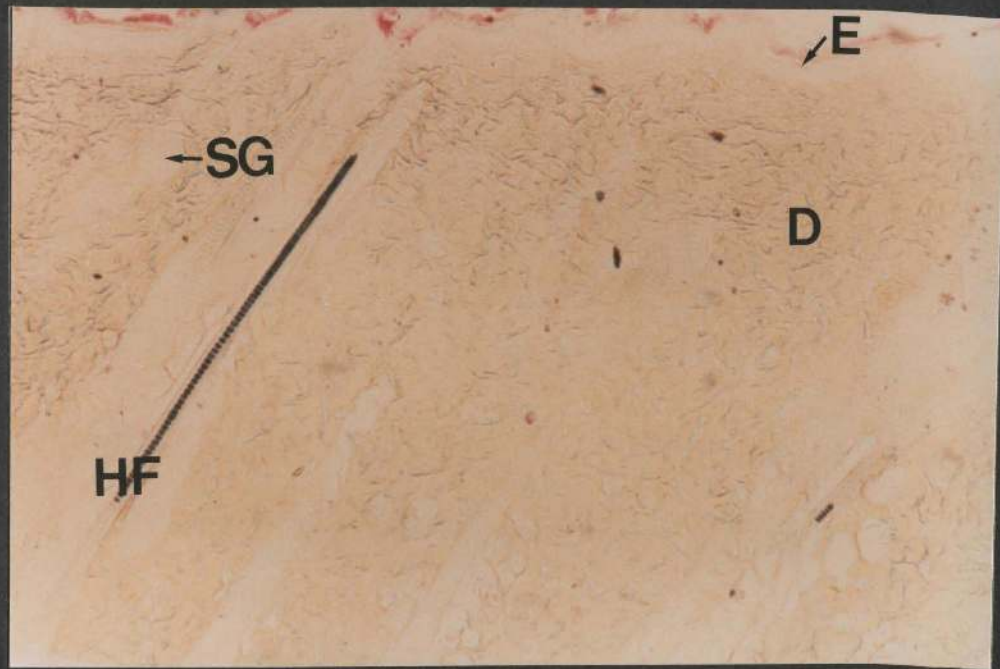
The tracer has formed a red film over the surface of the skin. No penetration is seen in the epidermis (E), the hair follicles (HF), the sebaceous glands (SG), or in the dermis (D).

Figure 60

Negative iontophoresis of 1% (W/V) eosin water- and alcohol-soluble in absolute ethanol at 30 milliamperes for 15 minutes

A cryostat section stained with tartrazine (x 80)

Hair follicles (HF) and their associated sebaceous glands (SG) are clearly stained with eosin, although very little or no staining is evident in the epidermis (E). The dermis (D) does not contain eosin.





### 3.2.2 Aniline blue water-soluble (Acid blue 22)

The aim of the following experiments was to investigate the effect of iontophoresis on the penetration of another anionic dye from the surface into the skin. Aniline blue water-soluble was selected because it has a high solubility in water and is insoluble in absolute alcohol.

The dye was prepared in distilled water to a concentration of 5% and applied locally (Figure 61) or introduced by negative iontophoresis (Figure 62). An additional set of experiments was carried out to investigate the influence of positive iontophoresis on the penetration of this anionic dye (Figure 63).

#### Figure 61

Local application (control) of a 5% aqueous aniline blue water-soluble solution for 15 minutes

A cryostat section stained with tartrazine (x 160)

The tracer forms a blue-greenish film over the surface of the skin. The tracer does not however, penetrate into the epidermis (E), the hair follicles (HF), the sebaceous glands (SG), or into the dermis (D).

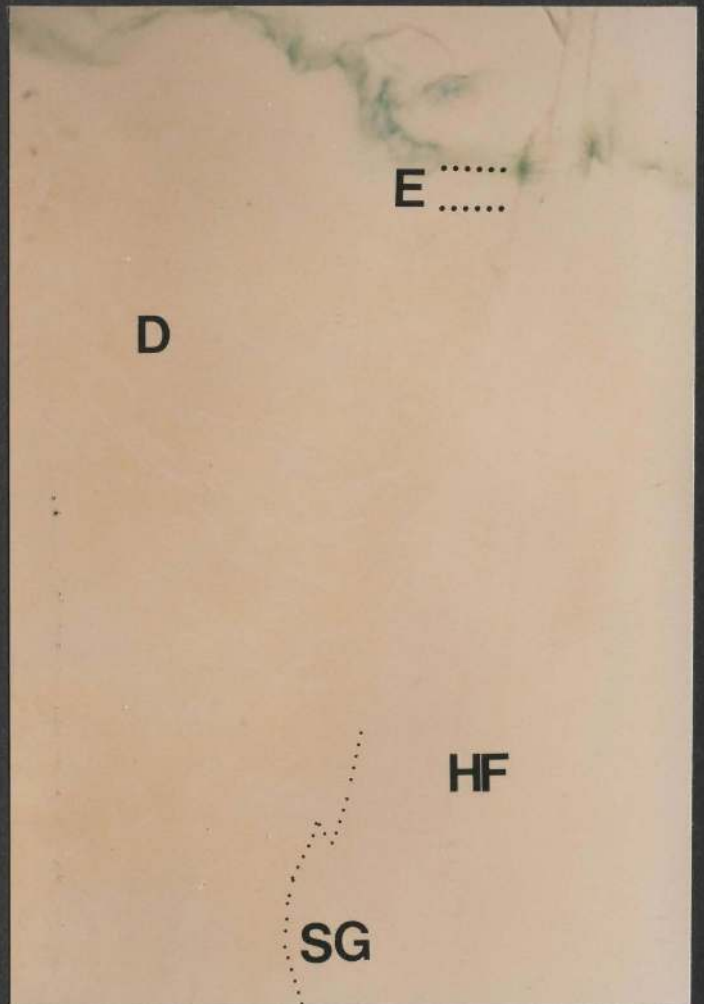


Figure 62

Negative iontophoresis of a 5% aqueous aniline blue water-soluble solution at 30 milliamperes for 15 minutes

A cryostat section stained with tartrazine (x 160)

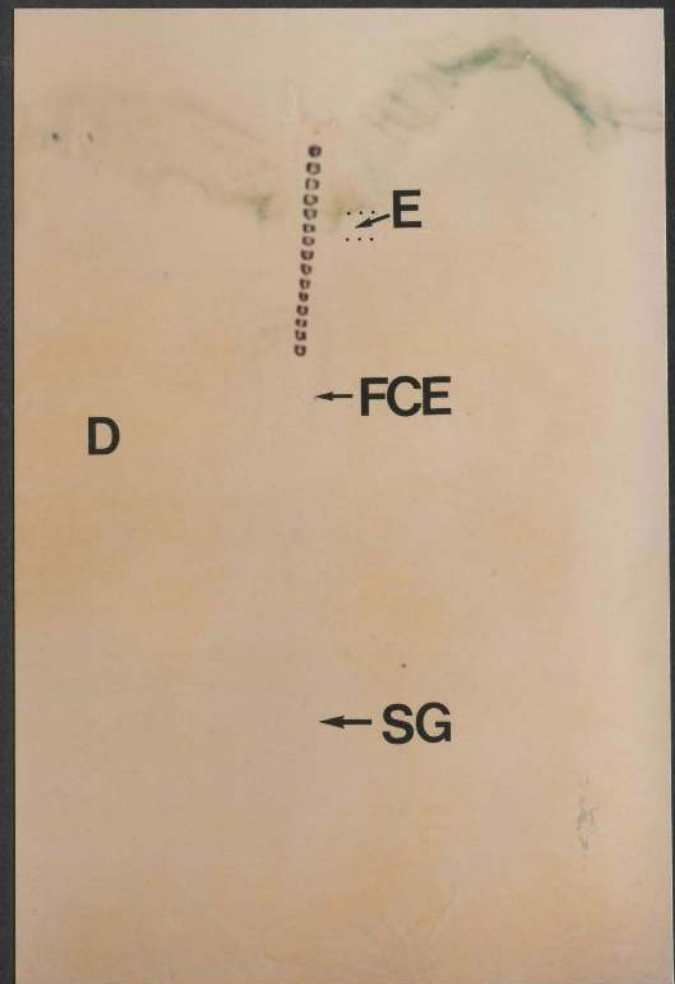
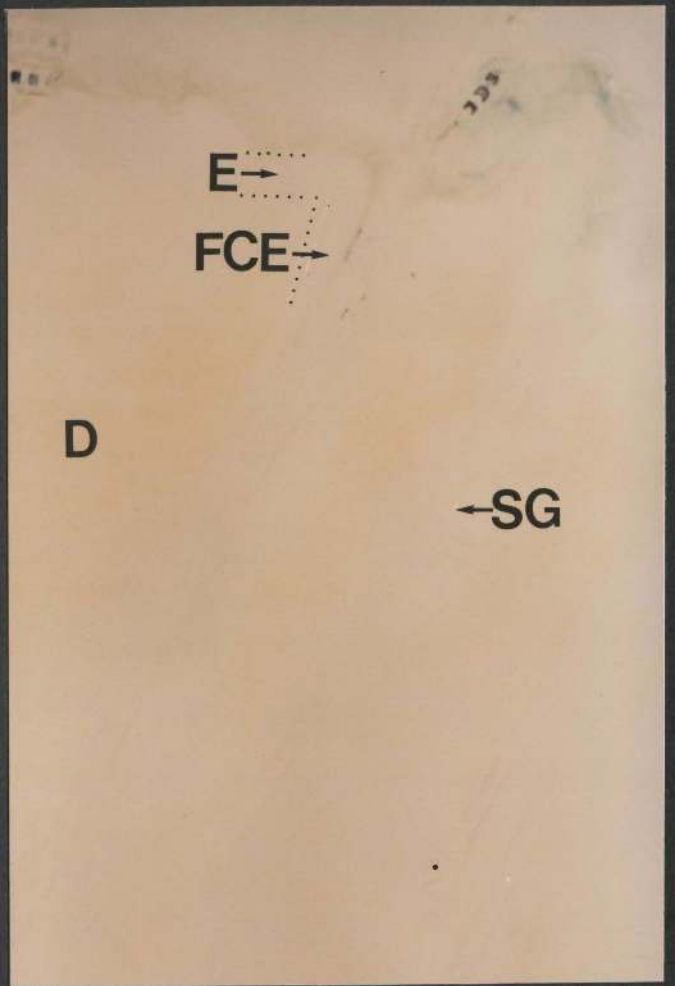
The penetration of the blue tracer through the skin is minimal. The dye is confined to the surface of the skin and does not penetrate into the epidermis (E), the follicular canal epidermis (FCE), the sebaceous glands (SG) or into the dermis (D).

Figure 63

Positive iontophoresis of a 5% aqueous aniline blue water-soluble solution at 30 milliamperes for 15 minutes

A cryostat section stained with tartrazine (x 160)

As in Figure 62, no penetraton is evident in the epidermis (E), the follicular canal epidermis (FCE), the sebaceous glands (SG) or in the dermis (D).



### 3.2.3 Picric acid

This yellow acid dye of the nitro group is highly soluble in absolute alcohol (9.0%) and less soluble in water (1.2%). Furthermore, it is characterized by having lower molecular and anionic weights than any other organic dye used in the penetration trials.

The dye was prepared in absolute ethanol to a concentration of 6% (V/V) by mixing 6 mls of the picric acid solution (as supplied) with 94 mls of absolute alcohol. This solution was then applied locally or introduced by negative iontophoresis.

#### Figure 64

Local application (control) of 6% (V/V) picric acid solution in absolute ethanol for 15 minutes

A cryostat section (x 32)

Picric acid is not visible in any of the structures identified in this section which include the dermis (D), the hair follicles (HF), the sebaceous glands (SG) and the hypodermis (H).

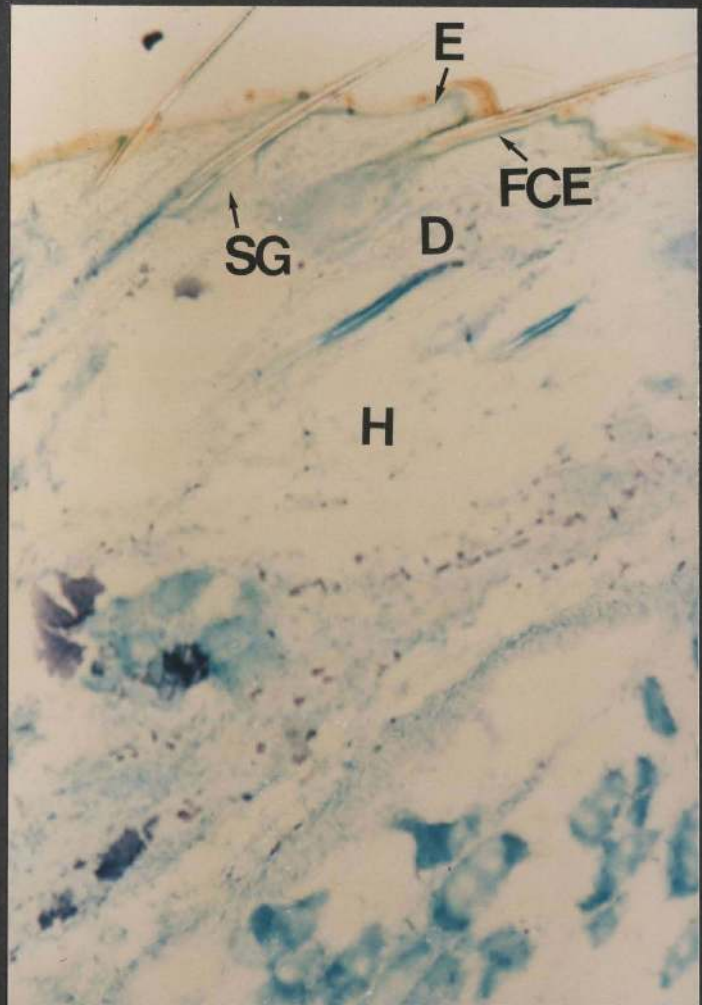
#### Figure 65

Negative iontophoresis of 6% (V/V) picric acid solution in absolute ethanol at 30 milliamperes for 15 minutes

A cryostat section stained with 0.1% aqueous toluidine blue for approximately 1-3 seconds (x 32)

The yellow tracer is visible in the epidermis (E), the follicular canal epidermis (FCE) and in the sebaceous glands (SG). The tracer is less evident in the dermis (D) and the hypodermis (H).





### 3.2.4 Alizarin red S

This red acid dye of the anthraquinone chemical group is characterized by a low molecular weight (342.26), a high solubility in water (6.5%) and a much lower solubility in absolute alcohol (0.1%).

The dye was prepared in distilled water to a concentration of 1% and applied locally or introduced by negative iontophoresis.

#### Figure 66

Local application (control) of a 1% aqueous alizarin red S solution for 15 minutes

A cryostat section stained with tartrazine (x 16)

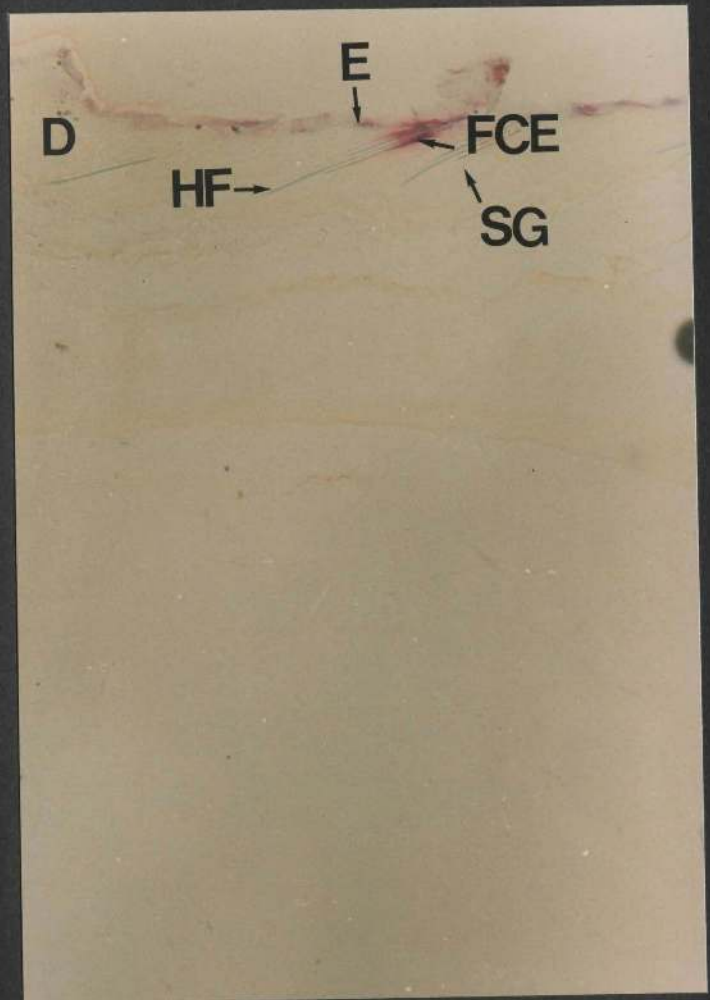
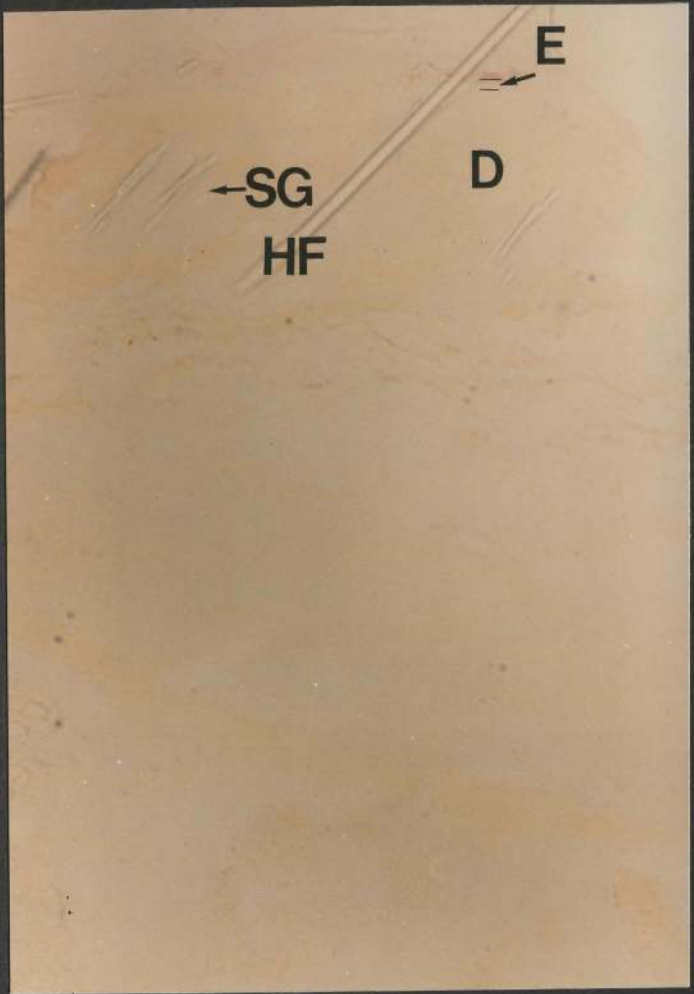
A light reddish colour is visible on the surface of the skin adjacent to the orifices of the hair follicles. The epidermis (E) appears as a colour-free band. No penetration is evident in the hair follicles (HF), the sebaceous glands (SG) or in the dermis (D).

#### Figure 67

Negative iontophoresis of a 1% aqueous alizarin red S solution at 30 milliamperes for 15 minutes

A cryostat section stained with tartrazine (x 16)

The staining of the epidermis (E) is not uniform along its surface but is characterized by alternating dark and pale segments of varying extent. Although the follicular canal epidermis (FCE) is filled with the red dye, the tracer does not extend any deeper into the follicles (HF) or into the sebaceous glands (SG). No staining is observed in the bulk of the dermis (D), except for that part immediately adjacent to the follicular canal epidermis.





### 3.2.5 Trypan blue

The aim of the following experiments was to investigate the influence of iontophoresis on the penetration of an additional acid dye, trypan blue, from the surface into the skin. This dye is characterized by a low solubility in water (1%) and a lower solubility in absolute alcohol (0.02%)

Trypan blue was dissolved in distilled water to a concentration of 0.5% and applied locally or introduced iontophoretically.

Figures 68a and 68b

Local application (control) of a 0.5% aqueous trypan blue solution for 15 minutes

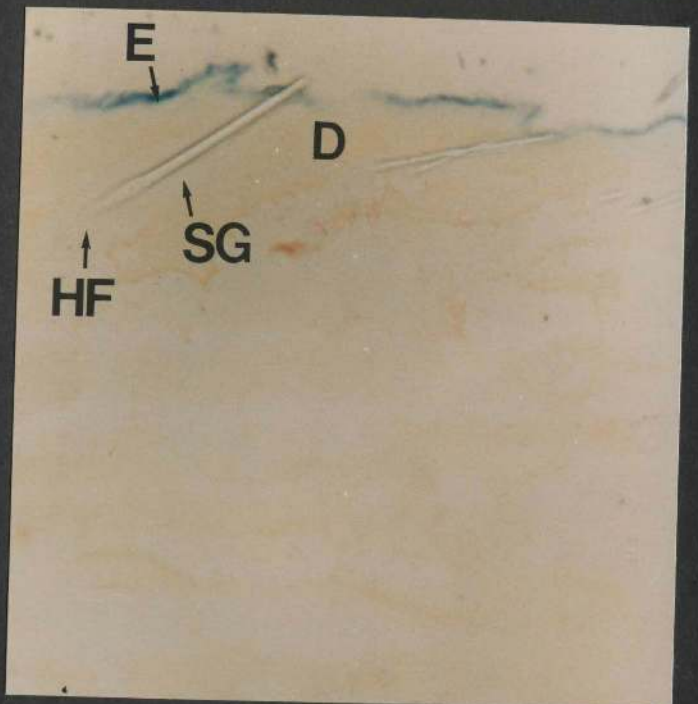
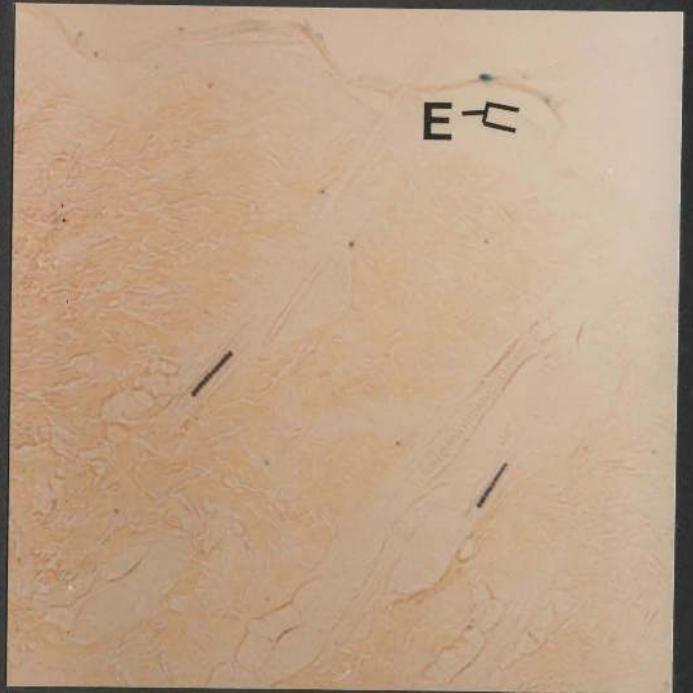
Figure 68a: A cryostat section stained with tartrazine (x 16)  
The tracer is visible in the superficial part of the skin. No penetration is observed in the hair follicles (HF), the sebaceous glands (SG) or in the dermis (D).

Figure 68b: A cryostat section stained with tartrazine (x 80)  
In addition to the features described in Figure 68a, this section shows that no penetration has taken place into the epidermis (E).

Figure 69

Negative iontophoresis of a 0.5% aqueous trypan blue solution at 30 milliamperes for 15 minutes

A cryostat section stained with tartrazine (x 16)  
Very little staining is observed in the epidermis (E), and the hair follicles (HF), but is seen occasionally in the dermis (D) immediately beneath the epidermis. No penetration is evident in the sebaceous glands (SG).



### 3.3 Neutral dyes

The aim of the following sets of experiments was to investigate the effect of iontophoresis on the penetration of neutral (lipid-soluble) dyes from the surface into the skin. Sudan black B was selected as a representative of such a class of compounds.

Sudan black B was prepared in absolute ethanol to a concentration of 0.1%. For comparative purposes this alcoholic solution was applied locally or by iontophoresis according to the following Table :-

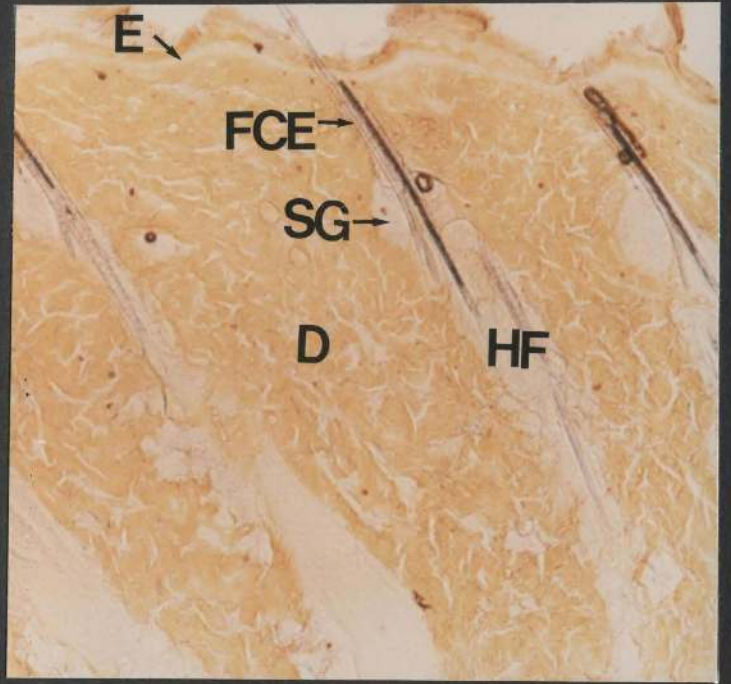
Experiment	Current (milliamperes)	Duration (minutes)	Figure
Local application	0	15	70
Positive iontophoresis	30	15	71
Negative iontophoresis	30	15	72

Figure 70

Local application (control) of 0.1% (W/V) sudan black B in absolute ethanol for 15 minutes

A cryostat section stained with tartrazine, mounted in aquamount and photographed immediately after mounting (x 40)

A brownish stain (sudan black B) is visible in the follicular canal epidermis (FCE), the sebaceous glands (SG) and in the lower follicular walls (HF). No staining is observed in the epidermis (E) or in the dermis (D).



## Figure 71

Positive iontophoresis of 0.1% (W/V) sudan black B in absolute ethanol at 30 milliamperes for 15 minutes

A cryostat section stained and mounted as in Figure 70 (x 40)

The tracer is visible on the surface of the skin, but only slightly so in the sebaceous glands (SG) and the hair follicles (HF). No tracer is seen in the epidermis (E) or in the dermis (D).

The location and distribution of the tracer is similar to that described in Figure 70.

## Figure 72

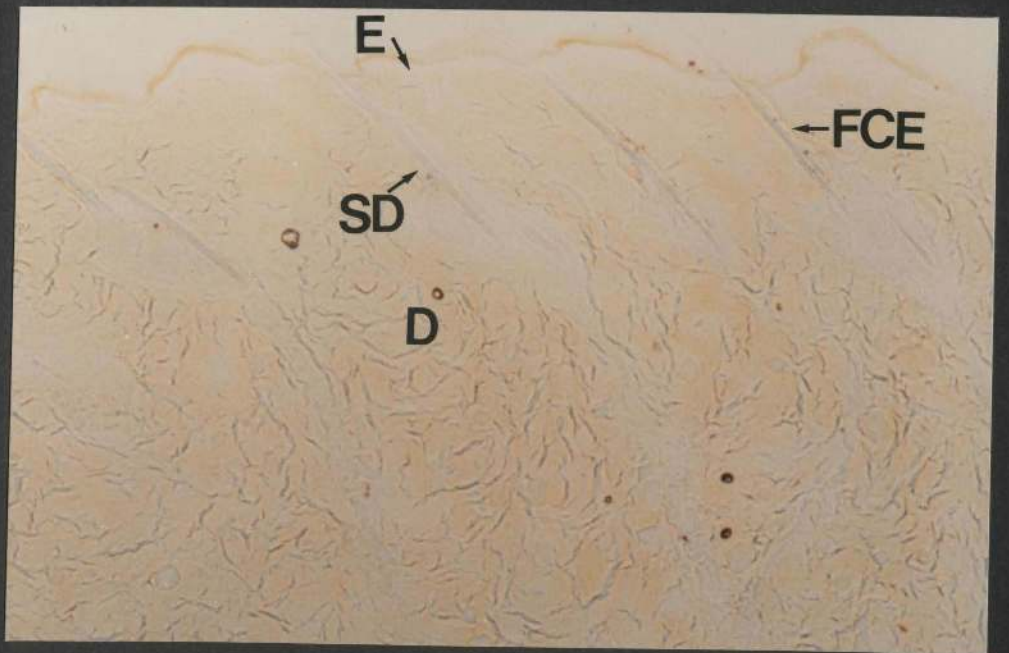
Negative iontophoresis of 0.1% (W/V) sudan black B in absolute ethanol at 30 milliamperes for 15 minutes

A cryostat section stained and mounted as in Figure 70 (x 40)

The dye is slightly visible in the follicular canal epidermis (FCE) and in the regions of the ducts of the sebaceous glands (SD). Other structures, including the epidermis (E) and the dermis (D), are devoid of the tracer.

The extent of penetration of sudan black B in this section resembles once again that described in Figure 70.





### 3.4 Compound dyes

Since Jenner's stain contains cationic (methylene blue) and anionic (eosin) portions, it seemed to be ideal for investigating the effect of both positive and negative iontophoresis on the penetration of such a stain into the skin.

Jenner's stain was prepared in absolute ethanol to a concentration of 0.5% and applied to the surface of the skin locally or by iontophoresis as presented in the following Table :-

Experiment	Current (milliamperes)	Duration (minutes)	Figure
Local application	0	15	73
Positive iontophoresis	30	15	74
Negative iontophoresis	30	15	75

All the cryostat sections were mounted in a water-based embedding medium (Aquamount, Gurr microscopy materials, BDH) and photographed immediately afterwards.



Figures 73a and 73b

Local application (control) of 0.5% (W/V) Jenner's stain in absolute ethanol for 15 minutes

Figure 73a: A cryostat section (x 32)

A mixture of red (eosin) and blue (methylene blue) colours is seen in the superficial part of the skin.

Figure 73b: A cryostat section stained with tartrazine (x 32)

It is apparent that the bluish-red stain is present on the surface of the skin. In addition, a very pale blue colour (methylene blue) may be observed in the epidermis (E), but it does not extend into the underlying connective tissue (D). Both the hair follicles (HF) and the sebaceous glands (SG) remain unstained.



## Figure 74

Positive iontophoresis of 0.5% (W/V) Jenner's stain in absolute ethanol at 30 milliamperes for 15 minutes

A cryostat section (x 32)

A blue colour (methylene blue portion of the stain) is evident in the epidermis (E), the follicular canal epidermis (FCE), some sebaceous glands (SG), and in the dermis (D) immediately adjacent to these structures. The penetration is not uniform through the skin, that is, some parts of the epidermis and some hair follicles show very little or no staining. However no red colour (eosin portion of the stain) is visible in this section.

## Figure 75

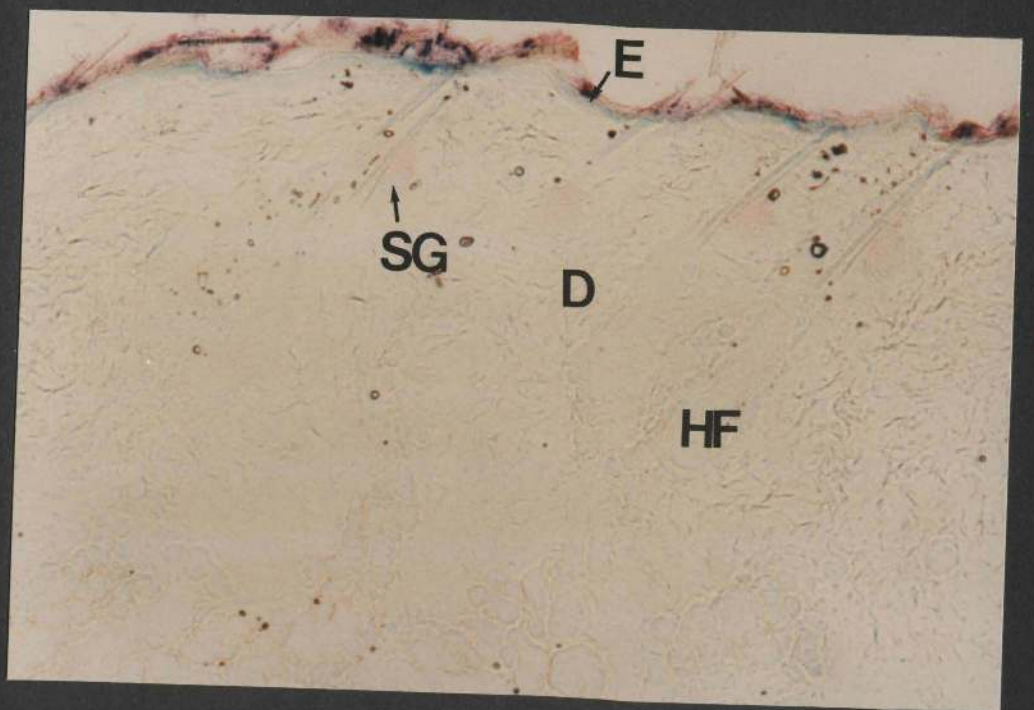
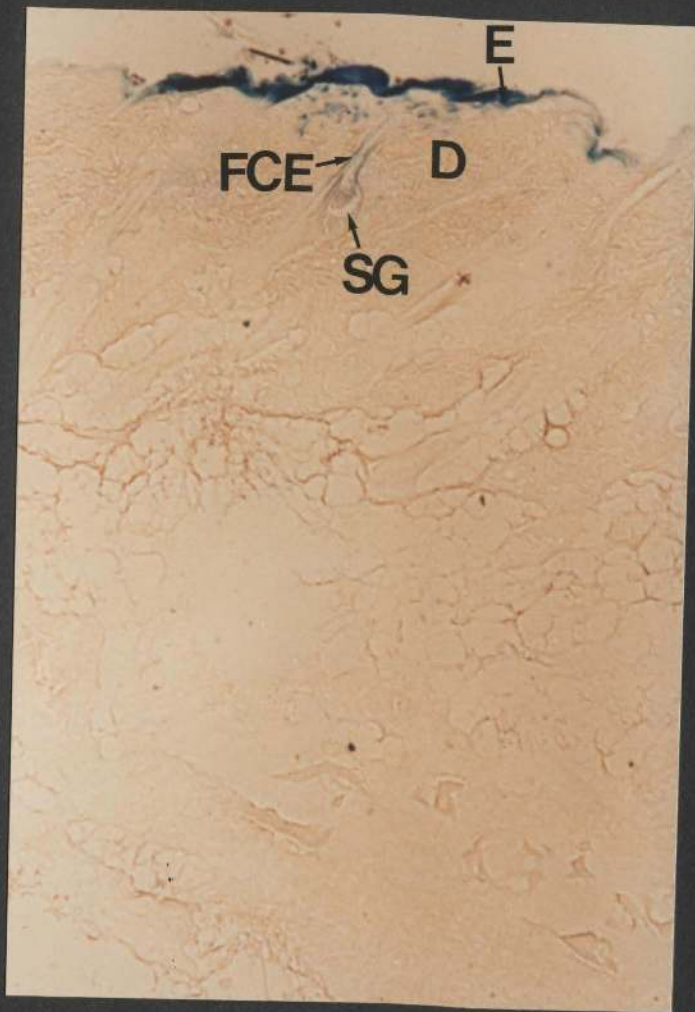
Negative iontophoresis of 0.5% (W/V) Jenner's stain in absolute ethanol at 30 milliamperes for 15 minutes

A cryostat section (x 32)

The bluish-red dye is visible on the surface of the skin. A pale blue stain (methylene blue portion) is seen in the epidermis (E) and occasionally in the follicular canals, a result similar to that described in Figure 73.

Significantly, a red colour (eosin portion of the stain) is evident in the sebaceous glands (SG).

Other structures, including the hair follicles (HF) and the dermis (D), remained relatively unstained.



**VOLUME**

**2**

Th A 811

1812

1812

1812

1812



CONTINUATION  
OF  
CHAPTER 3  
(RESULTS)





### 3.5 Lanthanum

Many materials have the property of being electron-dense and thus can be visualized directly in ultrathin sections examined with the electron microscope. These materials include lanthanum, horseradish peroxidase and ferritin. Lanthanum is undoubtedly the most popular tracer substance and has been used to study the external surface coat of cardiac (Martinez, Palomo *et al.*, 1973) and epidermal (Krawczyk, 1976) cells. It has also been used to study the intercellular spaces and junctional complexes of many tissues, including the heart and the liver (Revel and Karnovsky, 1967; Goodenough and Revel, 1970), the exocrine pancreas (Leeson and Leeson, 1982), oral epithelium (Shimono and Clementi, 1976), adipose tissue (Blanchette-Mackie and Scow, 1982), and the skin (Hashimoto, 1971). Furthermore, lanthanum has also served to investigate the permeability of the endothelium of blood vessels (Haack *et al.*, 1981), and the permeability of the amniotic epithelium (King, 1983). Finally, and most significantly, lanthanum has been used in determining the site and nature of the cutaneous barrier (Elias and Friend, 1975; Wolff and Schreiner, 1968), as well as barriers in other epithelia such as keratinized and non-keratinized oral epithelium (Squier and Rooney, 1975; Squier and Edie, 1983). The methods used in these barrier studies include topical application and intradermal injection of solutions containing a lanthanum salt as well as incubation of tissue samples in solutions containing lanthanum. All of these methods have been adopted in the present study.

The following experiments were undertaken to investigate (1) the extent of penetration of this electron-dense tracer from the surface into the skin following local application and iontophoresis, (2) factors which may affect such penetration, including the concentration of the tracer substance in the presenting vehicle and the type of vehicle used, (3) preferential route(s) of penetration into the skin, and (4) the site of the cutaneous barrier. In all these experiments, skin specimens were prepared for transmission electron microscopy according to the procedures described elsewhere (page 101). Penetration was judged by the location and distribution of electron-dense deposits in stained or unstained ultrathin sections. To confirm such findings, energy-dispersive X-ray (EDX) analyses were carried out using the scanning electron microscope on the "faces" of resin blocks from which the ultrathin sections were produced.

### 3.5.1 Intradermal injection

A 1% aqueous lanthanum nitrate solution was injected intradermally and biopsies were taken 15 minutes later. The results obtained are shown in Figures 76 a - i.

Figure 76a: A scanning electron microscope image taken from the "face" of a resin block. The structures present in this micrograph include the epidermis (E), sebaceous glands (SG) and parts of the hair follicles (HF). The various epidermal layers are clearly identified and include the stratum corneum (SC), the stratum granulosum (SG) containing keratohyalin granules, the stratum spinosum (SS) and the stratum basale (SB).

EDX analyses were carried out on different sites in the epidermis, the sebaceous glands and the hair follicles, and some of the analyzed areas are outlined by the electron beam (arrows). In addition, areas on the block-face immediately adjacent to the skin were also analyzed. The spectra obtained are shown following the micrograph. By comparing the spectrum obtained from the embedding medium alone with those obtained from the embedding medium plus skin, it appears that the lanthanum peaks are originating from the skin specimen.

With regard to its location within the skin, EDX analyses confirmed that lanthanum was present in the epidermis, the sebaceous glands and in the hair follicles. The precise localization of lanthanum within these structures was determined by the transmission electron microscope.



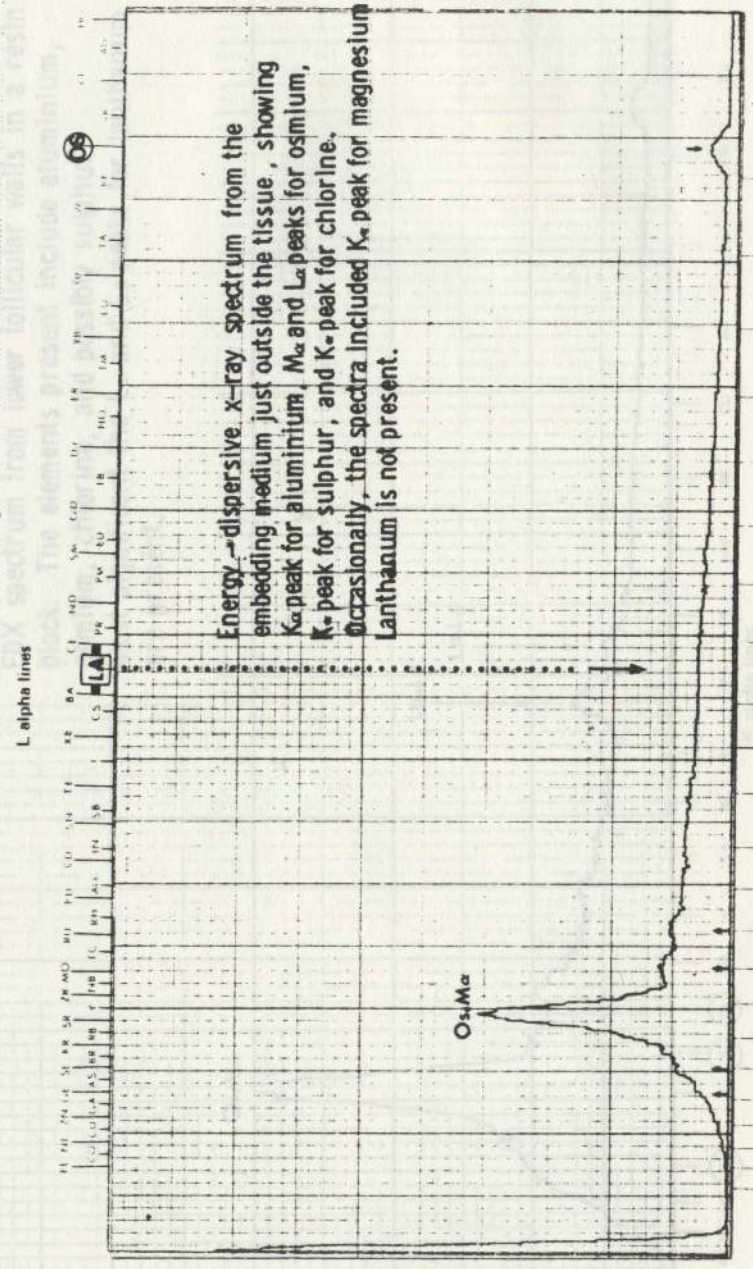
1529 100.00 SAUEM

15KV



Laboratory .....  
 Sample ..... **Intracutaneous injection of a 1 percent aqueous lanthanum nitrate solution.** .....  
 KeV ..... **15** .....  
 Seconds ..... **100** .....  
 Take off Angle ..... **33** .....  
 Date .....

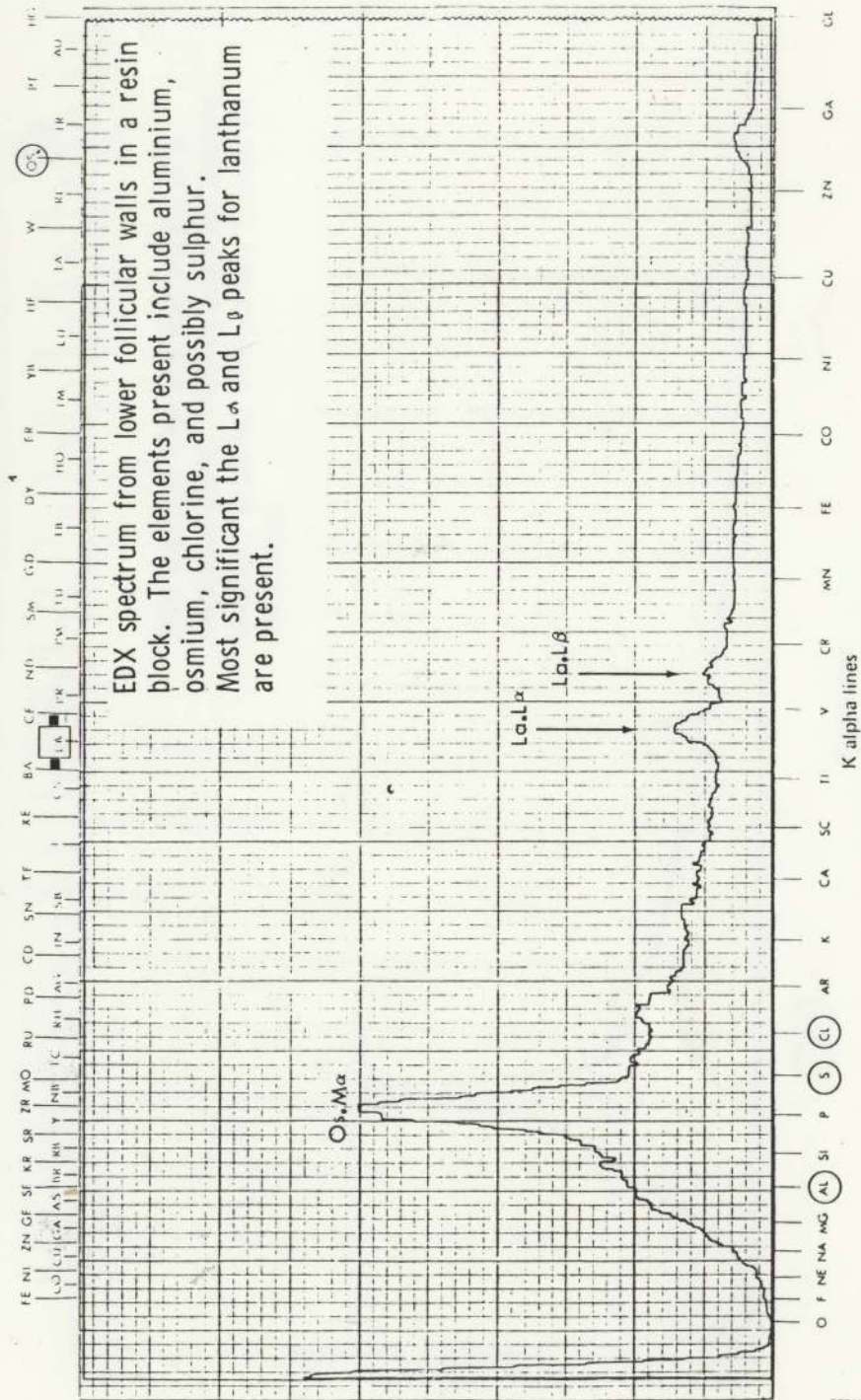
Researcher .....



Energy-dispersive x-ray spectrum from the embedding medium just outside the tissue, showing  $K_{\alpha}$  peak for aluminium,  $M_{\alpha}$  and  $L_{\alpha}$  peaks for osmium,  $K_{\alpha}$  peak for sulphur, and  $K_{\alpha}$  peak for chlorine. Occasionally, the spectra included  $K_{\alpha}$  peak for magnesium. Lanthanum is not present.

Laboratory St. Andrews University S.E.M. Unit. Researcher ..... Date .....  
 Gatty Marine Lab.  
 Sample ..... Intracutaneous injection of a 1 percent aqueous lanthanum nitrate solution .....  
 KeV ..... 15 ..... Seconds ..... 100 ..... Take off Angle ..... 33° .....

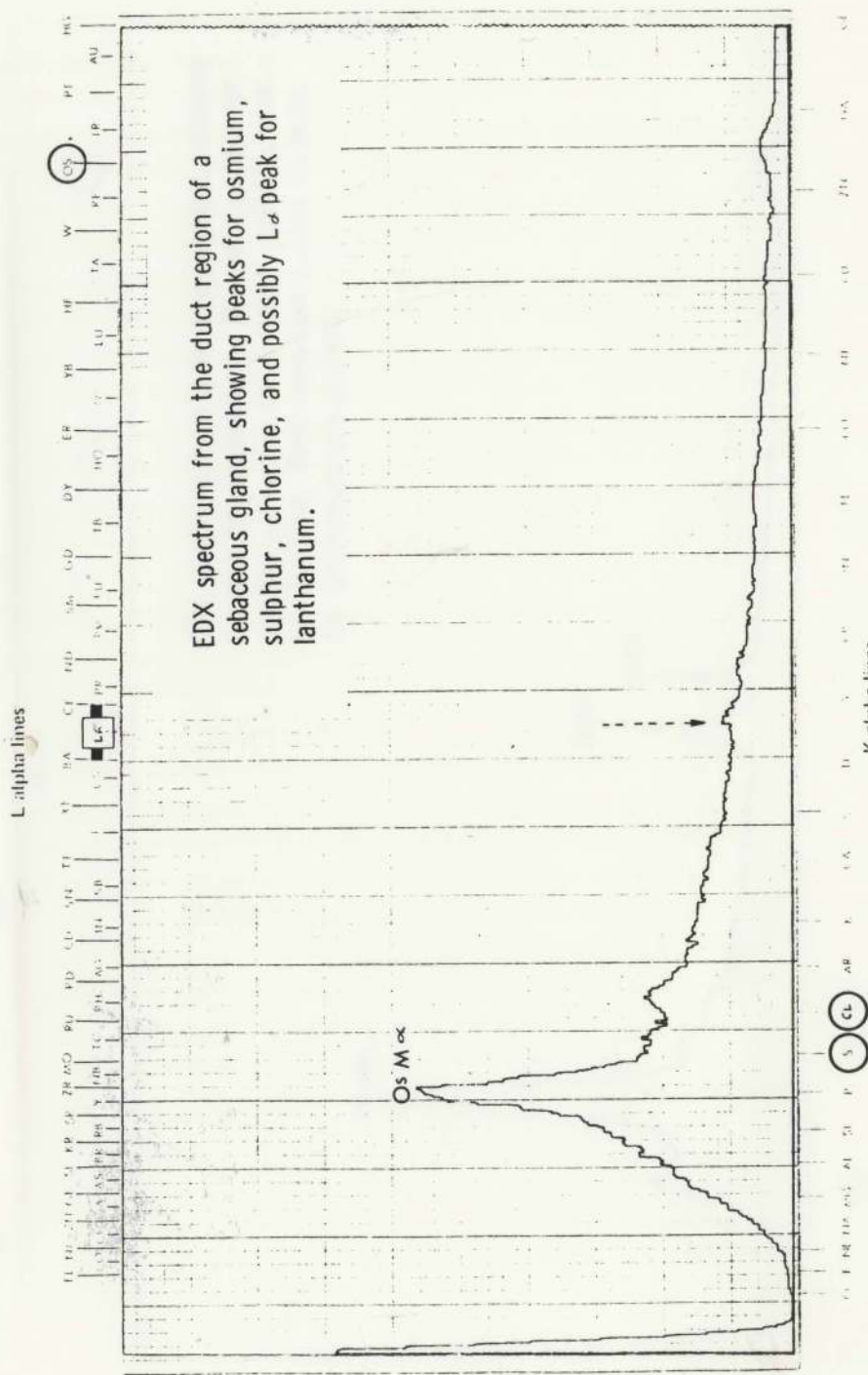
L alpha lines



EDX spectrum from lower follicular walls in a resin block. The elements present include aluminium, osmium, chlorine, and possibly sulphur. Most significant the  $L\alpha$  and  $L\beta$  peaks for lanthanum are present.



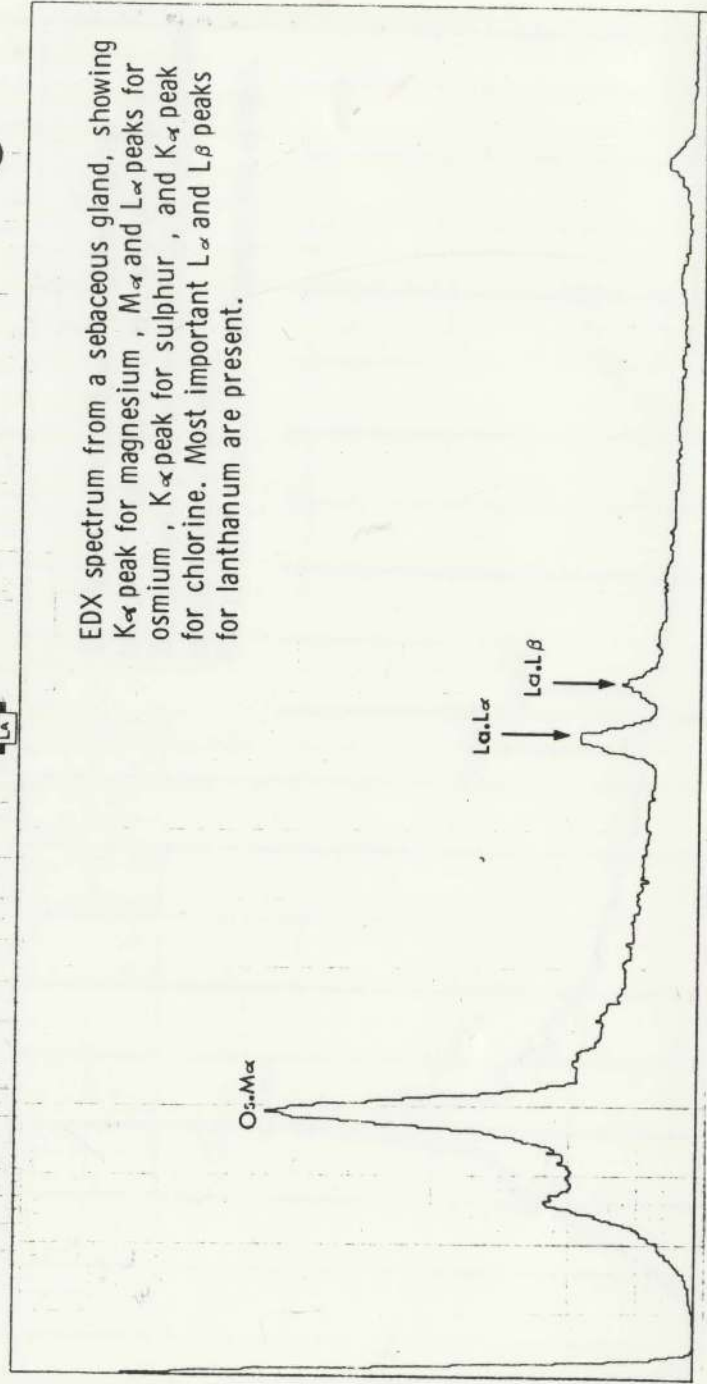
Laboratory **St. Andrews University S.E.M. Unit.** Date .....  
**Gatty Marine Lab.** Researcher .....  
 Sample **Intracutaneous injection of a 1 percent aqueous lanthanum nitrate solution.** Take off Angle **33°**  
 KeV **15** Seconds **100**





Intracutaneous injection of a 1 percent aqueous lanthanum nitrate solution. 33°

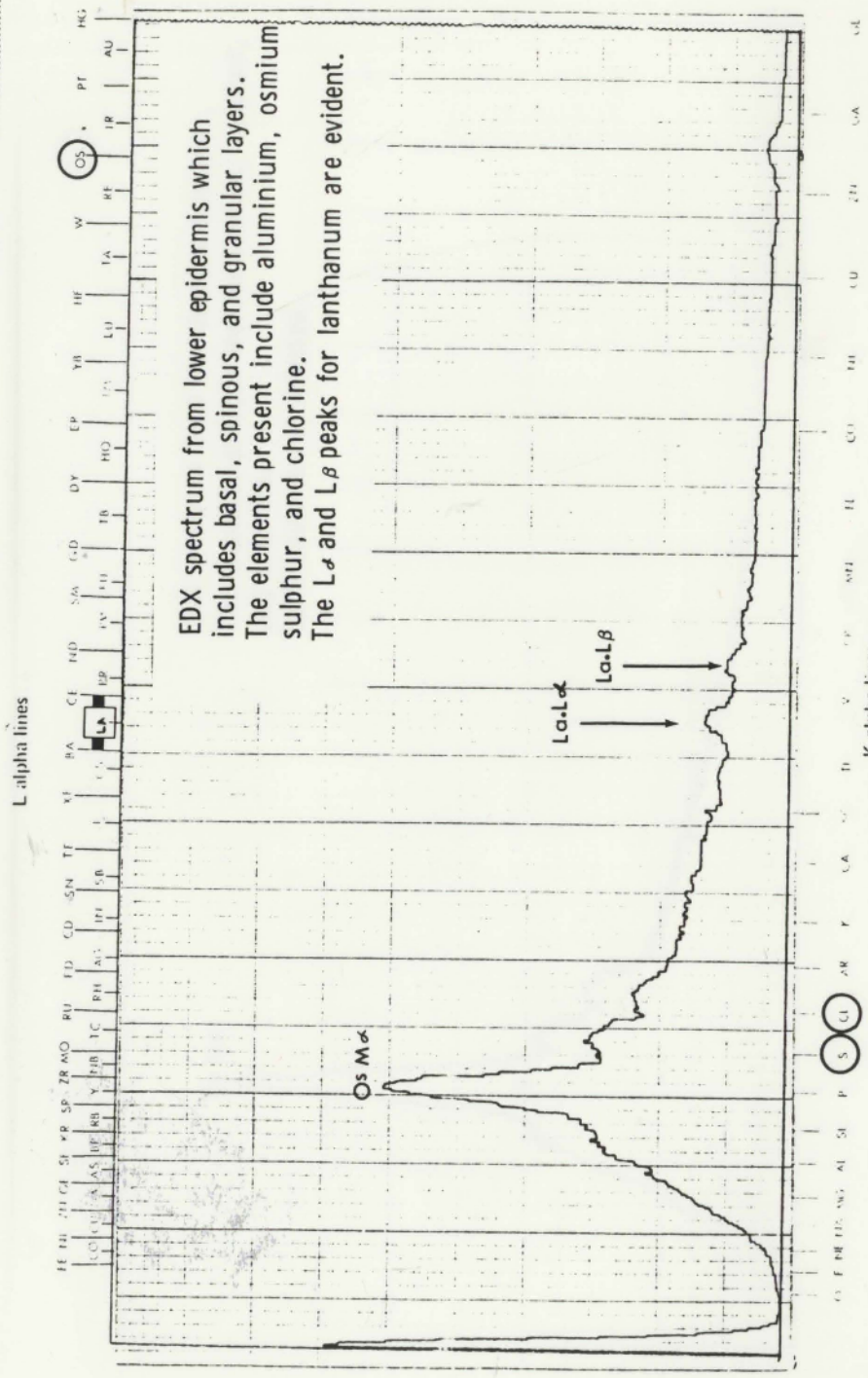
100



EDX spectrum from a sebaceous gland, showing K $\alpha$  peak for magnesium, M $\alpha$  and L $\alpha$  peaks for osmium, K $\alpha$  peak for sulphur, and K $\alpha$  peak for chlorine. Most important L $\alpha$  and L $\beta$  peaks for lanthanum are present.

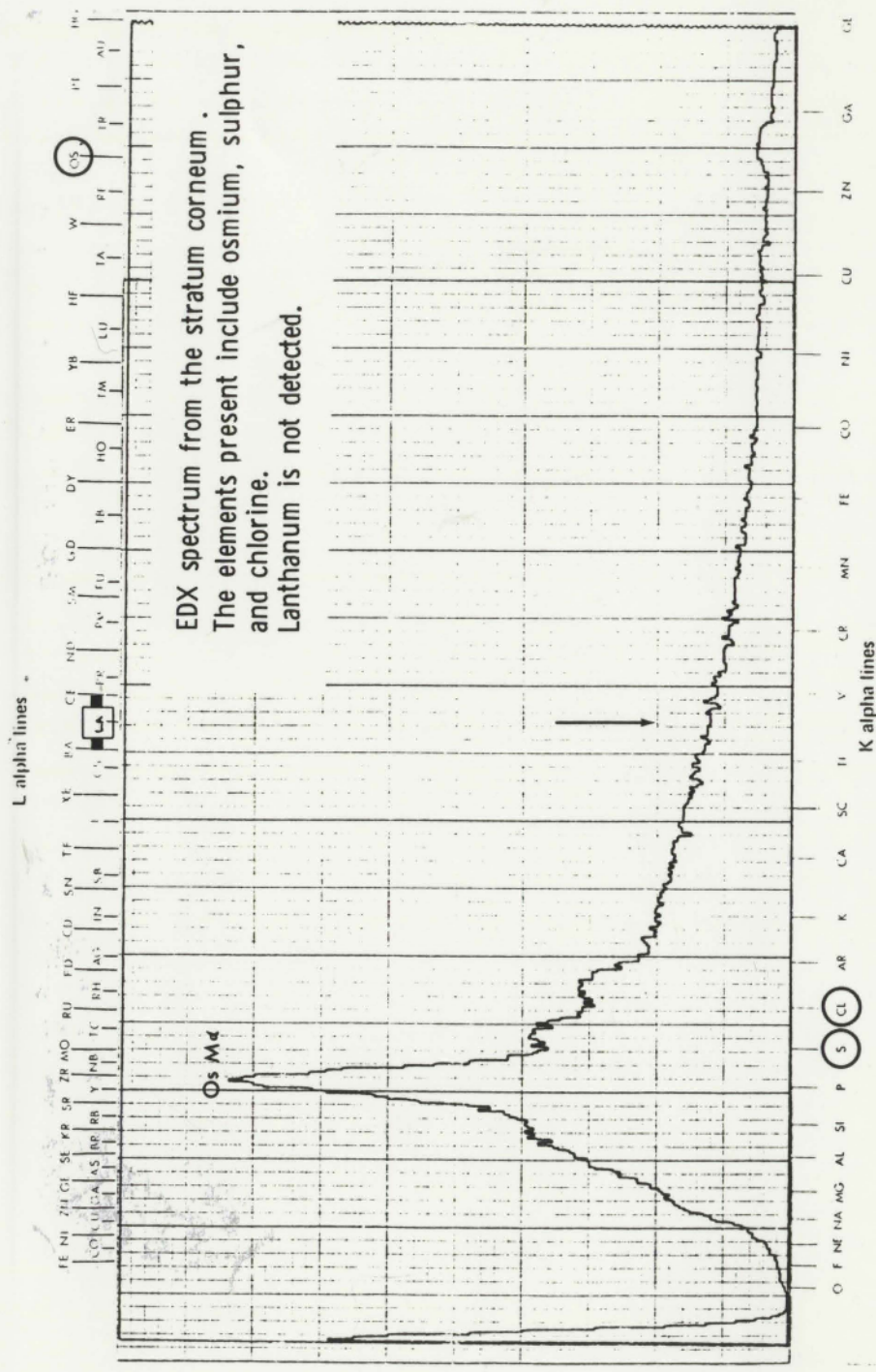
MS 5 dl

Laboratory **St. Andrews University S.E.M. Unit.** Date .....  
**Catty Marine Lab.** Researcher .....  
 Sample **Intracutaneous injection of a 1 percent aqueous lanthanum nitrate solution.**  
 KeV **15** Seconds **100** Take off Angle **33°**



EDX spectrum from lower epidermis which includes basal, spinous, and granular layers. The elements present include aluminium, osmium sulphur, and chlorine. The  $L\alpha$  and  $L\beta$  peaks for lanthanum are evident.

Laboratory **St. Andrews University S.E.M. Unit.** Researcher: \_\_\_\_\_ Date: \_\_\_\_\_  
**Gatty Marine Lab.**  
 Sample **Intracutaneous injection of a 1 percent aqueous lanthanum nitrate solution.**  
 KeV **15** Seconds **100** Take off Angle **33°**



**EDX spectrum from the stratum corneum.**  
 The elements present include osmium, sulphur,  
 and chlorine.  
 Lanthanum is not detected.

Figure 76b: This transmission electron micrograph from the lower region of a hair follicle features portions of outer root sheath cells (ORS) (x 14,000).

Lanthanum is present in the intercellular spaces, including regions of desmosomal attachments (D). Occasionally small patches of the dense material are seen inside the cells close to the plasma membranes (arrow). The X-ray analysis confirmed that lanthanum was present in the lower region of the hair follicle.



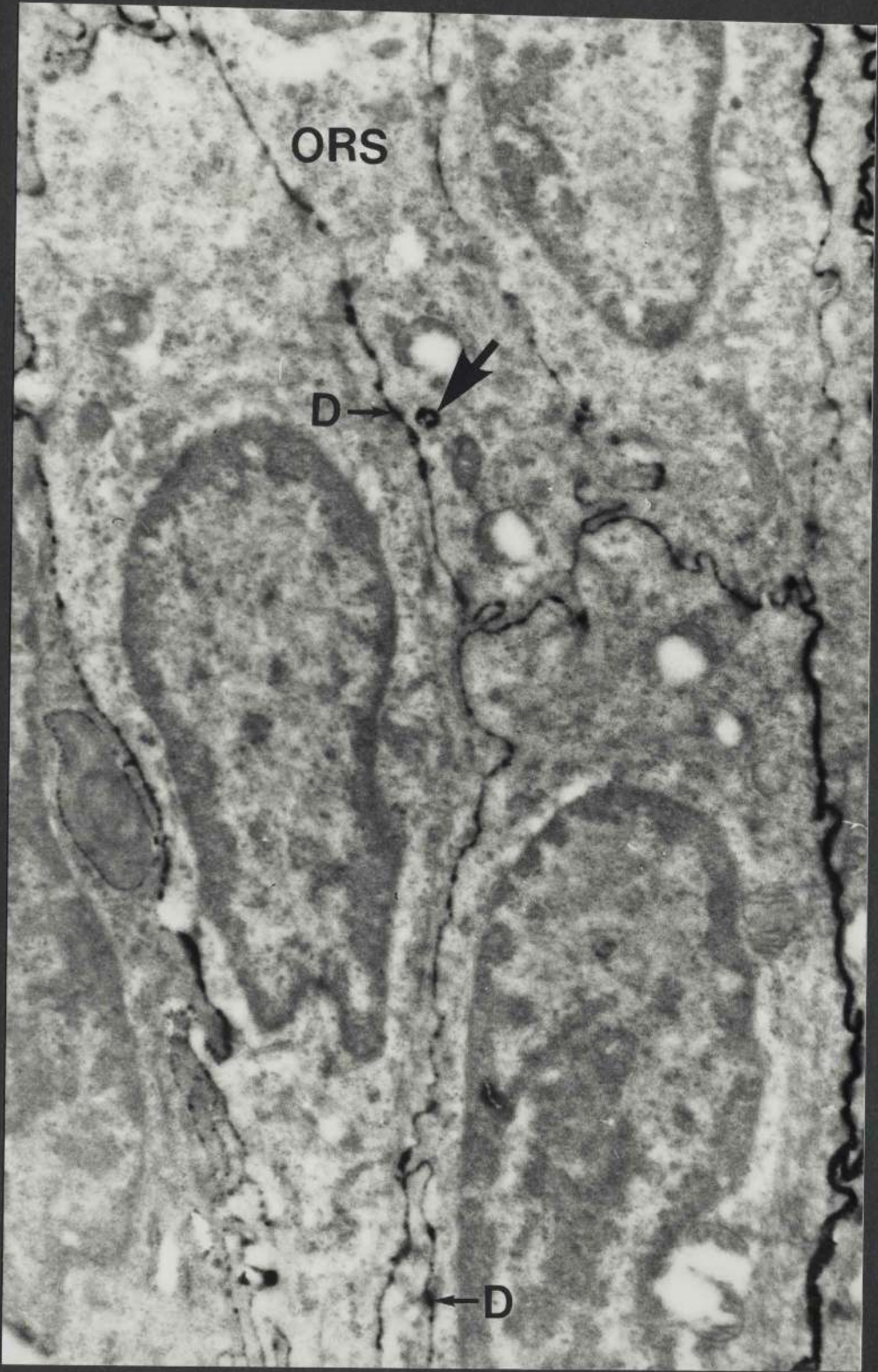


Figure 76c: This transmission electron micrograph is from a tangential section of a hair follicle just below the level of the base of a sebaceous gland (SG) (x 9,280).

A hair shaft is visible in the centre of the field. It consists of a cortex (CO), which forms the bulk of the hair, surrounded by a cuticle (CU) whose free margins are directed upwards. Adjacent to the hair is the inner root sheath consisting of Henle's layer (HE), Huxley's layer (HU) and the inner root sheath cuticle (CI). The outer root sheath (ORS) is surrounding the inner root sheath.

Lanthanum (arrows) is present in the intercellular spaces in the outer and inner root sheaths, except those of the cuticle of the inner root sheath.



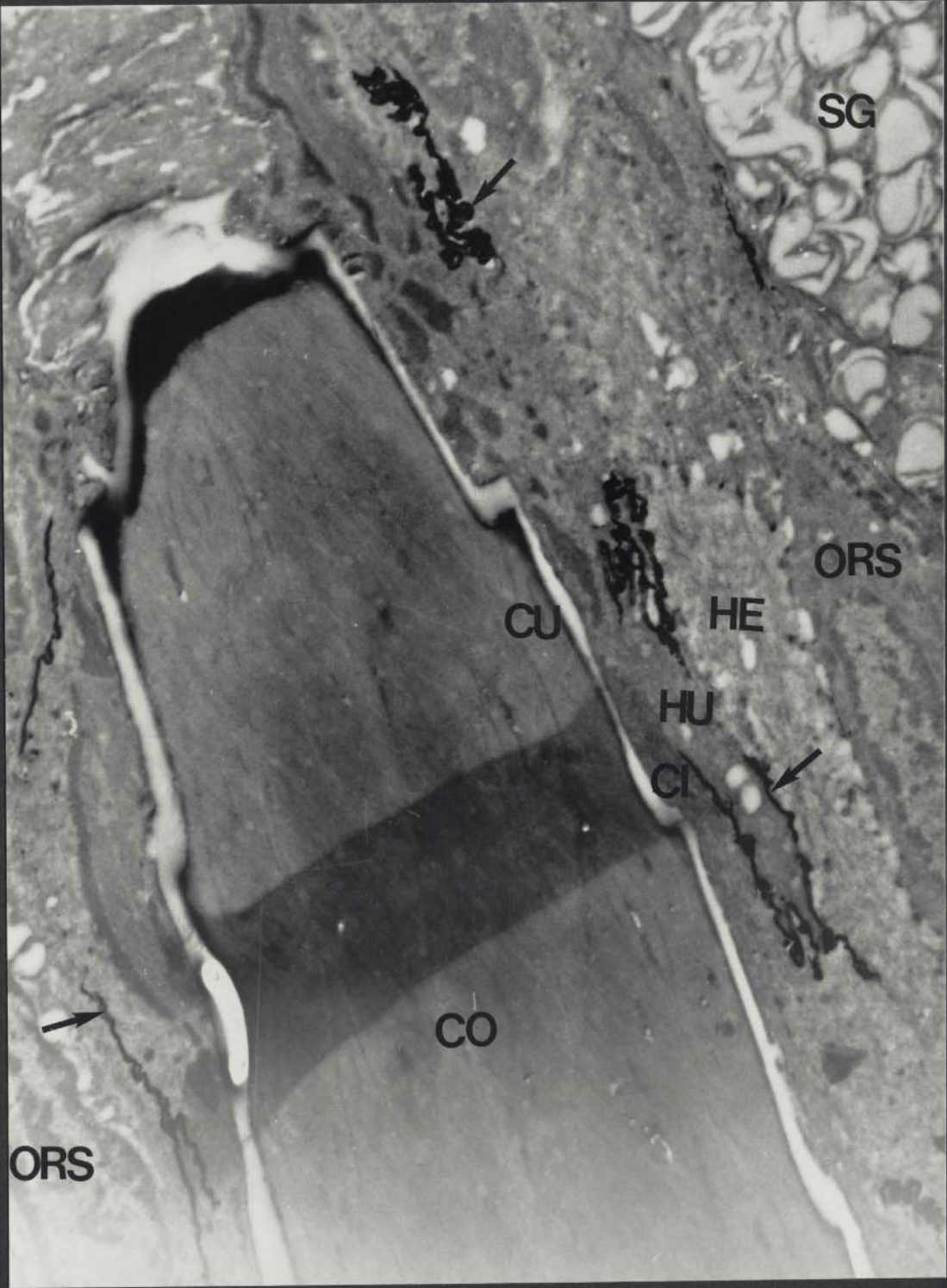




Figure 76d: This micrograph presents a section of a hair follicle at the level of the entry of the duct (SD) of a sebaceous gland into the follicle canal (x 9,280).

At this level both the stratum corneum (SC) of the follicular canal epidermis and the inner root sheath (IRS) terminate.

Lanthanum (arrows) is evident in the intercellular spaces between the cells of the outer root sheath (ORS). It appears that the tracer does not extend between the keratinized cells of the duct of the sebaceous gland. It is difficult to determine whether or not lanthanum is present within the lumen of this duct due to the lack of contrast resulting from the presence of cellular debris in this region of the gland.

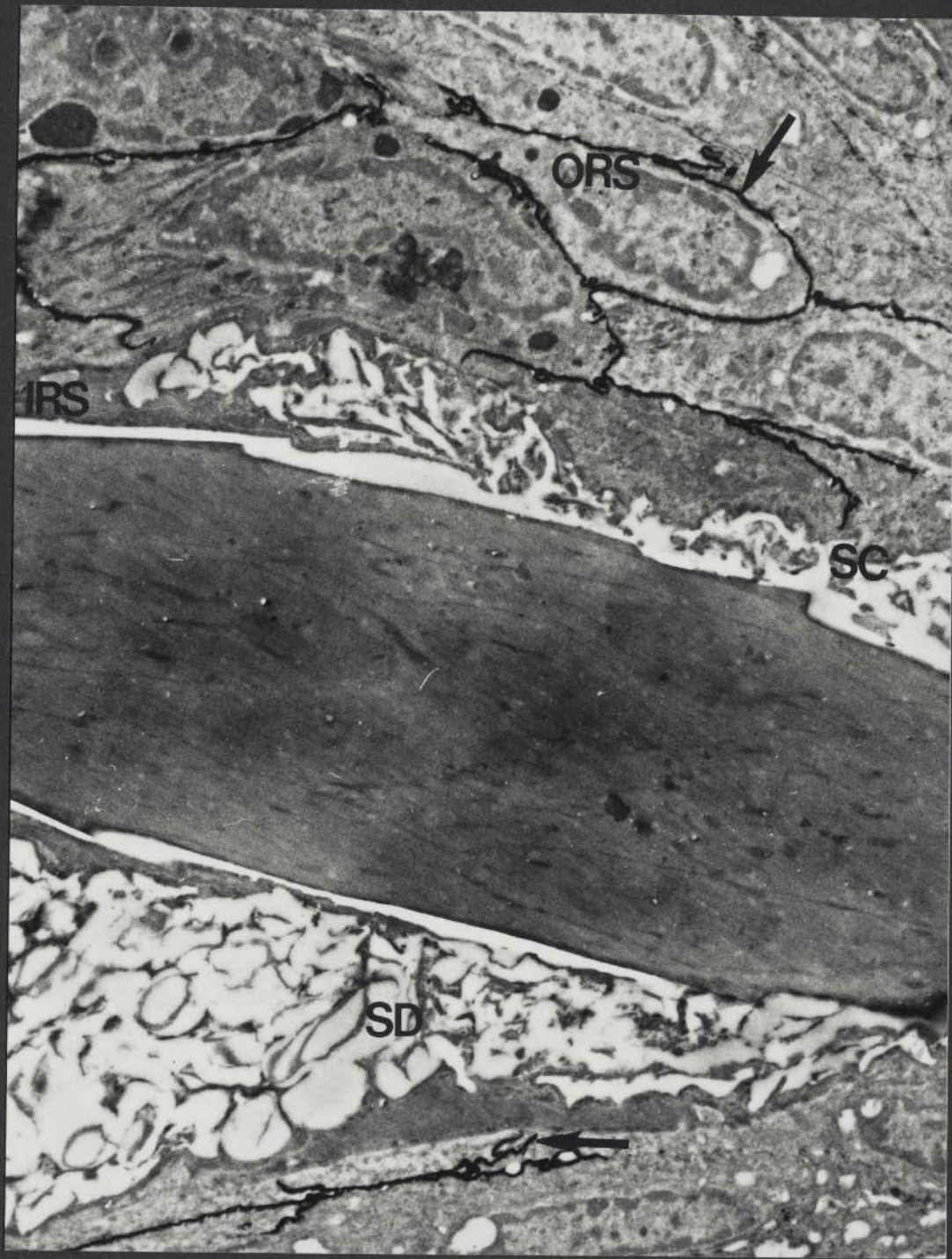


Figure 76e: This micrograph is from a section at the periphery of a sebaceous gland. It illustrates sebaceous cells at different stages of maturation. (x 8,352).

In the undifferentiated or peripheral cell (P) the nucleus is flat and elongated. No lipid droplets are present in these cells. PD is a partially differentiated cell, the cytoplasm of which contains a small number of lipid droplets (Li) of varying sizes. The interior of a fully differentiated or mature cell (FD) is packed with lipid droplets of roughly similar sizes. Occasionally a cloudy substance, probably squalene, is seen within the lipid droplets. Lanthanum is visible in the intercellular spaces between peripheral and partially differentiated sebaceous cells. The hemidesmosomes (Hd) uniting the peripheral sebaceous cells to the underlying basal lamina also contain tracer. Furthermore, lanthanum has permeated the desmosomal attachments (D) uniting adjacent sebaceous cells.



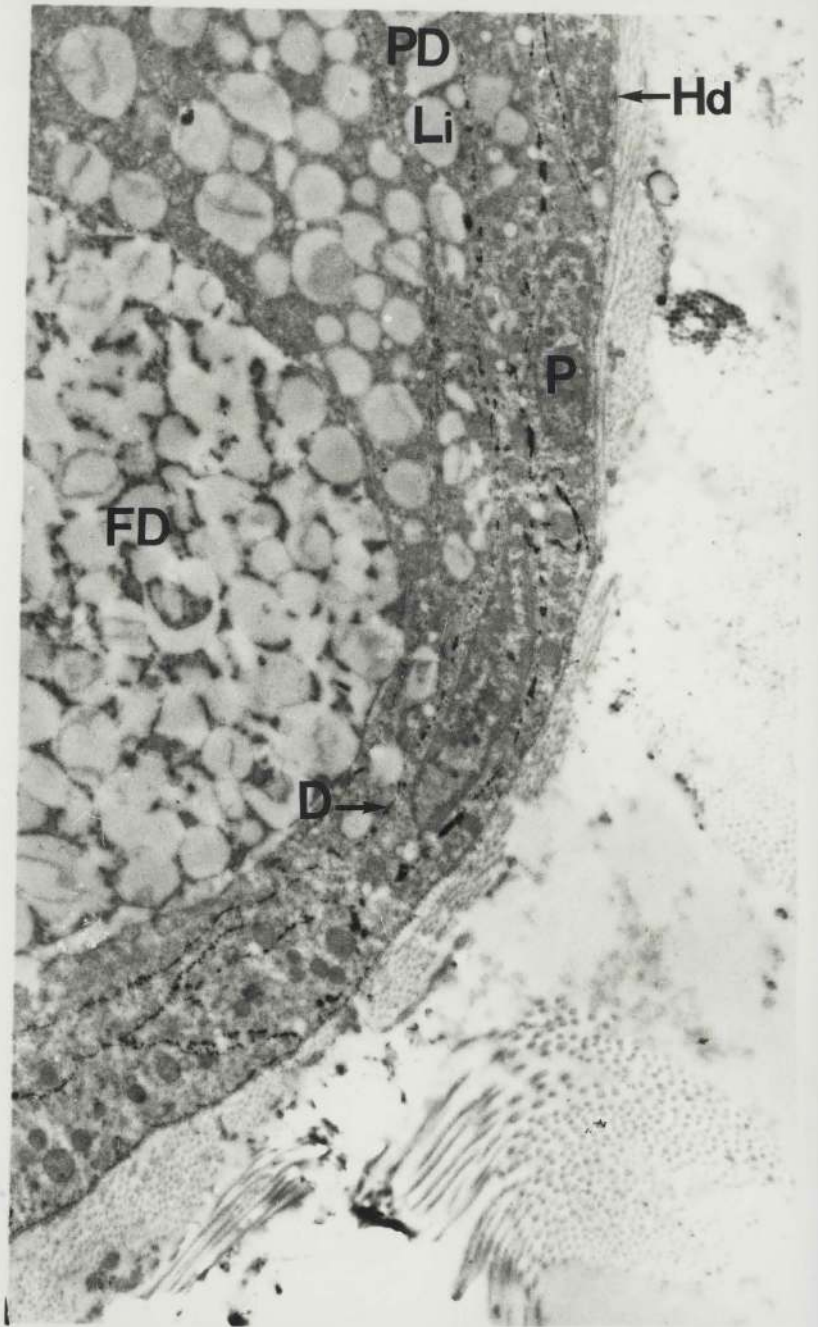


Figure 76f: This micrograph features portions of partially (PD) and fully (FD) differentiated sebaceous cells situated towards the duct region (x 9,280).

The nucleus (N) of the fully differentiated cell is dense and irregular in outline due to compression by adjacent lipid droplets (Li).

Lanthanum is confined to the intercellular spaces between partially and fully differentiated sebaceous cells (arrows).

Energy-dispersive X-ray analysis confirmed the presence of lanthanum in the sebaceous glands.

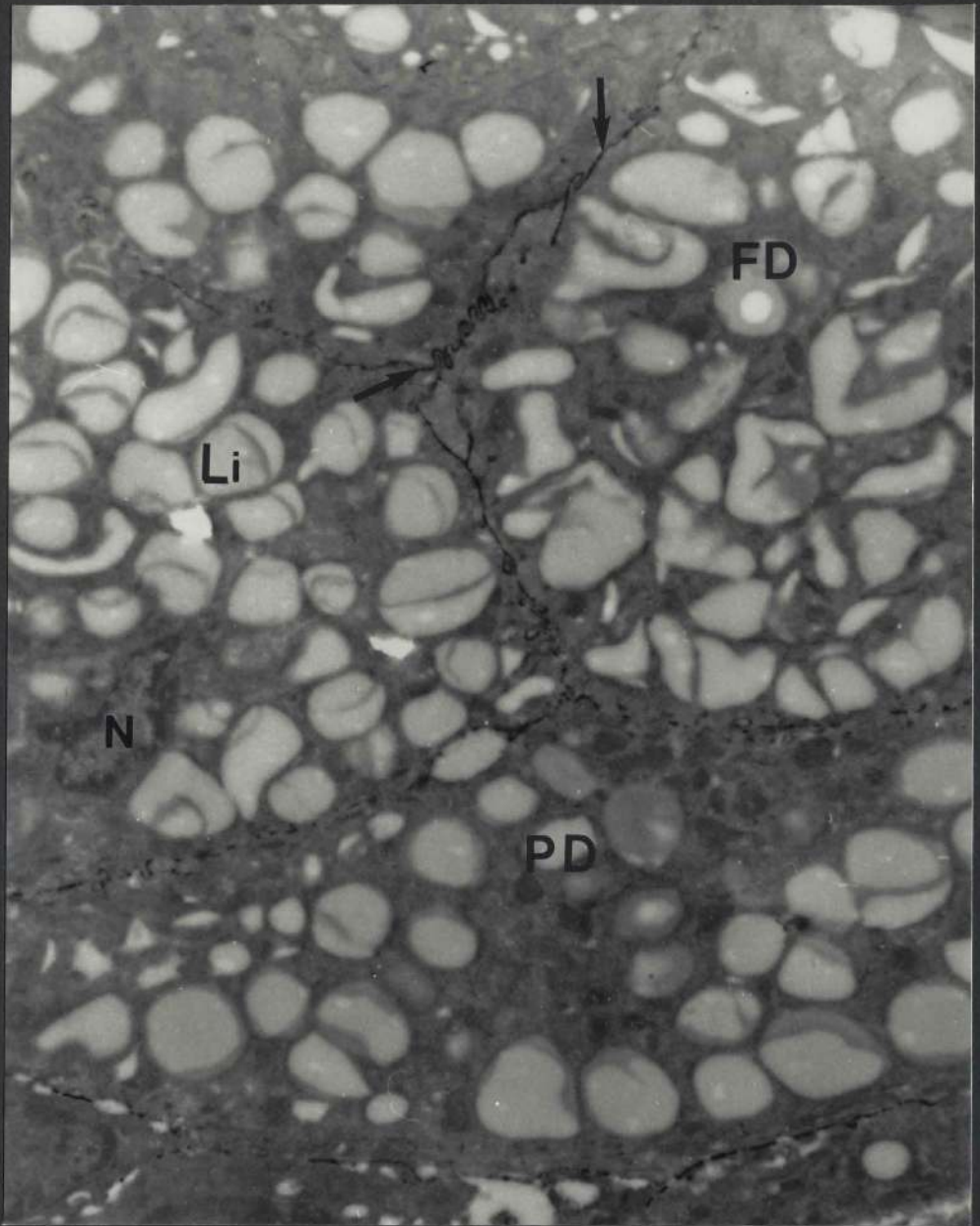


Figure 76g: Two transmission electron micrographs from the follicular canal epidermis of two hair follicles.

Micrograph 1. Included in this field are the viable layers of the hair canal epidermis (x 8,352).

Lanthanum is present in all intercellular spaces between basal (SB) and spinous (SS) cells of the canal epidermis. C indicates collagen in the dermis and Kh keratohyalin granules in the granular layer.

Micrograph 2. This field, obtained from the corneal (SC) and granular (SG) layers of a follicular canal epidermis, is of interest in that it shows lanthanum has entered the intercellular spaces between the granular cells, but does not extend into the intercellular space between the stratum granulosum and the stratum corneum or into the stratum corneum itself. The superficial surface of the stratum corneum is free from the tracer (x 11,136).

Energy-dispersive X-ray analysis confirmed the presence of lanthanum in the follicular canal epidermis.



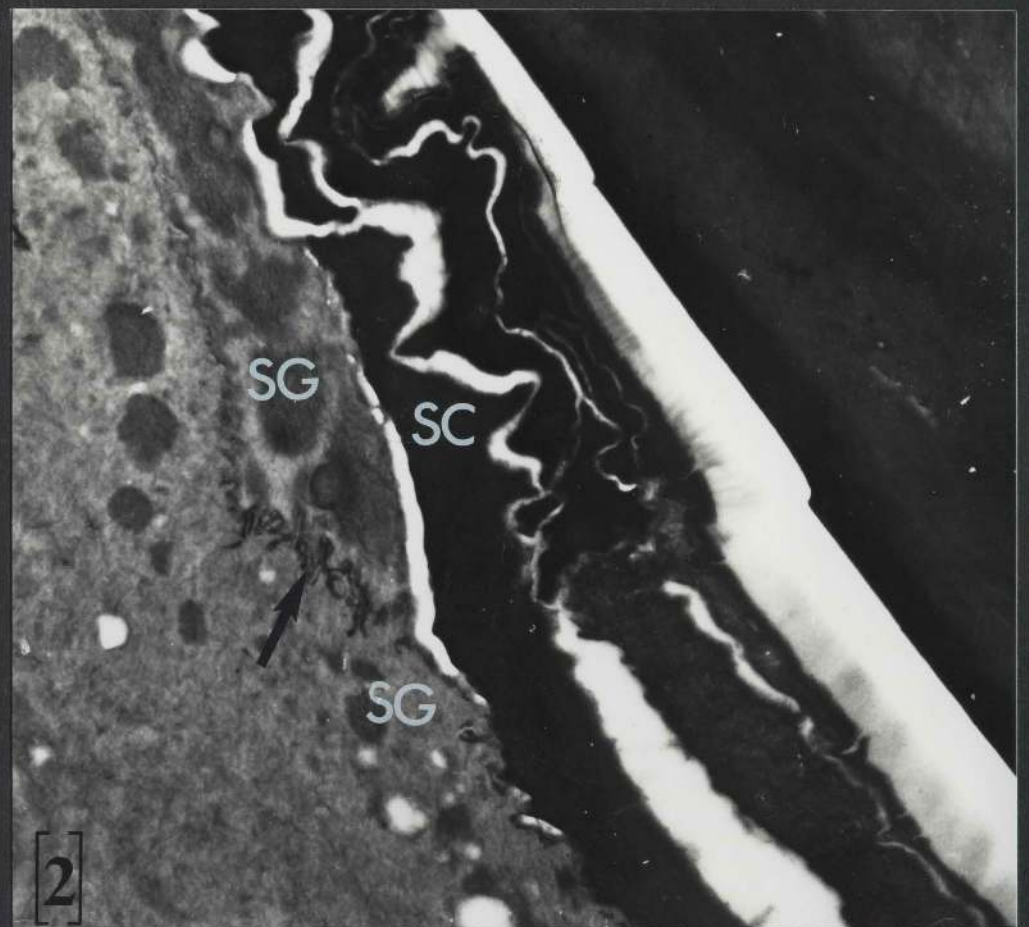
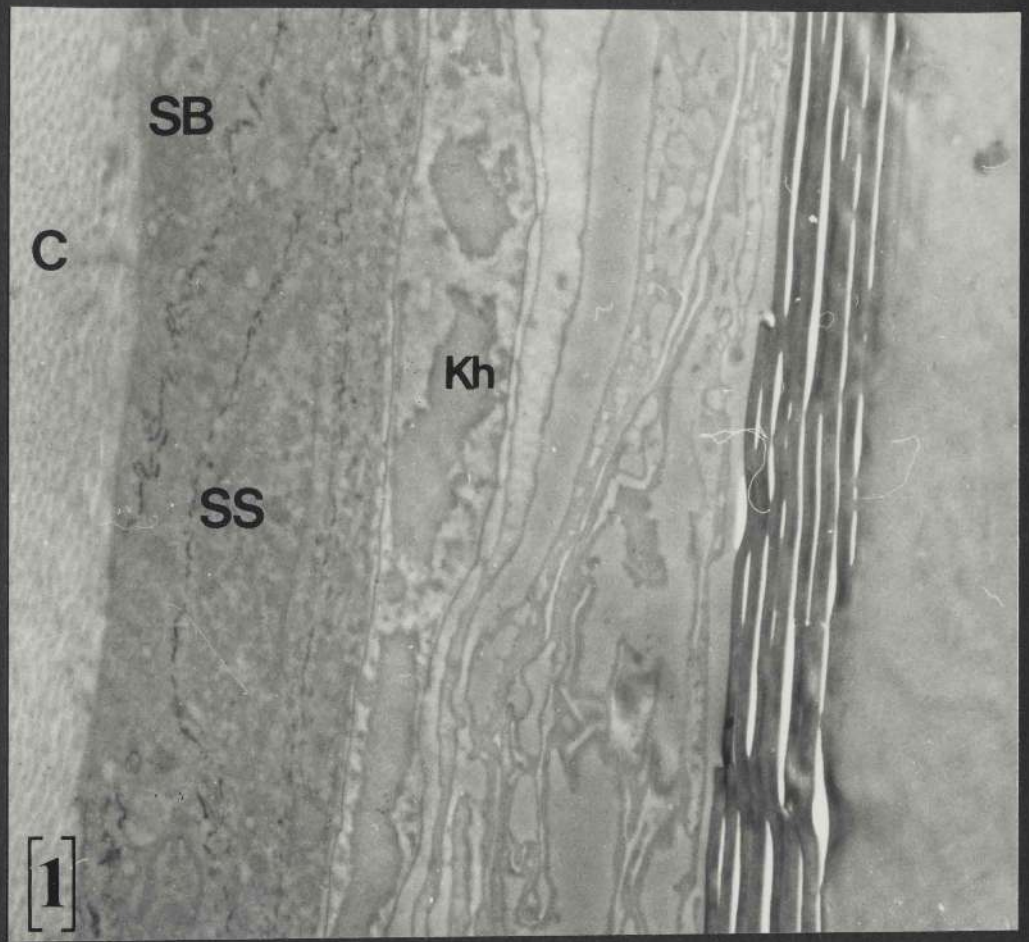


Figure 76h: This field features a portion of the deeper part of the lower epidermis and the papillary layer of the dermis. The former includes basal (SB) and spinous (SS) cell layers, and the latter contains collagen (C) (x 8,352).

Lanthanum has accumulated in all spaces between the basal and spinous cells, and in the region of the epidermal-dermal junction (EDJ). Furthermore, the tracer has permeated desmosomal attachments (D) uniting adjacent cells. These cells appear generally free from tracer; however, occasionally a small patch of electron-dense material (arrow) is seen inside the cells.

Energy-dispersive X-ray spectrum contained lanthanum when the analyzed area consisted of epidermis.



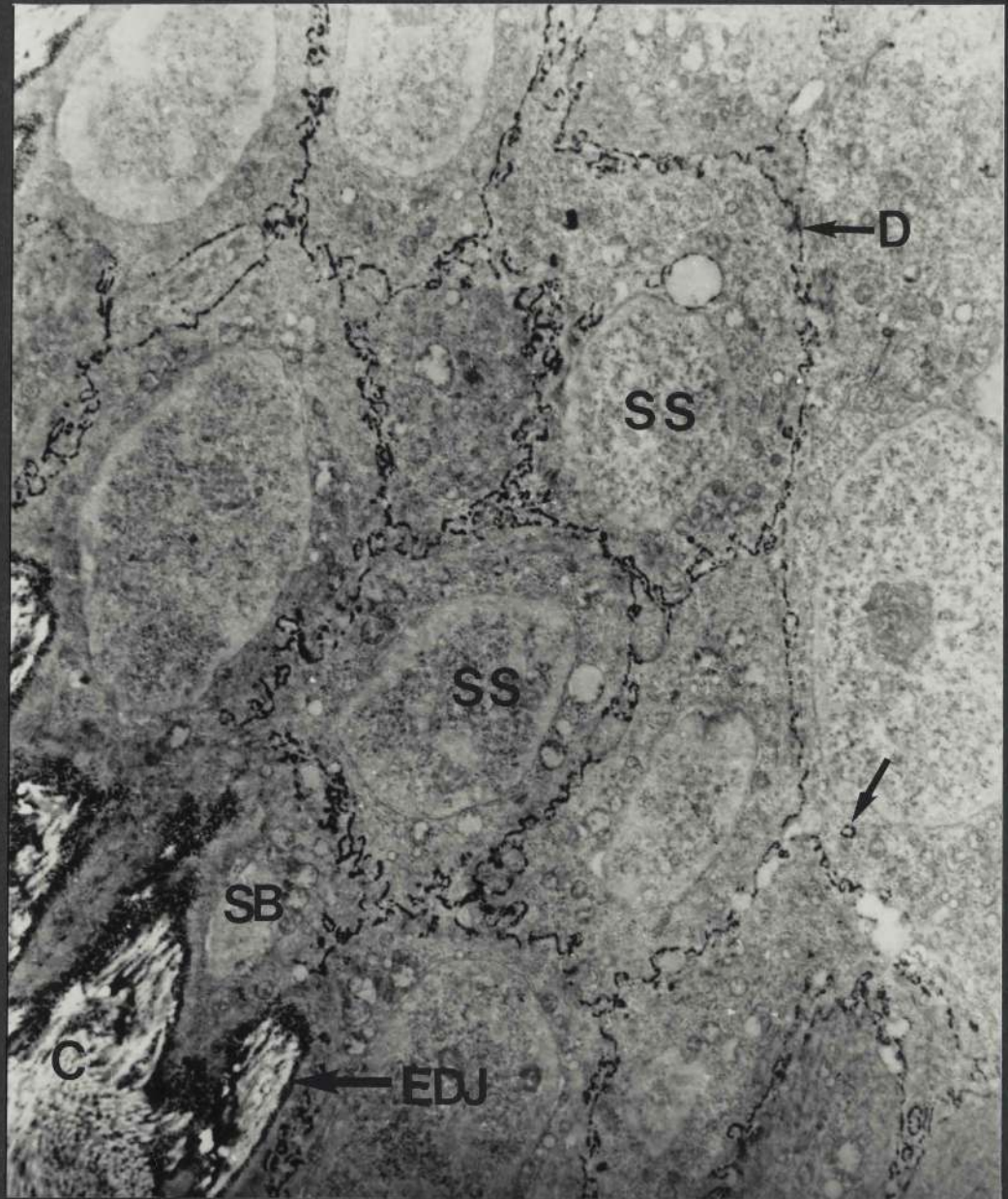


Figure 76i: This field spans a part of the epidermis and includes the upper part of the stratum spinosum (SS), the stratum granulosum (SG), the stratum corneum (SC) and keratohyalin granules (Kh) in the granular layer (x 11,136).

It is apparent that lanthanum is not only visible in the spaces between the spinous cells, but also in the intercellular spaces between the granular cells (arrow). However, no lanthanum has entered the intercellular space between the stratum granulosum and the stratum corneum or the spaces between the corneal cells themselves.

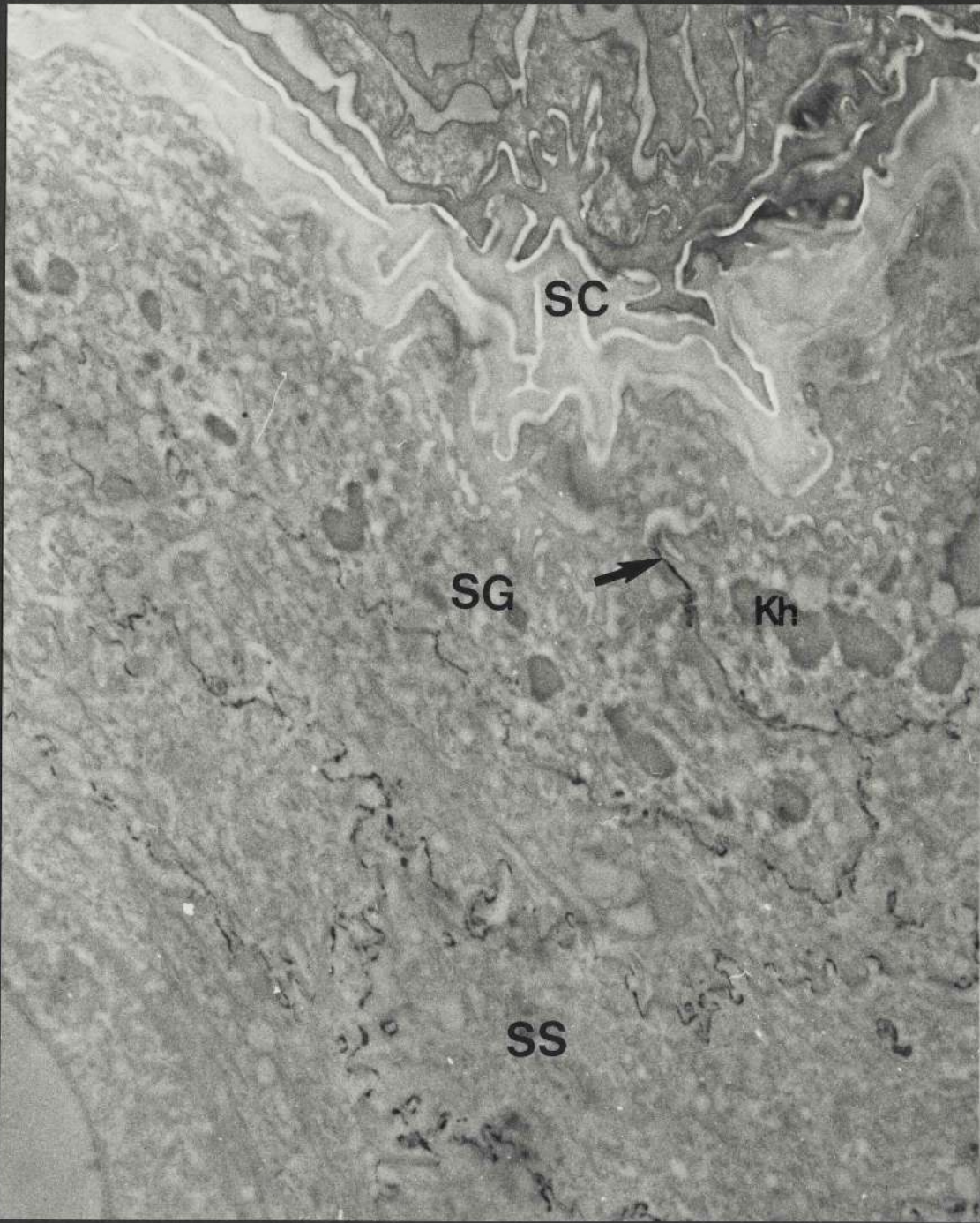
Finally, the tracer is not present on the surface of the stratum corneum.

#### Summary of results

Following intradermal injection, lanthanum permeates all the intercellular spaces between cells in the outer root sheath in the lower follicular walls. At a higher level, the tracer is evident in the intercellular spaces of the outer root sheath, and extends into the spaces between cells in Henle's and Huxley's layers of the inner root sheath, but not into those of the sheath cuticle. The tracer permeates all intercellular spaces in the sebaceous glands, including those lying towards the duct region.

In addition, lanthanum enters the epidermis and the follicular canal epidermis, accumulating in all intercellular spaces between basal, spinous, and granular cells. The level at which penetration is halted appears to be the intercellular space between the stratum granulosum and the stratum corneum. Energy-dispersive X-ray analysis confirmed the presence of lanthanum in hair follicles, sebaceous glands, and the epidermis.





### 3.5.2 Incubation method

Pieces of ventral (abdominal) skin were incubated in primary aldehyde fixative containing lanthanum nitrate (1% w/v) for 2.5 hours. They were subsequently washed for 15 minutes in cacodylate buffer and treated for 1 hour with the secondary osmium fixative, lanthanum nitrate being added to these two solutions to a concentration of 1%. The specimens were then dehydrated, embedded in araldite and sectioned on the ultramicrotome as described previously. The results obtained are shown in Figures 77 a - e. EDX analyses were carried out on the "faces" of the resin blocks following ultrathin sectioning, and the results obtained are reported in Figures 77 a - e.

Figure 77a: In this transmission electron micrograph, portions of the outer (ORS) and inner (IRS) root sheaths of a hair follicle at the base of a sebaceous gland (SG) are seen (x 8,352).

Lanthanum is evident in the intercellular spaces of the outer root sheath. The tracer has extended into the spaces between cells in Henle's (HE) and Huxley's (HU) layers of the inner root sheath but only occasionally appears in the sheath cuticle (C).

The EDX spectrum, which was obtained from the face of the araldite block from which this micrograph was produced, contained peaks for lanthanum when the analyzed area consisted of the follicular walls below the level of the sebaceous gland.



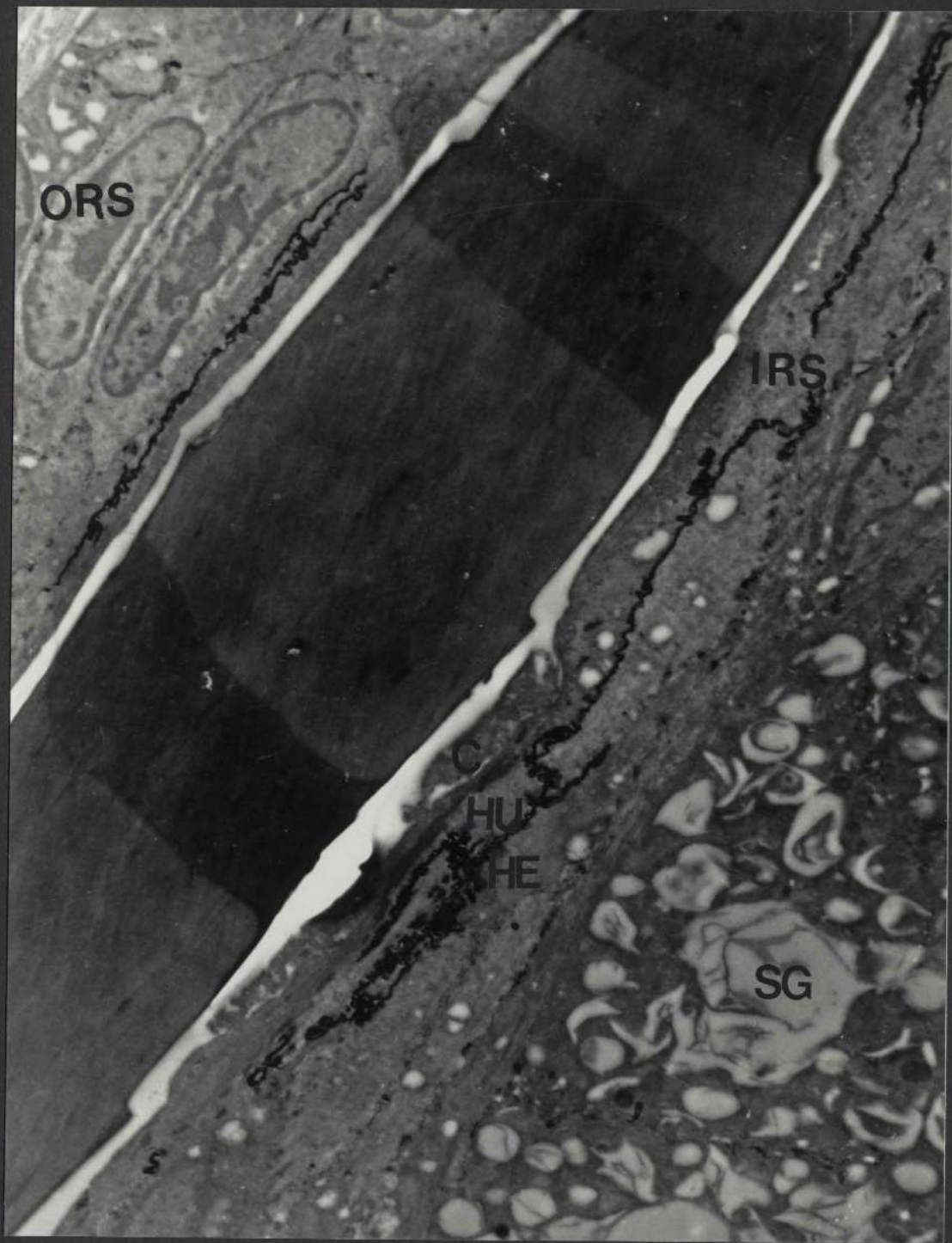


Figure 77b: Here is illustrated a segment of a sebaceous gland close to the region of its duct. Towards the upper right hand corner of the field may be seen a ruptured fully differentiated cell (FD) discharging into the duct. PD is a partially differentiated cell (x 9,280).

Lanthanum (arrows) is present between partially and fully differentiated sebaceous cells, and within parts of the desmosomes (D).

The tracer was detected in the EDX spectrum when analysis was carried out on the sebaceous gland from which the above section was obtained.



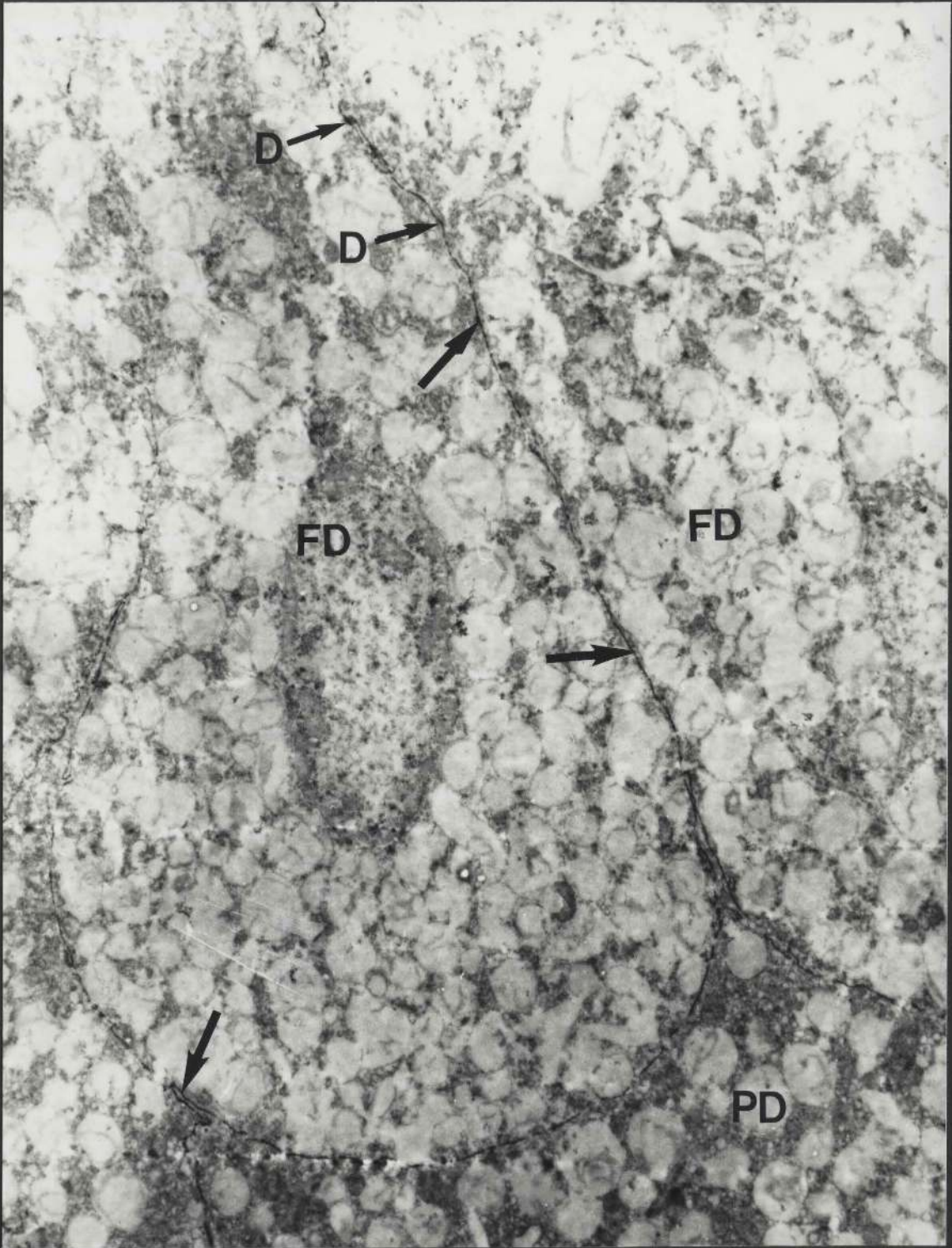


Figure 77c: This micrograph (x 8,352), obtained from the follicular canal epidermis is of great interest in that it shows that lanthanum has not only permeated the intercellular spaces of the stratum basale (SB) and the stratum spinosum (SS), but has also entered the intercellular space between two granular cells (SG) (large arrows).

The intercellular spaces of the stratum corneum (SC) do not contain lanthanum.

Another interesting feature of this micrograph is that it shows a crowding of membrane-coating granules (MCG) in the intercellular space between the stratum granulosum and the stratum corneum. This region is in fact the level at which the migration of lanthanum has been halted.

The EDX spectrum confirmed the presence of lanthanum when the analyzed area consisted of viable layers of the follicular canal epidermis. No lanthanum was detected however, when the probed area contained stratum corneum alone.



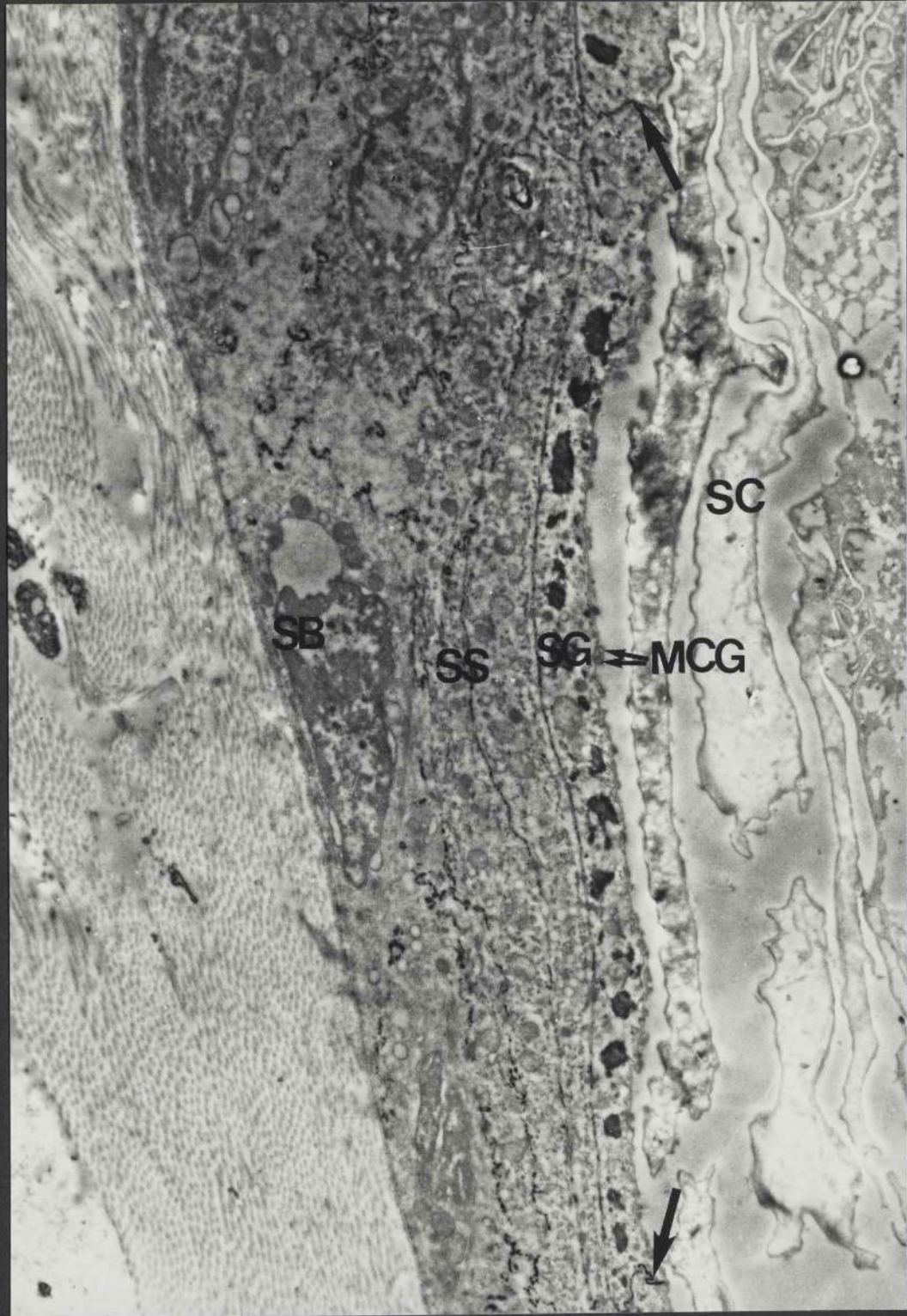


Figure 77d: This micrograph of the deeper layers of the epidermis illustrates that lanthanum is present in all the intercellular spaces in the stratum basale (SB) and stratum spinosum (SS), and within the intercellular junctional complexes (D) between adjacent cells (x 8,352).

The EDX spectrum of the viable epidermal layers contained peaks for lanthanum.



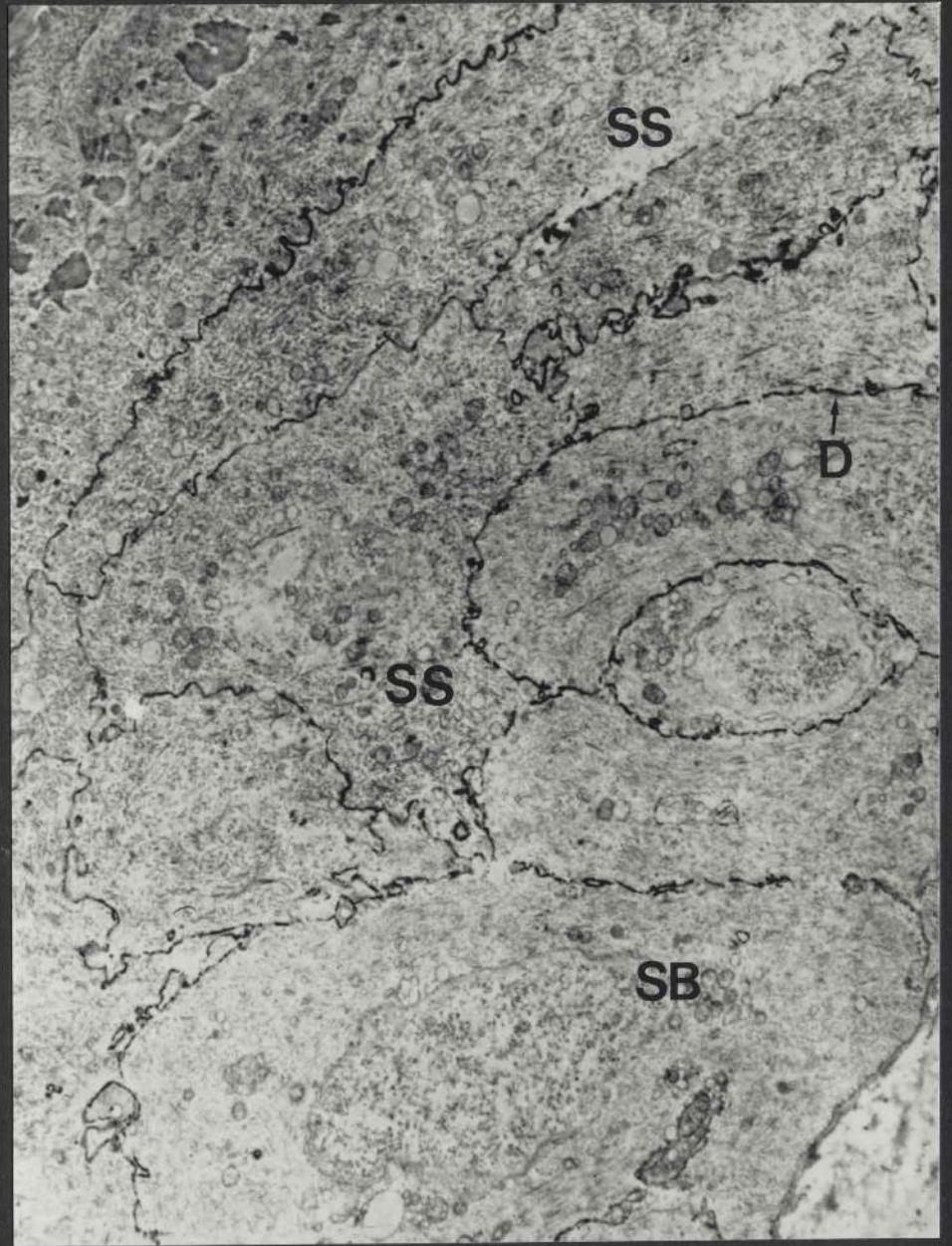




Figure 77e: This field spans the upper epidermis and includes the upper part of the stratum spinosum (SS), the stratum granulosum (SG), and lower corneal layers (SC) (x 10,208).

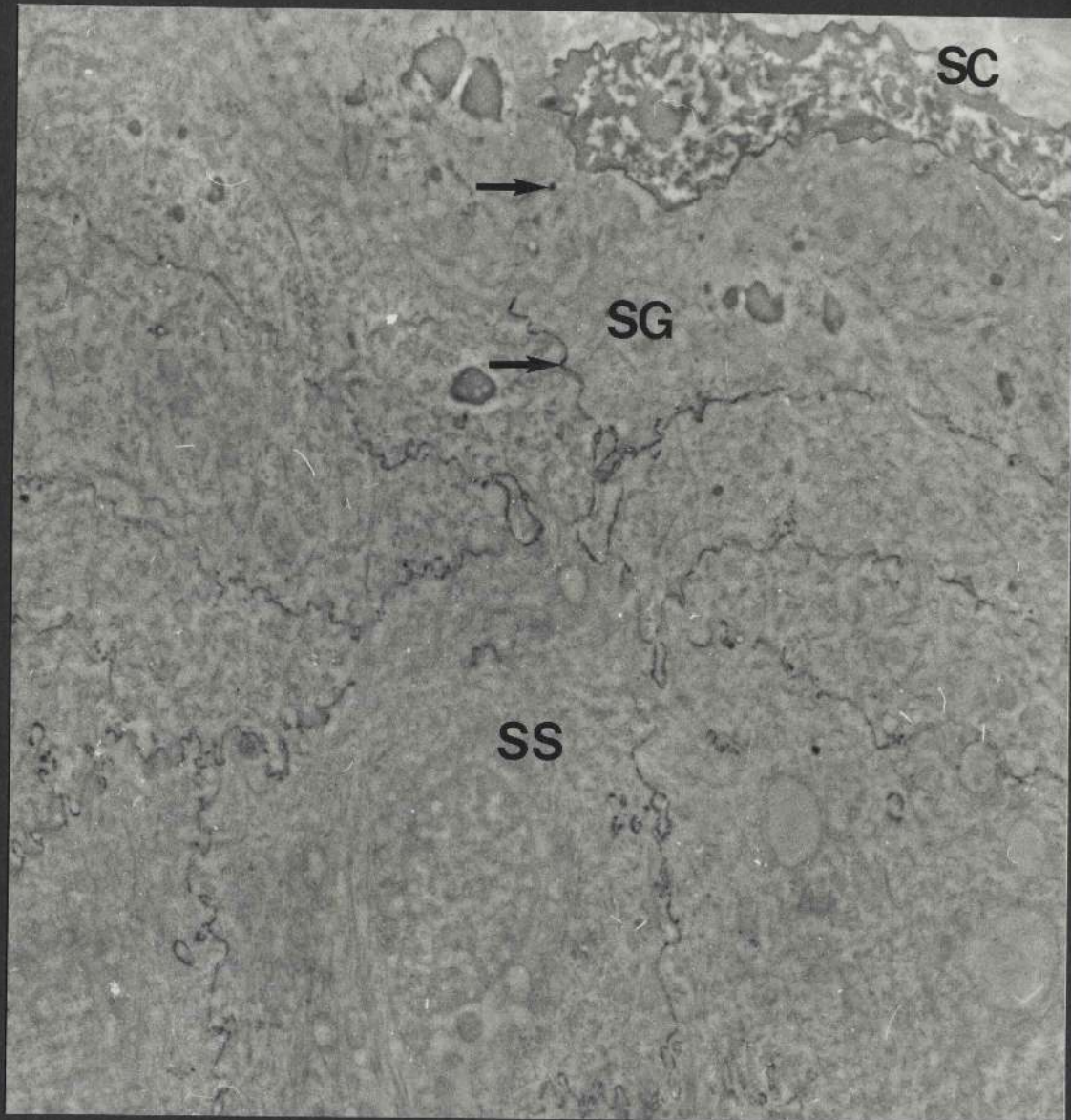
It is apparent that lanthanum has not only entered the spaces between spinous cells, but has also extended into the intercellular spaces between adjacent granular cells (arrows).

No lanthanum has entered the intercellular space between the granular layer and the basal horny layer, or the intercellular spaces in the stratum corneum.

Lanthanum was not present in the EDX spectrum when the analyzed area consisted of the stratum corneum alone.

#### Summary of results

The location and distribution of lanthanum in the hair follicles, sebaceous glands, and epidermis following the incubation method is very similar to that seen when lanthanum is injected intradermally (Figures 76 a - i).



### 3.5.3 Effect of concentration

The following experiments were undertaken to investigate the extent of the penetration of lanthanum from the surface into the skin as a function of the tracer concentration.

Lanthanum nitrate was prepared in distilled water to a concentration of 1% and 2%. These solutions were applied locally (control) or introduced by iontophoresis. The results obtained are shown in Figures 78 (a - d), 79 (a - c) and 80 (a - c). EDX analyses were carried out on the resin blocks and the results obtained are reported with each figure.

## Figure 78 (a - d)

Local application of a 1% aqueous lanthanum nitrate solution for 15 minutes

Figure 78a: Two transmission electron micrographs from the epidermis

Micrograph 1: Included in this field is the stratum corneum (SC) (x 8,352). No lanthanum is evident in the intercellular or in the intracellular regions. A remnant of the intercellular substance (IS) is seen.

Micrograph 2: This features the stratum basale (SB), the stratum spinosum (SS) and the stratum granulosum (SG) of the epidermis (x 8,352). No electron-dense material is seen inside or between the epidermal cells.

EDX analyses of the araldite blocks from which the above sections were produced confirmed the absence of lanthanum from the stratum corneum and the subjacent epidermal layers. However, lanthanum was detected occasionally when the analysis was performed on the surface of the skin.



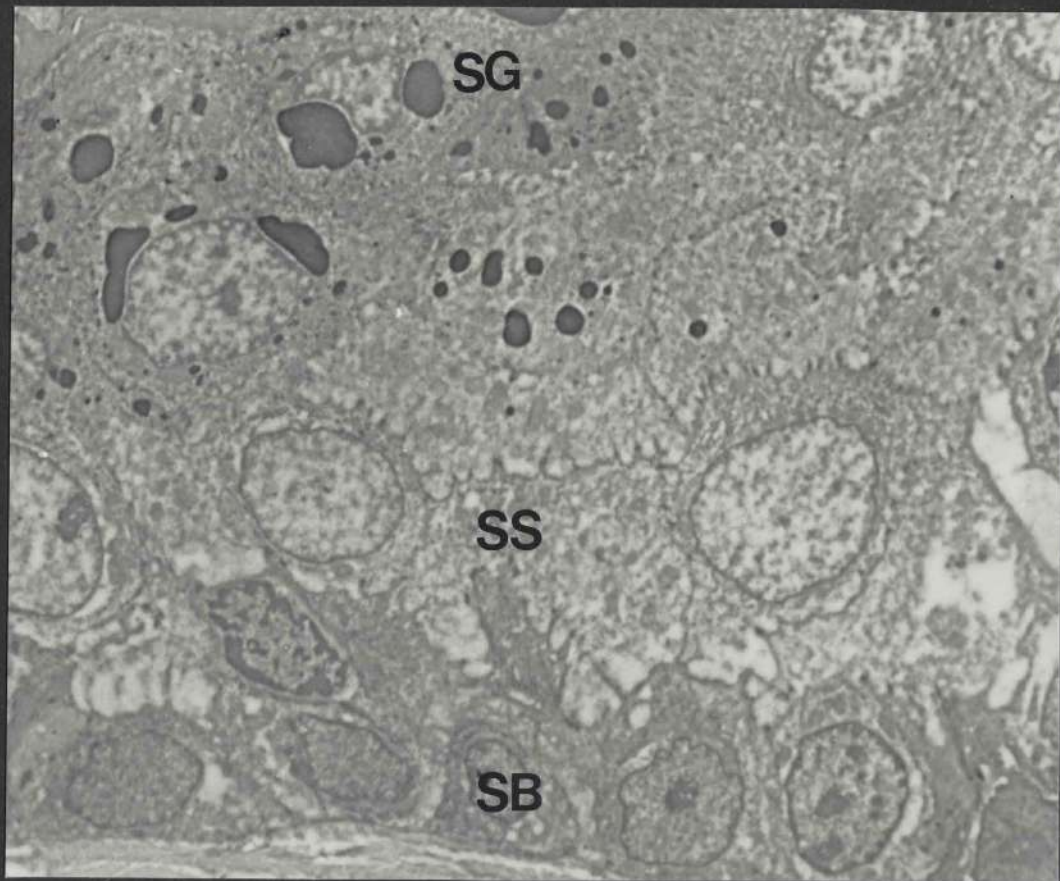
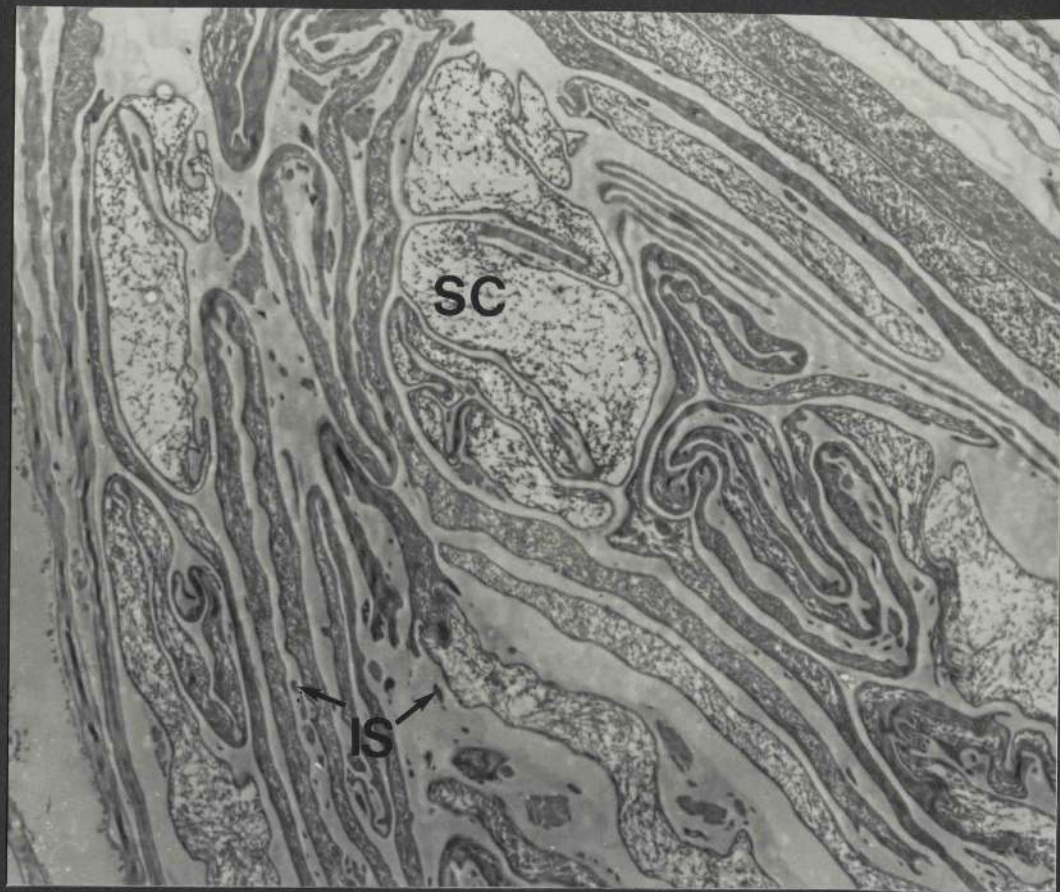


Figure 78b: This micrograph features the lower part of the follicular canal epidermis and a sebaceous gland towards the duct region (x 8,352). No electron-dense material is present in the horny (SC) or prickle (SS) cell layers of the follicular canal epidermis.

The intracellular regions of the mature (fully differentiated) sebaceous cells (FD) do not contain tracer and the intercellular spaces in the gland are also devoid of lanthanum.

Lanthanum was not detected in the EDX spectrum obtained from the araldite block-face containing the view above.



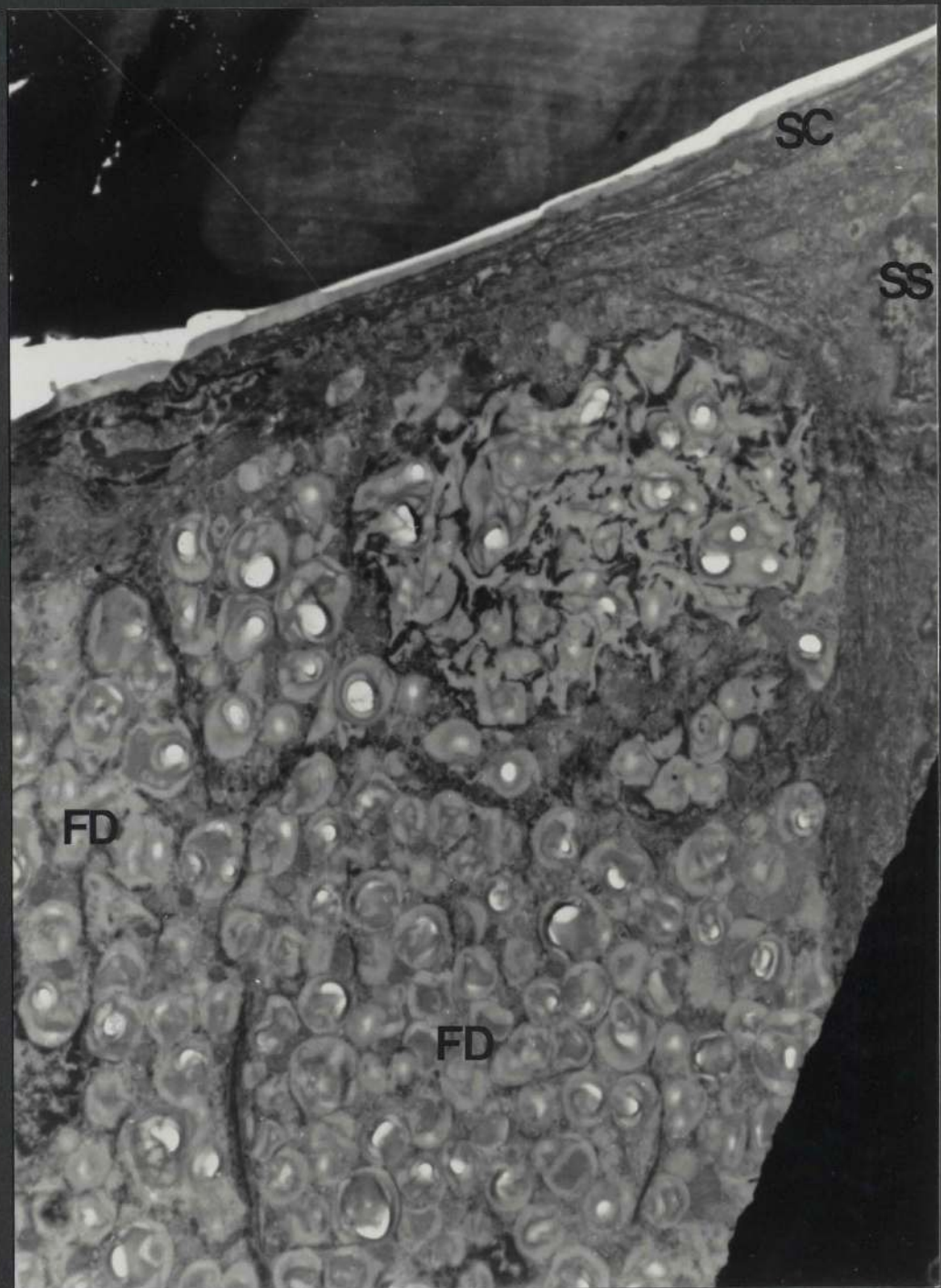




Figure 78c: This micrograph is a section of a sebaceous gland showing portions of fully differentiated (FD) sebaceous cells (x 8,352). No electron-dense deposits are present either inside or between the sebaceous cells.

The EDX spectrum obtained did not show a peak for lanthanum.

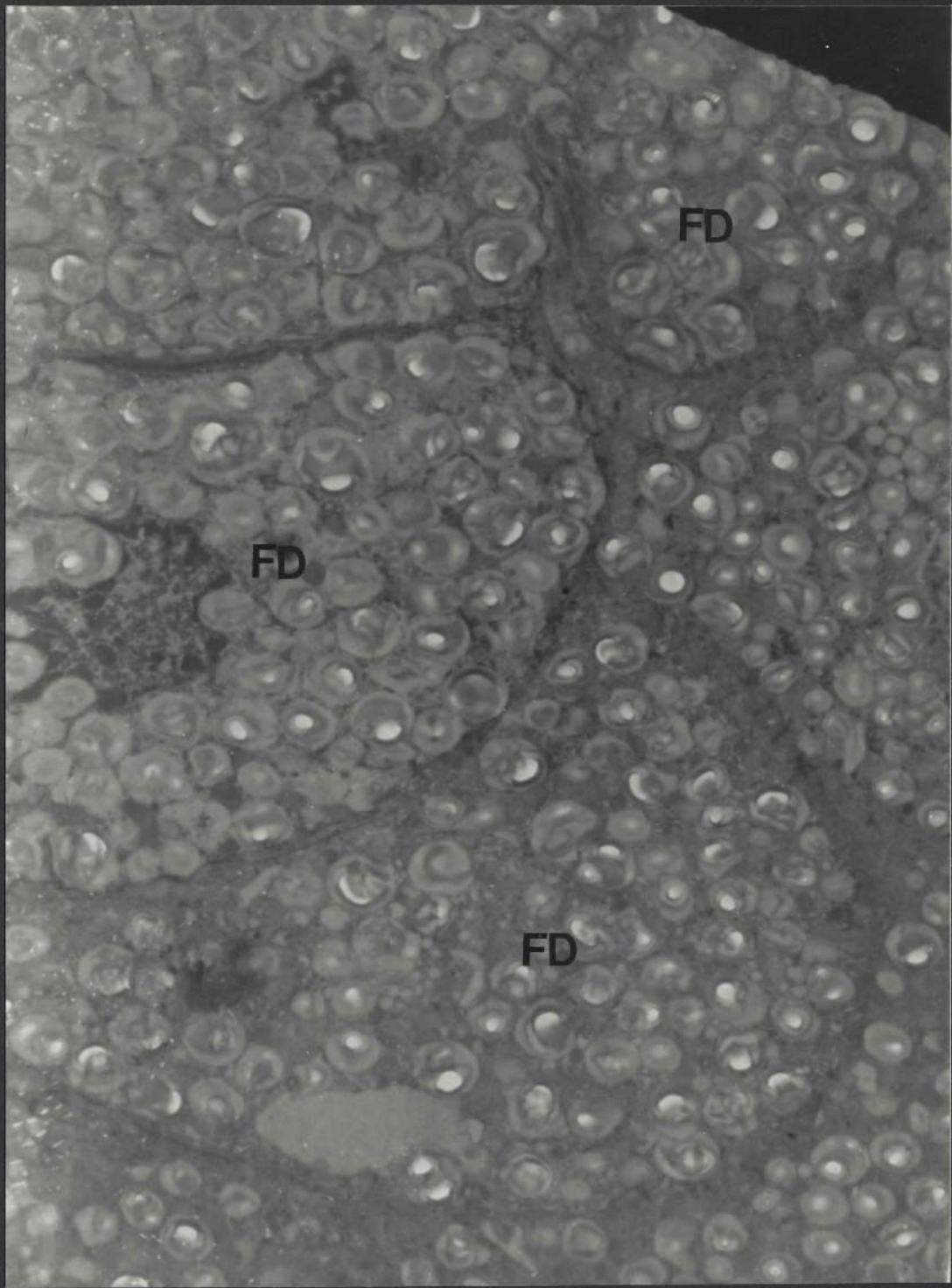


Figure 78d: This field spans the lower part of a hair follicle and includes the outer root sheath (ORS) and the cortex of the hair shaft (CO) (x 8,352).

The intercellular spaces (IS) in the lower follicular wall appear to be empty, that is, lanthanum is not present in these spaces.

The EDX spectrum confirmed the absence of lanthanum in such a field.

#### Summary of results

The penetration of lanthanum from a 1% aqueous solution is negligible following local application. The tracer is found on the surface of the skin, but not in the epidermis, the sebaceous glands or in the hair follicles. The EDX analyses confirmed the morphological findings.

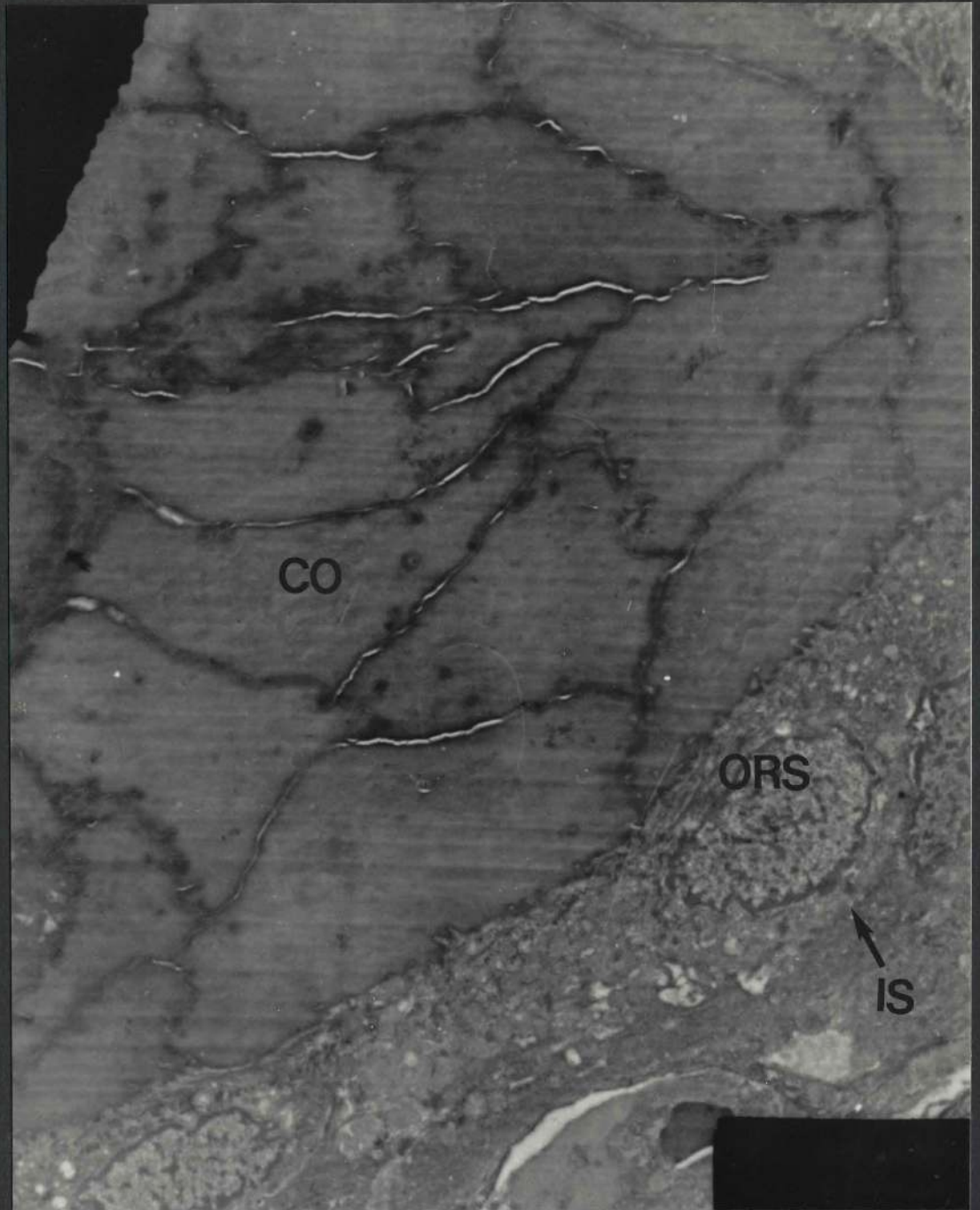


## Figure 79 (a - c)

Positive iontophoresis of a 1% aqueous lanthanum nitrate solution at 30 milliamperes for 15 minutes (x 8,352)

Figure 79a: A transmission electron micrograph of full-thickness epidermis (x 8,352)

This illustrates that a few irregular deposits of lanthanum are present in the intercellular space between the two most superficial layers of the stratum corneum (SC), where it accumulates over the surfaces of the cells (arrow).

The tracer has not extended into the intercellular spaces in the lower corneal layers, the stratum granulosum (SG), the stratum spinosum (SS), or into the stratum basale (SB).

There is some loss of the fine intracellular detail when compared, for example, to that seen in the epidermis following local application (Figure 78a). In this case, the nuclei (N) of the lower epidermal cells are more compact and irregular in outline. There is a coagulation and condensation of the cytoplasmic matrix which appears as a grayish dense cloud. Finally, there is some widening of the intercellular spaces especially in the lower epidermal layers.

EDX spectra indicated lanthanum when the analyzed area consisted of the superficial layers of the stratum corneum. No lanthanum was detected, however, in the lower layers of the stratum corneum or in the viable epidermal layers.



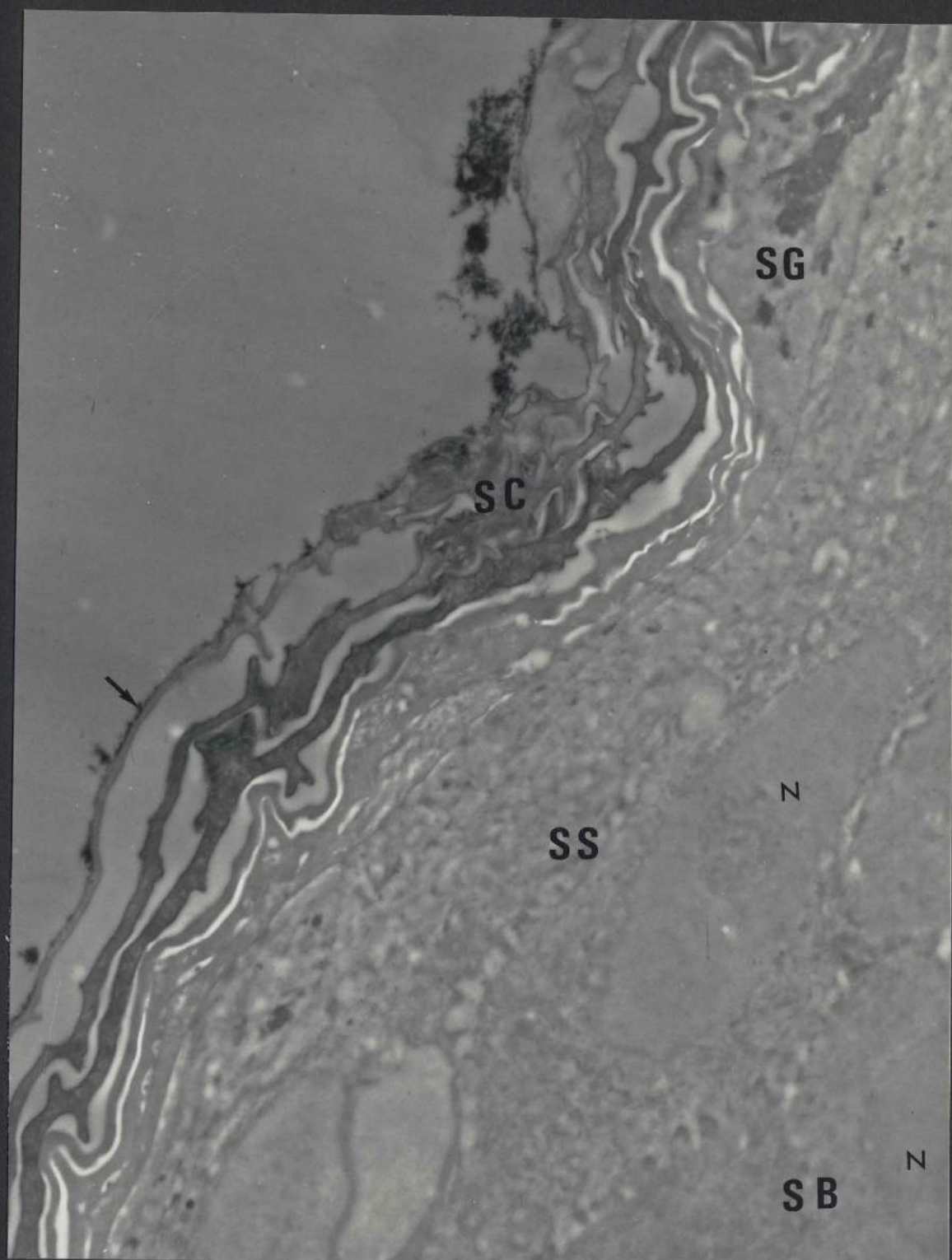




Figure 79b: This micrograph is from the periphery of a sebaceous gland surrounded by collagen fibres (C). Within the gland, peripheral (P) and partially differentiated (PD) sebaceous cells are seen (x 8,352).

The intercellular spaces (ICS) in the gland do not contain lanthanum. Moreover, no lanthanum is visible inside the sebaceous cells.

Apart from slight coagulation of the cytoplasmic matrix, no distinct ultrastructural changes are observed in the glands when compared to those seen in Figure 78c.

EDX analysis confirmed the absence of lanthanum in the gland.

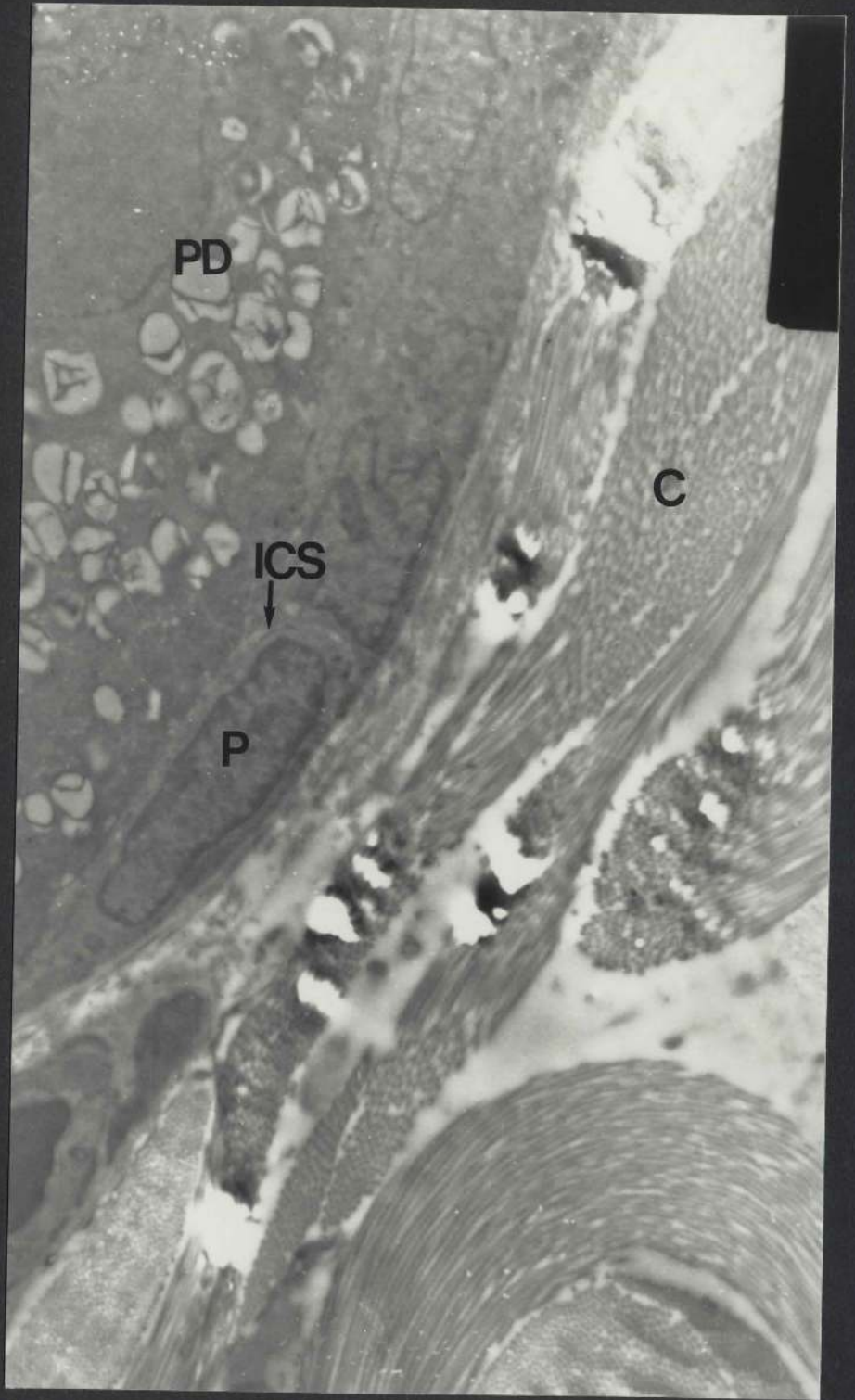


Figure 79c: This field from the lower part of a hair follicle features some outer root sheath cells (ORS) connected to each other by desmosomal attachments (D) (x 8,352).

No electron-dense material is found inside or between the cells in the outer root sheath. Lanthanum was not present in the EDX spectrum obtained from such a region.

### Summary of results

Following iontophoresis of a 1% aqueous lanthanum nitrate solution, the tracer is only present in the intercellular spaces in the two superficial corneal layers. The tracer is not found in the lower parts of the stratum corneum or in the underlying (deeper) epidermal layers. No lanthanum is found in the hair follicles or the sebaceous glands.

From these observations it appears that 1% lanthanum in aqueous solution does not penetrate significantly further when introduced by iontophoresis than it does when applied locally.

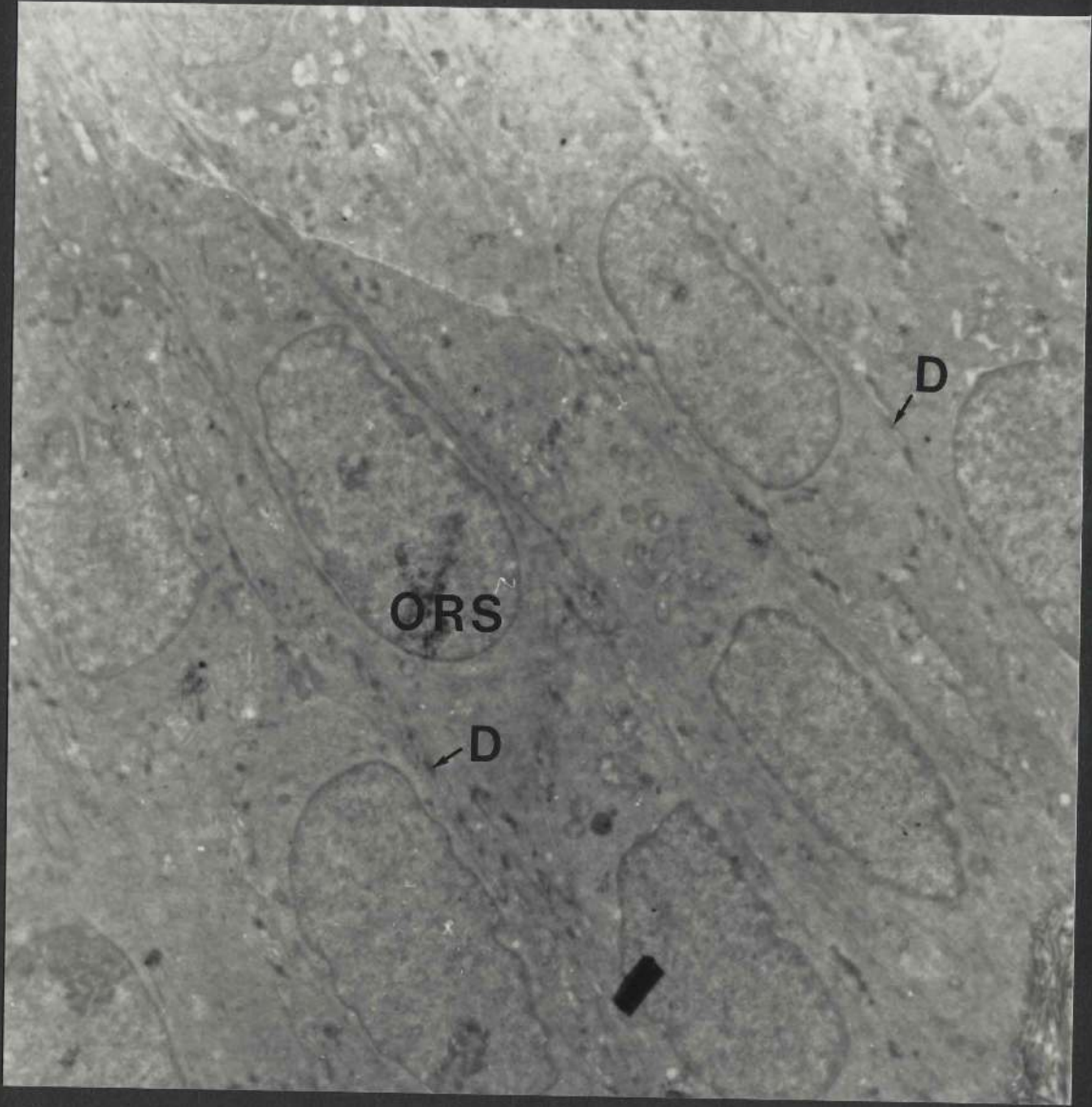


## Figure 80 (a - c)

Positive iontophoresis of a 2% aqueous lanthanum nitrate solution at 30 milliamperes for 15 minutes

Figure 80a: This micrograph spans the superficial epidermal layers which include the stratum corneum (SC), and a portion of a granular cell (SG) in which membrane-coating granules (MCG) and a small part of a keratohyalin granule (Kh) are seen (x 12,064).

A uniform dense deposit of lanthanum (arrows) is visible on the superficial surfaces of the upper two corneocytes. Lanthanum does not extend into the deeper intercellular spaces (ICS) and is not evident inside the corneal cells.

The EDX spectrum contained lanthanum when the analyzed area was confined to the upper layers of the stratum corneum, but no tracer was detected when the analyzed area consisted of the deeper layers of the stratum corneum.



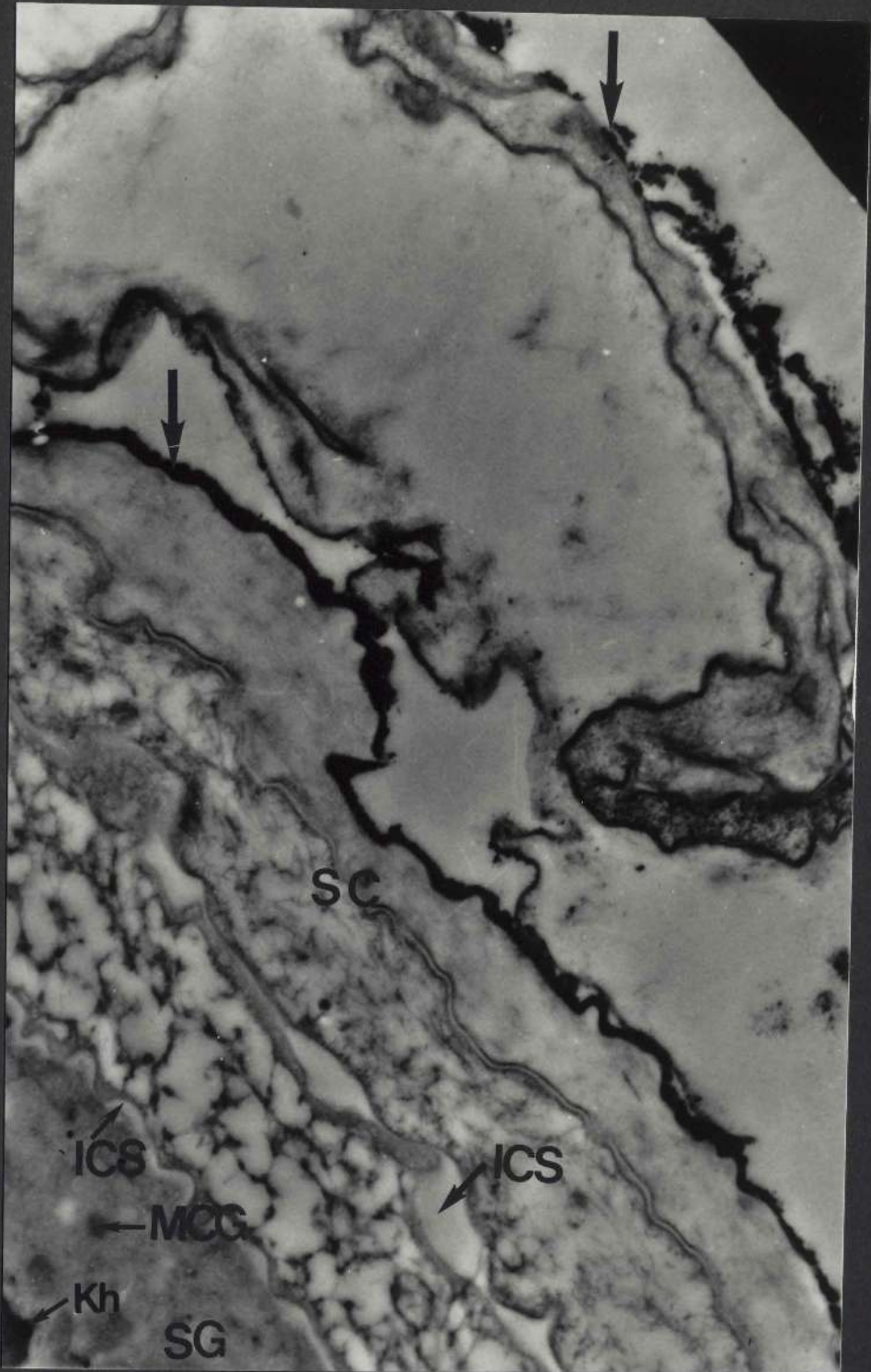




Figure 80b: A transmission electron micrograph (x 7,424) The structures present in this field include a part of the stratum granulosum (SG) with its characteristic keratohyalin granules (KH), the stratum spinosum (SS), and the stratum basale (SB) of the epidermis.

No lanthanum is evident in the viable epidermal layers and was not detected in the corresponding EDX spectrum.



Figure 80c: In this field from the base of a sebaceous gland, peripheral cells (P) and partially differentiated cells (PD) are seen (x 8,352).

No lanthanum has entered the intercellular spaces (ICS) in the gland. The interior of the sebaceous cells is devoid of lanthanum also.

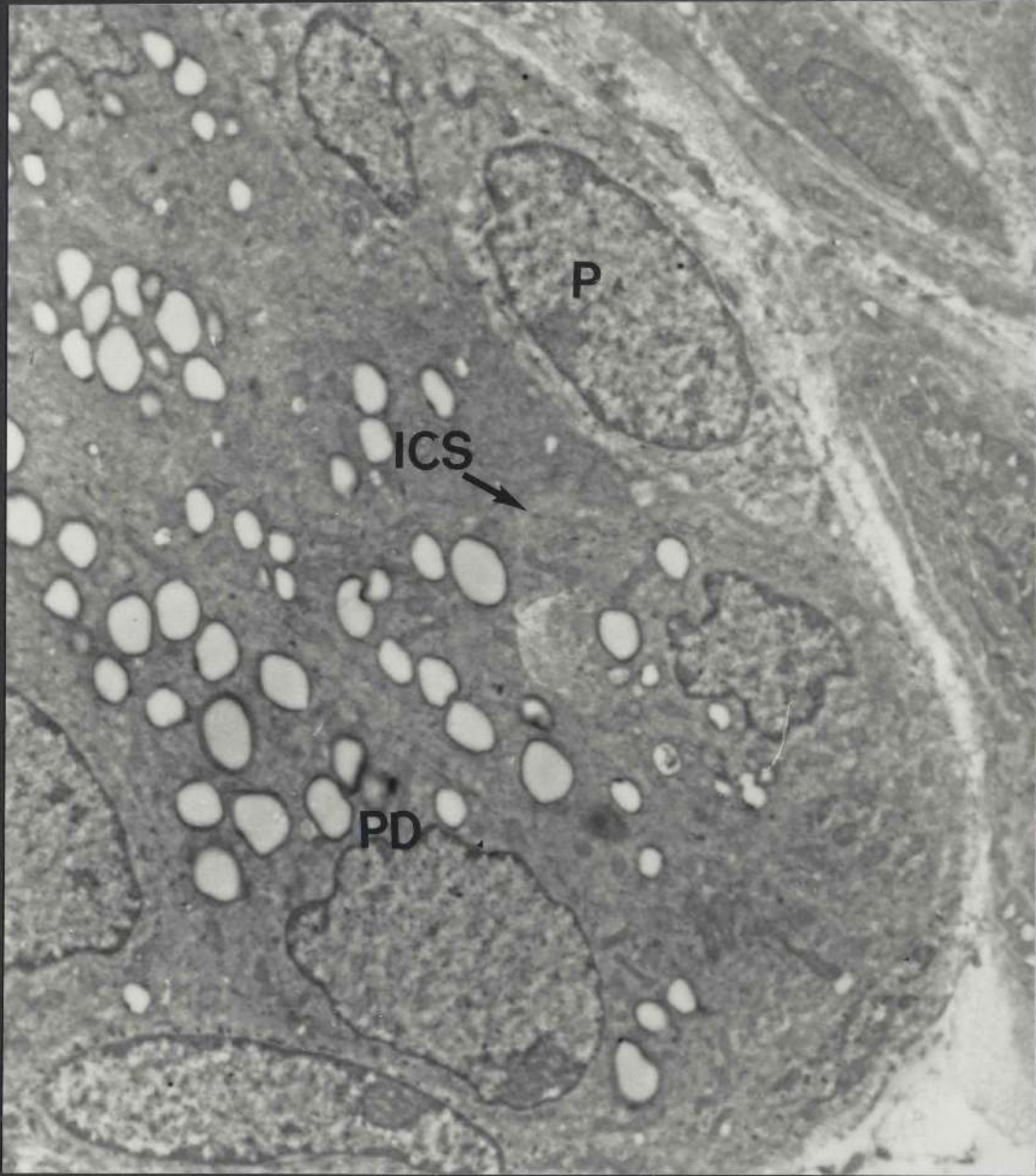
The EDX spectrum did not contain lanthanum when analysis was carried out on the resin block from which the view opposite was obtained.

#### Summary of result

Following iontophoresis of a 2% aqueous lanthanum nitrate solution, the tracer is only evident in the intercellular spaces in the upper two corneal layers. No penetration takes place into the lower corneal layers, the viable epidermal layers, the hair follicles or the sebaceous glands.

Increasing the concentration of lanthanum nitrate from 1% to 2% therefore only results in a heavier electrodeposition of the tracer in the intercellular spaces in the upper layers of the stratum corneum. Consequently, the extent of penetration of the tracer is similar in this case to that observed with a 1% solution (Figures 79a - 79c).





#### 3.5.4 Effect of removal of surface lipid

The aim of this experiment was to investigate the effect of the removal of the surface lipid on the penetration of lanthanum from the surface into the skin by iontophoresis. The surface lipid film was removed by gentle and regular wiping with cotton wool into which diethyl ether had been applied. This procedure lasted for approximately two minutes, following which the tracer was applied to the skin with iontophoresis.

#### Figure 81 (a - c)

Positive iontophoresis of a 1% aqueous lanthanum nitrate solution at 30 milliamperes for 15 minutes (x 8,352).

Figure 81a: This micrograph illustrates the full-thickness epidermis. One may note the condensation of the nuclei (N) and the coagulation of the cytoplasmic matrix in the basal (SB) and prickle (SS) cells (x 8,352).

Dense deposits of lanthanum (arrow) are present on the surface of the skin. However, the tracer has not entered the intercellular spaces in the stratum corneum (SC) or in the lower epidermal layers. Furthermore, lanthanum is not evident inside the cells.

The EDX spectrum contained lanthanum when analysis was confined to the surface of the skin, but no tracer was detected in the epidermis.



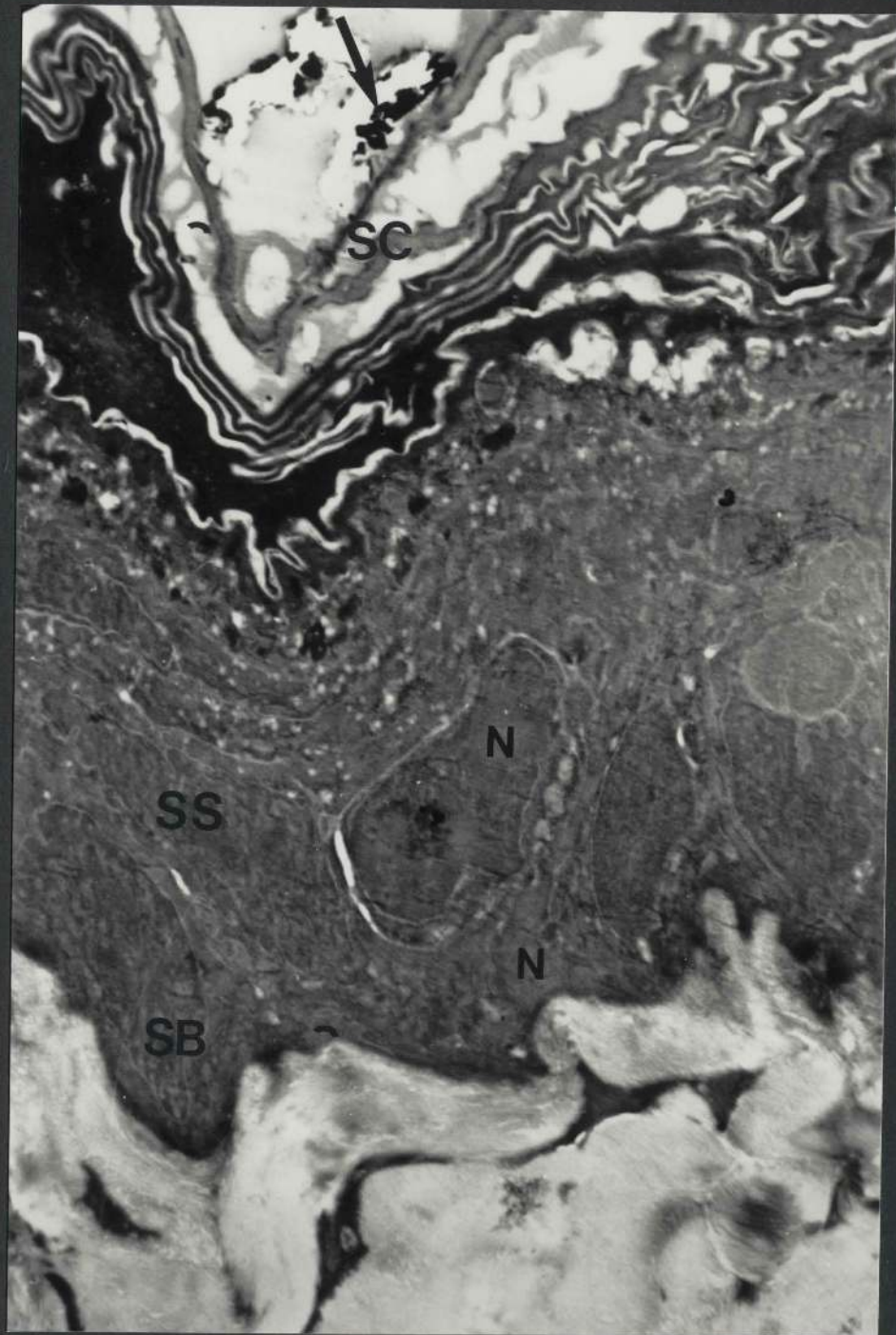




Figure 81b: The structures present in this micrograph include the stratum corneum (SC), the stratum granulosum (SG), and the stratum spinosum (SS) of the follicular canal epidermis (x 8,352).

A light irregular deposit of lanthanum (arrows) is seen on the surface of the stratum corneum. No penetration of the corneal or the other epidermal layers is evident.

The EDX spectrum showed a small peak for lanthanum when the surface of the follicular canal epidermis on either side of the pilary canal (P) was analyzed. No lanthanum was detected within the follicular canal epidermis.

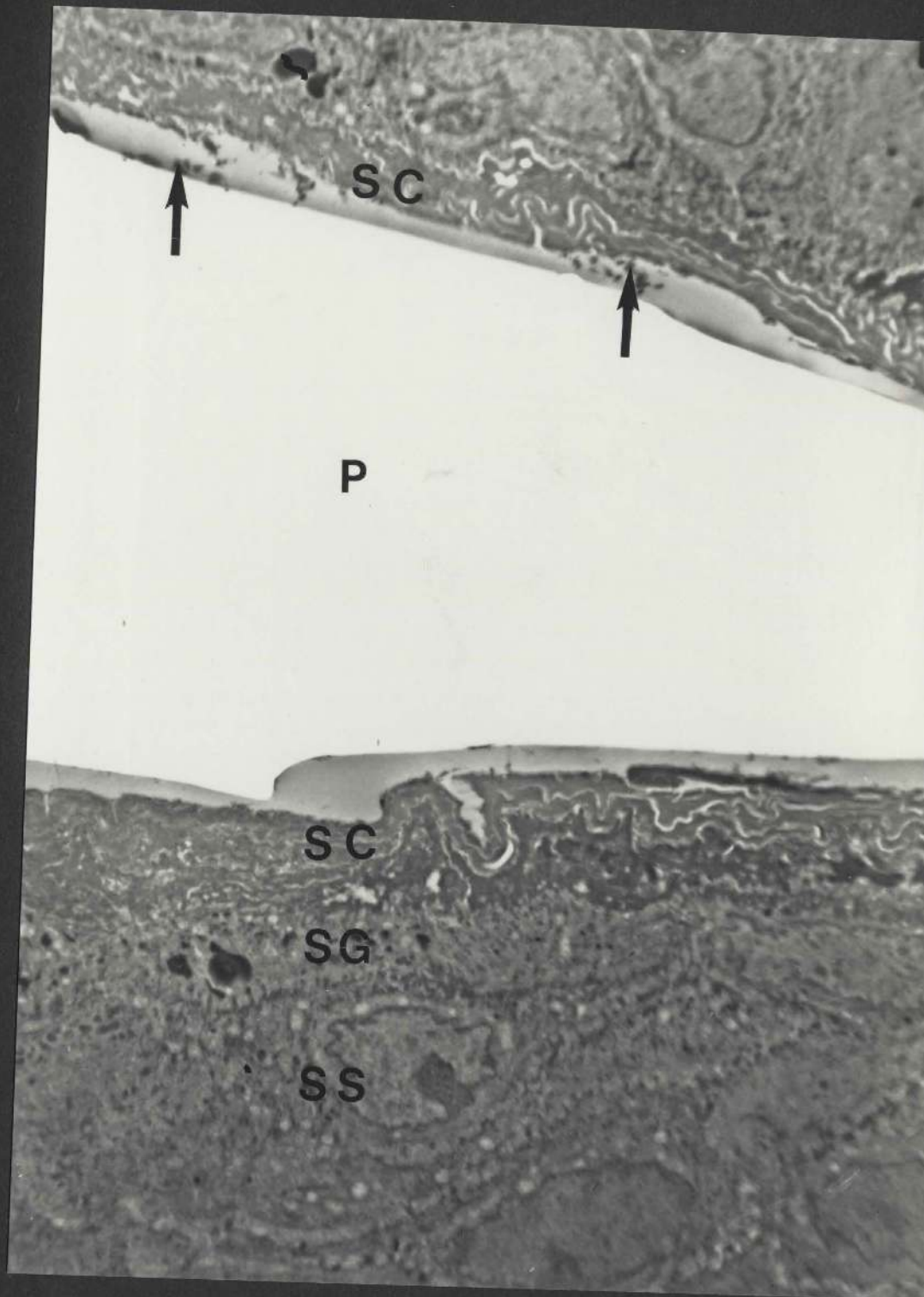


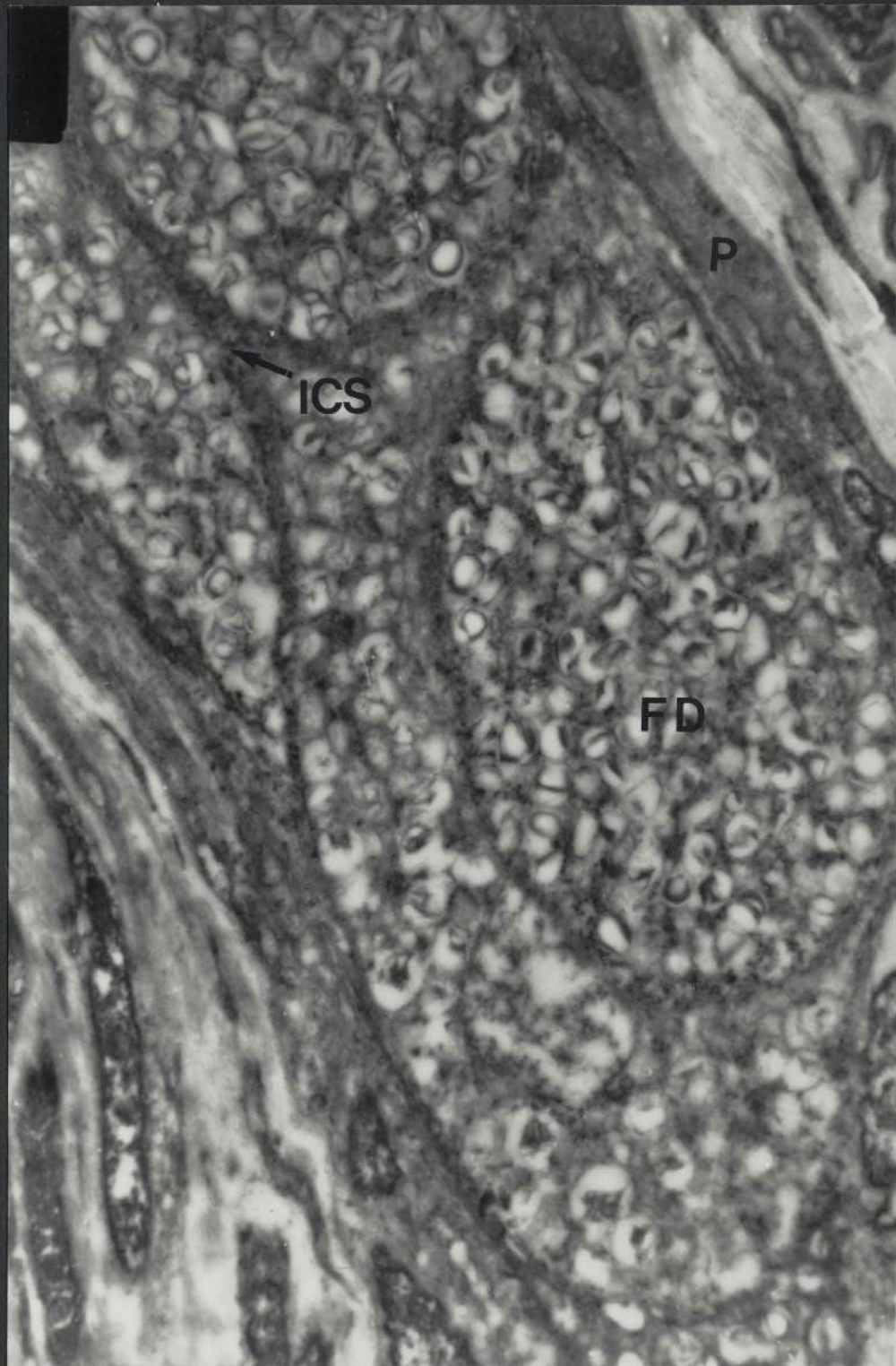
Figure 81c: This electron micrograph shows a portion of a sebaceous gland and includes peripheral (P) and fully differentiated (FD) sebaceous cells (x 9,280).

No electron-dense material is evident in the intercellular spaces (ICS) between the sebaceous cells, or inside the cells.

The EDX spectrum from the sebaceous gland did not contain lanthanum.

#### Summary of results

The only differences between these results and those obtained in similar experiments but without pretreatment with ether (Figure 79) is that, in this case, lanthanum is visible on the surface of the stratum corneum of the follicular canal epidermis. However, as in Figure 79, the tracer does not penetrate the epidermis, the follicular infundibulum or into the sebaceous glands.



### 3.5.5 Effect of vehicle

The following experiments were undertaken with the object of determining the effect of incorporating a detergent or an accelerant with the tracer in solution on the penetration of the tracer by iontophoresis. In addition, experiments were carried out to investigate the effect of using absolute ethanol as an alternative vehicle to water on skin penetration by iontophoresis.

3.5.5.1 Accelerants Dimethyl sulphoxide (DMSO) was selected as a representative of this class of materials. The test solution consisted of 1% (W/V) lanthanum nitrate in 60% aqueous DMSO. It was prepared by dissolving a gram of the tracer salt in 40 mls of distilled water to which 60 mls of DMSO solution were then added. Immediately following the addition of DMSO there was a rise in the temperature (exothermic process) of the final colourless test solution. The solution was left to cool therefore, and then used for penetration studies.

Figure 82 (a-c)

Positive iontophoresis of 1% (W/V) lanthanum nitrate in 60% aqueous DMSO at 30 milliamperes for 15 minutes

Figure 82a: This field spans the full-thickness epidermis which is composed of the horny (SC), the granular (SG), the prickle (SS) and the basal (SB) layers (x 8,352).

A continuous layer of lanthanum (arrows) is present on the surface of the skin. The tracer has not entered the stratum corneum or the deeper epidermal layers.

EDX analysis contained peaks for lanthanum only when it was performed on the skin surface.

One may note the condensation and elongation of the nuclei in the basal and prickle cells, and the widening of the intercellular spaces.



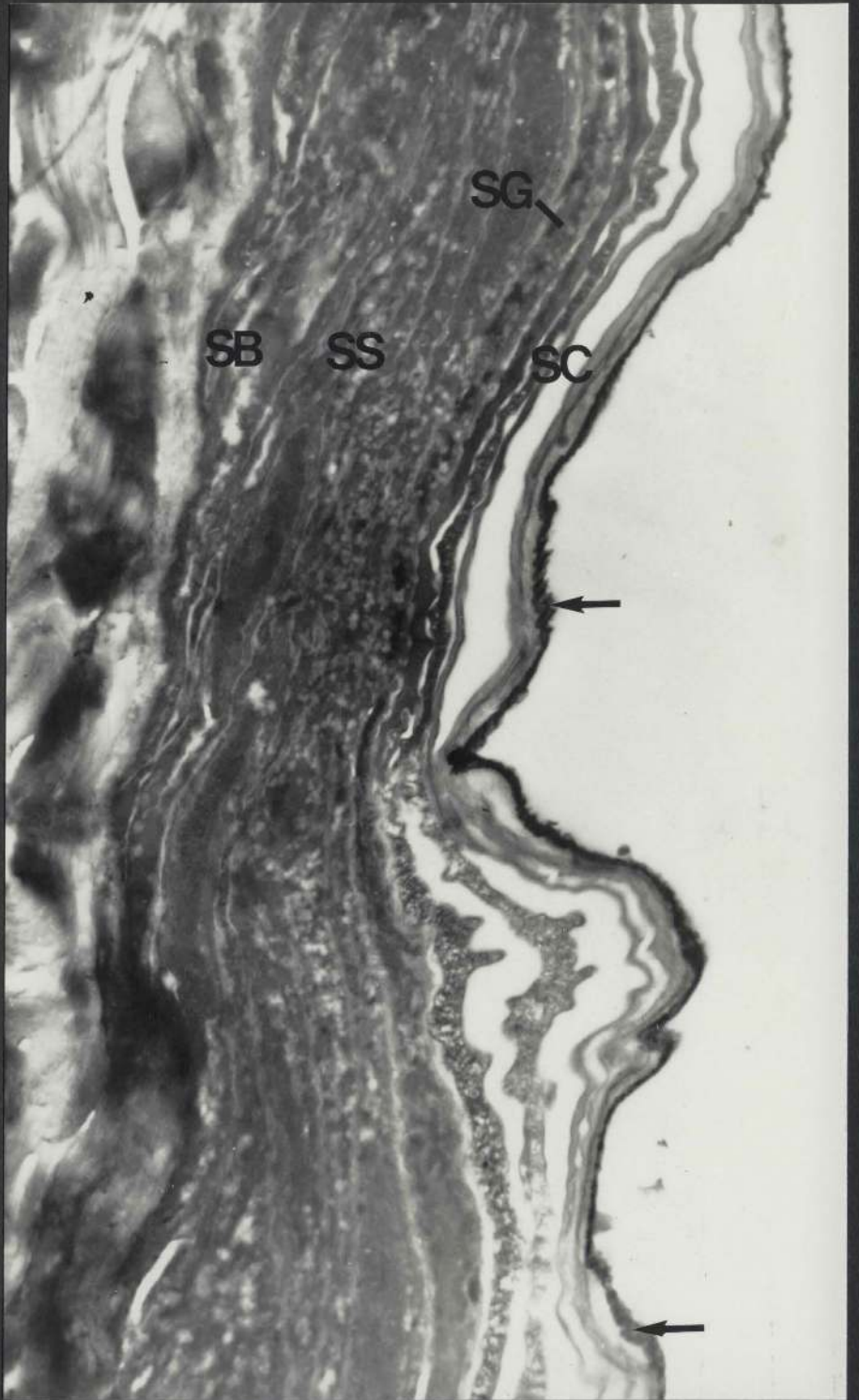




Figure 82b: This electron micrograph features a portion of the infundibulum of a hair follicle. The stratum corneum (SC), the stratum granulosum (SG), the stratum spinosum (SS), and the stratum basale (SB) are seen (x 9,280).

A light deposit of lanthanum (arrow) is seen on the surface of the stratum corneum adjacent to the hair shaft (H). No lanthanum is visible in the intercellular spaces in the stratum corneum or in other epidermal strata.

A very small, or no peak for lanthanum was observed in repeated EDX spectra obtained from the surface of the stratum corneum.

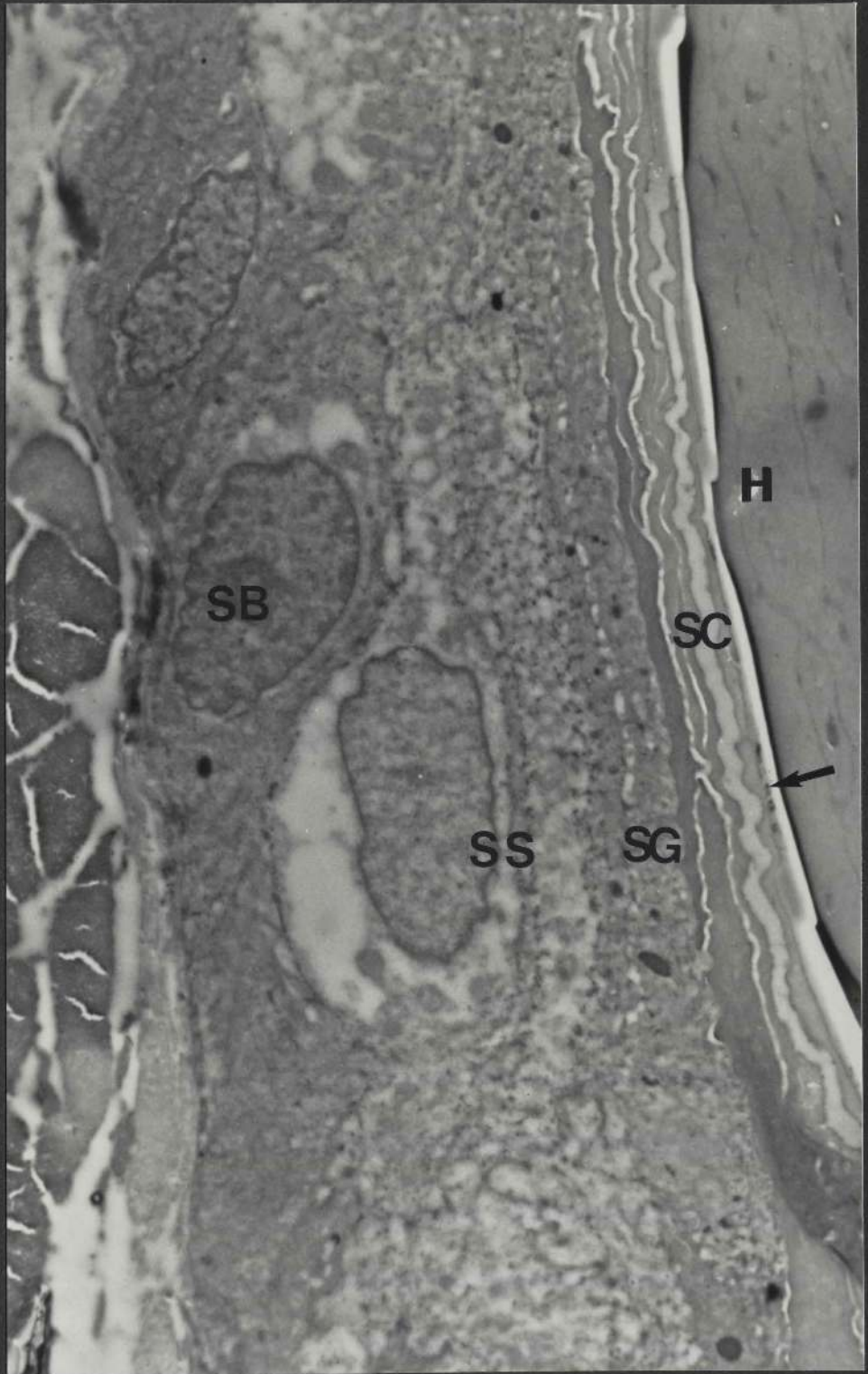


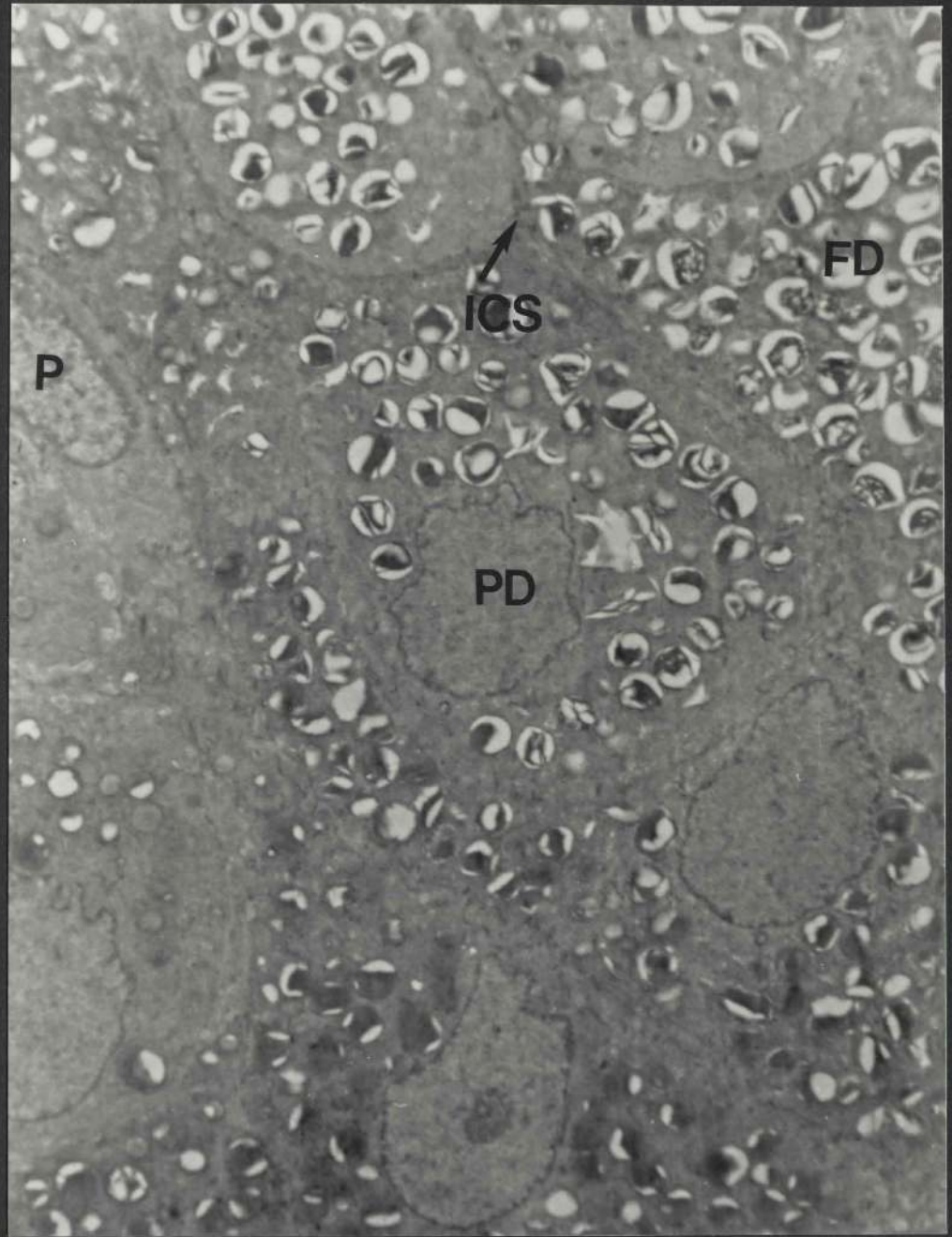
Figure 82c: Partially differentiated (PD), fully differentiated (FD), and peripheral (P) sebaceous cells are seen in this micrograph (x 8,352).

No lanthanum has penetrated into the intercellular spaces (ICS) between the sebaceous cells. In addition, the interior of the cells does not contain the tracer. No lanthanum was detected in the sebaceous gland following EDX analysis.

#### Summary of results

The incorporation of DMSO with lanthanum in solution results in a heavy deposit of lanthanum on the surface of the skin. No penetration is evident in the epidermis, the hair follicles or in the sebaceous glands.

The location of lanthanum in this case is similar to that obtained when the tracer is introduced from an aqueous vehicle alone (Figure 79).



3.5.5.2 Detergents The effect of incorporating a detergent with lanthanum in solution on the penetration of the electron-dense tracer from the surface into the skin was next investigated.

20 mls of tween 20 were added to 100 mls of 1% lanthanum nitrate in distilled water and subjected thereafter to iontophoresis as shown overleaf.



## Figures 83 (a - c)

Positive iontophoresis of 1% lanthanum nitrate (W/V), 20% tween 20 (V/V) in distilled water at 30 milliamperes for 15 minutes

Figure 83a: This micrograph features the full-thickness epidermis. Horny (SC), granular (SG), prickle (SS) and basal (SB) layers are seen (x 8,352).

A few deposits of lanthanum (arrow) are visible in the intercellular space between the two most superficial horny cells. No lanthanum has penetrated the intercellular spaces in the deeper layers of the stratum corneum or those in the remaining epidermal strata.

The EDX spectrum showed lanthanum when analysis was confined to the two outermost layers of the stratum corneum. The spectrum obtained from the deeper part of the stratum corneum and the subjacent viable epidermis did not contain tracer.

Figure 83b: This electron micrograph shows a portion of the upper part of a follicular infundibulum. The stratum corneum (SC), the stratum granulosum (SG) and the stratum spinosum may be seen (x 8,352).

No lanthanum is evident on the surface of the stratum corneum. Moreover, no penetration is evident in the stratum corneum itself or in the other epidermal strata. The EDX spectrum did not contain peaks for lanthanum.



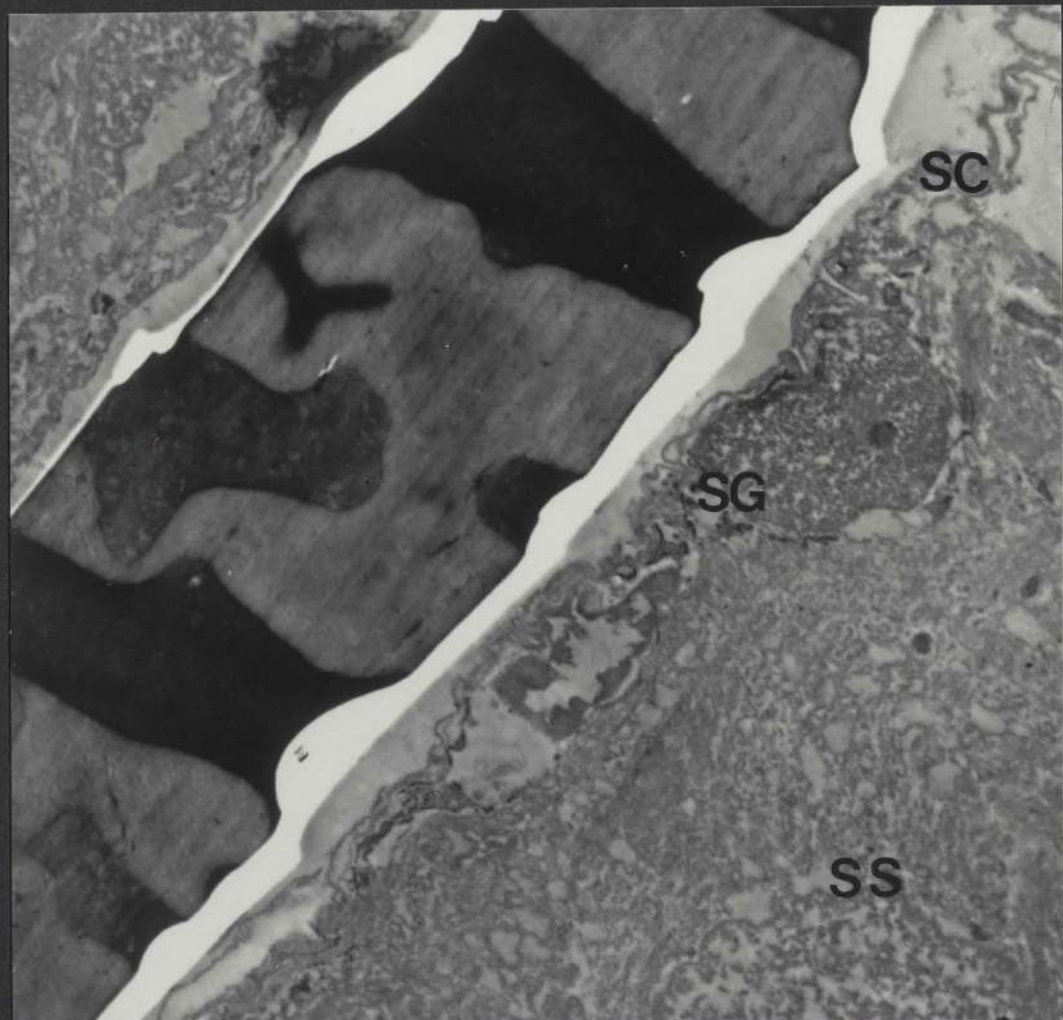
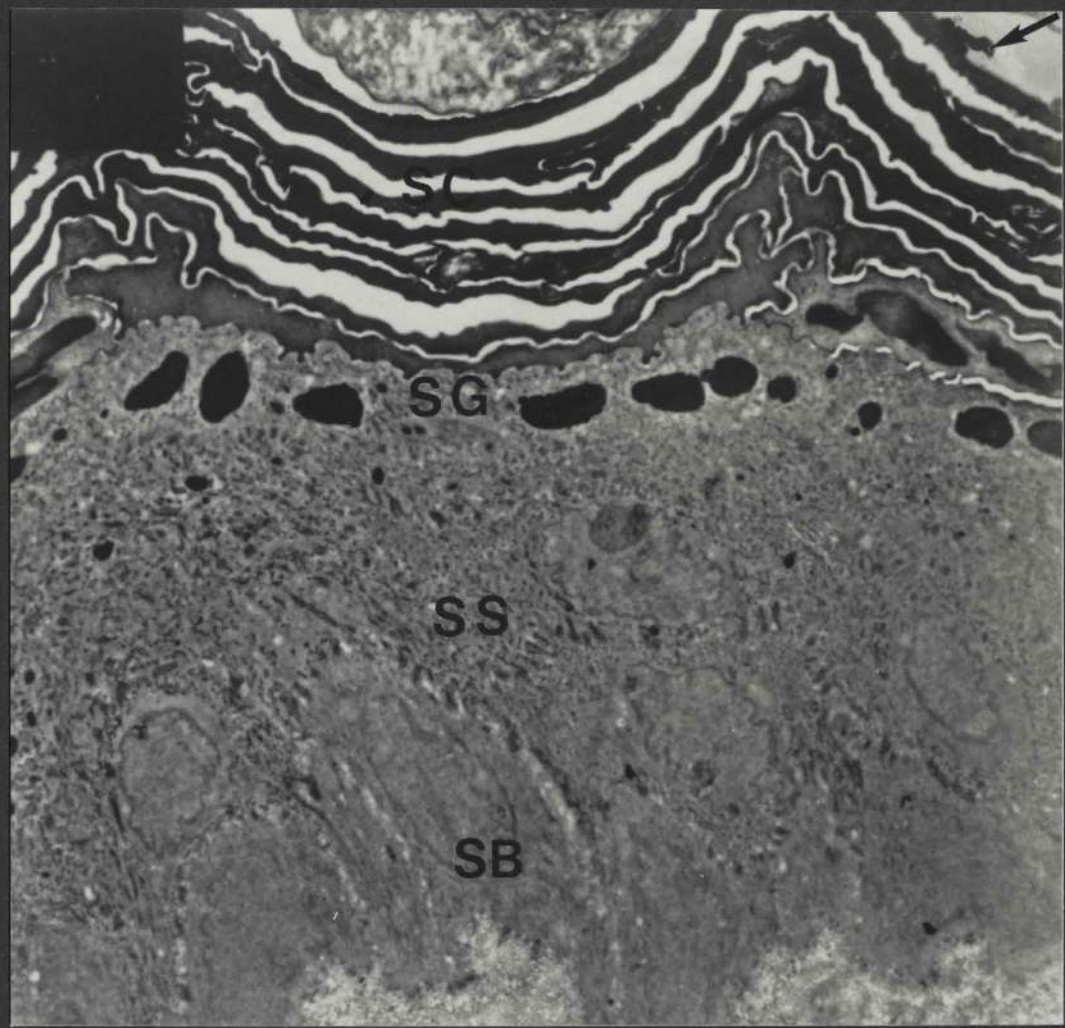
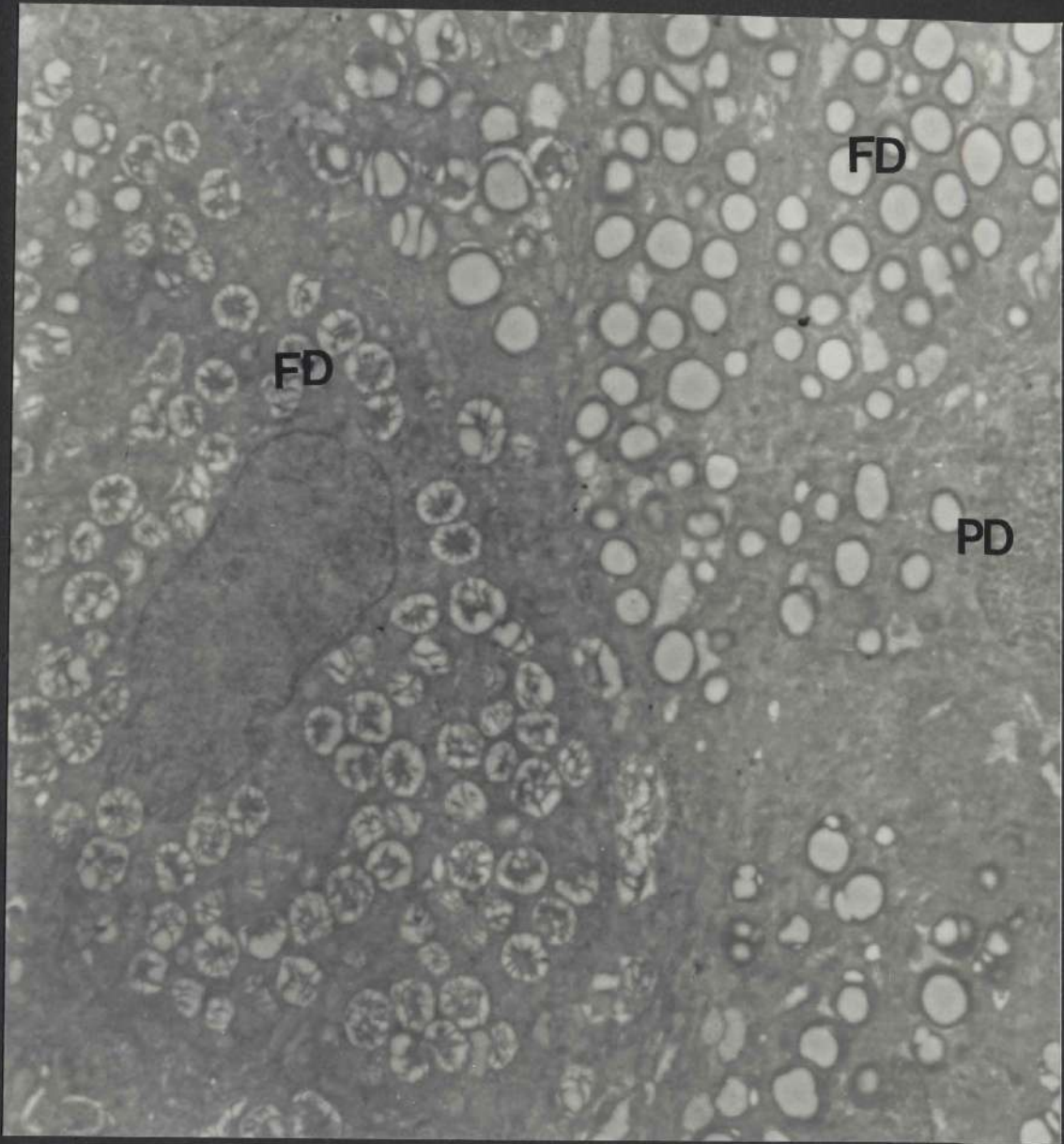


Figure 83c: This electron micrograph is from a section of a sebaceous gland. It illustrates partially differentiated (PD) and fully differentiated (FD) sebaceous cells (x 9,280).

No tracer is found inside or between the sebaceous cells and was not detected in the EDX spectrum.

### Summary of results

Following iontophoresis of the tracer-detergent solution, the tracer is visible in the intercellular spaces in the two superficial corneal layers, but not in the lower layers of the stratum corneum, the hair follicles or the sebaceous glands. The extent of penetration in this case is very similar to that obtained when lanthanum is introduced from an aqueous vehicle alone (Figure 79).





3.5.5.3 Organic solvents The following experiment was designed to investigate the effect of using absolute ethanol as a vehicle on the penetration of the tracer from the surface into the skin. Lanthanum nitrate was prepared in absolute ethanol to a concentration of 1% and applied locally or introduced by iontophoresis.

Figure 84 (a and b)

Local application (control) of 1% (W/V) lanthanum nitrate in absolute ethanol for 15 minutes

Figure 84a: This micrograph features the stratum corneum (SC), the stratum granulosum (SG) and the stratum spinosum (SS) of the epidermis (x 10,208).

Light deposits of lanthanum (arrow) are found on the surface of the skin. However, no electron-dense material is found in or between the cells in the stratum corneum or in the deeper epidermal layers.

No lanthanum was indicated in the EDX spectrum obtained from the epidermis.

The location and distribution of lanthanum in the follicular infundibulum are similar to those described in Figure 84a.

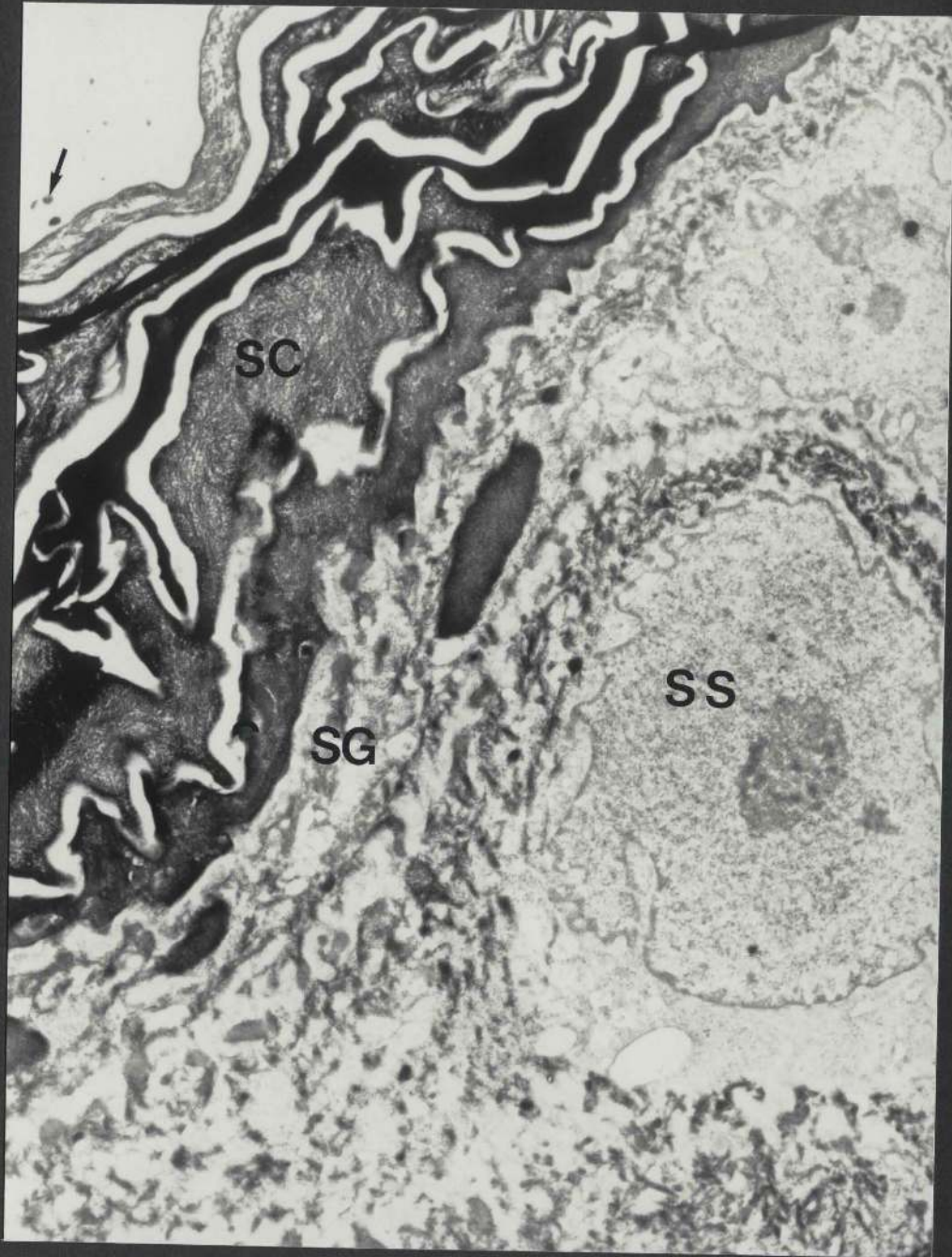
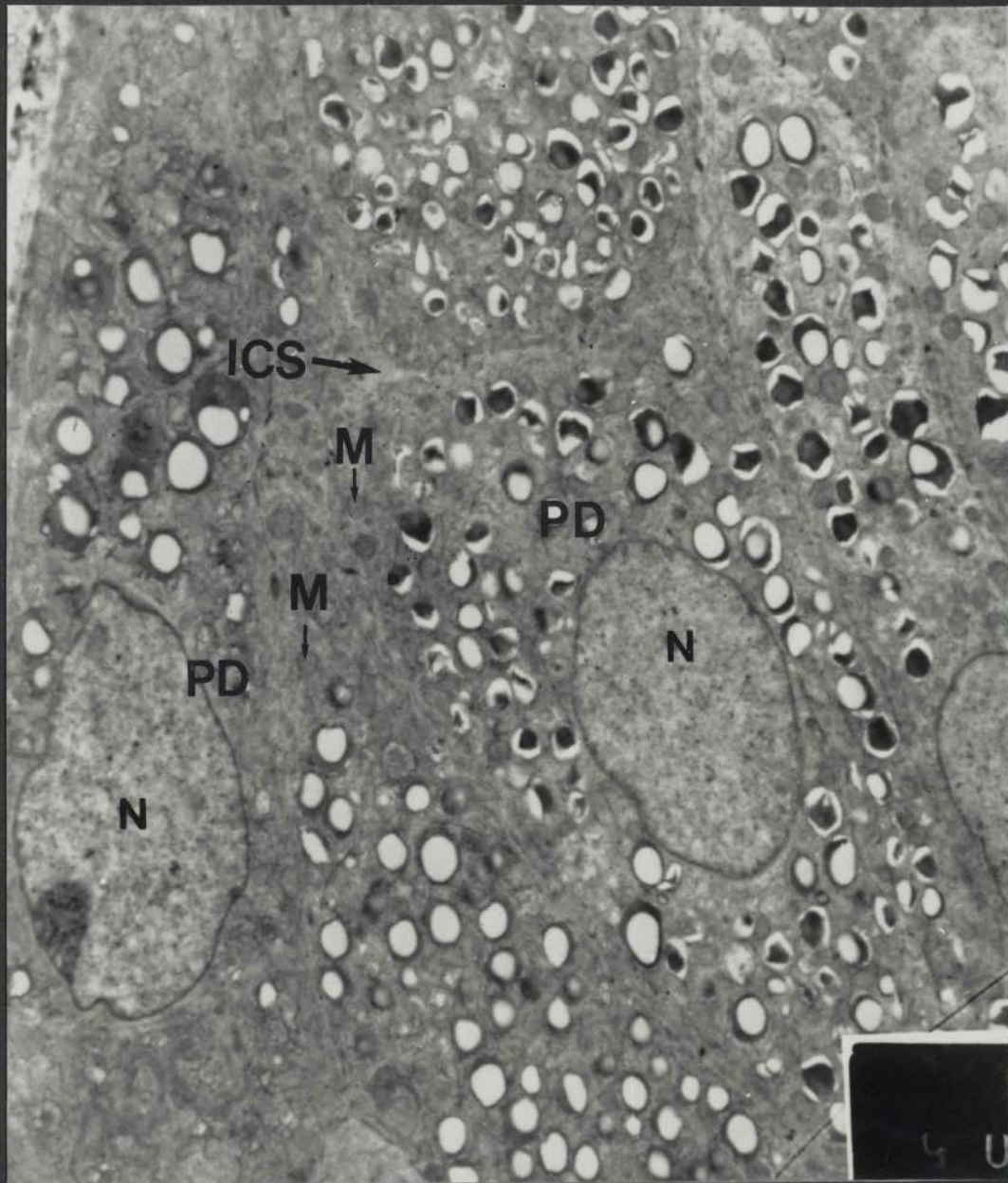


Figure 84b: This micrograph is from a section through the body of a sebaceous gland and illustrates portions of partially differentiated sebaceous cells (PD) (x 9,280). The fine intracellular details are preserved. The nuclei (N) of those cells are oval and regular in outline. Mitochondria (M) may be seen in the cytoplasm.

No lanthanum is present in the intercellular spaces (ICS) or inside the sebocytes and was not detected in the EDX spectrum obtained from the resin block-face containing the field shown.





## Figure 85 (a - d)

Positive iontophoresis of 1% (W/V) lanthanum nitrate in absolute ethanol at 30 milliamperes for 15 minutes

Figure 85a: This field shows the upper part of the epidermis which includes the stratum corneum (SC), the stratum granulosum (SG) and the upper part of the stratum spinosum (SS) (x 8,352)

The tracer is visible in all the intercellular spaces of the stratum corneum, including those between the two innermost corneal layers. Arrows indicate the location of the tracer. For the most part, the corneocytes appear to be free from tracer. The intercellular space between the basal corneal layer and the upper granular layers, as well as those in the viable epidermal layers, appear to be devoid of lanthanum also.

The EDX spectrum contained peaks for lanthanum when the analyzed area consisted of the stratum corneum. No tracer was detected in the viable epidermal layers.





Figure 85b: A transmission electron micrograph taken from the infundibulum of a hair follicle which includes the corneal (SC), the granular (SG), the spinous (SS) and the basal (SB) layers. A hair shaft (H) is seen adjacent to the stratum corneum (x 8,352).

Heavy regular deposits of lanthanum are clearly seen in the intercellular spaces in the outer corneal layers. A lighter deposit of the tracer may also be seen in the intercellular spaces of the inner corneal layers. In addition, patches of lanthanum are evident in the other epidermal layers (arrows) and the intracellular matrix of the outermost two or three corneal layers appears to contain lanthanum.

Severe histological changes may be seen, and these include condensation and elongation of the nuclei in the basal and spinous layers, widening of the intercellular spaces, and coagulation of the cytoplasmic matrix. EDX analysis did not only detect lanthanum in the stratum corneum, but also in the other epidermal layers.



Figure 85c: This micrograph is a longitudinal section of two neighbouring hair follicles at the level of the sebaceous ducts. Towards the upper right hand part of the field may be seen the hair shaft (H) of one of the follicles, surrounded by the stratum corneum (SC) of the follicular canal epidermis. Remnants of sebum (S) may be seen in the pilary canal (x 7,424).

A few deposits of an electron-dense material (arrows) are suspected to be mixed with the sebum in the pilary canal. However, the EDX spectrum from such a region did not indicate the presence of lanthanum.



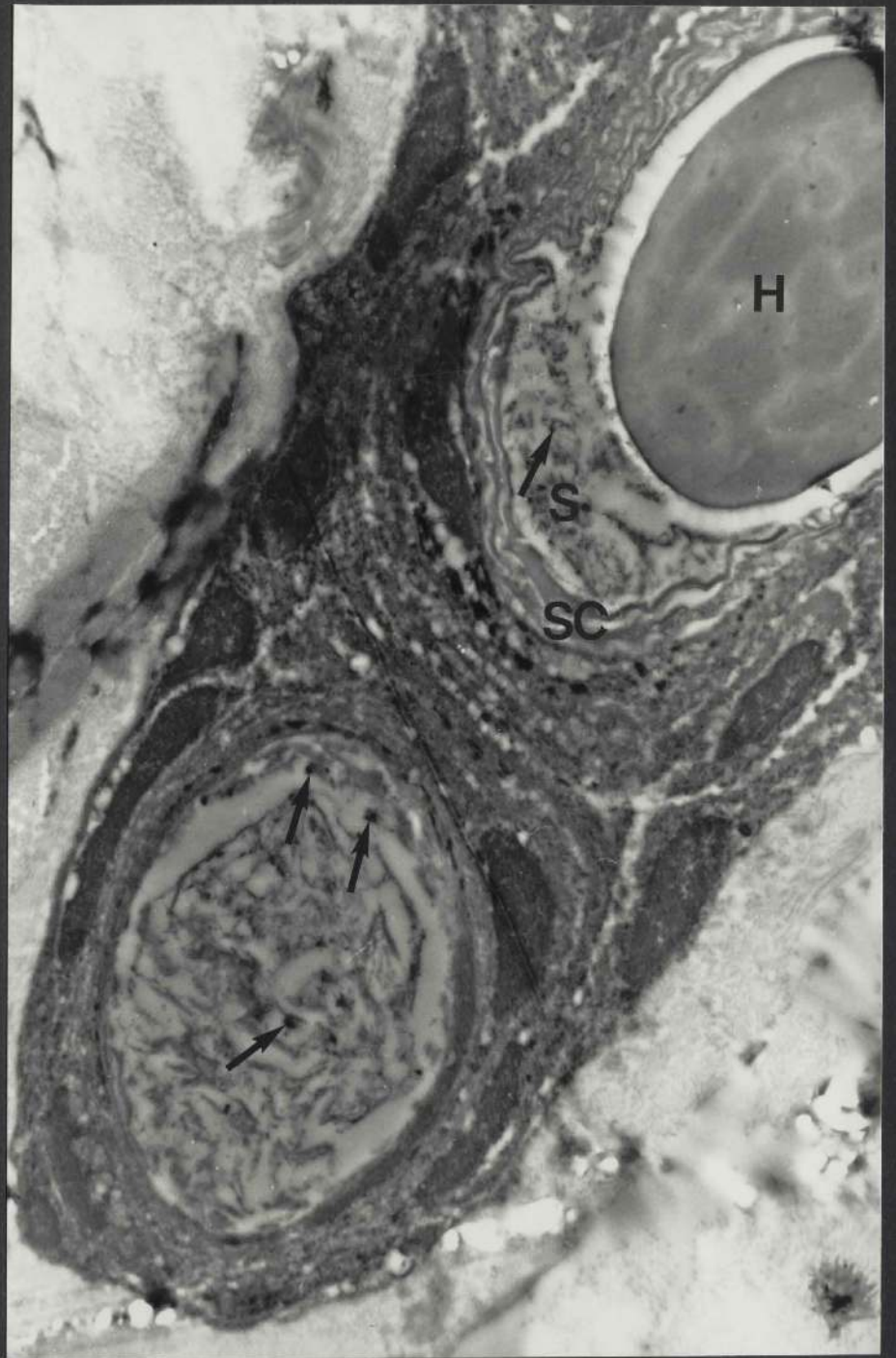
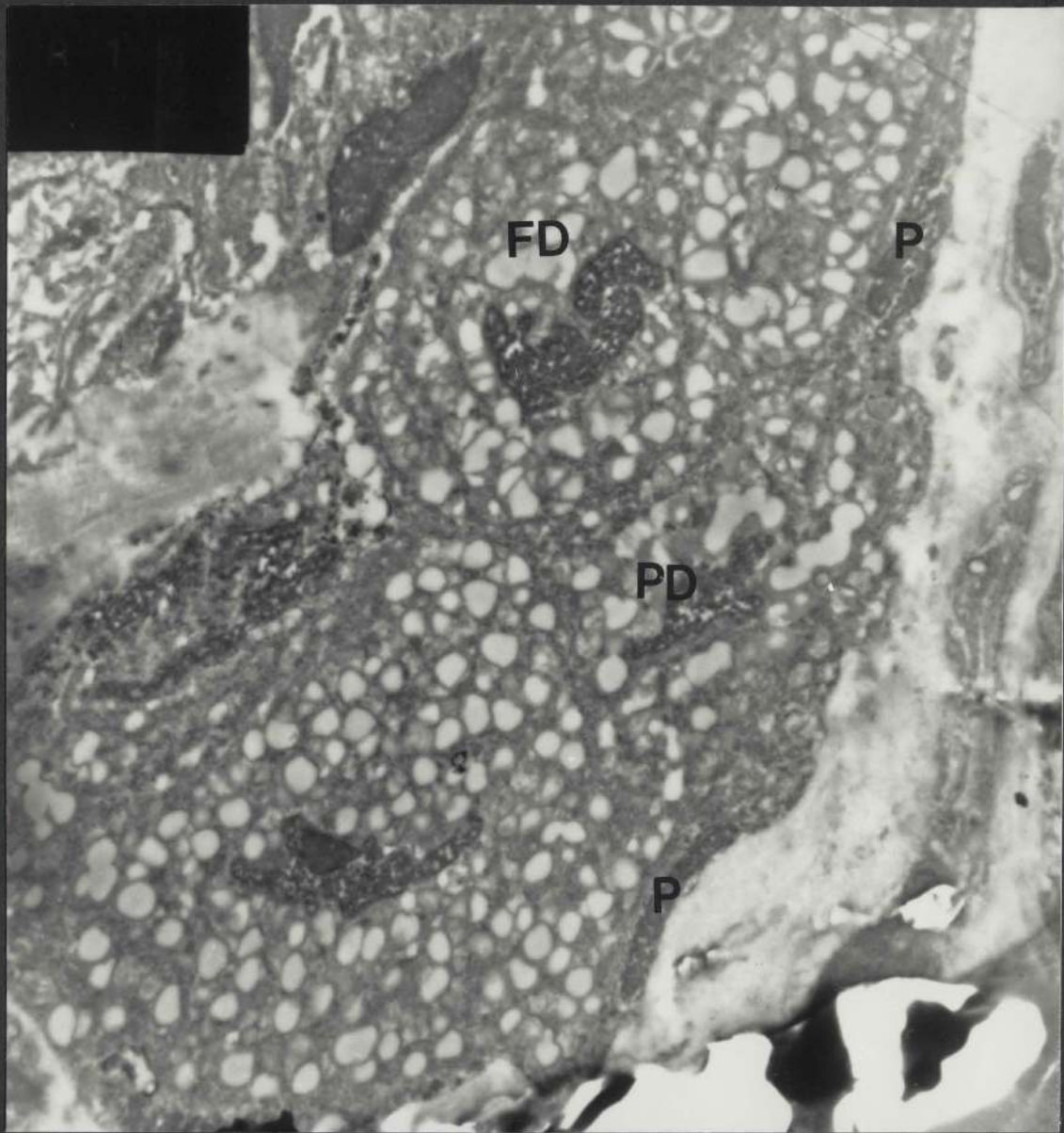


Figure 85d: This is an illustration of a segment of a sebaceous gland featuring sebaceous cells at different stages of maturation (x 7,424).

No electron-dense material is evident in any of the intercellular spaces between peripheral (P), partially differentiated (PD), and fully differentiated (FD) sebaceous cells. Furthermore, no lanthanum is seen inside the cells. The EDX spectrum of such a gland did not contain a peak for lanthanum.

Note the condensation and elongation of the nuclei (N) of the peripheral cells.



## Summary of results

Without the flow of current, the penetration of lanthanum from alcohol is negligible. Following iontophoresis, the penetration of the tracer through the stratum corneum of the epidermis down to, but not into, the intercellular space between the basal corneal layer and the upper granular layers is complete. This penetration appears to be mainly through the intercellular spaces, although small patches of dense material can occasionally be seen within some corneal cells.

The tracer has also penetrated the stratum corneum and extended into the inner epidermal layers of the follicular infundibulum. The tracer is seen inside and between cells in the outer layers of the stratum corneum, but is confined mainly to the intercellular spaces in the inner corneal layers and the viable epidermis.

Some electron-dense material is present in the ducts of the sebaceous glands; however, this can not be identified as lanthanum by the energy-dispersive X-ray analysis.

Although iontophoresis substantially increases the penetration of lanthanum into the skin, significant histological changes are seen accompanying such a penetration.



### 3.6 Silver

Silver, like lanthanum, is electron-dense and can be visualized directly in ultrathin sections and thus has been employed in electron microscopy. For example, Hayward and Hackemann (1973) applied a silver technique to ultrathin sections to investigate the chemical and structural nature of membrane-coating granules and the cell surface coat of human oral epithelium. Aqueous solutions of silver nitrate have been used as a stain for ribosomal proteins (Smith and Stuart, 1971).

Taking advantage of its electron density and high water solubility, silver nitrate was used as an additional tracer to investigate further the site of the cutaneous barrier and to explore its skin penetration by iontophoresis. Solutions of silver nitrate were injected intradermally, applied topically or subjected to iontophoresis. In all these experiments skin specimens were processed for transmission electron microscopy. As with lanthanum, penetration from within the skin to the surface and in the opposite direction was judged by the location and distribution of regular electron-dense deposits in ultrathin sections. EDX analyses were carried out, using the scanning electron microscope, on the "faces" of the resin blocks from which the ultrathin sections were produced.

It was observed that shortly following contact with the silver nitrate solution, the skin always became darker.

### 3.6.1 Intradermal injection

A 1% aqueous silver nitrate solution was injected intradermally and biopsies were excised 15 minutes later. The results obtained are shown in Figure 86 (a - f).

Figure 86a: A scanning electron microscope image from the face of a resin block following ultrathin sectioning. EDX analyses were carried out on different sites in the epidermis (E), the hair follicles (HF) and the sebaceous glands (SG). Some of the analyzed areas are outlined by the electron beam (arrows). EDX analysis was also carried out on an area of the block-face just outside the tissue. By comparing the spectrum obtained from the resin with those obtained from the resin plus the skin, signals arising from the skin alone can be identified. The spectra obtained are shown overleaf. The elements present in the resin may include peaks for magnesium, aluminium, osmium, sulphur and chlorine. The spectra obtained from the resin plus skin include, in addition to the above elements, peaks for silver. Thus it appears that the silver peaks are originating from the skin.

With respect to its penetration, silver was detected in the epidermis, the sebaceous glands and the hair follicles. The precise localization of silver in these structures was determined from ultrathin sections.



15KV

1550

100.0U

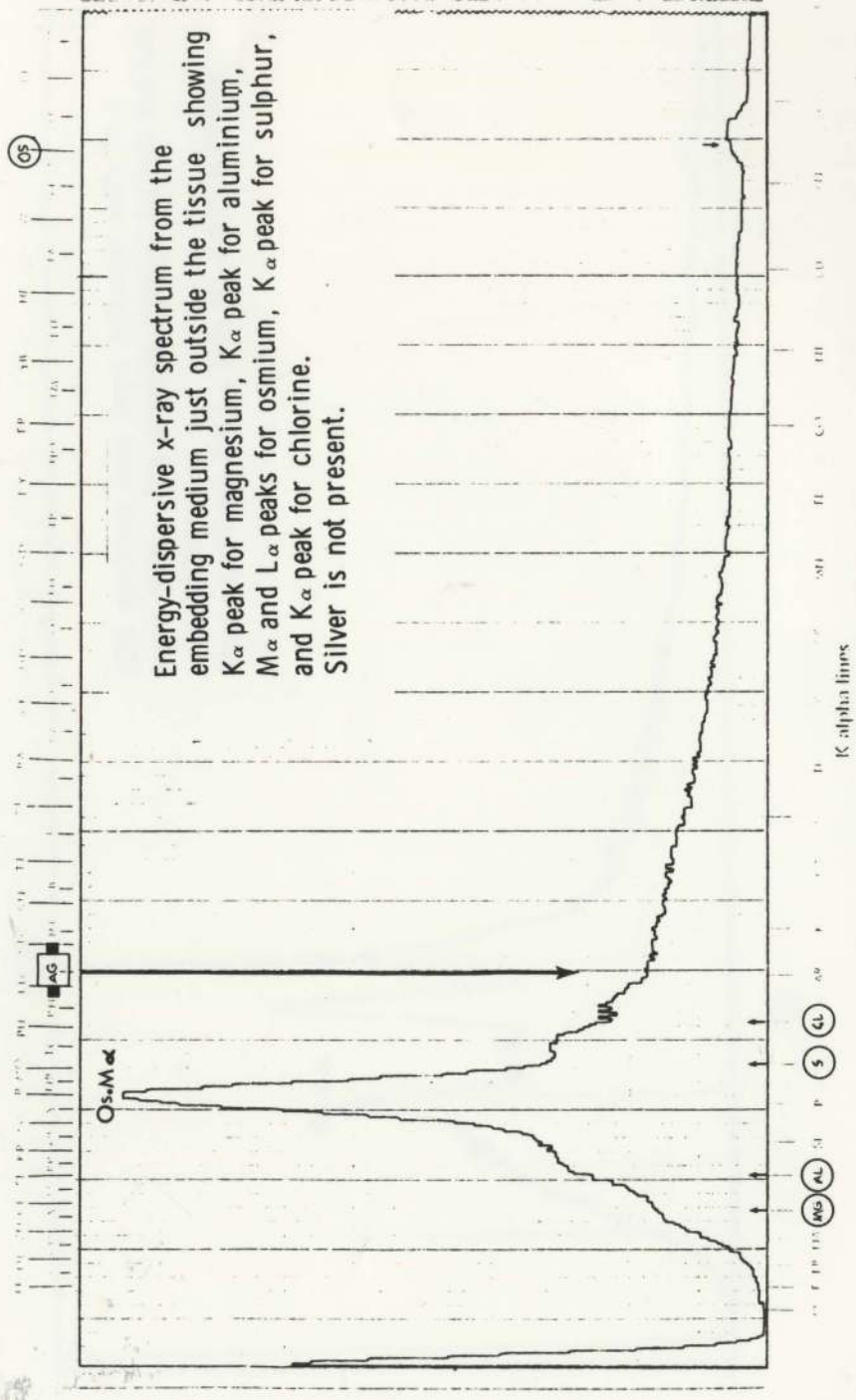
SAUEM



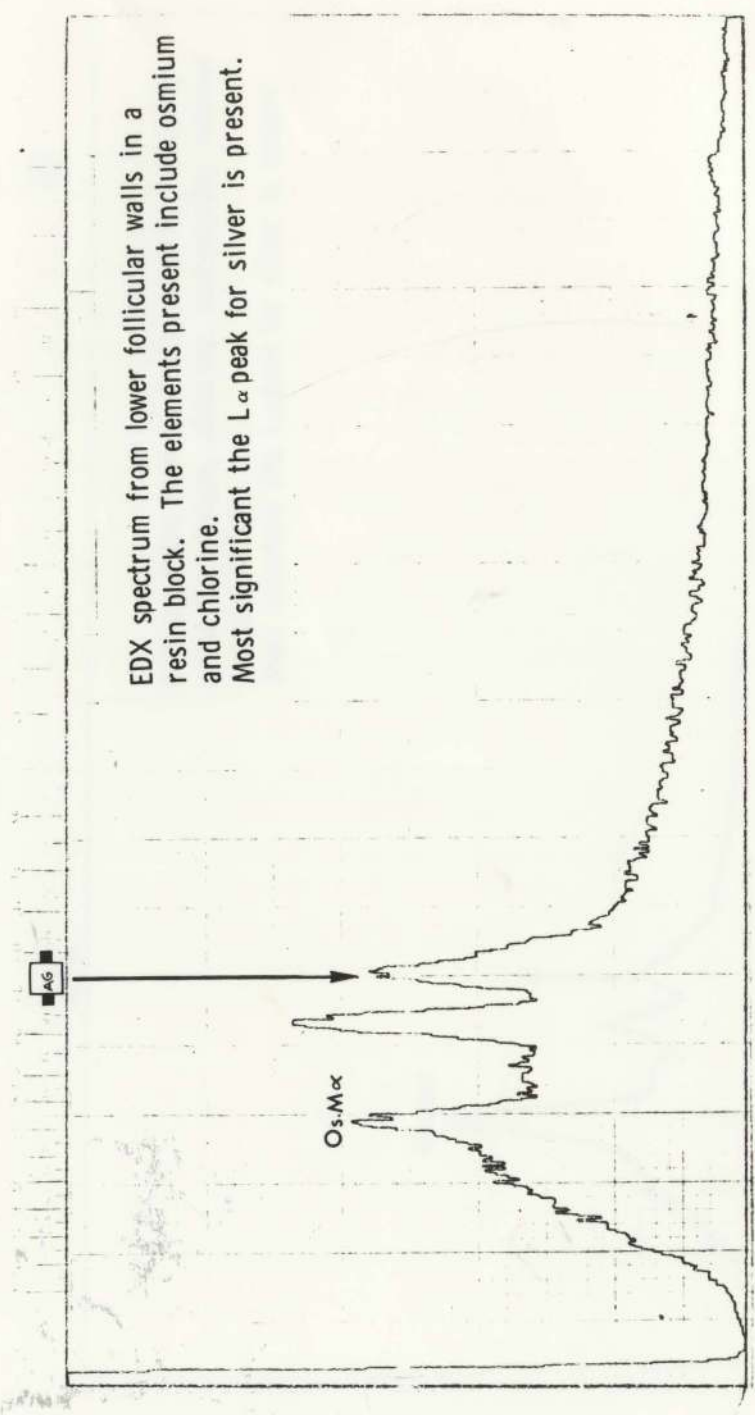
St. Andrews University S.E.M. Unit.  
 Catty Marine Lab.

Sample ..... Intracutaneous injection of a 1 percent silver nitrate in distilled water.  
 KeV ..... 15  
 Seconds ..... 100  
 Take off Angle ..... 33°

L. alpha lines



Laboratory  
 Sample  
 15  
 Intracutaneous injection of a 1 percent aqueous silver nitrate solution.  
 33°  
 Researcher  
 100  
 L alpha lines  
 33°



EDX spectrum from lower follicular walls in a resin block. The elements present include osmium and chlorine. Most significant the  $L_{\alpha}$  peak for silver is present.

(CL)

L alpha lines

Counts

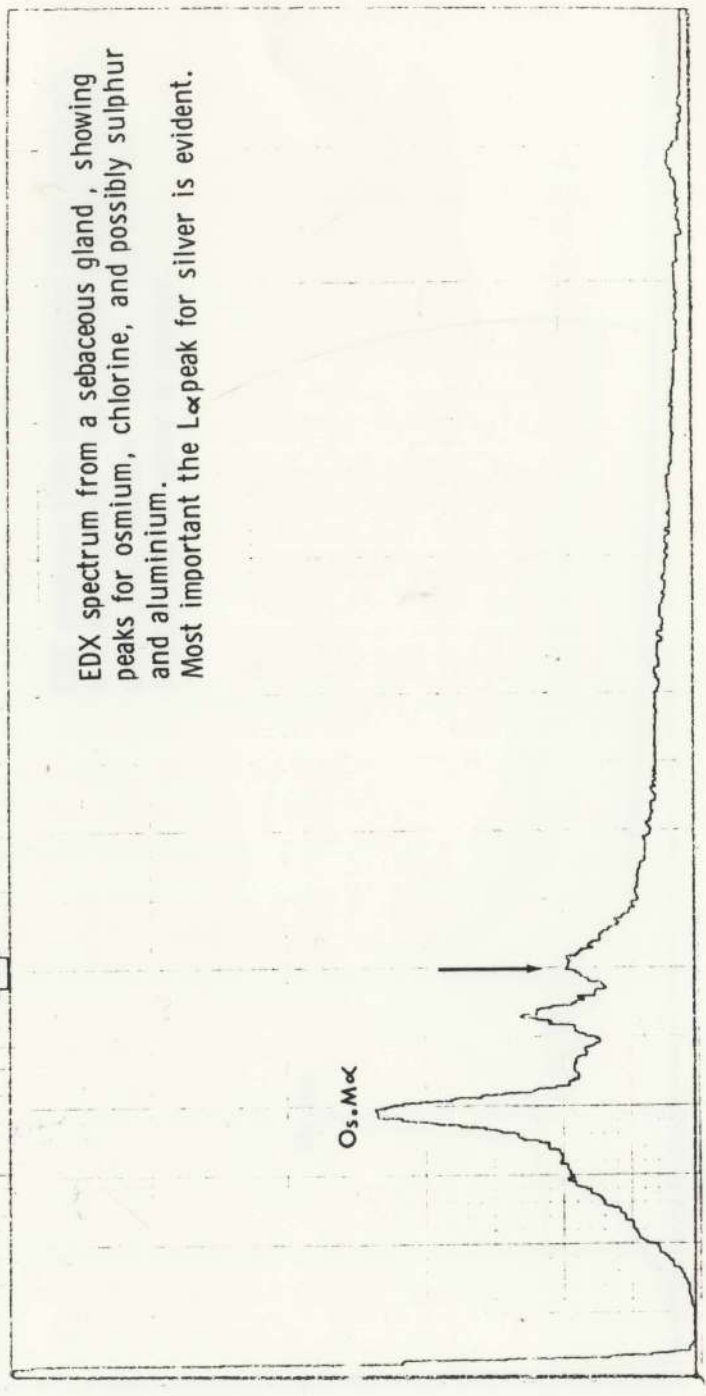


15 Intracutaneous injection of a 1 percent aqueous silver nitrate solution. 33°

100  
Seconds  
Counts/minutes

OS

Ag



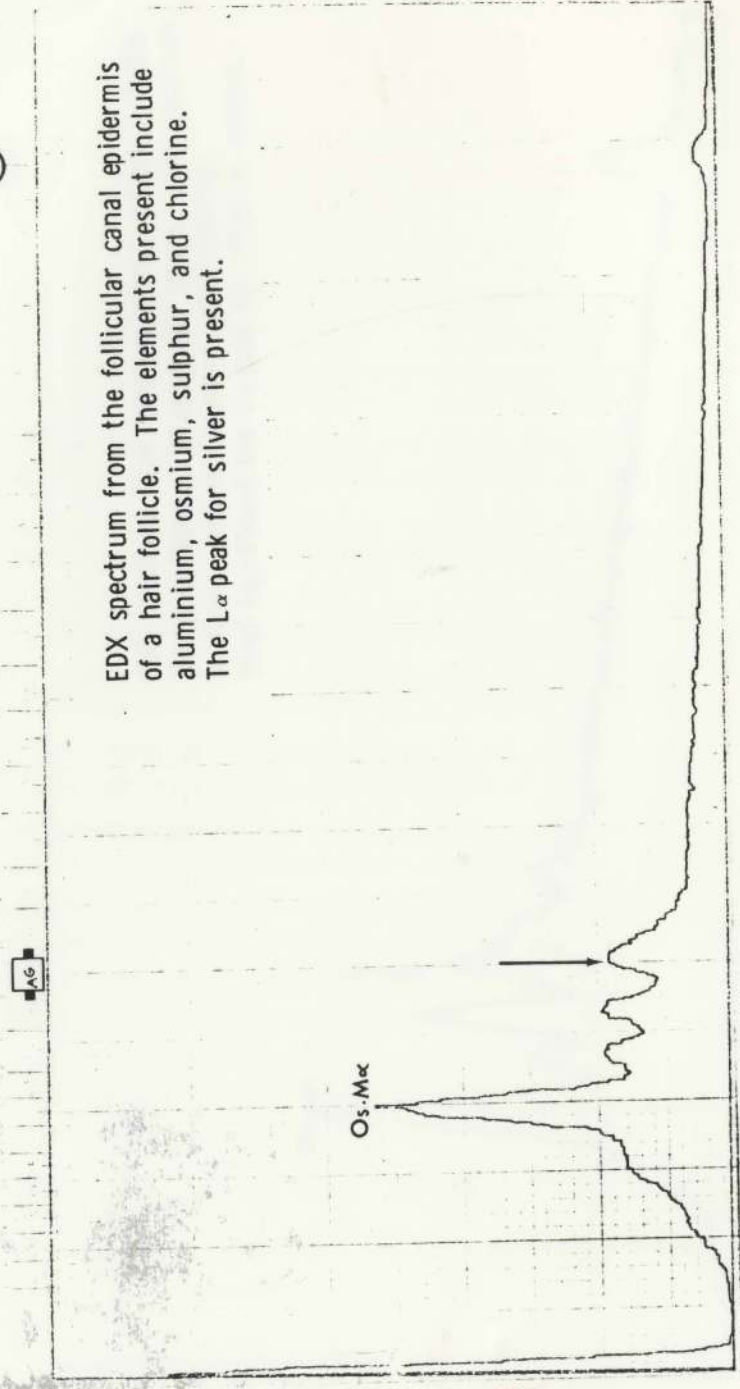
EDX spectrum from a sebaceous gland, showing peaks for osmium, chlorine, and possibly sulphur and aluminium. Most important the L $\alpha$  peak for silver is evident.

S CL

OS

CL

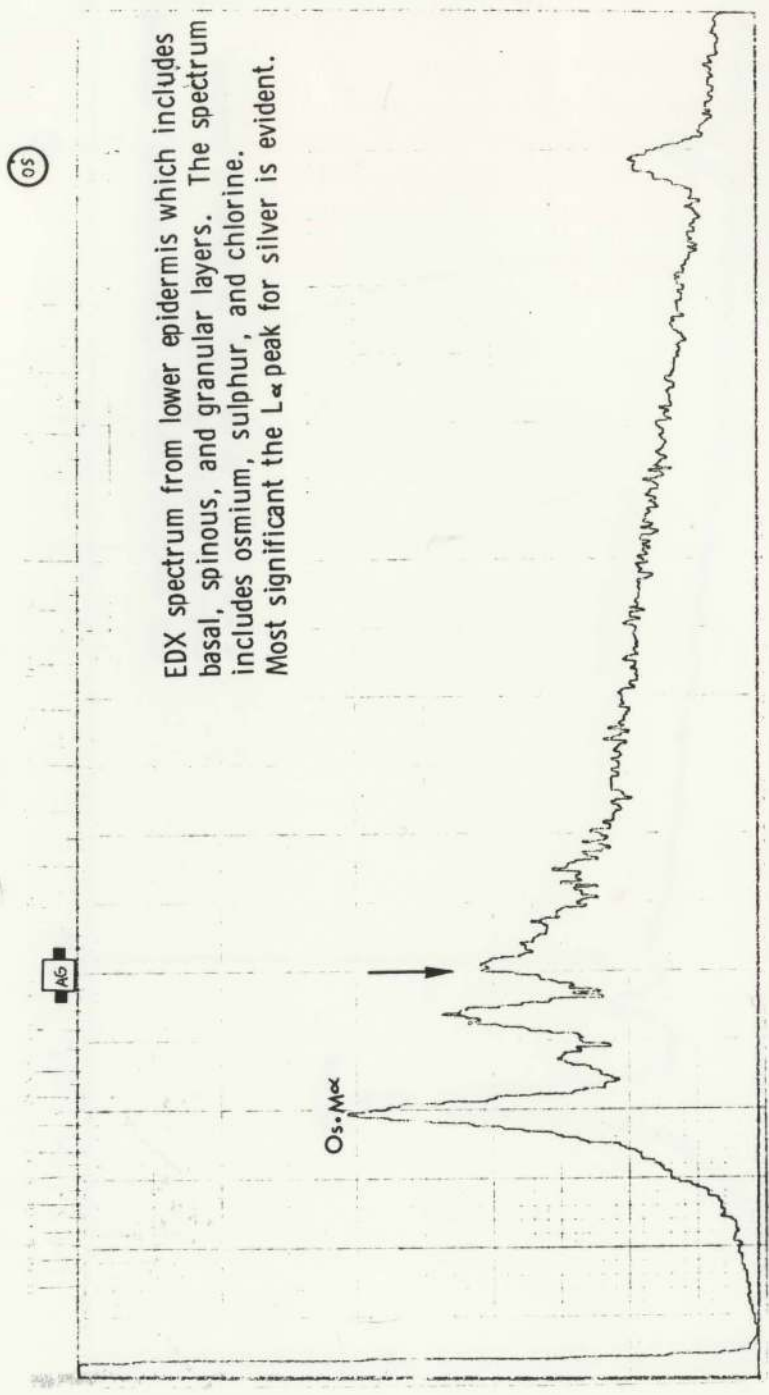
Laboratory .....  
 Sample .....  
 No. ....  
 Researcher .....  
**Intracutaneous injection of a 1 percent aqueous silver nitrate solution.**  
 15 .....  
 100 .....  
 33° .....  
 Subject .....  
 Tissue or sample .....  
 L. applications .....



EDX spectrum from the follicular canal epidermis  
 of a hair follicle. The elements present include  
 aluminium, osmium, sulphur, and chlorine.  
 The L<sub>α</sub> peak for silver is present.



Laboratory: Base metal:  
 Intracutaneous injection of a 1 percent aqueous silver nitrate solution. Take off angle: 33°  
 15 Seconds: 100  
Alpha lines:

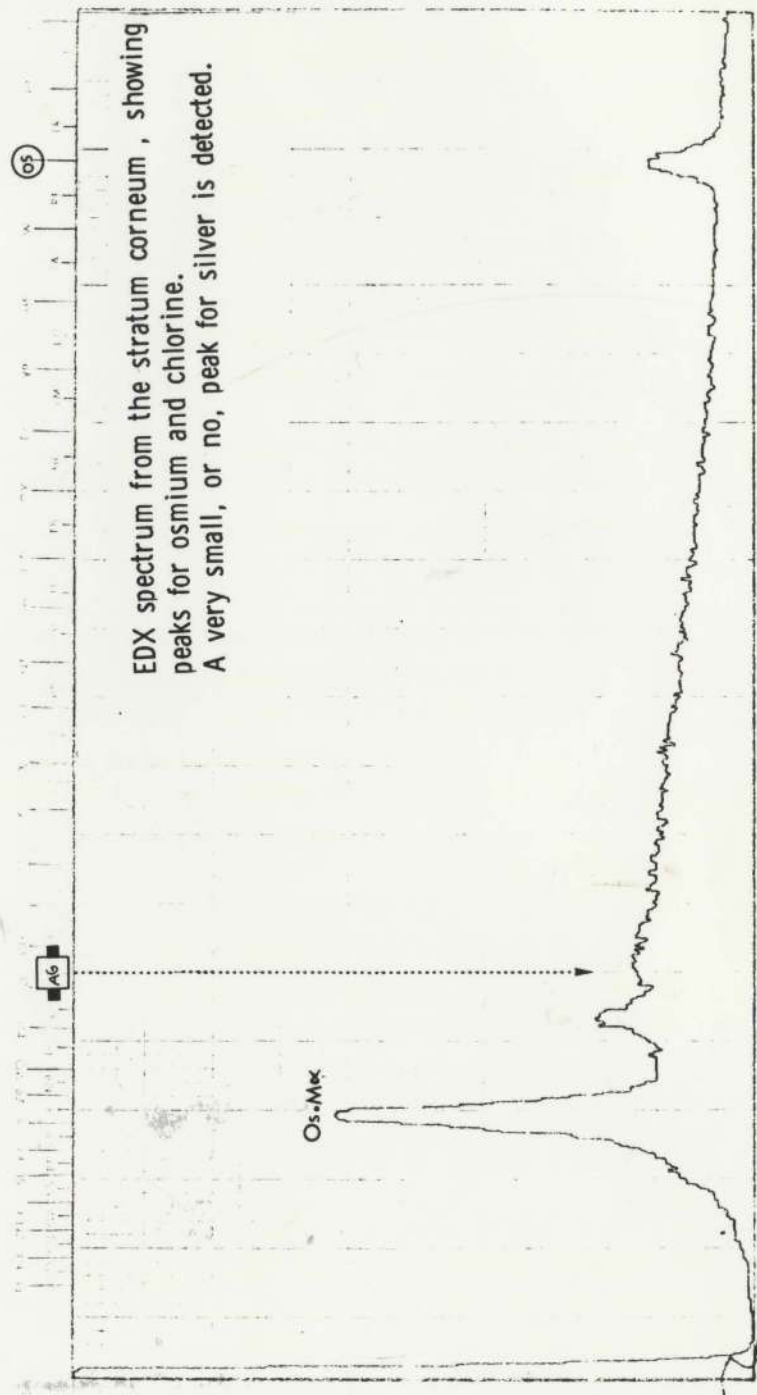


EDX spectrum from lower epidermis which includes basal, spinous, and granular layers. The spectrum includes osmium, sulphur, and chlorine. Most significant the  $L_{\alpha}$  peak for silver is evident.



Label:   
 Sample: **Intracutaneous injection of a 1 percent aqueous silver nitrate solution.**   
 KeV: **15**   
 Seconds: **100**   
 Take-off Angle: **33°**   
 Date:

L alpha line



EDX spectrum from the stratum corneum , showing  
 peaks for osmium and chlorine.  
 A very small, or no, peak for silver is detected.

Figure 86b: A transmission electron micrograph from the lower region of a hair follicle featuring cells in the outer root sheath (ORS) (x 8,352).

Regular electron-dense deposits of silver are visible in all the intercellular spaces between the cells, including regions of desmosomal attachments (DS) as well as hemidesmosomal complexes (H) uniting the cells of the outer root sheath to the underlying basement membrane (BM).

Moreover, the dense material is evident intracellularly in the cytoplasm and nuclei of the cells (arrows). Patches of the dense material are also seen in the dermis (D). The EDX spectrum contained  $L\alpha$  peak for silver when the analysis was performed on an area containing the region of the hair follicle from which this micrograph was produced.

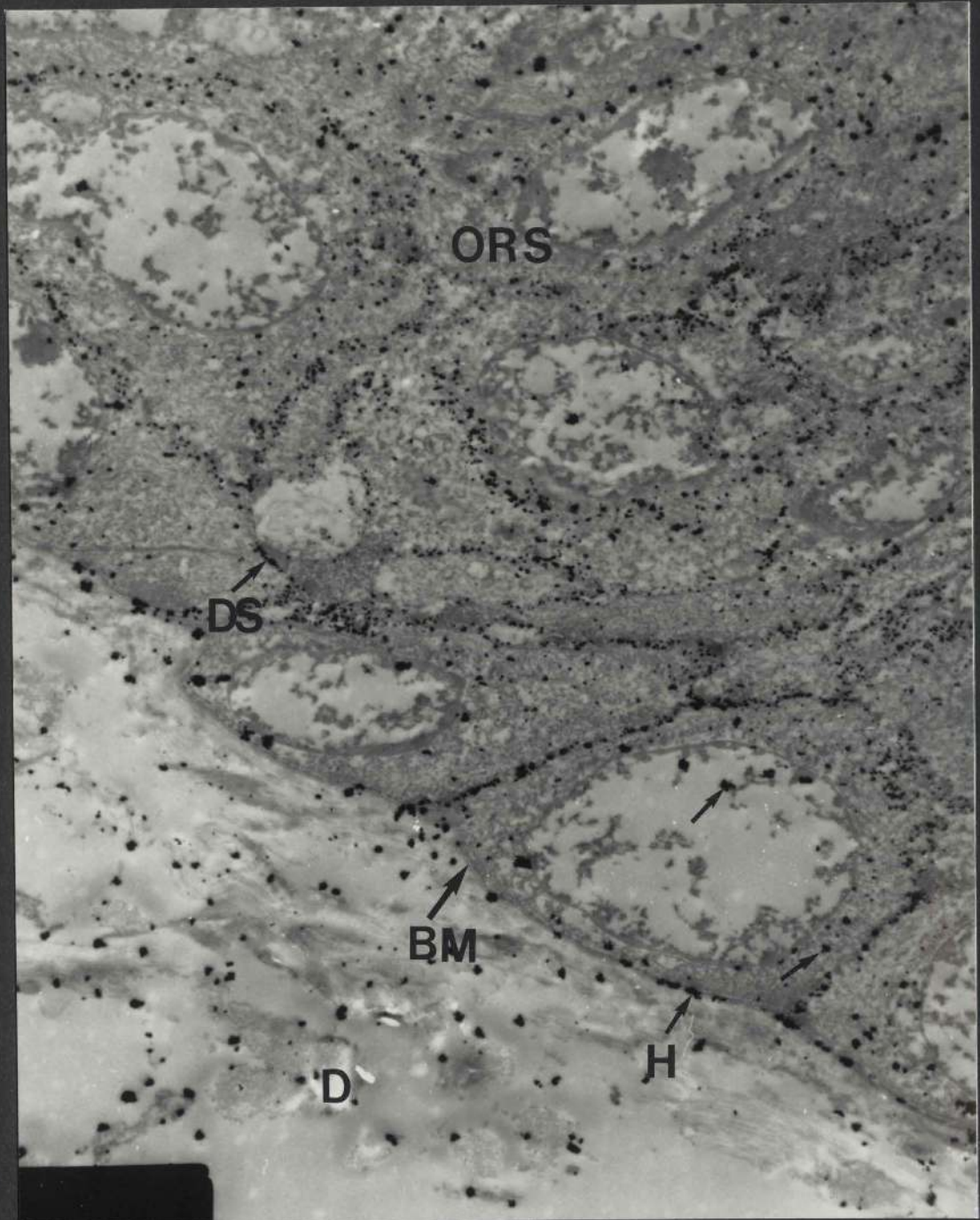


Figure 86c: This is a tangential section of a hair follicle at the level of the entry of the duct of a sebaceous gland into the follicle (x 8,352).

Electron-dense material (silver) may be seen mixed in with the remnants of sebum (S), and on the surface of the cuticle of the hair (H). Small patches of silver are also seen on and within the disintegrating stratum corneum (SC) of the follicular infundibulum. Arrows indicate the location of silver.

The EDX spectrum contained silver when the analysis was carried out on the area of the block-face from which this micrograph was produced.

Figure 86d: This micrograph illustrates sebaceous cells at different stages of maturation (x 8,352).

An electron-dense material is evident in the spaces between the sebaceous cells, and within the cytoplasm between the lipid droplets (Li) of the fully differentiated (FD) and the partially differentiated (PD) cells. Arrows indicate the location of the tracer.

EDX analysis confirmed the presence of silver in the sebaceous gland.



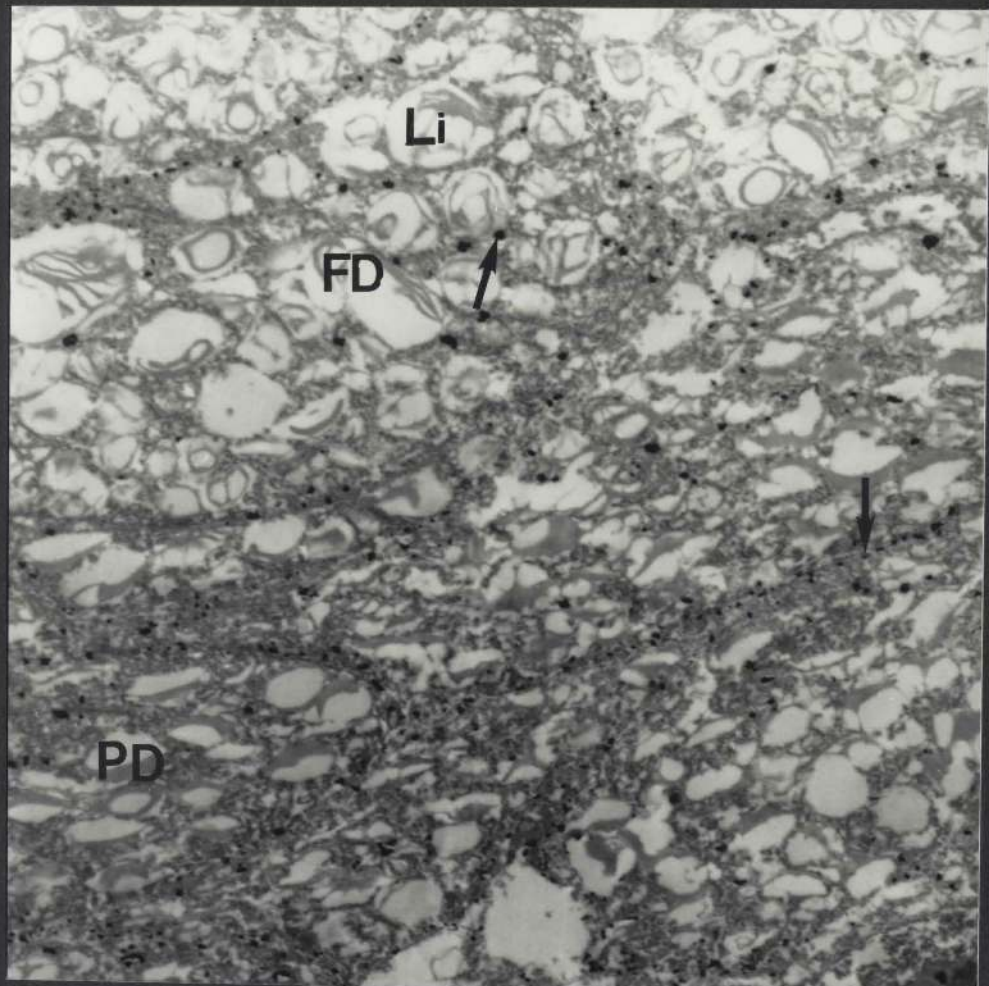
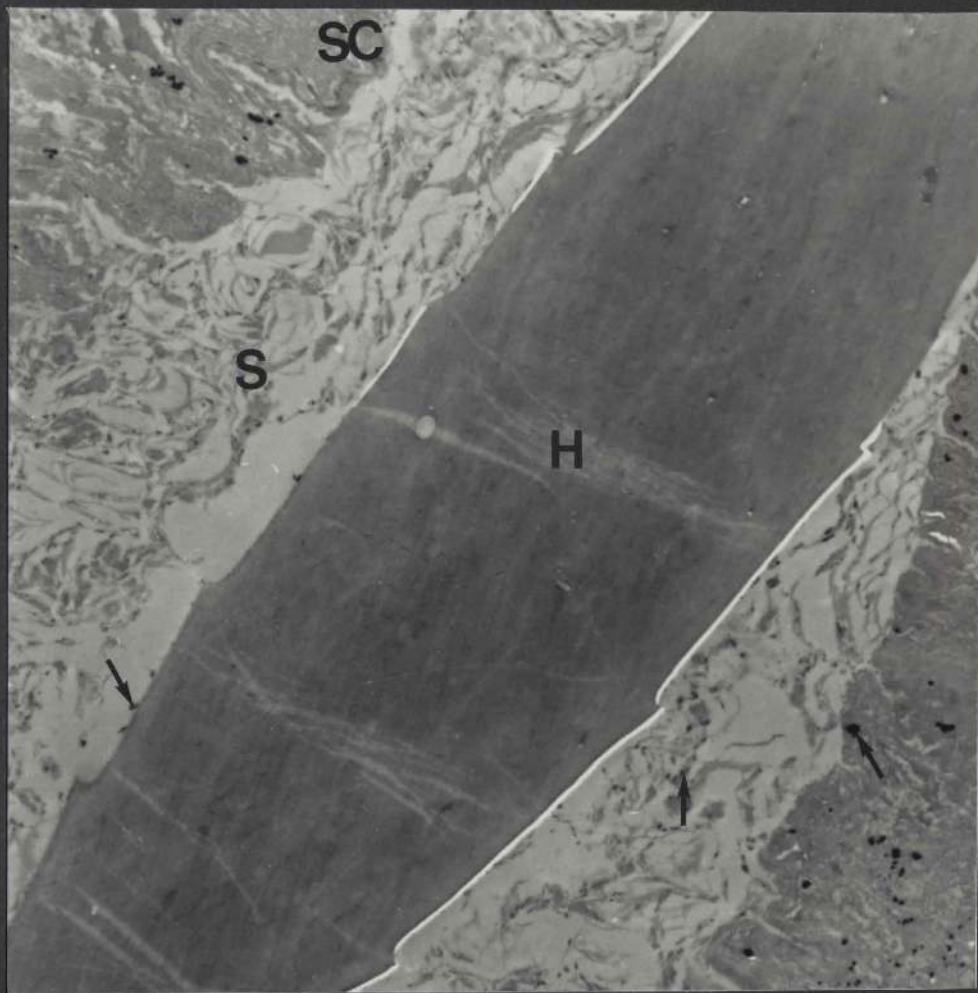


Figure 86e: Two transmission electron micrographs taken from the follicular canal epidermis of two hair follicles.

The micrograph opposite features the viable layers of the follicular canal epidermis (x 9,280). It shows silver granules in the inter- and intra- cellular regions of the basal (SB), the spinous (SS) and the granular (SG) layers of the follicular infundibulum.

This field shows the other layers of the wall of the follicular infundibulum (x 10,208).

It is apparent that silver has extended into the intercellular space between the two basal corneal cells (SC). Moreover, a small patch of silver is seen inside one of the basal corneocytes. The remainder of the stratum corneum, however, is free from silver granules. No silver is seen on the surface of the stratum corneum.

EDX analysis confirmed the presence of silver in the follicular infundibulum.



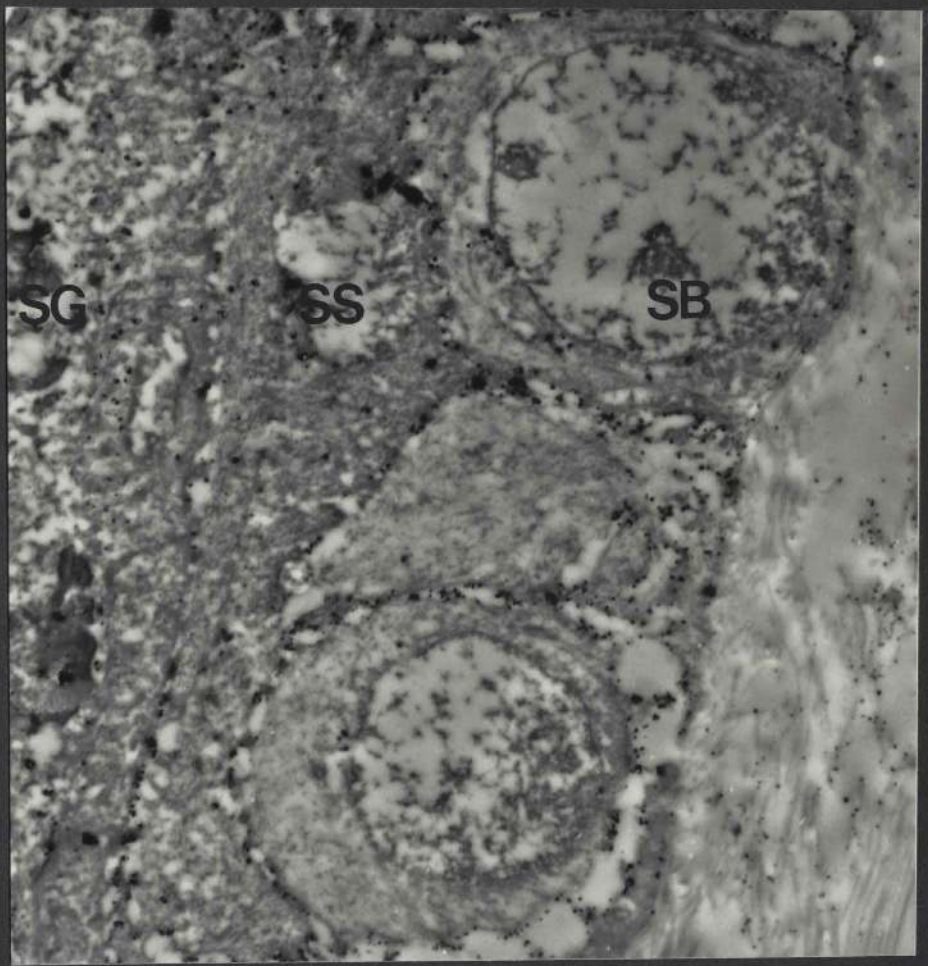


Figure 86f: The structures shown in this micrograph include the basal (SB), the spinous (SS), the granular (SG) and the horny layers of the epidermis (x 7,424).

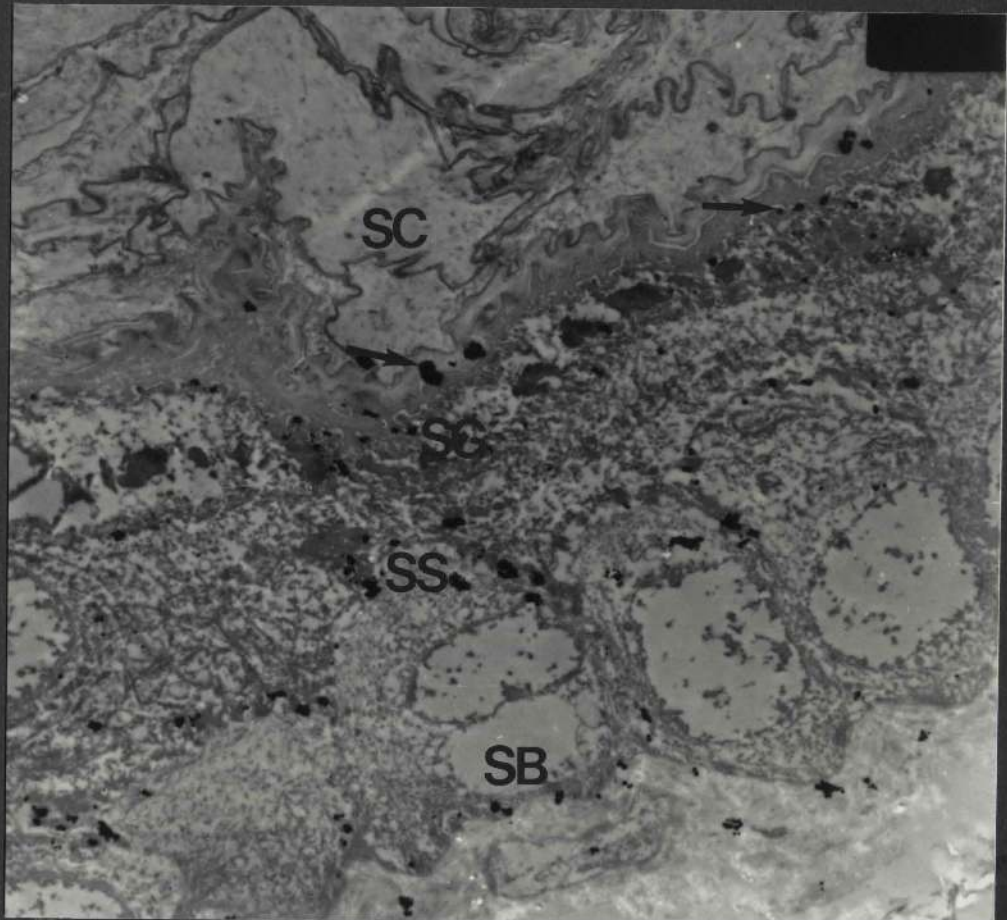
This micrograph is of interest in that it shows that silver is not only visible in the intercellular and intracellular regions of the basal, spinous and granular layers, but is also seen in the intercellular region between the superficial granular and the basal corneal layers. Moreover, the tracer migrates into the two deepest corneal layers, but not into the other layers in the stratum corneum.

The EDX spectrum contained peaks for silver when the analysis was carried out on the viable epidermis and the deeper corneal layers.

#### Summary of results

Following intradermal injection, the tracer is seen inside and between the cells of the outer root sheath. The silver granules are also found in all the inter- and intra- cellular regions in the sebaceous glands, and in the region of the sebaceous duct. Silver is also seen within and between the cells in the stratum basale, the stratum spinosum and the stratum granulosum. The tracer extends into the intercellular space between the superficial granular and the basal corneal layers and, furthermore, extends into the two deepest corneal layers. However, no tracer is found in the other layers of the stratum corneum. The EDX analyses confirmed these findings.





### 3.6.2 Effect of concentration

The following group of experiments was carried out to investigate the effect of changing the tracer concentration on the penetration of the tracer from the surface into the skin.

Silver nitrate was prepared in distilled water to a concentration of 2, 4 or 8%. Each of these solutions was then applied locally or with iontophoresis. The results obtained are shown in Figures 87 to 92.

#### Figure 87 (a - c)

Local application (control) of a 2% aqueous silver nitrate solution for 15 minutes

Figure 87a: This micrograph features the stratum corneum (SC), the stratum granulosum (SG), the stratum spinosum (SS) and the stratum basale (SB) of the epidermis (x 10,208).

A few deposits of silver are found on the surface of the skin (arrow), but these do not extend into the stratum corneum.

A very small or no peak for silver was obtained when EDX analysis was carried out on the stratum corneum.



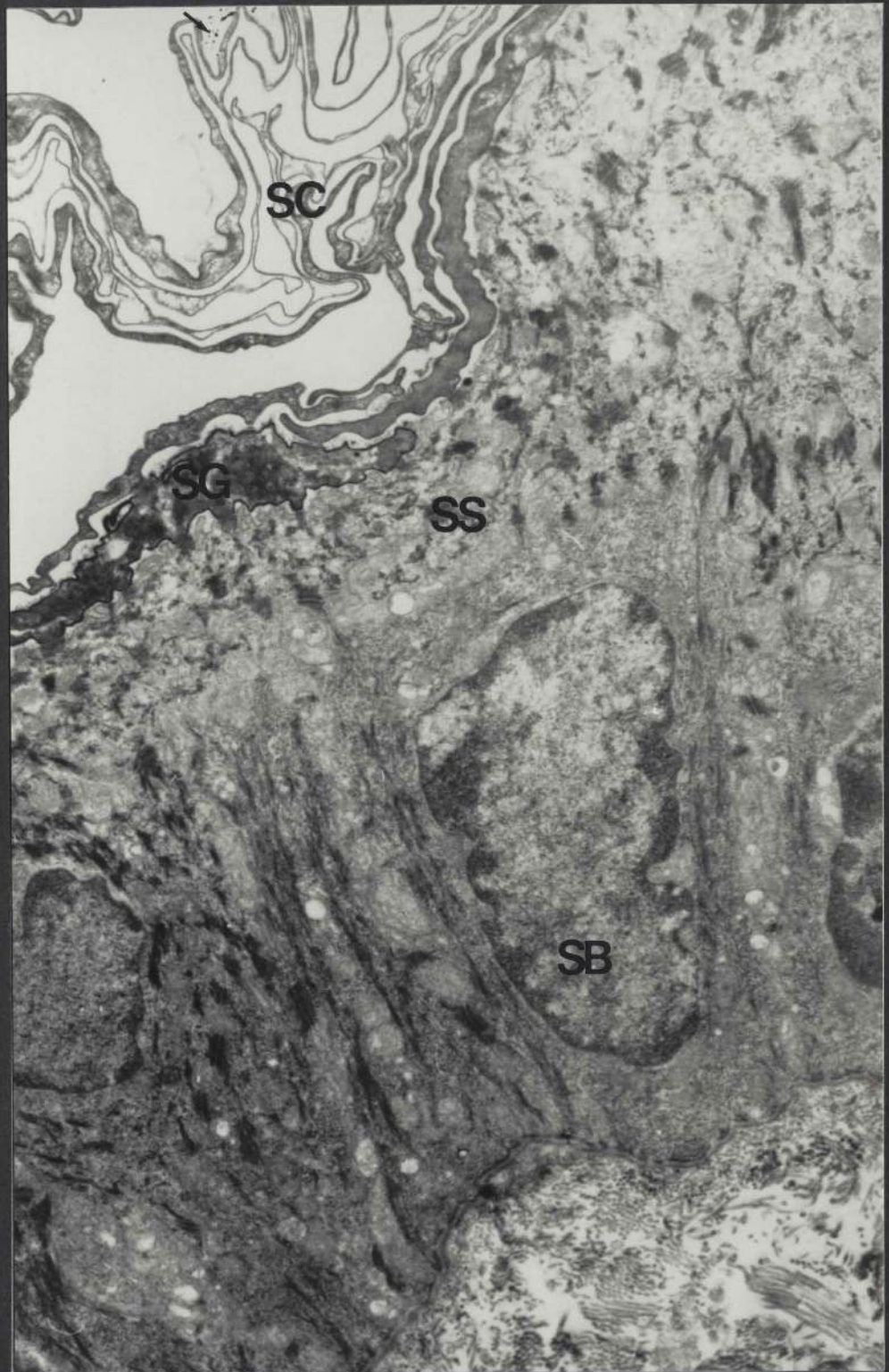


Figure 87b: This micrograph shows the follicular canal epidermis at the level of entry of the sebaceous duct (x 8,352).

Silver is not present on the surface of the stratum corneum (SC). The stratum corneum, the stratum granulosum identified by its keratohyalin granules (Kh), the stratum spinosum(SS) and the stratum basale (SB) do not contain tracer. No tracer is evident in the region of the sebaceous duct (SD).

The EDX spectrum from the follicular canal epidermis did not contain a peak for silver.





Figure 87c: A segment of a sebaceous gland exhibiting peripheral (P) and partially differentiated (PD) cells (x 12,992)

The intercellular and intracellular regions do not contain tracer.

Silver was not detected by EDX analysis of the sebaceous gland.

#### Summary of results

Following local application of a 2% aqueous silver nitrate solution, the penetration of the tracer is negligible. The tracer is visible on the surface of the skin only and does not extend into the hair follicles or the sebaceous glands.

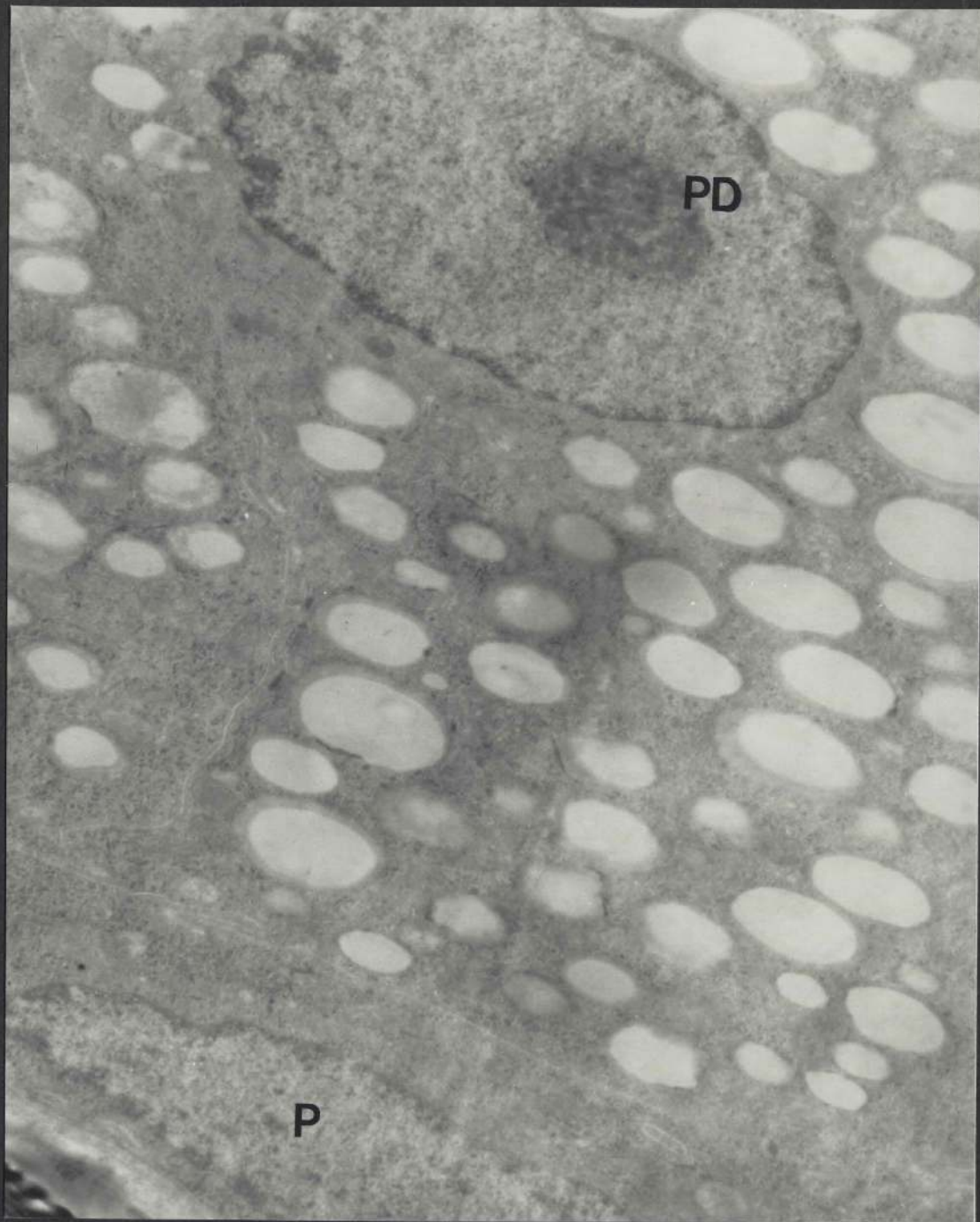


## Figure 88 (a - c)

Positive iontophoresis of a 2% aqueous silver nitrate solution at 30 milliamperes for 15 minutes

Figure 88a: This micrograph illustrates the basal (SB), the spinous (SS), the granular (SG) and the horny (SC) layers of the epidermis (x 9,280).

The tracer is found in all the layers of the stratum corneum, excluding the two innermost corneal layers.

The other epidermal layers are free from tracer. One may note the condensation of the nuclei (N) in the basal and spinous layers. The EDX spectrum contained a peak for silver when analysis was confined to the stratum corneum.



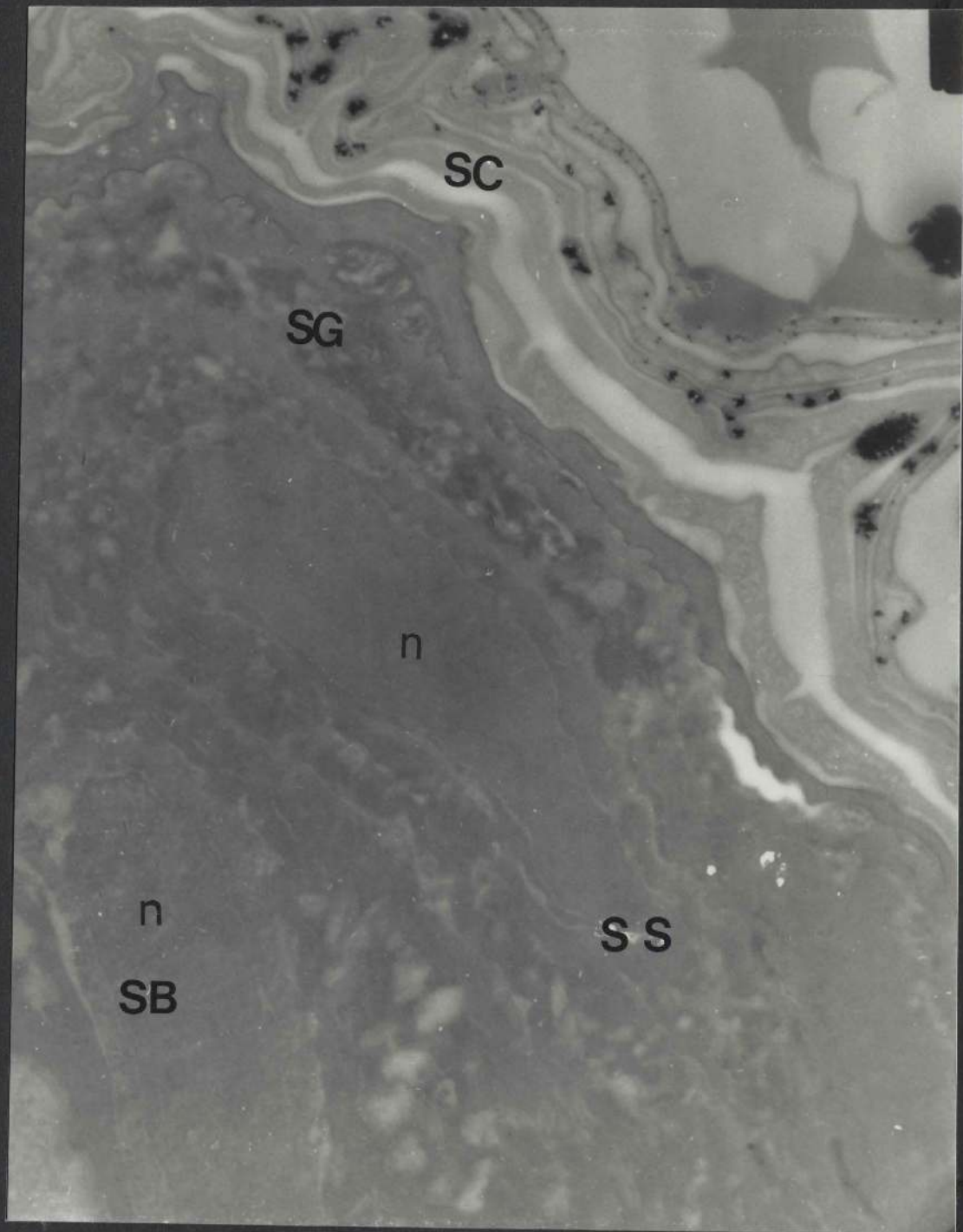


Figure 88b: This micrograph is obtained from two neighbouring hair follicles at the level of entry of a sebaceous duct (SD). One may note the disintegration of the stratum corneum (SC) at this level. The hair shaft is preserved in one of the follicles, but is missing from the other (x 8,352).

No tracer is visible in the region of the sebaceous duct (SD) or on the surface of the stratum corneum.

The EDX spectrum did not contain silver when analysis was performed on the area from which this micrograph was produced.





Figure 88c: This micrograph shows a portion of a sebaceous gland (SG) at a lower level than that seen in Figure 88b (x 8,352).

The intercellular and intracellular regions of the gland do not contain silver.

Silver was not detected in the corresponding EDX spectrum.

### Summary of results

Following iontophoresis, the tracer penetrates most of the layers of the stratum corneum. However, no tracer is found in the deeper epidermal layers, the follicular infundibulum or the sebaceous glands.



## Figure 89 (a - c)

Local application of a 4% aqueous silver nitrate solution for 15 minutes

Figure 89a: This field spans the full thickness of the epidermis (x 8,352).

A few isolated patches of an electron-dense material (arrow) are found on the surface of the skin, but these do not extend into the stratum corneum (SC) or into the deeper epidermal layers (DE).

A small  $L\alpha$  peak for silver was detected from the surface of the skin with EDX analysis.

Figure 89b: This field is taken from the follicular infundibulum (x 9,280).

No electron-dense material is found on or in the stratum corneum (SC).

The EDX spectrum did not contain a peak for silver.



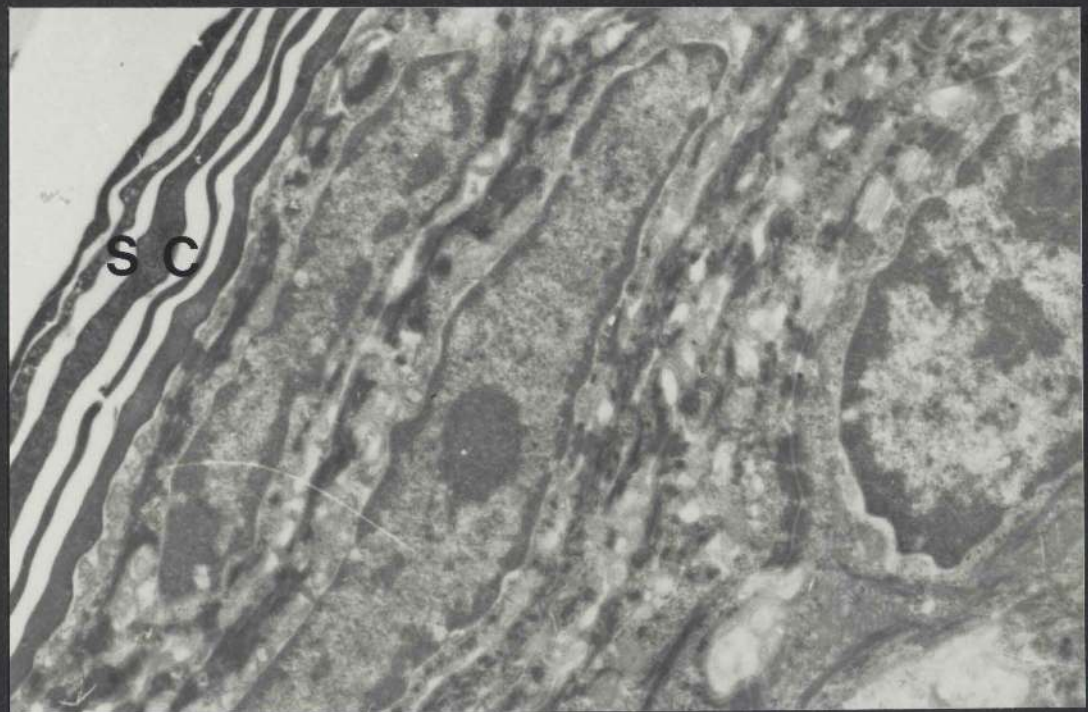
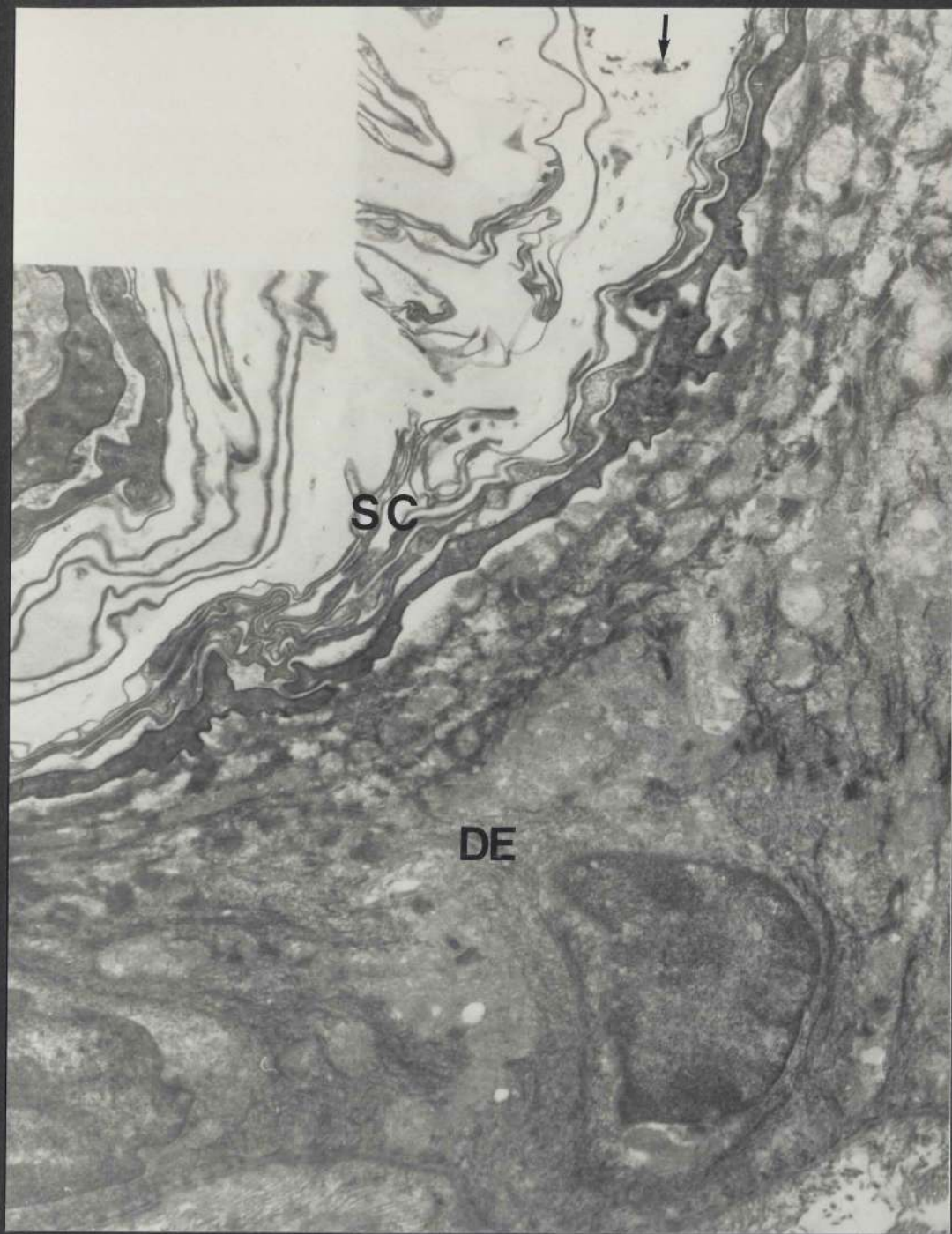


Figure 89c: A portion of a sebaceous gland is illustrated in this micrograph and includes peripheral (P) and partially differentiated (PD) sebaceous cells (x 12,000).

No electron-dense tracer is evident in the sebaceous gland.

No silver was found in the EDX spectrum.

#### Summary of results

The penetration of silver from a 4% aqueous solution is negligible. No tracer is found in the stratum corneum or in the deeper epidermal layers. The sebaceous glands are also free from silver.

The results are similar in this case to those obtained when a 2% aqueous silver nitrate solution is applied locally for the same duration of time (Figure 87 a - c).



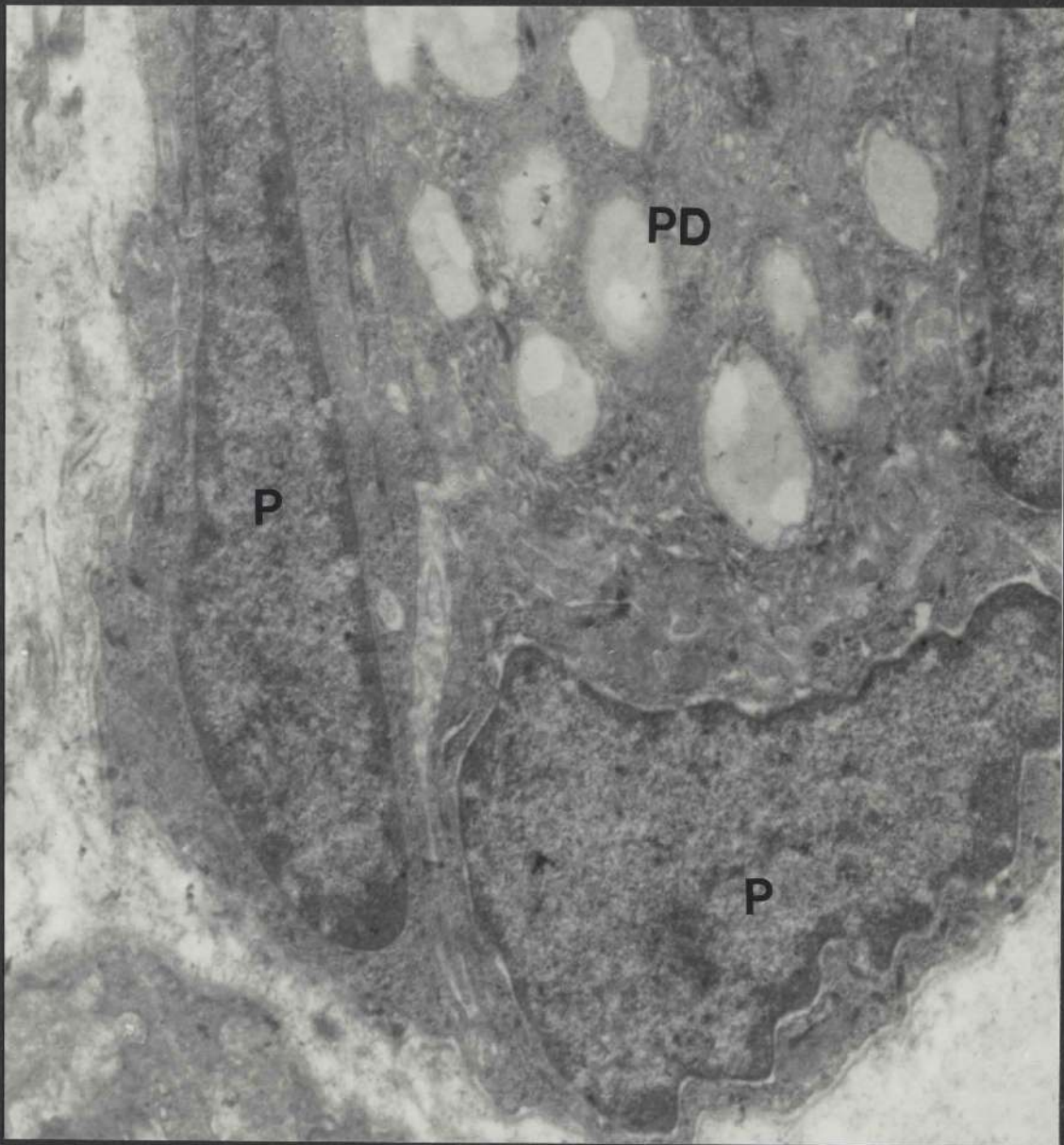


## Figure 90 (a - e)

Positive iontophoresis of a 4% aqueous silver nitrate solution at 30 milliamperes for 15 minutes

Figure 90a: This micrograph shows the stratum corneum (SC), the stratum granulosum (SG), the stratum spinosum (SS) and the stratum basale (SB) of the epidermis (x 9,280).

Silver has penetrated the full thickness of the stratum corneum in which deposits of silver are seen in the spaces between the corneal cells. The distribution of silver within the corneal cells is not uniform, that is, some cells contain a large amount of silver while other cells contain relatively little or no silver. The tracer has also extended into the intercellular space between the basal corneal and the superficial granular layers. Furthermore, the tracer has penetrated into the stratum granulosum, the stratum spinosum and the stratum basale where it is clearly seen in the intercellular spaces in these strata. Arrows indicate the location of silver.

The EDX spectrum contained a large  $L\alpha$  peak for silver when the epidermis was analyzed.

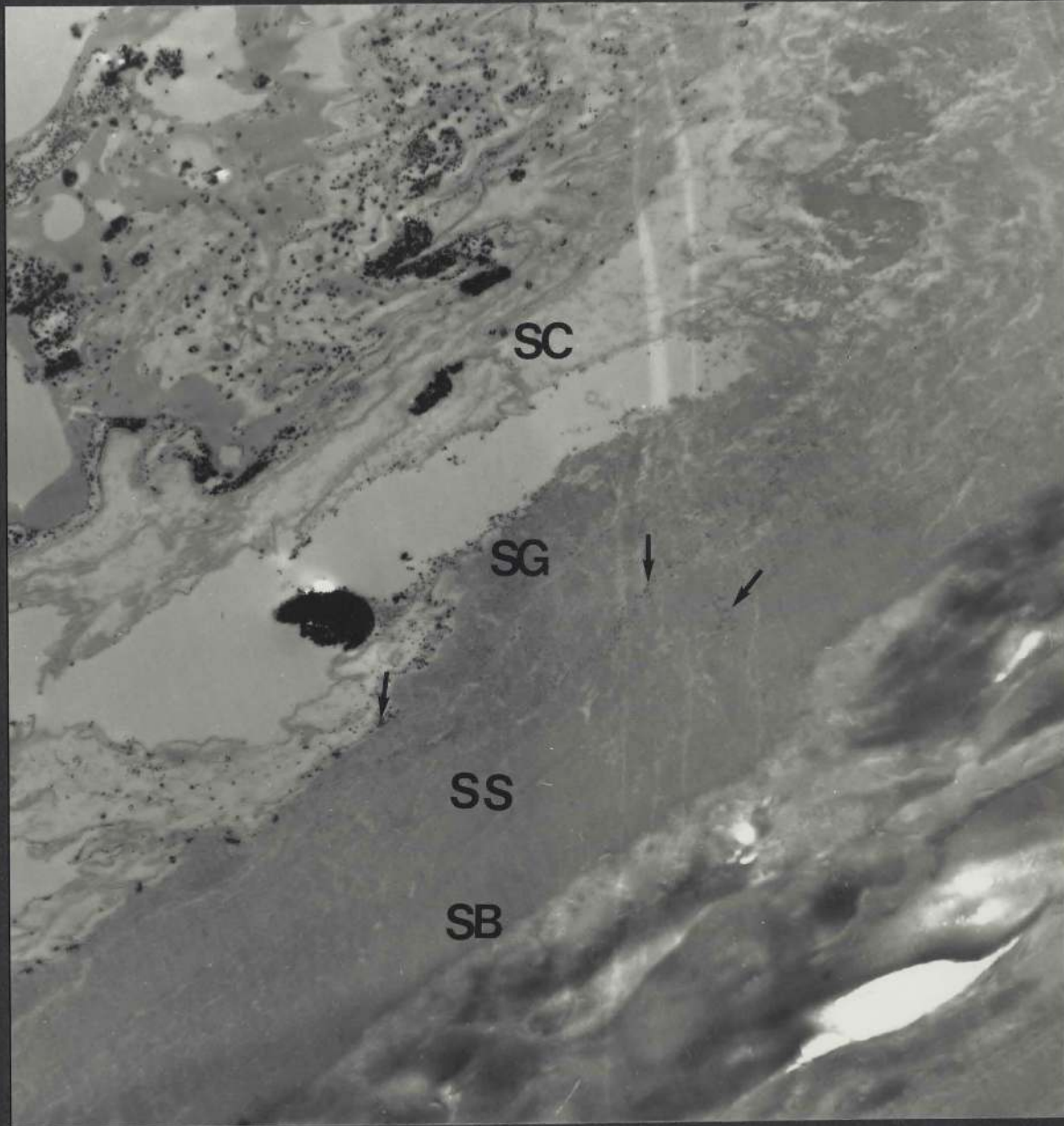


Figure 90b: The structures shown in this micrograph include the basal (SB), the prickle (SS), the granular (SG) and the horny (SC) layers of the follicular infundibulum. Towards the top of the field a portion of a hair shaft (H) may be seen (x 9,280).

The tracer has penetrated the stratum corneum and extended into the adjacent stratum granulosum. Although some cells contain a few silver granules, the deposition of the tracer appears to be mainly in the intercellular spaces.

The EDX spectrum from such a region contained a large peak for silver.





Figure 90c: This micrograph shows the lower part of the follicular canal epidermis at the level of the sebaceous duct. The basal (SB), the spinous (SS), and the granular (SG) layers of the canal epidermis are seen. The stratum corneum (SC) is disintegrating and passing into the sebum (S).

Small electron-dense deposits are seen mixed in with the sebum, and lying adjacent to the surface of the stratum corneum. Arrows indicate the location of silver. No silver is evident within the epidermal layers at this level.

The EDX spectrum showed a small peak for silver

Figure 90d: This micrograph is from a sebaceous gland, and shows peripheral (P), partially differentiated (PD) and fully differentiated (FD) sebaceous cells (x 8,352).

Both the intercellular and intracellular regions of the gland do not contain tracer.

The corresponding EDX spectrum confirmed the absence of silver in the gland.



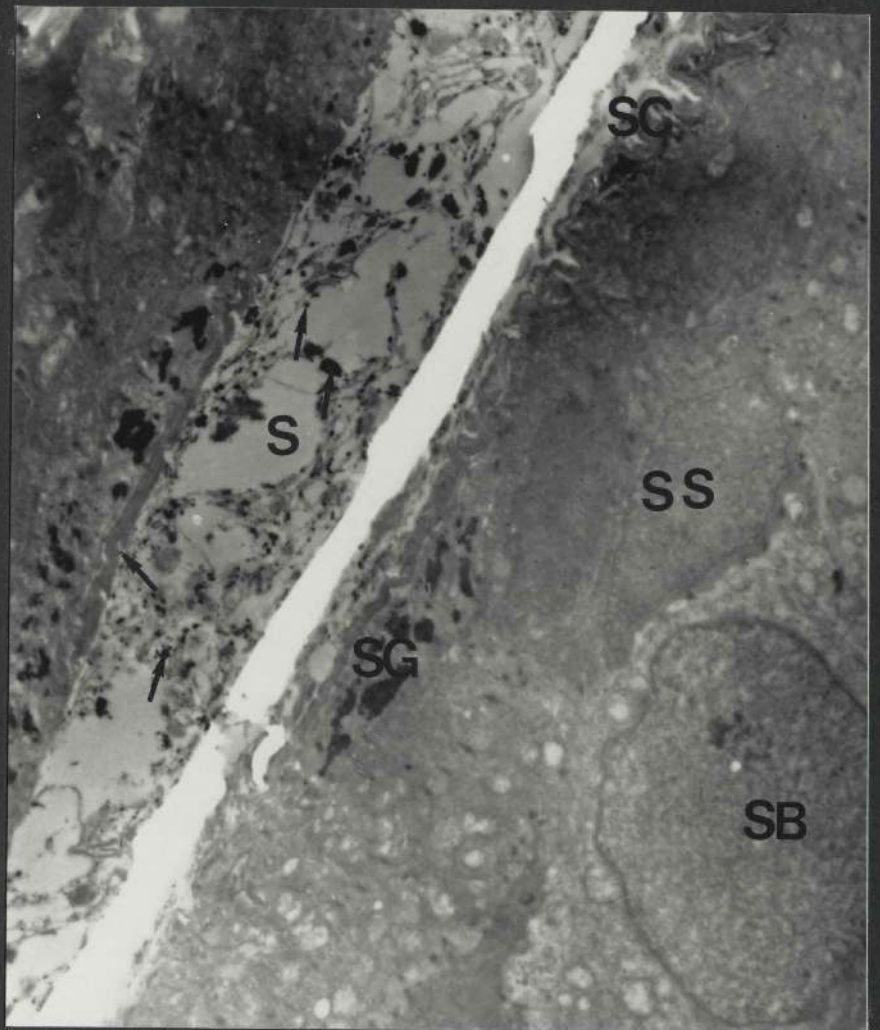


Figure 90e: This micrograph serves to illustrate that no silver is visible in the outer (ORS) or inner (IRS) root sheaths of a hair follicle (x 4,640).

EDX analysis confirmed the absence of silver from such regions.

#### Summary of results

The tracer is found throughout the full extent of the epidermis and the upper parts of the follicular infundibulum.

Although some dense granules of silver are seen within the region of the sebaceous duct, the tracer does not extend into the body of the gland itself. The follicular walls below the level of the sebaceous gland do not contain silver.

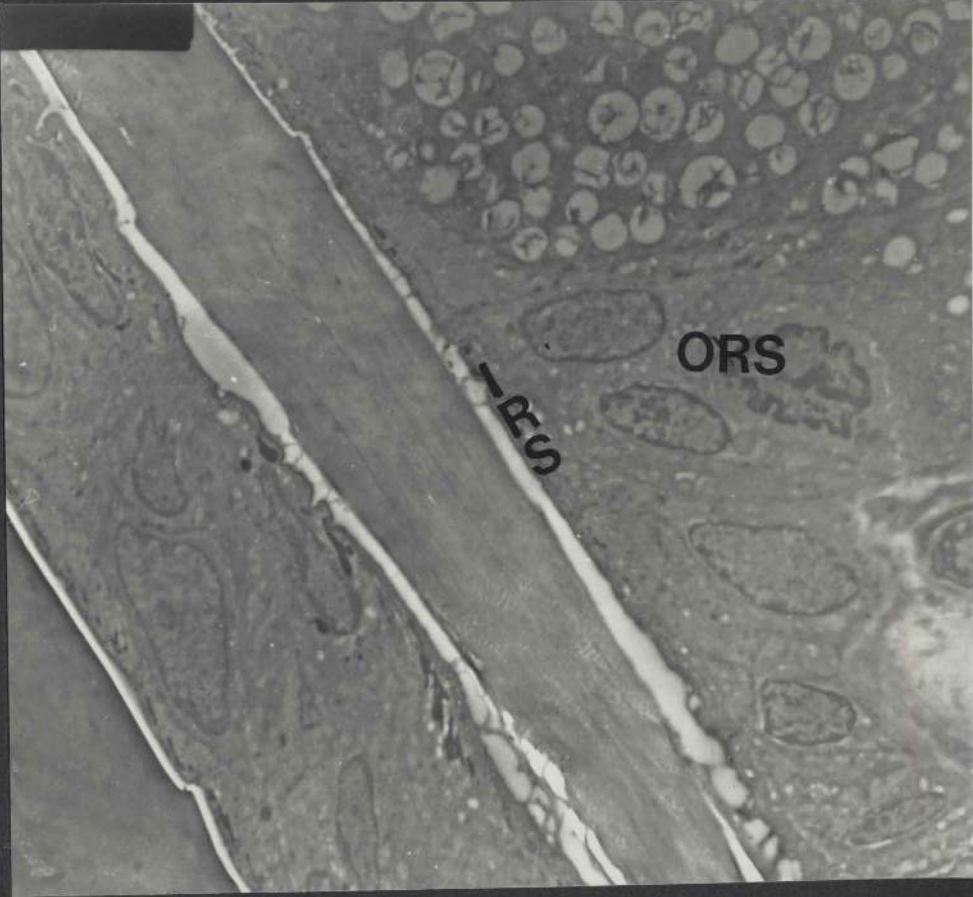




## Figure 91 (a - c)

Local application (control) of a 8% aqueous silver nitrate solution for 15 minutes

Figure 91a: This micrograph shows a portion of the follicular infundibulum at the level of its orifice, and includes parts of the stratum corneum (SC) and the stratum granulosum (SG) (x 7,424).

Scant deposits of silver are seen on the surface of the stratum corneum of both the epidermis and the follicular canal epidermis. Arrows indicate the location of such deposits. No tracer is visible in the stratum corneum or in the other epidermal layers.

The corresponding EDX spectrum did not include a peak for silver.



Figure 91b: This electron micrograph illustrates the follicular canal epidermis at a lower level than that shown in Figure 91a (x 9,280).

Some deposits are seen in the intercellular spaces in the two outermost corneal layers (arrows) but they do not extend into the other layers of the stratum corneum (SC). Furthermore, no electron-dense deposits are seen in the stratum granulosum (SG), the stratum spinosum (SS) or the stratum basale (SB).

EDX analysis did not contain a peak for silver.



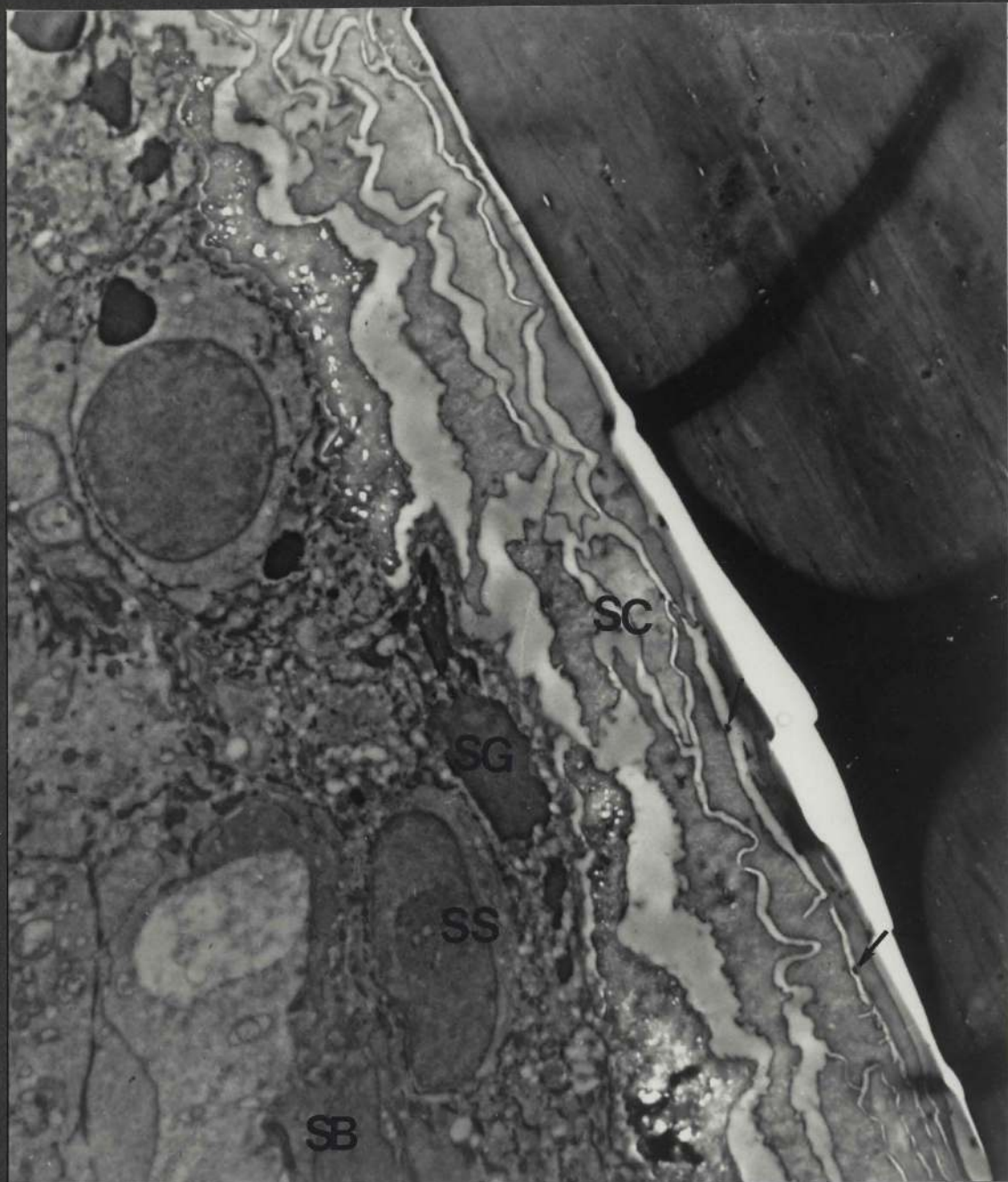


Figure 91c: A transmission electron micrograph of a sebaceous gland featuring partially (PD) and fully (FD) differentiated sebocytes (x 8,352).

No silver is present inside or between the sebaceous cells.

The EDX spectrum obtained from such a region did not include a peak for silver.

#### Summary of results

Without iontophoresis, the penetration of silver from a 8% aqueous silver nitrate solution is minimal. Isolated deposits of tracer are evident in the outer layers of the stratum corneum of the epidermis and the follicular infundibulum. However, no tracer is found in the sebaceous glands.

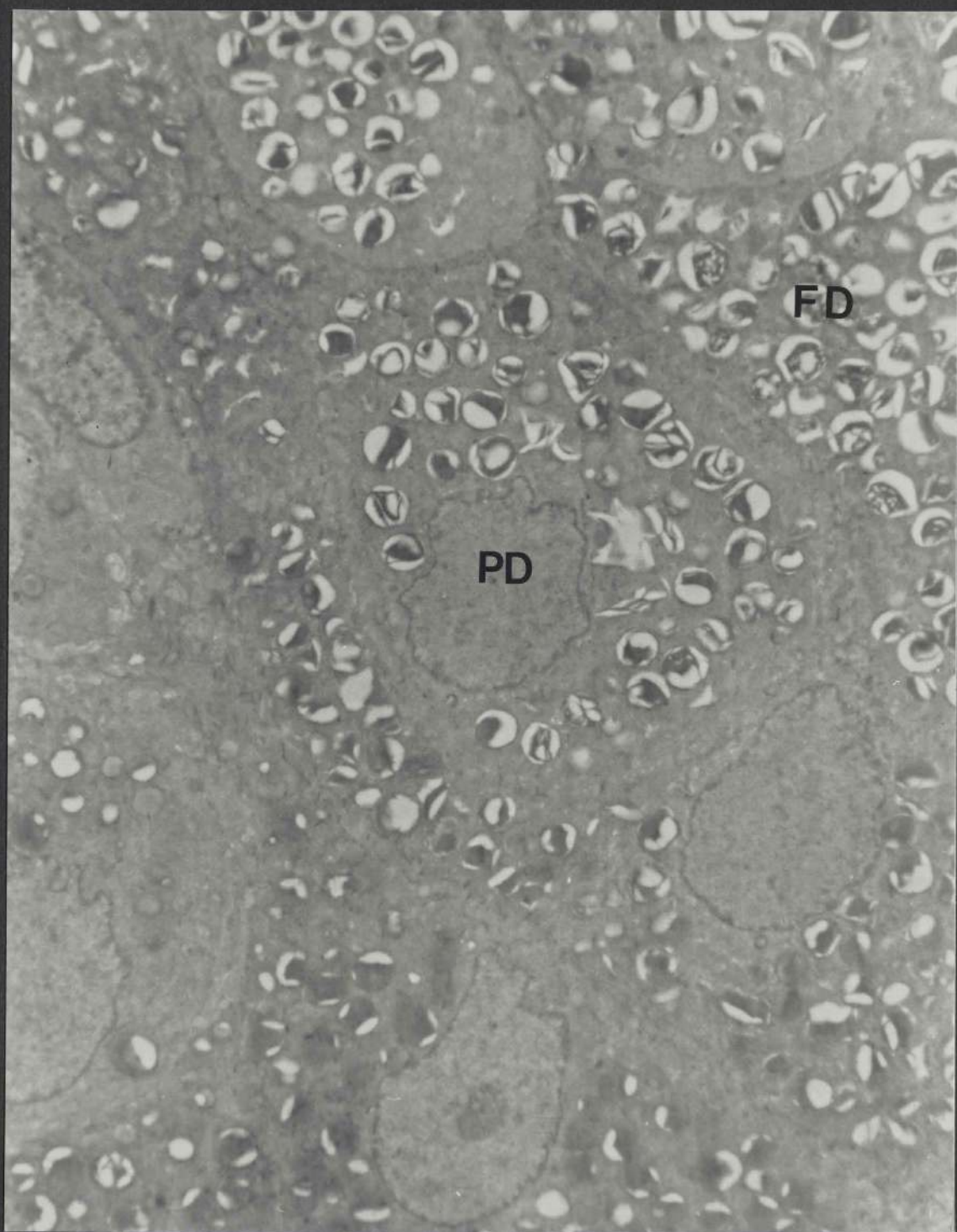




## Figure 92 (a - c)

Positive iontophoresis of a 8% aqueous silver nitrate solution at 30 milliamperes for 15 minutes

Figure 92a: This micrograph spans the upper part of the epidermis and includes the stratum corneum (SC), the stratum granulosum (SG) and the stratum spinosum (SS) (x 9,280).

Cells in the superficial layers of the stratum corneum are heavily loaded with silver granules (large arrow). The tracer has accumulated mainly in the intercellular spaces in the deeper layers of the stratum corneum, although it is occasionally seen inside some cells (small arrows). Silver is not evident in the stratum granulosum. The epidermis appears in general as a dense gray mass, and there is a marked widening of the intercellular spaces (ICS).

EDX analysis confirmed the presence of silver in the stratum corneum. A very small or no peak for silver was detected in the stratum granulosum.

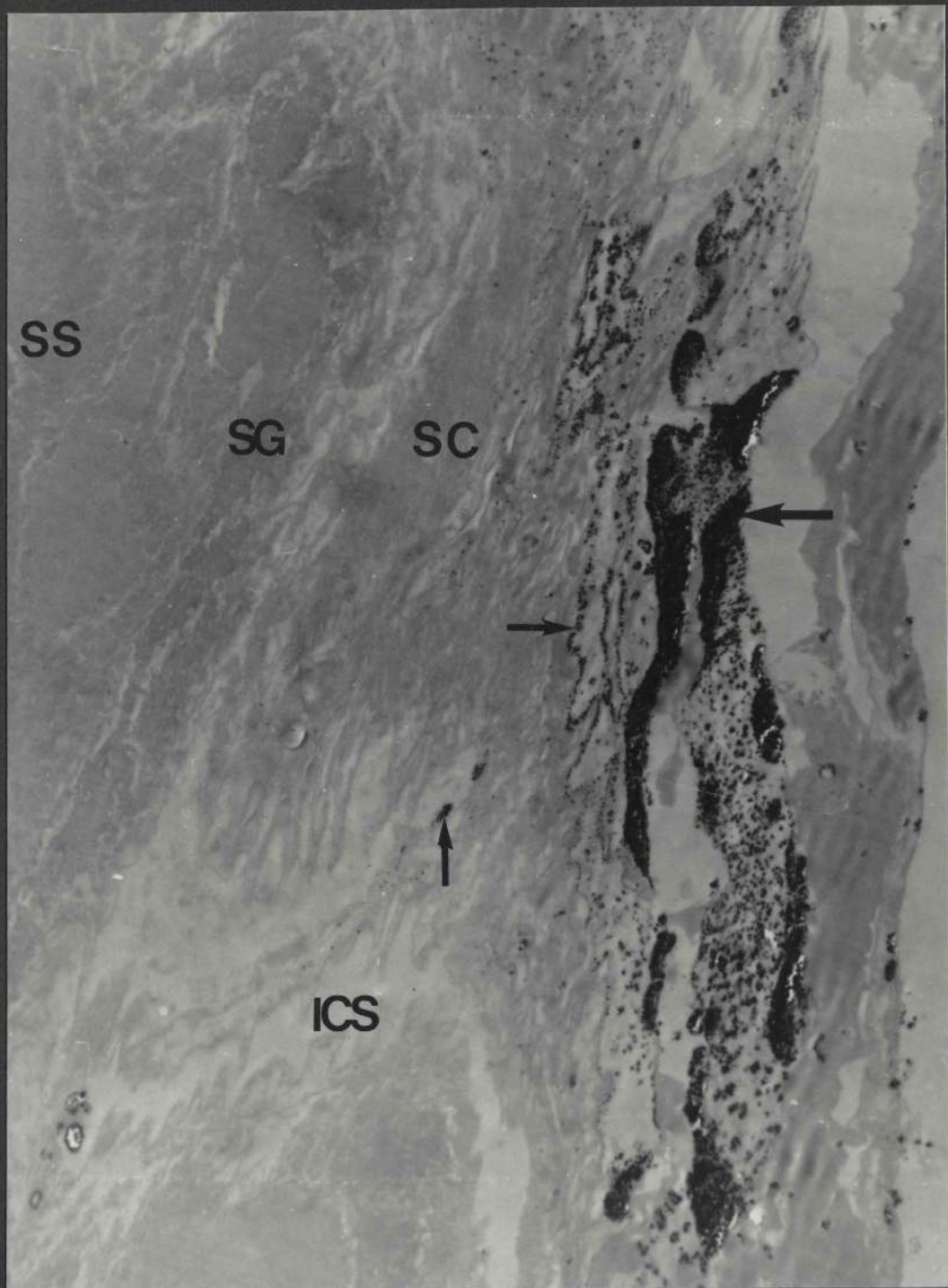


Figure 92b: This micrograph shows the lower part of a follicular canal epidermis (x 9,280).

The deposition of silver is so heavy that it is somewhat difficult to identify the individual layers. The stratum basale (SB) is identified by being adjacent to the dermis (D), and (SC) is the most superficial layer of the stratum corneum. The tracer is evident in both the inter- and the intra- cellular regions in the superficial half of the epidermis. In the other half, the deposition appears to be concentrated in the intercellular spaces (ICS) rather than in the intracellular regions.

A very large  $L\alpha$  peak for silver was seen in the EDX spectrum obtained from such a region.



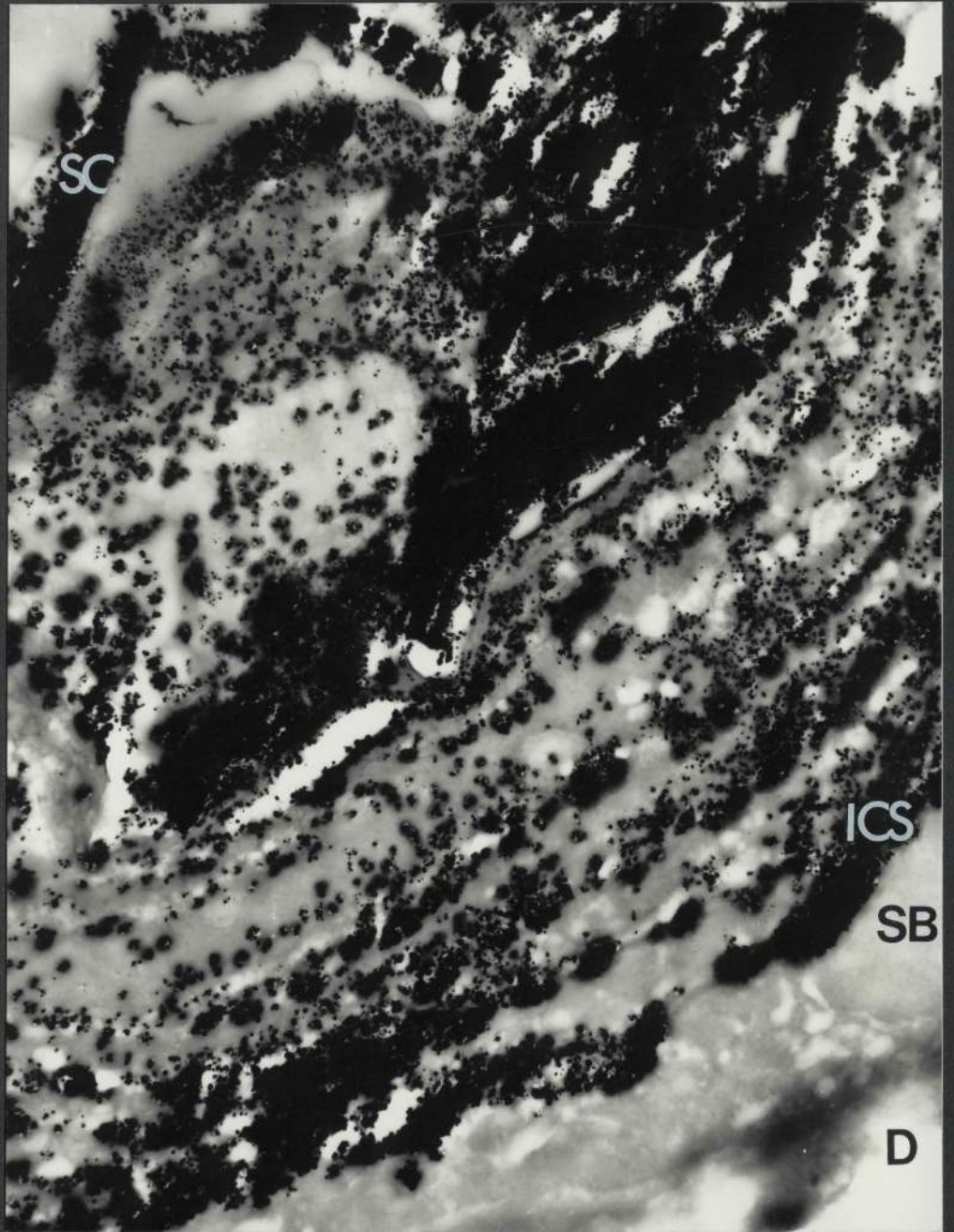


Figure 92c: Illustrated in this micrograph is a portion of a sebaceous gland (x 10,208).

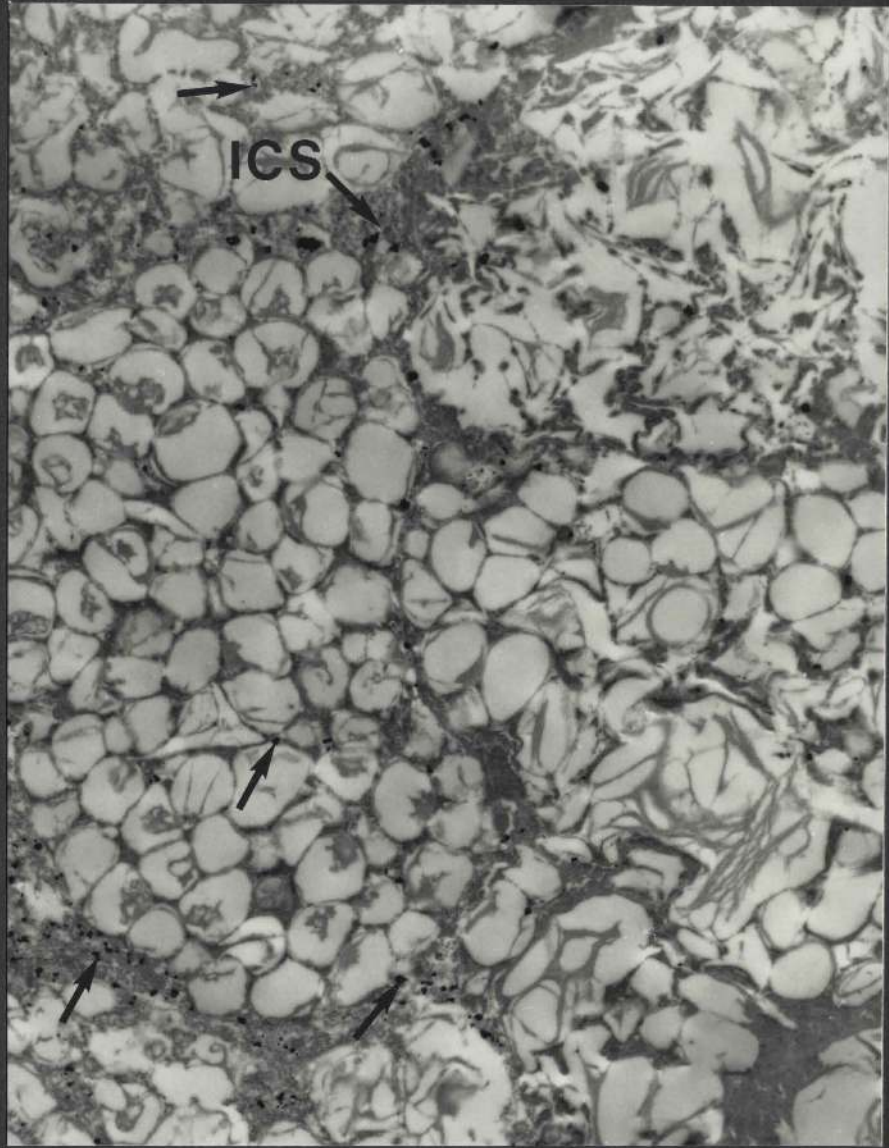
This micrograph is of interest in that it shows that silver has penetrated into the sebaceous glands. The tracer is evident in the intercellular spaces (ICS) and is also present inside the cells in the cytoplasmic strands between the lipid droplets. Towards the upper right hand corner of the micrograph, the tracer is seen mixed with sebum.

The EDX spectrum obtained from the gland contained a peak for silver.

#### Summary of results

Following iontophoresis, the tracer penetrates the stratum corneum of the epidermis but it is not identified with certainty in the lower epidermal layers. Penetration of the tracer through the walls of the follicular infundibulum is complete and in addition, it passes into the sebaceous glands.





### 3.6.3 Effect of vehicle (Accelerants)

The following experiment was carried out to investigate the effect of incorporating dimethyl sulphoxide (DMSO) with silver nitrate in solution on the penetration of silver into the skin by iontophoresis.

2 grams of silver nitrate were dissolved in 40 mls of distilled water. To this 60 mls of DMSO were added, following which there was an increase in the temperature of the final solution. Following cooling, the test solution was subjected to positive iontophoresis as shown below.

Figure 93 (a - c)

Positive iontophoresis of 2% silver nitrate in DMSO at 30 milliamperes for 15 minutes

Figure 93a: The structures present in this micrograph include the stratum corneum (SC), the stratum granulosum (SG) with its keratohyalin granules (Kh) and a portion of the stratum spinosum (SS) (x 10,208).

The tracer is visible throughout the stratum corneum excluding the two innermost corneal layers. No tracer is evident deep to the stratum corneum.

The EDX analysis confirmed these histological findings.



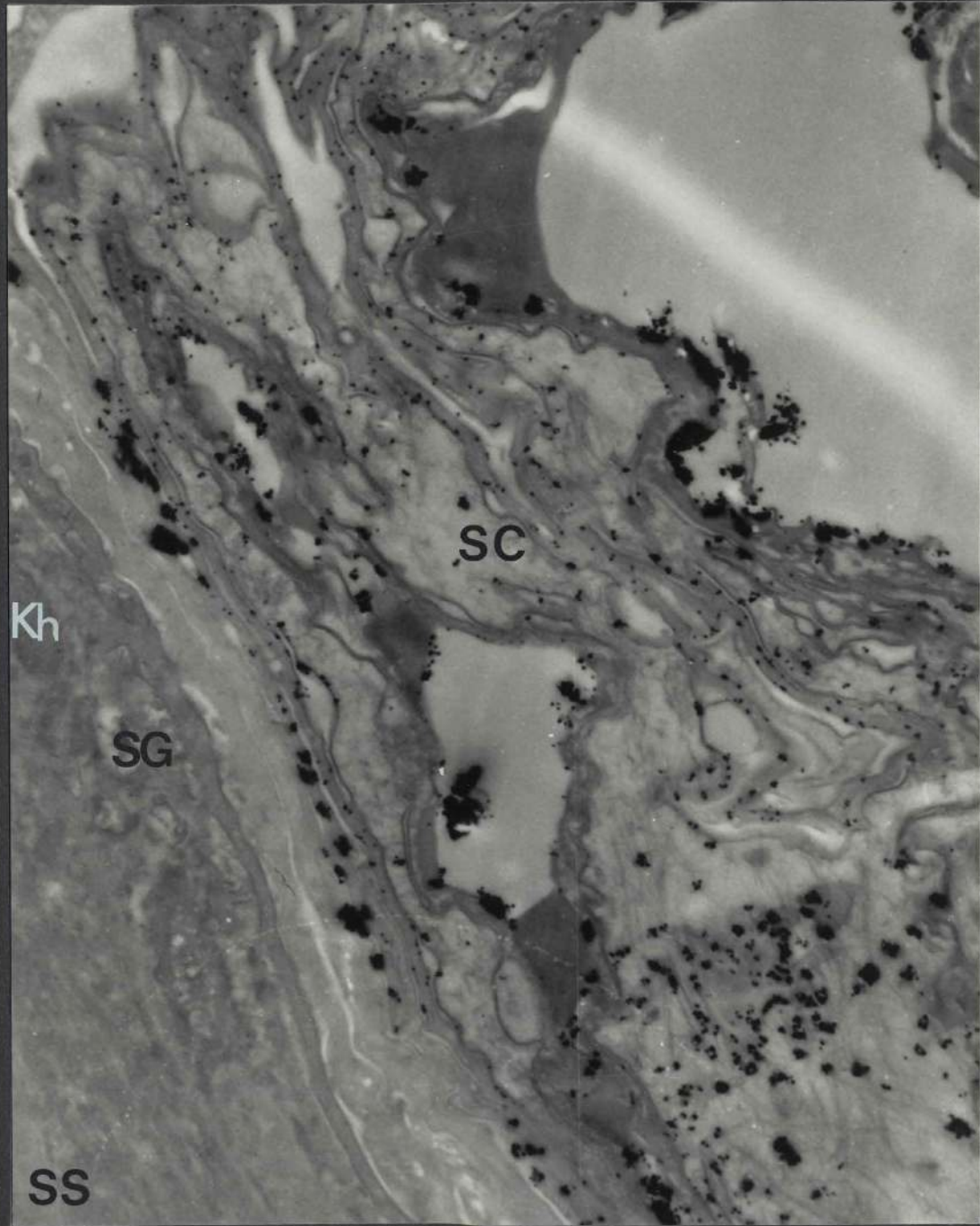


Figure 93b: This is a section of a hair follicle just above the level of entry of a sebaceous duct. Remnants of sebum (S) are seen in the pilary canal (x 10,208).

Small electron-dense deposits may be seen mixed with the sebum. Moreover, the deposits are present on the surface of the stratum corneum (SC) of the follicular canal epidermis (large arrows) and occasionally within the most superficial corneal cell (small arrows). However, no penetration is evident into the remainder of the stratum corneum, the stratum granulosum (SG) or the stratum spinosum (SS).

A small  $L\alpha$  peak for silver appeared in the EDX spectrum when analysis was carried out on the region of the sebaceous duct.



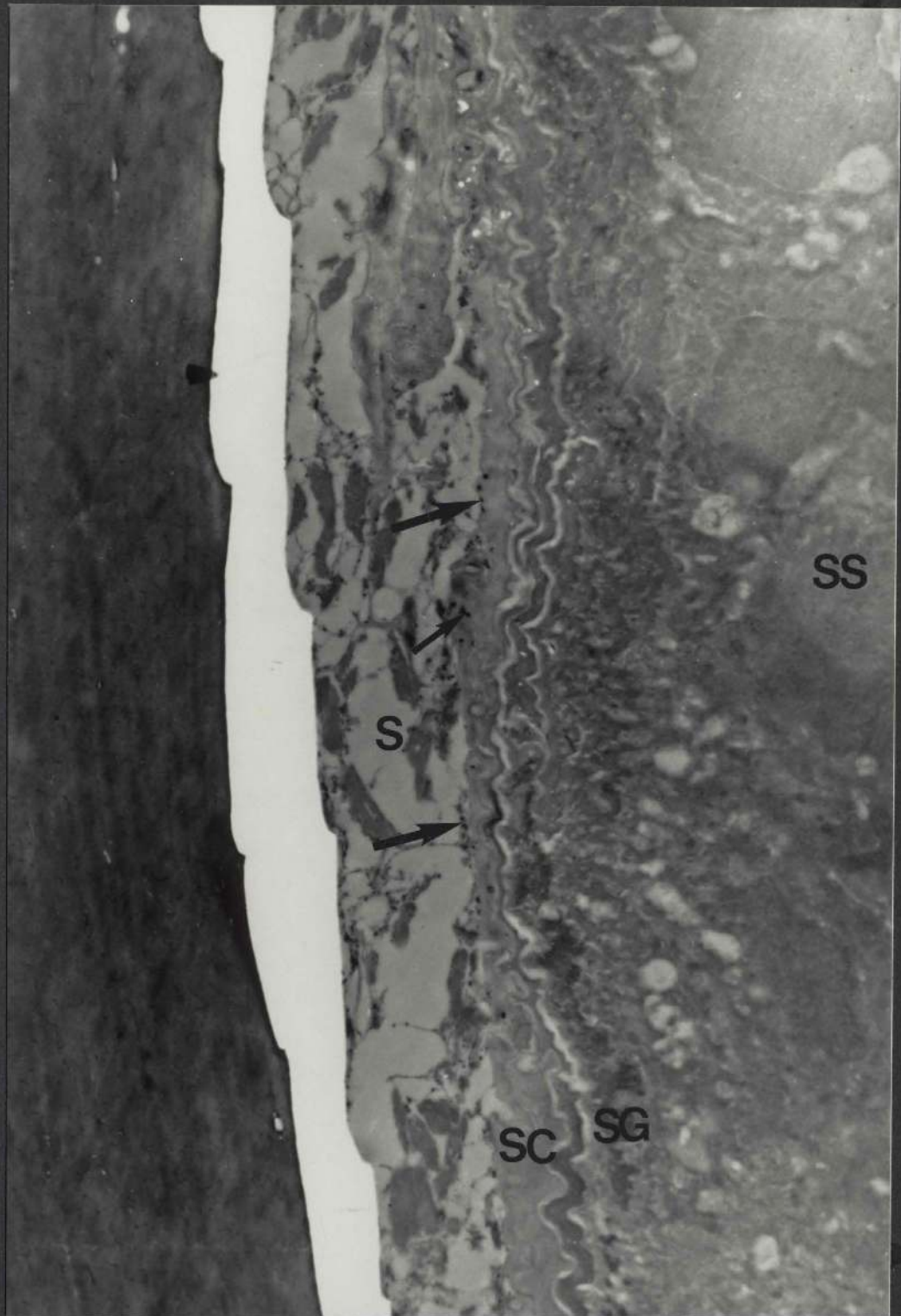


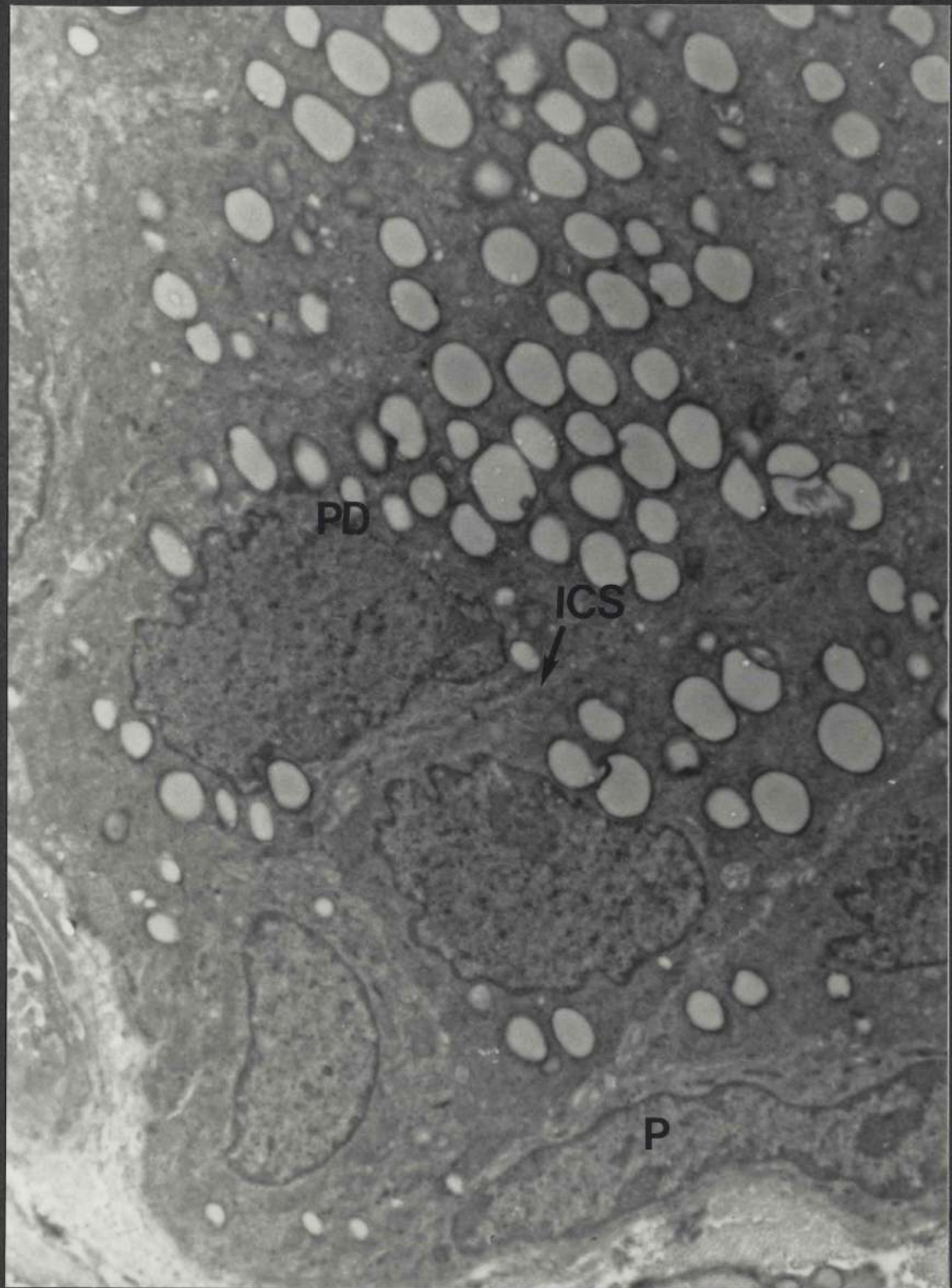
Figure 93c: This micrograph features a part of a sebaceous gland and shows peripheral (P) and partially differentiated (PD) sebaceous cells (x 9,280).

The intercellular spaces (ICS) and the intracellular regions do not contain silver granules.

The corresponding EDX spectrum did not contain silver when the sebaceous gland was analyzed.

#### Summary of results

The addition of DMSO to the tracer in solution results in the presence of silver on the surface of the stratum corneum of the follicular canal epidermis, and occasionally within the superficial squame. Apart from this, the extent of penetration through the epidermis, the follicular canal epidermis and the sebaceous glands is similar to that observed when the tracer is introduced by the same experimental protocol but from water alone (Figure 88 a - c).





#### 3.6.4 Effect of removal of surface lipid

The effect of the removal of surface lipid on skin penetration by iontophoresis was investigated. The surface lipid was removed by gentle wiping of the skin surface with cotton wool soaked in diethyl ether. Thereafter, a 2% aqueous silver nitrate solution was subjected to iontophoresis.

#### Figure 94 (a - c)

Positive iontophoresis of a 2% aqueous silver nitrate solution at 30 milliamperes for 15 minutes

Figure 94a: This micrograph features the full thickness of the epidermis (x 8,352).

The tracer is visible in the upper layers, but not in the deeper layers of the stratum corneum (SC). The viable epidermal layers (VE) do not contain tracer.

EDX analysis confirmed the presence of silver in the upper layers of the corneum and its absence from the deeper layers.

Figure 94b: This micrograph features the corneal (SC), the granular (SG), the spinous (SS) and the basal (SB) layers of the follicular infundibulum (x 7,424).

A few electron-dense spots are seen on the surface of the stratum corneum (arrow), but these do not extend into the stratum corneum or into the other epidermal layers.

No silver was seen in the spectrum obtained from such a region.

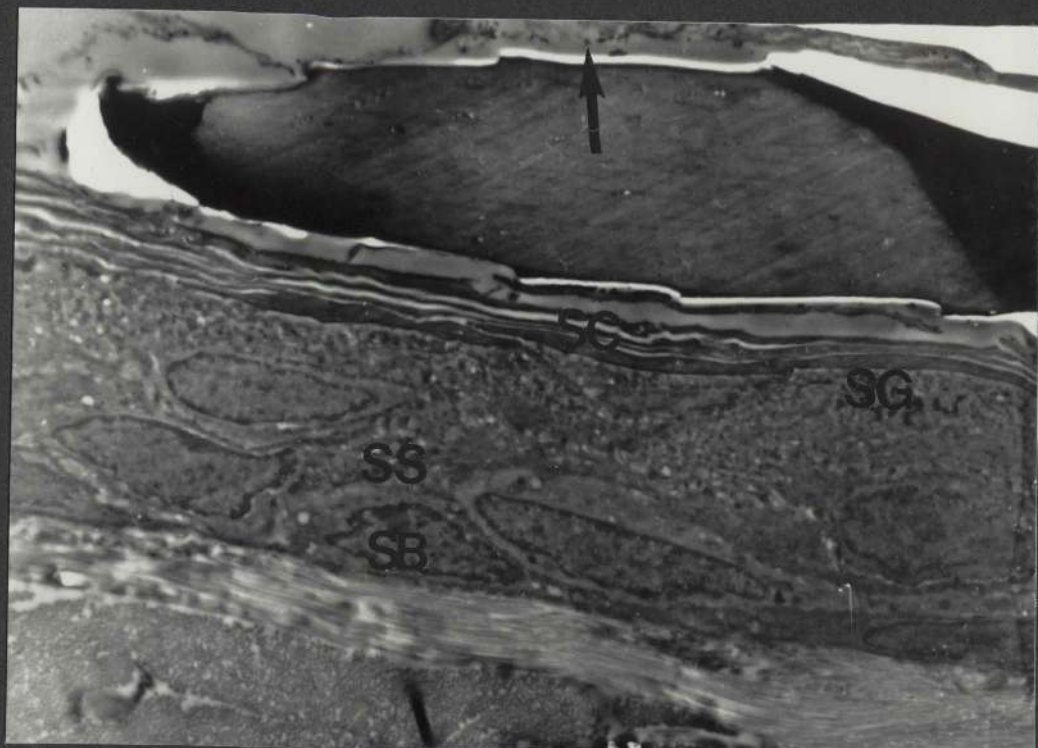
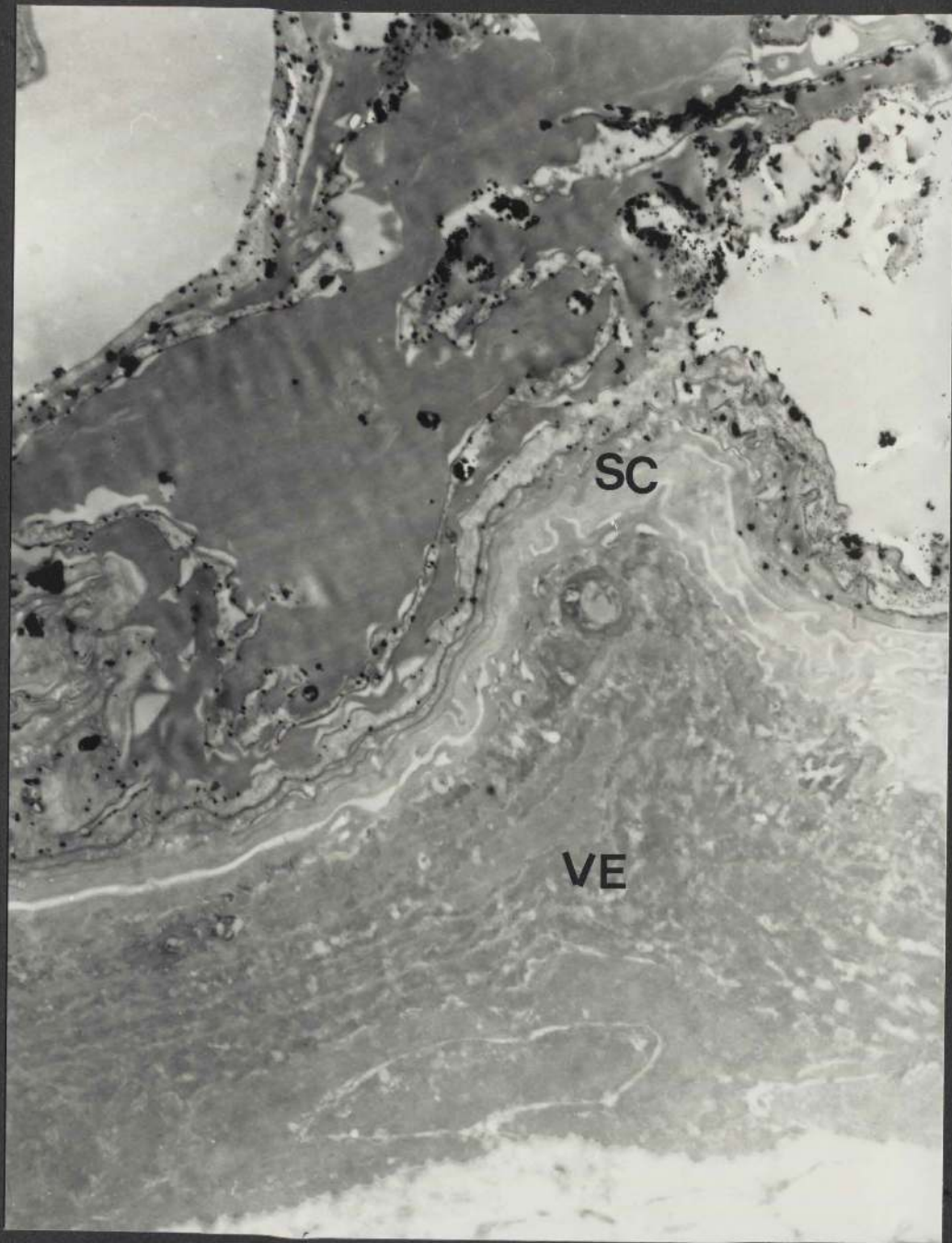




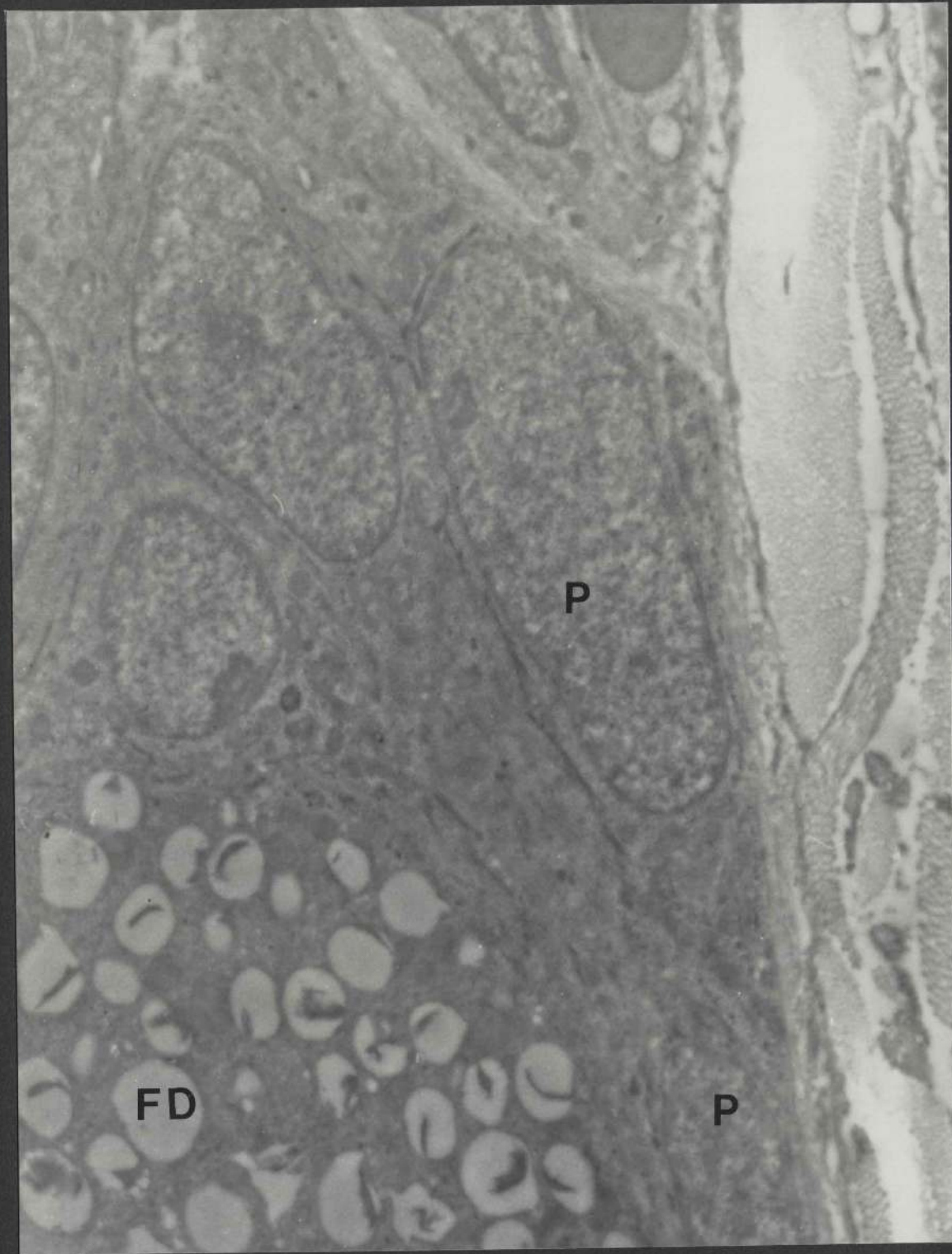
Figure 94c: This micrograph shows a portion of a sebaceous gland featuring peripheral (P) and fully differentiated (FD) sebaceous cells (x 10,208).

No electron-dense deposits are present in the intercellular or the intracellular regions of the gland.

EDX analysis confirmed the absence of silver in the gland.

#### Summary of results

The extent of penetration of silver into the skin following the removal of surface lipid does not differ significantly from that observed without the removal of the surface lipid (Figure 88 a - c).



### 3.7 Ruthenium red

Ruthenium red is an inorganic, intensely coloured dye. It is also called ammoniated ruthenium oxychloride. In solution, the ruthenium red is a hexavalent cation and is reported to be  $[(\text{NH}_3)_5\text{Ru}-\text{O}-\text{Ru}(\text{NH}_3)_4-\text{O}-\text{Ru}(\text{NH}_3)_5]^{+6}$  (Fletcher *et al.*, 1961; Clausen *et al.*, 1971). It is usually prepared with chloride as the counter ion. A number of articles are available which describe the physico-chemical properties of this material (Sterling, 1970; Luft, 1971 a,b). It is a red powder and is supplied in vials each containing 0.1 g.

Ruthenium red is commonly used as an intercellular tracer in electron microscopy (Luft, 1964; Szubinski and Luft, 1971; Dierichs, 1979; Baldwin, 1981). However, its use in the present study for that purpose appeared to be limited. The best explanation for this is provided by Luft (1971a, b). This author processed tissues according to routine electron microscopy techniques with ruthenium red being introduced at one point only in the processing sequence, namely before, during or after osmium fixation. He reported that no reaction characteristic of ruthenium red, that is electron-dense deposits, developed when the ruthenium red was introduced before or after the osmium fixation. However, when ruthenium red was used together with the osmium fixative the results in the electron microscope were those of the typical ruthenium reaction in that electron-dense deposits were evident. Therefore, it appears that ruthenium red itself is not electron-dense, and that if electron-dense deposits of ruthenium red are to be observed in ultrathin sections then the tracer must be used "instantaneously" with the osmium tetroxide fixative. Osmium tetroxide itself is very harmful and great care must be taken during

the handling of this material. For safety reasons, therefore, the osmium solution was not used together with the ruthenium red during the present *in vivo* penetration trials. Thus, it was more likely that no electron-dense deposits would be observed in the ultrathin sections.

Nevertheless, an attempt was made to investigate the penetration of ruthenium red through the skin from within to the surface and in the opposite direction. A 1% aqueous ruthenium red solution was prepared by dissolving 0.3 g of the tracer in 30 mls of distilled water. This solution was injected intradermally, applied topically or introduced with iontophoresis. Because of the importance of the ruthenium red-osmium fixative reaction, the excised skin was quickly cut into small pieces and these were placed immediately in the osmium fixative, omitting the primary aldehyde fixation. The specimens were then dehydrated, embedded and sectioned according to normal procedures (p 101).

Due to its characteristic red colour, the localization of ruthenium red in the skin following injection, topical application and iontophoresis was also studied with the light microscope using unfixed cryostat sections.

X-ray analysis was also carried out using energy-dispersive (EDX) and wavelength-dispersive (WDX) X-ray systems.

The results obtained are shown in Figures 95, 96 and 97.

## Figure 95 (a - f)

Intradermal injection of a 1% aqueous ruthenium red solution

Figure 95a: A cryostat section (x 32)

A red colouration is visible in the epidermis (E), the hair follicles (HF), the sebaceous glands (SG) and the dermis (D). The hypodermis (H) and the subjacent striated muscle (SM) are also stained. The precise determination of the localization of the tracer within the layers of the epidermis is not possible.



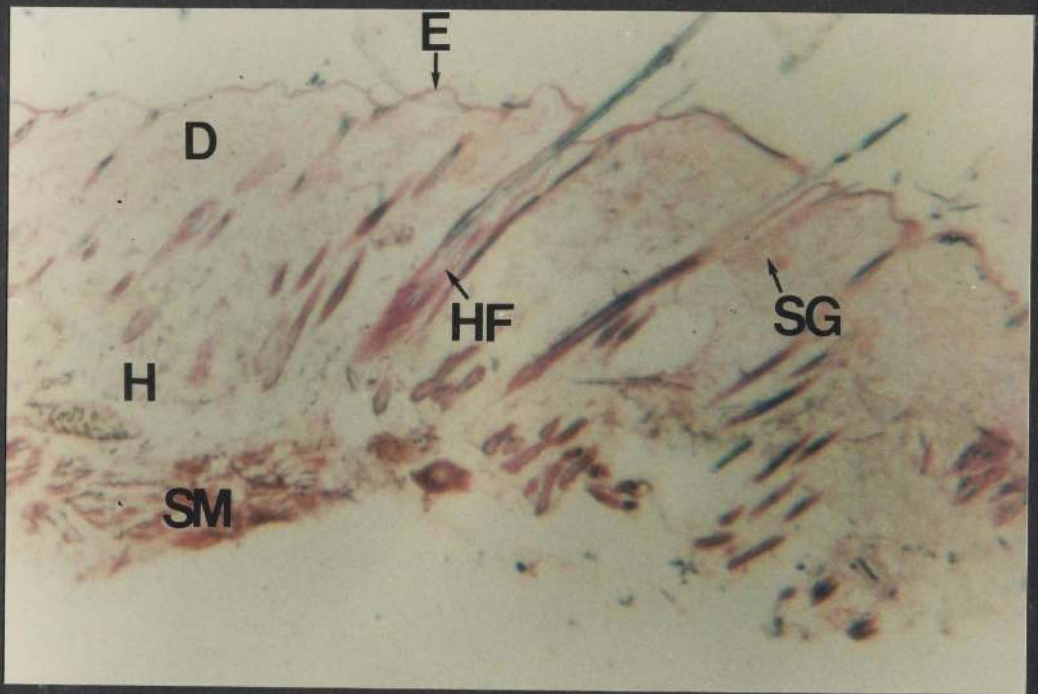
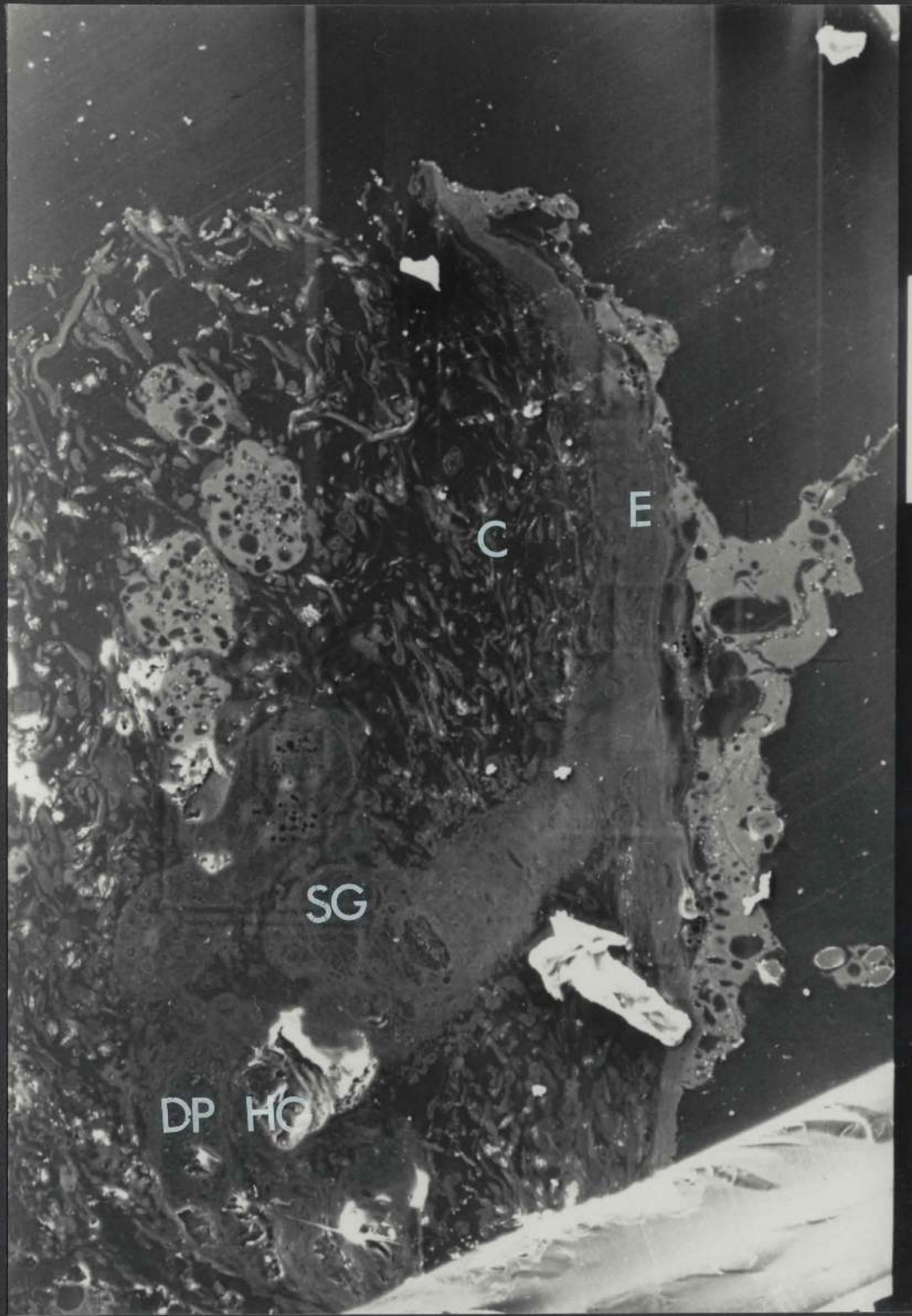


Figure 95b: A scanning electron microscope image from the face of a resin block following ultrathin sectioning.

This field illustrates the epidermis (E), the sebaceous glands (SG) and collagen fibres (C) in the dermis. Also included in this field is a hair follicle in a stage of quiescence (telogen); the cells of the dermal papilla (DP) are arranged as a ball which is located outside the follicle and immediately below the base of the hair germ (HG).

Energy-dispersive X-ray analysis was performed on various skin structures and on an area of the block-face just outside the tissue so that signals originating from the skin could be identified.

The spectrum obtained (see overleaf) from such analysis showed, among others, a peak at an energy value of 2.600 KeV. Two elements were identified at this value, chlorine (K alpha) and ruthenium (L alpha). Since overlapping of peaks had occurred it was not possible by this method of analysis to decide whether ruthenium was present. Therefore, the wavelength-dispersive X-ray (WDX) system was used as an alternative method of analysis (see Figure 95c).



15KV

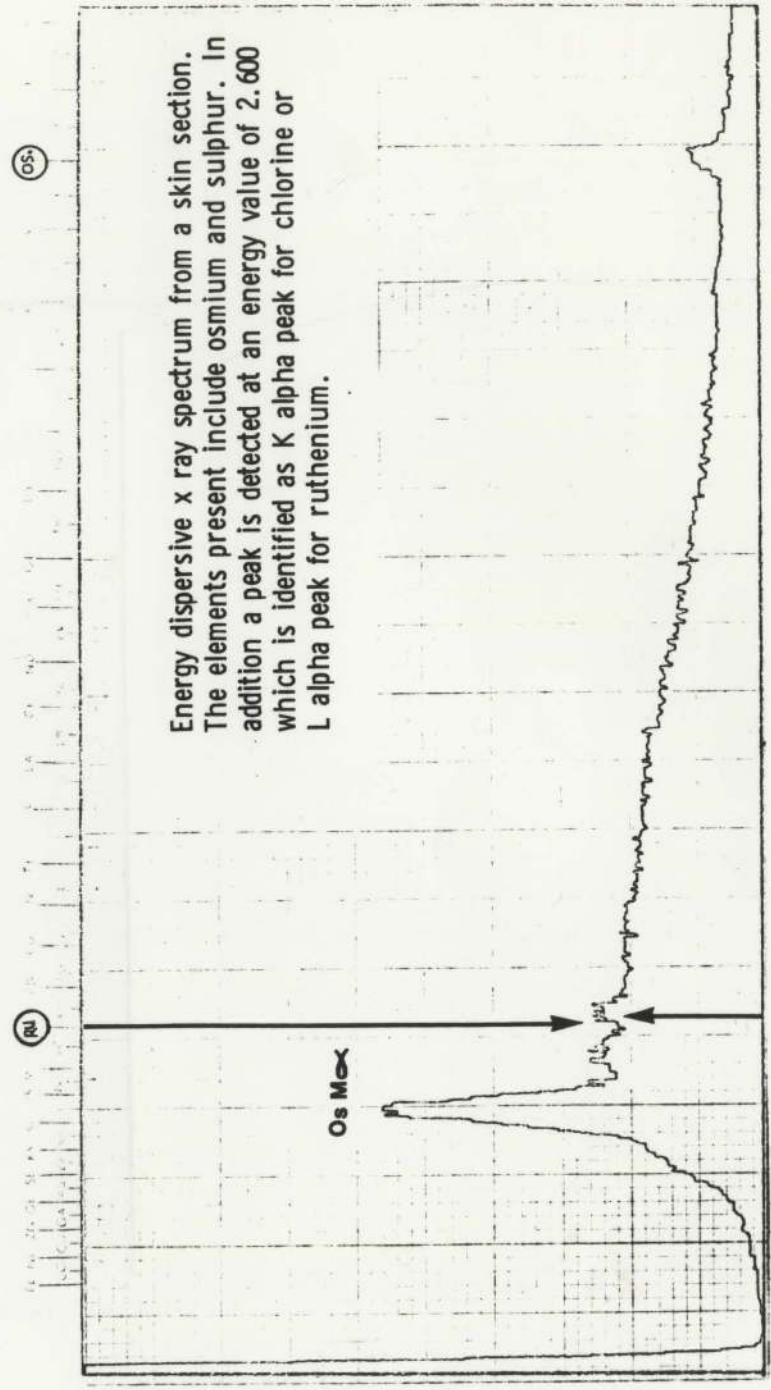
1567

100.00

SAUEM



Laboratory .....  
 Sample .....  
 15 .....  
 Researcher .....  
 Intracutaneous injection of a 1 percent ruthenium red in distilled water. 33  
 100 .....  
 Seconds .....  
 Take off Angle .....  
 L alpha lines



Energy dispersive x ray spectrum from a skin section. The elements present include osmium and sulphur. In addition a peak is detected at an energy value of 2.600 which is identified as K alpha peak for chlorine or L alpha peak for ruthenium.

Figure 95c: WDX analysis was carried out on 4u araldite sections and on 20u cryostat sections using the Jeol Superprobe 733 SEM operating at 15 KV. The diameter of the analyzing beam was 50u. The crystal of the probe was allowed to rotate from  $146^{\circ}$  to  $157^{\circ}$ . If a peak was obtained at an angle of diffraction of  $147.99^{\circ}$  this was the  $L\beta 1$  peak for ruthenium. A peak at  $155.21^{\circ}$  was the  $L\alpha 1$  peak for ruthenium whilst a peak at  $151.43^{\circ}$  was the  $K\alpha 1$  peak for chlorine.

Illustrated opposite are three skin sections following WDX analyses.

The above two are carbon-coated araldite sections (A and B)

A (X 160)

The structures present include the stratum corneum (SC), the stratum granulosum (SG) and the deeper epidermal layers (DE). The electron beam has marked the areas on which analyses were carried out.

B (X 80).

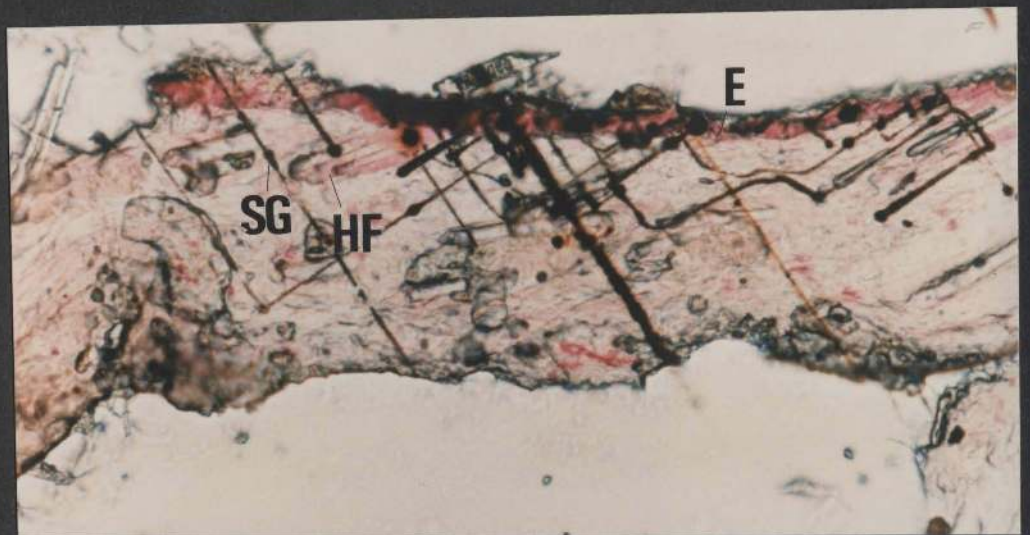
The beam has marked the areas on which analyses were carried out which include the epidermis (E), the hair follicles (HF) and the sebaceous glands (SG).

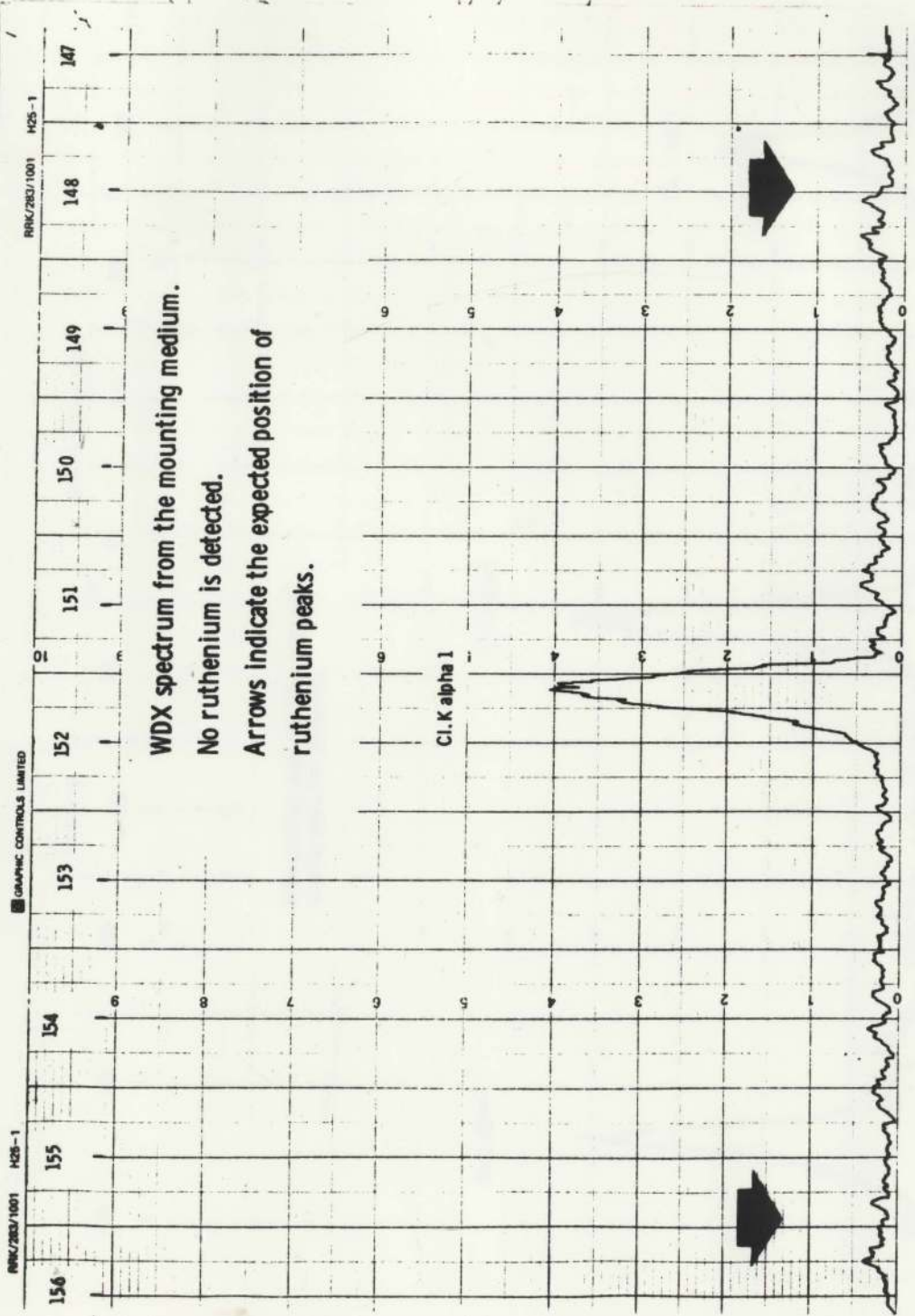
That below is a carbon-coated cryostat section (X 16).

The beam has marked the analyzed areas which include the epidermis (E), the hair follicles (HF) and the sebaceous glands (SG).

Both sections proved positive in terms of the detection of ruthenium and the WDX spectra obtained are shown overleaf. Following intradermal injection, ruthenium is detected in the hair follicles, the sebaceous glands and the epidermis.





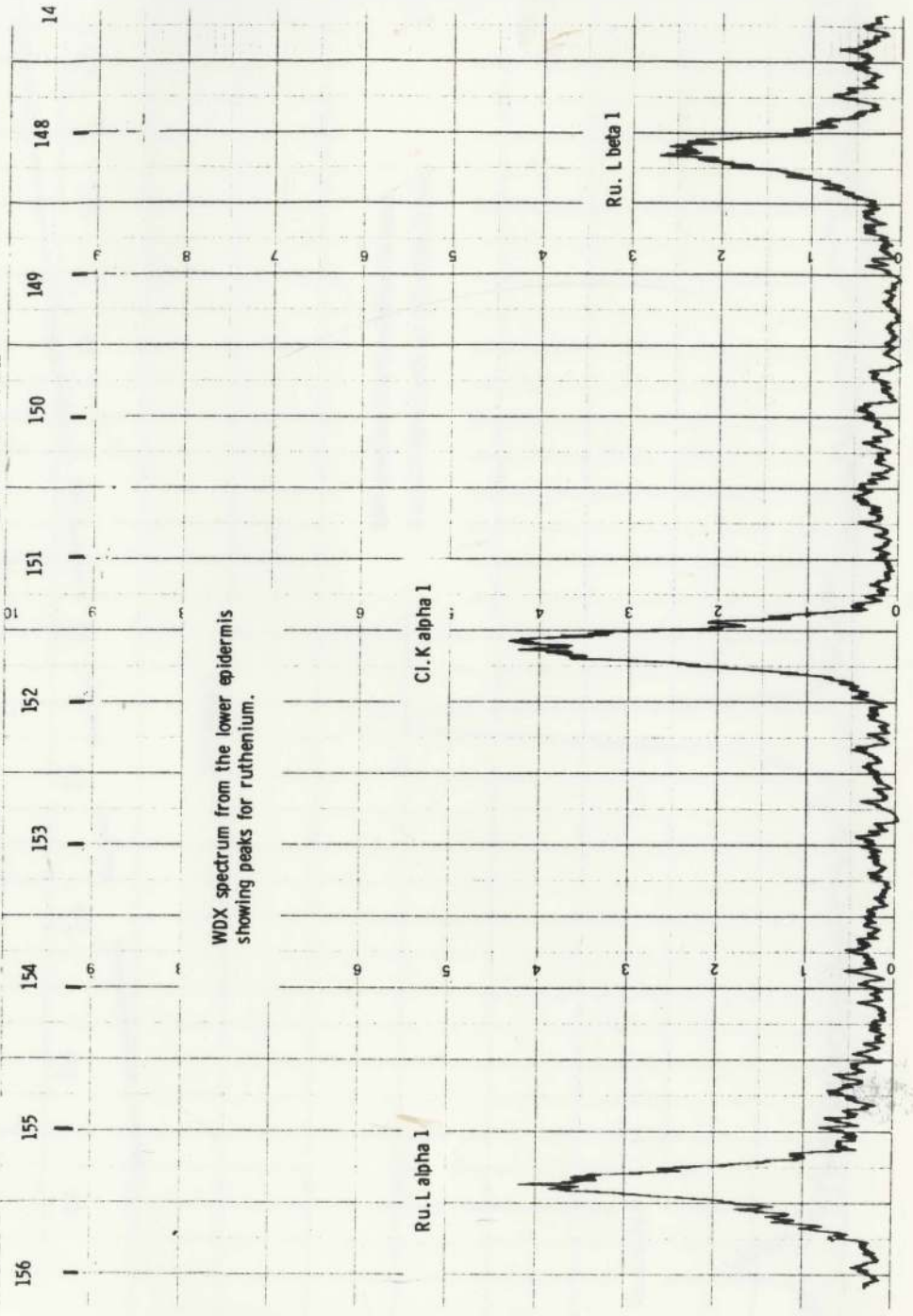


GRAPHIC CONTROLS LIMITED

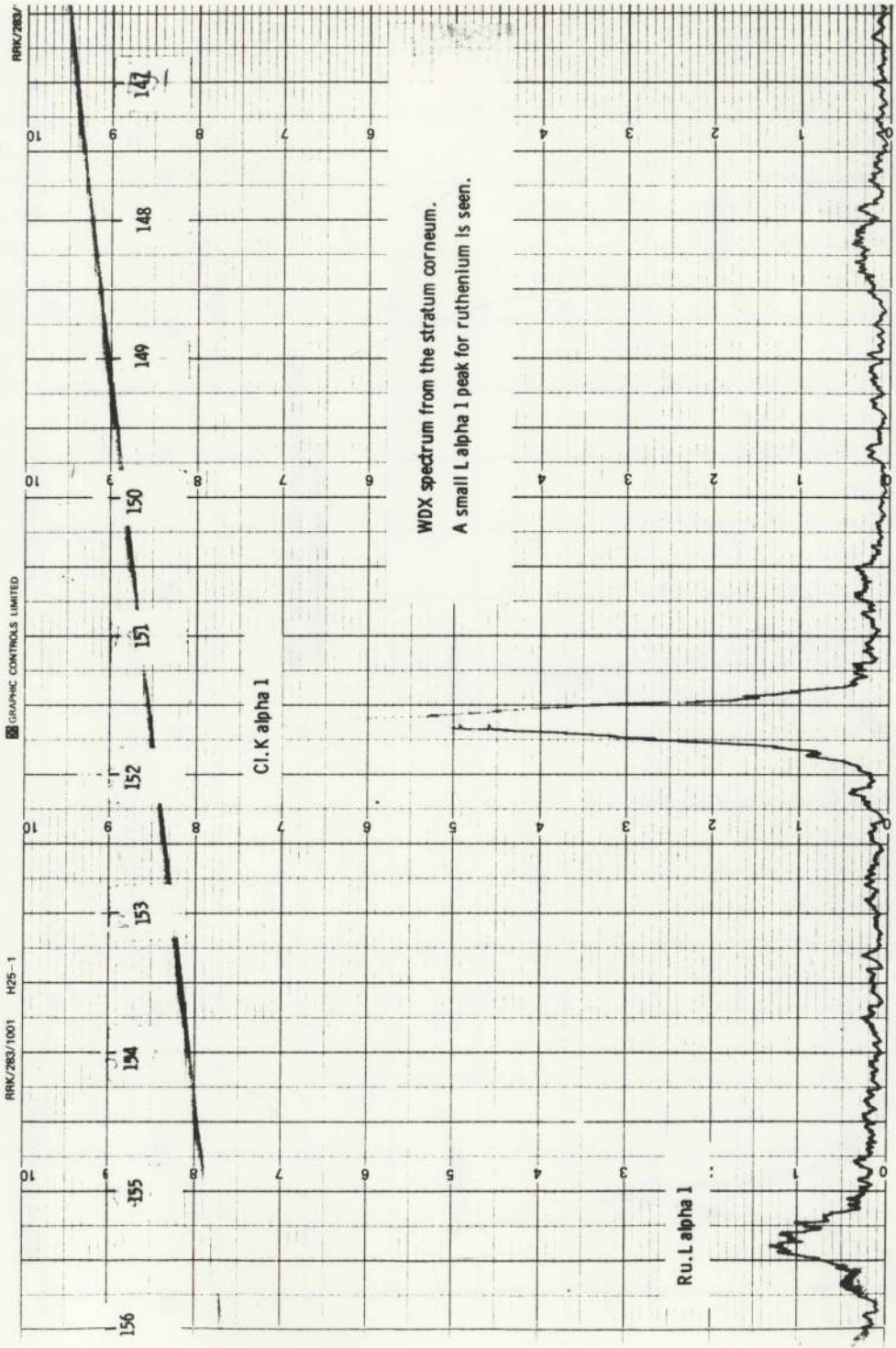


GRAPHIC CONTROLS, LIMITED

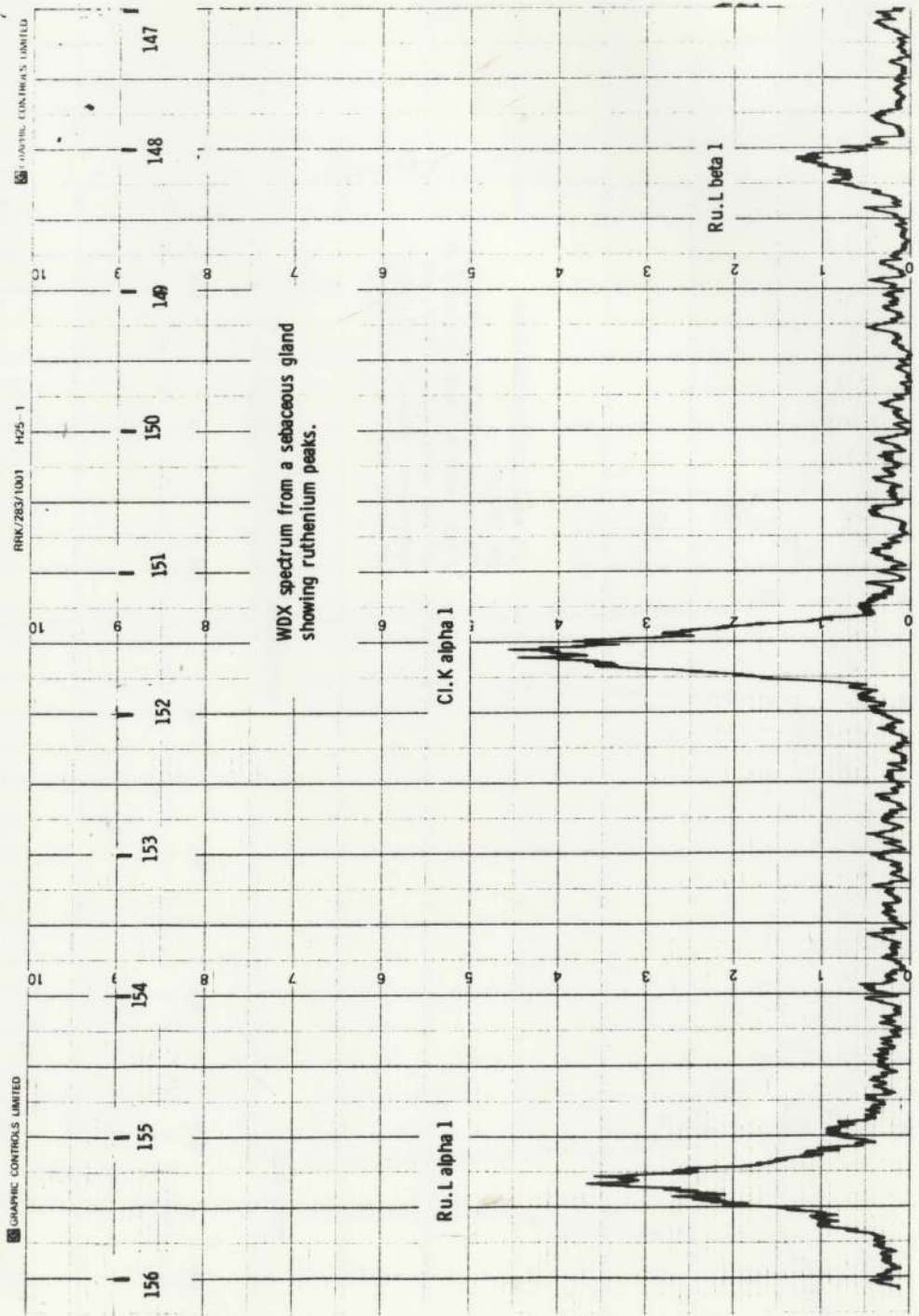
RRK/282/1001 H75-1



WDX spectrum from the lower epidermis showing peaks for ruthenium.



WDX spectrum from the stratum corneum.  
 A small L alpha 1 peak for ruthenium is seen.





GRAPHIC CONTROLS LIMITED

RRK/283/1001 H25-1

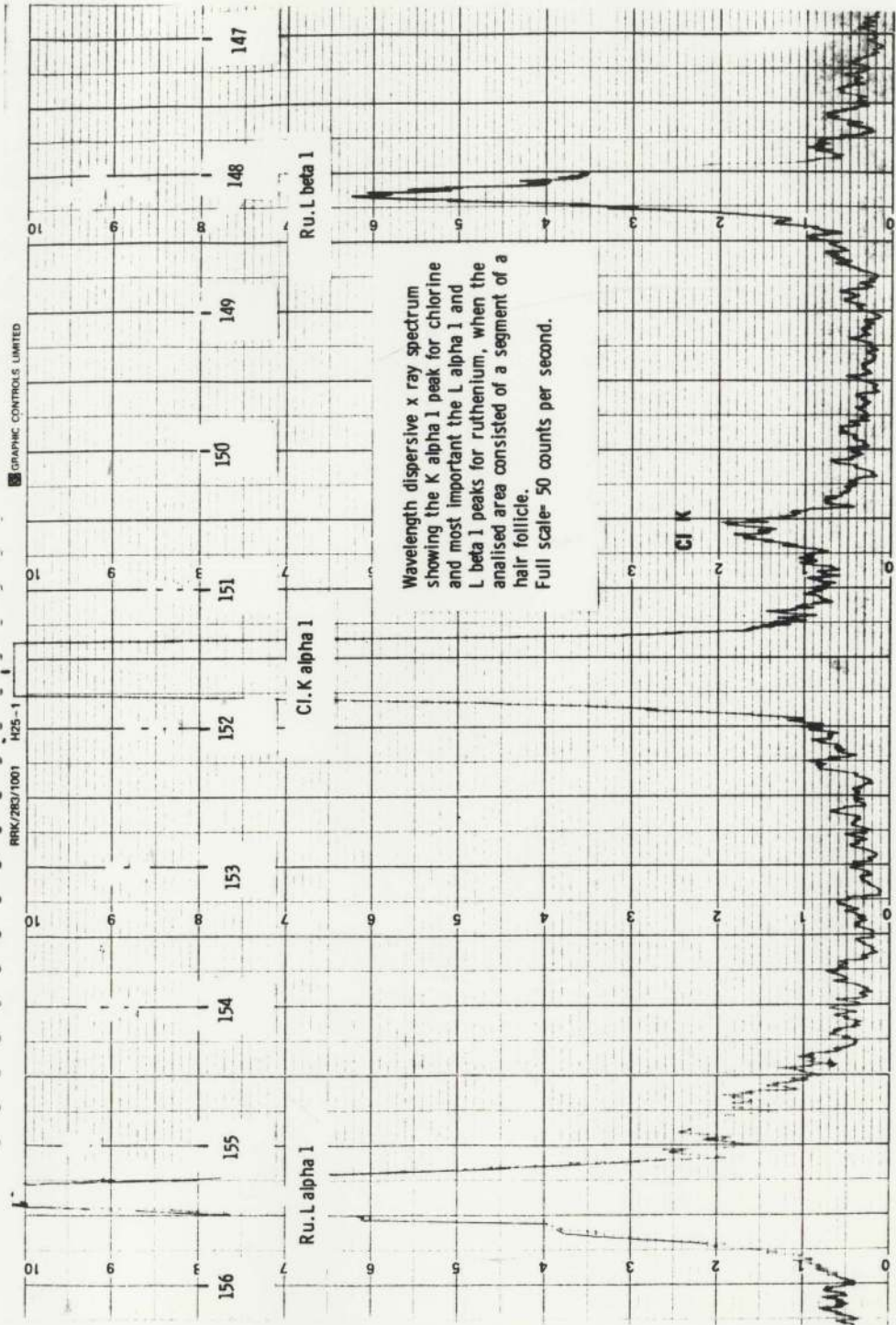


Figure 95d: This is a transmission electron micrograph featuring portions of partially (PD) and fully (FD) differentiated sebocytes (x 11,136).

Electron-dense material is seen in the intercellular spaces (ICS) between three sebaceous cells (upper arrows). The precipitation of the dense material is not uniform throughout the intercellular spaces, and furthermore is not seen consistently in all the ultrathin sections examined. Small patches of dense material are also occasionally seen scattered between the lipid droplets (lower arrows).

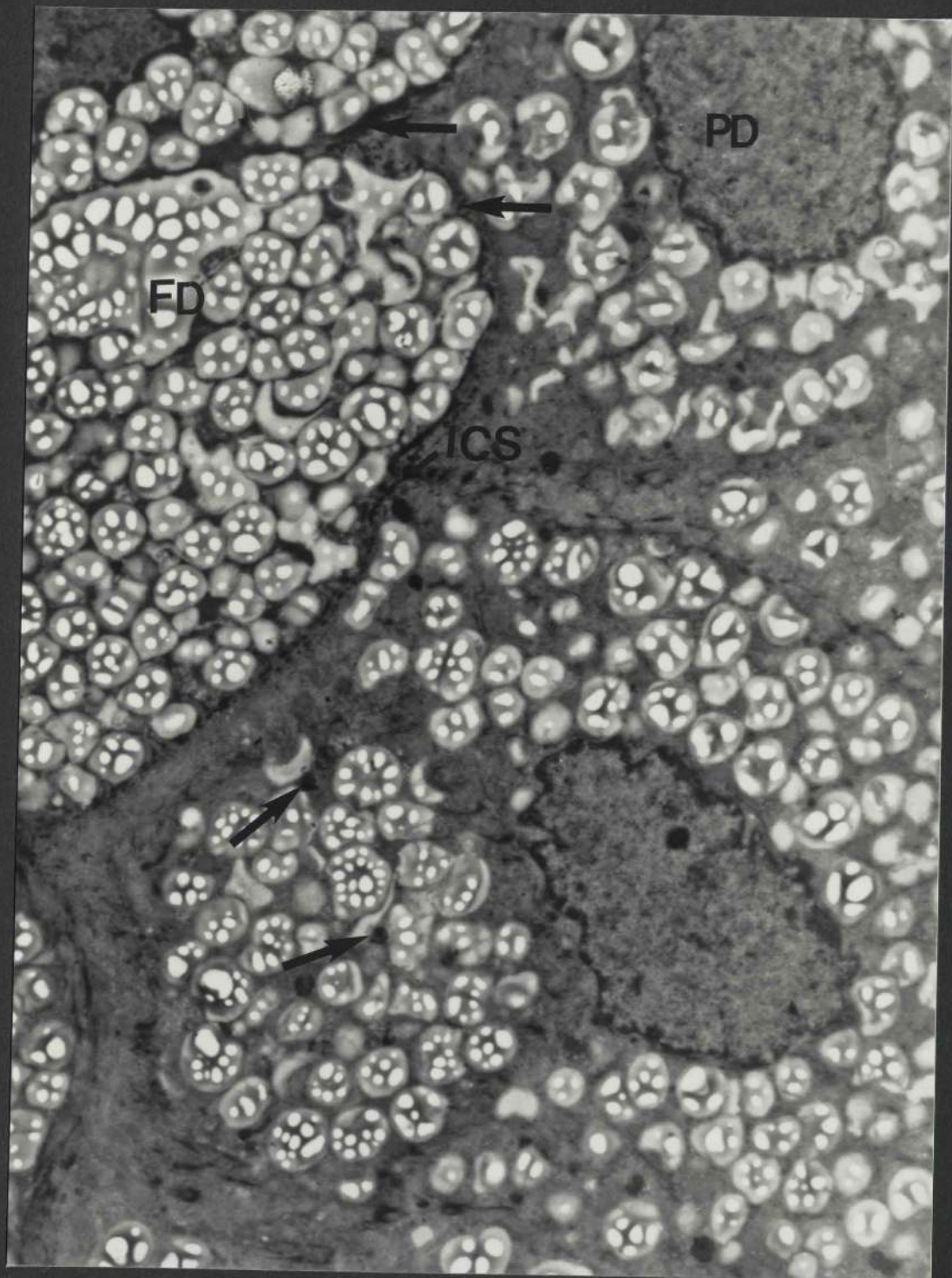


Figure 95e: This micrograph shows a part of the follicular canal epidermis. Some basal (SB), spinous (SS), granular (SG) and corneal (SC) cells are seen (x 8,352).

Deposits of an electron-dense material are present in the intercellular spaces between basal, spinous and granular cells (small arrows). Some cells contain small aggregations of the dense material. The large arrow indicates the location of such dense deposits.

The intercellular spaces in the stratum corneum appear to be empty. Furthermore, no tracer is found on the surface of the stratum corneum.

Figure 95f: This micrograph is a section of the epidermis and includes the basal (SB), the spinous (SS), the granular (SG) and the horny (SC) cell layers (x 8,352).

No regular pattern of electron-dense material is observed in the epidermis. However, some patches of dense deposits are seen scattered within the lower epidermal layers (arrows), but not in the stratum corneum. Such deposits were not seen in all the ultrathin sections examined. The intercellular spaces (ICS) often appear empty in places.



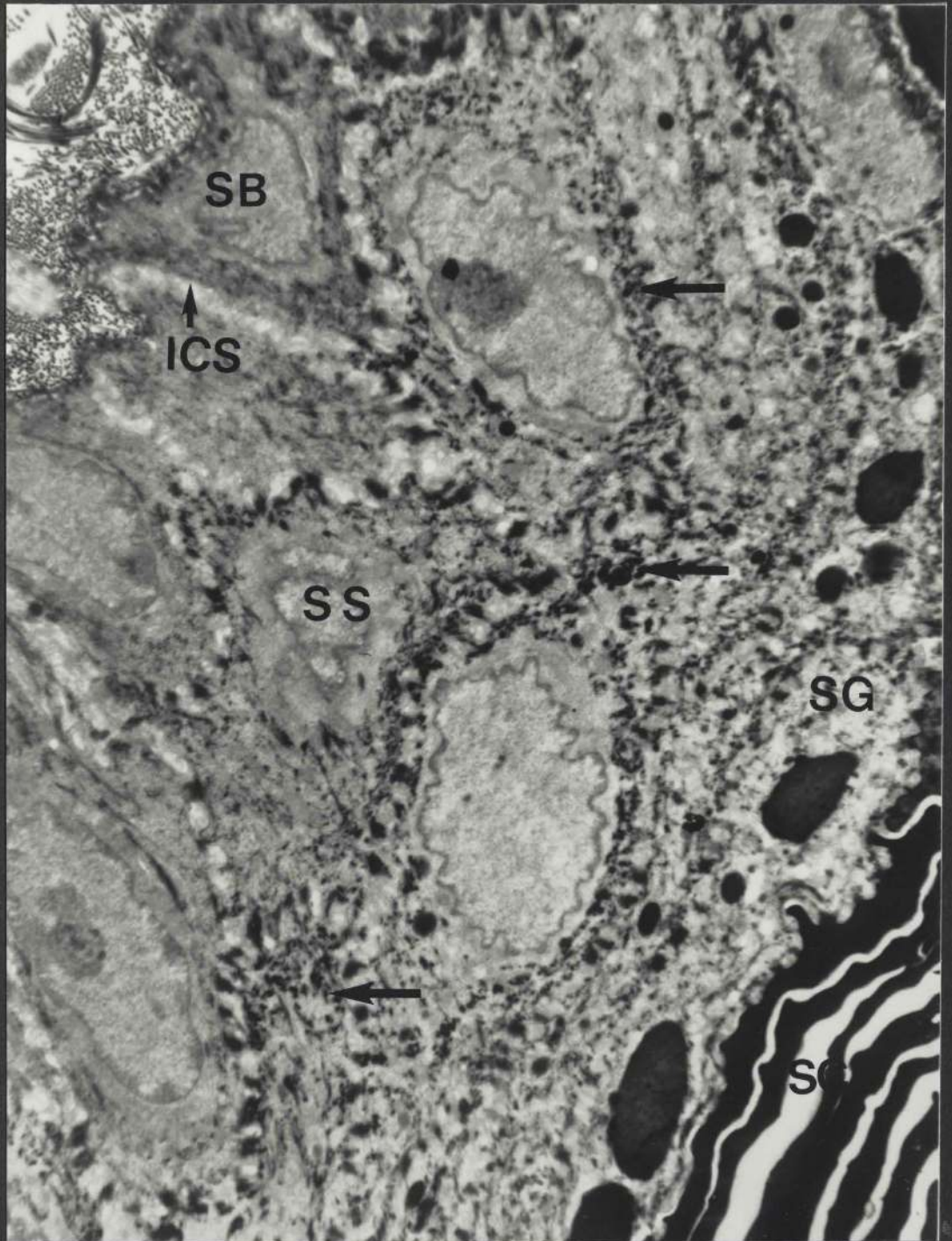
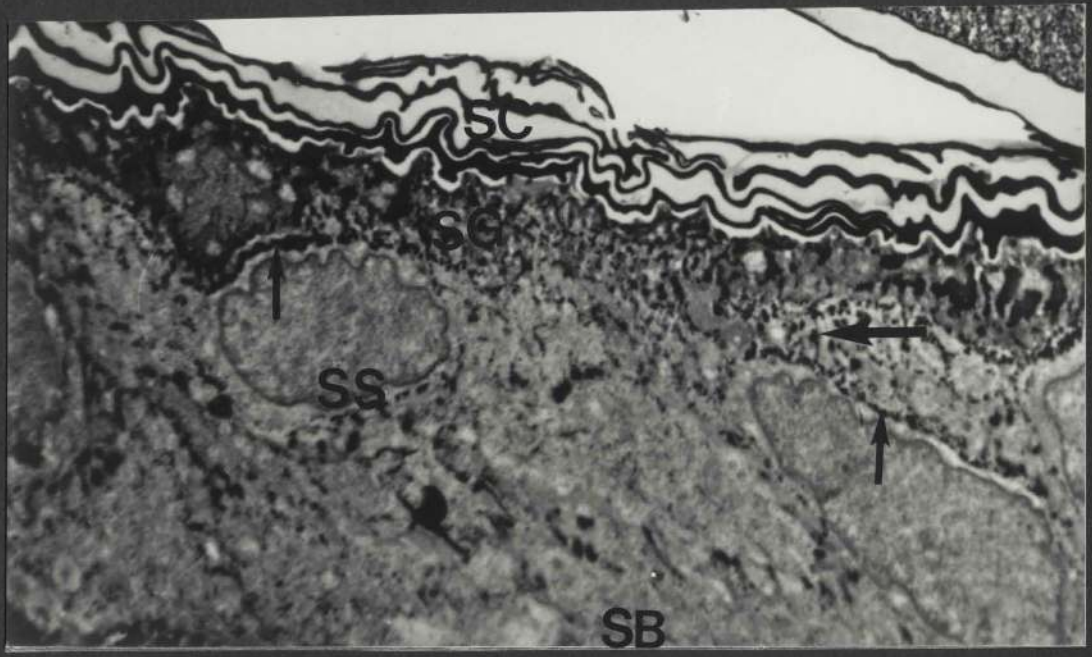




## Figure 96 (a - c)

Local application (control) of a 1% aqueous ruthenium red solution for 15 minutes

## Figure 96a:

Above: A cryostat section (x 32)

The penetration of ruthenium red into the skin following local application is minimal. A red colouration is occasionally visible in the upper part of the skin.

Below: A similar cryostat section to that shown above but stained with haematoxylin and eosin (x 32)

This shows the skin structures which are not seen clearly in the previous section. These include the epidermis (E), the hair follicles, (HF), the sebaceous glands (SG), the dermis (D) and the hypodermis (H). By comparison, it appears that the red colouration seen in the previous section is confined to the surface of the epidermis.

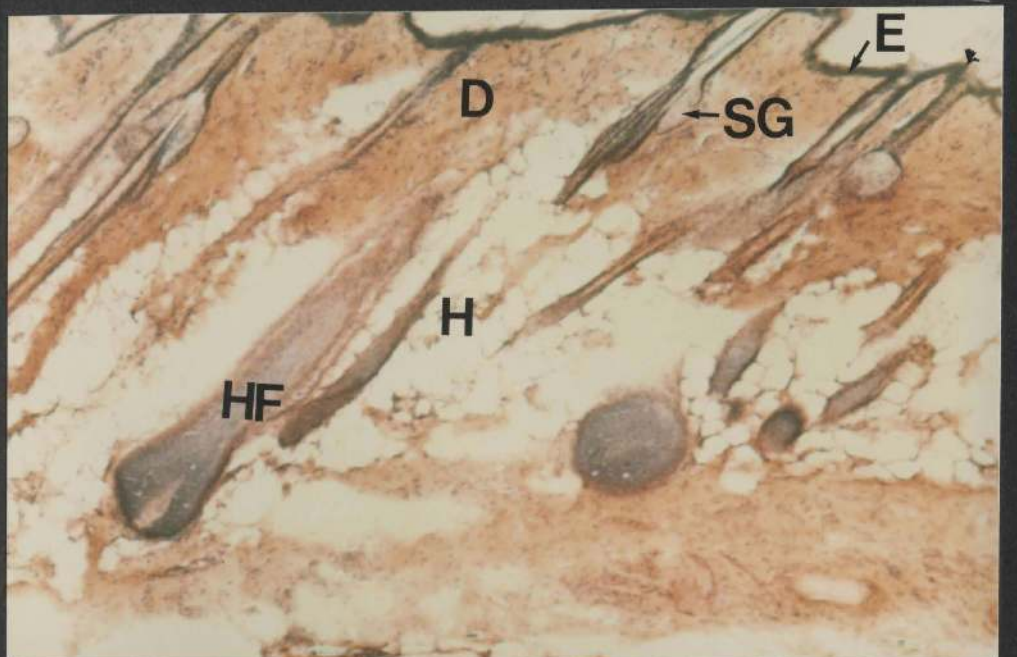
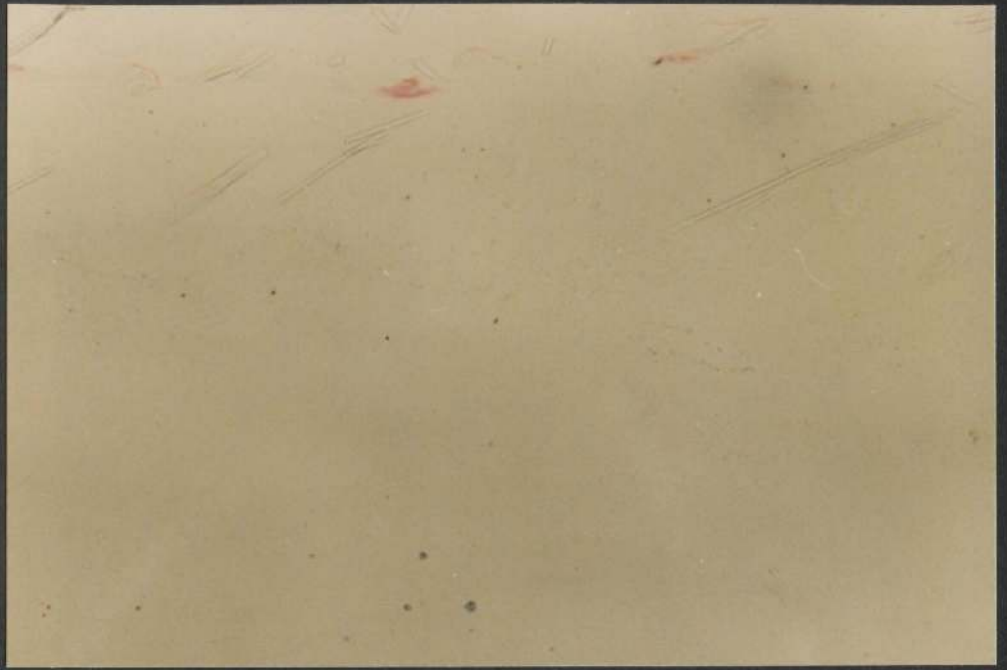
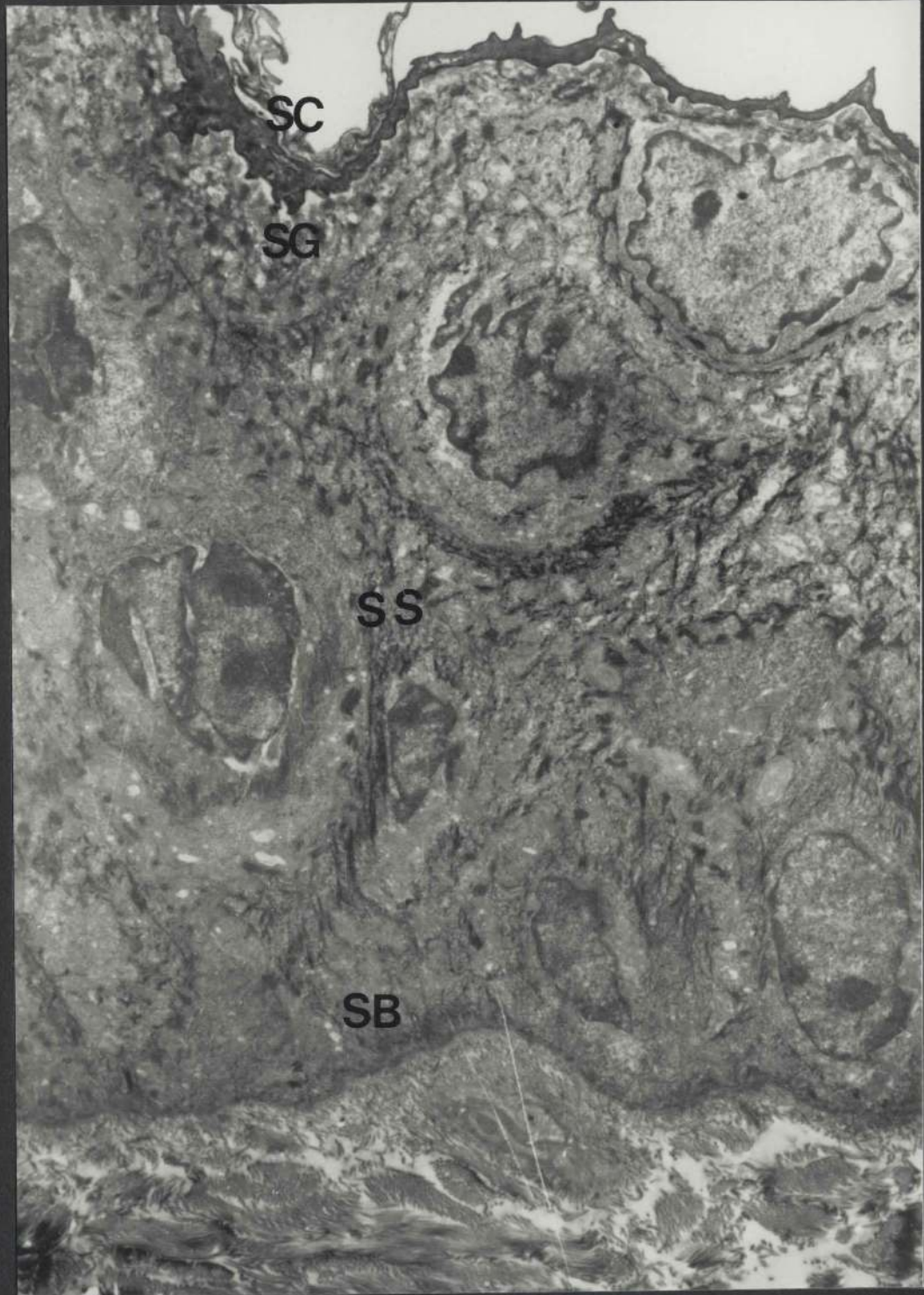


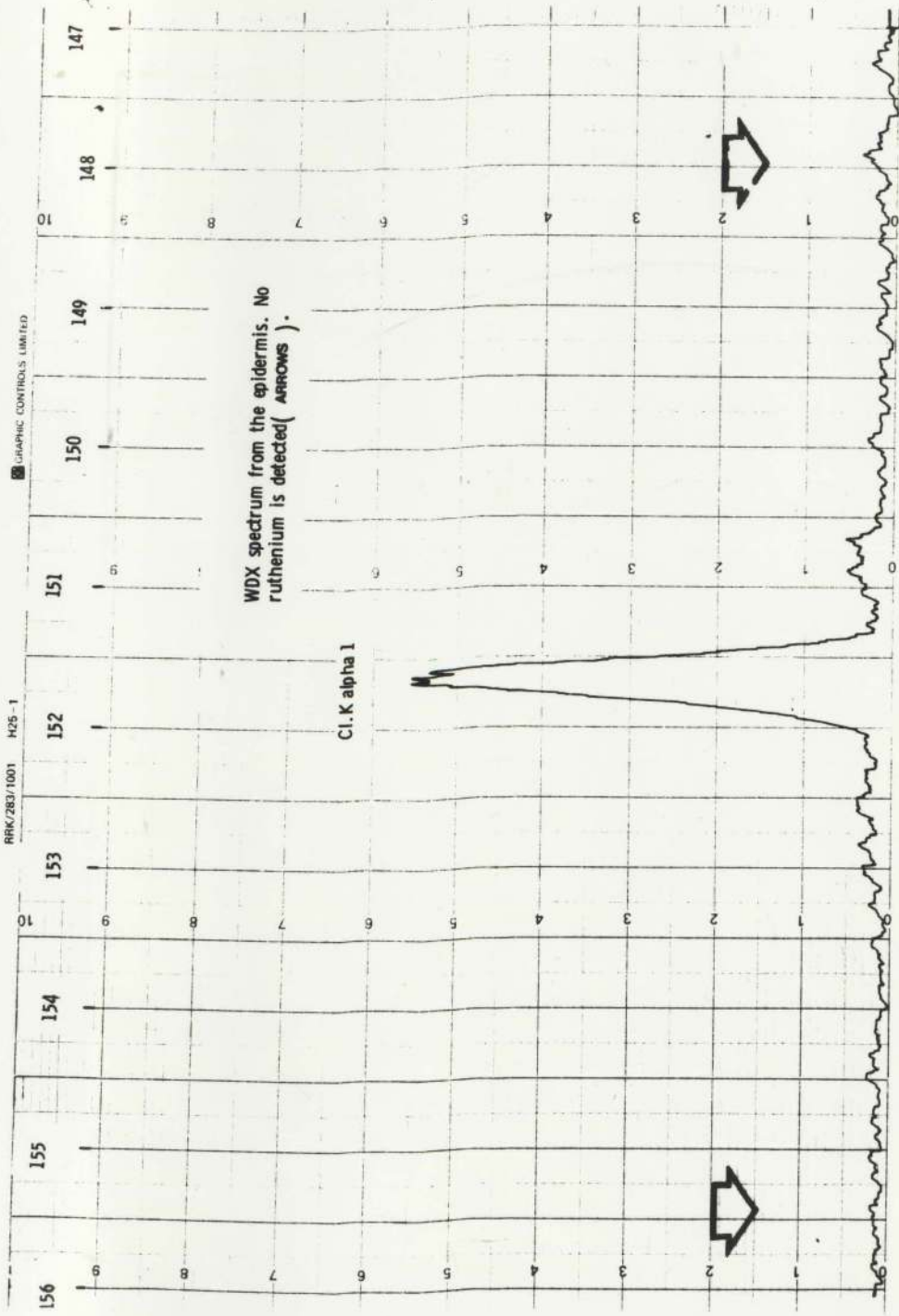
Figure 96b: This micrograph shows the stratum corneum (SC), the stratum granulosum (SG), the stratum spinosum (SS) and the stratum basale (SB) of the epidermis (x 8,352).

No electron-dense material is found in the intercellular or in the intracellular regions in the stratum corneum or in the deeper epidermal layers.

The WDX spectrum (see overleaf) obtained from a semithin araldite section containing a view similar to that shown opposite did not contain peaks for ruthenium.







447 1481

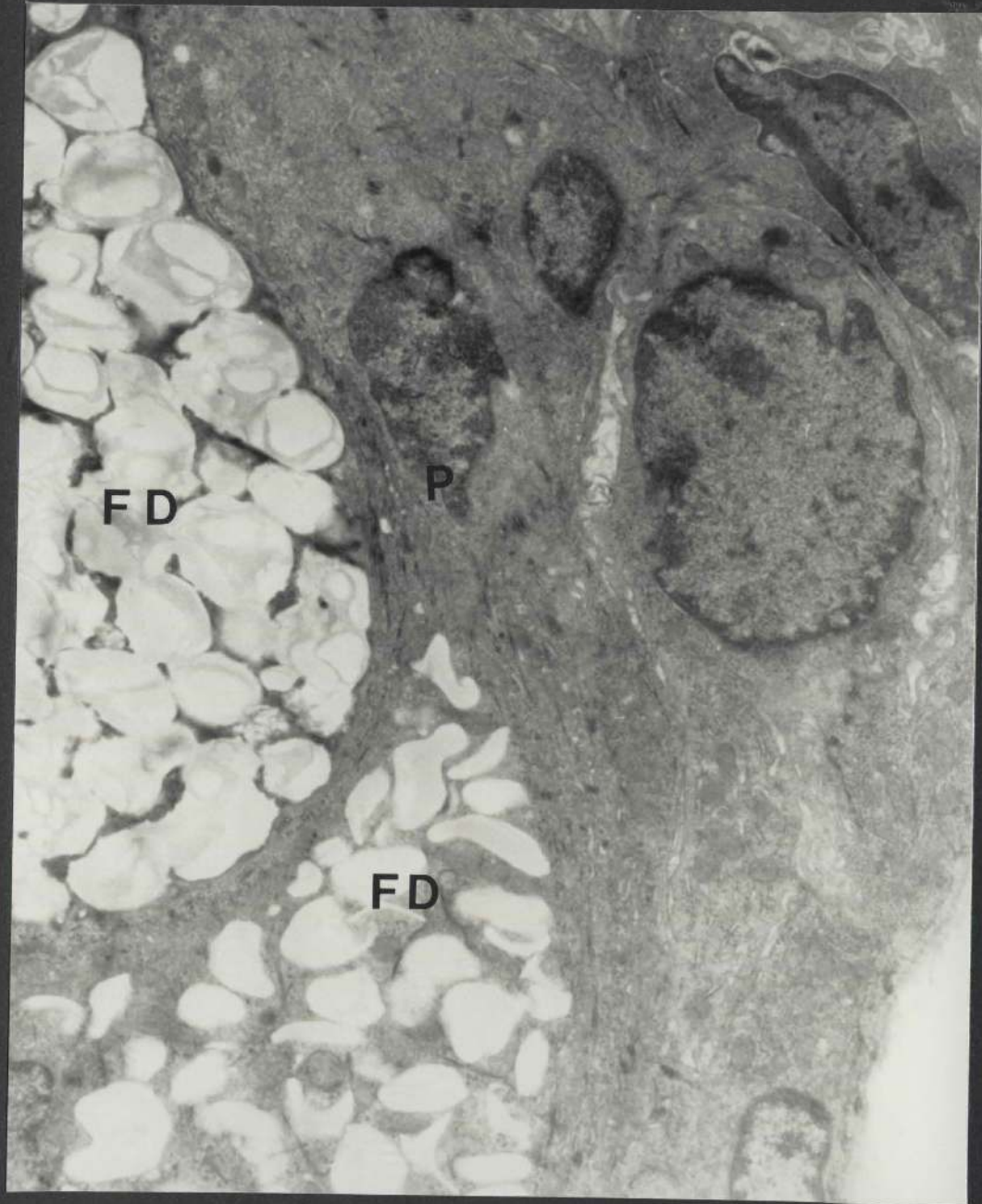
447 1481



Figure 96c: This electron micrograph features the periphery of a sebaceous gland towards the duct region. The structures present include peripheral (P) and fully differentiated (FD) sebaceous cells (x 10,208).

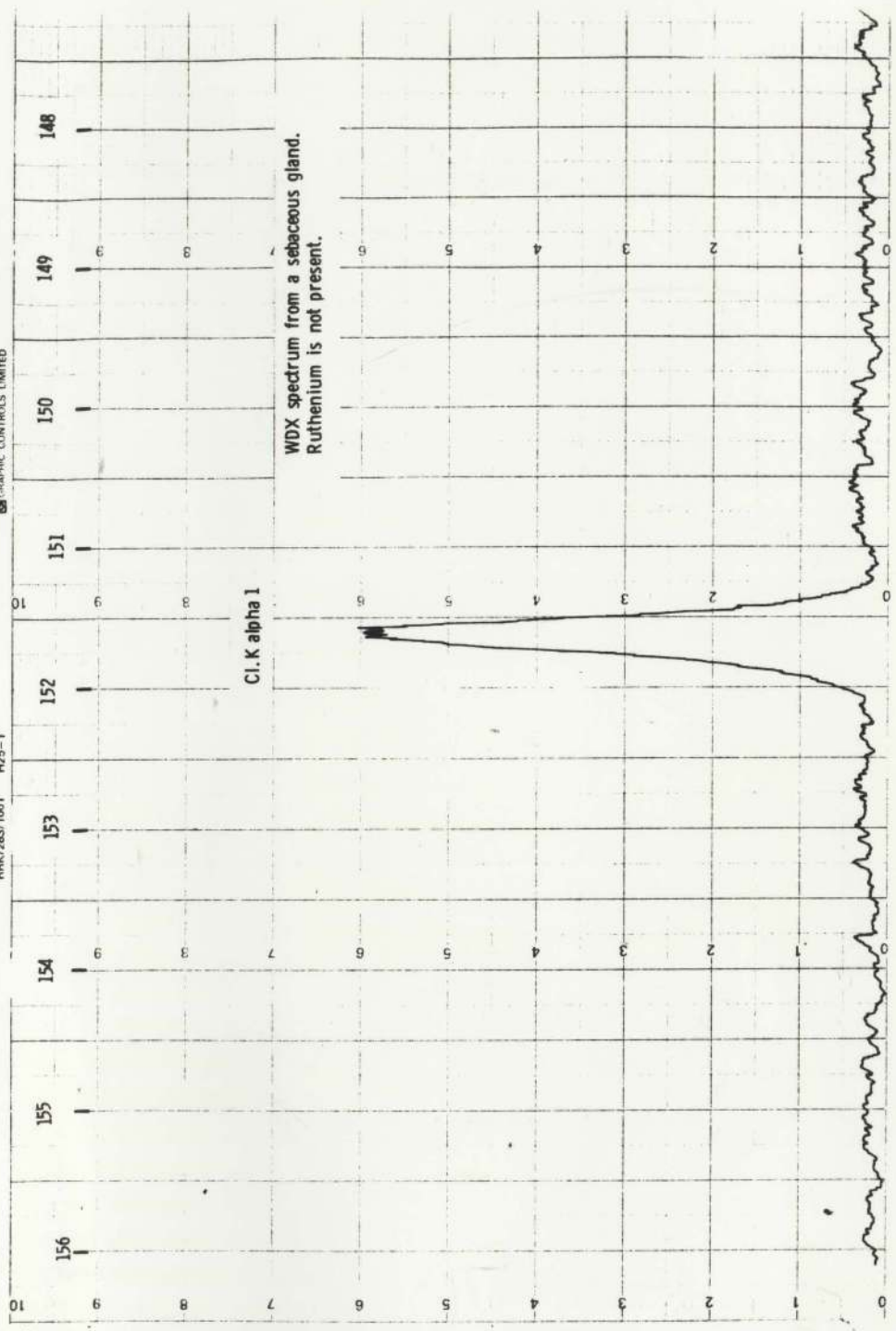
No electron-dense material is found inside or around the sebaceous cells.

The corresponding WDX spectrum did not contain ruthenium.



GRAPHIC CONTROLS LIMITED

RRK/263/1001 H25-1



WDX spectrum from a sebaceous gland.  
Ruthenium is not present.

Cl. K alpha 1

Figure 97 (a - e)

Positive iontophoresis of a 1% aqueous ruthenium red solution at 30 milliamperes for 15 minutes

Figure 97a: A cryostat section (x 32)

The penetration of ruthenium red into the skin and the underlying tissues is complete. A red colouration is visible in the epidermis (E), the hair follicles (HF), the sebaceous glands (SG), the dermis (D), the hypodermis (H) and the striated muscle (SM).



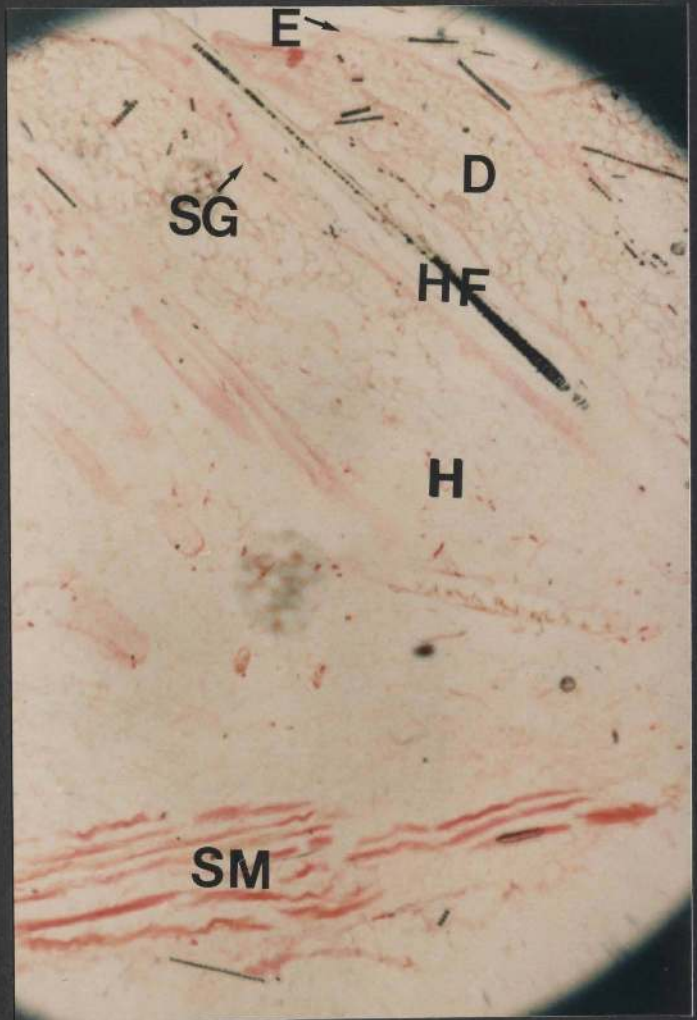




Figure 97b: This micrograph illustrates the stratum basale (SB), the stratum spinosum (SS), the stratum granulosum (SG) and the stratum corneum (SC) of the epidermis (x 8,352).

No electron-dense deposits are seen in the epidermis. The nuclei of the cells in the stratum basale and the stratum spinosum are dense and "granular" in appearance with irregular outlines. In addition, there is coagulation of the cytoplasmic matrix resulting in the loss of the fine intracellular detail.

The WDX spectrum obtained from a semithin araldite section containing a similar view to the one shown opposite contained peaks for ruthenium (see overleaf).



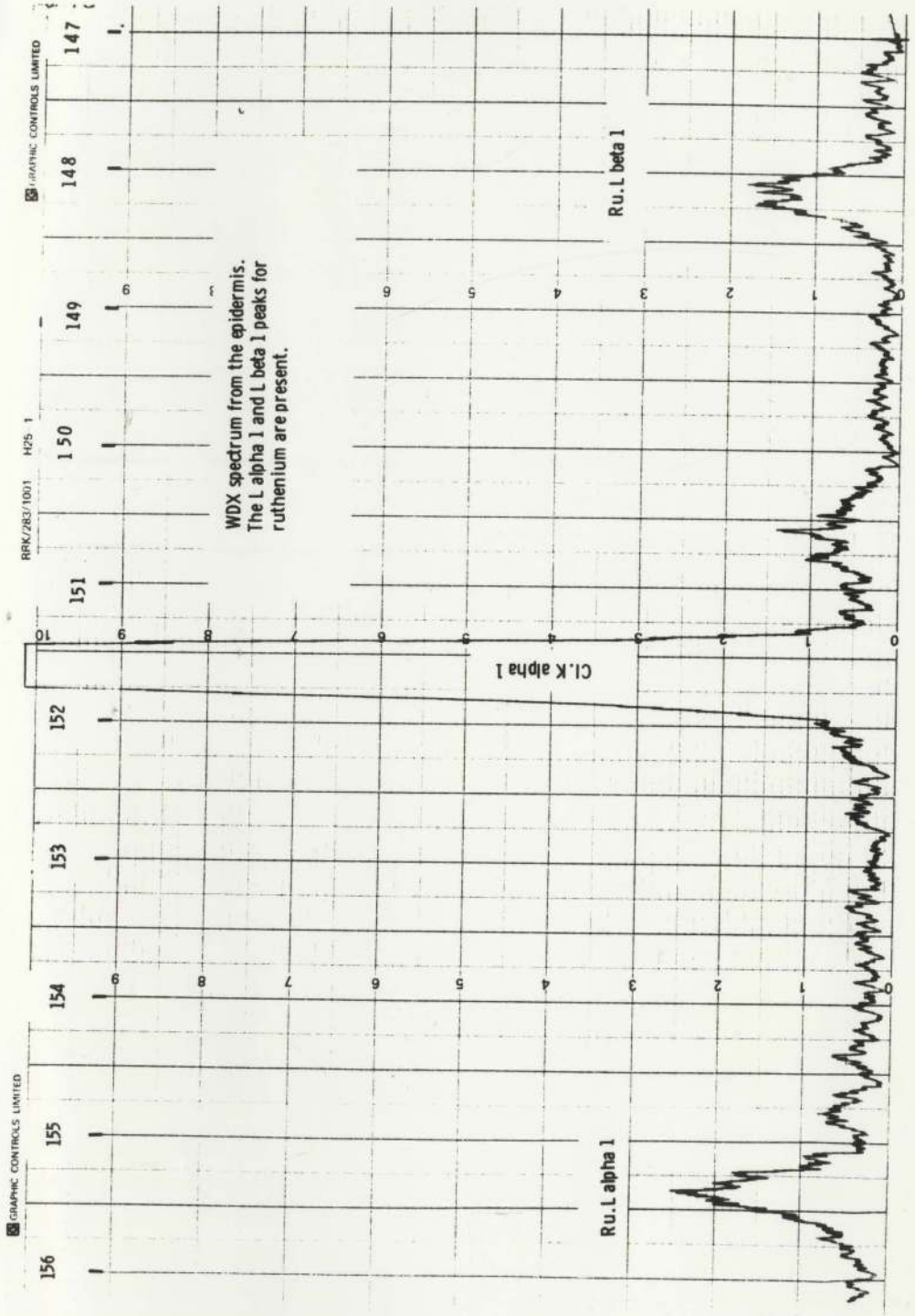


Figure 97c: This micrograph shows a portion of the follicular infundibulum and includes the basal (SB), the spinous (SS), the granular (SG) and the corneal (SC) layers. Towards the upper right hand corner of the field, a segment of a hair shaft (H) is seen (x 8,352).

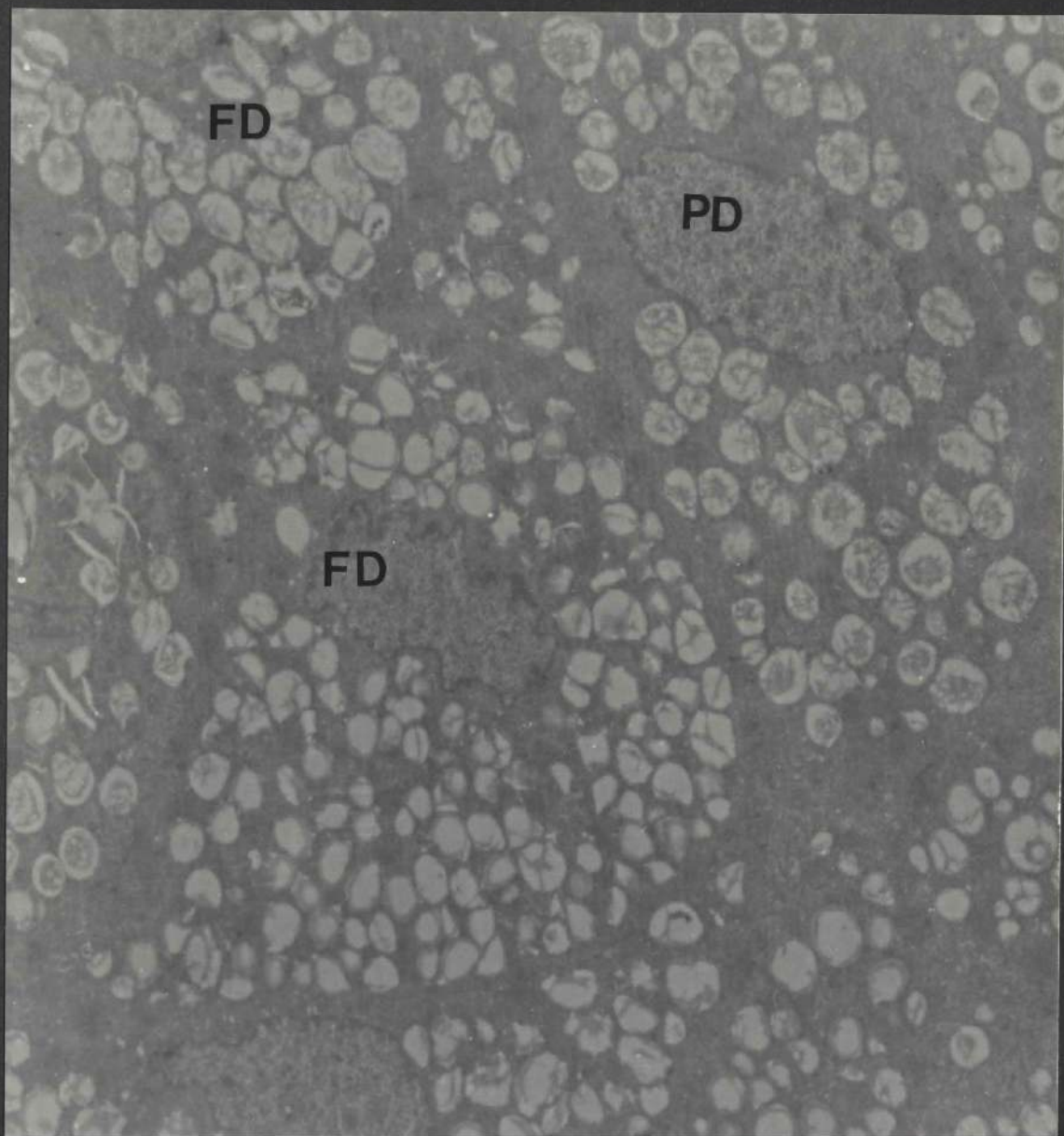
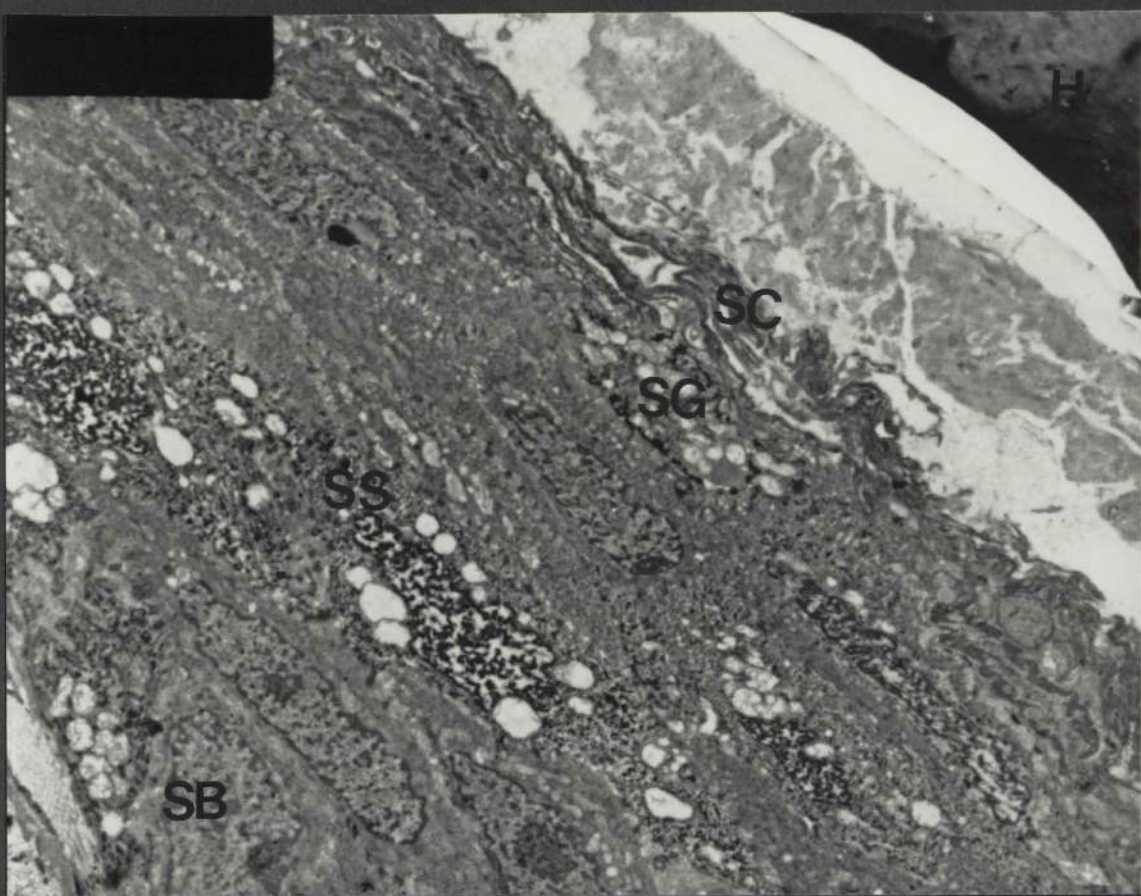
Once again, no electron-dense deposits are seen in the infundibulum. One may note the distinct "granulation" of the nuclei and the cytoplasm in the deeper layers of the epidermis.

The WDX spectrum obtained from the follicular infundibulum contained peaks for ruthenium (see overleaf).

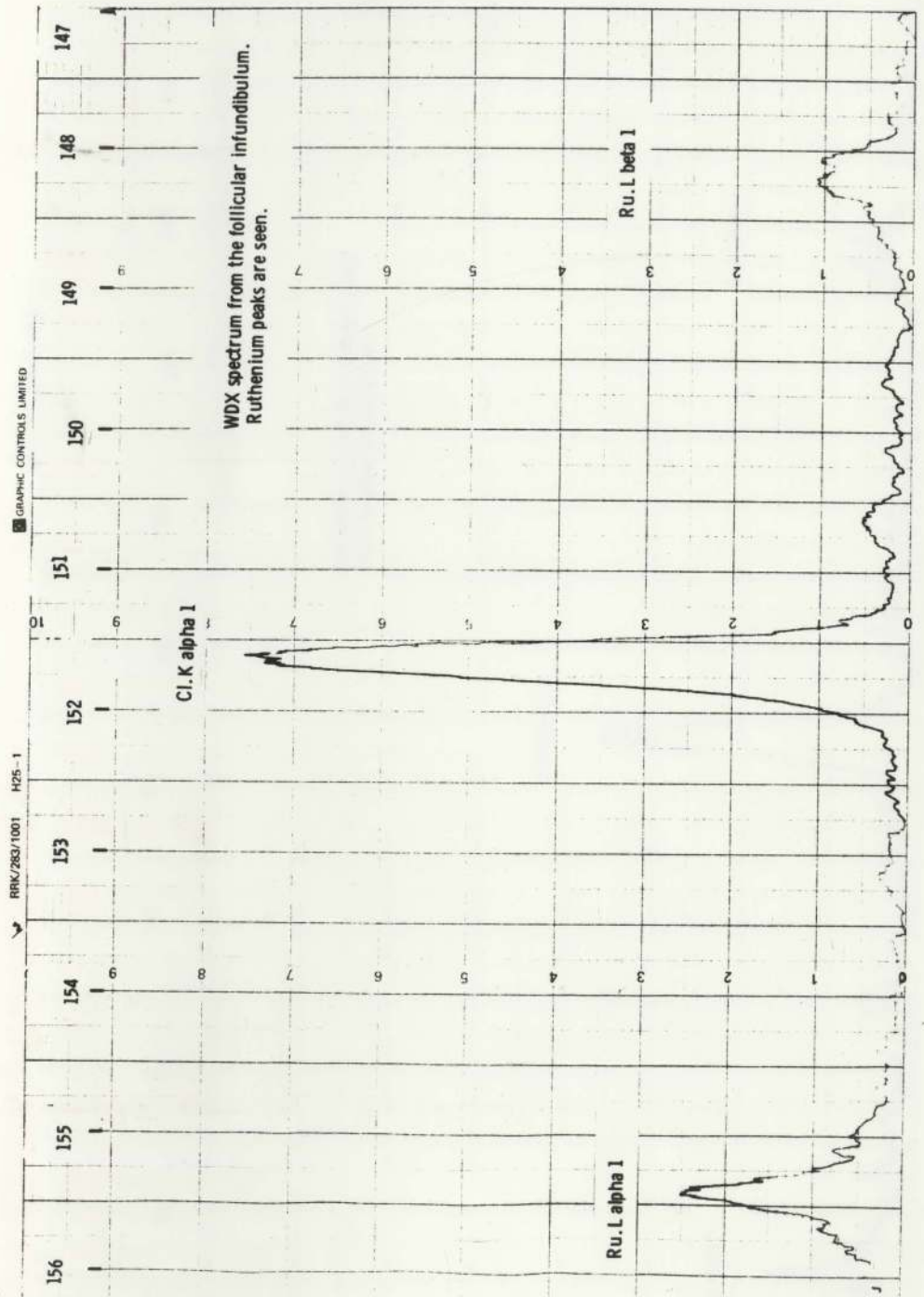
Figure 97d: A segment of a sebaceous gland exhibiting partially (PD) and fully (FD) differentiated sebocytes (x 10,208).

No electron-dense material is present in the sebaceous glands. However, the WDX spectrum obtained from the gland contained peaks for ruthenium (see overleaf).









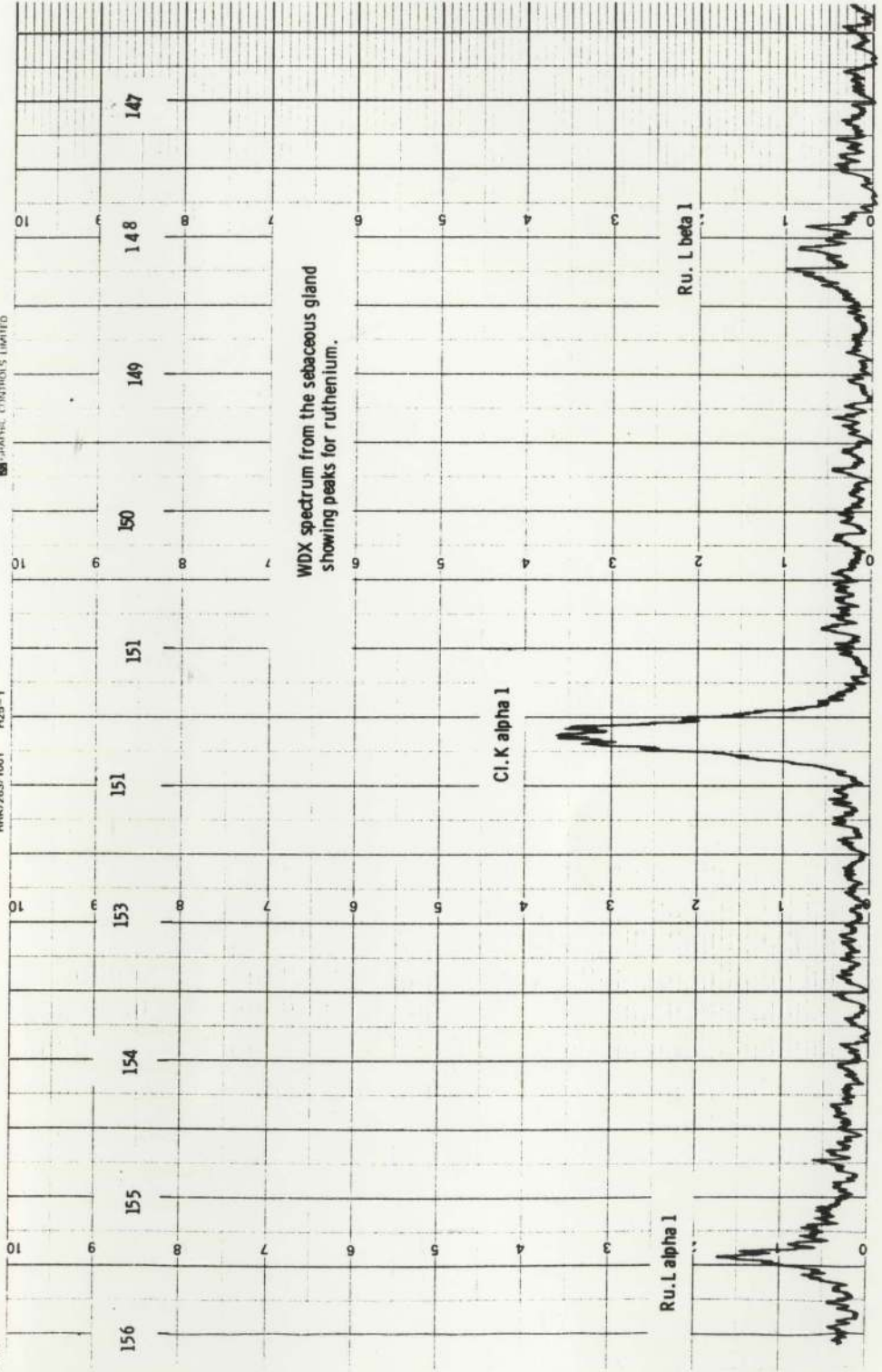
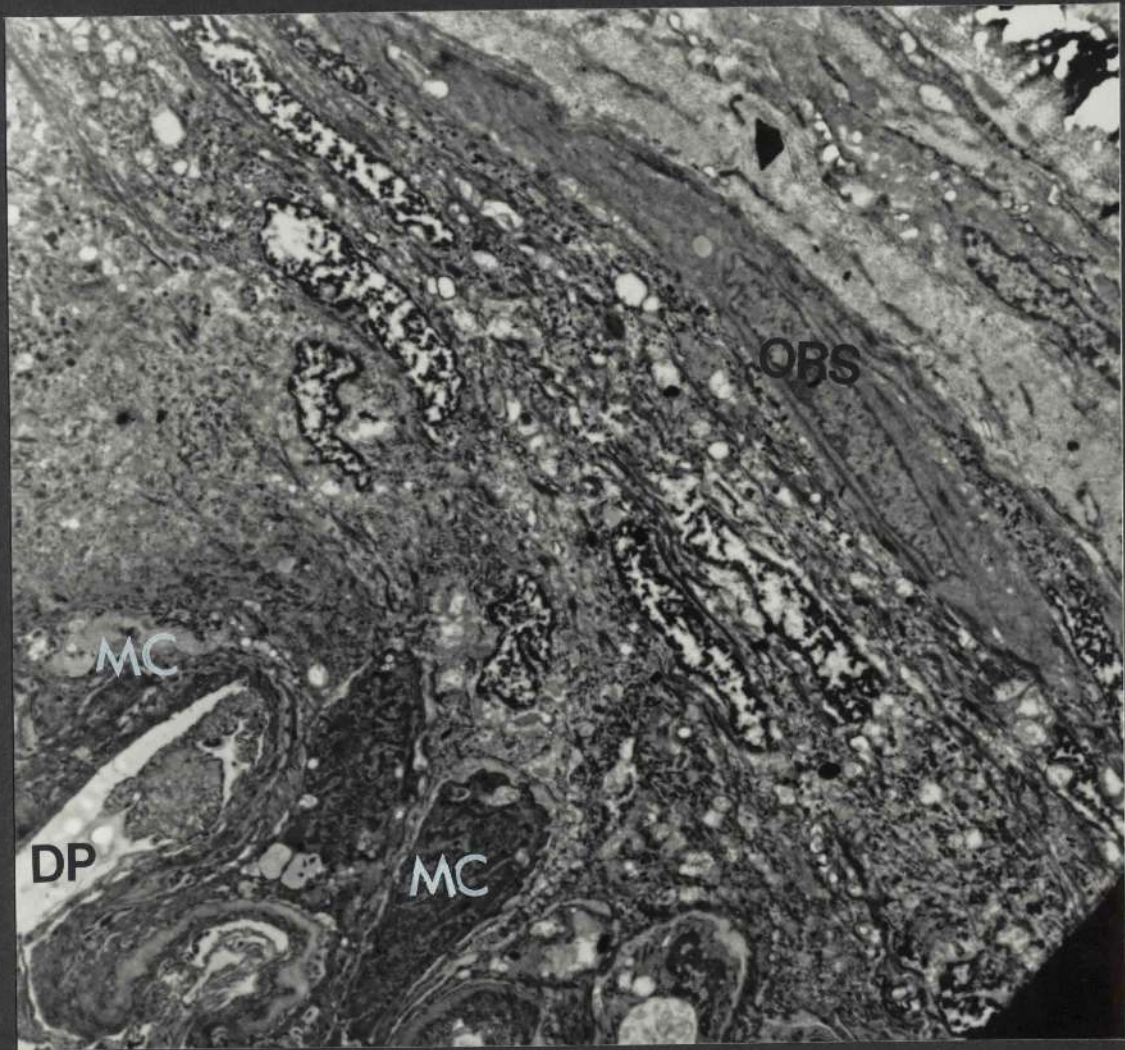
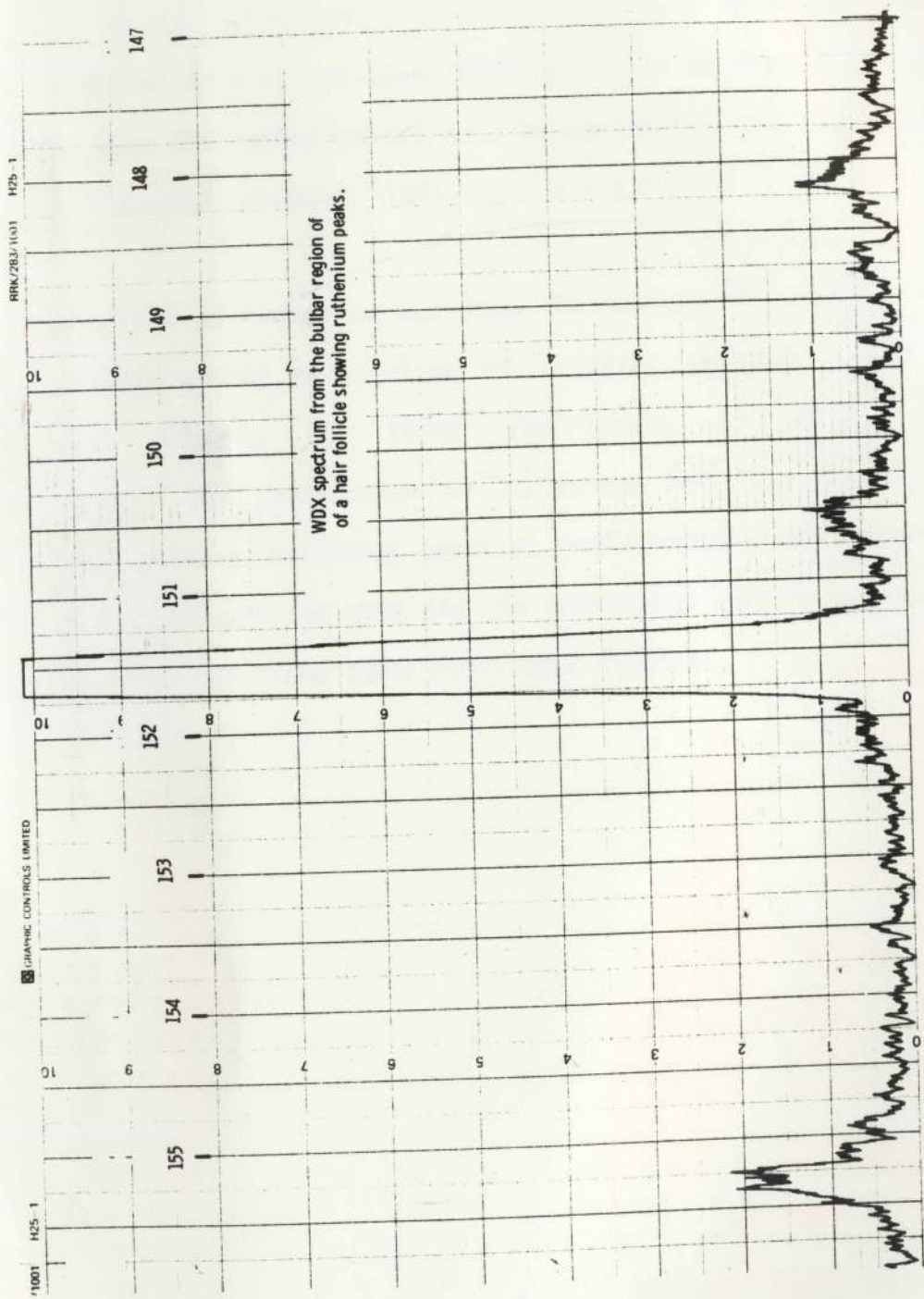


Figure 97e: This electron micrograph is from the lower part of a hair follicle at the level of the bulb. The structures present include the dermal papilla (DP), the matrix cells (MC) and cells of the outer root sheath (ORS) (x 8,352).

The bulbar region of the hair follicle does not contain a deposition of electron-dense material. However, the WDX spectrum contained peaks for ruthenium (see overleaf).









### Summary of results (Figures 96 and 97)

Examination of the skin with the transmission electron microscope was considered to be unsatisfactory in that no electron-dense deposits were seen in the ultrathin sections. This confirmed the previous reports that if an electron-dense material is to be seen in ultrathin sections, then the ruthenium red must be applied to the tissue in the presence of osmium tetroxide (Luft, 1971 a and b).

The penetration of ruthenium red from the surface into the skin was rather determined by examination of cryostat sections. The most significant finding of these experiments is that without iontophoresis, the penetration of ruthenium red into the skin is negligible, whereas following positive iontophoresis the penetration of the tracer through the skin and the underlying tissues is complete. The WDX spectra confirmed these histologic findings.

**VOLUME**

**3**



TR 11812

30

RECEIVED

11 11 11

CONTINUATION  
OF  
CHAPTER 3  
(RESULTS)

### 3.8 Copper

Solutions containing copper sulphate ( $\text{CuSO}_4$ ) have been used to study the penetration of copper ions ( $\text{Cu}^{2+}$ ) into the skin (Pereyra, 1945). The tracer itself cannot be observed directly in tissue sections, but histochemical tests are available to localize the tracer in tissues. These tests consist of immersing tissue sections in solutions which cause the formation of coloured compounds with the tracer. Two histochemical tests for copper were applied in the present study, these being Mallory's haematoxylin method (p 94) and the ruboanic acid method (p 94). The former was employed by Pereyra (1945) to demonstrate copper in skin sections.

The following group of experiments was undertaken to test the extent of the penetration of copper ions from the surface into the skin with and without iontophoresis, to investigate some of the factors which may influence such penetration, and to observe preferential route(s) of entry into the skin. The histochemical tests were applied to unfixed cryostat sections of skin. EDX analysis using the Jeol JSM-35CF scanning electron microscope was carried out on the cryostat sections to confirm the histologic findings. In addition to the above experiments, solutions of copper sulphate were injected intradermally in order to evaluate the sensitivity of both the histochemical tests and the EDX analysis in demonstrating copper in unfixed cryostat sections.



### 3.8.1 Intradermal injection

A 1% aqueous copper sulphate solution was injected intradermally. Biopsies were taken 15 minutes after the injection and sectioned with the cryostat. Some sections were analyzed with the EDX system and others were subjected to histochemical tests. The results obtained are shown in Figure 98 (a and b).

Figure 98a: A scanning electron microscope image from a cryostat section

EDX analysis was carried out on the epidermis (E), the hair follicles (HF), the sebaceous glands (SG) and the dermis (D). In addition, an area on the glass slide consisting of mounting medium just outside the skin was also analyzed. By subtraction, signals arising from the skin alone were identified. The spectra obtained are shown overleaf. A number of elements are seen in the spectrum from the mounting medium. These include aluminium, silicon, phosphorus, sulphur, chlorine, calcium and possibly sodium and magnesium, but no copper is present in the mounting medium. On the other hand, the spectra obtained from the skin sections include the  $K\alpha$  peak for copper in addition to some of the elements mentioned above. Thus it appears that the copper signals are arising from the skin specimens.

Using such analysis, copper is detected in the epidermis, the hair follicles, the sebaceous glands and the dermis.

20KY

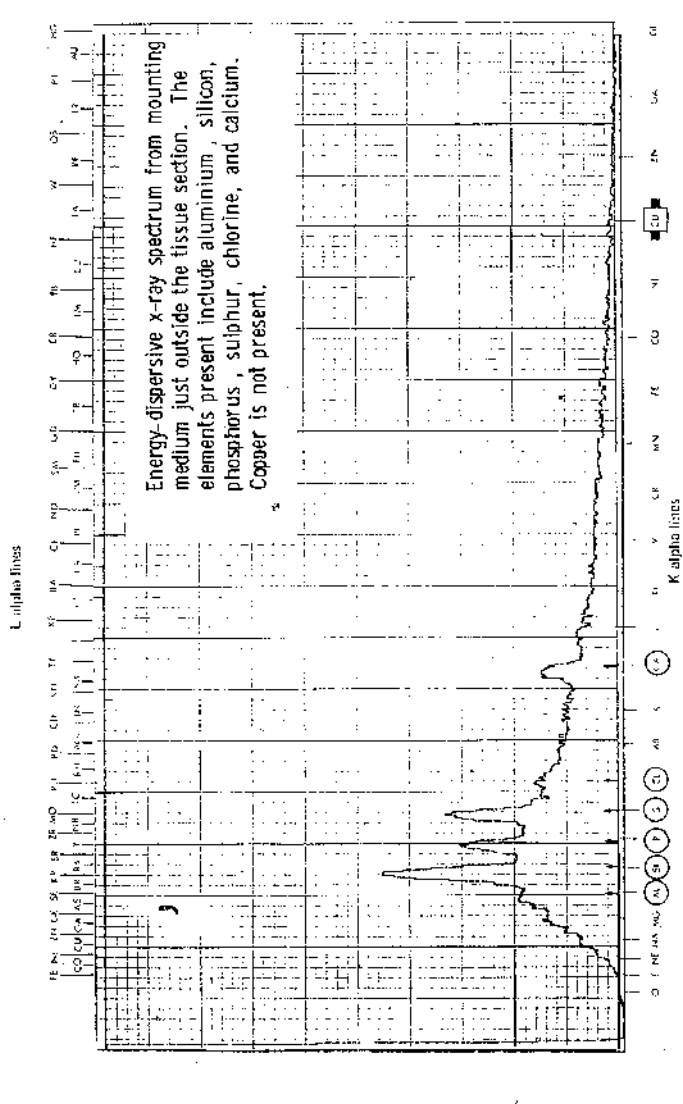
1796

100.0U

SAUEM



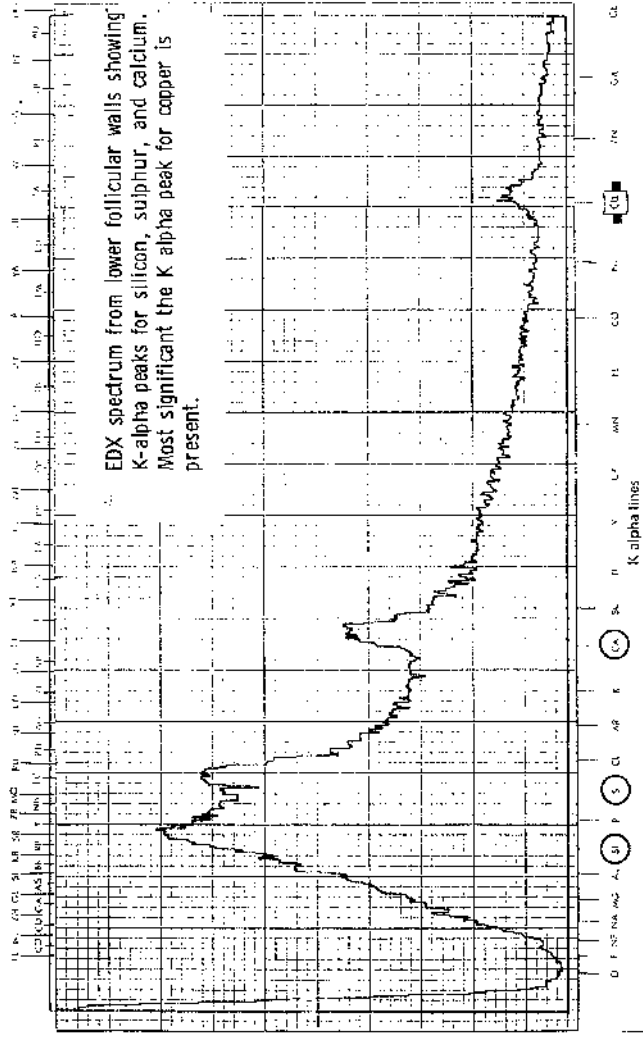
St. Andrews University S.E.N. Unit, Dabr  
 Laboratory Research  
 Gatty Marine Lab.  
 Sample **Intracutaneous injection of a 1 percent aqueous copper sulphate solution**  
 KeV **15** 33  
 Seconds **100** 33  
 Take-off Angle



Energy-dispersive x-ray spectrum from mounting medium just outside the tissue section. The elements present include aluminium, silicon, phosphorus, sulphur, chlorine, and calcium. Copper is not present.

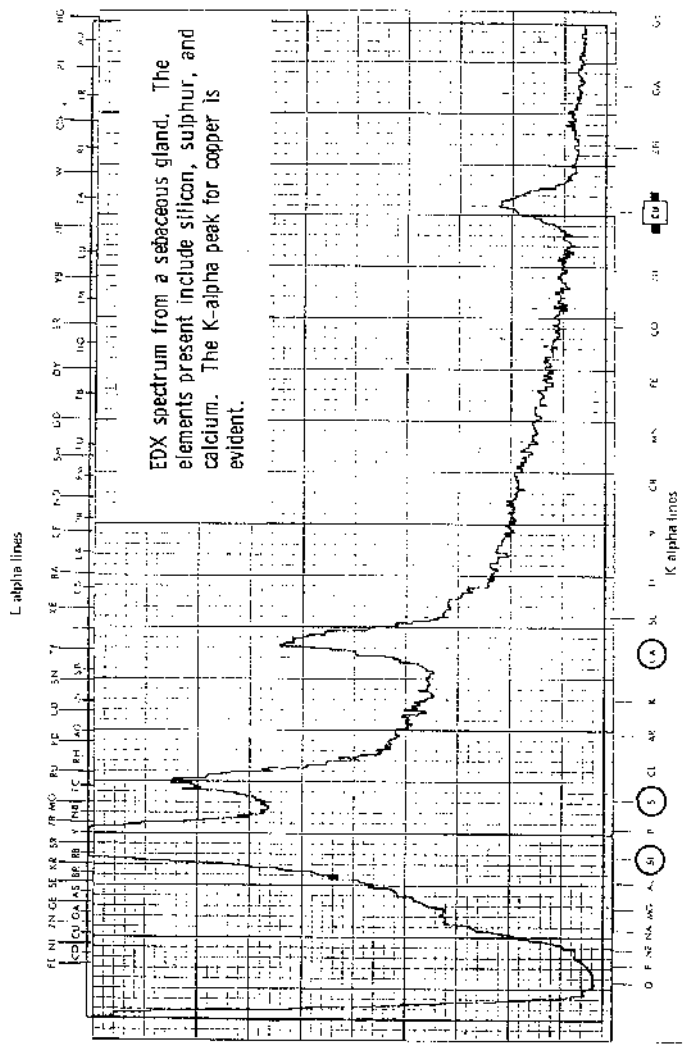
Laboratory St. Andrews University S.E.K. Unit.      Date                       
Gatty Marine Lab.      Received                       
 Sample intravenous injection of a 1 percent aqueous copper sulphate solution.  
 KeV 15      Seconds 100      Take off Angle 33

L alpha lines



EDX spectrum from lower follicular walls showing  
 K-alpha peaks for silicon, sulphur, and calcium.  
 Most significant the K alpha peak for copper is  
 present.

Laboratory St. Andrews University S.E.A. Unit. Researcher ..... Date .....  
Getty Machine Lab.  
 Sample Intracutaneous injection of a 1 percent aqueous copper sulphate solution.  
 KeV 15 Seconds 100 Tube off Angle 33

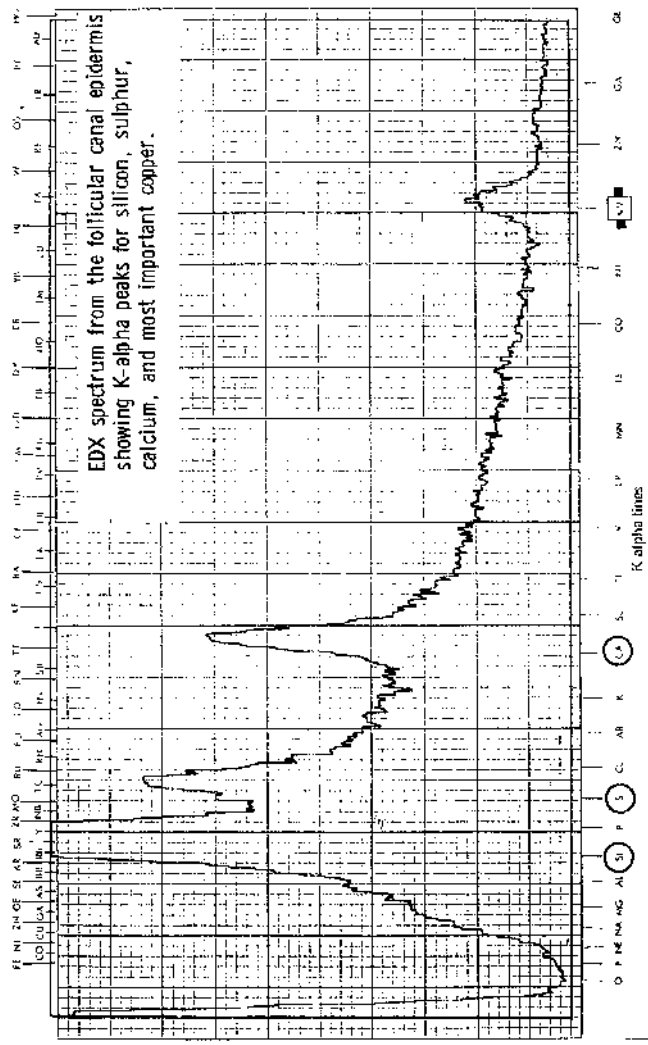


EDX spectrum from a sebaceous gland. The elements present include silicon, sulphur, and calcium. The K-alpha peak for copper is evident.



Laboratory St. Andrews University S.E.M. Unit, Date                       
Carby Machine Lab. Researcher                       
 Sample Intracutaneous injection of a 1-percent aqueous copper sulphate solution.  
 KeV 15 Seconds 100 Take off Angle 33

L alpha lines



St. Andrews University S.E.M. Unit. Date .....  
 Laboratory Gatty Marine Lab. Researcher .....  
 Sample ..... **Intracutaneous injection of a 1 percent copper sulphate solution.** 33  
 KeV ..... 15 Seconds ..... 100  
Take off Angle .....

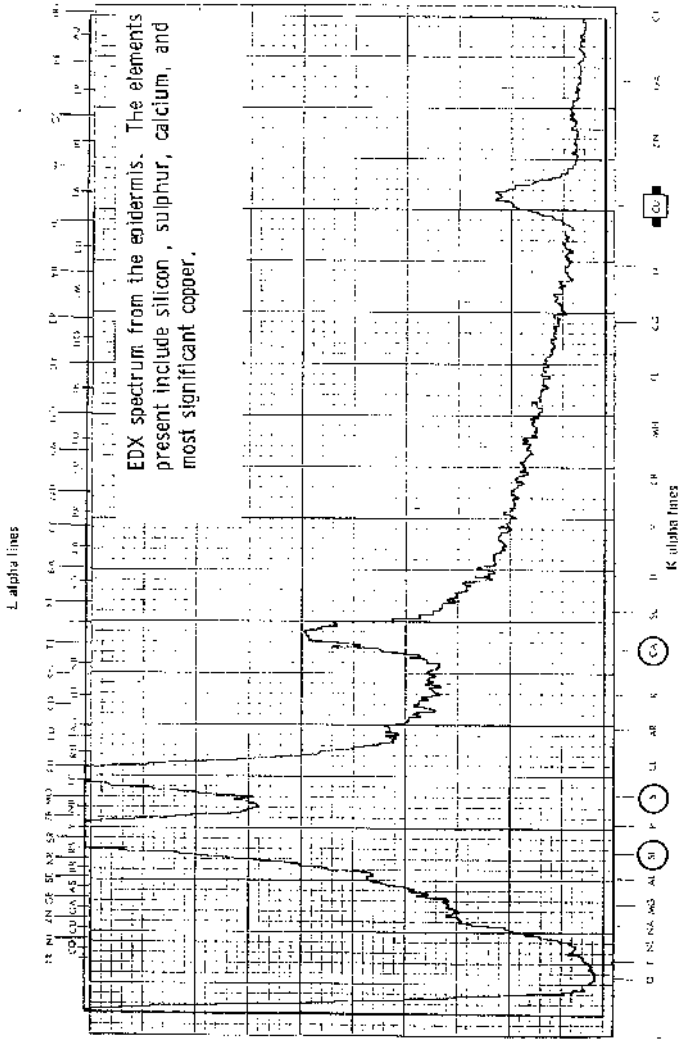


Figure 98b: A cryostat section subjected to Mallory's haematoxylin histochemical method (x 80).

Following such a technique, blue-black deposits are seen throughout the skin section. Copper is evident in the epidermis (E), the hair follicles (HF), the sebaceous glands (SG) and the dermis (D). However, it is difficult to determine at which level within the epidermis the superficial migration of copper ions is halted.

From Figures 98a and 98b it is clear that both the histochemical and the EDX methods are sensitive enough to demonstrate and detect copper in unfixed cryostat sections.



### 3.8.2 Effect of current intensity

In order to investigate the efficiency of iontophoresis regarding the introduction of copper ions into and through the skin, a 1% aqueous copper sulphate solution was applied to the surface of the skin and subjected to positive iontophoresis at different values of current intensity. The extent of penetration following iontophoresis was checked against a control, that is, a similar application but without the flow of current. The experimental conditions are summarized in the following Table:-

Figure	Current intensity (mA)	Duration of application (Min)
99 (a and b)	0	15
100	30	5
101	30	10
102	30	15



## Figure 99 (a and b)

Local application (control) of a 1% aqueous copper sulphate solution for 15 minutes

Figure 99a: A cryostat section stained with Mallory's haematoxylin technique for copper (x 100).

A few deposits of copper are visible on the surface of the skin and at the follicular orifices. The hair follicles (HF), the sebaceous glands (SG) and the dermis (D) do not indicate a reaction for copper. There is a colour-free zone situated between the superficial part of the skin containing the copper reaction and the dermis which is stained with haematoxylin. The extent of the colour-free zone is indicated by the dotted lines.

Figure 99b: A similar cryostat section to that shown above but stained with standard haematoxylin and eosin (x 100).

It appears that, by comparing this figure with that shown in 99a, the colour-free zone seen in Figure 99a consists of the entire epidermis (E), probably excluding the most superficial squames of the stratum corneum.

The EDX analysis carried out on similar cryostat sections confirmed the absence of copper in the skin.

## Figure 100

Positive iontophoresis of a 1% aqueous copper sulphate solution at 30 milliamperes for 5 minutes

A cryostat section stained with Mallory's haematoxylin method for copper (x 40).

A reaction for copper is visible in the epidermis (E), the follicular canal epidermis (FCE) and the upper parts of the sebaceous glands (SG). Judging by the intensity of the copper reaction, it appears that the penetration of copper ions through the epidermis is not uniform but is more intense in areas adjacent to the hair follicles. Moreover, the tracer has passed from the surface into the sebaceous glands before passing from the epidermis into the dermis (D).

The EDX analysis confirmed the presence of copper in the structures mentioned above.

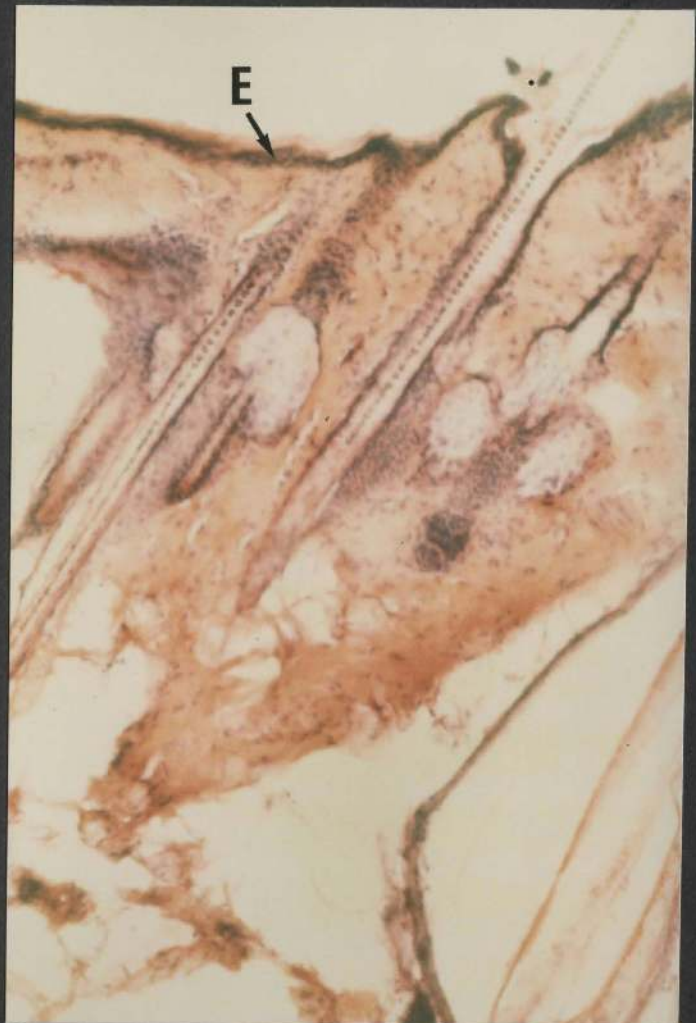
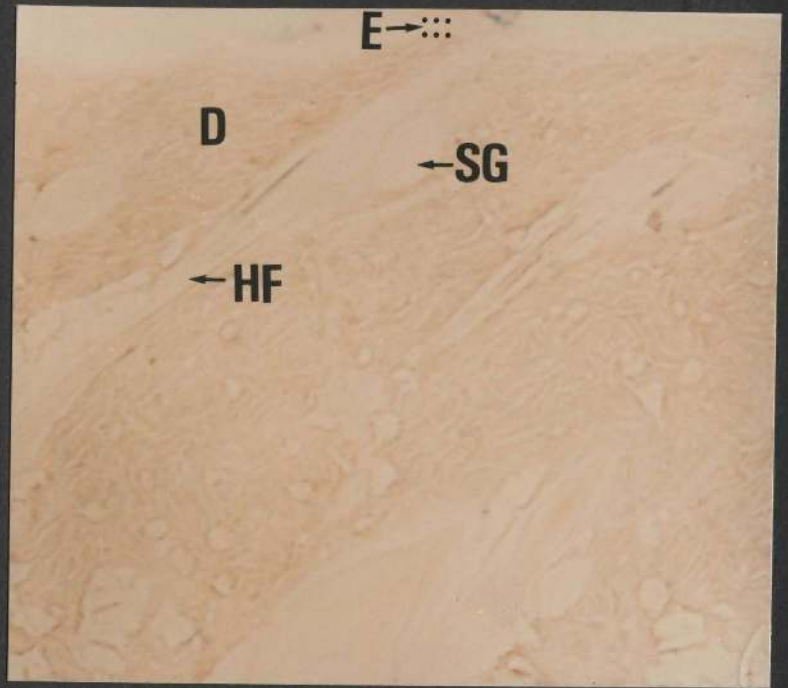
## Figure 101

Positive iontophoresis of a 1% aqueous copper sulphate solution at 30 milliamperes for 10 minutes

A cryostat section stained as in Figure 100 (x 32)

Copper is evident in the epidermis (E) and the sebaceous glands (SG), and in the hair follicles (HF) down to a short distance below the level of the glands. The penetration through the dermis (D) is deeper in areas adjacent to the hair follicles.

The EDX analysis confirmed the histological findings.





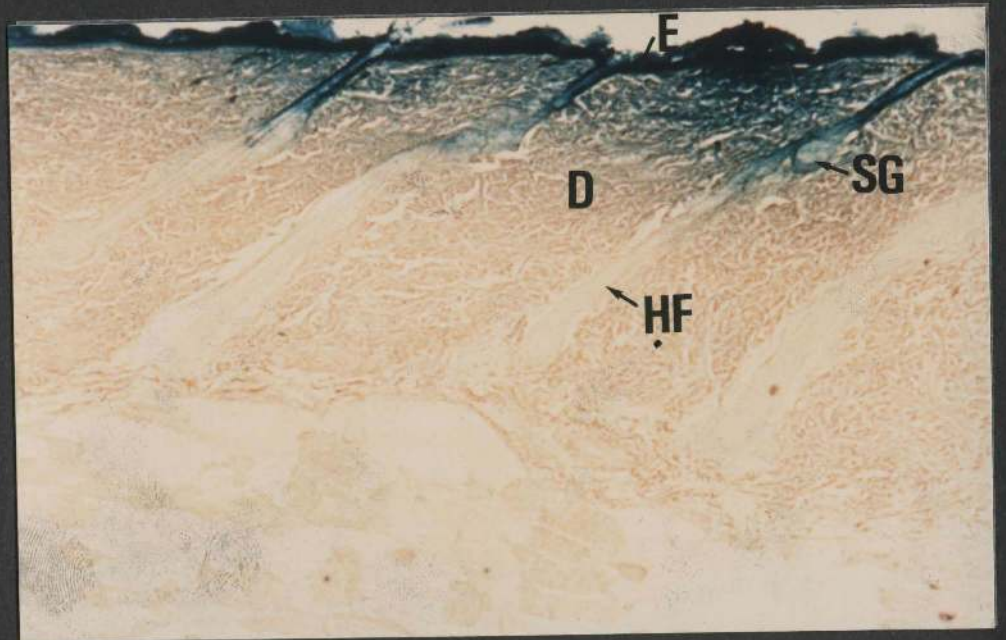
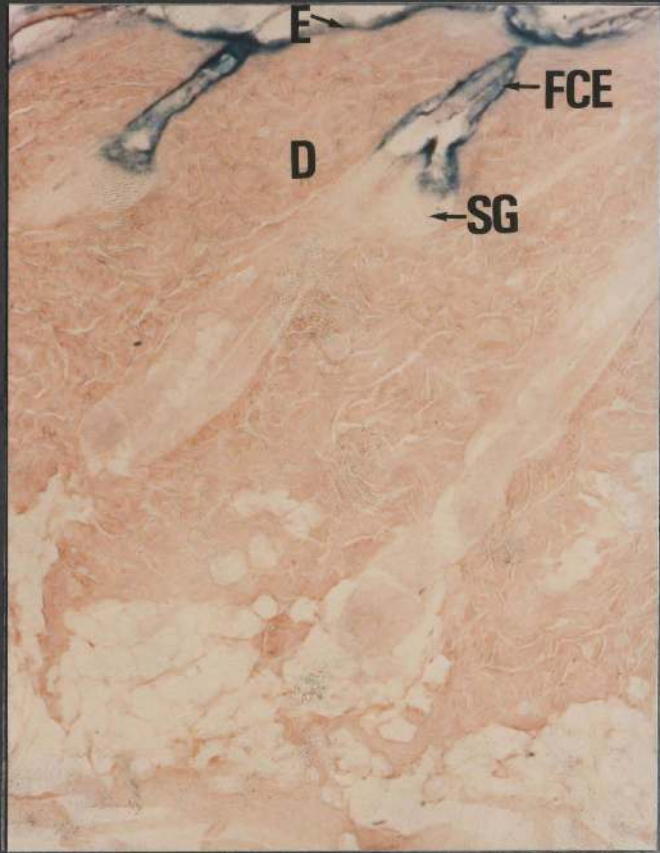


## Figure 102

Positive iontophoresis of a 1% aqueous copper sulphate solution at 30 milliamperes for 15 minutes

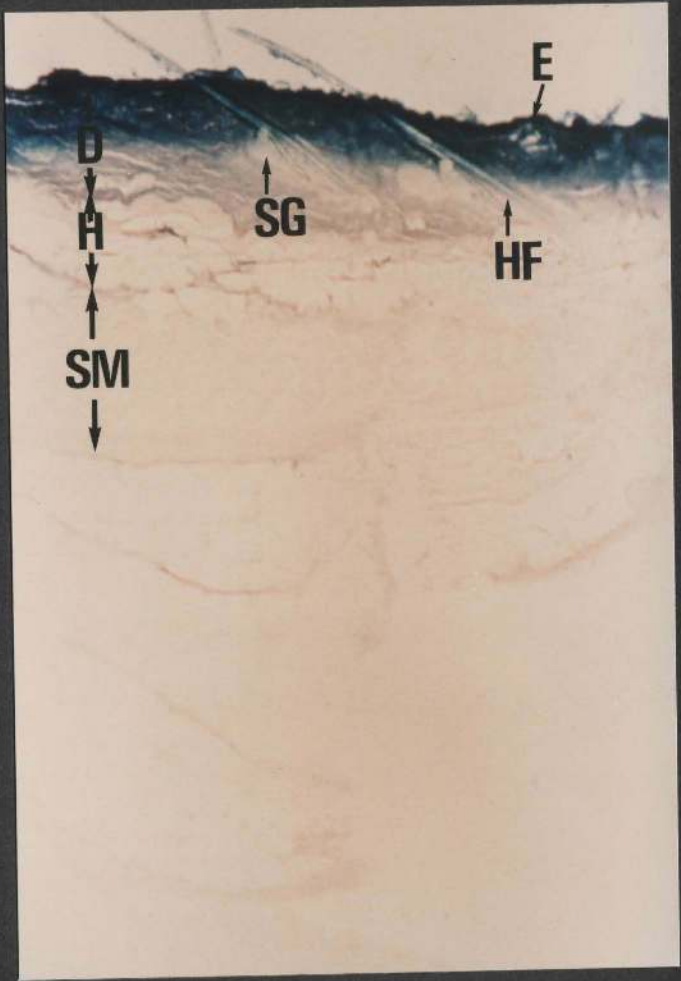
A cryostat section stained with Mallory's haematoxylin technique (x 16)

The penetration of the tracer through the skin and the subcutaneous tissue is complete. A positive reaction for copper is visible in the epidermis (E), the hair follicles (HF), the sebaceous glands (SG) and the dermis (D). Having entered deep to the skin, copper is also visible in the hypodermis (H). The limit of the penetration of copper into the tissue appears to be at the level of the hypodermis and the striated muscle (SM) deep to it.

As judged by the intensity of the reaction product, the structures at and above the level of the sebaceous glands are more heavily penetrated by copper than those below the level of these glands.

The EDX analysis confirmed the above histological findings.





### 3.8.3 Effect of concentration

The following experiments were designed to study the effect of changing the concentration of the tracer in the presenting vehicle on the penetration of the tracer into and through the skin by iontophoresis. In the previous section (3.8.2) the tracer was introduced from a 1% aqueous solution by topical application (Figure 100) or by positive iontophoresis using a current of 30 mA over a duration of 15 minutes (Figure 102). In order to investigate the effect of changing the concentration on skin penetration, copper sulphate was prepared in distilled water to three additional concentrations, namely 4, 8 and 12%. These solutions were applied locally or introduced by iontophoresis according to the following Table:-

Figure	Concentration (%)	Current intensity (mA)	Duration of application (Min)
103	4	0 (control)	15
104 (a and b)	4	30	15
105	8	0 (control)	15
106 (a and b)	8	30	15
107	12	0 (control)	15
108	12	30	15

EDX analysis confirmed the histological findings in all cases.

## Figure 103

Local application (control) of a 4% aqueous copper sulphate solution for 15 minutes

A cryostat section stained with Mallory's haematoxylin method (x 32)

A few copper products are seen in the superficial part of the epidermis adjacent to the hair follicles and within the follicular orifices. However, the tracer has not extended into the hair follicles (HF), the sebaceous glands (SG) or the dermis (D).

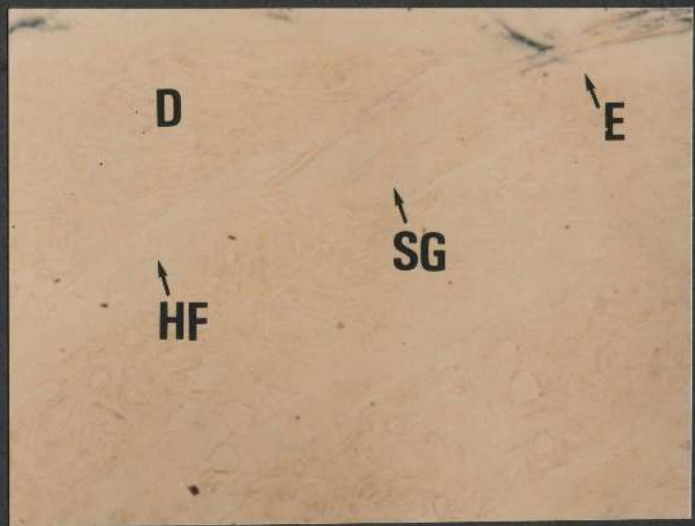


## Figure 104 (a and b)

Positive iontophoresis of a 4% aqueous copper sulphate solution at 30 milliamperes for 15 minutes

Figure 104a: A cryostat section stained with Mallory's haematoxylin method (x 16)

Copper is visible in the epidermis (E), the hair follicles (HF), the sebaceous glands (SG), the dermis (D), the hypodermis (H) and the striated muscle (SM). Copper is also present in the superficial parts of the muscle of the body wall (BW).

Figure 104b: A paraffin section treated with the rubeanic acid technique for copper (p 94), and stained with tartrazine (x 16)

Black deposits of copper rubeanate are visible in the epidermis (E), the hair follicles (HF), the sebaceous glands (SG), the dermis (D), the hypodermis (H) and the striated muscle (SM). The tracer is also seen in the superficial parts of the muscle of the body wall (BW). The location of copper is similar therefore to that shown in Figure 104a.



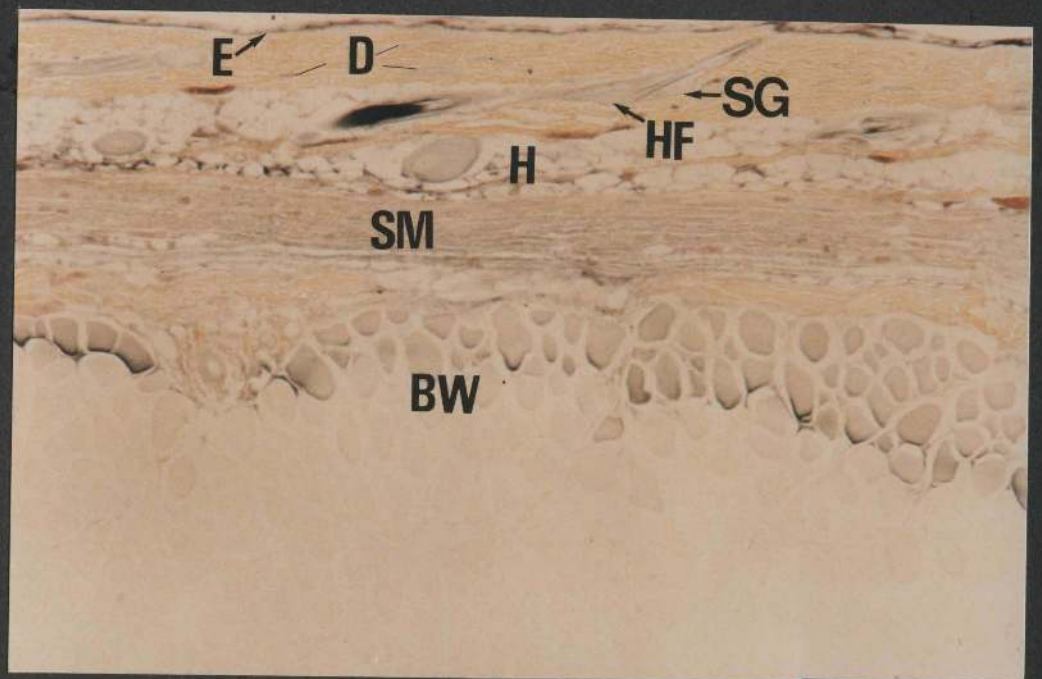
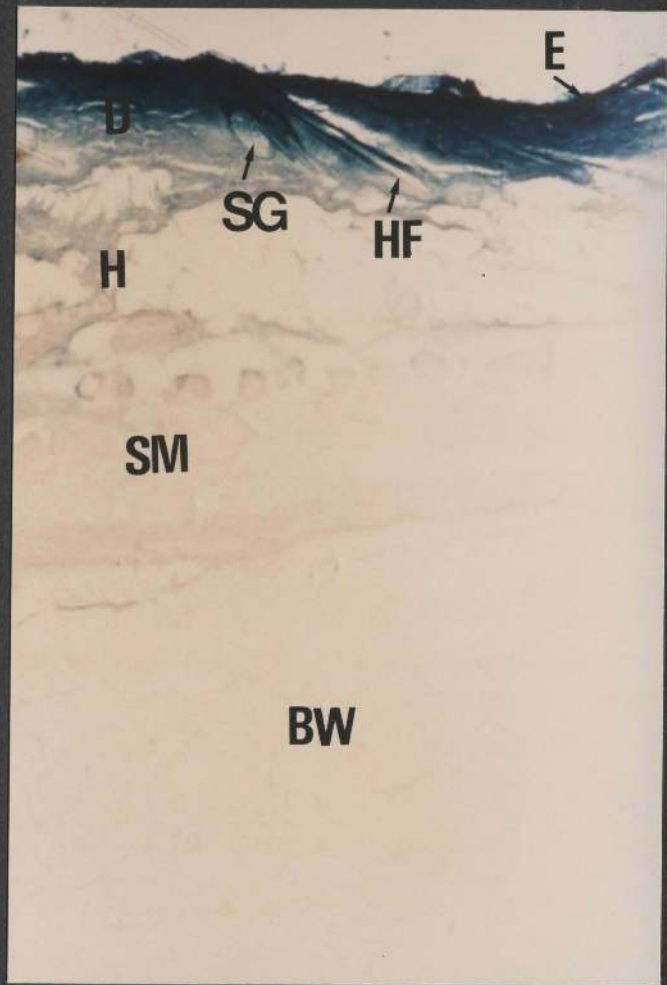


## Figure 105

Local application (control) of a 8% aqueous copper sulphate solution for 15 minutes

A cryostat section stained with Mallory's haematoxylin technique (x 40)

The reaction for copper is evident on the surface of the skin and in parts of the epidermis (E) adjacent to the follicular orifices. Although copper is visible in the upper part of each follicular infundibulum, it does not extend any deeper into the hair follicles (HF) or the sebaceous glands (SG). No tracer is evident in the dermis (D).

## Figure 106 (a and b)

Positive iontophoresis of a 8% aqueous copper sulphate solution at 30 milliamperes for 15 minutes

Figure 106a: A cryostat section stained with Mallory's haematoxylin method for copper (x 16)

A very intense reaction for copper is evident in the epidermis (E), the hair follicles (HF), the sebaceous glands (SG) and the dermis (D). The reaction for copper is so strong that in certain areas it is difficult to identify clearly the skin structures. All the structures located deep to the skin contain copper, namely, the hypodermis (H), the striated muscle (SM), and the body wall (BW).

Figure 106b: A paraffin section subjected to the rubeanic acid method for copper and stained with tartrazine (x 16)

Copper is visible in the epidermis (E), the hair follicles (HF), the sebaceous glands (SG), the dermis (D), the hypodermis (H), the striated muscle (SM), and in the body wall (not shown). The extent of penetration is similar therefore in this section to that described above.







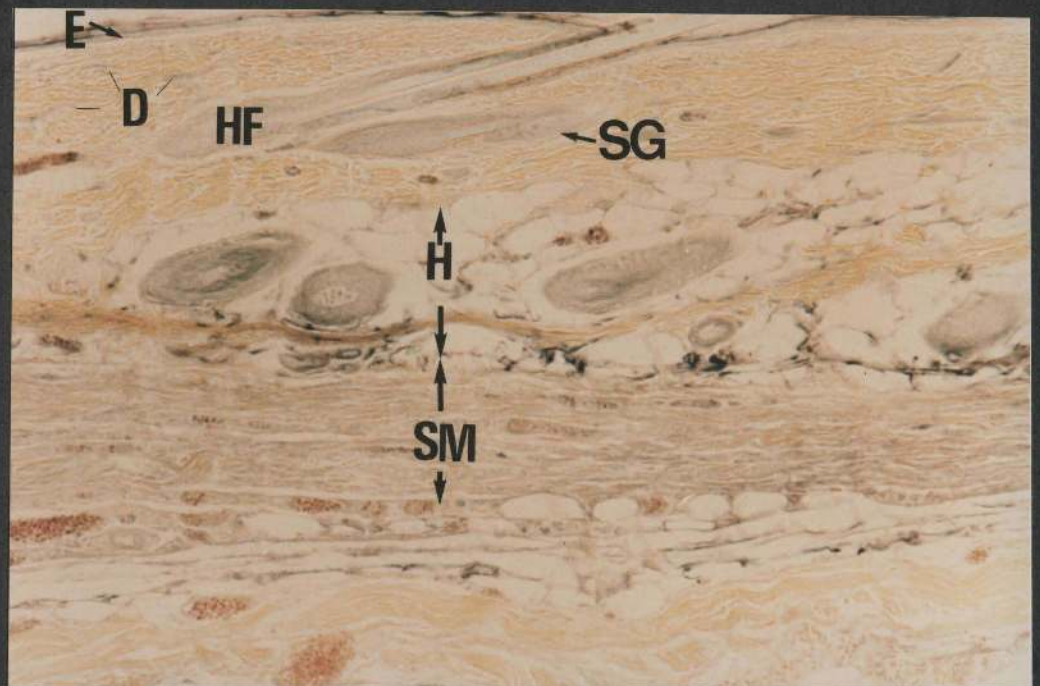
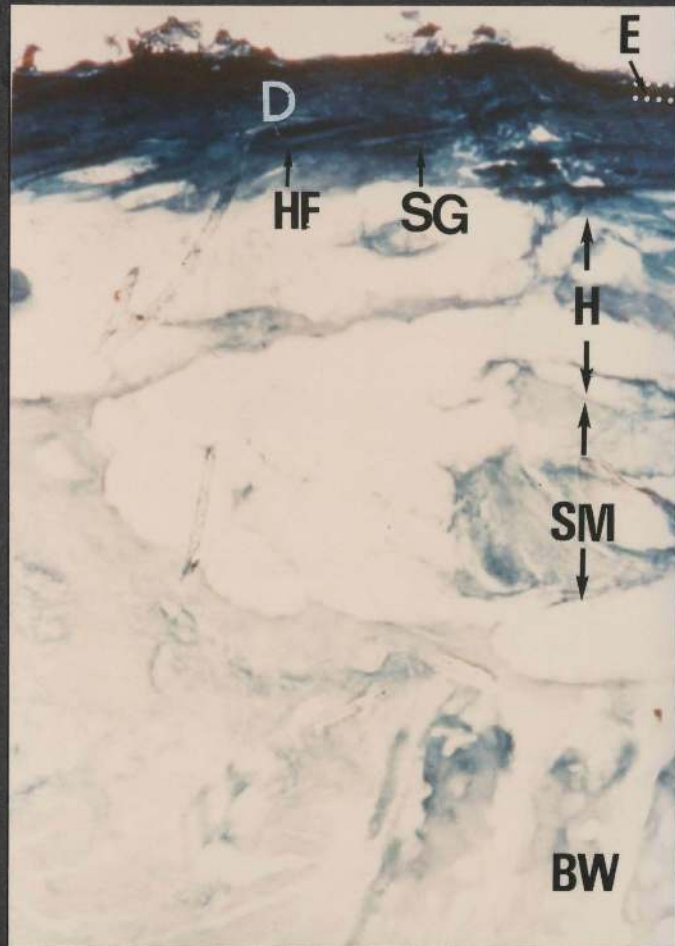




## Figure 107

Local application (control) of a 12% aqueous copper sulphate solution for 15 minutes

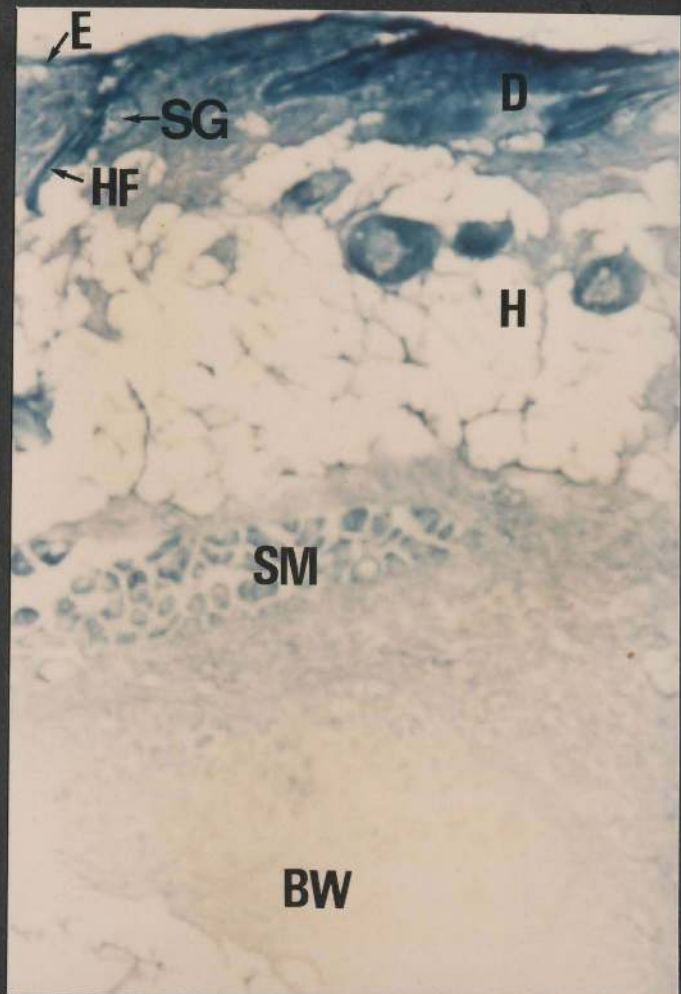
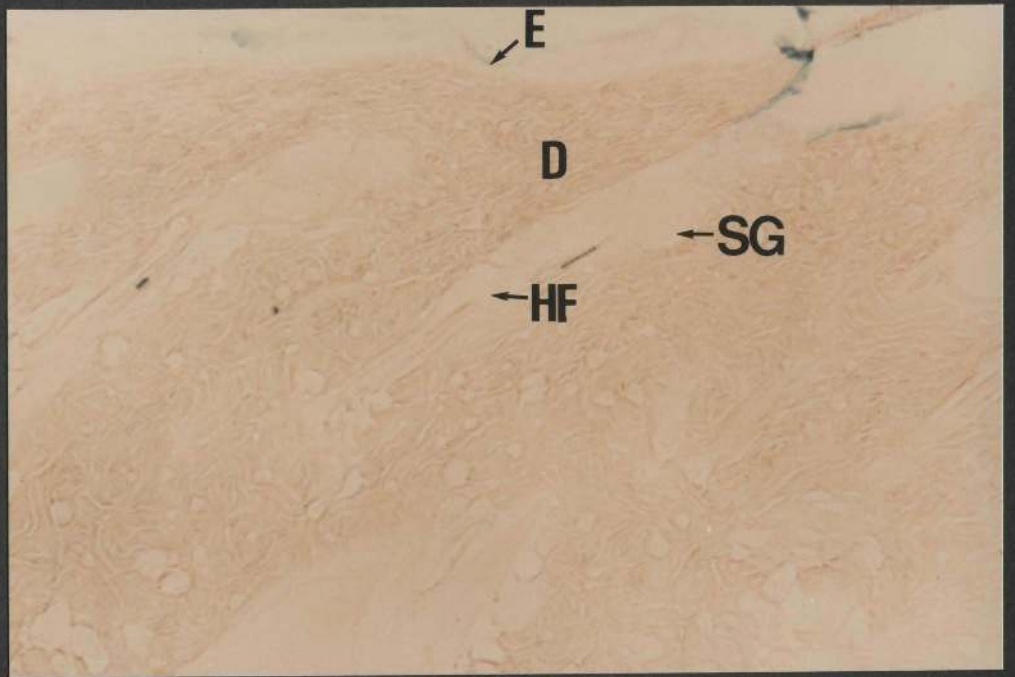
A cryostat section stained with Mallory's technique for copper (x 40). Although the tracer is visible on the surface of the skin and in the upper part of a follicular infundibulum, copper does not penetrate any deeper into the epidermis (E), the hair follicles (HF) or the sebaceous glands (SG). No tracer is evident in the dermis (D).

## Figure 108

Positive iontophoresis of a 12% aqueous copper sulphate solution at 30 milliamperes for 15 minutes

A cryostat section stained with Mallory's technique for copper (x 16). The tracer is visible in the epidermis (E), the hair follicles (HF), the sebaceous glands (SG), the dermis (D), the hypodermis (H), the striated muscle (SM), and in the upper parts of the body wall (BW).

The extent of penetration is reduced in this case as compared to that shown in Figure 106, and the reaction for copper is more intense in Figure 106.



### 3.8.4 Effect of vehicle

The following experiments were undertaken to study the effect of changing the vehicle in which the tracer was prepared on the penetration of the tracer into the skin by iontophoresis. According to the nature of the vehicle, these experiments were grouped into two categories; namely, accelerants and detergents.

#### 3.8.4.1 Accelerants

The effect of DMSO on the penetration of copper ions into the skin was investigated by dissolving 4 grams of copper sulphate in a solution of 30 mls of DMSO and 70 mls of distilled water.

The test solution was then applied locally (Figure 109) or subjected to iontophoresis (Figure 110).

## Figure 109

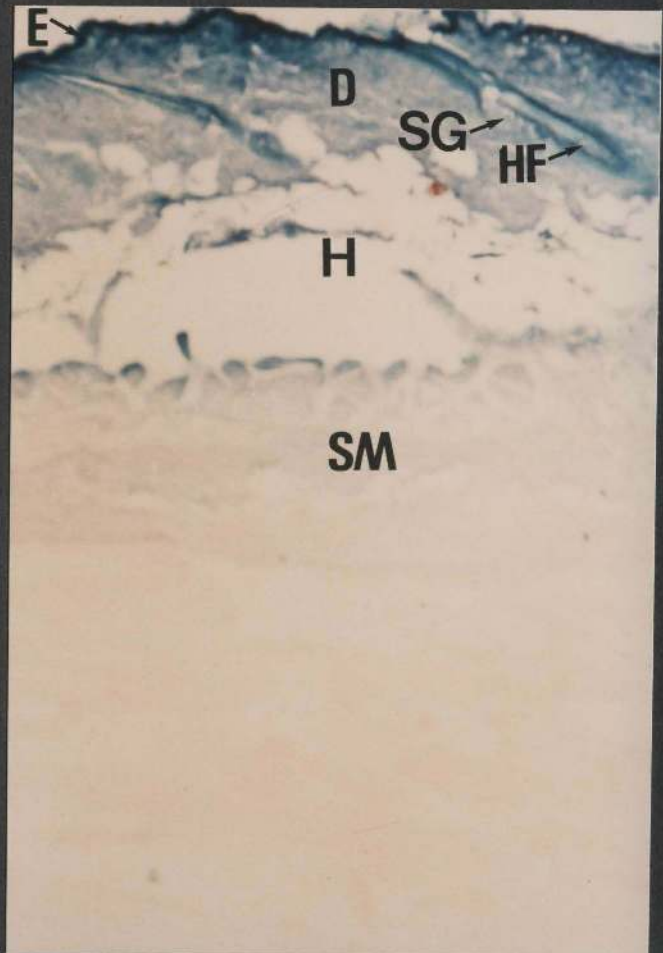
Local application of 4% (W/V) copper sulphate in DMSO/water vehicle for 15 minutes

A cryostat section stained with Mallory's method for copper (x 40)  
Copper is seen on the surface of the skin and in those parts of the epidermis (E) adjacent to the follicular orifices. Although the tracer is visible in the upper part of each follicular infundibulum, it does not extend any deeper into the hair follicles (HF) or into the sebaceous glands (SG). No tracer is evident in the dermis (D).

## Figure 110

Positive iontophoresis of 4% (W/V) copper sulphate in DMSO/water vehicle at 30 milliamperes for 15 minutes

A cryostat section stained with Mallory's technique for copper (x 16)  
The tracer is evident in the epidermis (E), the hair follicles (HF), the sebaceous glands (SG), the dermis (D), the hypodermis (H), and in the most superficial parts of the striated muscle (SM). The extent of penetration is similar in this case to that seen when the tracer is introduced from the aqueous vehicle alone (Figure 104).





#### 3.8.4.2 Detergents

The following experiments were undertaken to investigate the effect of incorporating sodium lauryl sulphate (SLS) with copper sulphate in solution on the penetration of copper ions into the skin by iontophoresis.

4 grams of copper sulphate and 0.5 grams of SLS were dissolved in 100 mls of distilled water. This solution was then applied locally (Figure 111) or introduced by iontophoresis (Figure 112). Since SLS is an anionic (negatively charged) detergent, the test solution was subjected first to negative iontophoresis using a current of 30 milliamperes over a duration of 5 minutes, followed immediately by positive iontophoresis using the same intensity of current but for 15 minutes.

## Figure 111

Local application (control) of 0.5% SLS/4% copper sulphate in distilled water for 15 minutes

A cryostat section stained with Mallory's method for copper (x 80)  
Copper is visible on the surface of the skin and in the follicular orifices. No penetration is evident in the epidermis (E), the hair follicles (HF) or the sebaceous glands (SG).

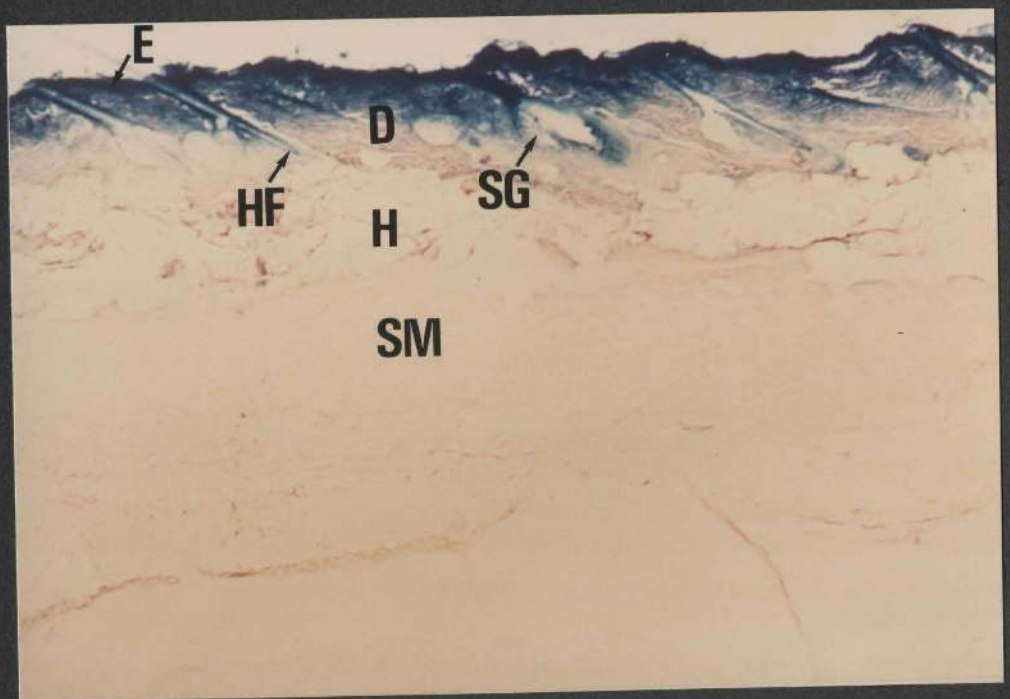
## Figure 112

Negative/positive iontophoresis of 0.5% SLS/4% copper sulphate in distilled water

A cryostat section stained as in Figure 111 (x 16)

The tracer is evident in the epidermis (E), the hair follicles (HF), the sebaceous glands (SG), the dermis (D) and the hypodermis (H).

It appears that the tracer does not extend into the striated muscle (SM) as it does when introduced from an aqueous vehicle alone (Figure 104).



### 3.9 Iron

Experiments were carried out with ferric chloride solutions to investigate the penetration of the trivalent cation from the surface into and through the skin following iontophoresis. In these experiments the concentration of the ferric chloride and the vehicle in which it was prepared were varied. Control experiments consisted of the application of the tracer solution to the surface of the skin but without the flow of a current.

Two histochemical tests were employed to demonstrate the location of iron in unfixed cryostat sections, these being Mallory's haematoxylin method and Per1's (Prussian blue) method. The former is specific both for copper and iron, while the latter is specific for iron only. EDX analyses were carried out to confirm the histological findings. As with copper, in order to test the ability of both the histochemical and the EDX methods to demonstrate iron in cryostat sections, the tracer solution was injected intradermally.

### 3.9.1 Intradermal injection

A 1% aqueous ferric chloride solution was injected intradermally. Specimens were removed 15 minutes later and sectioned with the cryostat. Some sections were analyzed with the EDX system (Figure 113a) and others were subjected to a selected histochemical test (Figure 113b).

Figure 113a: A scanning electron microscope image from a cryostat section

EDX analyses were made on the epidermis (E), the hair follicles (HF), the sebaceous glands (SG) and the dermis (D). For comparison, areas just outside the tissue were also analyzed. The spectra obtained are shown overleaf. That obtained from the surrounding medium does not include iron, whereas the spectra obtained from the skin consistently include peak(s) for iron. Thus iron signals are originating from the skin.

The tracer was detected in the epidermis, the hair follicles, the sebaceous glands and the dermis.

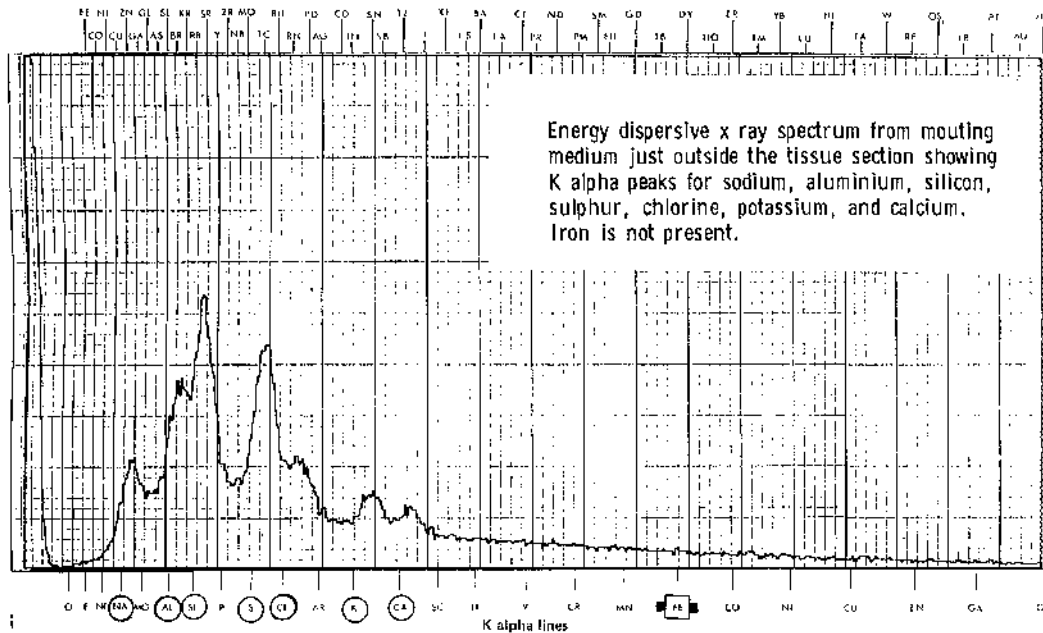


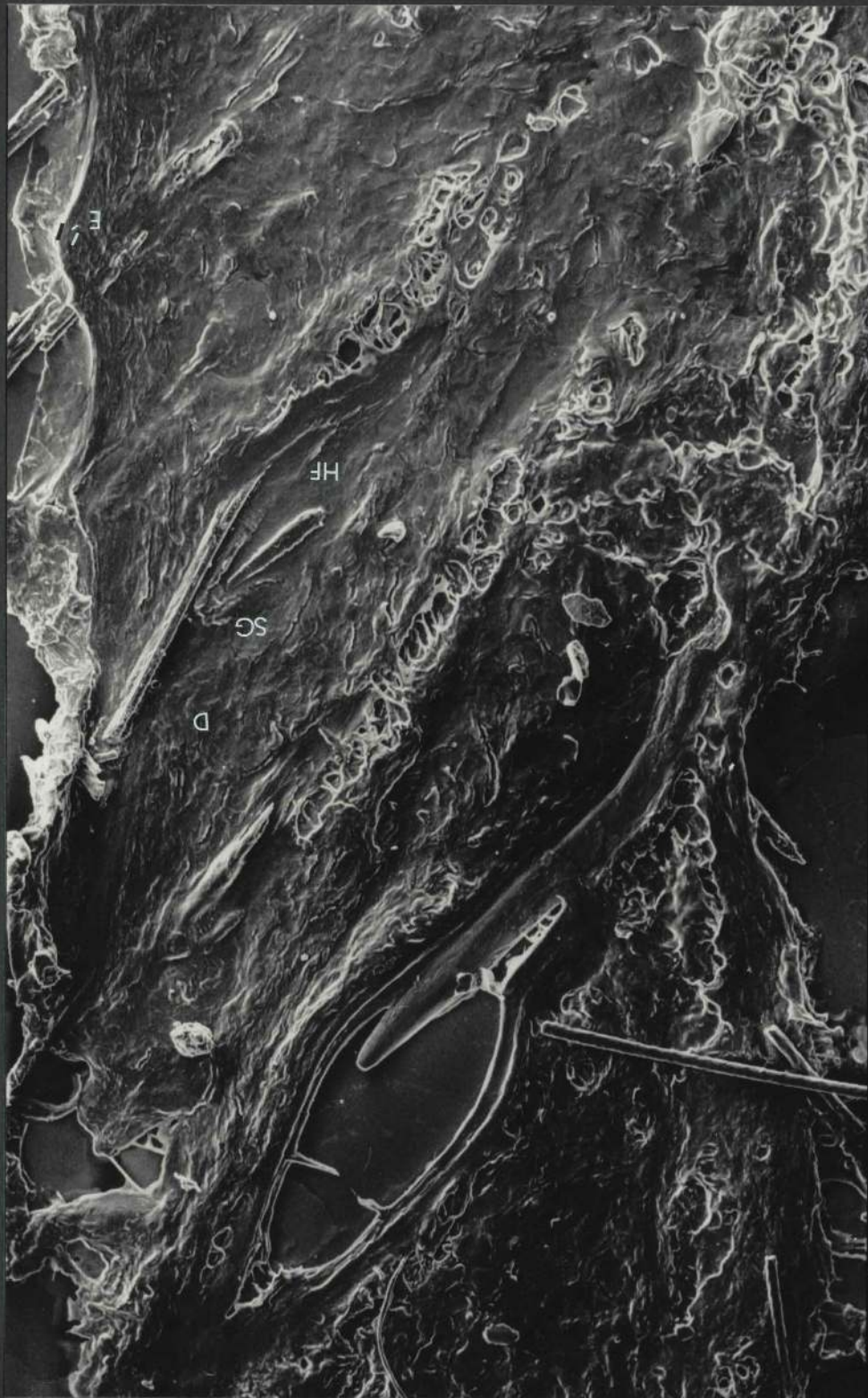
Laboratory St. Andrew University S.E.M. Unit. Researcher .....

Sample Intracutaneous injection of a 1 percent aqueous ferric chloride solution. Date .....

KaV 15 Seconds 100 Take off Angle 33

L alpha lines

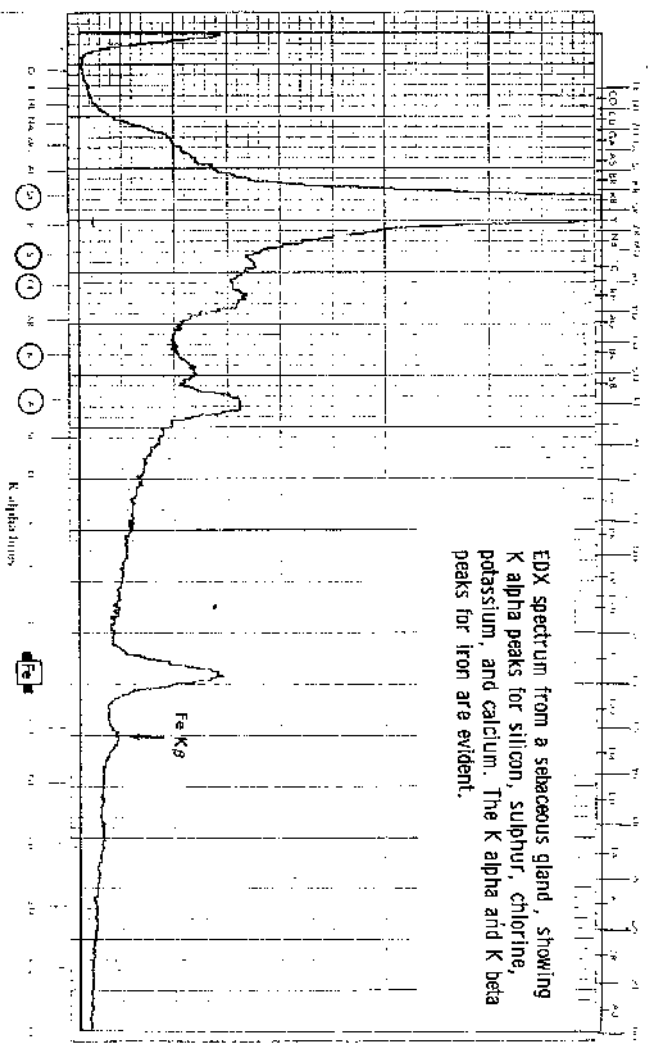




15KV 2116 100.0U SAUEM



Laboratory **St. Andrew's University, S. B. M. Inst.** Recorder **Reedular** Page **.....**  
 Sample **Intracutaneous injection of a 1 percent aqueous ferric chloride solution.**  
 KeV **15** Scale **100** Tick interval **33**  
 L alpha lines



EDX spectrum from a sebaceous gland, showing K alpha peaks for silicon, sulphur, chlorine, potassium, and calcium. The K alpha and K beta peaks for iron are evident.

Laboratory St. Andrews University, St. E.M. Unit 5

Researcher

Date

Sample 15 Intra-cutaneous injection of a 1 percent aqueous ferric chloride solution.

Key

Scoring 100

Tilt of Angle 33

L alpha lines

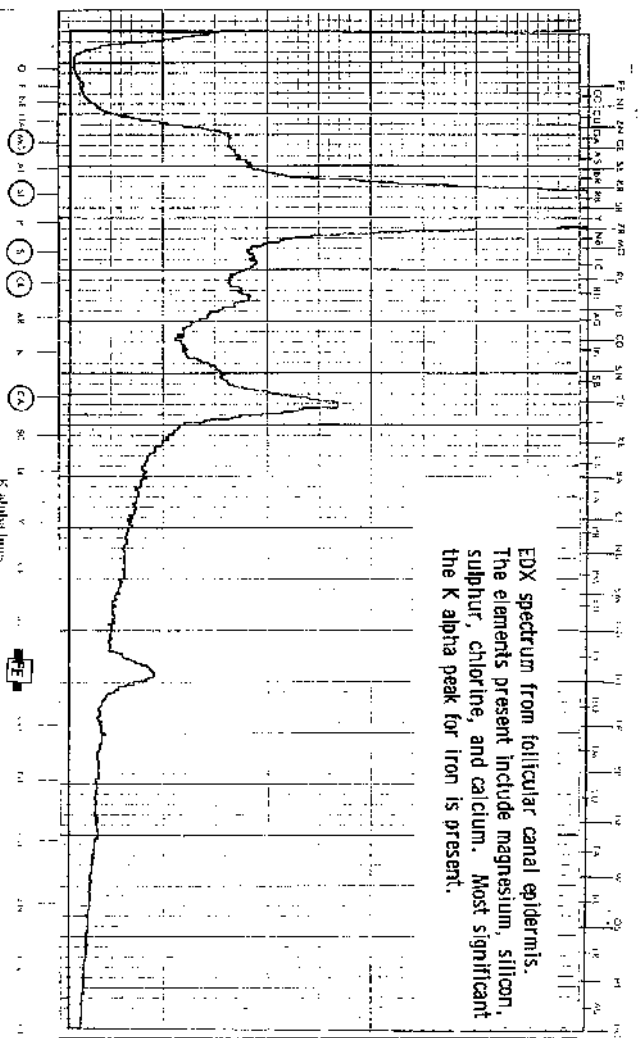


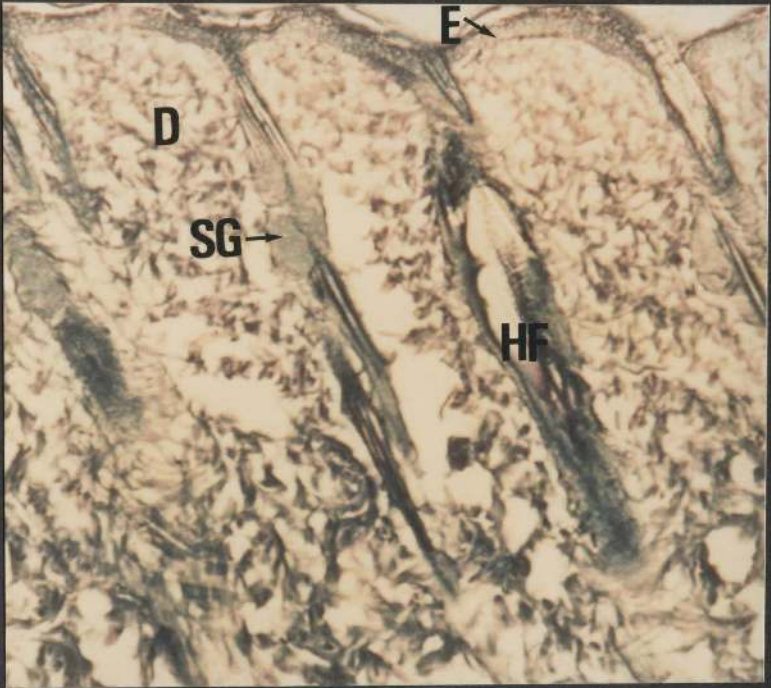




Figure 113b: A cryostat section stained with Mallory's haematoxylin method for iron (x 40)

As judged by the location of the reaction product, iron is visible in the epidermis (E), the hair follicles (HF), the sebaceous glands (SG) and the dermis (D). It is difficult to determine at which level within the epidermis the superficial migration of the tracer is halted.

The location and distribution of the tracer within the skin in this section is consistent with the spectra obtained following the EDX analysis.



## 3.9.2 Effect of concentration

The following experiments were performed to evaluate the effect of changing the concentration of the tracer substance in the presenting vehicle on the penetration of the tracer from the surface into the skin. Ferric chloride was prepared in distilled water to a concentration of 1% and 4%. These solutions were applied locally or introduced by iontophoresis according to the following Table:-

Figure	Concentration %	Current Intensity (mA)	Duration of Application (Min)
114 (a and b)	1	0 (control)	15
115	1	30	15
116	4	0 (control)	15
117	4	30	15

## Figure 114 (a and b)

Local application (control) of a 1% aqueous ferric chloride solution for 15 minutes

Figure 114a: A cryostat section stained with Perl's method for iron (x 80)

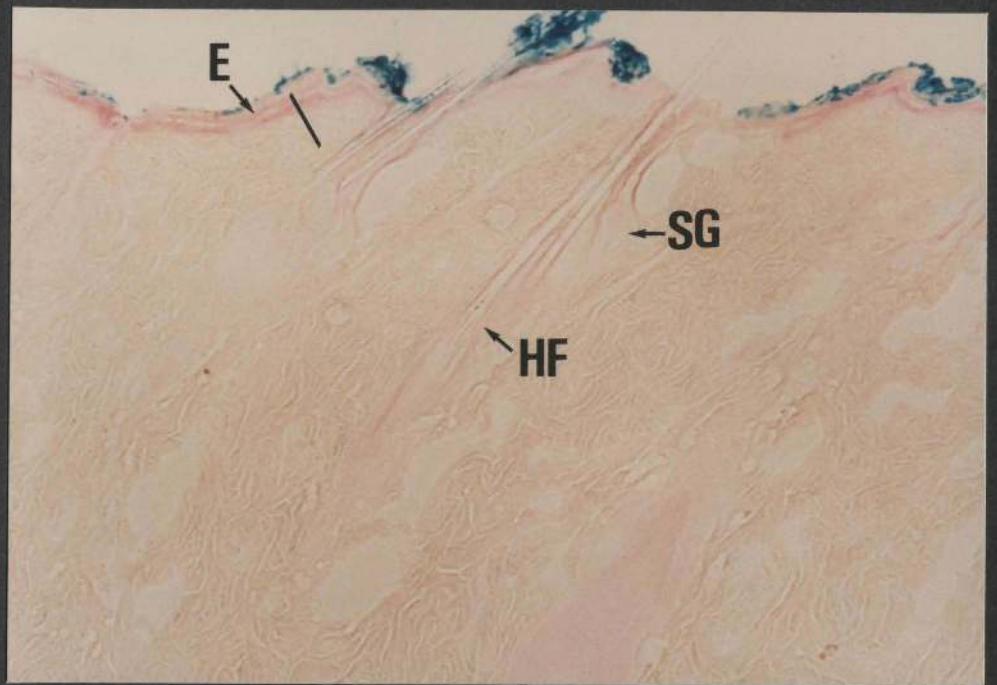
Ferric ferrocyanide (Prussian blue) is visible on the surface of the skin and in the orifices of the hair follicles. No reaction for iron is evident in the epidermis (E), the hair follicles (HF) or the sebaceous glands (SG).

Figure 114b: A cryostat section stained with Mallory's haematoxylin method (x 32)

The tracer is seen on the surface of the skin and in the ostia of the hair follicles. No penetration is evident in the epidermis (E), the hair follicles (HF) or the sebaceous glands (SG).

The location of the tracer is similar in this case to that shown in Figure 114a.





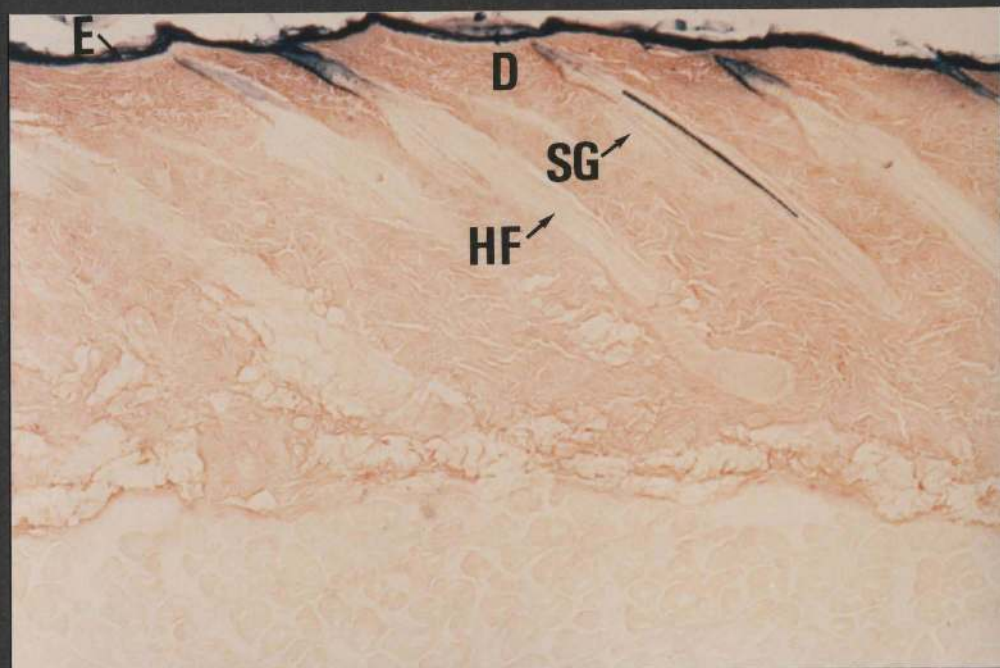


## Figure 115

Positive iontophoresis of a 1% aqueous ferric chloride solution at 30 milliamperes for 15 minutes

A cryostat section stained with Mallory's haematoxylin technique (x 40)

The reaction for ferric iron is evident in the epidermis (E) and the follicular canal epidermis. Dermal areas (D) adjacent to the follicular canal epidermis also contain some tracer, whereas interfollicular regions of the dermis at the same level remain free from the tracer. No penetration is evident in the lower walls of the hair follicles (HF) or the sebaceous glands (SG).

## Figure 116

Local application (control) of a 4% aqueous ferric chloride solution for 15 minutes

A cryostat section stained with Perl's technique (x 40)

The tracer is visible on the surface of the skin. No reaction for iron is evident in the epidermis (E), the hair follicles (HF), the sebaceous glands (SG) or the dermis (D).

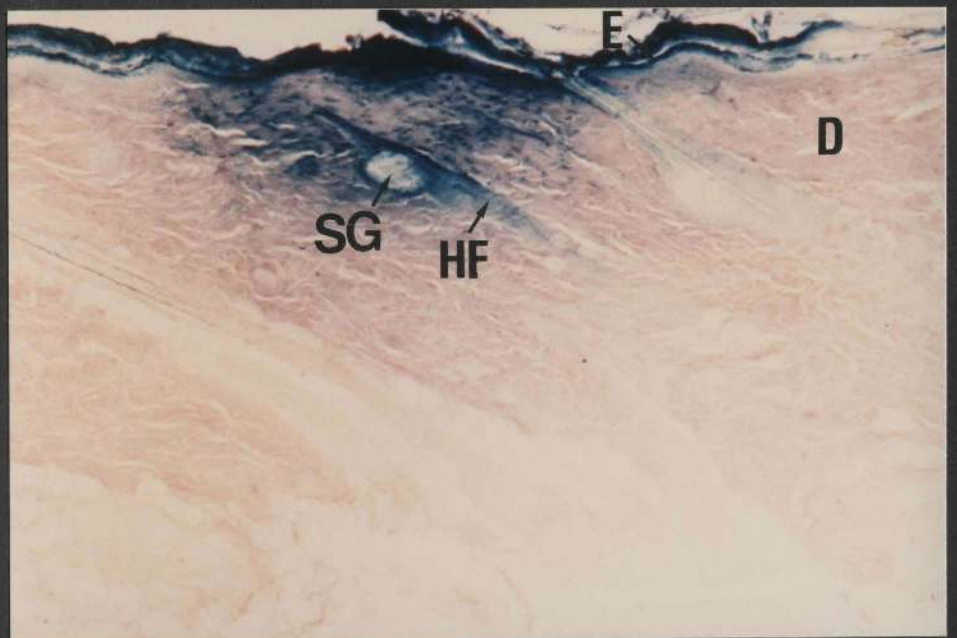
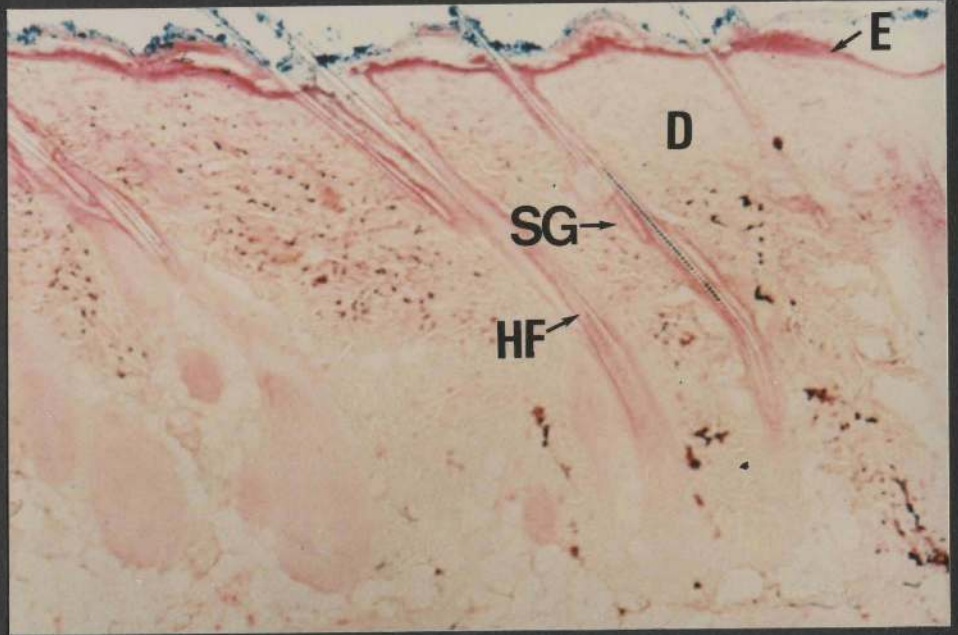
## Figure 117

Positive iontophoresis of a 4% aqueous ferric chloride solution at 30 milliamperes for 15 minutes

A cryostat section stained with Mallory's haematoxylin method (x 40)

The tracer is visible in the epidermis (E), the sebaceous glands (SG) and the hair follicles (HF) down to or slightly below the level of the bases of the sebaceous glands. Dermal areas (D) at and above the level of the glands and in close relation to the hair follicles also contain the reaction for iron.







### 3.9.3 Effect of vehicle

The following experiments were carried out to investigate the effect of preparing ferric chloride in a solution containing the accelerant DMSO, and the effect of using absolute ethanol as an alternative vehicle to water on the penetration of the tracer from the surface into the skin.

EDX analyses confirmed the histological findings at all times.

#### 3.9.3.1 Accelerants

4 g of ferric chloride were dissolved in a solution containing 60 mls of DMSO and 40 mls of distilled water. This was applied to the surface of the skin with and without iontophoresis.

#### Figure 118

Local application (control) of 4% ferric chloride in a DMSO/water vehicle for 15 minutes

A cryostat section stained with Perl's technique (x 32)

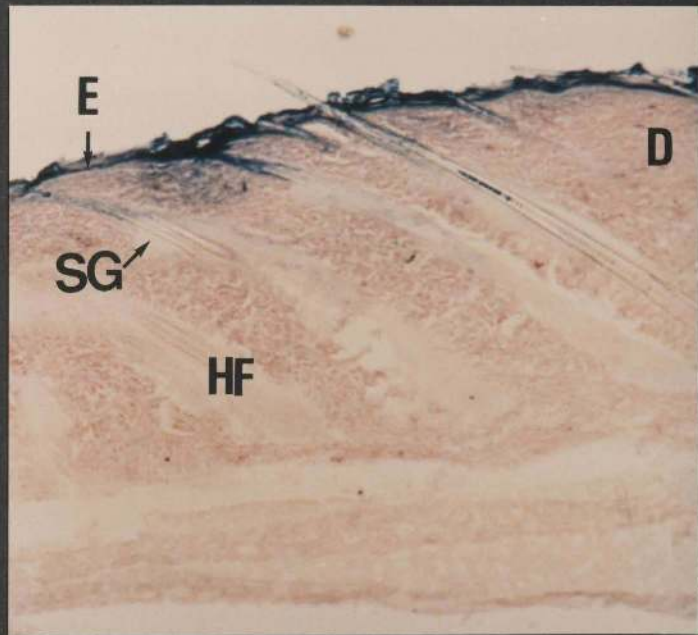
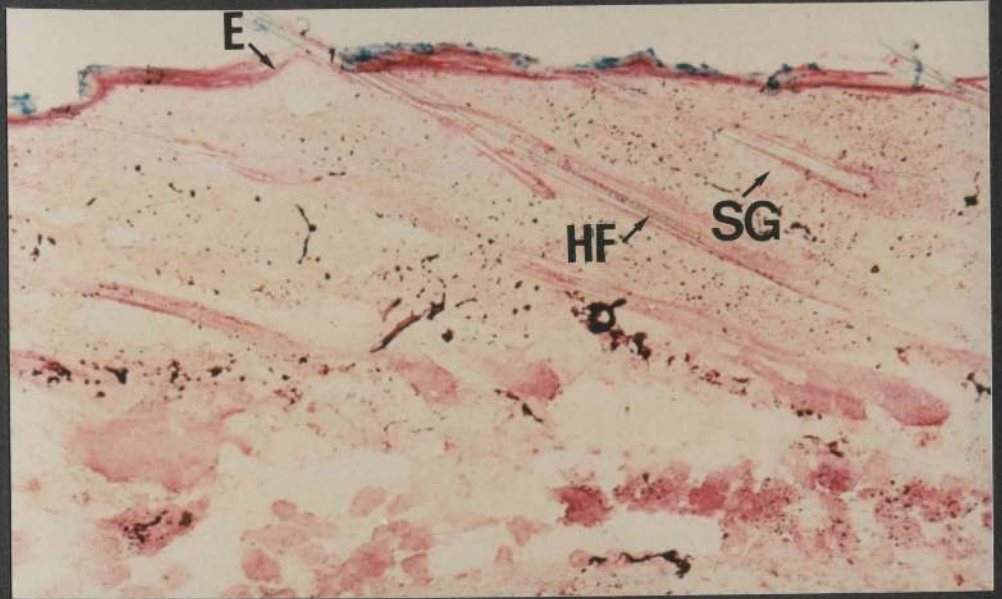
The tracer is evident on the surface of the skin, but not in the epidermis (E), the hair follicles (HF) or the sebaceous glands (SG).

#### Figure 119

Positive iontophoresis of 4% ferric chloride in a DMSO/water vehicle at 30 milliamperes for 15 minutes

A cryostat section stained with Mallory's haematoxylin technique (x 32)

A strong reaction for ferric iron is evident in the epidermis (E), the follicular infundibulum and in the dermal areas (D) adjacent to these structures. A relatively weak reaction is seen in the sebaceous glands (SG) and in the middle one third of the hair follicles (HF).



### 3.9.3.2 Alcohols

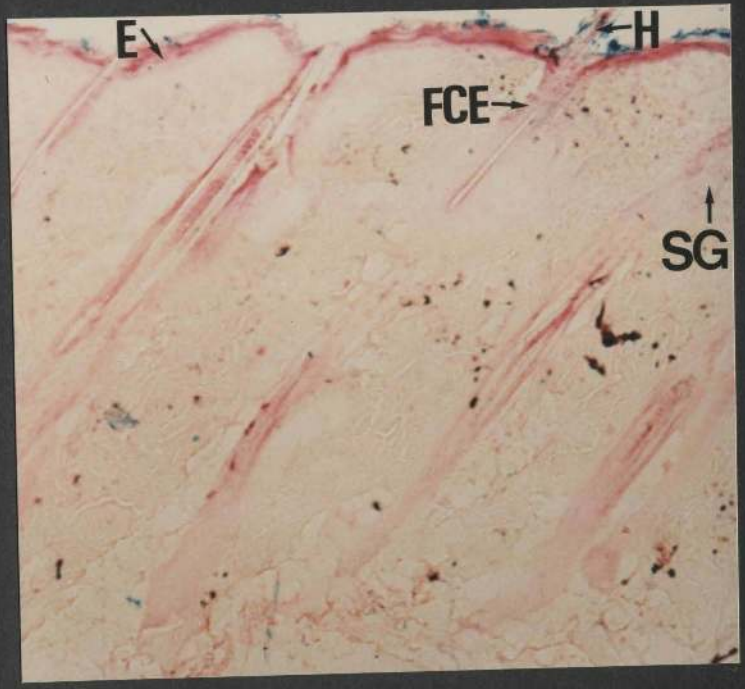
4 grams of ferric chloride were dissolved in 100 mls of absolute ethanol and applied to the surface of the skin with or without iontophoresis.

#### Figure 120

Local application (control) of 4% (W/V) ferric chloride in absolute ethanol for 15 minutes

A cryostat section stained with Perl's method for iron (x 40)

The tracer is found on the surface of the skin, but not in the epidermis (E). A weak reaction for iron is occasionally seen in the follicular canal epidermis (FCE) and in some of the sebaceous glands (SG).



## Figures 121 (a and b)

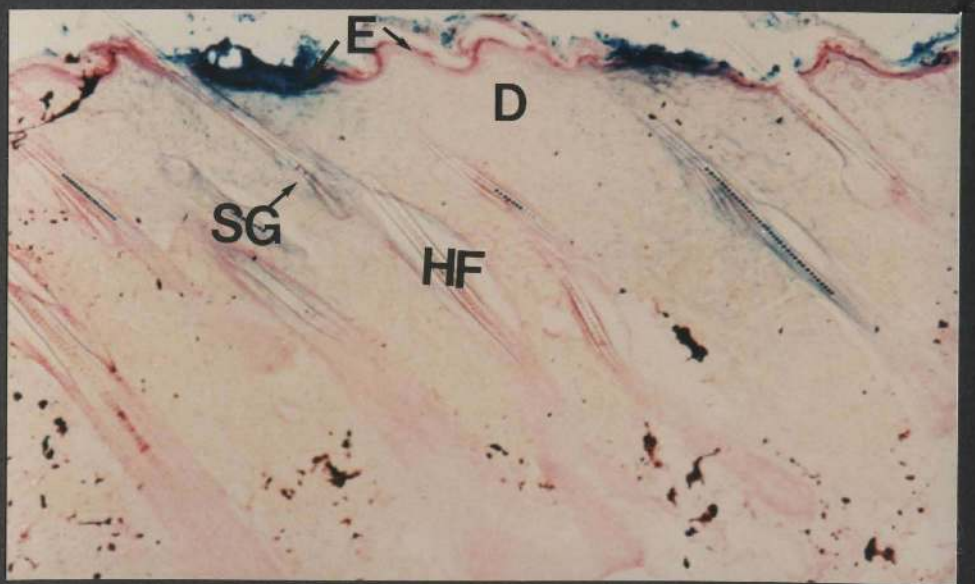
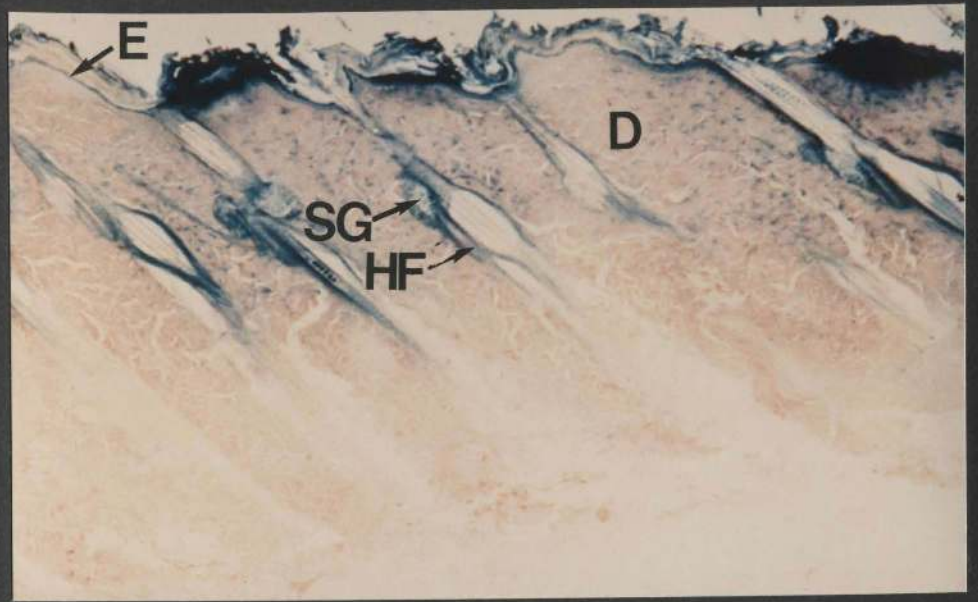
Positive iontophoresis of 4% (W/V) ferric chloride in absolute ethanol at 30 milliamperes for 15 minutes

Figure 121a: A cryostat section stained with Mallory's method (x 32)  
A positive reaction for the tracer is seen in the epidermis (E), the hair follicles (HF) especially in the upper halves of the follicles, the sebaceous glands (SG) and the superficial half of the dermis (D).

Figure 121b: A similar cryostat section to that shown above but stained with Perl's technique (x 32)

The location of the tracer in the epidermis (E), the hair follicles (HF), the sebaceous glands (SG) and the dermis (D) is similar to that shown in Figure 121a.





### 3.10 Iodine

It has been suggested that inorganic anions such as chlorides, bromides and iodides can be introduced into the skin by negative iontophoresis. The most popular inorganic anion used for penetration trials is iodine. Shaffer and Zackheim (1947) reported the successful treatment of sporotrichosis of the limbs by iodide-iontophoresis. Tas and Feige (1958) demonstrated the penetration of radioactive iodide ( $I^{131}$ ) through the skin following topical application by detection of activity in urine specimens.

On the other hand, the demonstration of non-radioactive, inorganic anions in tissue sections by histochemical methods is a difficult technique (Pearse, 1961). Although Turchini (1930) described a method (starch test) whereby iodine could be demonstrated in tissues, Lison (1936, 1953) concluded that it was almost impossible to localize diffusible iodide or bound iodine by means of histochemical methods. Jenkinson *et al.* (1974) also carried out a starch test on histologic sections but failed to demonstrate iodine in the skin following iontophoresis.

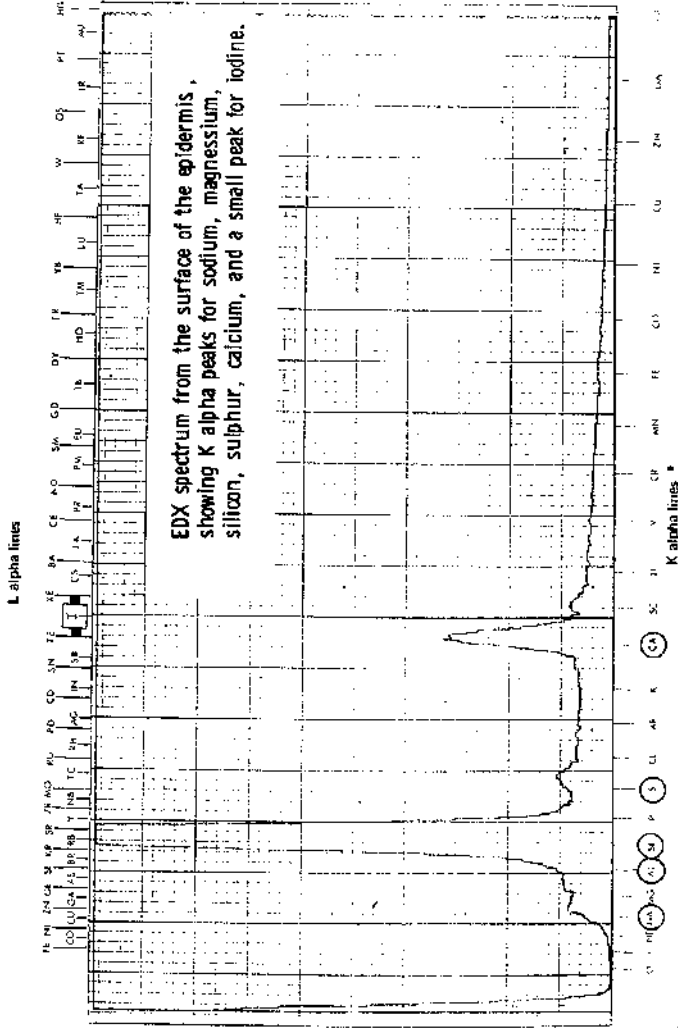
In the present study experiments were carried out using a 2% aqueous solution of potassium iodide to investigate the penetration of iodide ions into the skin. The test solution was applied locally to the skin for a duration of 15 minutes, or introduced with negative iontophoresis using a current intensity of 30 mA over a period of 15 minutes. In view of the above reports, penetration was judged by EDX analysis only made on unfixed cryostat sections. The spectra obtained are shown overleaf. No L alpha peak for iodine was present in the

spectrum obtained from the mounting medium or in the spectra obtained from the skin after local application.

Following iontophoresis, a small peak was detected occasionally on the surface of the skin. From this it would appear that the penetration of iodine into the skin is not facilitated by iontophoresis. However, further investigations are required to confirm this conclusion, and these include, for example, autoradiography (see p 414 ).

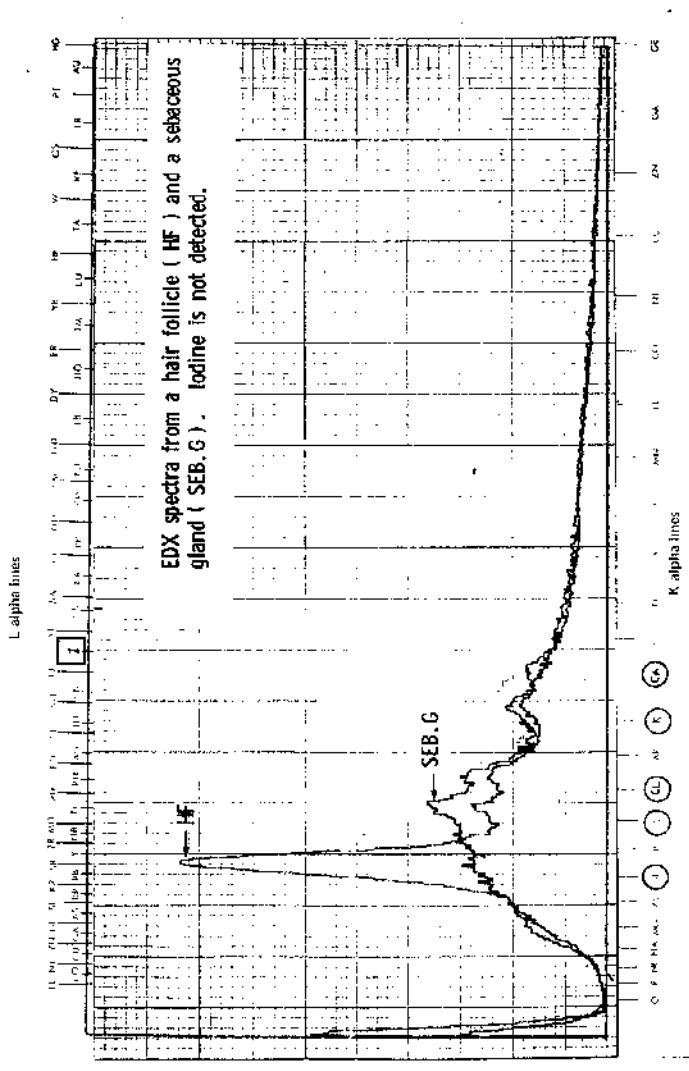


Laboratory **St. Andrews University S.E.M. Unit,** Researcher **.....** Date **.....**  
**Catty Marine Lab.**  
 Sample **Local application of a 2 percent aqueous potassium iodide solution for 15 minutes.**  
 eV **15** Seconds **100** Take off Angle **33**





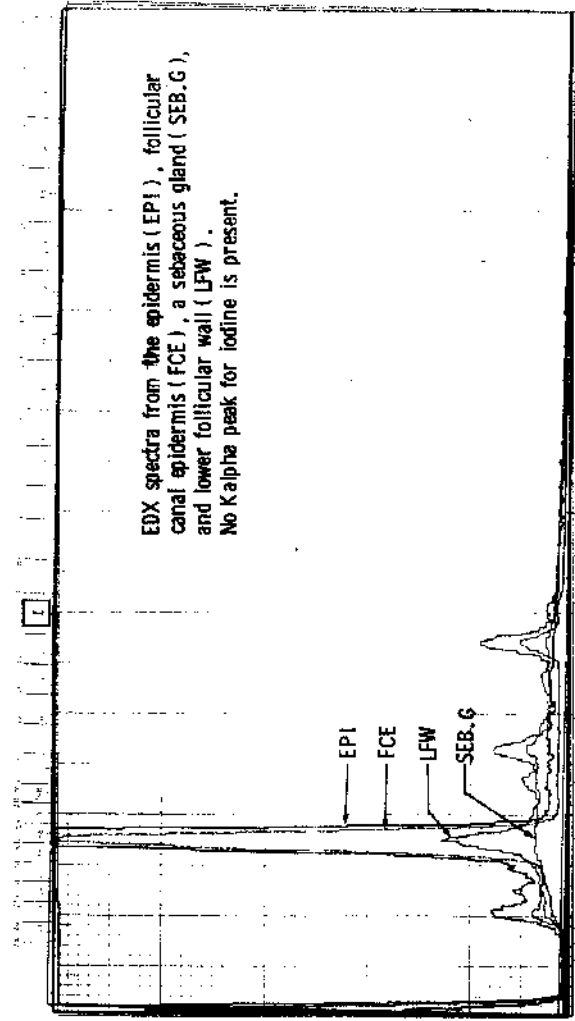
Laboratory St. Andrews University S.A.M. Unit Date                       
Gatty Marine Lab Report No.                       
 Sample Local application of a 2 percent aqueous potassium iodide solution for 15 minutes.  
 eV 15 Seconds 100 Take off Angle 33



EDX spectra from a hair follicle (HF) and a sebaceous gland (SEB. G). Iodine is not detected.

LABORATORY ..... Heberather ..... Padin  
 Sample 15 Negative iontophoresis of a 2 percent aqueous potassium iodine solution at 30 mA for 15 minutes.  
 KGV 100 ..... Seconds ..... 33 ..... Take off Angle ..... 33 .....

L-alpha lines



EDX spectra from the epidermis (EPI), follicular  
 canal epidermis (FCE), a sebaceous gland (SEB.G),  
 and lower follicular wall (LFW).  
 No K alpha peak for iodine is present.

(M) (S) (E) (G) (CA)

Waldenström

Link by the ... Ltd. A. No. ... 1985

### 3.11 Tissue changes

Smit (1936) reported definite changes in the nasal tissues of the dog and the guinea pig following iontophoresis. These included coagulative necrosis of the epithelium, early stages of inflammation with polymorphonuclear leukocytes which were later replaced by round cells, atrophy and loss of mucous glands, metaplastic changes in glands and ducts, formation of stratified squamous epithelium which later returned to normal ciliated columnar, fibrosis of the submucosa, dehydration of edematous tissue, fibrosis of the blood vessels and, in some cases, cartilaginous necrosis. Suzuki (1956) elucidated the histological changes in the skin of the guinea pig under both electrodes following iontophoresis. Under the cathode, (1) the subcutaneous tissue below the epidermis was swollen and the connective tissue was transparent and loose when compared to that under the anode, (2) the epidermis showed a marked desquamation, with fissures in the Malpighian layer, and (3) the capillaries were dilated and ecchymotic areas were noted. Under the anode, (1) the tissues between the epidermis and the muscularis were atrophied and condensation and turbidity of the connective tissue fibres were noted, (2) cellular aggregations were noted in the dermis, and (3) the irregularity in the contour of the epidermis appeared to be less marked when compared to controls. Midtgaard (1986) reported that iontophoresis caused a local electro-chemical coagulation of proteins in the treated areas which would explain why the effect of iontophoresis can last for several weeks since this is the time it takes for the cells subjected to the current to be replaced by new cells.

In the present study, certain histological changes were observed in semithin and ultrathin araldite sections of the skin under the iontophoresis electrode. The following skin sections are included to highlight these changes. The histological appearance of untreated skin is also included.

### 3.11.1 Untreated skin

Specimens of ventral (abdominal) skin were removed and fixed, embedded and sectioned according to the procedure described previously (p 101). The appearance of the untreated skin is shown in Figures 122 (a and b) and 123 (a - c).

Figure 122a: A semithin (0.5  $\mu$ ) araldite section stained with toluidine blue (x 120)

The general morphology of the epidermis is seen. The stratum basale (SB) consists of a single layer of columnar cells adjacent to the basal lamina (BL). Above the basal layer is the stratum spinosum consisting of several layers of polygonal cells. The cells in the stratum granulosum (SG) are flat and contain keratohyalin granules. The outermost layer is the stratum corneum (SC).

Figure 122b: A semithin (0.5  $\mu$ ) araldite section stained with toluidine blue (x 120)

This section includes a sebaceous gland. Cells at different stages of maturation are seen. These include peripheral (undifferentiated) (P), partially differentiated (PD) and fully differentiated (FD) sebaceous cells. Towards the duct (D), the fully differentiated cells rupture to form sebum.



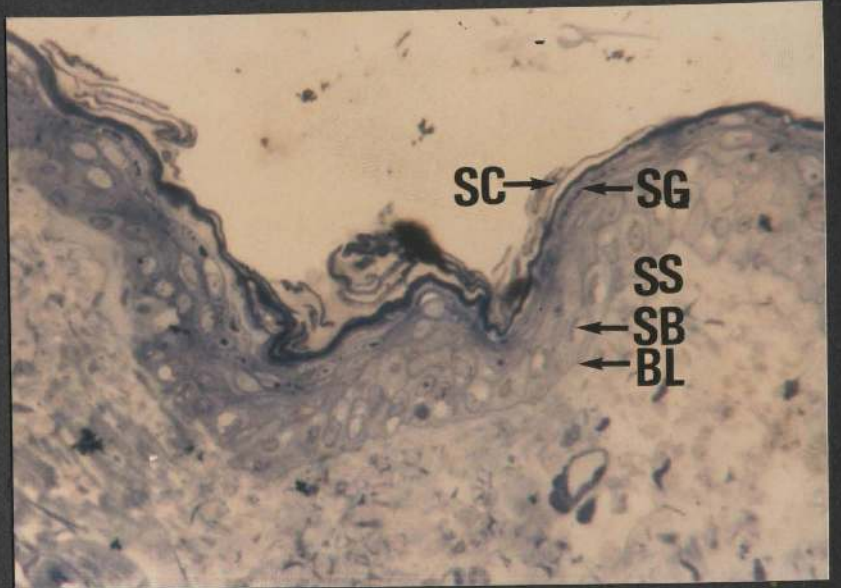


Figure 123a: An electron micrograph (x 12,064)

This represents a segment of the stratum corneum which shows the keratin pattern in the corneal cells. Two membrane-coating granules (MCG) and the intercellular components of desmosomes (D) can be seen. The major part of the intercellular spaces appears electron-optically empty.

Figure 123b: An electron micrograph (x 8,352)

This features a section of the epidermis. Below the stratum corneum (SC) is the stratum granulosum (SG) containing keratohyalin granules. The stratum spinosum (SS) consists of about four or five layers of cells with "spines or prickles", and many tonofilaments in the cytoplasm. Beneath the stratum spinosum is the basal cell layer (SB).



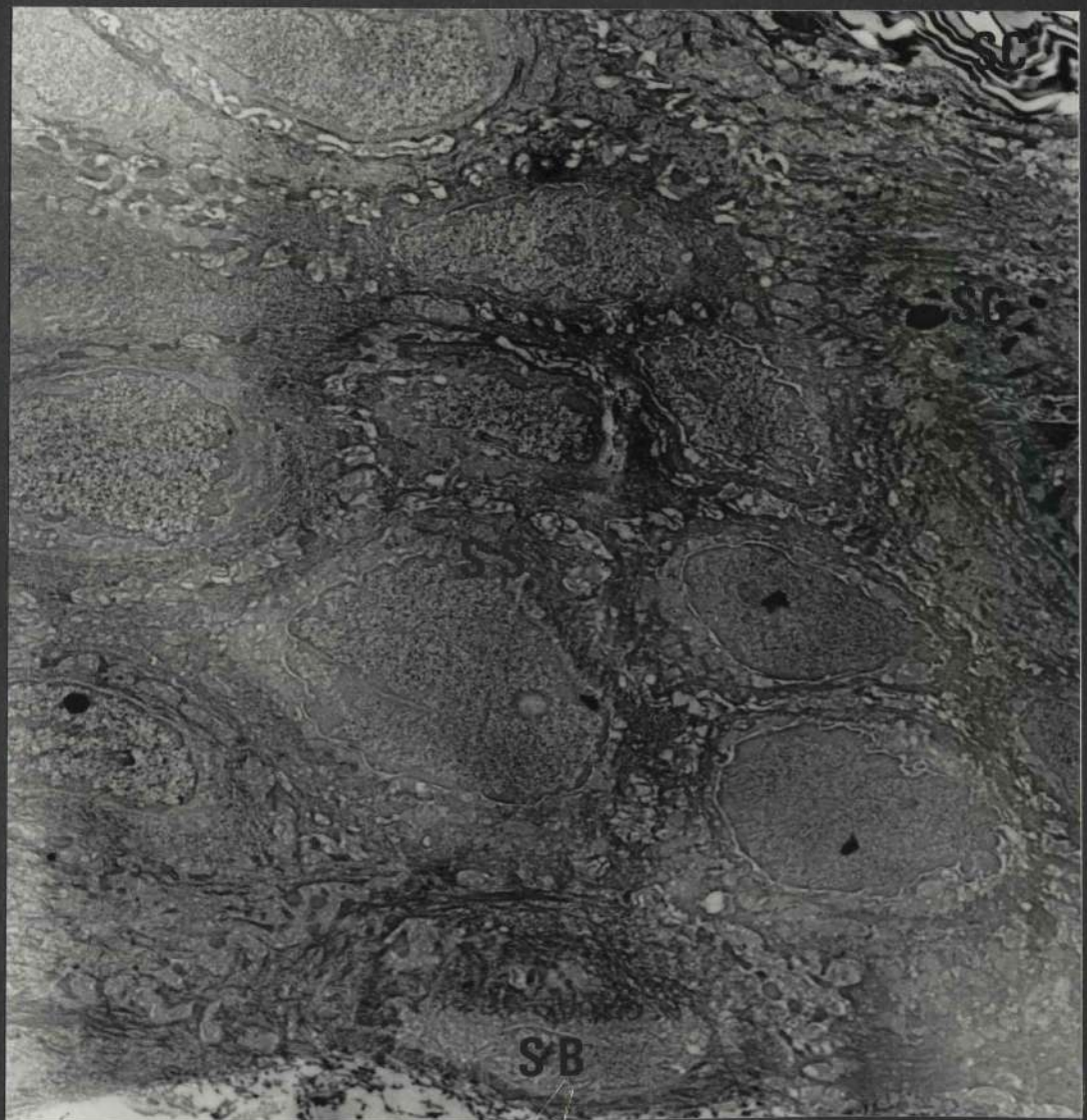
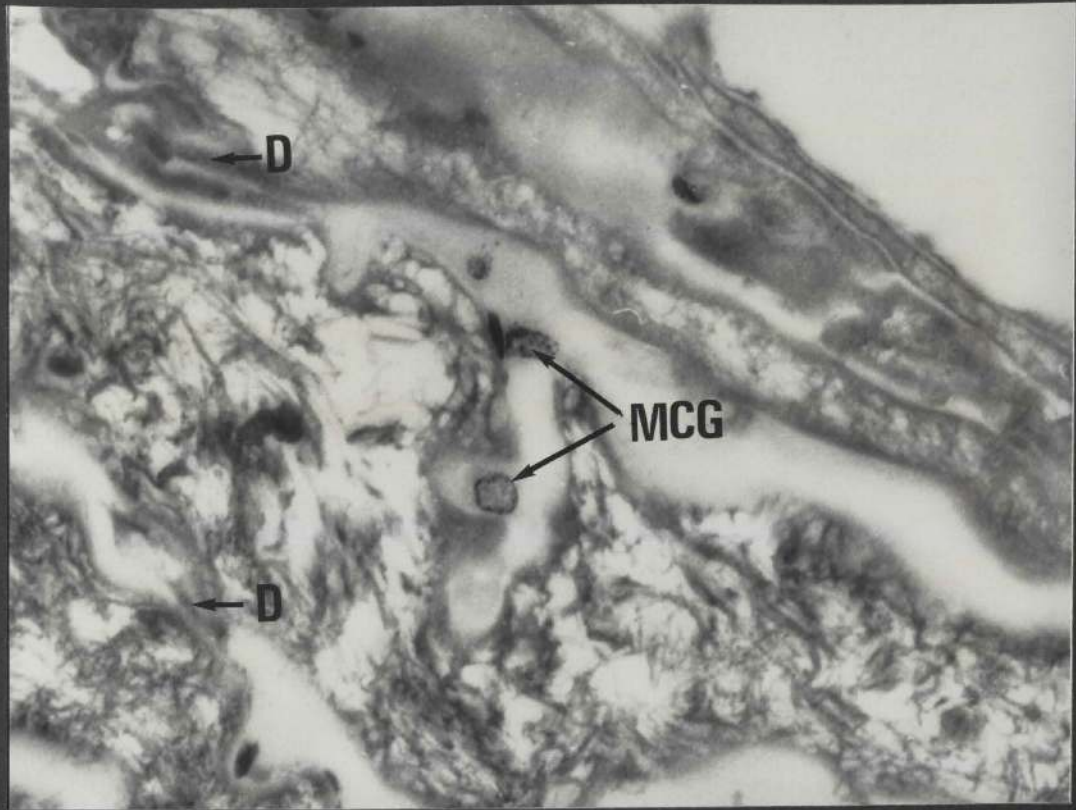


Figure 123c: An electron micrograph (x 8,352)

This micrograph features a portion of a hair follicle at the level of the sebaceous duct (SD). The structures present include a hair shaft (H) and the lower part of the follicular canal epidermis (FCE). The keratinized stratum corneum (SC) of the FCE terminates at the duct region.

Towards the duct, a fully mature sebaceous cell (FD) is about to rupture.

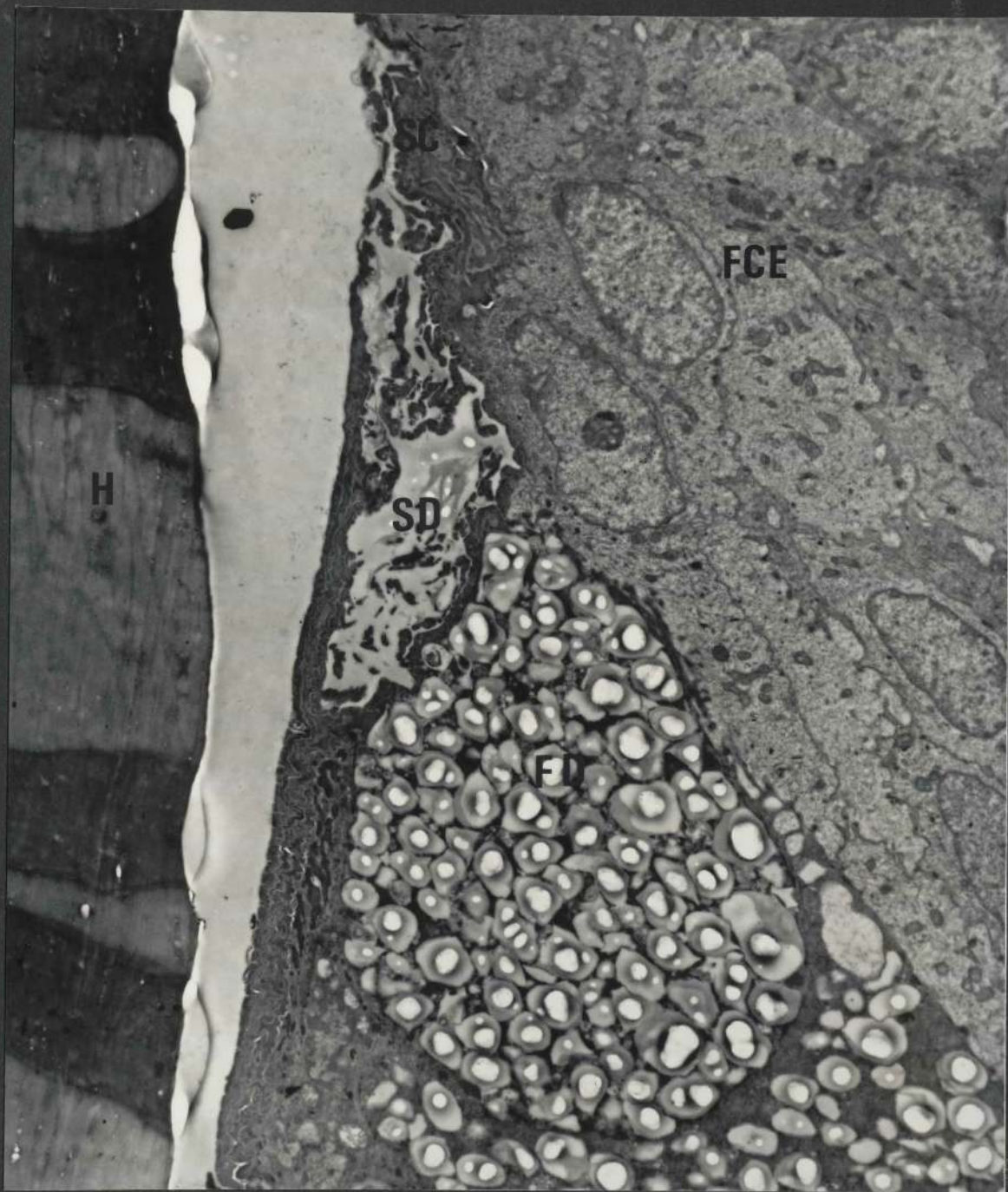
### 3.11.2 The skin following local application of a 1% aqueous lanthanum nitrate solution

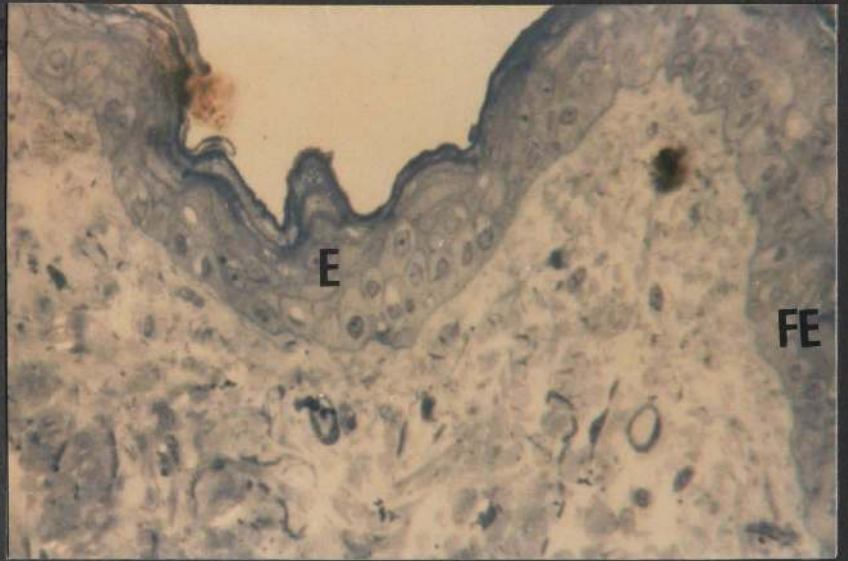
#### Figure 124

A semithin (0.5  $\mu$ ) araldite section stained with toluidine blue (x 120)

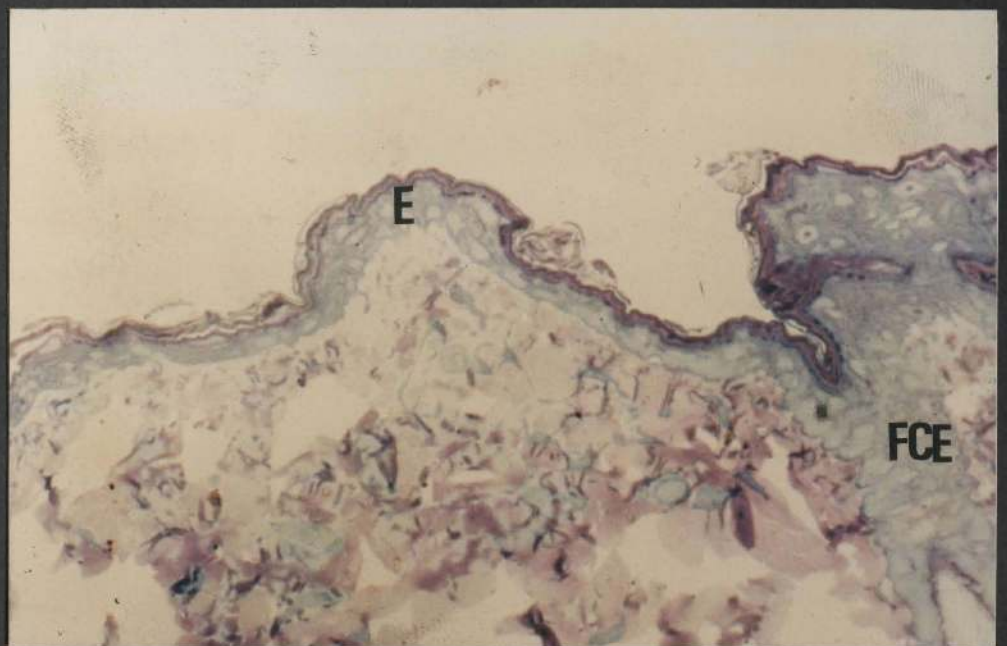
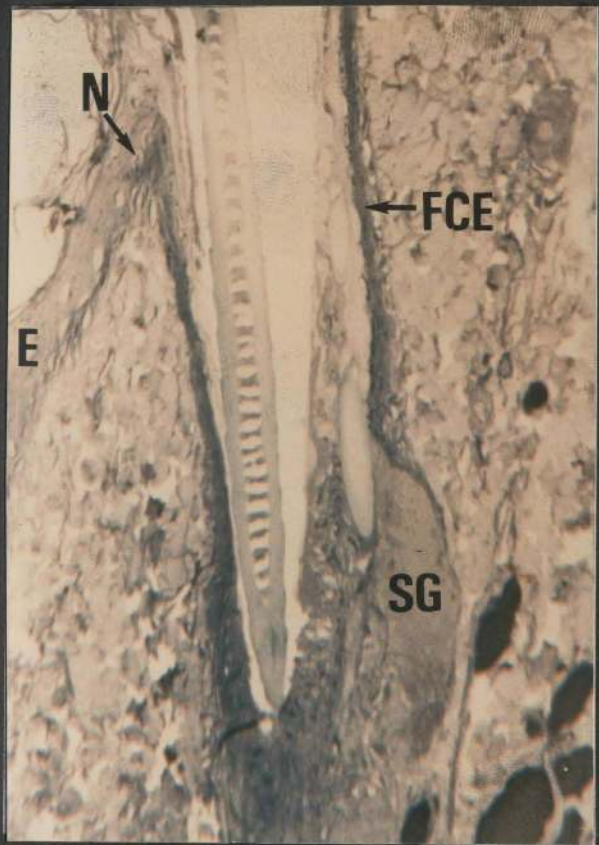
Included in this section are the epidermis (E) and the follicular canal epidermis (FE). The appearance of these structures is similar to that of untreated skin shown in Figure 122a. Furthermore, there is no significant difference in the appearance of the epidermis, the hair follicles and the sebaceous glands following local application of various other test solutions (for example, Figure 78(a - d), 84 (a and b), 87 (a - c) and 89 (a - c) when compared to those of untreated skin (Figures 123 (b - c)).











### 3.11.3 The skin following iontophoresis

#### 3.11.3.1 Positive iontophoresis

Figure 125a: A semithin (0.5 u) araldite section (x 80)

This section is from an experiment in which a 1% aqueous lanthanum nitrate solution was subjected to positive iontophoresis at 30 milliamperes for 15 minutes. The epidermis (E) appears as a condensed layer with many vacuoles. The nuclei (N) in the lower epidermal layers appear as dense, rod-shaped bodies surrounded by empty sacs. The follicular canal epidermis is dense and compact. There is a loss of the normal histological appearance of the sebaceous gland (SG) when compared to that seen in Figure 122b (untreated skin).

Figure 125b: A semithin (0.5 u) araldite section (x 100)

This section is from an experiment in which 1% lanthanum nitrate in absolute ethanol was subjected to positive iontophoresis at 30 milliamperes for 15 minutes. The epidermis (E) and the follicular canal epidermis (FE) appear as a gray dense mass. There is a loss of the fine cellular detail observed in the untreated skin (Figure 122a).

A large number of transmission electron micrographs (for example, Figures 79 (a - c), 85 (a - d) and 90 (a - e)) have been shown which demonstrate the ultrastructural changes observed in the epidermis, the hair follicles and the sebaceous glands following positive iontophoresis. These changes include condensation and elongation of the nuclei, coagulation of the cytoplasm and widening of the intercellular spaces as compared to untreated skin (Figure 123 (a - c)).

### 3.11.3.2 Negative iontophoresis

The materials used in the present study for negative iontophoresis included anionic dyes and iodide ions which could not be visualized in the transmission electron microscope. Nevertheless, in order to evaluate the changes which occurred in the skin following negative iontophoresis, specimens were taken from an area subjected to negative iontophoresis of a 2% aqueous potassium iodide solution at 30 milliamperes for 15 minutes. These specimens were processed for electron microscopy and the sections are shown in Figure 126 (a - c).

Figure 126a: A semithin (0.5  $\mu$ ) araldite section stained with toluidine blue (x 120)

This shows the epidermis (E) and the follicular canal epidermis (FE). The stratum basale (SB), the stratum spinosum (SS), the stratum granulosum (SG) and the stratum corneum (SC) are clearly identified. No distinct histological changes are seen in this section when compared to that seen in Figure 122a.



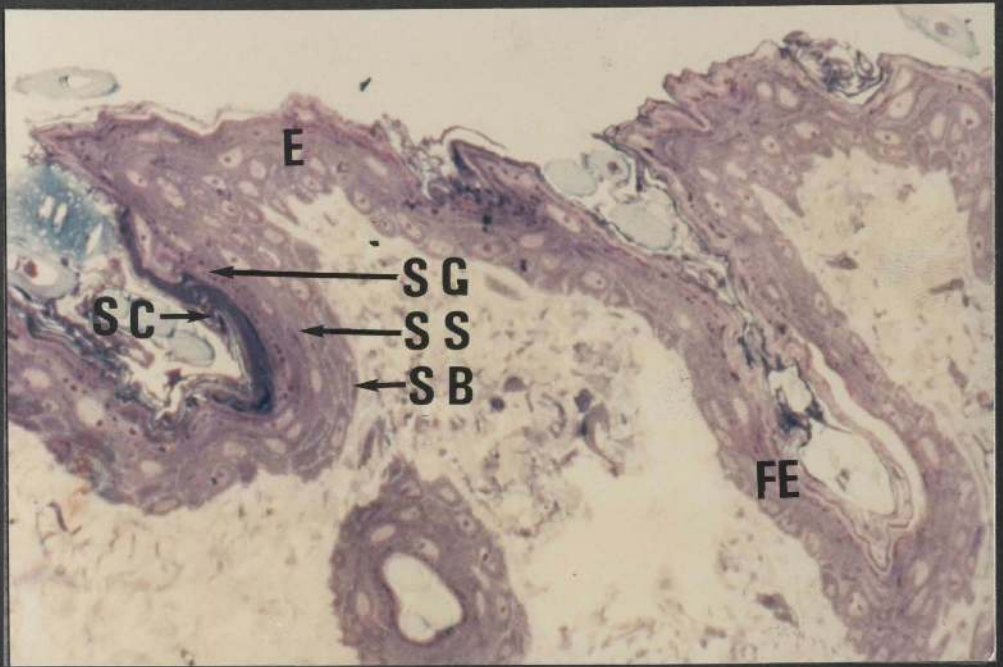


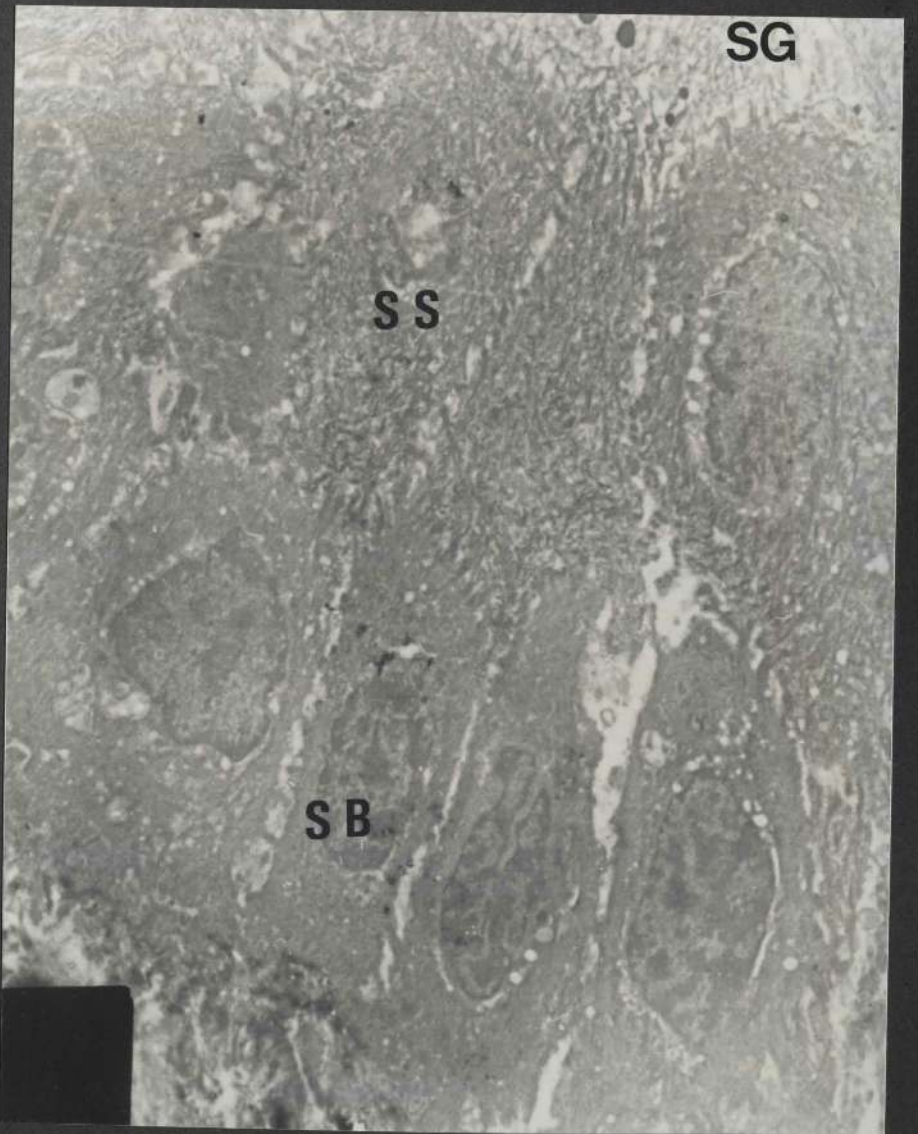
Figure 126b: A transmission electron micrograph (x 8,352)

A segment of the stratum corneum (SC) is presented in this micrograph. The appearance of the stratum corneum is similar to that shown in normal skin (Figure 123a).

Figure 126c: A transmission electron micrograph (x 1,136)

This field spans the basal (SB), the spinous (SS) and the granular layers (SG) of the epidermis. Widening of the intercellular spaces and slight coagulation of the cytoplasmic matrix are seen. However, the fine morphological details of the nuclei (N) are preserved. From this it appears that the morphological changes observed in this case are less marked compared to those seen following positive iontophoresis.





CHAPTER 4  
*DISCUSSION*

## CONTENTS

	Page	
<b>4.1</b>	<b>Initial observations</b>	304
4.1.1	The skin surface	304
4.1.2	Current intensity	305
4.1.3	Vehicles used	306
<b>4.2</b>	<b>Justification of methods used and significance of results</b>	306
4.2.1	Elimination of factors affecting skin penetration	307
4.2.2	Evaluation of some factors affecting skin penetration	307
4.2.3	Demonstration of tracers in skin sections	308
4.2.3.1	Organic dyes	308
4.2.3.2	Inorganic tracers	309
4.2.4	X-ray analysis	311
<b>4.3</b>	<b>Evaluation of extent of penetration</b>	313
<b>4.4</b>	<b>Efficacy of iontophoresis</b>	314
<b>4.5</b>	<b>Variation in penetration caused by the specification of the apparatus</b>	316
4.5.1	Thickness of the electrode dressing	316
4.5.2	Condition of iontophoresis electrode	318
<b>4.6</b>	<b>Penetration through treated and untreated skin</b>	319
<b>4.7</b>	<b>Effect of variation in current density on skin penetration</b>	321
<b>4.8</b>	<b>Polarity effect</b>	324
4.8.1	Penetration of ionic materials	324
4.8.2	Effect of reversing the current	326



4.8.3	Effect of iontophoresis on the penetration of non-ionic materials	328
4.8.4	The extent of penetration as a function of the polarity of the test material	330
4.8.5	Penetration of inorganic ions	332
4.9	The effect on concentration on skin penetration by iontophoresis	332
4.10	The effect of aprotic solvents on skin penetration by iontophoresis	341
4.11	The effect of detergents on skin penetration by iontophoresis	344
4.12	The effect of organic solvents on skin penetration by iontophoresis	349
4.13	Physico-chemical factors influencing skin penetration by iontophoresis	354
4.13.1	Solubility characteristics of the penetrant	354
4.13.2	pH of the test solution	357
4.13.3	Diffusivity of the test material	360
4.13.4	Ionic and molecular weights of penetrants	362
4.13.5	The size of the hydrated ion	364
4.14	Tracer-tissue interaction	366
4.15	Mode of action of iontophoresis	370
4.16	The location and nature of the cutaneous barrier	376
4.16.1	The role of the surface lipid	376
4.16.2	The role of the stratum corneum and sebum in the follicular canal	378
4.16.3	The epidermal-dermal junction	395

<b>4.17</b>	<b>Routes of entry</b>	<b>396</b>
4.17.1	Trans-appendageal versus trans-epidermal penetration	396
4.17.2	Transcellular versus intercellular penetration	408
<b>4.18</b>	<b>Advantages and disadvantages of iontophoresis</b>	<b>411</b>
<b>4.19</b>	<b>Suggestion for future investigations</b>	<b>413</b>

## 4.1 Initial observations

### 4.1.1 The skin surface

During the course of the present study the surface of the skin used for penetration trials was always examined before excision. With regard to organic dyes, it was observed that following local application of all solutions of the dyes tested, the surface of the skin stained very lightly but fairly uniformly and there was no clear evidence of marked selective absorption of the dyes by any particular skin structure. Following iontophoresis, however, the surface of the intact treated area showed a distinct dye colouration conforming to the size and shape of the iontophoresis electrode. This observation was particularly evident with dyes such as methylene blue, toluidene blue, chrysoidine Y, pyronin Y, eosins, picric acid and alizarin red S. When a current of low intensity (5, 10 or 15 milliamperes) was employed for a short duration of time (up to 10 minutes), selective penetration was observed, that is, the dye colouration was more accentuated at the follicular orifices. But when a current of relatively higher intensity (20, 25 or 30 milliamperes) was employed the colouration of the surface of the treated area was intensely deep and uniform throughout the treated area and thus no selective penetration into the skin could be identified. Similar observations were also evident when a coloured solution of inorganic tracers, for example ruthenium red, was used for penetration studies. Following iontophoresis of all the materials used, the treated skin always showed a harder surface than the neighbouring skin and this phenomenon was used in particular to distinguish the treated skin from

neighbouring skin when a colourless solution of inorganic tracer, such as a solution of lanthanum nitrate, was used for penetration trials.

#### 4.1.2 Current intensity

It was noticed that when the current intensity was increased from zero to a selected value, after a few moments the current intensity first decreased below and then increased above the selected value. Accordingly readjustment of the resistors was necessary to bring the current intensity back to the selected value, at which the current remained fairly constant providing that the electrodes were not allowed to dry. These changes in the current amperage were very slight when a weak current (5, 10 or 15 mA) was used, whereas with a relatively strong current (20, 25 or 30 mA) the changes in the amperage reading were frequently of the order of 5 mA. It has been suggested that the initial decrease and then increase in the current intensity is due to first an increase and then a decrease in the skin resistance respectively (report of the Council on Pharmacy and Chemistry and the Council on Physical Therapy, 1941; Rothmans, 1943). In addition, it was observed that when a current exceeding 40 mA was used for a duration of 20 minutes, small cuts and bruises were occasionally seen on the treated area. In contrast when a current of 30 mA was used over a duration of 15 minutes no damage was observed in the treated skin and therefore these values were used as standards.

#### 4.1.3 Vehicles used

When distilled water was used as the vehicle, approximately 25 to 40 mls of tracer solution were used. This volume included (1) the amount of solution which penetrated into the skin (if penetration occurred), (2) the amount of solution removed by cotton wool from the skin surface plus the amount which could not be removed and which remained visible on the surface, (3) the amount of solution which remained in the absorbent pad of the iontophoresis electrode and (4) the amount of solution which occasionally escaped down the flank of the animal during experimentation. From this it is clear that the major disadvantage of using iontophoresis is controlling the amount of ionic materials penetrating the skin. In contrast to the aqueous vehicle which remained in a global form on the surface of the skin, when absolute ethanol was used as the vehicle it diffused rapidly over the skin surface and was quickly absorbed by the skin. As a result when a tracer compound was prepared in the alcohol a significantly larger volume (approximately 150 mls) was used during experimentation to prevent the iontophoresis electrode from drying out and to ensure that there was always excess solution on the surface of the skin.

#### 4.2 Justification of methods used and significance of results

Many methods are available to investigate skin penetration (p 14). The use of microscopically detectable tracers provides a useful method for demonstrating penetration, visualizing the pathways that tracers take in penetrating the skin, and for revealing the presence of any barrier to penetration. The use of cryostat sections and ultrathin sections has been employed by previous investigators in studying skin



penetration (and cutaneous barrier) (Elias *et al.*, 1977; Hayward, 1983; Squier, 1984), and these have been adopted in the present study. Many factors are known to influence skin penetration (page 37), and in order to be able to draw fundamental conclusions and to obtain accurate data it is essential to restrict the experimental system so that some factors that influence penetration are eliminated while others are evaluated.

#### 4.2.1 Elimination of factors affecting skin penetration

Throughout the present study, experiments have been performed on intact, undamaged abdominal skin of anaesthetized, male albino rats of the same age and weight. The rats were kept in the same conditions of temperature, humidity and light and were fed the same diet. Therefore many potential factors affecting skin penetration such as sex, skin condition, age and weight of the animal, site of application, species variations, blood flow, and seasonal variation were eliminated from the discussion of the major contributors to bringing about variations in the results.

#### 4.2.2 Evaluation of some factors affecting skin penetration

Some of the factors which influence skin penetration, and which have been investigated in the present study, are the concentration of the test material in the vehicle, the intensity of the current used, the duration of application and the type of vehicle used. In order to obtain meaningful results, the method used was carefully thought out. Firstly, the effect of the flow of current on skin penetration was checked against a control, that is, against an identical experiment

but without the flow of current. Secondly, in order to investigate the effect of one of the afore-mentioned factors on skin penetration, all variables were kept constant while the one being investigated was varied. By doing so, any variations in the results could be attributed to the one variable. Thirdly, each experiment was repeated on average three times, and a large number of sections (cryostat or ultrathin) were selected from different sites of the treated area and examined to determine the extent of penetration of a particular tracer. Finally, the procedures used to prepare the skin for microscopical examination were standardized.

#### 4.2.3 Demonstration of tracers in skin sections

##### 4.2.3.1 Organic dyes

In order to avoid relocation of the dyes used for penetration trials in the skin due to fixation, studies were made on unfixed cryostat sections. Cryomicroscopy was adopted because it is the most direct method for revealing the site of deposition of the test materials in the skin. The exact determination of the location of a tracer dye within the histologically differentiated layers of the epidermis and the hair follicles was difficult when studies were made on unfixed sections, particularly when the dye solution was applied to the surface of the skin without iontophoresis (as, for example, in Figures 1a, 44a and 59). In order to determine more accurately the tracer level within the skin structures some sections were stained additionally in tartrazine (for example, Figures 1b, 44b and 60) or haematoxylin and eosin (for example, Figures 1d, 39c and 42b) and compared to similar sections which were not additionally stained. It is interesting to note that such additional stainings, which were

accompanied by rinsing, dehydration and mounting, did not result in the extraction of the tracer dyes used for penetration trials from the cryostat sections. Furthermore, following a particular set of experiments the location and distribution of the dye used for penetration trials were consistent in most of the cryostat sections examined. Thus relocation of the dye within the skin as a result of preparative techniques (page 89) appeared to be minimal.

#### 4.2.3.2 Inorganic tracers

Lanthanum and silver were used as tracers to investigate the site of any cutaneous barrier and to test their penetration into the skin by iontophoresis. The location and site of deposition of the tracers within the skin were determined by examination of ultrathin sections since these tracers share the property of being electron-dense. The question arose as to whether or not the routine procedure of fixation, dehydration, embedding and sectioning used to prepare specimens for electron microscopic examination (page 96) caused relocation or loss of the tracers concerned. Squier and Edie (1983) carried out studies on the localization of lanthanum which examined ultrathin sections in the transmission electron microscope and analyzed freeze-dried sections by microprobe X-ray analysis. They came to the conclusion that the routine procedure applied for processing tissues for electron microscopy did not affect the distribution and localization of lanthanum in tissues and so validated the routine procedure for studies of epithelial permeability. With regard to silver, it is also probable that such a procedure did not alter significantly its position in the skin since the localization and site of deposition of silver were identical in the vast majority of the ultrathin sections examined following a particular experiment.

Various solutions containing copper sulphate or ferric chloride were used for penetration trials, and the deposition of metal tracers in the skin was determined by histochemical tests applied to skin sections. These tests were the Mallory's haematoxylin method which is specific for both copper and iron, the rubeanic acid method which is specific for copper, and the Prussian blue (Perl's) method which is specific for iron. All these methods were sensitive enough to reveal copper and iron in the skin sections. Regardless of which histochemical test was employed, the location of these tracers in the skin was consistent in the cryostat sections examined from a particular experiment and its repetition subsequently. Thus it appears that the procedures applied in the histochemical tests did not alter significantly the localization of the tracer in the skin sections. Furthermore, since all the specimens were handled in the same way, the results obtained are valid for comparative studies.

The localization of ruthenium red in the skin following penetration trials was determined from unfixed cryostat section because of the characteristic red colour of the tracer. The visualization of the tracer in ultrathin sections was not possible because osmium tetroxide could not be used simultaneously with the tracer during the penetration trials (page 250). However, the marked "granulation" of the nuclei and the cytoplasmic matrix observed in ultrathin sections of the epidermis and the hair follicles following iontophoresis (Figure 97 b - e), and the absence of such granulation in skin treated with lanthanum iontophoresis (Figure 79 a - c), may be regarded as an indication that penetration of ruthenium red took place into the epidermis and the hair follicles.

#### 4.2.4 X-ray analysis

The aim of X-ray analysis is to provide information about elements normally present or artificially introduced in tissues *in vivo*. The removal of tissues from their normal environment and the exigencies of sample preparation for analysis inevitably mean that diffusible constituents tend to be displaced. However, numerous reports (Chandler, 1977; Erasmus 1978; Hall, 1979; Roomans, 1979; Hayat, 1980; Goldstein *et al.*, 1981; Moreton, 1981; Morgan, 1985) are available which describe various preparative techniques to minimize elemental translocation and loss from the specimen. The most popular techniques are those which use freeze-dried ultrathin cryosections and ultrathin frozen-hydrated cryosections. These have been employed to investigate the presence of a tracer in skin (Squier and Edie, 1983), to observe the fine structure of epidermal keratinocytes (Suzuki and Kakimi, 1985), and to analyze the diffusible substances in the skin (Warner *et al.*, 1985). The electron microprobe is a direct method for the characterization of electron-dense regions of ultrathin sections examined in the transmission electron microscope (Hall, 1979), and has been employed by Nemanic and Elias (1980) in the visualization of pathways across the stratum corneum.

In the present study, work was undertaken to determine if energy-dispersive X-ray (EDX) analysis was sensitive enough to detect the presence of metal tracers in the skin with the preparative methods used. Analyses were carried out on cryostat sections of skin and on the resin "block faces" containing the skin specimens following ultrathin sectioning. To evaluate the significance of such analyses, the analyzed area consisted of skin or the mounting medium (glass



slide or resin). In order to avoid variations in analysis due to instrumentation, the SEM used was standardized at 30° take-off angle, 100 counts per second and an accelerating voltage of 15 KV. When peak-overlap occurred (Figure 95b), the wavelength-dispersive X-ray (WDX) system was used as an alternative method and the analyses were made on semithin araldite sections. The spectra included with Figures 76a, 86a, 95c, 96 b and c, 97 b, c, d and e, 98a and 113a are examples of the results obtained with the EDX and the WDX analyses. They were obtained from the mounting medium alone or from skin sections following intradermal injections of solutions containing metal tracers. The results obtained with X-ray analysis following iontophoresis and local application (that is, without iontophoresis) are reported throughout Chapter Three. These results indicated that :

- (1) Although the shape of the spectra varies, the elements detected are very consistent.
- (2) The spectra obtained from the glass slides adjacent to the cryostat skin sections may include peaks for aluminium, silicon, phosphorus, sulphur, chlorine, calcium, potassium and magnesium, while the spectra obtained from resin block areas adjacent to the skin specimens may include peaks for magnesium, sulphur, chlorine, osmium and aluminium. It is possible that the elements detected in these spectra arise from different sources. For example, they may arise from the vacuum grease used within the microscope column (Pohla *et al.*, 1983) or from the embedding media themselves.
- (3) The spectra obtained from different skin sites without iontophoresis are similar to those obtained from the mounting media.
- (4) The spectra obtained from different skin sites following iontophoresis or intradermal injection of tracers are similar to those

obtained from the mounting media but, in addition, they consistently include peaks for the metals used as tracers.

From the above it appears that although no specific characterization about the overall elemental content of the skin can be made, the method used in the present study was sensitive enough to detect the metals used for penetration trials. Thus, X-ray analyses were carried out to confirm the presence or absence of a metal tracer in the skin, although the precise determination of the location of tracers within the skin structures (epidermis, hair follicles and sebaceous glands) was made by histological observations. However, it was noted that when an examination was made on a resin block face containing a skin specimen following ultrathin sectioning, determination of the site of deposition of a tracer within the skin structures was feasible because the identification of the various strata in the epidermis and the hair follicles was possible (Figure 76a).

#### 4.3 Evaluation of extent of penetration

For descriptive purposes, the following have been used to indicate

the approximate extent or degree of penetration of tracers into and through the skin:

- (-) = no penetration
- (-/+ ) = no or some penetration
- (+) = some penetration
- (++) = moderate penetration
- (+++ ) = good penetration

However, reference should always be made to the histological sections shown in **Chapter Three** with regard to the precise location and site of deposition of a tracer within the skin.

#### 4.4 Efficacy of iontophoresis

In order to evaluate the efficacy of iontophoresis in introducing cations and anions into and through the skin, solutions of organic and inorganic tracers were subjected to positive or negative iontophoresis in accordance with the polarity of the tracer, using standard values of current intensity (30 mA) and duration of application (15 min). The extent of penetration of each tracer following iontophoresis was compared to a control, that is, to a similar experiment without the flow of current. Some of the experimental data and the results obtained are summarized in Tables 4.1 and 4.2.

It is clear that the penetration of all the tracers used was negligible in the control experiments, whereas penetration occurred following iontophoresis. Since the concentration, vehicle and duration of application were the same for each tracer, differences between the control and iontophoresis experiments can be attributed to

Table 4.1 Efficacy of Iontophoresis - Organic Tracers

Solution	Type of experiment	Figure	Extent of penetration					
			Epidermis	Hair follicles	Subcutaneous glands	Dermis	Hypodermis	
2% aqueous methylene blue in ethanol	Control	1	-	-	-	-	-	
	Positive Iontophoresis	19	+++	+++	+++	+++	+++	
2% methylene blue in ethanol	Control	39	-/+	-/+	-	-	-	
	Positive Iontophoresis	43	+++	+++	+++	+++	+++	
2% aqueous colloidine blue	Control	44	-	-	-	-	-	
	Positive Iontophoresis	42	+++	+++	+++	+++	+++	
1% eosin in ethanol	Control	56	-	-	-	-	-	
	Negative Iontophoresis	60	-/+	+++	++	-/+	-	
6% picric acid in ethanol	Control	64	-	-	-	-	-	
	Negative Iontophoresis	65	++	++	++	+	+	

Control - local (topical) application

Table 4.2 Efficacy of Iontophoresis - Inorganic (anodal) cations

Solution	Type of experiment	Figure	Extent of penetration					
			Epidermis	Hair follicles	Sweat glands	Dermis	Hypodermis	
8% aqueous copper sulphate	Control	105	-	-/+	-	-	-	
	Positive Iontophoresis	106 (a,b)	+++	+++	+++	+++	+++	
4% aqueous ferric chloride	Control	116	-	-	-	-	-	
	Positive Iontophoresis	117	++	++	++	++	-	
4% ferric chloride in ethanol	Control	120	-	-/+	-/+	-	-	
	Positive Iontophoresis	121 (a,b)	++	+++	+++	++	+	
1% aqueous ruthenium red	Control	96a	-	-	-	-	-	
	Positive Iontophoresis	97a	+++	+++	+++	+++	+++	
8% aqueous silver nitrate	Control	91 (a-c)	-	-	-	-	-	
	Positive Iontophoresis	92 (a-c)	++	+++	++	++	++	

Control = local (topical) application



the only variable, which was the flow of current. In other words, these findings indicate that penetration has occurred as a result of the flow of the current, and not to simple absorption by the skin from the pad soaked with the tracer solution.

In the early literature, increased penetration of an ionic material as a result of the flow of an electric current was judged mainly by the physiological response of the body to that material. For example, Inchley (1921) applied to animal skin solutions of the cations atropine, strychnine and cocaine by positive iontophoresis which resulted in paralysis of the cranial nerves, twitching, convulsion and heart failure. No such physiological reactions resulted from local application alone. The same author also investigated the penetration of calcium ions through the skin by detecting the clotting time of a drop of blood. After positive iontophoresis, the clotting time was reduced as compared to the control value and this was attributed to the penetration of calcium ions through the skin and into the general circulation. In turn, Abramson (1938) investigated the penetration of histamine and ragweed pollen by iontophoresis and this was judged by weal production. Other workers (Abramson and Gorin, 1940 ; Abramson and Engle, 1942) investigated the penetration of many organic dyes, including the cations methylene blue, basic fuchsin and patent blue and the anions eosin Y, neutral red, and acid fuchsin, as well as metal ions such as silver following iontophoresis. These studies simply examined the surface of the intact skin, but it has been pointed out that such studies only demonstrated the uptake of the test materials through the orifices of the epidermal appendages but did not actually demonstrate penetration into the skin (Rothman, 1954). Clark *et al.*, (1942) studied the penetration of various sulfonamides

following iontophoresis by colorimetical measurements of the test materials in the filtrates of macerated tissues. O'Malley *et al.* (1954) and O'Malley and Oester (1955) investigated the penetration of various radioactive materials ( $P^{32}$ ,  $Na^{24}$ ,  $Ca^{45}$ ) by means of radioactivity counts carried out on the liver, kidney, blood and urine. More recently, Hornquist *et al.* (1984) investigated the effect of the flow of current on the penetration of many drugs including phenylephrine, clonidine and isoprenaline by the production of blanching, piloerection and erythema. All the publications cited above have reported enhanced penetration following iontophoresis. In contrast, only a few studies have demonstrated in histological sections the enhanced penetration by iontophoresis and these are limited to tholium X ions (Fleischmajer and Witten, 1955) and copper ions (Pereyra, 1945). The present study, therefore, has provided much-needed histologic evidence that the penetration of many organic and inorganic ions into and through the skin is facilitated by the galvanic current.

#### 4.5 Variation in penetration caused by the specifications of the apparatus

##### 4.5.1 Thickness of the electrode dressing

Many investigators (Cumberbatch, 1933; Cross, 1936; Clyton, 1952; Liventsev, 1964) have reported that endogenous ions, particularly sodium and chloride ions, migrate from within the skin to the surface during iontophoresis thus permitting the formation of sodium hydroxide and hydrogen at the negative electrode, and hydrochloric acid and oxygen at the positive electrode. If these are produced in sufficient

concentrations they have a caustic effect on the skin such as the production of iontophoretic burns (Molitor and Fernandez, 1939). This occurs whenever the metal electrode touches the skin surface. In order to prevent this, the surface of the skin should be separated from the electrode by a piece of cloth which absorbs the substances produced on the surface of the skin (Liventsev, 1964). However, the thickness of the cloth is of importance in iontophoresis studies.

In the initial stages of the present work, pads of different thicknesses were applied on to the iontophoresis electrode in order to select the most suitable one for penetration studies. The thickness of the pad applied to the return electrode was kept as constant as possible. Following a number of trials, and as judged by the extent of penetration, it was decided that a pair of folded medical tissues enclosed in a sheath of absorbent material (see page 68) was the most suitable and therefore was used throughout as the standard dressing. However, to demonstrate the effect of changing the thickness of the absorbent pad on skin penetration, a 2% aqueous methylene blue solution was subjected to positive iontophoresis using a relatively thick cotton pad which had been applied on to the iontophoresis electrode. The results obtained are summarized in Table 4.3. Following the treatment, the dye was not seen generally in any skin structure located below the level of the sebaceous glands (Figure 29), whereas when the same dye solution was applied to the skin using a standard dressing the penetration of the dye through the skin and the subcutaneous tissues was complete (Figure 19). Thus it is apparent that the extent of penetration into and through the skin can be reduced significantly by increasing the thickness of the dressing around the iontophoresis electrode. This is probably because thicker

Table 4.3 Thickness of the electrode dressing

Figure	Type of dressing	Current intensity (mA)	Duration (min)	Extent of penetration				
				Epidermis	Hair follicles	Sebaceous glands	Dermis	Hypodermis
29	Thick (12 mm)	30	15	+	+	+	+	-
19	Standard (3 mm)	30	15	+++	+++	+++	+++	+++

pads have a higher electrical resistance which retards the flow of the current as compared to thin pads. Thus, a very thick pad, although providing a good reservoir, will not allow full passage of the current and this in turn retards penetration. On the other hand, a very thin pad, although allowing good passage of current, provides a poor reservoir effect and in addition may not completely prevent contact between the metal electrode and the skin surface. For practical purposes, therefore, the absorbent pad should be thin enough to allow a good flow of current, yet thick enough to prevent contact between the electrode and the skin surface and to ensure that there is always excess test solution on the surface of the skin.

#### 4.5.2 Condition of iontophoresis electrode

A contaminated electrode (Figure 30a) was deliberately used in the introduction of a 2% aqueous methylene blue solution into the skin. The results are shown in Table 4.4. The extent of penetration of the dye (Figure 30b) was significantly reduced as compared to that seen when the same dye solution was introduced using a clean electrode (Figure 19). This is probably because the current does not flow freely from the contaminated surface of the electrode (Liventsev, 1964). Furthermore, penetration into the skin was not uniform when a contaminated electrode was used. In some areas penetration was deep, while in others penetration was shallow. This is probably a result of variation in the extent of contamination over the surface of the electrode in that penetration is deeper in skin areas under less contaminated areas of the electrode (see Figure 30a).



Table 4.4 Condition of iontophoresis electrode

Figure	State of electrodes	Current intensity (mA)	Duration (min)	Extent of penetration				
				Epidermis	Hair follicles	Sebaceous glands	Dermis	Epyodermis
30b	Contaminated	30	15	(++) or (+)	(++) or (-/+)	(++) or (-/+)	(+) or (-/+)	-
19	Standard (clean)	30	15	+++	+++	+++	+++	+++

#### 4.6 Penetration through treated and untreated skin

Treated skin is that under the iontophoresis electrode, while that outside the iontophoresis electrode and adjacent to the treated skin is untreated skin.

Experiments were carried out to determine whether penetration following iontophoresis was confined to treated skin or whether it also occurred in untreated skin. A 2% aqueous methylene blue solution was subjected to positive iontophoresis and specimens were selected from different parts within the treated area, as well as from untreated skin. The results are shown in Table 4.5 which shows that penetration into and through the skin and the subcutaneous tissue was as deep and intense at the edges and the corners as it was in the centre of the treated area. McEwan Jenkinson *et al.* (1974) also reported that the intensity of staining of the sebaceous glands was uniform in the different regions of the treated area. The present study has shown that not only the staining of the sebaceous glands but also the extent of penetration into and through the skin and the subcutaneous tissue is uniform over the area under the iontophoresis electrode. This uniformity of penetration occurs probably because the distribution of the current is fairly even over the treated area which, in turn, is brought about by making the electrode dressings as uniform (free from folds) as possible and by keeping the electrodes parallel to each other and to the skin surface.

In the untreated skin, the penetration of the same dye solution was negligible (Figure 25 a and b), a result which is similar to that obtained with the control experiment (Figure 1 a - d). This finding

Table 4.5 Penetration of 2% aqueous methylene blue into different sites of skin following positive iontophoresis

Figure	Site of skin	Extent of penetration					
		Epidermis	Hair follicles	Sebaceous glands	Dermis	Hypodermis	
20	Treated skin. Area (1) diagram 3.1, p 133	+++	++	+++	+++	++	
21	Treated skin. Area (2) diagram 3.1, p 133	+++	++	+++	+++	++	
22	Treated skin. Area (3) diagram 3.1, p 133	+++	++	+++	+++	++	
23	Treated skin. Area (4) diagram 3.1, p 133	+++	++	+++	+++	++	
24	Treated skin. Area (5) diagram 3.1, p 133	+++	++	+++	+++	++	
25 (a,b)	Untreated skin. Areas (6) and (7), diagram 3.1, p 133	-	-	-	-	-	

suggests that penetration of the dye from the surface into the skin occurs only in the treated skin and not from the surface of neighbouring areas. Furthermore, the finding that the entire thickness of untreated skin is devoid of stain may also suggest that having penetrated into the treated skin, the dye does not diffuse horizontally from within the deep tissues under the iontophoresis electrode into adjacent deep tissues, but is confined to the tissues under the iontophoresis electrode. The great concentration of the current (see page 64) in all tissues beneath the iontophoresis electrode ensures penetration into these tissues. Although the current also traverses the tissues outside the electrode and passes throughout the body, it appears that in these regions the current is weakly diffused and is not strong enough to cause migration of the dye into the untreated skin. Thus the lateral (horizontal) diffusion suggested by Rothman (1955) appears to have not taken place in these penetration studies.

The above findings highlight the great advantage of using iontophoresis as an experimental and therapeutic tool, in that it deposits ionic materials just where their effect is particularly desired. Thus, for therapeutic purposes, it is possible to use electrodes of varying shapes and sizes in accordance with the areas to be treated. Indeed, different designs of iontophoresis electrodes have been employed in the treatment of many skin conditions (Liventsev, 1964; McEwan Jenkinson *et al.*, 1974; Hornqvist *et al.*, 1984).

#### 4.7 Effect of variation in current density on skin penetration

Current density is defined as the product of current per unit area and duration of application. This may be represented as:

$$\text{Current density} = \frac{\text{Intensity of current (mA)} \times \text{Duration of application (min)}}{\text{Surface area of treated skin (cm}^2\text{)}}$$

The surface area of treated skin is the area through which the current flows and therefore equals the surface area of the iontophoresis electrode.

It has been commonly believed that the extent of penetration of ions into the skin is directly correlated with the current density (Browne, 1931; Abramson and Gorin, 1939; Report of the Council on Pharmacy and Chemistry and the Council on Physical Therapy, 1941). A number of more recent studies have confirmed this concept. For example, McEwan Jenkinson *et al.* (1974) applied positive iontophoresis of methylene blue to diseased skin of cattle and dogs and reported that the rate of recovery of an infected area was correlated with the current density. They found that with high current densities the recovery was fast whereas with low current densities, additional treatments were necessary before betterment was appreciated. Hornqvist *et al.* (1984) studied skin reactions such as blanching and erythema following iontophoresis of many drugs including phenylephrine, clonidine and



isoprenaline, and found increased physiological responses as the current density was increased.

In the present study experiments have been undertaken to investigate histologically the effect of variation in current density on the extent of penetration of organic (methylene blue and toluidine blue) and inorganic (copper) tracers into and through the skin. Since the same iontophoresis electrode was used throughout, the surface area of the treated skin remained constant, being equal to that of the iontophoresis electrode ( 12.25 cm<sup>2</sup>). Thus the effect of variation in current density on skin penetration was investigated directly by varying either the current intensity and/or the duration of application, the tracer compound being prepared in the same vehicle to a fixed concentration. The results obtained are summarized in Tables 4.6 and 4.7.

From Table 4.6 it appears that:

- (1) The penetration of methylene blue is negligible without the flow of current.
- (2) With iontophoresis, the least effective penetration is observed when the dye is introduced using a current of 5 mA over a duration of 5 minutes. The penetration of the dye increases thereafter by increasing the current intensity and/or by increasing the duration of application. Methylene blue shows the most effective penetration when it is introduced by iontophoresis using a current of 30 mA for a duration of 15 minutes.
- (3) The extent of penetration into and through the skin is generally the same when the dye solution is applied to the skin surface at the same current density. For example, the extent of penetration using a



current intensity of 5 mA for 10 minutes is very similar to that seen using a current intensity of 10 mA for 5 minutes. In both cases the current density is  $4.08 \text{ mA}\cdot\text{min}\cdot\text{cm}^{-2}$ , and therefore these two are grouped together in the same horizontal column. Similarly, with a current density of  $12.25 \text{ mA}\cdot\text{min}\cdot\text{cm}^{-2}$  the extent of penetration of methylene blue through the skin is the same when the dye solution is introduced, for example, using a current intensity of 10 mA for 15 minutes, 15 mA for 10 minutes, or 30 mA for 5 minutes.

Similarly, toluidine blue, prepared as a 2% aqueous solution, also shows enhanced penetration with increased current density (Figures 44 to 46).

In order to determine if a similar observation is applicable to inorganic ions, a 1% aqueous copper sulphate solution has been subjected to positive iontophoresis using different values of current density (Table 4.7). From this Table, it can be seen that penetration increases as the current density increases.

In conclusion, it would seem justified to state that the extent of penetration of organic and metal ions into and through the skin, as well as the underlying tissues, is directly proportional to the current density when the penetrant ion is introduced from the same vehicle and at a fixed concentration. This finding is in conformity with a number of similar observations in the literature (Browne, 1931; Abramson and Gorin, 1939; O'Malley and Oester, 1955; Harris, 1959; McEwan Jenkinson *et al.*, 1974; Hornqvist *et al.*, 1984). The simplest explanation for this phenomenon is that the rate of repulsion of the ions from the solution in contact with the iontophoresis electrode

Table 4.7 Penetration of copper ions through the skin following positive iontophoresis in relation to current density

Figure	Current intensity (mA)	Duration of application (min)	Current density mA.min/cm <sup>2</sup>	Extent of penetration					
				Epidermis	Hair follicles	Sebaceous glands	Dermis	Hypodermis	
100	30	5	12.25	+	+	+	-/+	-	
101	30	10	24.49	++	++	++	+	-	
102	30	15	36.73	+++	+++	+++	+++	+++	

into the skin increases as the current density increases. This is based on Faraday's law which, in essence, states that when a current is passed through an electrolyte, the amount of material deposited at either electrode is proportional to the quantity of electricity which passes through the system. However, the amount of ionic material driven into the skin does not necessarily conform exactly to the amount expected under Faraday's law since biological membranes are present. O'Malley and Oestler (1955) reported that the amount of  $P^{32}$  deposited in the tissues of the rat by iontophoresis was roughly proportional to the quantity of electricity used but this was not a direct linear relationship.

#### 4.8 Polarity effect

##### 4.8.1 Penetration of ionic materials

According to the principle of electrolytic dissociation and the basic rule of attraction and repulsion, it is commonly believed that when a galvanic current is applied to ions in solution, cations are repelled by the positive electrode and migrate toward the negative electrode while anions move in the opposite direction. Thus, theoretically, only one electrode should assist the penetration into the skin of a charged material during iontophoresis. That positive ions are delivered by positive iontophoresis and negative ions are delivered by negative iontophoresis (Harris, 1959) has received a substantial support. A few examples are listed in the following Table:



Positively charged materials introduced by positive iontophoresis	Authors
Methylene blue	Jenkinson et al, 1974; Abramson and Gorin, 1940.
Patent blue and basic fuchsin	Abramson and Gorin, 1940
Histamine	Kovacs, 1937; Baker, 1939; Abramson and Gorin, 1939
Acetyl-beta-methylcholine	Kramer, 1937; Baker, 1939; Craig and Kraff, 1943; Jacoby and Berbrucke, 1942; Martin et al, 1937
Phenylephrine, clonidine and isoprenaline	Hornqvist et al, 1984
Atropine, strychnine and aconitine	Inchley, 1921
Copper	Baker, 1939; Finzi, 1912; Jorsild and Plensner, 1940's; Knox, 1943; Pereyra, 1945; Watkins, 1962
Aluminium	Deuschle, 1943
Thorium X	Elschmajer and Witten, 1955
Calcium and Iron	Finzi, 1912; Inchley, 1921
Magnesium, zinc, calcium, lithium, adrenalin, aconitine, codeine, streptomycin and quinine	Liventsev, 1964
Silver	Abramson and Eagle, 1942
Zinc	Watkins, 1962
Calcium and sodium	O'Malley et al, 1955
Negatively-charged materials introduced by negative iontophoresis	
Neutral Red, eosin Y, sodium protosol, sodium indigo tetrasulphonate, sodium phenolsulphonethalate and acid fuchsin	Abramson and Gorin, 1940
Azosulfamide	Abramson and Engle, 1942
Cyanide and salicylates	Inchley, 1921
Ragweed pollen	Abramson, 1938
Sulfonamides	Clark et al., 1942
Bromide, caffeine, salicylate, sulphate, phosphate, iodide and phosphorus	Liventsev, 1964, Watkins; 1962; O'Malley et al., 1955

Consistent with the above, additional studies (Bierman and Licht, 1952; Harris, 1959; McEwan Jenkinson *et al.*, 1974; Gangarosa, 1983) have indicated that no penetration occurs when cations are applied to the skin from the negative electrode or when anions are applied to the skin from the positive electrode. Interestingly, however, a few studies have indicated otherwise. For example, Ehrenwald (1942) reported that histamine, which is a cation, could be introduced into the skin by negative iontophoresis, whilst Abramson (1938) reported that ragweed pollen, which is an anion, could be introduced into the skin by positive iontophoresis.

Experiments have been undertaken in the present study to determine the effect of the polarity of the tracer on skin penetration. Jenner's stain is a compound dye consisting of methylene blue and eosin Y. Gurr (1960) reported that the eosin (red) portion of the stain acted as an acid dye while the methylene blue portion behaved as a basic dye. In the present study, a solution of this stain was applied to the surface of the skin without iontophoresis, with positive iontophoresis, or with negative iontophoresis. Without iontophoresis, the penetration of the dye solution was minimal (Figure 73 a and b). Following positive iontophoresis only a blue colouration (methylene blue) was evident in the epidermis, the follicular infundibula and the sebaceous glands (Figure 74). Following negative iontophoresis, only a red colouration (eosin) was observed in the follicular infundibula, the sebaceous glands and occasionally in the epidermis (Figure 75). These results offer additional evidence that cations can be introduced into the skin by positive iontophoresis and that anions can be introduced by negative iontophoresis, but not vice versa. Additional experiments have confirmed this view. When introduced from aqueous

solution using fixed values of current intensity and duration of application, the cationic dye methylene blue penetrated the skin and the subcutaneous tissue following positive iontophoresis (Figure 19) whereas the penetration of the dye was negligible following negative iontophoresis (Figure 28 a and b). Flesch *et al.*, (1951) reported that eosin Y was a positively charged dye and did not show penetration into and through the skin following positive iontophoresis. However, a substantial body of data is available reporting that eosin Y is a negatively charged (anionic) dye (Gurr, 1960, 1971; Lillie, 1969; the Merck group, 1985). Thus the failure of eosin Y to penetrate into the skin as reported by Flesch *et al.* (1951) may be explained in terms of incorrect selection of the polarity of the iontophoresis electrode.

#### 4.8.2 Effect of reversing the current

Ehrenwald (1942) introduced the cation histamine into the skin by positive iontophoresis during the treatment of various conditions, and reported that the effect of treatment could be intensified by a second application with reversal of the current, that is, negative iontophoresis following the first application of positive iontophoresis. Furthermore, Abramson and Gorin (1940) reported that following its introduction into the skin by positive iontophoresis, histamine could be successfully recovered from the skin by negative iontophoresis.

In view of the above reports, experiments were carried out to investigate the effect of reversing the current at regular intervals on skin penetration as compared to the direct method. A 2% aqueous methylene blue solution was subjected to positive iontophoresis,

followed by negative iontophoresis, then a second positive iontophoresis and finally a second negative iontophoresis, all using the same current intensity (15 mA) and duration of application (5 minutes). The results are summarized in Table 4.8.

The extent of penetration following repeated reversal of the current (Figure 26) was not significantly different to that obtained when the same dye solution was subjected to a single, direct positive iontophoresis with a current density of  $12.24 \text{ mA}\cdot\text{min}\cdot\text{cm}^{-2}$  (Figures 7 and 9). This is probably because the current density of the latter is in fact the algebraic sum of the current densities of the two positive iontophoresis applications used in the experiment involving the reversal of current. Negative iontophoresis appears to have no effect. This is equivalent to saying that reversing the current at regular intervals does not result in enhancement or retardation of penetration as compared to the direct method.

To further evaluate this, an additional set of experiments was carried out with the same dye solution but with a different experimental protocol. The dye solution was subjected to positive iontophoresis using a current of 15 mA for a duration of 5 minutes, followed by negative iontophoresis using the same values of current intensity and duration of application. The results are presented in Table 4.9.

The extent of penetration in this case (Figure 27) was similar to that seen when the same dye solution was subjected to a single but direct positive iontophoresis with a current density of  $6.12 \text{ mA}\cdot\text{min}\cdot\text{cm}^{-2}$  (Figures 4 and 8). Once again, this demonstrates that the introduction of negative iontophoresis to the experimental protocol

Table 4.8 Penetration of methylene blue as a function of reversing the current

Figure	Type of iontophoresis	Current intensity (mA)	Duration of application (min)	Current density mA. min./cm <sup>2</sup>	Extent of penetration					
					Epidermis	Hair follicles	Sebaceous glands	Dermis	Hypodermis	
26	Positive	15	5	6.12	+++	++	+++	++	-	
	Negative	15	5	6.12						
	Positive	15	5	6.12						
7	Positive	10	15	12.24	+++	++	+++	++	-	
	Positive	15	10	12.24	+++	++	+++	++	-	



Table 4.9 Penetration of methylene blue as a function of reversing the current

Figure	Type of iontophoresis	Current intensity (mA)	Duration of application (min)	Current density mA.min./cm <sup>2</sup>	Extent of penetration					
					Epidermis	Hair follicles	Sebaceous glands	Dermis	Hypodermis	
27	Positive	15	5	6.12	+	+	+	+	-	
	Negative	15	5	6.12						
4	Positive	5	15	6.12	+	+	+	+	-	
8	Positive	15	5	6.12	+	+	+	+	-	

has no effect on penetration. In addition, this finding shows that once penetrated into the skin by positive iontophoresis, methylene blue cannot be recovered from the skin by negative iontophoresis. This is probably because the dye no longer exists in the ionic form and has been deposited in an insoluble form as a result of binding to negatively-charged tissue loci (page 366).

#### 4.8.3 Effect of iontophoresis on the penetration of non-ionic materials

It is commonly held that only charged materials can be introduced into the skin under the influence of an electric current (Harris, 1959; Watkins, 1962; Liventsev, 1964). However, it has been reported (Gangarosa *et al.*, 1980) that both positive and negative iontophoresis of aqueous sodium chloride solutions containing [<sup>3</sup>H] thymidine (dThd) or the antiviral agent [<sup>3</sup>H] 9.β.D. arabinofuranosyladenine (Ara-A) greatly enhances the penetration of these non-electrolytes (dThd and Ara-A) through the skin of the mouse as compared to local application.

In view of the above, experiments were undertaken to investigate the effect of iontophoresis on the penetration of non-ionic dyes into the skin. These dyes are virtually insoluble in water, but are soluble in lipid solvents and lipids, and for this reason are widely used for the demonstration of lipids in tissues (Montagna and Noback, 1947; Lillie, 1969; Dixon, 1970; Bancroft and Stevens, 1977). Sudan black B was selected as a representative of such dyes. It was prepared in absolute ethanol to a concentration of 0.1% and applied to the skin

surface either without iontophoresis, with positive iontophoresis, or with negative iontophoresis. The results are shown in Table 4.10.

Without iontophoresis, a brownish-black colouration was visible in the sebaceous glands and hair follicles, but no staining was seen in the epidermis (Figure 70). Similar results were observed using another sudan dye, namely sudan IV, when prepared in ethanol and applied to the surface of the skin of the guinea pig (Ebling *et al.*, 1981). The extent of penetration of the dye solution following positive (Figure 71) and negative (Figure 72) iontophoresis did not differ significantly from that seen without iontophoresis (Figure 70). From this it appears that iontophoresis does not result in an enhancement or a retardation of the penetration of non-ionic materials (sudan black B) into the skin. Consistent with this, Hill *et al.* (1977) reported that one of the preconditions of using iontophoresis for therapeutic and practical purposes was that the test material must be ionized or modified to carry a charge. Cutner (1949) used penicillin iontophoresis in the treatment of certain disorders (paronychia) and acknowledged that such treatment was ineffective because penicillin was present in a non-ionic form in the solutions used.

Although sudan black B has been reported to be composed of two components, one being soluble in neutral lipids and the other being a slightly basic dye favouring phospholipid staining (Bancroft and Stevens, 1977), it appears that the slightly basic component of the dye is insignificant in terms of enhancing dye penetration by positive iontophoresis.

Table 4.10 Penetration of sudan black B into the skin

Figure	Type of experiment	Extent of penetration					
		Epidermis	Hair follicles	Sebaceous glands	Dermis	Hypodermis	
70	Control	-	++	++	-	-	
71	Positive iontophoresis	-	+ or ++	++	-	-	
72	Negative iontophoresis	-	+ or ++	++	-	-	

#### 4.8.4 The extent of penetration as a function of the polarity of the test material

According to Rein (1926) a negative charge "on" the skin surface facilitates the passage of positively charged dyes and retards the passage of negatively charged dyes by iontophoresis. This was disputed by Abramson and Gorin (1940) who indicated that there was no correlation between the charge on the skin with the passage into the skin of ionic dyes by iontophoresis, and maintained that both cationic and anionic dyes could be introduced into the skin by such a technique.

Consistent with the report of Abramson and Gorin (1940), the present work has shown that the skin permits the passage of both cationic and anionic dyes by positive and negative iontophoresis respectively (Table 4.1). However, when penetration occurs there appears to be a relation between the sign which the dye ions carry and their extent of penetration into and through the skin. The following Table (4.11) summarizes the extent of penetration of various dyes when solutions of these are presented to the skin using the standard iontophoresis procedure, that is, using a current intensity of 30 mA and a duration of application of 15 minutes.

From this Table it can be readily appreciated that, in general, cationic dyes are better penetrants than anionic dyes in that the epidermis and the pilosebaceous units are stained much more intensely with cationic dyes than with anionic dyes. Furthermore, having penetrated the epidermis and the hair follicles, the cationic dyes appear not only in the dermis but also in the subcutaneous tissues,



Table 4.11 The extent of penetration as a function of the polarity of the test material

Dye	Solution	Figure	Extent of penetration following iontophoresis				
			Epidermis	Hair follicles	Sebaceous glands	Dermis	Hypodermis
C A T I O N I C	1% aqueous methylene blue	34	+++	+++	+++	+++	+++
	2% aqueous methylene blue	19	+++	+++	+++	+++	+++
	2% methylene blue in alcohol	43	+++	+++	+++	+++	+++
A N I O N I C	2% aqueous toluidine blue	45	+++	+++	+++	+++	+++
	1% aqueous eosin water- and -alcohol soluble	58	-/+	+	-/+	-	-
I O N I C	1% eosin water- and alcohol-soluble in ethanol	60	-/+	+++	++	-/+	-
	6% picric acid in ethanol	65	++	++	++	+	+

whereas anionic dyes are confined mainly to the epidermis and its appendages. There are two possible explanations for this observation; the first relates to the movement of the vehicle containing the tracer in an electric field whilst the second relates to the staining properties of the skin.

It was generally held (Calvery *et al.*, 1946; Rothman, 1954) that the movement of water into the body was accelerated by the positive electrode and retarded by the negative electrode. This was believed to be the reason for the success of cations and the failure of anions to pass into the skin by iontophoresis. But relatively recently Gangarosa *et al.* (1980) presented evidence that both positive (anodal) and negative (cathodal) iontophoresis were effective in enhancing the penetration of water into the skin as compared to controls, and that positive iontophoresis was much more effective in increasing the penetration of water into the skin than negative iontophoresis. Since, in accordance with the polarity, cations are applied to the skin with positive iontophoresis and anions are applied with negative iontophoresis, the enhanced penetration of water into the skin by positive rather than by negative iontophoresis is the more likely reason for the effective penetration of cationic dyes and cations in general and the less effective penetration of anionic dyes and anions in general. Furthermore, the basophilia of the epidermis and its appendages (Montagna and Noback, 1947; Dixon, 1970) probably explains why basic dyes penetrate from these structures into the dermis much more easily than acidic dyes.

Certain ultrastructural changes were observed in the skin following iontophoresis, which included widening of the intercellular spaces, loss of fine cellular detail as a result of coagulation and

condensation of the cytoplasmic matrix and nuclear materials, and a reduction in the thickness of the epidermis. It is interesting to note that these changes were clearly evident following positive iontophoresis (Figures 79 (a - c), 85 (a - d) and 125 (a and b) whereas following negative iontophoresis the morphological changes were less obvious (Figure 126 a, b and c). This may be regarded as indicative of the marked effect of the current on the skin following positive rather than negative iontophoresis.

#### 4.8.5 Penetration of inorganic anions

In the present study, experiments were carried out using solutions of potassium iodide to investigate the penetration into the skin of iodide ions following local application and negative iontophoresis. In view of earlier reports, (see page 293), penetration was judged by energy-dispersive X-ray analysis on unfixed cryostat sections. The spectra obtained with both methods of application did not differ significantly (see page 293). Thus it may be speculated that the penetration of iodide ions is not significantly enhanced by iontophoresis as compared to controls. However, further investigations (page 414) are required to confirm this conclusion.

#### 4.9 The effect of concentration on skin penetration by iontophoresis

One of the well-documented factors which influences percutaneous penetration is the concentration of the penetrant in the presenting vehicle. The common view that an increase in the concentration of the penetrant results in an increase in penetration has been demonstrated using methyl salicylate (Cotley *et al.*, 1960), many alcohols

(Treherne, 1956; Blank, 1964), and steroids (Maibach and Feldmann, 1959). Tregear (1966) and Idson (1975) have listed other examples. In all the afore-mentioned reports the effect of concentration on skin penetration was investigated either by means of local application of labelled compounds or by exposure of isolated skin to such compounds in a diffusion cell chamber.

In view of these reports, a study of the relationship between the concentration of the tracer and its penetration by iontophoresis was examined by varying the concentration of different tracers in a selected vehicle and observing the extent of penetration into and through the skin. The tracers were applied to the skin using the standard conditions for iontophoresis. The results obtained are summarized in Tables 4.12 and 4.13.

Following iontophoresis using a current intensity of 30 mA over a duration of 15 minutes, the penetration of methylene blue was as extensive with a 1% (Figure 34) as with a 2% (Figure 19) solution. Using a 3% aqueous solution (Figure 38) the staining was very intense but the penetration was markedly reduced when compared to that obtained with the 2% solution (Figure 19). When lower values of current intensity and duration of application were used, the dye showed a better penetration once again when presented from a 2% (Figures 6 and 10) rather than from either a 1% (Figures 32 and 33) or a 3% (Figures 36 and 37) aqueous solution. The histological findings therefore suggest that an initial increase in the concentration of the dye results in an increase in penetration, and that this holds until a particular value of concentration is reached (2%) above which a further increase in concentration results in a decrease in

Table 4.12 Penetration of methylene blue through the skin as a function of the dye concentration following iontophoresis

Solution	Figure	Current (mA)	Duration (min)	Extent of penetration					
				Epidermis	Hair follicles	Sebaceous glands	Dermis	Hypodermis	
1% aqueous solution	31	0	15	-	-	-	-	-	
	32	10	10	++	++	++	+	-	
	33	15	15	++	++	++	++	+	
	34	30	15	+++	+++	+++	+++	+++	
2% aqueous solution	1	0	15	-	-	-	-	-	
	6	10	10	++	++	++	+	+	
	10	15	15	+++	+++	+++	++	+	
	19	30	15	+++	+++	+++	+++	+++	
3% aqueous solution	35	0	15	-	-	-	-	-	
	36	10	10	++	++	+	+	-	
	37	15	15	++	++	++	++	+	
	38	30	15	+++	++	++	++	+	

penetration. Thus the ranking order with respect to the extent of penetration of methylene blue as a function of a change in concentration may be given as 2% > 1% > 3%. These results are in agreement with those of McEwan Jenkinson *et al.* (1974) who reported that 2% aqueous methylene blue showed better penetration into the sebaceous glands than did 1%, 5% or 10% aqueous solutions. In addition, the present study has shown that the penetration into and through the skin and the subcutaneous tissues as a whole is affected by changes in the penetrant concentration (Table 4.12). In contrast to the above, Juhlin (1961b) found that the dose of epinephrine and l-norepinephrine introduced into the skin by iontophoresis was independent of the concentration used. This conclusion, however, was based simply on the intensity of the drug reaction which consisted of the formation of small round blanched spots with or without piloerection.

Other studies were undertaken to investigate further the relationship between concentration and penetration following iontophoresis by using metal ions as tracers (Table 4.13). When a 1% aqueous lanthanum nitrate solution was subjected to positive iontophoresis using a current of 30 mA over a duration of 15 minutes, lanthanum was observed in ultrathin sections as electron-dense deposits on the surface of the skin. These deposits did not extend into the stratum corneum of the epidermis or into the pilosebaceous units (Figure 79 a - c). Under similar conditions of iontophoresis, increasing the concentration of the tracer salt by two-fold did not render the skin permeable to lanthanum, that is, the localization of the electron-dense deposits (Figure 80 a - c) was similar to that seen when the tracer was introduced from a 1% aqueous solution. Thus the change in the



Table 4.13 Penetration of inorganic cations through the skin as a function of the concentration of the metal salt following positive iontophoresis

Solution	Type experiment	Figure	Extent of penetration				
			Epidermis	Hair follicles	Sebaceous glands	Dermis	Hypodermis and striated muscle
2% aqueous silver nitrate	Control	87 a-c	-	-	-	-	-
	Iontophoresis	88 a-c	+	-	-	-	-
4% aqueous silver nitrate	Control	89 a-c	-	-	-	-	-
	Iontophoresis	90 a-e	++	++	-/+	-	-
8% aqueous silver nitrate	Control	91 a-c	-	-	-	-	-
	Iontophoresis	92 a-c	++	+++	++	-	-
1% aqueous ferric chloride	Control	114 a,b	-	-	-	-	-
	Iontophoresis	115	+	+	-	+	-
4% aqueous ferric chloride	Control	116	-	-	-	-	-
	Iontophoresis	117	++	++	++	++	-
1% aqueous copper sulphate	Control	99 a,b	-	-	-	-	-
	Iontophoresis	102	+++	++	++	++	+
4% aqueous copper sulphate	Control	103	-	-/+	-	-	-
	Iontophoresis	104 a,b	+++	+++	+++	+++	++
8% aqueous copper sulphate	Control	105	-	+	-	-	-
	Iontophoresis	106 a,b	+++	+++	+++	+++	+++
12% aqueous copper sulphate	Control	107	-	-/+	-	-	-
	Iontophoresis	108	+++	+++	+++	+++	++

concentration of lanthanum nitrate is regarded as unimportant in terms of initiating skin penetration by lanthanum. Instead, these results confirm the impermeable nature of the skin to this particular electron-dense tracer.

In turn, aqueous solutions containing 2%, 4% and 8% silver nitrate were subjected to positive iontophoresis using a current of 30 mA for a duration of 15 minutes. The solutions were also applied locally to the surface of the skin without iontophoresis for 15 minutes (controls). The extent of the penetration of silver ions from the 2% (Figure 87 a - c), 4% (Figure 89 a - c) and 8% (Figure 91 a - c) solutions was the same in the control experiments. Following iontophoresis, however, the tracer was evident in the upper corneal layers of the epidermis when presented from a 2% solution (Figure 88 a - c), in the epidermis and the follicular infundibula when presented from a 4% solution (Figure 90 a - e), and in the epidermis, the follicular infundibula and the sebaceous glands when presented from 8% solution (Figures 92 a - c). Furthermore, the electrodeposition of silver in the skin was heavier from the 8% than from the 2% or 4% solution.

When ferric chloride was introduced from the same vehicle following iontophoresis, the metal tracer showed a better penetration when presented from a 4% (Figure 117) than from a 1% (Figure 115) solution. Without iontophoresis, the localization of the tracer in the skin sections was the same with a 1% (Figure 114 a and b) as with a 4% (Figure 116) solution.

Within the limits of these experiments, the above results indicate that a change in the concentration of silver nitrate or ferric chloride does not appear to alter the penetration of the tracer when aqueous solutions of these metal salts are applied to the skin for a short duration of time without the flow of a current. With iontophoresis, however, an increase in the concentration of the tracers results in an enhancement of their penetration. Similar results have been reported by several other workers using iontophoresis (Abramson and Alley, 1937; Erlanger, 1939; O'Malley and Oester, 1955). However, in these experiments the extent of penetration was judged simply by the rapidity of the development of a pharmacological response or by the detection of radioactivity in organs (liver and kidney) and fluids (blood and urine) of the body.

Finally, experiments were carried out to further validate the relationship between concentration and the extent of penetration following iontophoresis and local application by varying the concentration over a wide range. Copper sulphate was prepared in distilled water to four concentrations, namely, 1%, 4%, 8% and 12%, and these solutions were subjected to positive iontophoresis with a fixed current intensity (30 mA) for a fixed duration of application (15 minutes). By doing so, as with other tracers, differences in the extent of penetration could be attributed to the one variable which was the change in concentration of the penetrant.

The results indicate that the ranking order in terms of the extent of penetration of copper ions is as follows:

8% (Figure 106 a and b) > 12% (Figure 108) > 4% (Figure 104 a and b) > 1% (Figure 102).

This is equivalent to saying that the penetration is increased as the concentration of copper sulphate is increased from 1% to 4% and from 4% to 8%. When the concentration is increased further to 12%, there is a reduction in penetration as compared to that seen with the 8% solution. Without the flow of current, the penetration of the metal ions from these solutions is similar (Figures 99 a and b, 103 and 107), although with the 8% solution (Figure 105) copper reaction was more evident in the upper parts of the follicular infundibula.

From these findings and those of methylene blue, it may be concluded that the extent of penetration of ionic tracers into and through the skin by iontophoresis is directly proportional to the concentration of the penetrating ion in the presenting vehicle until a particular "critical" value of concentration is reached, over and above which penetration becomes inversely proportional to the concentration of the penetrant ion. For copper this critical concentration appears to be at or around 8% when the tracer is prepared as aqueous copper sulphate solutions, while for methylene blue introduced from distilled water this critical concentration appears to be at or around 2%. The results reported here are in substantial agreement with those of Skog and Wahlberg (1964) who, by means of *in vivo* disappearance measurements and by organ analysis, found that the penetration of metal ions from radioactive metal compounds in aqueous solutions increased with increasing concentration up to a maximum value which appeared to be characteristic for each metal, and that the penetration diminished gradually thereafter as the concentration was further increased. Similar observations were reported by Blank (1964) who carried out an investigation on the penetration of a non-ionic alcohol (pentanol) from a non-ionic vehicle (olive oil) by means of a

diffusion chamber. He found that the flux of pentanol was nearly a straight-line function of concentration up to a particular value (IM), and that as the concentration of pentanol was increased above this value the flux did not continue to rise but levelled off and finally decreased as the concentration was further increased. A possible explanation for this pattern of penetration was provided by Blank (1969) who indicated that the initial increase in flux when the concentration of pentanol was increased initially was a result of adherence to Fick's law of diffusion (see page 44) and that this held only for relatively weak solutions. As the concentration of the penetrant became higher the forces of attraction between the penetrant molecules also became higher and this tended to prevent the transfer of the penetrant to the skin. In other words, the partition coefficient between the stratum corneum and the vehicle decreased as a result of a change in the chemical activity of the penetrant in the applied vehicle. This decrease in the partition coefficient resulted in a reduction in the concentration of the penetrant in the stratum corneum and hence the flux decreased in spite of the high concentration of the penetrant in the vehicle. However, since pentanol and olive oil are non-ionic, it is not clear if the same argument, that is an increase in penetration in accordance with Fick's law with a subsequent decrease in penetration due to a decrease in partition coefficient, can be applied to the penetration of metal ions such as copper ions and organic ions such as methylene blue when these are applied to the skin surface from an aqueous vehicle at different concentrations with iontophoresis. Certainly in accordance with Fick's law, Tregear (1966) reported that the penetration of potassium ions from an aqueous potassium chloride solution through excised rabbit skin increased as the concentration of the electrolyte

increased from 0.01 to 1.0%. Wahlberg *et al.* (1961) presented data showing that Fick's law held for mercuric ions applied from mercuric chloride solution to the skin of the guinea pig when the concentration of the electrolyte was varied from 0.1 to 1.0%. The proportionality between penetration rate and concentration (Fick's law) however, breaks down when a high concentration of the penetrant is applied to the skin. This break-down was believed to be a result of the interaction between the penetrant ions and the skin (Wahlberg and Skog, 1962). Blank and Gould (1961), however, reduced the protein-binding of ionic surfactants in different ways and found that there was no increase in penetration and concluded that protein-binding was not a major mechanism by which the skin regulated the penetration of ionic materials. Another possible explanation for the variation in penetration as the concentration is varied was provided by McEwan Jenkinson *et al.* (1974) who reported that the variation in the penetration of methylene blue following iontophoresis may be due to differences in the degree of ionization as the dye was prepared at different concentrations.

The process of dissolution of ionic compounds is essentially one of separation of the ions that are associated in the solid by the reduction of the strong electrostatic forces between the ions. When an ionic compound is dissolved in water, for example, the hydrogen (positive) side of a polar water molecule is strongly attracted to the anion at the surface of the solid and the oxygen (negative) side of a water molecule is strongly attracted to the cation at the surface of the solid. The water molecules surround individual cations and anions at the surface of the crystal thereby reducing the strong inter-ionic forces of attraction that bind the ions together in the crystal and



thus permitting them to move off into the water as hydrated ions. Several water molecules become associated with each ion in solution as a result of the electrostatic attraction between the charged ions and the dipole of the water, and such an attraction is referred to as an ion-dipole attraction.

Although the forces of inter-ionic attraction in solution are very greatly reduced by hydration of ions, they are not completely nullified, giving rise thereby to "residual" inter-ionic attraction by which a positive and a negative ion may actually touch, giving a solvated unit called an ion pair. The more dilute the solution, the greater the separation of oppositely charged ions and the less the residual inter-ionic attraction. Conversely, the higher the concentration of the ionic compound in the solvent, the less is the separation of the ions and the more the residual inter-ionic attraction. Thus, it may be postulated that the enhanced penetration of ionic tracers such as methylene blue and copper ions as the concentration of the tracer substances (methylene blue chloride and copper sulphate) is increased initially is probably due to the increased number of ions repelled by the iontophoresis electrode. The reduced penetration of ionic tracers as the concentration of the tracer substances becomes sufficiently high is probably due to a reduction of the rate at which the ions are repelled by the iontophoresis electrode, the so-called retarding or drag effect (O'Malley and Oester, 1955), as a result of a marked increase in the residual inter-ionic forces of attraction between the ions in solution due to ions aggregation. Furthermore, the more concentrated the solution of an electrolyte substance, the poorer the conductance of

the solution. For clinical purposes, therefore, it is more desirable to use weak solutions during iontophoresis (Harris, 1959).

#### 4.10 The effect of aprotic solvents on skin penetration by iontophoresis

Dimethyl sulphoxide (DMSO) was selected in the present study as a representative of this class of materials as it is the most widely known penetration accelerant through the skin *in vivo* and *in vitro* of numerous substances (Stoughton and Fritsh, 1964; Kligman, 1965a,b; Elfbaum and Laden, 1968a; Allenby *et al.*, 1969a,b; Sekura and Scala, 1969). DMSO exhibits an unusual concentration dependence in that a particular value of DMSO concentration (50-70%) is necessary before skin permeability is enhanced or the penetration rate of DMSO itself can be measured (Allenby *et al.*, 1969a; Sekura and Scala, 1969; Idson, 1975).

However, unlike the afore-mentioned reports, the effect of DMSO on skin penetration by iontophoresis has not been investigated. Since DMSO is miscible with water and is capable of bringing into solution a large variety of substances, including metal salts (Scheuplein and Bronaugh, 1983), the effect of making DMSO a constituent of the vehicle on the penetration of metal tracers into the skin by iontophoresis was tested. Lanthanum nitrate, silver nitrate and ferric chloride were prepared in 60% DMSO in water to a concentration of 1%, 2% and 4% respectively. Copper sulphate was prepared in 30% DMSO in water to a concentration of 4%. These solutions were applied locally or introduced by standard positive iontophoresis and the results compared with those obtained from similar experiments in which

water alone was used as the vehicle. These results are summarized in Table 4.14.

Following positive iontophoresis, the incorporation of DMSO in the vehicle results in a heavy electrodeposition of lanthanum on the surface of the skin, but does not render the skin permeable to the tracer (Figure 82 a - c). However, the failure of lanthanum to penetrate into the skin from the DMSO/water vehicle cannot be attributed wholly to a non-accelerant action of DMSO since the tracer does not penetrate into the skin when presented under similar conditions but from water alone. (Figure 79 a - c).

The extent of silver penetration into the stratum corneum following iontophoresis from a DMSO/water vehicle (Figure 93a) is not significantly different to that seen when the tracer is introduced from water alone (Figure 88a). The addition of DMSO results in a heavier deposition of silver in the superficial corneal layers, but the two deepest corneal layers are devoid of electron-dense material when the tracer is presented from either vehicle. Although silver is seen mixed with remnants of sebum in the pilary canal and on the surface of the stratum corneum when the tracer is presented from the DMSO/water vehicle (Figure 93b), no penetration is evident into the follicular canal epidermis or into the sebaceous glands when either vehicle is used (Figures 93b, 93c, 88b and 88c).

It is apparent from Figures 103 and 109 that the localization of copper in the skin following topical application is the same when the tracer is introduced from water alone or from water and DMSO. Furthermore, there is no significant difference in the extent of

Table 6.14 Effect of DMSO on skin penetration by iontophoresis using a current of 30 mA over a duration of 15 minutes

Solution	Type of experiment	Figure	Extent of penetration				
			Epidermis	Hair follicles	Sebaceous glands	Dermis	Epidermis and deeper tissues
1% lanthanum nitrate in water	Iontophoresis	79 a-c	-	-	-	-	-
1% lanthanum nitrate in DMSO/water vehicle	Iontophoresis	82 a-c	-	-	-	-	-
2% silver nitrate in water	Iontophoresis	88 a-c	+	-	-	-	-
2% silver nitrate in DMSO/water vehicle	Iontophoresis	93 a-c	+	+	-	-	-
4% copper sulphate in water	Control	103	-	-/+	-	-	-
4% copper sulphate in DMSO/water vehicle	Iontophoresis	104 a,b	+++	+++	+++	+++	++
4% ferric chloride in water	Control	109	-	-/+	-	-	-
4% ferric chloride in water	Iontophoresis	110	+++	+++	+++	+++	++
4% ferric chloride in DMSO/water vehicle	Control	116	-	-	-	-	-
4% ferric chloride in DMSO/water vehicle	Iontophoresis	117	++	++	++	++	-
4% ferric chloride in DMSO/water vehicle	Control	118	-	-	-	-	-
4% ferric chloride in DMSO/water vehicle	Iontophoresis	119	++	++	++	++	-

copper penetration into and through the skin and the subcutaneous tissue when the tracer substance is prepared in the DMSO/water vehicle (Figure 110) or in water alone (Figure 104 a and b) following iontophoresis.

The localization of ferric iron following local application is the same whether the tracer salt is introduced from water (Figure 116) or from a 60% aqueous DMSO solution (Figure 118) in that in both cases the tracer is visible on the surface of the skin only. Following iontophoresis, the extent of penetration of the metal tracer into and through the skin is similar from a 60% aqueous DMSO solution (Figure 119) to that seen when the tracer is introduced from water alone (Figure 117). Having said that, a very weak reaction for iron was seen in the lower follicular walls when the tracer is presented from the DMSO/water vehicle as compared to no reaction when presented from water alone.

These results suggest that the addition of DMSO to the vehicle may be considered insignificant with respect to increasing the penetration of metal ions into and through the skin. There are at least four possible explanations for the non-accelerant action of DMSO as used in the present study. Firstly, the flow of current had no effect on the penetration of DMSO itself through the skin and thus no enhancement of penetration of tracers incorporated with the DMSO was observed. Secondly, the concentration of DMSO was not high enough to allow the aprotic solvent to exert its marked effect on the skin. This includes the displacement of bound water from the stratum corneum and its substitution by a looser, less associated solvent-protein structure (Scheuplein, 1978), the swelling and expansion of the protein fibres

in the stratum corneum (Elfbaum and Laden, 1968b) and lipid extraction (Elfbaum and Laden, 1968c). Sekura and Scala (1969) and Idson (1975) reported that local application of 50% to 70% was required to alter the permeability of the skin, whilst Scheuplein and Bronaugh (1983) have suggested that solvent proportions of DMSO in excess of 80% to 90% (almost pure DMSO) are necessary before skin permeability is appreciably enhanced. Thirdly, the redeposition of any substance extracted from the tissue as a result of evaporation of DMSO during its application (Scheuplein and Ross, 1970). Fourthly, the duration of contact was not long enough. For example, Elfbaum and Laden (1968c) only observed enhanced penetration of methylene blue from 80% DMSO after 24 hours of local application.

In conclusion, the present study has shown that the application of 30% and 60% DMSO as a constituent of the vehicle does not result in a substantial enhancement of penetration of metal ions, even following iontophoresis at 30 mA for 15 minutes.

#### **4.11 The effect of detergents on skin penetration by iontophoresis**

The effect of incorporating a detergent with a tracer in solution on the penetration of the tracer into the skin by iontophoresis was investigated. In order to select a suitable detergent for penetration trials a simple qualitative method was carried out which consisted of adding solutions of various detergents to the tracer in solution to see if precipitation occurred. Detergents which caused precipitation were eliminated. The non-ionic detergent tween 20 was found to be suitable for lanthanum penetration trials, while the anionic detergent



sodium lauryl sulphate was found to be suitable for copper penetration trials. The results obtained are summarized in Table 4.15.

The localization of lanthanum in ultrathin sections of skin subjected to positive iontophoresis at 30 mA for 15 minutes is the same with (Figure 83 a - c) or without (Figure 79 a - c) the addition of tween 20 to the aqueous lanthanum solution. In both cases electron-dense deposits are present on the surface of the skin, but do not extend deeper into the stratum corneum or into the body of the sebaceous glands. EDX analysis confirmed the superficial localization of lanthanum in tissue sections from both experiments. From these results it appears that the addition of tween 20 to lanthanum in solution has no effect on the impermeability of the skin to the electron-dense tracer. It is not unreasonable to suggest that in this case the flow of the current had no effect on the detergent itself because of its non-ionic nature. This result is in agreement with the view that non-ionic surfactants interact weakly with the skin and have little effect in promoting skin penetration (Scheuplein and Blank, 1971; Idson, 1975) or in promoting penetration through other biological tissues (Kawamura and Takala, 1961) following local application.

In contrast, other work has indicated that local application of anionic surfactants *in vitro* greatly increases the permeability of the skin. Bettley (1961) reported that exposure of isolated epidermis to 1% potassium palmitate in solution for a duration of 1-3 weeks markedly increased the permeability of the tissue to glucose and salicylate. Scheuplein and Ross (1970) demonstrated that treatment of isolated epidermis with 5% sodium lauryl sulphate for a duration of

Table 4.15 Effect of detergents on skin penetration by iontophoresis

Solution	Type of experiment	Figure	Extent of penetration				
			Epidermis	Hair follicles	Sebaceous glands	Dermis	Hypodermis and deeper tissues
1% lanthanum nitrate in water	Iontophoresis <sup>a</sup>	79 a-c	-	-	-		
	Iontophoresis <sup>a</sup>	83 a-c	-	-	-		
4% copper sulphate in water	Control	103	-	-/+	-	-	-
	Iontophoresis <sup>a</sup>	104 a, b	+++	+++	+++	+++	+++
	Control	111	-	-/+	-	-	-
4% copper sulphate + 0.5% SLS in water	Iontophoresis <sup>b</sup>	112	+++	+++	+++	++	+

a = positive iontophoresis  
 b = negative iontophoresis followed by positive iontophoresis

over 6 hours resulted in increased skin permeability to tritiated water. Below 6 hours no increase in permeability was observed with sodium lauryl sulphate, but with 5% sodium laurate an increase in skin permeability was observed after 2 hours of exposure only. Similarly, Frosch *et al.* (1980) observed *in vivo* a significant increase in penetration of dimethyl sulphoxide (DMSO) through intact human skin of sensitive subjects following local application of a 5% sodium lauryl sulphate solution for a duration of 24 hours by means of sealed chambers. The accelerating action of anionic detergents is a result of damage inflicted on the stratum corneum (the barrier layer) by the detergent. This damage consists of protein denaturation, membrane expansion, increased porosity of the tissue and loss of water-binding capacity (Scheuplein and Ross, 1970). After penetration of the barrier layer the anionic detergents can then damage the viable cells (Smeenk, 1969). That the permeability of the skin increases as the concentration of anionic detergents in the presenting vehicle is increased, or as the duration of contact with the skin is increased, has also been demonstrated previously (Bettley, 1961; Scheuplein and Ross, 1970). Ionic surfactants also enhance the permeability of other biological tissues such as the oral mucous membranes (Kawamura and Takata, 1961). It is clear that the enhanced penetration following local application reported by Bettley (1961), Scheuplein and Ross (1970) and Frosch *et al.* (1980) only developed after the skin had been exposed to the anionic detergents in solution over long periods of time. In all the afore-mentioned reports, the skin was exposed to the detergent in solution without iontophoresis.

Reports describing the effect of ionic detergents on skin penetration by iontophoresis are rare. Pereyra (1945) reported that the addition

of anionic detergents, including sodium lauryl sulphate, to copper sulphate in solution resulted in a substantial increase in the penetration of copper ions through the skin. In view of this, experiments were carried out to investigate this effect of anionic detergents on skin penetration by iontophoresis. An aqueous solution containing 4% copper sulphate and 0.5% sodium lauryl sulphate (SLS) was prepared and subjected firstly to negative iontophoresis using a current intensity of 30 mA for 5 minutes to take account of the anionic nature of the detergent. This was followed by positive iontophoresis using a current intensity of 30 mA for 15 minutes to take account of the cationic nature of the tracer. The extent of penetration of the tracer was compared to a similar experiment in which no detergent had been added. The results obtained are shown in Table 4.15.

The penetration of the tracer following topical application is similar from the SLS-tracer solution (Figure 111) to that seen from water alone (Figure 103), and in both cases the penetration is minimal. Although the extent of penetration of the tracer into and through the skin and the underlying tissues from the SLS/copper sulphate solution following negative/positive iontophoresis (Figure 112) is not significantly different to that seen when the tracer is introduced from water alone with direct positive iontophoresis (Figure 104 a and b), the reaction for copper in the skin is more intense when presented from water alone. This may indicate that the penetration of the tracer is slightly reduced, rather than enhanced, by the addition of the detergent possibly as a result of inter-ionic attraction between the copper cations and the lauryl sulphate anions.

It seems reasonable to assume that if a solution containing SLS is placed on the surface of the intact skin for a duration of 15 minutes, or is subjected to negative iontophoresis with a current of 30 mA over a duration of 5 minutes, penetration of the detergent into the stratum corneum at least will be necessary for it to exert its enhancement effect on the penetration of metal ions incorporated with it in the presenting vehicle. Since no enhanced penetration of copper was observed, the possibility remains that little (if any) of the lauryl sulphate anion as used in the present study penetrated the skin and thus the tissue was not affected by the detergent.

Pereyra (1945) found, firstly, that the addition of any one of the three anionic detergents which he investigated (sodium lauryl sulphate, dihexyl sodium sulfosuccinate and diamyl sodium sulfosuccinate) at a concentration of 1% to an aqueous solution containing 1% copper sulphate resulted in a significant increase in the penetration of the metal tracer from the surface into the skin and the penile tissues of the rabbit when subjected to direct positive iontophoresis using a current of 5 mA over a duration of 15 minutes. He also found, secondly, that no penetration occurred when the copper sulphate was introduced by the same iontophoresis but without the addition of the anionic detergent. He explained that the increased penetration of the tracer was the result of the prevention of chemical interaction between the copper ions and tissue proteins and that this prevention was brought about by the detergent. Inconsistent with this, Blank and Gould (1961) attempted subsequently to prevent binding of ionic material (anionic detergents) by the proteins of the stratum corneum by increasing the alkalinity of the vehicle, by using a 60% acetone solution which contained an electrolyte with a divalent cation

as a vehicle for the anionic surfactant, by pretreating the skin on the epidermal side with formaldehyde to block the amino groups, by pretreating the skin on the epidermal side with acetic anhydride in order to acetylate the amino groups and by saturating the amino groups with excess surfactant. They came to the conclusion that the ability of the proteins in the stratum corneum to bind ionic materials was not one of the major mechanisms whereby the skin prevents the penetration of these materials. Furthermore, it is hard to explain the penetration into the skin of negatively-charged ions such as lauryl sulphates from the positive electrode which was observed by Pereyra (1945). Moreover, the present study has demonstrated copper penetration with iontophoresis from aqueous copper sulphate solutions of different solute concentrations without the addition of detergents (Figures 100, 101, 102, 104, 105 and 107).

In conclusion, the present results show that no accelerating action on the penetration of copper ions into the skin results from the addition of sodium lauryl sulphate to the tracer in solution when the detergent is: (1) applied at a low concentration (0.5%) and the tracer/detergent solution is left in contact with the surface of the intact skin for a short period of time (15 minutes), (2) subjected to negative iontophoresis with a low current density (30 mA/5 minutes), or (3) remains in solution while the cationic tracer is being subjected to standard positive iontophoresis (30 mA/15 minutes).

#### 4.12 Effect of organic solvents on skin penetration by iontophoresis

The stratum corneum lipids are located in the intercellular substance, the plasma membranes and the intrafibrillar and intrafilamentous



matrix of keratin (Wheatley and Flesch, 1967). It seems clear that the lipid component of the stratum corneum is essential for its barrier properties (Goldsmith and Baden, 1970; Scheuplein and Black, 1971; Elias, 1981). In addition, Kitson and Van Lennep (1984) have also suggested that a barrier function is provided by sebum in the follicular infundibulum. Many investigators have shown that prolonged exposure of isolated skin or stratum corneum to lipid solvents greatly alters the membrane permeability. For example, Blank and Gould (1961) showed that none of the synthetic anionic surfactants which they used penetrated normal excised skin, whereas penetration occurred after the skin had been incubated in ethanol (95%), acetone (100%) or in a mixture of ethanol:ethyl ether (1:9) for a duration of 72 hours. In a similar study, Blank *et al.*, (1964) showed that little, if any, of the cationic detergent benzalkonium chloride penetrated normal excised skin, whereas following treatment with ethanol, acetone or an ethanol-ethyl ether mixture for a duration of 65-92 hours, the impermeability of the skin to the detergent decreased and thus penetration occurred. Scheuplein and Ross (1970) illustrated an increase in water permeability after excised stratum corneum had been held in continuous contact for a duration of up to 7 hours with ethanol, acetone, ether or a 2:1 chloroform:methanol mixture. The lipid solvent mixture had the largest effect because it was capable of extracting bound polar lipids and proteolipids as well as neutral lipids. Further support for the role of lipids in skin permeability is provided by studies which indicate that the barrier function is substantially, if not completely, restored when the extracted lipids are re-incorporated into the tissue (Onken and Moyer, 1963).

In view of the above reports, a study has been undertaken with the object of determining the effect of using absolute ethanol as an alternative vehicle to distilled water on skin penetration by organic and inorganic tracers when solutions of these are applied to the skin surface with or without iontophoresis. Ethanol was selected in preference to other lipid solvents because it is capable of bringing into solution many organic and inorganic electrolytes.

Methylene blue, eosin, lanthanum nitrate and ferric chloride were prepared, each to a fixed concentration, in absolute ethanol and in distilled water and applied to the surface of the skin with or without iontophoresis. The extent of penetration of each tracer from both vehicles is summarized in Table 4.16. Eosin was subjected to negative iontophoresis, while the others were subjected to positive iontophoresis.

Without the flow of current, there appeared to be some enhancement of penetration when methylene blue was presented from the alcohol (Figure 39 a - c) as compared to that obtained from the aqueous vehicle (Figure 1 a - d). Following iontophoresis using a current of 30 mA over a duration of 15 minutes, the penetration of methylene blue from the alcohol (Figure 43) was as deep as that seen from water (Figure 19), but the staining was more intense from the alcohol. At lower values of current intensity and duration of application, the penetration was slightly enhanced when the dye was presented from the alcohol (Figures 40, 41 and 42) than from water (Figures 2, 6 and 10).

Eosin showed a better penetration when presented to the skin surface from absolute ethanol (Figure 60) than from water (Figure 58)

4.16 Penetration of organic and inorganic materials from absolute ethanol and water by iontophoresis

Solution	Figure	Current (mA)	Duration (min)	Extent of penetration					
				Epidermis	Hair follicles	Sebaceous glands	Dermis	Hypodermis	
2% methylene blue in water	1	0	15	-	-	-	-	-	
	2	5	5	-/+	-/+	-	-	-	
	6	10	10	++	+	+	+	+/+	
	10	15	15	+++	++	++	++	+/+	
	15	30	15	+++	+++	+++	+++	+++	
2% methylene blue in alcohol	39	0	15	+	-/+	-	-	-	
	40	5	5	+	+	+	+	-	
	41	10	10	++	++	++	++	-/+	
	42	15	15	+++	+++	+++	+++	+	
1% eosin in water	43	30	15	+++	+++	+++	+++	+++	
	57	0	15	-	-	-	-	-	
1% eosin in alcohol	58	30	15	-/+	+	-/+	-	-	
	59	0	15	-	-	-	-	-	
1% lanthanum nitrate in water	60	30	15	-/+	+++	+++	-/+	-	
	78 a-d	0	15	-	-	-	-	-	
1% lanthanum nitrate in alcohol	79 a-c	30	15	-	-	-	-	-	
	84 a, b	0	15	++	++	-/+	-	-	
4% ferric chloride in water	85 a-d	30	15	++	++	++	++	++	
	116	0	15	-	-	-	-	-	
4% ferric chloride in alcohol	117	30	15	++	++	++	++	++	
	120	0	15	-	-	-	-	-	
4% ferric chloride in alcohol	121 a, b	30	15	++	-/+	+/+	+/+	+/+	

following negative iontophoresis, whereas the dye penetration from either vehicle was the same without the use of a current (Figures 57 and 59).

The localization of lanthanum in the ultrathin sections was the same whether the tracer was applied to the skin from water without iontophoresis (Figure 78 a - d), introduced by iontophoresis from distilled water (Figure 79 a - c) or applied to the skin from absolute ethanol without iontophoresis (Figure 84 a and b). In all these cases, lanthanum was seen as electron-dense deposits over the surface of the skin. When introduced from absolute ethanol with iontophoresis, however, lanthanum was able to penetrate into and through the epidermis, gaining access to regions from which it is normally excluded. The tracer was evident in the full extent of the stratum corneum of the epidermis (Figure 85a) and the follicular infundibulum (Figure 85b). Furthermore, the tracer was visible in the viable layers of the infundibulum, but the penetration of lanthanum into the sebaceous glands could not be confirmed clearly (Figure 85 c and d). This is the only instance in which the tracer was seen throughout the corneum and in the viable epidermal layers. Since no such penetration was observed when the tracer was applied to the skin from the alcohol without the flow of the current, it is possible that iontophoresis has facilitated the tracer penetration. Equally, since no penetration was observed when the tracer was introduced by the same iontophoresis but from water, it is possible that the alcohol has rendered the skin permeable to lanthanum. This is equivalent to saying that the penetration of lanthanum has resulted from both the use of alcohol as the vehicle and iontophoresis as the driving force.

As judged by the localization of the reaction for ferric iron in unfixed cryostat sections, there appeared to be a slight enhancement of penetration when the tracer was introduced from absolute ethanol (Figure 120) than from water (Figure 116) following topical application. Following iontophoresis, there was a marked enhancement of penetration from the alcohol (Figures 121 a and b) than from water (Figure 117).

The present study has shown therefore that ethanol can alter the permeability of skin *in vivo* following a short duration of contact (15 minutes) but with iontophoresis in that there is enhanced penetration of methylene blue, eosin, lanthanum and ferric iron from the alcohol as compared to water. This enhancement of penetration, however, is accompanied by severe morphological changes (Figure 85 a - d) which include a marked reduction in the thickness of the epidermis, severe condensation and elongation of nuclei and cytoplasm in the viable epidermal cells and in the sebaceous glands, a marked thinning of the individual corneal cells and widening of the intercellular spaces. These changes are also present, though less marked, when water is used as the vehicle (Figure 79 a - c). The results in the present study are in agreement with those of Harpuder (1948) who reported enhanced penetration of ions following iontophoresis by the use of alcohol, a significant difference being that Harpuder used alcohol at a concentration of 80 % while in the present study absolute ethanol was used.

The enhanced permeability of skin when the alcohol is used as the vehicle is probably due to the extraction of lipoidal substances from the skin (Flesch, 1962; Malkinson, 1965; Bettley, 1970), and this is

facilitated by the use of the current since no marked enhancement of penetration is evident without iontophoresis. Another possible explanation for the enhanced penetration is the more favourable partitioning of tracers from ethanol than from water to the skin, that is, the more favourable tissue-vehicle partition coefficient which is a measure of the relative solubility of the tracer in the tissue and the presenting vehicle (Blank, 1964; Bronaugh and Franz, 1986). Reducing the water content of the stratum corneum by dehydrating agents such as ethanol, reduces the corneum's plasticity and enhances its permeability (Malkinson, 1965).

#### **4.13 Physico-chemical factors influencing skin penetration by iontophoresis**

The major motivation of this section is to relate the contributions of the physico-chemical properties of a tracer substance to the extent of penetration of the tracer into and through the skin by iontophoresis. These physico-chemical properties include the solubility characteristics of the test material, the polarity of the test material, the diffusivity of the test material, the pH of the test solution, the size of the hydrated ion, and the ionic and molecular weights of the penetrant.

##### **4.13.1 Solubility characteristics of the penetrant**

It has long been recognised that the solubility characteristics of a substance greatly influence the ability of that substance to penetrate biological membranes. A certain degree of solubility in both lipids and water is thought to favour penetration (Rothman, 1943; Blank and



Scheuplein, 1964; Malkinson, 1964; Wills 1969; Winkelmann, 1969). Hence a number of cationic and anionic dyes with different solubilities in water and organic solvents have been used to study the relation between the solubility characteristics and the extent of penetration of the dyes into the skin following local application and iontophoresis. The dyes were prepared in water and/or absolute ethanol according to their solubility properties. In accordance with the polarity, cationic dyes were presented to the skin with positive iontophoresis while anionic dyes were presented to the skin with negative iontophoresis. All the solutions of the dyes were subjected to standard iontophoresis, that is using a current intensity of 30 mA over a duration of 15 minutes.

The extent of penetration of the cationic dyes is presented in Table 4.17, and the extent of penetration of the anionic dyes is shown in Table 4.18. Also included in these tables are the solubility values of each dye in different solvents (Gurr, 1960).

From Tables 4.17 and 4.18 it appears that not all the ionic dyes penetrated the skin following iontophoresis, and that when penetration does occur the extent of penetration into and through the skin varies with different dyes. These variations may at least in part be related to the solubility characteristics of the dyes. Of all the dyes tested, methylene blue, toluidine blue, eosin water- and alcohol-soluble and chrysoidin Y show the most effective penetration, and these dyes are characterized by good solubilities in water and in organic solvents. Dyes with a good solubility in organic solvents and a moderate solubility in water (picric acid), and dyes with a good solubility in water and a moderate solubility in organic solvents

Table 4.17 Penetration of cationic dyes into the skin

Dye	Solution	Type of Experiment	Figure	Extent of penetration						Approximate % solubility at 15° C			
				Dermis	Hair follicles	Sebaceous glands	Dermis	Hypodermis	Water	Organic solvents		Ethylene glycol (anhydrous)	
Methylene blue	2% in water	Control	1 a-d	-	-	-	-	-	9.5	6.0	6.5	10.0	
		Iontophoresis	19	+++	+++	+++	+++	+++					
	2% in ethanol	Control	39	+	-/+	-	-	-					
		Iontophoresis	43	+++	+++	+++	+++	+++					
Toluidine blue	2% in water	Control	44	-	-	-	-	-	3.25	1.75	3.5	5.5	
		Iontophoresis	46	+++	+++	+++	+++	+++					
		Control	47	-	-	-	-	-	9.5	0.5	1.85	4.35	
Pyronin Y	2% in water	Iontophoresis	48	++	+	-/+	+	-					
		Control	49	-	-	-	-	-					
Aniline blue alcohol-soluble	1% in ethanol	Iontophoresis	50	-	-/+	-	-	-	NIL	1.5	2.0	4.0	
		Control	51	-	-	-	-	-					
Chrysoidin Y	2% in water	Iontophoresis	52	++	++	++	++	++	5.5	4.75	6.0	9.5	

Table 4.18 Penetration of anionic dyes into the skin

Dye	Solution	Type of experiment	Figure	Extent of penetration						Approximate $\lambda$ solubility at 15° C			
				Epidermis	Hair follicles	Sebaceous glands	Dermis	Hypodermis	Gaver	Organic solvents	Cellulosive glycol (anhydrous)	Ethylene glycol (anhydrous)	
Rosin (7), water-soluble	4% in water	Control	53	-	-	-	-	-	-	44.0	2.0	25.0	27.5
		Iontophoresis	54	++	-/+	-	-	-	-				
Eosin (ethyl), alcohol-soluble	0.5% in in ethanol	Control	55	-	-	-	-	-	-	NH1	1.0	2.25	1.0
		Iontophoresis	56	+	-/+	-	-	-	-				
Eosin (methyl), water- and alcohol-soluble	1% in water	Control	57	-	-	-	-	-	-	10.0	7.5	5.0	8.0
		Iontophoresis	58	-/+	+	-/+	-	-	-				
		Control	59	-	-	-	-	-	-				
		Iontophoresis	60	-/+	+++	++	-/+	-	-				
Methylene blue water-soluble	5% in water	Control	61	-	-	-	-	-	-	50.0	NH1	4.5	7.8
		Regressive Iontophoresis	62	-	-	-	-	-	-				
		Positive Iontophoresis	63	-	-	-	-	-	-				
Picric acid	6% in ethanol	Control	64	-	-	-	-	-	-	1.2	9.0	15.0	5.6
		Iontophoresis	65	++	++	++	+	+	+				
Alizarin red S	1% in water	Control	66	-	-	-	-	-	-	5.5	0.1	1.75	2.25
		Iontophoresis	67	-/+	+	-	-	-	-				
Trypan blue	0.5% in water	Control	68	-	-	-	-	-	-	1.0	0.02	2.10	7.15
		Iontophoresis	69	-/+	-	-	-	-	-				

(alizarin red S, pyronin Y and eosin water-soluble) show moderate penetrations. Dyes with a good solubility in water but which are only slightly soluble or insoluble in organic solvents (aniline blue water-soluble) and dyes with a good solubility in organic solvents but which are only slightly soluble (trypan blue) or insoluble (eosin alcohol-soluble and aniline blue alcohol-soluble) in water show the least effective or no penetration. It is interesting to note that ionic dyes such as patent blue, basic fuchsin, neutral red and acid fuchsin, which are reported to penetrate the skin following iontophoresis (Abramson and Gorin, 1940), are characterized by good solubilities in water and organic solvents (Gurr, 1960, 1971). Treherne (1956) studied the permeability through the skin of a wide variety of compounds including glucose, urea, glycerol, thiourea, methanol and ethyl iodide, and reported that of these substances those with an ether:water partition coefficient nearest to 1.0 were most readily absorbed. In other words, maximum permeability was expected from those compounds which had about equal ether- and water- solubility. Stoughton *et al.* (1960) investigated the penetration of nicotinic acid and seven closely related derivatives and also found a good correlation between penetration and the relative solubilities of the test materials in ether and water. The solubility of a test material in lipid solvents was considered to be a good model for its solubility in tissue lipids (Treherne, 1956; Stoughton *et al.*, 1960). However, Blank (1964, 1969) suggested strongly that skin penetration depended on the relative solubility of the test material in the stratum corneum and the vehicle, that is, on the tissue:vehicle partition coefficient. Test materials which are more soluble in the stratum corneum than in the vehicles in which they are prepared will preferentially pass from the vehicle into the tissue.

It has been reported that water-soluble substances traverse the stratum corneum via water-filled channels and that lipid-soluble substances traverse the corneum via lipid pathways (Blank, 1969; Goldsmith and Baden, 1970; Scheuplein and Blank, 1971; Hurley, 1975; Elias, 1981). Thus it may be inferred that dyes which are characterized by good solubilities in water and organic solvents can utilize both the water and the lipid pathways and thus show the most effective penetration following iontophoresis.

#### 4.13.2 pH of the test solution

Blank and Gould (1961) studied the penetration of laurate anions from buffered solutions as a function of pH changes (pH 7 - pH 12) of solutions containing sodium laurate. They reported that penetration occurred from solutions whose pH was below 8.5 or above 10.5, but that very little or no penetration occurred from solutions buffered in the 8.5 - 10.5 pH range. They also reported that penetration from solutions in the pH range of 7 to 8.5 was a result of an increase in the lipophilicity of the test material, whereas penetration from solutions whose pH values were above 10.5 was believed to be due to damage inflicted on the stratum corneum by their high alkalinity. Alkaline solutions with high pH values destroy the tissue by hydrolyzing the keratin (Allenby *et al.*, 1969a). On the other hand, Bettley (1965), in a study of the effect of detergents on the penetration of sodium and potassium ions, could find no correlation with pH. There is evidence to indicate that the pH of a solution changes after the solution is applied to the surface of the skin. For example the pH of an aqueous sodium laurate solution drops from 10.1 to 8.6 after 5 hours of topical application (Blank and Gould, 1961).

Table 4.19 (a - c) shows the pH values of solutions containing tracer substances and the extent of penetration of the tracers into and through the skin following iontophoresis using a current intensity of 30 mA over a duration of 15 minutes. The extent of penetration of all these tracers was negligible without the flow of current (Figures 78 a - d, 84 a and b, 87 a - c, 89 a - c, 91 a - c, 99a, 103, 105, 107, 109 and 111) and therefore this has been excluded from the Tables.

The pH was measured using a glass electrode digital pH meter (Model 7065, Electronic Instruments Ltd, Kent), at room temperature (approximately 18<sup>o</sup> C) just prior to the application of the solutions on to the surface of the skin.

The data presented in Table 4.19 a and b suggest that there is a relationship between the extent of penetration and the pH of the solution if the same tracer substance is prepared in the same vehicle. For example, when silver nitrate is prepared in distilled water to various concentrations, the penetration of silver ions increases as the pH of the solutions decreases from 5.92 to 5.56 (Table 4.19a). Similarly, when copper sulphate is prepared in distilled water to three concentrations, namely 1%, 4% and 8%, the penetration of copper ions increases as the pH of the solutions decreases from 4.46 to 3.71 (Table 4.19b).

Although the pH of aqueous lanthanum nitrate solutions decreases from 5.02 to 4.94 as the concentration of the solute is increased from 1% to 2%, the change in the pH in this case is very slight when compared to that seen for copper and silver. Furthermore, lanthanum nitrate in solution exists as a combination of  $\text{La}^{3+}$ ,  $(\text{La}(\text{NO}_2))^{2+}$  and  $(\text{La}(\text{NO}_3)_2)^+$ ,



Table 4.19a Extent of penetration of silver as a function of pH of the test solution

Solution	Figure	pH readings	Average pH	Extent of penetration		
				Epidermis	Hair follicles	Sebaceous glands
2% silver nitrate in water	88 a-c	5.87 5.88 6.00	5.92	+	-	-
4% silver nitrate in water	90 a-e	5.51 5.63 5.69	5.61	++	++	-/+
8% silver nitrate in water	92 a-c	5.48 5.61 5.60	5.56	++	+++	++

Table 4.19b Extent of penetration of copper as a function of pH of the test solution

Solution	Figure	pH readings	Average pH	Extent of penetration					
				Epidermis	Hair follicles	Sebaceous glands	Dermis	Hypodermis and subjacent tissues	
1% copper sulphate in water	102	4.58	4.46	+++	++	++	++	+	
		4.47							
		4.35							
4% copper sulphate in water	104	4.07	4.03	+++	+++	+++	+++	++	
		4.02							
		3.99							
8% copper sulphate in water	106	3.84	3.71	+++	+++	+++	+++	+++	
		3.81							
		3.49							
12% copper sulphate in water	108	3.60	3.67	+++	+++	+++	+++	++	
		3.72							
		3.69							
4% copper sulphate in DMSO/water vehicle	110	4.05	3.97	+++	+++	+++	+++	++	
		3.89							
		3.97							
4% copper sulphate 0.5% SLS in water	112	4.19	3.95	+++	+++	+++	++	+	
		3.91							
		3.75							

Table 4.13c Extent of penetration of lanthanum as a function of pH of the test solution

Solution	Figure	pH readings	Average pH	Extent of penetration		
				Epidermis	Hair follicles	Sebaceous glands
1% lanthanum nitrate in water	79 a-c	5.10 4.98 4.99	5.02	-	-	-
2% lanthanum nitrate in water	80 a-c	4.87 4.95 5.00	4.94	-	-	-
1% lanthanum nitrate, 20% tween 20 in water	83 a-c	2.98 3.01 2.96	2.98	-	-	-
1% lanthanum nitrate in ethanol	85 a-c	3.76 3.63 3.56	3.65	++	++	-/+

although the ratio of these ionic species is not known (Moeller, 1963). Therefore, the failure of lanthanum to penetrate even when the tracer concentration is increased may be attributed to the presence of the two ion-pair  $[(\text{La}(\text{NO}_3)_2)^+$  and  $(\text{La}(\text{NO}_3))^{2+}]$ .

In addition, there is a relationship between the extent of penetration and the pH of the solution when different tracer substances are prepared in the same vehicle to a fixed concentration. For example, the penetration of copper ions from a 4% aqueous copper sulphate solution (pH 4.03) is better than that of silver from a 4% aqueous silver nitrate solution (pH 5.61). A reduction in the pH value indicates that better ionization has taken place.

In contrast, it appears that the relationship between the extent of penetration and the pH of the solution does not always hold when:

(1) the same tracer substance is prepared in different vehicles. For example: (a) copper shows a better penetration when copper sulphate is applied to the surface of the skin from water (pH 4.03) than from a DMSO/water vehicle (pH 3.97) or water containing SLS (pH 3.95), even though the pH of the latter two solutions is slightly lower than that of the first. (b) variations in the pH do not render skin permeable to lanthanum when the tracer salt is prepared in water (pH 5.02) or in water containing tween 20 (pH 2.98). Contrary to these findings, however, penetration of lanthanum into the skin takes place when lanthanum nitrate is prepared in ethanol (pH 3.65) whereas the penetration of the tracer is negligible when it is prepared in water (pH 5.02).

(2) The pH of the same electrolyte changes over a wide range. For example, although the penetration of copper ions from aqueous copper

sulphate solutions increases as the pH originally decreases from 4.46 to 3.71, a further decrease in pH to 3.67 does not result in enhanced penetration. The variation of the pH was brought about by variation in the concentration of the solute in the solvent, and the effect of solute concentration on penetration is discussed elsewhere (page 332).

In summary, variations in the extent of penetration are observed as the pH of the solutions changes when a tracer substance is prepared in the same vehicle. These changes are brought about by changing the concentration of the solute in the solvent. Furthermore, there appears to be a relationship between the pH and extent of penetration when different tracer substances are prepared in the same vehicle to a fixed concentration. No consistent relationship, however, is observed when a tracer substance is prepared in different vehicles.

#### 4.13.3 Diffusivity of the test material

One factor which is known to influence the penetration of a test material is the ease with which the material diffuses through the skin. It has been shown that butanol, which contains one hydroxy group, penetrates the skin 100 times faster than 2,3-butanediol which contains two hydroxy groups (Blank *et al.*, 1967). The diffusion constant of progesterone is 30 times greater than that of cortisol (Scheuplein *et al.*, 1969). The cortisol molecule differs from the progesterone molecule by the presence of three hydroxyl groups which cause the diffusion constant of cortisol to drop (Blank, 1969). These results led Blank (1969) to conclude that as polar groups were added to the test material, forces of attraction between these groups and polar sites within the skin, in particular the stratum corneum,

increased and the diffusivity of the material, therefore, decreased. Kawamura and Takata (1960) investigated the penetration of sodium, potassium and calcium ions into and through the oral mucosa of the dog and reported that although the three cations were able to pass and accumulate in the oral mucosa, only the monovalent cations ( $\text{Na}^+$  and  $\text{K}^+$ ) were able to pass into the submucosa. The failure of the divalent cation ( $\text{Ca}^{2+}$ ) to do so was attributed to a strong binding between  $\text{Ca}^{2+}$  and the tissue substances.

In view of the above reports, it is possible that the number of polar groups or the ionic valency which a test material attains in solution influences its extent of penetration into the skin by iontophoresis since the rate of migration of an ion in an electric field depends on the value of the charge that it carries (Morris, 1971).

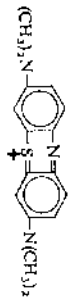
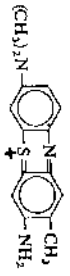
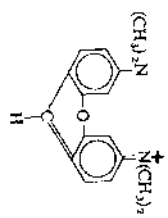
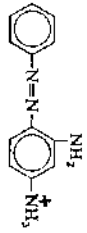
The extent of penetration of cationic and anionic dyes following standard positive and negative iontophoresis respectively, and the ionic structures of the dyes (Gurr, 1971) are shown in Table 4.20.

From Table 4.20, it appears that monovalent dyes (methylene blue, toluidine blue, pyronin Y, chrysoidine Y, picric acid and alizarin red S) are better penetrants than divalent (eosin BN and eosin Y) and polyvalent (aniline blue water-soluble) dyes. Thus it may be inferred that the extent of penetration may in part be related to the charge that the dye attains in solution.

The extent of penetration of inorganic cations following standard positive iontophoresis and the valencies of the cations are shown in Table 4.21. From this Table, it appears that  $\text{Cu}^{2+}$  has a better



Table 4.20 The extent of penetration of ionic dyes following standard iontophoresis as a function of their valency

Figure	Dye	Ionic structure	Valency	Extent of penetration					
				Epidermis	Hair follicles	Sweat glands	Dermis	Epidermis	
19	Methylene blue		+1	+++	+++	+++	+++	+++	
45	Toluidine blue		+1	+++	+++	+++	+++	+++	
48	Pyronin Y		+1	++	+	-/+	+	-	
52	Chrysoidine Y		+1	++	++	++	++	++	

Continuation of Table 4.20 The extent of penetration of ionic dye standards iontophoresis as a function of their valency

Figure	Dye	Ionic structure	Valency	Extent of penetration					
				Epidermis	Hair follicles	Sebaceous glands	Dermis	Hypodermis	
58	Eosin RN (water- and alcohol- soluble)		-2	-/+	+	-/+	-	-	
54	Eosin Y (water-soluble)		-2	++	-/+	-	-	-	
62	Amiline blue water-soluble		-2	-	-	-	-	-	
65	Picric acid		-1	++	++	++	+	+	
67	Aizaron red S		-1	-/+	+	-	-	-	

Table 4.21 Extent of penetration of inorganic cations following standard positive iontophoresis as a function of valency

Test solution	Tracer	Figure	Extent of penetration					
			Epidermis	Hair follicles	Sebaceous glands	Dermis	Hypodermis	
4% aqueous ferric chloride	Fe <sup>3+</sup>	117	++	++	++	++	-	
4% aqueous copper sulphate	Cu <sup>2+</sup>	104	+++	+++	+++	+++	++	
4% aqueous silver nitrate	Ag <sup>+</sup>	90	+	+	-/+			
1% aqueous copper sulphate	Cu <sup>2+</sup>	100	+++	++	++	++	+	
1% aqueous ferric chloride	Fe <sup>3+</sup>	115	+	+	-	+	-	
1% aqueous ruthenium red (RR) chloride	RR <sup>+6</sup>	97a	+++	+++	+++	+++	+++	

penetration than  $\text{Fe}^{3+}$  when salts of these cations are prepared in distilled water to fixed concentrations (1% and 4%). However, a relationship between valency and the extent of penetration cannot be applied to all ionic tracers since ruthenium red, which is a hexavalent cation and was reported to be  $[(\text{NH}_3)_5\text{Ru}-\text{O}-\text{Ru}(\text{NH}_3)_4-\text{Ru}(\text{NH}_3)_5]^{+6}$  (Fletcher *et al.*, 1961; Clausen, 1971 *et al.*) shows a similar penetration to  $\text{Cu}^{2+}$  and a better penetration than  $\text{Fe}^{3+}$ . Furthermore, both  $\text{Cu}^{2+}$  and  $\text{Fe}^{3+}$  showed better penetration than  $\text{Ag}^+$ . In conclusion, a possible, but by no means definite relationship exists between the polarity of the tracers examined and their extent of penetration into the skin.

#### 4.13.4 Ionic and molecular weights of penetrants

Little is known about the effect of the molecular weight of a test material on skin penetration. It has been reported that low viscosity and small particle-size increase penetration, presumably because physical contact with the surface of the skin is more complete (Bettley, 1970). Helium, with a low molecular weight, passes through the skin very rapidly while human serum albumin passes through the skin very slowly indeed (Tregear, 1966). However, within a smaller range of molecular size there appears to be no correlation between molecular weight and penetration (Tregear, 1966; Baker, 1979) because other factors are more important. For example, although Scheuplein and Blank (1971) noted an increase in the permeability of skin to primary alcohols  $\text{C}_1$  to  $\text{C}_8$  (methanol to octanol) with increasing rather than decreasing molecular weight, this variation in penetration was attributed to variations in the solubility characteristics of the alcohols concerned.

In the present study, there appears to be a possible (but not definite) relationship between the molecular and ionic weights and the extent of penetration following standard iontophoresis. The molecular and ionic weights of the organic dyes tested for penetration trials are shown in Appendix A, while the extent of penetration is shown in Tables 4.1 and 4.2 (page 314). Of the cationic dyes tested, methylene blue, toluidine blue, pyronin Y and chrysoidin Y show good or moderate penetration into the skin whereas aniline blue alcohol-soluble does not show any penetration. The latter dye is characterized by higher molecular and ionic weights than those of the former four dyes. Likewise, of the anionic dyes tested, eosin water- and alcohol-soluble, picric acid, alizarin red S and eosin water-soluble show moderate penetration into the skin following negative iontophoresis, whereas aniline blue water-soluble, trypan blue and eosin alcohol-soluble show the least effective or no penetration. The molecular and ionic weights of the former four dyes are lower than those of the latter three dyes. However, when comparison is made between individual dyes this relationship between molecular and ionic weights and extent of penetration does not hold. For example, toluidine blue shows a very effective penetration into the skin and the subcutaneous tissue following iontophoresis whereas pyronin Y does not, although the two dyes have almost the same molecular and ionic weights. Similarly, eosin water- and alcohol-soluble shows a better penetration following iontophoresis than alizarin red S, although the latter dye has lower molecular and ionic weights.

In summary, no obvious correlation between molecular and ionic weights and the extent of penetration following iontophoresis has been detected.

#### 4.13.5 The size of the hydrated ion

In its pure state, water is a non-conductor of electric currents. When ionic substances are dissolved in it, the aqueous solutions thus formed become conducting liquids called electrolytes. When an electrolyte-producing substance is added to water, it dissolves and immediately begins to dissociate into its component charged ions until an equilibrium is reached between the amount of substance dissolved and the number of ions which remains in the undissociated state. The process of dissociation is called ionization, during which water interacts with the ions in a specific manner. The interaction between water molecules and the ions is a complicated process and is described in great detail by Marcus (1985). The following is a summary treatment of such interaction. The individual ion in solution is surrounded by a shell of water. The number of water molecules associated with the ion is called the hydration number, and if other solvents are used then it is called the solvation number. The hydration (or solvation) number varies with the properties of the ion, namely size and charge. The hydration number is divided into a primary hydration number (also called first hydration shell) and a secondary hydration number (also called secondary hydration shell). The former is the number of water molecules which are immediate neighbours of the ion and the latter is the number of water molecules which are the next nearest neighbours of the ion. Beyond the second hydration shell the water molecules are indistinguishable in their behaviour from those in pure water, hence they constitute the bulk water.



Table 4.22 lists some physical properties of cations used as tracers in the present study. The extent of penetration of the metal cations following iontophoresis (see Table 4.2, page      and Table 4.19 (a-c), page 357) is given as  $\text{Cu}^{2+} > \text{Fe}^{3+} > \text{Ag}^+ > \text{La}^{3+}$ .

This is equivalent to saying that  $\text{Cu}^{2+}$  shows the most effective penetration while  $\text{La}^{3+}$  shows the least effective or no penetration. This variation in the extent of penetration may be related to the physical properties of the cations.  $\text{Cu}^{2+}$  is characterized by a small ionic radius and a small number of water molecules associated with it. Although  $\text{Fe}^{3+}$  has a slightly smaller ionic radius than that of  $\text{Cu}^{2+}$ , there are more water molecules associated with  $\text{Fe}^{3+}$  than  $\text{Cu}^{2+}$ , that is,  $\text{Fe}^{3+}$  has a higher hydration number than that of  $\text{Cu}^{2+}$ . Although  $\text{Ag}^+$  has the smallest hydration number, it has the largest ionic radius which may result in its reduced penetration as compared to  $\text{Cu}^{2+}$  and  $\text{Fe}^{3+}$ . On the other hand,  $\text{La}^{3+}$  has a large ionic radius and the largest hydration number and as a result shows the least effective or no penetration. Therefore, it may be possible that metal ions which have small ionic radii and small hydration numbers show the most effective penetration, whereas those which have large ionic radii and/or large hydration numbers show a less effective or no penetration. The increased hydration number makes the effective size of the ion greater than the effective size of the water-filled channels in the stratum corneum and as a result causes retardation or prevention of penetration (Blank and Gould, 1961). The amount of  $\text{Au}^{198}$  driven into the skin of the rat by iontophoresis was greater than that of  $^{131}\text{I}$ -labelled albumin and was attributed to variations in the particle size, that of  $\text{Au}^{198}$  being 0.005  $\mu$  while that of the albumin was 0.0275  $\mu$  (O'Malley and Oester, 1955). The rate of

Table 4.22 Physical properties of metal tracers

Ion	Primary hydration number (Marcus, 1985)	Ionic hydration number (Marcus, 1985)	Ionic radius (nm) (Harrison, 1972)
Ag <sup>+</sup>		3.1	0.126
Cu <sup>2+</sup>	4 or 6	9.8	0.069
Fe <sup>3+</sup>	6	18.8	0.064
La <sup>3+</sup>	8 or 9	21.5	0.114*

\* From Switzer (1978)

migration of ions in an electric field is governed by the volume of the hydrated ion; the smaller the volume, the faster the rate of migration of ions (Morris, 1971). Bierman and Licht (1952) reported that the depth to which ionic migration took place by iontophoresis depended on the atomic weight of the elements, that is, ions of elements of low atomic weight migrated faster than those of high atomic weight. Therefore, since  $\text{Cu}^{2+}$  and  $\text{Fe}^{3+}$  show better penetration into and through the skin than  $\text{Ag}^+$  and  $\text{La}^{3+}$ , the variation in the extent of penetration may in part be attributed to the lower atomic weights of copper and iron (see Appendix II).

#### 4.14 Tracer-tissue interaction

When ionic dyes pass into solution they ionize. A basic dye gives cationic or positively charged coloured dye ions and negatively charged colourless (usually chloride) ions, whilst an acidic dye gives anionic or negatively charged coloured dye ions and positively charged colourless (usually sodium) ions. This occurs over pH ranges that are used in Histology, that is, pH 3 - pH 10. Thus the terms basic and acidic as applied to dyes have no relevance to pH and it seems better if the term cationic dye is used for a basic dye and anionic dye is used for an acidic dye (Drury and Wallington, 1980). In practice, these terms are used interchangeably.

Like ionic dyes, biological tissues contain electrically charged groups; negatively charged sites include phosphoryl, sulphuryl, carboxyl and hydroxyl groups, while positively charged sites include the basic amino groups. When ionic dyes come into contact with a biological tissue, cationic (basic) dyes bind to negatively charged

(basophilic) tissue loci, and anionic (acidic) dyes bind to positively charged (acidophilic) tissue loci. Although this chemical binding may result from the formation of Van der Waal's forces, hydrogen bonds and covalent bonds (Bancroft and Stevens, 1977), electrostatic binding appears to be the most predominant reaction (Bancroft and Stevens, 1977; Drury and Wallington, 1980). Electrostatic attraction is also called coulombic attraction and salt link.

The ionic dyes used in the present study for penetration trials persisted in all the cryostat sections examined without (for example, Figures 4a, 33a, 41a and 59) or with additional staining in tartrazine (for example, Figures 4b, 33b and 41b), haematoxylin and eosin (for example, Figures 31b and 39c), eosin (for example, Figures 30b, 51 and 52) or toluidine blue (for example, Figure 65). The selection of the dyes used for the staining of the cryostat sections was made so that the colour of each stain would not interfere with the colours of the dyes used for penetration trials. The additional staining of the cryostat sections, which is accompanied by rinsing, dehydration and mounting of the sections, did not result in translocation or loss of the dyes used for penetration trials as compared to sections which were not stained additionally. This may indicate that some kind of chemical binding exists between the tissue structures and the dyes subjected to iontophoresis. This contention is further supported by the finding that once methylene blue is introduced into the skin by positive iontophoresis, it cannot be recovered from the skin by negative iontophoresis (Figures 26 and 27). This suggests that the dye no longer exists in its ionic form within the skin but is likely to be bound to the tissue. From the discussion mentioned above, it is probable that, having penetrated into the intact skin by

iontophoresis, cationic and anionic dyes bind electrostatically to oppositely-charged ionic sites in the skin, that is, cationic dyes are reduced by basophilic tissue loci while anionic dyes are oxidized by acidophilic loci to insoluble forms. This binding ensures thereby the persistence of the dyes in the cryostat sections. Additional support for dye-tissue chemical binding has come from studies such as those of Abramson and Gorin (1940) and Abramson and Engle (1942) who reported that dyes introduced into the skin by iontophoresis remained clearly visible in the skin for as long as two weeks after application. Similarly, McEwan Jenkinson *et al.* (1974) reported that organic dyes were clearly evident in the skin several days after iontophoresis. This duration coincides with the time it takes for the cells subjected to iontophoresis to be replaced by new ones (Mitdgaard, 1986).

Substances that dissolve in tissues are known as lysochromes. Most of these are lipid-soluble and are thus used for the demonstration of lipids in tissues. The most widely-used lipid-soluble dyes are the sudan dyes, sudan III, sudan IV and sudan black B. It is generally believed that these dyes pass preferentially from the solvent in which they are prepared into the tissue lipids because they have higher solubilities in the lipids. This type of staining is called staining by elective solubility (Dixon, 1970; Bancroft and Stevens, 1977; Drury and Wallington, 1980). With regard to sudan black B, which has been used in the present study for penetration trials, it has been mentioned already (page 329) that this dye comprises two distinct fractions. The first is soluble in neutral lipids and the second is a slightly basic dye favouring phospholipids and thus the dye is capable of staining both hydrophobic and hydrophilic lipids (Bancroft and Stevens, 1977). Therefore, in addition to staining by elective

solubility, the possibility of a chemical binding between sudan black B and the tissues (Gurr, 1960) cannot be eliminated.

Although the extent of penetration of  $\text{Ag}^+$ ,  $\text{Cu}^{2+}$  and  $\text{Fe}^{3+}$  into and through the skin following iontophoresis varies with the individual tracer, the location and distribution of each tracer is consistent in most of the ultrathin or cryostat sections examined following a particular experiment and its repetition. This may indicate that translocation and relocalization of the tracers as a result of the preparative techniques used are minimal. Therefore, as with the ionic dyes, it is likely that, having penetrated into and through the skin, the cations  $\text{Ag}^+$ ,  $\text{Cu}^{2+}$  and  $\text{Fe}^{3+}$  are deprived of their charges, that is, they are reduced to insoluble forms (report of the Council on Pharmacy and Chemistry and the Council on Physical Therapy, 1941; Harris, 1959; Liventsev, 1964). This is probably brought about via electrostatic binding to negatively-charged tissue loci.

The chemistry of lanthanum salts has been extensively discussed by Moeller (1963). Lanthanum has different chemical forms depending on the method used to prepare the tracer solution. The tracer is generally used in the form of nitrate or chloride salts. At a concentration of 1% in solutions used as fixatives in electron microscopy, lanthanum is thought to exist mainly as colloidal particles of lanthanum hydroxide, each with a diameter of about 2 nm (Revel and Karnovsky, 1967). Particles of colloid do not pass through membranes of normal cells but contrast their surfaces and the narrow slits between them. This property led to the use of lanthanum for studying the structure of intercellular junctions (Revel and Karnovsky, 1967). When lanthanum salts are prepared in fixative



solutions, aqueous sodium hydroxide is normally added to the fixatives to bring the pH of the fixatives close to that of the tissue, and to facilitate the formation of colloidal lanthanum hydroxide. More recent studies, however, have indicated that the physical state of lanthanum in solution depends on the pH of the solution. Schatzki and Newsome (1975) carried out column chromatography, ultrafiltration and conductivity measurement studies of fixative solutions containing lanthanum and concluded that during titration with sodium hydroxide approximately 80% of the lanthanum existed as charged particles of less than 500 daltons at pH 7.7 and below, whilst the other 20% consisted of larger, possibly colloidal particles. Subsequent studies (Sharov, 1981) have confirmed that the tracer exists in the ionic form ( $\text{La}^{3+}$ ) until the pH of the solution reaches 7.8, above which colloidal lanthanum is formed. In aqueous solutions, lanthanum is present as  $\text{La}^{3+}$  with an ionic radius of 1.14 Å (Switzer, 1978). Martin and Richardson (1979) gave a value of 1.16 Å. The interaction between lanthanum and biological tissues has been reported to be via electrostatic binding of the ionic lanthanum ( $\text{La}^{3+}$ ) to anionic sites on the cell surface (Schatzki and Newsome, 1975; Haack *et al.*, 1981; Shaklai and Tarassoli, 1982).

#### 4.15 Mode of action of iontophoresis

It is commonly held that ionic species in aqueous solutions do not penetrate the skin or may do so only in very small amounts (Malkinson, 1964; Wills, 1969; Scheuplein and Blank, 1971). Rothman (1954) listed many examples demonstrating the impermeable nature of skin to non-physiological cations such as lithium, rubidium, caesium and strontium, as well as physiologically occurring cations such as sodium

and calcium when salts of these metals were applied to the surface of the skin from aqueous solutions. The ionization of a weak electrolyte has long been known to radically decrease its permeability and the much greater permeability of salicylic acid than sodium salicylate has often been discussed (Rothman, 1944, 1955). Consequently, quantitative data are scarce since very few ionic permeability constants have been successfully measured (Scheuplein and Bronaugh, 1983). On the other hand, Tregear (1966) reported that ions of either sign ( $K^+$  and  $Br^-$ ) penetrated the skin of the rabbit nearly as rapidly as water and as rapidly as many covalent substances. However, these data are insufficient to provide a basis for understanding ionic permeability through the skin (Scheuplein and Bronaugh, 1983).

Many factors are believed to cause the low permeability of the skin to ions, and these include:

(1) Steric hindrance, that is, the stable hydration sphere around each ion which makes it virtually a polyhydroxylic ion. This may prevent the penetration of the ion simply by making the effective size of the ion greater than the effective size of the water-filled channels in the stratum corneum (Blank and Gould, 1961).

(2) The absence of a highly specialized transport mechanism in the metabolically inactive stratum corneum (Malkinson, 1965).

(3) The presence of lipids in the stratum corneum which make difficult the establishment of continuous aqueous pathways through the tissue along which water-soluble electrolytes can penetrate (Blank and Gould, 1961).

(4) The interaction of the penetrating ions with co-ions, counterions and fixed charges in the tissue (Scheuplein and Bronaugh, 1983). Under normal conditions the net charge on the protein fibres in the

stratum corneum is believed to be electronegative. Thus ions will either be repelled or combined electrostatically by the proteins in the stratum corneum and in both cases penetration will be prevented even when the aqueous pathway is continuous (Blank and Gould, 1961).

The present study has shown that organic and inorganic ionic tracers do not penetrate the skin readily when they are applied in solution to the surface of the skin for a total duration of 15 minutes (Tables 4.1 and 4.2, page 314). In addition, the present study (Tables 4.1 and 4.2) as well as other studies (Finzi, 1912; Inchley, 1921; Abramson and Gorin, 1940; Fleischmajor and Witten, 1955; Harris, 1959; McEwan Jenkinson *et al.*, 1974) have shown that the impermeability of the skin to electrolytes can be changed significantly by the use of a galvanic current.

Different theories have been suggested to explain the increased penetration of ionic species into the skin by iontophoresis. Rein, in a series of papers (cited by Calvery *et al.*, 1946), believed that the most important mechanism involved in the penetration of ions was electrosmosis, that is, the transfer of water across the skin in an electric field. Water moves into the skin from an anode placed in contact with the surface of the skin and this is termed electro-endosmosis. Cations also move in this field and in the same directions so that the over-all effect is an enhancement of penetration. Following negative iontophoresis, however, there is practically no penetration of anions into the skin because the electrosmotic stream is outward, that is electro-exosmosis, which opposes the inward movement of ions. This hypothesis was questioned by Abramson and Gorin (1940) who claimed to have transferred

successfully both positive and negative ionic dyes into the skin by iontophoresis as judged by the development of "pore pattern" (page 406). However, Rothman (1954) indicated that the pore pattern did not demonstrate skin penetration by the dyes, but only the uptake of dyes by the pores of the epidermal appendages.

Abramson and Gorin (1939) postulated that with respect to the movement of ions and charged particles into the skin, three factors which may be summed up algebraically were operative. The first was the simple migration of the ions in an electric field, the second was the electrosmotic flow of the liquid as a whole and the third was diffusion under a concentration gradient. This was presented as

$$V = V_E + V_D$$

$$= (V_i + V_s) + V_D$$

where  $V$  was the actual velocity of the particle and  $V_E$  was the resultant velocity due to the electrical field, which equalled the sum of the ionic velocity of the particle ( $V_i$ ) and the electro-osmotic velocity of the vehicle ( $V_s$ ).  $V_D$  was the diffusion velocity (Abramson and Gorin, 1939, 1940). Consequently, these authors reported that the ducts and canals of the epidermal appendages were not filled completely with sweat or sebum but also contained air. When an electrical potential was applied across the skin, the electro-osmotic forces displaced the air with the liquid used for the iontophoresis study. The ducts then contained an unbroken column of liquid, that is, a liquid bridge in contact with the test liquid on the surface of the skin and with the dermal gels and fluids. Following this, penetration occurred whenever concentration gradients existed and the extent of penetration was determined by the electro-osmotic velocity ( $V_s$ ) and the velocity of the test ions ( $V_i$ ).

In its pure state, water does not conduct a galvanic current. When an electrolyte-producing substance is dissolved in water, the aqueous solution thus formed becomes a conducting liquid. Recent studies (Gangarosa *et al.*, 1980) have shown that both positive (anodal) and negative (cathodal) iontophoresis result in enhanced penetration of water into the skin when a small amount of sodium chloride is dissolved in the water as compared to controls, and that positive iontophoresis is much more effective in increasing the penetration of water into the skin than is negative iontophoresis. Water-soluble substances are believed to penetrate the stratum corneum via water-filled channels while lipid-soluble substances penetrate via the corneum's lipid system (Scheuplein and Blank, 1971). Substances with good lipid and water solubility are most easily absorbed by the skin (Rothman, 1943; Winkelmann, 1969). In addition, hydration is known to enhance the permeability of the stratum corneum (page 42). Therefore, it may be suggested that two events occur simultaneously during iontophoresis. The first is the shifting of water through the skin with the current and the second is the migration of ions in the electric field. Water moves inward into the stratum corneum of the epidermis and the cornified membrane of the hair follicle during both positive and negative iontophoresis, with positive iontophoresis producing the larger effect. The entry of the first few water molecules greatly reduces the resistance of the tissues to the flow of the current. The application of water on the surface of the skin "even for a second", which will not allow the water to penetrate, nevertheless, causes a great increase in the loss of resistance of the corneum (Tagami *et al.*, 1980). While aqueous pathways are being established across the cornified tissues, simultaneously ions in the solution migrate from the iontophoresis electrode into the skin,

provided that the electrode is connected to the positive pole for cations or to the negative pole for anions. The overall result is enhancement of penetration. However, since not all ionic tracers used in the present study penetrated the skin following iontophoresis (Tables 4.17 and 4.18), it is highly probable that iontophoresis accelerates the extent of penetration of ionic materials once these are allowed entry into the skin. What determines whether or not penetration will occur seems to be the physico-chemical properties of the tracers and the vehicles, and their interactions with the skin. Consistent with this, Scheuplein (1965) reported that the swelling and softening of the keratin filaments following a sufficient period of contact with water, which was accompanied by a partial dissolution of the stratum corneum and the establishment of large "holes" through which diffusion could occur, did not obviate the far greater effect of solubility characteristics. However, once penetration occurs, then the extent of penetration of ionic tracers into and through the skin is influenced by the current intensity and the duration of current flow.

Other theories are available which describe the enhanced penetration of "non-electrolytes" into the skin by iontophoresis. In these studies (Gangarosa *et al.*, 1980) dilute aqueous NaCl solutions containing [ $^3\text{H}$ ]-9- $\beta$ -D-arabinofuranosyladenine (Ara-A) and [ $^3\text{H}$ ]thymidine (tThd) were subjected to iontophoresis, and this resulted in the enhancement of the penetration of the non-electrolytes. Gangarosa *et al.* (1980) assumed that the non-electrolytes move passively in association with water or with the moving sodium and chloride ions. However, they did not exclude the possibility that the Ara-A and tThd might have a slight degree of



ionization, and that the ions formed would move into the tissue by the normal process of iontophoresis. In the present study, positive and negative iontophoresis did not result in the enhancement or retardation of the penetration of non-ionic dyes, namely sudan black B (Figures 71 and 72) as compared to controls (Figure 70). Thus the enhanced penetration of non-electrolytes resulting from the use of iontophoresis could not be substantiated.

#### 4.16 The location and nature of the cutaneous barrier

The prime function of mammalian skin is to interpose a barrier between the internal environment and external events. This barrier limits egress of physiological fluids and limits ingress of noxious or undesirable substances.

In the present study experiments have been undertaken to re-evaluate the location and nature of the cutaneous barrier. They will be discussed in three parts: the role of the surface lipid, the role of the stratum corneum and sebum in the follicular canal, and the role of the epidermal-dermal junction.

##### 4.16.1 The role of the surface lipid

The present study has shown that the removal of surface lipid by swabbing the surface of the skin with lipid solvents in cotton wool does not render the skin permeable to lanthanum (Figure 81 a - c). Furthermore, the extent of penetration of silver ions into the stratum corneum following iontophoresis is the same with (Figure 94 a - c) or without (Figure 88 a - c) the removal of surface the lipid. These

results offer additional support to the general view that the surface lipid plays very little or no role in percutaneous penetration (Winsor and Burch, 1944; Laug *et al.*, 1947; Blank and Gould, 1961; Blank *et al.*, 1964; Tregear, 1966).

#### 4.16.2 The role of the stratum corneum and sebum in the follicular canal

Different experimental techniques have been used to investigate the location and nature of the cutaneous barrier. Measurements of percutaneous perfusion combined with stripping and separation experiments have long suggested that the barrier is located in the stratum corneum of the epidermis (Berenson and Burch, 1951; Monash and Blank, 1958; Malkinson, 1958). This is supported further by the observed reduction in permeability as the stratum corneum regenerates following stripping experiments (Monash and Blank, 1958; Matoltsy *et al.*, 1962; Komatsu and Suzuki, 1982). Biophysical analysis of percutaneous absorption (Scheuplein and Blank, 1971) coupled with the finding that the stratum corneum lipids are located intracellularly and surround the keratin filaments (Swanbeck and Thyresson, 1962; Goldsmith and Baden, 1970) have indicated that the cutaneous barrier is provided by the contents of the corneal cells. Judging by its high structural rigidity and marked chemical resistance, Matoltsy (1961) reported that the plasma membrane of corneocytes should not be eliminated as a part of the cutaneous barrier. Another approach in determining the site of the cutaneous barrier has come from studies that reveal the location of tracer substances within skin sections some time after exposure of isolated or intact skin to the tracer in solution. Intercellular tracers such as lanthanum, horseradish peroxidase and ferritin which are detectable with the electron microscope have been employed (Elias and Friend, 1975; Elias *et al.*, 1977) and the results have shown that the cutaneous barrier is in large part provided by the lipid-rich intercellular substance in the stratum corneum and the stratum granulosum. Similar findings have

been reported for keratinized oral epithelium (Squier, 1973; Squier and Rooney, 1976).

In the present study, lanthanum was used as a vital tracer by studying its movement through the intact skin following intradermal injections of aqueous lanthanum nitrate solutions, or alternatively by using it as an *in vitro* tracer by making lanthanum nitrate a constituent of the fixative solutions into which excised skin specimens were incubated. The most striking feature of lanthanum as an intercellular tracer was the similarity of its distribution within the skin following intradermal injection (Figure 76 a - i) and the incubation method (Figure 77 a - e). Consequently, the results obtained using these two methods will be discussed together. In the ultrathin sections examined with both methods, in some cases the intercellular spaces were partially filled with tracer and in others heavy deposition of lanthanum was seen. Nevertheless, the extent of tracer movement was the same.

With regard to the epidermis, lanthanum freely permeated all the intercellular regions (spaces) in the stratum basale, stratum spinosum and, more significantly, in the stratum granulosum, but the tracer did not enter the region (intercellular space) between the superficial granular and the basal corneal layers (Figures 76h and 76i, 77d and 77e). In addition, with the incubation method no tracer entered from the cut ends of the skin specimens or from the surface into the intercellular regions between the cornified cells (Figure 77e). From this it appears that the granular-corneal interface and the corneum's intercellular spaces are not "open" to the tracer. One possible interpretation of this suggests a barrier provided by intercellular

junctional complexes. These intercellular junctions are specialized regions of contact between the opposed plasma membranes of adjacent cells, and include the tight junction (zonula occludens), the desmosome (macula adherens, fasciae or zonula adherens) and the gap junction (nexus, communicating junction). A detailed description of the anatomical features and physiological functions of these junctions has already been reported (Staehein, 1974; Shimono and Clementi, 1976; Hirokawa, 1982). Gap junctions are most plentiful in the basal layer of the epidermis. They decrease progressively in number as the keratinocytes migrate outward to the stratum granulosum, and none has been described in the stratum corneum (Shimono and Clementi, 1976). Lanthanum has been shown to permeate gap junctions in the viable epidermis (Elias *et al.*, 1977; Leach and Oliphant, 1983).

The most prominent membrane junctional structure in the epidermis is the desmosome. Unlike gap junctions, desmosomes normally occupy more of the plasma membrane surface area in the upper layers of the epidermis than in the more basal layers (Elias *et al.*, 1977). Desmosomes were thought to play a role in the regulation of intercellular permeability as Wolff and Honigsmann (1971) reported that desmosomes were not permeated by Thorotrast. They also reported that the distance between the outer leaflet of the cell membrane and the intercellular contact layer (M-line) of the desmosome measured less than 100 Å, and that the diameter of the individual Thorotrast particles approached this order of magnitude. Thus the size of the Thorotrasts and the effective enlargement of the tracer particles by hydration may have accounted for the inability of Thorotrast to enter these structures. However, lanthanum has been shown to permeate desmosomes in the viable epidermis (Wolff and Schreiner, 1968; Squier

and Rooney, 1976). Furthermore, following intradermal injection of the intercellular tracer horseradish peroxidase which permeated the intercellular spaces in the viable layers of keratinized and non-keratinized oral epithelium, it was also evident between the outer leaflets of the plasma membranes in the regions of desmosomes (Squier, 1973). Shakhai and Tavassoli (1982) reviewed many articles on the use of lanthanum as an electron microscopic tracer and concluded that, with the exception of the tight junction, all intercellular junctions, namely desmosomes, gap and septate junctions were in direct communication with the extracellular space and, therefore, could be delineated by lanthanum as it penetrated and precipitated in the extracellular space. In other tissues, namely the exocrine pancreas, lanthanum has been shown to penetrate gap junctions and desmosomes but not tight junctions (Leeson and Leeson, 1982).

Although desmosomes persist into the stratum corneum, in this layer their appearance in freeze-fracture replicas and in ultrathin sections is different from that in the subjacent viable layers (Brody, 1969; Shimono and Clementi, 1976; Elias, 1981;). For example, in the region of corneal desmosomes the intercellular space is occupied by an opaque homogeneous material and the usual distinct attachment plaques are absent. Furthermore, there is a reduction in the number of intramembranous particles in the freeze-fractured cornified desmosome. It is not clear whether this modification reflects in any way a barrier property to intercellular transport across the stratum corneum.

Although tight junctions are known to function as barriers in non-keratinizing epithelia (Staehelein, 1974; Leeson and Leeson, 1982) and



are impermeable to lanthanum because of the fusion of the outer layers of the two adjacent plasma membranes which results in total obliteration of the intercellular space (Shaklai and Tavassoli, 1982), their role in keratinizing epithelia is open to question. A few studies have established the presence of tight junctions in the upper layers of the murine oesophagus (McNutt, 1973), rat oral mucosa (Shimono and Clementi, 1976), and human epidermis (Caputo *et al.*, 1975), and have suggested a role in regulating tissue permeability. Contrary to these findings, however, many studies of various tissues including the epidermis, the oesophagus and the vagina of newborn and adult humans and mice (Elias and Friend; 1975; Elias *et al.*, 1977) have shown that true tight junctional elements are either absent, or too fragmentary to constitute an effective barrier in keratinizing tissues.

Still another membrane structure has been described at the interface of the stratum corneum and stratum granulosum and has been termed "the distal tight junction of the stratum granulosum" (Hashimoto, 1971). They were thought to limit the outward passage of lanthanum, but the same author pointed out that lanthanum did not enter the stratum corneum from the lateral cut surfaces of the skin blocks following incubation of the blocks in solutions containing lanthanum, and that tight junctions were not present in the keratinized layer. Thus the distal tight junctions of the stratum granulosum do not explain the impermeability of the stratum corneum to lanthanum and, furthermore, subsequent studies (Elias *et al.*, 1977; Elias, 1981) have indicated that it is erroneous to term such structures "tight junctions" since they bear only a superficial resemblance to true tight junctions. In

view of these reports, it seems likely that junctional complexes play a relatively minor role in impeding tracer movement.

Another possible interpretation for the blockage of tracer movement into the granular-corneal interface and the corneum's intercellular spaces suggests a barrier substance located in these intercellular spaces. This has received wide support (Schreiner and Wolff, 1969; Squier, 1973; Lavker, 1976; Squier and Rooney, 1976; Elias *et al.*, 1977, 1979; Elias and Brown, 1978; Elias, 1981; Hayward 1983; Squier and Edie, 1983; Lampe *et al.*, 1983; Bowser and White, 1985; Grayson *et al.*, 1985). The intercellular barrier substance originates from the excreted contents of membrane-coating granules, and is composed of a variety of free fatty acids, polar and neutral lipids and possibly glycolipids (Gray and Yardley, 1975; Elias *et al.*, 1979), rather than phospholipids as originally proposed (Hashimoto, 1971). The concept of an intercellular barrier substance has received further support by studies done on fetal rats *in utero* which showed that lanthanum diffuses freely through all the intercellular spaces in the epidermis prior to exocytosis of membrane-coating granules, and that tracer movement ceases after the granules have been expelled into the intercellular spaces (Hayward, 1983). In addition, Squier (1984) has shown that horseradish peroxidase penetrates all the intercellular spaces of the stratum corneum after the intercellular substance has been removed by chondroitinase ABC. Without the removal of the intercellular substance the marker does not gain access to the stratum corneum. Consistent with this, Hashimoto (1971) demonstrated that following treatment with phospholipase C, which digests the extracellular granules, the granules attached to the plasma membranes and the contents of the intracytoplasmic granules, lanthanum permeated

the regions between keratinized nail cells. Without such treatment the tracer was excluded from these regions.

Although it is generally accepted that the barrier to intercellular passage is provided by the intercellular substance, there has been some uncertainty with regard to the precise level at which the outward movement of intercellular tracers is halted. Elias *et al.* (1977) carried out tracer studies on oesophageal and epidermal membranes and found that in the oesophagus lanthanum permeated through the intercellular spaces to reach the interface of the stratum granulosum and the stratum corneum. In the epidermis the tracer movement stopped in the mid-to-upper stratum granulosum. In a similar study Elias and Friend (1975) reported that in the epidermis of the neonatal mouse in which the stratum granulosum is four to six layers thick, lanthanum, horseradish peroxidase and thorium dioxide percolated superficially from the dermis, through the epidermal intercellular spaces, to the mid-to-upper stratum granulosum. Since these tracers were highly water-soluble, these authors concluded that the cutaneous barrier was actually formed **beneath** the stratum corneum (mid-to-upper stratum granulosum), and that this barrier impeded outward tracer movement and regulated transepidermal water loss. Squier (1973) and Wolff and Honigsmann (1971) also favoured the upper layers of the stratum granulosum as the level at which the upward tracer migration was stopped.

On the other hand, other studies have illustrated that lanthanum (Hashimoto, 1971; Montagna and Parrakal, 1974) and ferritin (Olson *et al.*, 1969) show an intercellular permeation up to the level of the intercellular space between the stratum granulosum and the stratum

corneum. Consistent with this, the present study has shown that all the intercellular spaces of the stratum granulosum of the epidermis are permeated by lanthanum and that the level at which the superficial migration is halted is the granular-corneal interface (Figures 76i and 77e). This coincides with the observed aggregations of membrane-coating granules in the intercellular space between the basal corneal and the superficial granular layers (Figure 77c). The present findings, therefore, suggest that the stratum granulosum does not function as an effective barrier to the outward passage of water-soluble intercellular markers and, more significantly, to transepidermal water loss. The stratum granulosum of the epidermis of rat abdominal skin as seen in the present study (Figures 76i, 77e) is one or two layers thick as compared to 4-6 layers in neonatal mouse skin (Elias and Friend, 1975). Interestingly, however, the thickening of the stratum granulosum which follows treatment of psoriasis with tar therapy is not accompanied by an increase in resistance to permeability (Winkelmann, 1969).

The finding that the tracer is excluded from the granular-corneal interface and from all the intercellular spaces in the stratum corneum, along with its presence in all the spaces between granular cells, may indicate that the intercellular substance in the stratum granulosum differs from that in more superficial intercellular regions. It has been shown that following extrusion, the material derived from membrane-coating granules undergoes both chemical (Elias *et al.*, 1977) and structural (Elias and Friend, 1975) modifications as it ascends into the upper intercellular spaces. Indeed, only then does the material achieve its full degree of impermeability (Hayward, 1983). These modifications include the coalescence of individual

granules to form broad lamellae, and a shift in composition from polar to neutral lipids. Elias and Friend (1975) indicated that it was the outward progression of the lamellar material throughout the interstices of the stratum corneum that explained the persistence of the impermeability of this layer to water-soluble intercellular tracers.

In the light of the present results, it is not unreasonable to conclude that the intercellular substance in the stratum corneum and in the granular-corneal interface provides or forms **physiological tight junctions** which impede the movement of water-soluble intercellular tracers and perhaps regulate epidermal water loss.

Thus far, lanthanum has been described as an intercellular tracer. The presence of lanthanum between the cells may be due to the precipitation of the tracer to an insoluble form in the intercellular spaces (Revel and Karnovsky, 1967) or to the binding of the tracer to anionic sites on the external surface coat of the epidermal cells (Krawczyk, 1976; King, 1983). On a few occasions the tracer was observed in the interior of some cells, especially those in the lower layers of the stratum spinosum (Figure 77 h and d) and in the outer root sheath (Figure 76b). The uptake of lanthanum by an active transport process such as vesicular formation is one possible explanation of its intracellular location following intradermal injection *in vivo*. The intracellular localization of intercellular tracers such as Thorotrast and ferritin is believed to be a result of phagocytic properties of viable keratinocytes (Olson *et al.*, 1969; Wolff and Honigsmann, 1971). Shakhai and Tavassoli (1982) and Blanchette-Mackie and Scow (1982) regarded intracellular lanthanum to

be evidence for the continuity or the direct communication between some cellular organelles and the intercellular space.

Within the sebaceous glands, lanthanum freely permeates all the intercellular spaces between the peripheral, the partially differentiated and the fully differentiated sebaceous cells (Figures 76e, 76f and 77b). Similar results have been reported previously by Jackson *et al.* (1983) and by Kitson and Van Lennep (1984). Lanthanum was also found in the regions between the sebaceous duct cells but did not extend between the keratinized ones (Figure 76d). Using ultrathin sections and freeze-fracture techniques, Kitson *et al.* (1978) and Kitson and Van Lennep (1984) provided evidence for the presence of desmosomes and gap junctions and for the absence of tight junctions in the sebaceous glands. Jackson *et al.* (1983) concluded that there was no intercellular barrier to lanthanum which could pass therefore from the dermis to the sebum. Thus, as in the epidermis, the intercellular junctions may be excluded as an effective barrier in the sebaceous glands to the intercellular movement of water-soluble tracers, and perhaps to water itself.

The above findings raise the question of the nature of the permeability barrier in the sebaceous glands. Kitson and Van Lennep (1984) suggested that the secreted sebaceous lipids formed a barrier to water exchange between the gland and the skin surface. The secretion of lipids by the holocrine process may be considered in physical terms to be the inversion of an oil-in-water emulsion to form a water-in-oil emulsion. This corresponds to the transition from the cellular part of a sebaceous gland, where lipids are dispersed within an aqueous phase, to the sebaceous duct and follicular canal where



lipids form the continuous phase. As a result there is no continuous aqueous phase that allows water movement between the sebaceous glands and the skin surface. From this, it appears that the barrier presented by the sebaceous glands to the external environment differs from that provided by the epidermis.

In the lower follicular walls, lanthanum was clearly evident in the intercellular spaces in the outer root sheath and in the regions between cells in Henle's and Huxley's layers, but the tracer was less evident in the intercellular spaces in the cuticle of the inner root sheath (Figures 76b, 76c and 77a). These results closely resemble those shown by Hashimoto and Shibasaki (1976). These authors also reported the existence of hemidesmosomes, desmosomes and gap junctions, and the absence of tight junctions in the hair follicles. In the follicular canal epidermis, which is continuous with the surface epidermis, lanthanum was evident in the intercellular spaces between all cells in the viable layers and could often be followed from the basal layer up to, but not into, the granular-corneal interface (Figures 76g and 77c). Moreover, no tracer was observed in the stratum corneum. As with the surface epidermis, therefore, the presence of lanthanum in all the intercellular spaces in the stratum granulosum and its absence in the stratum corneum may be considered as additional support for the permeable nature of the former and the impermeable nature of the latter.

With regard to inward penetration, lanthanum was observed on the surface of the skin only following both local application (Figure 78 a - d) and iontophoresis (Figure 79 a - c). Increasing the concentration of the tracer in the vehicle (Figure 80 a - c), the

addition of DMSO to the tracer in the vehicle (Figure 82 a - c), or the addition of a non-ionic detergent to the tracer solution (Figure 83 a - c) did not render skin permeable to lanthanum when these solutions were applied onto the skin with iontophoresis. In all the cases the tracer was effectively excluded from the stratum corneum of both the surface epidermis and the follicular canal epidermis, confirming the impermeable nature of the corneum. Equally, the tracer was also excluded from the sebaceous duct regions and the sebaceous glands themselves, and thus it may be inferred that the sebum in the pilary canal prevents the movement of the tracer from the surface into the glands. Therefore, although sebum on the surface of the skin does not participate in the barrier function, sebum in the follicular infundibulum or the so-called follicular reservoir (Kligman and Shelley, 1958) appears to participate in the barrier function.

Taking advantage of its electron-density and high water solubility, silver has been used as an additional tracer to further investigate the barriers to outward and inward flow through the skin.

Following intradermal injection, silver was seen in all the intercellular and intracellular compartments in the stratum basale, the stratum spinosum and the stratum granulosum (Figure 86f), although the nuclei of some basal and spinous cells appeared as electron-translucent spaces containing no silver deposits. Having crossed the granular-corneal interface, silver was evident in the innermost one or two corneal layers where it was seen as a few dense patches dispersed mainly between the basal corneocytes (Figure 86f). No silver entered the higher corneal layers. The relative failure of silver to appear in the intracellular compartments of the basal corneocytes, as

compared to its free transcellular flow in the subjacent epidermal layers, may be a result of the modifications which the plasma membranes undergo as the keratinocytes enter the stratum corneum (see page 30-31) and/or the impermeable nature of the cytoplasmic matrix of the corneocytes (see pages 27-30). These findings coupled with those of lanthanum may suggest that the location and nature of the barrier presented by the epidermis to the outward flow of tracers may differ in accordance with the physiochemical nature of the tracers (Wolff and Honigsmann, 1971). The barrier to the superficial migration of silver, which selectively stains the corneum's intercellular substance (Hayward and Hackemann, 1973) and is able to cross intact plasma membranes of viable epidermal cells, appears to be at the base of the stratum corneum and possibly consists of both the plasma membranes of the corneocytes and their cellular contents. In contrast, the barrier to the superficial migration of the intercellular tracer lanthanum appears to be at the granular-corneal interface and consists of the intercellular substance derived from the expelled contents of membrane-coating granules. Since lanthanum nitrate and silver nitrate are highly water-soluble and were prepared in water when injected into the skin, it may be hypothesized that the inner limit of the barrier function to the regulation of transepidermal water loss resides in the intercellular substance in the granular corneal interface and the innermost one or two corneal layers.

In the sebaceous glands, silver was seen in all the intercellular spaces between the cells and, having crossed the plasma membranes, it appeared within the cytoplasm between the lipid droplets (Figure 86d). At the level of entry of the sebaceous duct into the pilary canal, the tracer was seen as fine dense deposits mixed with remnants of sebum

and on the surface of the cuticle of the hair shaft (Figure 86c). Thus it appears that no barrier exists in the sebaceous gland to silver which can pass from the dermis to the sebum via both the inter- and intra- cellular regions.

In the lower follicular walls, silver was evident inside and between the outer root sheath cells (Figure 86b). At the base of the follicular infundibulum, silver was seen as fine deposits on the outer surface of the cornified cells (Figure 86c) suggesting that silver had moved passively with the sebum into the base of the pilary canal and passed from the sebum to bind to the surface of the cornified cells. Throughout the follicular infundibulum the tracer had permeated all the intercellular and intracellular regions of the stratum basale, stratum spinosum and stratum granulosum and, furthermore, was evident at the granular-corneal interface (Figure 86e). It was not observed throughout the stratum corneum except for the innermost corneal layer where a few silver deposits were observed (Figure 86e). The same argument therefore which applies to the surface epidermis may be applied to the follicular infundibulum, that is, the presence of an intercellular and an intracellular barrier in the base of the stratum corneum which prevents the outward migration of ions.

Local applications of aqueous silver nitrate solutions confirmed the impermeable nature of the intact skin. Under no circumstances did the water-soluble tracer gain access either to individual cornified cells (excluding the most superficial squames) or to the intercellular spaces between them in both the surface epidermis (Figures 87a, 89a and 91a) and the follicular infundibulum (Figures 87b, 89b and 91b). No tracer was seen in the sebaceous duct region or in the sebaceous

glands themselves (Figures 87b, 87c, 89c and 91c). Furthermore, even with iontophoresis, silver was not visible in the glands when the tracer was introduced from a 2% (Figure 88c) or from a 4% (Figure 90d) aqueous solution. Therefore, although silver may diffuse passively or move with the sebum as the latter is expelled from the sebaceous gland into the base of the pilary canal following intradermal injection, the tracer is not allowed to pass from the surface through the pilary canal and into the sebaceous glands, suggesting a barrier function for sebum in the pilary canal.

The debate surrounding the stratum corneum as the epidermal barrier has pivoted mainly on the question as to whether the barrier is located in the lower part of the stratum corneum, or resides in the whole of the corneum. The studies of Blank (1953) and Marzulli (1962) showed that as the cornified epithelium was stripped with adhesive tape very little change in permeability was observed until the base of the stratum corneum was reached and stripped, when there was an abrupt increase in permeability. They concluded that the major barrier was not the entire cornified epithelium but was in the lower part of the stratum corneum. Another possible interpretation of these results is to argue that the bulk of the stratum corneum is a uniformly good barrier. The abrupt increase as the lower part of the corneum is removed indicates that this part of the corneum is quite impermeable but not necessarily more impermeable than the upper layers, and this has been acknowledged by Blank (1965). Other stripping experiments by Monash (1957) and by Monash and Blank (1958) supported the concept of the barrier being located in the bulk of the corneum. Another approach in determining the site of the barrier within the stratum corneum has come from studies that reveal the location of tracer

substances within the corneum some time after topical application. The results of such studies were summarized by Kligman (1964) and Malkinson (1964). The largest concentration is found in the upper layers of the corneum with decreasing or undetectable concentrations in the lower corneal layers. Malkinson (1964) believed that this was an indication of the barrier being in the lower stratum corneum. Kligman (1964) believed that it was a reflection of a barrier gradient of increasing resistance from superficial to deep, corresponding to increasing cohesiveness of the cells, and that all the layers of the stratum corneum contributed to its barrier function. Thus the question of the location of the barrier within the stratum corneum remains in dispute and some favour the lower layers of the corneum as the barrier layer (Hurley, 1975; Blake *et al.*, 1981; Bowser and White, 1985) while others favour the bulk of the stratum corneum as the barrier layer (Idson, 1975; Scheuplein and Bronaugh, 1983). There is little doubt that the cells of the stratum corneum are not all histologically identical. Brody (1962) sub-divided the stratum corneum into three sublayers on the basis of differences in staining characteristics, as examined in the transmission electron microscope, and these were termed the basal, the intermediate, and the superficial corneal layers. Brody (1964) also identified two types of corneocytes within an individual sublayer and these were designated cell type A, in which the keratin pattern completely filled the cytoplasm of the cell, and cell type B in which electron-optically empty spaces occurred in varying number and size between the keratin fibrils. King *et al.* (1979) reported a reduction in the height of the individual corneocyte as these cells progressed towards the surface. However, it is not clear whether these morphological features reflect in any way variations in the barrier property across the stratum corneum.



In an attempt to contribute some resolution to the above dispute, silver nitrate was prepared in different vehicles to different concentrations and these solutions were applied locally or introduced iontophoretically. Only when silver was introduced from an 8% aqueous solution with iontophoresis was a variation in the amount of deposition established across the stratum corneum. The upper corneal layers were saturated with silver granules while the lower corneal layers contained relatively few silver deposits (Figure 92a). This may, as mentioned above, be interpreted in two ways. Either the individual layers of the stratum corneum are equally permeable but a particular layer becomes saturated before the subjacent layer, or the lower layers are less permeable than the upper layers. It is interesting to note that some corneocytes were heavily loaded with silver while adjacent cells **in the same cell layer** contained relatively few silver deposits (Figure 92a). This may be attributed to variations in the morphological features of cells in the same corneal layer (Brody, 1964, 1973). However, the distribution and localization of silver deposits in the upper and the lower corneal layers was generally uniform following iontophoresis of a 2% aqueous silver nitrate solution (Figure 88a), a 4% aqueous silver nitrate solution (Figure 90a) and a 2% silver nitrate in 50% aqueous DMSO solution (Figure 93a). These findings strongly suggest that whether the penetration through the stratum corneum is complete or not, the upper and lower layers of the stratum corneum are probably equally permeable. In addition, silver did not penetrate superficially above the basal corneal layer when aqueous tracer solutions were injected intradermally, nor did the tracer penetrate below the superficial corneal layer following topical application of different preparations

of silver nitrate (Figures 86e, 86f, 87a, 89a, 91a). These results may suggest that the epidermal barrier to silver ions is provided by the whole of the stratum corneum.

In summary, although some investigators have considered the stratum granulosum to be the barrier layer (MacKee *et al.*, 1945; Squier, 1973; Elias and Friend, 1975; Elias *et al.*, 1977), the present study has shown that both the inter- and the intra- cellular compartments of the stratum granulosum are readily penetrated with metal tracers following intradermal injections of the tracer solution or incubation of skin biopsies in solutions containing the tracer. Furthermore, the present study has provided additional evidence that (1) the cutaneous barrier to inward and outward flow of materials is provided by the stratum corneum of the epidermis (Monash and Blank, 1958; Tregear, 1966; Idson, 1975; Scheuplein and Bronaugh, 1983), possibly including the intercellular substance in the granular-corneal interface, and (2) if penetration through the stratum corneum occurs, then the corneal layers are equally permeable (Kligman, 1964). Finally, the present results have confirmed the barrier role previously suggested for sebum (Kitson and Van Lennep, 1984).

#### 4.16.3 The epidermal-dermal junction

No firm evidence exists that the structures of the epidermal-dermal junction (see page 8) act as a barrier to the diffusion of water, electrolytes and other low molecular weight materials. Indeed, it would be difficult to imagine a barrier to these materials at this level since the avascular epidermis depends upon the dermis for its nutrition. Furthermore, several studies have demonstrated the passage

of materials across the epidermal-dermal junction. Horseradish peroxidase, a water-soluble protein marker with a molecular weight of approximately 40,000, readily crosses this junction (Squier, 1973). Lanthanum (Wolff and Schreiner, 1968), ferritin (Elias and Friend, 1975) and Thorotrast (Wolff and Honigsmann, 1971) have also been shown to traverse the junction. Consistent with this, the present study has shown that lanthanum (Figure 76h) and silver (Figure 86 e and f) readily traverse the epidermal-dermal interface and appear within the epidermis following intradermal injections.

#### 4.17 Routes of entry

##### 4.17.1 Trans-appendageal versus trans-epidermal penetration

Three routes are available for the passage of materials from the surface into the skin: (1) the hair follicles, together with their associated glands, (2) the ducts and coils of the sweat glands and (3) the surface epidermis. There has been a division of opinion as to which one of these is the principal route of entry. Some favour the epidermal appendages as the major route of penetration while others favour the epidermis as the principal pathway of entry, and there is substantial data in the literature which support both opinions (page 34). In view of this, a consideration of the relative importance of the role of trans-appendageal versus trans-epidermal penetration is of importance.

Ionic dyes such as methylene blue and eosin, and metal salts such as copper sulphate, ferric chloride and silver nitrate, as well as the organic non-electrolyte sudan black B, have been used as tracers in

the present study. Solutions of these tracers were applied to the intact skin with or without the flow of a current. Utilization of cryostat and electron microscopy techniques has made it possible to demonstrate the penetration and sites of deposition of these tracers within the skin under different experimental conditions, and thus make possible the visualization of preferential route(s) of entry.

The way in which a 2% aqueous methylene blue solution penetrates the skin can be pictured histologically in detail from Figures 1 - 19. These represent the site of deposition of the dye in cryostat sections of skin when the dye solution is applied locally or introduced iontophoretically using different values of current intensity and duration of application. The experimental procedures and the extent of penetration are summarized in Table 4.6, (page 322).

Without iontophoresis, the penetration of the dye was negligible (Figure 1). With the minimum current density used ( $2.04 \text{ mA}\cdot\text{min}/\text{cm}^2$ ) there was a selective staining and hence penetration of the follicular infundibula by methylene blue (Figure 2). The dermis immediately adjacent to the follicular infundibula was also stained. The staining of the epidermis was not continuous but was interrupted by colour-free segments of varying extent. With a current density of  $4.08 \text{ mA}\cdot\text{min}/\text{cm}^2$ , the dye passed into the sebaceous glands while the penetration through the epidermis was still incomplete (Figures 3 and 5). This clearly indicates that the follicular infundibula and the sebaceous glands are primarily responsible for the transport of the dye into the skin.

As the current density was further increased, the dermal areas adjacent to the follicular infundibula and the sebaceous glands became intensely stained (Figures 4 and 8). Although the epidermis showed a more uniform colouration, dermal regions just below the epidermis and between the follicles remained unstained. From this it appears that the presence of the dye in the dermis is due to the horizontal passage of the tracer from the follicular infundibula and the sebaceous glands.

With a current density of 8.16 - 10.20 mA.min./cm<sup>2</sup>, the dye passed from the epidermis into the superficial part of the dermis situated between the follicles (Figures 6, 11 and 14). The staining of the dermis was very intense in areas adjacent to the follicular infundibula and the sebaceous glands, whereas the staining was less intense or absent in similar areas situated between the follicles. At a current density of 12.25 mA.min./cm<sup>2</sup>, all dermal areas at and above the level of the sebaceous glands became stained, probably as a result of penetration from the epidermis, the follicular infundibula and the sebaceous glands. Simultaneously, the dye extended down the follicles to the level at which the dermis merged with the hypodermis. Furthermore, the dermal areas adjacent to the lower parts of the hair follicles were also stained in contrast to similar areas situated between the follicles which remained relatively unstained. This indicates that the dye has passed horizontally from the lower follicular walls into the adjacent tissues.

As the current density was further increased from 16.33 to 18.37 and 20.41 mA.min./cm<sup>2</sup>, most of the dermis became stained (Figures 10, 12 and 15). Frequently the penetration of the dye extended into the

superficial part of the hypodermis adjacent to the hair follicles. In other words, the penetration of the dye through the hypodermis is deeper in areas containing hair follicles. This is another indication for penetration from the lower follicular walls. As the current density was yet further increased, the penetration of the dye was complete in many hair follicles, the dermis and in the superficial part of the hypodermis (Figures 13 and 18). With the maximum current densities used, 30.61 and 36.73 mA.min./cm<sup>2</sup>, the dye was visible in the panniculus carnosus muscle, having penetrated the skin and the hypodermis (Figures 16 and 19).

This orderly sequence of events is summarized diagrammatically in Figure 4.1 and indicates clearly that the pilosebaceous units constitute the major route of entry of methylene blue into the skin.

In further studies, methylene blue was prepared in distilled water to concentrations of 1% and 3%, and in absolute ethanol to a concentration of 2%. When these solutions were subjected to positive iontophoresis, the dye was clearly evident in the hair follicles, the sebaceous glands and the dermis immediately adjacent to these structures, whereas dermal regions located between the follicles remained relatively unstained (Figures 36 and 40). These results once again indicate clearly that the penetration of methylene blue into the skin is preferentially trans-follicular.

Additional studies were undertaken to further define the contribution of the pilosebaceous units to skin penetration. When different types of the anionic dye eosin were prepared in water or ethanol and subjected to standard negative iontophoresis, the tracer was clearly



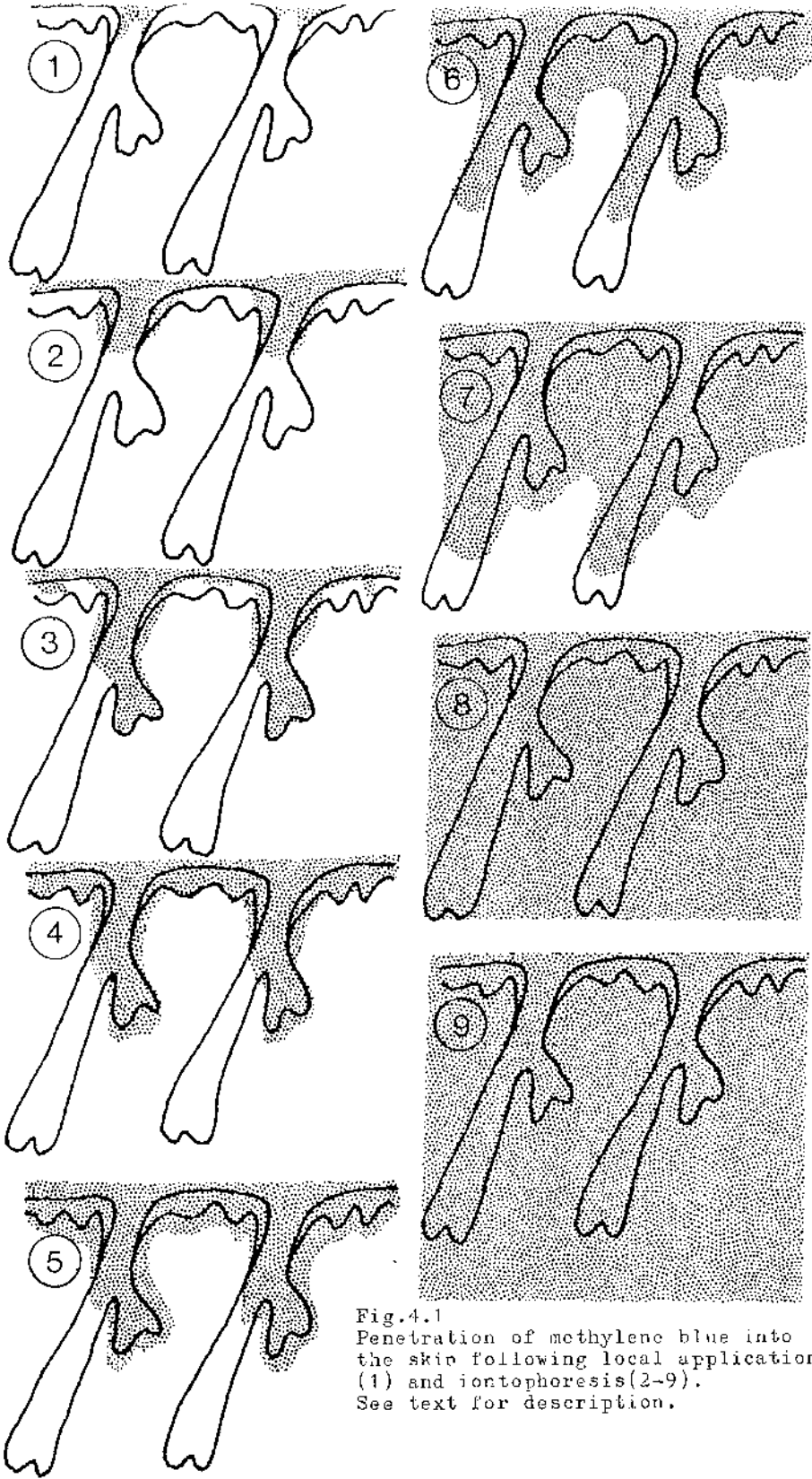


Fig.4.1  
Penetration of methylene blue into  
the skin following local application  
(1) and iontophoresis(2-9).  
See text for description.

evident in the hair follicles and their associated sebaceous glands (Figures 58 and 60) while the penetration through the epidermis was either absent (Figures 58 and 60) or minimal (Figures 54 and 56). Following local application of 0.1% sudan black B in ethanol for a duration of 15 minutes, the non-ionic tracer was seen in the hair follicles and the sebaceous glands, whereas the epidermis remained unstained (Figure 70). These findings, coupled with those of methylene blue, clearly show that the pilosebaceous units are the major avenue of entry of cationic, anionic and non-ionic organic dyes.

Further studies were carried out to investigate the preferential route(s) of penetration of metal ions into and through the skin. A 1% aqueous copper sulphate solution was subjected to positive iontophoresis using a current of 30 mA over a duration of 5 or 10 minutes. With the 5 minute duration, the tracer penetrated from the surface into the follicular infundibula and the sebaceous glands while the penetration through the epidermis was incomplete (Figure 100). With the 10 minute duration, although the penetration of the tracer was complete in the epidermis, the follicular infundibula and the sebaceous glands, the penetration of the tracer through the dermis was deeper in areas containing hair follicles (Figure 101). These results suggest that the pilosebaceous units are the major route of penetration of metal ions into the skin. Additional support for trans-follicular penetration was provided by the studies in which ferric ions were used as the tracer. Various preparations of ferric chloride were applied to the skin with standard positive iontophoresis. From a 1% aqueous solution, the follicular infundibula contained reaction for iron and, in addition, the penetration of the tracer extended into the dermal areas adjacent to the follicular

infundibula. Similar areas situated between the follicles were devoid of the tracer (Figure 115). From a 4% aqueous solution, the reaction product progressed to the sebaceous glands and the dermis surrounding them, but the penetration through the epidermis was incomplete (Figure 117). When the tracer substance was prepared in ethanol to a concentration of 4%, the tracer was visible in the epidermis, the hair follicles, the sebaceous glands, and in dermal areas adjacent to the hair follicles (Figure 121).

In conclusion, therefore, these studies indicate strongly that the pilosebaceous units are the major pathway for the penetration of not only organic dyes but also metal ions.

There have been some reports on the routes by which chemical compounds penetrate the skin. The *in vitro* penetration studies of Treherne (1956), Tregear (1960), Blank and Gould (1959) and Scheuplein (1966) were all measurements of steady state fluxes, which required exposure of isolated membranes to the penetrant in solution over long periods of time. All concluded that the stratum corneum was the major route of entry through the skin. Tregear (1961) applied tri-n-butyl phosphate *in vivo* to the flank of the pig either to hairless regions or directly to the hair follicles and showed that penetration was trans-epidermal with no comparable transport through the hair follicles. On the other hand, other *in vivo* permeability studies, which are commonly rapid measurements, are consistent with trans-follicular penetration. For example, Shelley and Melton (1949) observed perifollicular weals within minutes of histamine application. Histological studies of percutaneous penetration of dyes have also demonstrated that follicular penetration occurs within 5 minutes after

compound application (MacKee *et al.*, 1945). Neither group of investigators, however, demonstrated the constant predominance of a single route of entry, and this led Scheuplein (1967) and Scheuplein and Blank (1971) to suggest that trans-appendageal entry predominated during the initial stages of diffusion, and that the trans-epidermal pathway predominated once the stratum corneum was saturated with the penetrant. However, the present study offers evidence that the pilosebaceous units remain the major route of entry for even when the epidermis is saturated with the tracers, penetration into the dermis and the hypodermis is deeper in areas containing hair follicles.

It appears that at least four factors are involved in determining the role of trans-follicular versus trans-epidermal penetration: these are, firstly, the density of the hair follicles, secondly, the morphological features of the epidermis and its appendages, thirdly, the electrical property of the skin, and fourthly, the physico-chemical properties of the test material.

The density of the hair follicles:

This is the number of hair follicles in a given area (usually  $1 \text{ cm}^2$ ) of skin surface.

Different values have been estimated for the density of hair follicles in different species and in different regions of the body. A few examples are shown in the following Table:

Species	Site	Number of hair follicles per cm <sup>2</sup>	Author(s)
Man	Cheek	880	Szabo (1958)
	Forearm	60	Tregear (1966)
	Abdomen	11	Bronaugh et al. (1982)
	Back	80	Cunliffe and Cotterill (1975)
	Forehead	360	Cunliffe and Cotterill (1975)
Pig	Flank Back	40 11	Tregear (1966) Bronaugh et al. (1982)
Rabbit	Flank	700-3,000	Tregear (1966)
Rat	Back	289	Bronaugh et al. (1982)
Mouse	Back	658	Bronaugh et al. (1982)
Hairless mouse	Back	75	Bronaugh et al. (1982)

It has been suggested that in skin with relatively few hair follicles, the surface area of the stratified epithelium available for absorption within the hair follicles is small relative to that on the skin surface, while in densely-haired skin the opposite is true (Tregear, 1966). It is therefore probable that penetration is mainly trans-follicular (if the penetrant gets down the follicle) in densely-haired skin, while penetration is trans-epidermal in skin with a relatively low density of follicles (Tregear, 1961, 1962). The relationship of follicular density and the surface area available for penetration within the follicles as compared to that on the surface, with respect to skin penetration, has been discussed by a number of other investigators. For example, Scott (1957) demonstrated by means of autoradiography that the penetration of radioactive sulphur through normal human skin in areas with relatively low follicular densities was mainly through the epidermis. No preferential absorption through the hair follicles was noted. However, in skin affected with acne vulgaris, although the sulphur penetrated the epidermis as in the normal case, a larger and more persistent concentration was observed in the hair follicles which was attributed to the relatively greater surface area of the epithelium lining the involved follicles. Frosch *et al.* (1980) investigated the permeability of different regions of human subjects to dimethyl sulphoxide and found that the region of the forehead had the highest permeability while the mid-ventral forearm and the ventral wrist had the lowest permeabilities. They concluded that the greater permeability of the forehead region was due to the high density of appendageal shunts. Supporting evidence for the trans-follicular penetration in densely-furred skin was provided by Ebling *et al.* (1981) who applied ethanol containing sudan IV to the flank of the rat *in vivo* and found that the sebaceous glands received



the materials by way of the pilosebaceous orifices rather than by trans-epidermal absorption. Montagna (1954) found that vitamin A in different vehicles also penetrated the intact skin of the guinea pig by way of the pilosebaceous canals and the sebaceous glands. Sulzberger (1960) demonstrated the trans-follicular penetration of ink through the skin of the mouse following an hour of topical application. Therefore, the high follicular density in rat skin may be a contributory factor to the preferential trans-follicular penetration observed in the present study.

#### Morphological features:

The higher permeability of the pilosebaceous units may be related to their morphological features. Even though the epidermis and the follicular canal epidermis are continuous and are basically similar in proliferation, keratinization and exfoliation, they differ nonetheless. The stratum corneum is less developed in the hair follicle than it is on the surface of the skin (Bettley, 1970). Within the epidermis, the keratohyalin granules are irregular and large and the horny cells are strongly attached to each other. In the follicular infundibulum, the keratohyalin granules are round and small and the horny cells do not seem to be strongly adherent to each other and are easily exfoliated (Montagna and Parakkal, 1974). From an anatomical point of view, the lumen of the sebaceous excretory duct may provide an "open" gate for penetration if the test material is allowed entry into the follicles.

#### The electrical property of the skin:

The skin has a very high electrical resistance which was originally attributed to the stratum granulosum and the stratum lucidum of the epidermis (Calvery *et al.*, 1946; Rothman, 1954). Recent evidence, however, has shown that the site of the electrical resistance of the skin resides in the stratum corneum and that the epidermal appendages have relatively a very low resistance (Tregear, 1966; Grice *et al.*, 1975; Yamamoto and Yamamoto, 1976; Edelberg, 1977; Grice and Verbov, 1977; Tagami *et al.*, 1980). This probably explains the enhanced penetration through the hair follicles when an electrical potential is applied across the skin. Rothman (1954) suggested that the promotion of absorption by the flow of an electric current was via the hair follicles, and the present findings support this view.

#### Physico-chemical property of the test material:

Because electrolytes are known to be poor penetrants of the epidermis, Scheuplein and Bronaugh (1983) speculated that shunt diffusion through the epidermal appendages played a significant role in the transport of this class of materials into the skin. The present study has provided histological evidence that the pilosebaceous units are indeed the major route for entry of charged dyes and metal ions into the rat skin by iontophoresis. The hair follicles also appear to be the easy port of entry of non-ionic materials into the skin. The trans-follicular penetration of sudan IV (Ebling *et al.*, 1981) and sudan black B (Figure 70) may be related to the sudanophilic nature of the lipids in the hair follicles. Similarly, the penetration of vitamin A into the sebaceous glands was attributed to the lipophilicity of the penetrant by Montagna (1954).

Thus far, the epidermis and the hair follicles have been discussed as routes for penetration. The third possible route of entry is the ducts of the sweat glands and this type of penetration is termed transudoriferous. The role of sweat ducts as a preferential route for penetration cannot be discussed fully in the present study since the skin of the usual experimental animals (rat, rabbit, guinea pig, etc.) is devoid of sweat glands (Tregear, 1962). Available data conflict in terms of the importance of sweat ducts as a major part of entry of materials into the skin. Abramson and Gorin (1940) and Abramson and Engle (1942) demonstrated the rapid penetration of methylene blue through the sweat ducts in the human palms *in vivo* by iontophoresis. There was no comparable transport through the surface epidermis as judged by the development of a "particular pattern", that is, the dye was confined to the acrosyringium of the sweat glands which appeared as blue "spots" distributed over an unstained skin surface. In the course of time, the blue spots developed within them paler areas, the individual spot as a whole then taking on the appearance of a "doughnut" in which the pale area in the centre of the doughnut was the orifice of the sweat gland. These workers also reported that this pore pattern could be obtained with basic dyes like patent blue and basic fuchsin as well as acidic dyes like eosin Y, sodium prontosil, sodium indigo tetra sulphionate, acid fuchsin and sodium phenolsulphanephthalein. However, Flesch *et al.* (1951) showed that the sweat pore patterns were readily erased from intact skin by the scraping-off of the horny layer with a scalpel, and that the penetration through the sweat ducts could not be demonstrated histologically. Furthermore, palmar skin, which contains a larger number of sweat glands than elsewhere, was found to be less permeable to tributyl phosphate (Marzulli, 1962) and other materials, excluding

water (Tregear, 1966), than skin of other regions. Holzle and Braun-Falco (1984) treated hyperhidrosis of the axillary eccrine sweat glands by aluminium ions from aluminium chloride solutions by overnight local applications. The number of applications varied from a single application every two to three weeks to three applications per week, while the treatment period ranged from 6 to 40 months. They came to the conclusion that metal ions did not penetrate into the coils and ducts of the sweat glands following prolonged contact with the skin surface, but rather formed an obstructive conglomerate that completely plugged the acrosyringium of the eccrine glands. This in turn led to the desired functional (loss of secretion) and structural (atrophy of secretory cells) changes. On the other hand, Witten et al (1951, 1953) demonstrated (*in vivo*) by means of topical application and autoradiography the penetration of thorium X from various vehicles into the epidermis, the hair follicles and, more significantly, into the ducts and coils of sweat glands, with no comparable radioactivity being detected throughout the dermis. Blank and Gould (1959) studied the penetration of a radioactive anionic surfactant through isolated human abdominal skin and observed a very dense activity in the epidermis, the sebaceous glands and the sweat glands and a weaker activity throughout the dermis. However, they could not decide whether the ions reached the epidermal appendages directly from the surface or through the epidermis with subsequent diffusion through the dermis and accumulation in the appendages.

Iontophoresis of tap water has been used in the treatment of hyperhidrosis of the palms, soles and axilla (Shrivastava and Singh, 1977; Midtgaard, 1986). The effect of such treatment has been attributed to a local electro-chemical coagulation of proteins in the

areas where the current is applied (Midtgaard, 1986). But the role of iontophoresis in driving ions preferentially into the ducts and coils of sweat glands remains to be established. Furthermore, the significance of using aqueous solutions of metal salts rather than tap water in the treatment of hyperhidrosis with iontophoresis remains to be examined.

#### 4.17.2 Transcellular versus intercellular penetration

The penetration of materials through the epidermis, the follicular infundibula and the sebaceous glands can either be transcellular (through the cells) or intercellular (between the cells). With regard to the epidermal barrier, some workers provided evidence that penetration through the stratum corneum was transcellular (Crouse, 1965; Blank, 1969; Goldsmith and Baden, 1970; Scheuplein and Blank, 1971; Baden *et al.*, 1976), while others provided evidence for intercellular penetration (Elias and Friend, 1975; Elias and Brown, 1978; Nemanic and Elias, 1980; Elias, 1981). According to the condition of the skin, Scott (1957) reported that the penetration of radioactive sulphur through the stratum corneum was intercellular in normal skin and transcellular in involved skin (seborrhoeic dermatitis, acne vulgaris and psoriatic lesion). According to the chemical nature of materials, Tregear (1962) speculated that ions penetrated the corneum via the intercellular route while covalent compounds penetrated via the transcellular route.

In the present study, solutions of electron-dense tracers, namely lanthanum and silver, were applied to the skin with iontophoresis with the object of determining the relative importance of intercellular and

transcellular penetration not only through the epidermis, but also through the follicular infundibula and the sebaceous glands.

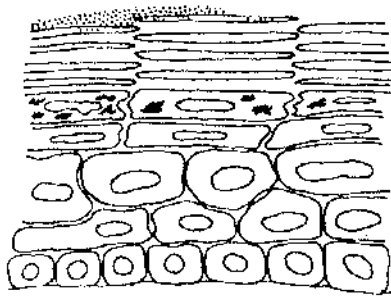
When introduced from ethanol with standard positive iontophoresis, lanthanum was able to penetrate inwards into the stratum corneum of the epidermis, gaining access to regions from which it is normally excluded without the flow of current (Figure 84a). Despite the occasional presence of electron-dense material in some cells in the upper layers of the stratum corneum, the deposition of lanthanum in the intercellular compartment was very prominent throughout the stratum corneum (Figure 85a). A similar result was observed for the follicular canal epidermis and, furthermore, the tracer was evident in the intercellular spaces in the viable layers of the epidermis (Figure 85b). The presence of the tracer in the sebaceous glands was suspected but not proven (Figure 85 c and d). These findings suggest that the penetration through the stratum corneum (excluding the outermost one or two layers) of both the epidermis and the follicular infundibula is predominantly intercellular.

Silver nitrate was prepared in distilled water to a concentration of 2% or 4%. Each of these solutions was applied locally for a duration of 15 minutes or subjected to positive iontophoresis using a current intensity of 30 mA for 15 minutes. The penetration of the tracer from either solution was negligible without the flow of current, that is, the tracer was only visible on the surface of the skin and in the outermost corneal layer (Figures 89a and 91a). Furthermore, silver was not seen in the follicular infundibula (Figures 89b and 91b) or in the sebaceous glands (Figures 89c and 91c). Following iontophoresis, however, although silver deposits were seen inside some cells in the



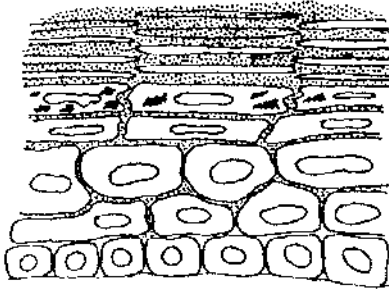
upper layers of the stratum corneum, the deposition of silver in the intercellular spaces was very prominent throughout the stratum corneum (Figures 90a and 92a). In addition, the tracer was also visible in the viable epidermal layers in which it was mainly confined to the intercellular spaces (Figure 90a). This is not surprising since the intercellular regions in the viable epidermis are "open" for the exchange of fluids between the epidermis and the dermis. These findings indicate that the penetration of the tracer occurs mainly via the intercellular route. Harris (1959) used silver iontophoresis in the treatment of painful small joints in the hands and feet resulting from rheumatoid arthritis and osteoarthritis and reported that the penetration of silver into the epidermis was facilitated by the galvanic current. However, he did not indicate whether silver was located intercellularly or intracellularly within the epidermal layers.

The location and distribution of the tracer in the follicular canal epidermis when presented from a 4% solution (Figure 90b) closely resembled those described for the epidermis (Figures 90a and 92a). The deposition of silver in the follicular canal epidermis from an 8% solution was so intense that the identification of the various epidermal layers proved difficult (Figure 92b). However, the penetration of the tracer in this case was transcellular in the outer epidermal layers and intercellular in the inner epidermal layers. The way in which silver ions appear to penetrate the stratum corneum is summarized in Figure 4.2. When present in the sebaceous glands, the tracer was seen in the cytoplasm between the lipid droplets of the sebocytes and in the intercellular regions (Figure 92c) although the deposition was slightly heavier in the latter. Nonetheless, this may



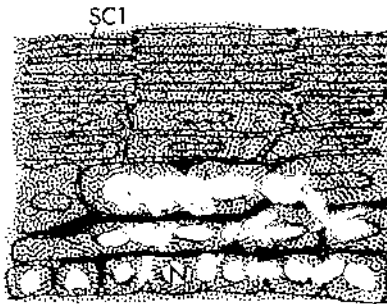
The tracer is visible on the surface of the skin and in the most superficial corneal layer.

Figures 89a and 91a



The tracer passes through all the intercellular spaces in the stratum corneum and into the intercellular spaces in the viable epidermal layers. The tracer is only visible inside some cells in the outer layers of the stratum corneum.

Figures 90a, 90b and 92a.



The deposition of the tracer in the epidermis is so dense that identification of the various epidermal layers is difficult.

SC1 is the outermost corneal layer and N is the nucleus of a basal cell.

Figure 92b

Fig.4.2.  
Penetration of silver into the epidermis following local application and iontophoresis.

indicate that penetration into the gland occurs equally well through the inter- and intra- cellular compartments. It is interesting to note that the tracer was seen inside the sebaceous glands and the follicular infundibula before it passed from the stratum corneum into the subjacent layers of the interfollicular epidermis (Figures 92 a, b and c), suggesting a trans-follicular penetration.

In conclusion, the present findings suggest that the penetration of lanthanum and silver through the stratum corneum of the interfollicular and intrafollicular epidermis is preferentially intercellular, while that through the sebaceous glands is probably transcellular.

#### 4.18 Advantages and disadvantages of iontophoresis

The use of iontophoresis as a therapeutic and an experimental tool embodies many advantages which include:

(1) While electrolytes are known to be poor penetrants (Blank and Gould, 1961; Blank *et al.*, 1964; Scheuplein and Bronaugh, 1983), iontophoresis may be a very effective technique by which ionic materials can be introduced into and through the skin.

(2) The surface of the skin is unbroken following iontophoresis whereas conventional procedures used to study, for example, allergic skin reactions may include scratching of the skin and rubbing the test material into the wound so formed.

(3) The current intensity and duration of application can be varied over a wide range.

(4) There is excellent uniformity in the distribution of the penetrant ions through the skin (see, for example, Figures 2 - 19).

(5) Since penetration occurs only in that area of skin under the iontophoresis electrode (Figures 20 - 25), the electrode can be designed in accordance with the shape and size of the area to be treated, thus ensuring penetration only where it is desired.

(6) No discomfort or pain is felt by the animal (McEwan Jenkinson *et al.*, 1974) or the human subject (Abramson and Engle, 1942) during the treatment, provided that certain precautions are taken into consideration. These include the selection of appropriate values of current intensity and duration of application, and the presence of electrode dressings. It is interesting to note that, in dental practice, iontophoresis is not only effective in the treatment of various conditions but also in producing a good mucosal anaesthesia (Gangarosa, 1983), thus eliminating pain, anxiety and fear of injections, particularly in children.

(7) The prolonged persistence of electrically introduced ionic materials in the treated area. This has been demonstrated by a number of investigators, for example, Juhlin (1961a) who subjected the skin of the human forearm to epinephrine and norepinephrine iontophoresis and observed the characteristic blanching reaction. Two days later trypsin was introduced by iontophoresis and the blanching was limited to the pretreated areas which suggested that the catecholamines had remained in the skin for two days after their introduction by iontophoresis. Abramson and Gorin (1940) and Abramson and Engle (1942) also reported the persistence of electrically-repelled materials in the skin several days after treatment.

(8) The technique can be used in the treatment of many skin and other surface tissue conditions which do not respond to routine therapy (see page 55).

(9) Iontophoresis enables certain aspects of percutaneous penetration of ionic chemicals to be investigated which otherwise could not be easily studied. For example, Blank and Gould (1959) studied the penetration of a radioactive anionic surfactant through isolated human abdominal skin, and the position of the radioactive chemical within the skin was determined by autoradiography. The tracer solution was left in contact with the surface of the skin for 22 hours. They observed a very dense activity in the epidermis, sebaceous glands, sweat glands and the blood vessels in the upper dermis, while a weaker activity was seen throughout the dermis. However, they could not say whether the surfactant had reached the sebaceous glands through the hair follicles directly, or through the epidermis with subsequent diffusion through the dermis to the sebaceous glands. In contrast, by the use of iontophoresis the penetration trials can be carried out on intact skin, the duration of application is reduced significantly as compared to that mentioned above and the avenues of entry can be established by varying the intensity of the current and/or the duration of application.

The only disadvantage of iontophoresis appears to be controlling the exact amount of material introduced during iontophoresis. Nevertheless, the total amount introduced and the rate of introduction can be varied significantly by changing the current intensity and/or the duration of treatment.

#### 4.19 Suggestion for future investigations

The use of microscopically detectable tracer substances provides an important method for establishing the pathway(s) that tracers take in

penetrating the skin and for revealing the presence of any barrier to penetration. In the present investigation the localization and site of deposition of test materials have been determined directly on cryostat sections if the tracer was a coloured material (organic dyes and ruthenium red), on ultrathin sections if the tracer was electron-dense (lanthanum and silver), or on cryostat sections when the tracer had a specific histochemical test (copper and iron).

Another method which may be employed in such investigations is autoradiography. Compounds labelled with radioisotopes have found wide application in dermatological research, particularly in the field of percutaneous absorption (Pinson, 1952; Scott and Kalz, 1956; Malkinson, 1958, 1960; Blank and Gould, 1959; Solomon and Lowe, 1979; Reifenrath *et al.*, 1984). Quantitative penetration of radioactive materials through the skin may be studied by detection of these compounds in body fluids, tissues or excreta, and pathways of penetration can be determined by autoradiography. Thus it may be suggested that autoradiography is a good method which can be employed to investigate the penetration and route(s) of penetration of materials by iontophoresis. Indeed, this has been employed in the past but only occasionally. For example, Fleischmajer and Witten (1955) demonstrated by means of autoradiographs the enhanced penetration of thorium X through the epidermis by iontophoresis, but penetration through the follicles and sweat glands was not mentioned. Furthermore, it is highly desirable to employ autoradiography in studying the penetration of inorganic anions such as iodides, bromides and chlorides, since it is hard to carry out successful histochemical tests to reveal their location in tissues, particularly in skin sections following iontophoresis.



# *CONCLUSIONS*

## Conclusions

(1) Electrolytes in solution do not penetrate the intact skin following local (topical) application for a duration of 15 minutes.

(2) The penetration of many ionic materials into the skin is facilitated by iontophoresis.

(3) Cationic dyes and metal cations are introduced into the skin by positive iontophoresis. However, the penetration of non-ionic dyes into the skin is not influenced by the flow of current.

(4) The penetration of ionic tracers into the skin occurs only in the treated area under the iontophoresis electrode. No penetration occurs from the surface of neighbouring areas.

(5) The penetration of tracers is as deep and intense at the edges and corners as it is in the centre of the treated area.

(6) Reversing the polarity of the iontophoresis electrode at regular intervals does not result in enhancement or retardation of penetration of ionic tracers.

(7) Once introduced into the skin by the correct (that is, positive or negative) iontophoresis, the tracers cannot be recovered from the skin by reverse iontophoresis.

(8) Cations penetrate the skin more extensively than anions following positive and negative iontophoresis respectively.

(9) The removal of surface lipid is not followed by enhanced tracer penetration by iontophoresis.

(10) The addition of accelerants (dimethyl sulphoxide) and detergents (sodium lauryl sulphate and tween 20) to tracers in aqueous solutions does not result in an enhancement of tracer penetration by iontophoresis as compared to aqueous vehicle alone.

(11) The use of absolute ethanol as an alternative vehicle to water results in an enhancement of tracer penetration by iontophoresis. However, such penetration is accompanied by marked morphological changes as compared to those seen when water is used as the vehicle.

(12) An initial increase in the concentration of tracer substances results in an increase in the penetration of the tracers by iontophoresis up to a particular concentration which is characteristic for each tracer. Thereafter, further increase in their concentrations results in a reduced penetration.

(13) The extent of penetration of a tracer is influenced by the current density. The stronger the current intensity and/or the longer the duration of application, the deeper the penetration.

(14) The penetration of ionic tracers into the skin is determined by the physico-chemical properties of the tracer. These include the solubility characteristics, the ionic weight and size, the diffusivity and the valency of the tracer, and the pH of the tracer solution.

(15) The whole of the stratum corneum of the epidermis is the major barrier to cutaneous penetration by electrolytes. In addition, a barrier function is suggested for sebum in the follicular canals.

(16) The penetration of organic and inorganic ions into the skin as a whole is preferentially transfollicular.

(17) The penetration of electron-dense tracers into the stratum corneum is preferentially intercellular, while that into the sebaceous glands is transcellular.

# *REFERENCES*

- Abbott, N. J., Temin, S. C. and Park, C. (1968).  
The stress-strain behavior of wool in various swelling media.  
*Text. Res. J.*, **38**: 1026-1039.
- Abramson, H. A. (1938).  
Skin reaction. IV. Iontophoresis of Allergens and Histamine.  
*J. Mount Sinai Hospit.*, **5**: 134-137.
- Abramson, H. A. and Alley, A. (1937).  
Skin reactions. I. Mechanism of histamine iontophoresis from aqueous media.  
*Arch. Phys. Therap.*, **18**: 327-332.
- Abramson, H. A. and Engle, M. G. (1942).  
Skin reactions. XII. Patterns produced in the skin by electrophoresis of dyes.  
*Arch. Dermatol. Syphil.*, **44**: 190-200.
- Abramson, H. A. and Gorin, M. H. (1939).  
Skin reactions. VII. Relationship of skin permeability to electrophoresis of biologically active materials into the living human skin.  
*J. Physiol. Chem.*, **43**: 335-346.
- Abramson, H. A. and Gorin, M. H. (1940).  
Skin permeability.  
*Cold Spring Harbor Symp. Quant. Biol.*, **8**: 272-278.
- Ackerman, A. B. (1975).  
Structure and function of the skin. In "Dermatology", (Eds: Moschella, S. L., Pillsbury, D. M. and Hurley, H. J.). W. B. Saunders and Co., Philadelphia and London. pp 1-68.
- Ainsworth, M. (1960).  
Methods for measuring percutaneous absorption.  
*J. Soc. Cosmet. Chem.*, **11**: 69-78.
- Allen, T. D. and Potten, C. S. (1974).  
The fine structural identification and organization of the epidermal proliferative unit.  
*J. Cell. Sci.*, **15**: 291-319.
- Allen, T. D. and Potten, C. S. (1975).  
Desmosomal form, fate and function in mammalian epidermis.  
*J. Ultrastruct. Res.*, **51**: 94-105.
- Allenby, A. C., Creasey, N. H., Edgington, A. G., Fletcher, J. and Schock, C. (1969b).  
Mechanism of action of accelerants on skin penetration.  
*Brit. J. Dermatol.*, **81** (Suppl. 4): 47-55.
- Allenby, A. C., Fletcher, J., Schock, C. and Tees, T. F. S. (1969a).  
The effect of heat, pH and organic solvents on the electrical impedance and permeability of excised human skin.  
*Brit. J. Dermatol.*, **81**: (Suppl. 4): 31-39.

- Anjo, D. M., Feldmann, R. J. and Maibach, H. I. (1980).  
Methods for predicting percutaneous penetration in man. In  
"Percutaneous Absorption of Steroids", (Eds: Mauvais-Jarvis, P.,  
Vickers, C. F. H. and Wepierre, J.). Academic Press, London.  
pp 31-51.
- Axelrod, D. J. and Hamilton, J. G. (1947).  
Radio-autographic studies of the distribution of lewisite and  
mustard gas in skin and eye tissues.  
*Amer. J. Pathol.*, 23: 389-411.
- Ayres, P. J. W. and Hooper, G. (1978).  
Assessment of the skin penetration properties of different  
vehicles for topically applied cortisol.  
*Brit. J. Dermatol.*, 99: 307-317.
- Bahr, G. F. (1954).  
Osmium tetroxide and ruthenium tetroxide and their reactions  
with biologically important substances.  
*Exper. Cell Res.*, 7: 457-479.
- Baker, F. (1939).  
Indications and technique of iontophoresis.  
*Arch. Phys. Therap.*, 20: 197-207.
- Baker, H. (1968).  
The effects of dimethyl sulphoxide, dimethyl formamide and  
dimethyl acetamide on the cutaneous barrier to water in human  
skin.  
*J. Invest. Dermatol.*, 50: 283-288.
- Baker, H. (1979).  
The skin as a barrier. In "Textbook of Dermatology", (Eds:  
Rook, A., Wilkinson, D. S. and Ebling, F. J. G.). Vol. 1, 3rd  
edn, Blackwell Sci. Pub., Oxford. pp 289-298.
- Baldwin, K. M. (1981).  
Cell-to-cell tracer movement in cardiac muscle. Ruthenium red  
vs lanthanum.  
*Cell Tiss. Res.*, 221: 279-294.
- Bancroft, J. D. and Stevens, A. (1977).  
"Theory and Practice of Histological Techniques." Churchill  
Livingstone, Edinburgh and London.
- Berenson, G. S. and Burch, G. E. (1951).  
Studies of diffusion of water through dead human skin.  
*Amer. J. Trop. Med.*, 31: 842-853.
- Bettley, F. R. (1961).  
The influence of soap in the permeability of the epidermis.  
*Brit. J. Dermatol.*, 73: 448-454.
- Bettley, F. R. (1963).  
Irritant effect of soap in relation to epidermal permeability.  
*Brit. J. Dermatol.*, 75: 113-116.



- Bettley, F. R. (1965).  
The influence of detergents on epidermal permeability.  
*Brit J. Dermatol.*, **77**: 98-100.
- Bettley, F. R. (1970).  
The epidermal barrier and percutaneous absorption. In "An Introduction to the Biology of the Skin", (Eds: Champion, R. H., Gillman, T., Rook, A. J. and Sims, R. T.). Blackwell Sci. Pub., Oxford. pp 342-354.
- Bettley, F. R. and Donoghue, E. (1960).  
Effect of soap on the diffusion of water through isolated human epidermis.  
*Nature*, **185**: 17-20.
- Bierman, W. and Licht, S. (1952).  
"Physical Medicine in General Practice". 3rd edn, Cassell and Co. Ltd, London. pp 178-235.
- Blake, M., Garcia, M. L., Thorvaldsen, J., Wolfram, L. and Yare, R. (1981).  
Variations in properties across the thickness of stratum corneum.  
*Bioengineering and Skin*, **3**: 141.
- Blanchette-Mackie, E. and Scow, R. O. (1982).  
Continuity of intracellular channels with extracellular space in adipose tissue and liver demonstrated with tannic acid and lanthanum.  
*Anat. Rec.*, **203**: 205-219.
- Blank, I. H. (1952).  
Factors which influence the water content of the stratum corneum.  
*J. Invest. Dermatol.*, **18**: 443-440.
- Blank, I. H. (1953).  
Further observations on factors which influence the water content of the stratum corneum.  
*J. Invest. Dermatol.*, **21**: 259-269.
- Blank, I. H. (1964).  
Penetration of low-molecular weight alcohols into skin. I. The effect of concentration of alcohol and type of vehicle.  
*J. Invest. Dermatol.*, **43**: 415-420.
- Blank, I. H. (1965).  
Cutaneous barriers.  
*J. Invest. Dermatol.*, **45**: 249-256.
- Blank, I. H. (1969).  
Transport across the stratum corneum.  
*Toxicol. Appl. Pharmacol. Supp.*, **3**: 23-29.

- Blank, I. H. and Gould, E. (1959).  
Penetration of anionic surfactants (surface active agents) into skin. I. Penetration of sodium laurate and sodium dodecyl sulfate into excised human skin.  
*J. Invest. Dermatol.*, **33**: 327-336.
- Blank, I. H. and Gould, E. (1961).  
Penetration of anionic surfactants into skin. II. Study of mechanisms which impede the penetration of synthetic anionic surfactants into skin.  
*J. Invest. Dermatol.*, **37**: 311-315.
- Blank, I. H., Gould, E. and Theobald, A. (1964).  
Penetration of cationic surfactants into skin.  
*J. Invest. Dermatol.*, **42**: 363-366.
- Blank, I. H. and Scheuplein, R. J. (1964).  
The epidermal barrier. In "Progress in the Biological Sciences in Relation to Dermatology", (Eds: Rook, A. J. and Champion, R. H.). Cambridge University Press, London. Vol. 2, 2 edn. pp 245-261.
- Blank, J. H., Scheuplein, R. J. and MacFarlane, D. J. (1967).  
Mechanism of percutaneous absorption. III. The effect of temperature on the transport of non-electrolytes across the skin.  
*J. Invest. Dermatol.*, **49**: 582-589.
- Boden, H. P., Lee, L. D. and Kubilus, J. (1976).  
Intra- and extracellular cementing substances.  
*J. Soc. Cosmet. Chem.*, **27**: 433-441.
- Bolliger, A. and Gross, R. (1954).  
Non-keratins of avian and mammalian skin flakes.  
*Aust. J. Exp. Biol. Med. Sci.*, **32**: 747-756.
- Bowser, P. A. and White, R. J. (1985).  
Isolation, barrier properties and lipid analysis of stratum compactum, a discrete region of the stratum corneum.  
*Brit. J. Dermatol.*, **112**: 1-14.
- Bradbury, J. H. and Champan, G. V. (1964).  
The chemical composition of wool. I. The separation and microscopic characterization of components produced by ultrasonic disintegration.  
*Aust. J. Biol. Sci.*, **17**: 960-972.
- Breathnach, A. S. (1971).  
"An Atlas of the Ultrastructure of Human Skin."  
J. and A. Churchill, London.
- Breathnach, A. S. and Wylie, L. (1966).  
Osmium iodide positive granules in spinous and granular layers of guinea pig epidermis.  
*J. Invest. Dermatol.*, **47**: 58-60.

- Breathnach, A. S., Goodman, T., Stolinski, C. and Gross, M. (1973).  
Freeze-fracture replication of cells of stratum corneum of human epidermis.  
*J. Anat.*, **114**: 65-81.
- Briggaman, R. A. and Wheeler, E. (1975).  
The epidermal-dermal junction.  
*J. Invest. Dermatol.*, **65**: 71-84.
- Brody, I. (1959).  
The keratinization of epidermal cells of normal guinea-pig skin as revealed by electron microscopy.  
*J. Ultrastruct. Res.*, **2**: 482-511.
- Brody, I. (1960).  
The ultrastructure of the tonofibrils in the keratinization process of normal human epidermis.  
*J. Ultrastruct. Res.*, **4**: 264-297.
- Brody, I. (1962).  
The ultrastructure of the horny layer in normal and psoriatic epidermis as revealed by electron microscopy.  
*J. Invest. Dermatol.*, **39**: 519-528.
- Brody, I. (1964).  
Observations on the fine structure of the horny layer in the normal human epidermis.  
*J. Invest. Dermatol.*, **42**: 27-31.
- Brody, I. (1966).  
Intercellular space in normal human stratum corneum.  
*Nature*, **209**: 472-476.
- Brody, I. (1969).  
The modified plasma membranes of the transition and horny cells in normal human epidermis as revealed by electron microscopy.  
*Acta Dermatovener.*, **49**: 128-138.
- Brody, I. (1973).  
The ultrastructure of epidermis in lichen ruber planus as revealed by electron microscopy.  
*J. Ultrastruct. Res.*, **43**: 362-376.
- Bronaugh, R. L. and Franz, T. J. (1986).  
Vehicle effects on percutaneous absorption: *in vivo* and *in vitro* comparisons with human skin.  
*Brit. J. Dermatol.*, **115**: 1-11.
- Bronaugh, R. L., Stewart, R. F. and Congdon, E. R. (1983).  
Differences in permeability of rat skin related to sex and body site.  
*J. Soc. Cosmet. Chem.*, **34**: 127-135.
- Bronaugh, R. L., Stewart, R. F., Congdon, E. R. and Giles, A. L. (1982).  
Methods for *in vitro* percutaneous absorption studies. I. Comparison with *in vivo* results.  
*Toxicol. Appl. Pharmacol.*, **62**: 474-480.

- Browne, A. R. I. (1931).  
"Medical Electricity for Students." Oxford University Press,  
London. 3rd ed.
- Bulgin, J. J. and Vinson, L. J. (1967).  
The use of differential thermal analysis to study the bound  
water in stratum corneum membranes.  
*Biochem. Biophys. Acta*, **136**: 551-560.
- Burch, G. E. and Winsor, T. (1944).  
Diffusion of water through dead plantar, palmar and dorsal human  
skin and through toe nails.  
*Arch. Dermatol.*, **53**: 39-41.
- Burch, G. E. and Winsor, T. (1944).  
Rate of insensible perspiration locally through living and  
through dead human skin.  
*Arch. Intern. Med.*, **74**: 437-444.
- Calvery, H. Q., Draize, J. H. and Laug, E. P. (1946).  
The metabolism and permeability of normal skin.  
*Physiol. Rev.*, **26**: 495-540.
- Caputo, R., Peluchetti, D. and Monti, M. (1975).  
The junctions of normal human epidermis: A freeze-fracture  
study.  
*J. Invest. Dermatol.*, **64**: 282.
- Champion, R. H. (1970).  
Sweat glands. In "An Introduction to the Biology of the Skin",  
(Eds: Champion, R. H., Gillman, T., Rook, A. and Sims, R. T.).  
Blackwell Sci. Pub., Oxford. pp 175-183.
- Chandler, J. A. (1977).  
"X-Ray Microanalysis in the Electron Microscope". North-Holland  
Pub. Co., Oxford.
- Christophers, E. (1971).  
Cellular architecture of the stratum corneum.  
*J. Invest. Dermatol.*, **56**: 165-169.
- Clark, W. G, Strakosch, E. A. and Nordlum, C. (1942).  
Penetration of sulfonamides through intact skin by iontophoresis  
and other means of local application.  
*Proc. Soc. Exper. Biol. Med.*, **50**: 43-48.
- Clausen, C. A., Prados, R. A. and Good, M. L. (1971).  
A mossbauer study of ruthenium red.  
*Inorg. Nucl. Chem. Letters*, **7**: 485-489.
- Clayton, E. B. (1952).  
"Electrotherapy and Actinotherapy". Bailliere, Tindall and Cox;  
London, 2nd ed.
- Cook, H. C. (1974).  
"Manual of Histological Demonstration Techniques". Butterworths  
Co. (Pub.) Ltd, London.

- Cottey, V. F., Skerpac, J., Ederma, H. M., Zurzola, F. and Kuna, M. (1960).  
The percutaneous absorption of salicylates as measured by blood plasma levels in the rabbit.  
*J. Soc. Cosmet. Chem.*, 11: 97-116.
- Council on Pharmacy and Chemistry and the Council on Physical Therapy. (1941).  
Ion transfer (iontophoresis).  
*J. Amer. Med. Ass.*, 117: 360-361.
- Craig, R. L. and Kraff, H. (1943).  
The treatment of acute inflammatory pelvic masses of tubal origin by iontophoresis with acetyl Beta methylcholine chloride.  
*Amer. J. Obst. Gynecol.*, 45: 96-102.
- Cronin, E. and Stoughton, R. B. (1962).  
Percutaneous absorption, regional variations and the effect of hydration and epidermal strippings.  
*Brit. J. Dermatol.*, 74: 265-272.
- Cross, H. H. U. (1925).  
"Electro-Therapy and Ionic Medication". Charles Griffin Co. Ltd, London.
- Cross, H. H. U. (1936).  
"Electricity in Therapeutics - A Technical and Clinical Compendium". Crosby Lockwood and Son Ltd, London.
- Crouse, R. G. (1965).  
Keratin and the barrier.  
*Arch. Environ. Health*, 11: 522-528.
- Cumberbatch, E. P. (1933).  
"Essentials of Medical Electricity". Henry Kimpton, London. 7th ed.
- Cunliffe, W. J. and Cotterill, J. A. (1975).  
"The Acnes. Clinical Features, Pathogenesis and Treatment". W. B. Saunders Co. Ltd, London. pp 173-191.
- Cutner, M. (1949).  
The influence of red light and of ionization upon the penetration of the skin by penicillin.  
*Brit. J. Phys. Med.*, 12: 144-147.
- Deuschle, F. M. (1943).  
A suggested method for managing dental and aveolar infections.  
*Cincinnati J. Med.*, 23: 578-586.
- Dierichs, R. (1979)  
Ruthenium red as a stain for electron microscopy, some new aspects of its application and mode of action.  
*Histochemistry*, 64: 171-187.

- Dixon, K. (1970).  
Principles of some tinctorial and cytochemical methods. In "An Introduction to the Biology of the Skin", (eds: Champion, R. H., Gillman, T., Rook, A. and Sims R. T.). Blackwell Sci. Pub., Oxford. pp 35-60.
- Drury, R. A. B. and Wallington, E. A. (1980).  
"The Theory and Practice of Staining - Carleton's Histological Technique". Oxford University Press, Oxford. pp 107-124.
- Dugard, P. H. and Scheuplein, R. J. (1973).  
Effect of ionic surfactants on the permeability of human epidermis: an electrometric study.  
*J. Invest. Dermatol.*, **60**: 263-269.
- Dyson, J. N. (1936).  
"The Practice of Ionization". Henry Kimpton, London.
- Ebling, F. J. (1964).  
The hair follicle. In "Progress in the Biological Sciences in Relation to Dermatology - 2", (eds: Rook, A. and Champion, R. H.). The University Press, Cambridge. pp 303-323.
- Ebling, F. J. (1979).  
The normal skin. In "Textbook of Dermatology", (eds: Rook, A., Wilkinson, D. S. and Ebling, F. J. G.). Blackwell Sci. Pub., Oxford. Vol. 1, 3rd edn, pp 5-30.
- Ebling, F. J. and Rook, A. (1975a).  
The sebaceous glands. In "Textbook of Dermatology", (eds: Rook, A., Wilkinson, D. S. and Ebling, F. J. G.). Blackwell Sci. Pub., Oxford. pp 1526-1558.
- Ebling, F. J. and Rook, A. (1975b).  
Hair. *Ibid.*, pp 1559-1641.
- Ebling, F. J. G. (1970a).  
The embryology of skin. In "An Introduction to the Biology of the Skin", (eds: Champion, R. H., Gillman, T., Rook, A. J. and Sims, R. T.). Blackwell Sci. Pub., Oxford and Edinburgh. pp 23-24.
- Ebling, F. J. G. (1970b).  
Sebaceous glands. *Ibid.*, pp 184-196.
- Ebling, F. J. G. (1986).  
The normal skin. In "Textbook of Dermatology", (eds: Rook, A., Wilkinson, D. S., Ebling, F. J. G., Champion, R. H. and Burton, J. L.). Blackwell Sci. Pub., Oxford. Vol. 1, 4th edn. pp 5-38.
- Ebling, F. J., Randall, V. A. and Skinner, J. (1981).  
Local suppression of sebum secretion in rats by topical cyproterone acetate in ethanol.  
*J. Invest. Dermatol.*, **77**: 458-463.



- Edelburg, R. (1977).  
"Relation of electrical properties of skin to structure and physiologic state."  
*J. Invest. Dermatol.*, **69**: 324-327.
- Ehrenwald, H. J. (1942).  
Cranio-cerebral ionization.  
*Brit. J. Phy. Med. Indust. Hyg.*, **5**: 172-174.
- Elfbaum, S. G. and Laden, K. (1968a).  
The effect of dimethyl sulfoxide on percutaneous absorption: A mechanistic study, Part I.  
*J. Soc. Cosmet. Chem.*, **19**: 119-127.
- Elfbaum, S. G. and Laden, K. (1968b).  
The effect of dimethyl sulfoxide on percutaneous absorption: A mechanistic study, Part II.  
*J. Soc. Cosmet. Chem.*, **19**: 163-172.
- Elfbaum, S. G. and Laden, K. (1968c).  
The effect of dimethyl sulfoxide on percutaneous absorption: A mechanistic study, Part III.  
*J. Soc. Cosmet. Chem.*, **19**: 841-847.
- Elias, P. M. (1981).  
Lipids and the epidermal barrier.  
*Arch. Dermatol. Res.*, **270**: 95-117.
- Elias, P. M. and Brown, B. E. (1978).  
The mammalian cutaneous permeability barrier, defective barrier function in essential fatty acid deficiency correlates with abnormal intercellular lipid deposition.  
*Laboratory Investign.*, **39**: 574-583.
- Elias, P. M., Brown, B. E., Fritsch, P., Goerke, J., Gray, G. M. and White, R. J. (1979).  
Localization and composition of lipids in neonatal mouse stratum granulosum and stratum corneum.  
*J. Invest. Dermatol.*, **73**: 339-348.
- Elias, P. M., Cooper, E. R., Kore, A. and Brown, B. E. (1981).  
Percutaneous transport in relation to stratum corneum structure and lipid composition.  
*J. Invest. Dermatol.*, **76**: 297-301.
- Elias, P. M. and Friend, D. S. (1975).  
The permeability barrier in mammalian epidermis.  
*J. Cell. Biol.*, **65**: 180-191.
- Elias, P. M., McNutt, N. S. and Friend, D. S. (1977).  
Membrane alterations during cornification of mammalian squamous epithelia: A freeze-fracture, tracer and thin-section study.  
*Anat. Rec.*, **189**: 577-594.
- Erasmus, D. A. (1978).  
"Electron Probe Microanalysis in Biology". Chapman and Hall, London.

- Erlanger, G. (1936).  
On the scientific and practical value of ionization in ophthalmology, recent advances and researches.  
*Brit. J. Ophthalmol.*, 20: 213-229.
- Erlanger, G. (1939).  
Iontophoretic medication in ophthalmology.  
*Arch. Phys. Therap.*, 20: 16-24.
- Farbman, A. I. (1966).  
Plasma membrane changes during keratinization.  
*Anat. Rec.*, 156: 269-282.
- Feldmann, R. J. and Maibach, H. I. (1967).  
Regional variation in percutaneous penetration of C<sup>14</sup>-cortisol in man.  
*J. Invest. Dermatol.*, 48: 181-183.
- Ferguson, R. L. and Silver, S. D. (1947).  
Demonstration in skin of active chlorine from chlorine-liberating ointments.  
*Amer. J. Clin. Pathol.*, 17: 35-36.
- Finzi, N. S. (1912).  
Some experiments with ionic medication.  
*Arch. Roentgen Ray*, 1912/1913: 423-426.
- Fleischmajer, P. and Witten, V. H. (1955).  
Studies of thorium X applied to human skin. IV. Clinical and autoradiographic findings following the introduction by iontophoresis.  
*J. Invest. Dermatol.*, 25: 223-232.
- Fleming, N. (1943).  
Iontotherapy as an aid in ophthalmic therapeutics.  
*Brit. J. Ophthalmol.*, 28: 354-367.
- Flesch, P. (1962).  
The cementing substance of human horny layers.  
*J. Soc. Cosmet. Chem.*, 13: 113-118.
- Flesch, P., Goldstone, S. B. and Urbach, F. (1951).  
Palmar pore patterns: their significance in the absorption of dyes.  
*Arch. Dermatol. Syph.*, 63: 228-231.
- Fletcher, J. M., Greenfield, B. F., Hardy, C. J., Scargill, D. and Woodhead, J. L. (1961).  
Ruthenium red.  
*J. Chem. Soci.* pp 2000-2006.
- Foreman, M. I., Clanachan, I. and Kelly, I. P. (1983).  
Diffusion barriers in skin - a new method of comparison.  
*Brit. J. Dermatol.*, 108: 549-553.

- Fox, C., Tassoﬀ, J. A., Rieger, M. M. and Deem, D. E. (1962).  
Modification of the water holding capacity of callus by  
pretreatment with additives.  
*J. Soc. Cosmet. Chem.*, 13: 263-279.
- Fraser, R. B. D. (1969).  
Keratins.  
*Scient. Am.*, 221: 87-96.
- Fraser, R. B. D., MacRae, T. P. and Miller, A. (1965).  
X-ray diﬀraction patterns of -fibrous proteins.  
*J. Mol. Biol.*, 14: 432-442.
- Freeman, M. V., Alvarez, E. and Draize, H. (1950).  
Cutaneous absorption of phenol from intact and damaged skin.  
*Feder. Proc.*, 9: 273-274.
- Friel, A. R. (1919).  
The treatment of sepsis in the nose and ear by ionization.  
*Practitioner*, 103: 449-452.
- Frosch, P. J., Duncan, S. and Kligman, A. M. (1980).  
Cutaneous biometrics. I. The response of human skin to  
dimethyl sulphoxide.  
*Brit. J. Dermatol.*, 102: 263-274.
- Fukuyama, K. and Epstein, W. L. (1969).  
Sulfur-containing proteins and epidermal keratinization.  
*J. Cell Biol.*, 40: 830-838.
- Gangarosa, L. P. (1983).  
"Iontophoresis in Dental Practice". Quintessence Publishing Co.  
Inc., Chicago.
- Gangarosa, L. P., Park, N., Wiggins, C. A. and Hill, J. M. (1980).  
Increased penetration of nonelectrolytes into mouse skin during  
iontophoretic water transport (iontohydrokinesis).  
*J. Pharm. Exper. Therap.*, 212: 377-381.
- Gillman, T. (1970).  
The dermis. In "An Introduction to the Biology of the Skin",  
(eds: Champion, R. H., Gillman, T., Rook, A. J. and Sims, R.  
T.). Blackwell Sci. Pub., Oxford. pp 76-113.
- Goldsmith, L. A. and Baden, H. P. (1970).  
Uniquely oriented epidermal lipid.  
*Nature (Lond.)*, 225: 1052-1053.
- Goldstein, J. I., Newbury, D. E., Echlin, P., Joy, D. C., Fiori, C.  
and Lifshin, E. (1981).  
"Scanning Electron Microscopy and X-Ray Microanalysis". Plenum  
Press, New York and London.
- Goodenough, A. V. and Revel, J. P. (1970).  
A fine structural analysis of the intercellular junctions in the  
mouse liver.  
*J. Cell Biol.*, 45: 272-290.

- Gray, G. M. and White, R. (1978).  
Glycosphingolipids and ceramides in human and pig epidermis.  
*J. Invest. Dermatol.*, **70**: 336-341.
- Gray, G. M. and Yardley, H. J. (1975).  
Different populations of pig epidermal cells: isolation and  
lipid composition.  
*J. Lipid Res.*, **16**: 441-447.
- Grayson, S., Johnson-Winegar, A. D., Wintroub, B. U., Epstein, E. H.,  
Isseroff, R. R. and Elias, P. M. (1985).  
Lamellar bodies from neonatal mouse epidermis: Functional  
implications of lipid and enzyme content.  
*J. Invest. Dermatol.*, **84**: 329.
- Grice, K. and Verbov, J. (1977).  
Sweat glands and their disorders. In "Recent Advances in  
Dermatology - 4", (ed.: Rook, A.). Churchill Livingstone,  
Edinburgh. pp 155-198.
- Grice, K., Sattar, H. and Baker, H. (1972).  
Treatment of idiopathic hyperhidrosis with iontophoresis of tap  
water and poldine methosulphate.  
*Brit. J. Dermatol.*, **86**: 72-78.
- Grice, K., Sattar, H., Kasey, T. and Baker, H. (1975).  
An evaluation of Na<sup>+</sup>, Cl<sup>-</sup> and pH ion-specific electrodes in the  
study of the electrolyte contents of epidermal transudate and  
sweat.  
*Brit. J. Dermatol.*, **92**: 511-518.
- Guilleminot, W. H. (1906).  
"Handbook of Electricity in Medicine". Translated by Butcher,  
W. E. Rebman Ltd, London.
- Gurr, E. (1960).  
"Encyclopaedia of Microscopic Stains". Leonard Hill (Books)  
Ltd, London.
- Gurr, E. (1971).  
"Synthetic Dyes in Biology, Medicine and Chemistry". Academic  
Press, London.
- Haack, D. W., Bush, L. R., Shlafer, M. and Lucchesi, B. R. (1981).  
Lanthanum staining of coronary microvascular endothelium:  
effects of ischemia reperfusion, propranolol and atenolol.  
*Microvascular Res.*, **21**: 362-376.
- Hall, T. A. (1979).  
Biological X-ray microanalysis.  
*J. Microscopy*, **117**: 145-163.
- Hansen, J. R. and Yellin, W. (1972).  
NMR and infrared spectroscopic studies of stratum corneum  
hydration. In "Water Structure at the Water-Polymer Interface",  
(ed.; Jellinek, H. H. G.). Plenum Press, New York and London.  
pp 19-28.

- Harpuder, K. (1948).  
Electrophoretic therapy.  
*Occup. Therap. Rehabil.*, 27: 449-455.
- Harris, R. (1959).  
Iontophoresis. In "Therapeutic Electricity and Ultraviolet Radiation", (ed., Licht, S. H.). 2nd edn. The Williams and Wilkins Co., Baltimore. pp 146-168.
- Harrison, R. D. (1972).  
"Book of Data: Chemistry, Physical Science, Physics". Nuffield Advanced Science (Penguin Books Ltd), England.
- Hashimoto, K. (1971).  
Cementsome, a new interpretation of the membrane-coating granules.  
*Arch. Dermatol. Forsch.*, 240: 349-364.
- Hashimoto, K. and Shibasaki, S. (1976).  
Ultrastructural study on differentiation and function of hair. In "Biology and Disease of the Hair", (eds: Kobori, T., Montagna, W., Toda, K., Ishibashi, Y., Hori, Y. and Morikawa, F.). University Park Press, Baltimore. pp 23-57.
- Hayat, M. A. (1970).  
"Principles and Techniques of Electron Microscopy: Biological Applications". Van Nostrand Reinhold Co., New York. Vol. 1.
- Hayat, M. A. (1980).  
"X-Ray Microanalysis in Biology". University Park Press, Baltimore.
- Hayward, A. F. (1983).  
The permeability of the epithelium of the skin of fetal rats demonstrated with a lanthanum-containing solution.  
*J. Anat.*, 136: 379-388.
- Hayward, A. F. and Hackemann, M. (1973).  
Electron microscopy of membrane-coating granules and a cell surface coat in keratinized and non-keratinized human oral epithelium.  
*J. Ultrastruct. Res.*, 43: 205-219.
- Higuchi, T. (1960).  
Physical chemical analysis of percutaneous absorption process from creams and ointments.  
*J. Soc. Cosmet. Chem.*, 11: 85-96.
- Hill, J. M., Gangarosa, L. P. and Park, N. H. (1977).  
Iontophoretic application of antiviral chemotherapeutic agents.  
*Ann. N. Y. Acad. Sci.*, 284: 604-612.
- Hirokawa, N. (1982).  
The intramembrane structure of tight junctions: An experimental analysis of the single-fibril and two-fibril models using the quick freeze method.  
*J. Ultrastruct. Res.*, 80: 288-301.

- Holbrook, K. A. and Odland, G. F. (1974).  
Regional differences in the thickness (cell layers) of the human stratum corneum: An ultrastructural analysis.  
*J. Invest. Dermatol.*, **62**: 415-422.
- Hollender, A. R. and Fabricant, N. D. (1938).  
Nasal ionization, histological studies in relation to clinical evaluation.  
*Arch. Otolaryng.*, **27**: 452-468.
- Holzle, E. and Braun-Falco, O. (1984).  
Structural changes in axillary eccrine glands following long-term treatment with aluminium chloride hexahydrate solution.  
*Brit. J. Dermatol.*, **110**: 399-403.
- Hornqvist, R., Back, O. and Henriksson, R. (1984).  
Adrenoceptor-mediated responses in human skin studied by iontophoresis.  
*Brit. J. Dermatol.*, **III**: 561-566.
- Hume, W. J. (1985).  
Keratinocyte proliferative hierarchies confer protective mechanisms in surface epithelia.  
*Brit. J. Dermatol.*, **112**: 493-502.
- Hunt, G. (1966).  
Cited in "Physical Function of Skin", (ed: Tregear, R. T.), Academic Press, London. p 12.
- Hurley, H. J. (1975).  
Permeability of the skin. In "Dermatology" (eds: Moschella, S. L., Pillsbury, D. M. and Hurley, H. J.). Vol. 1. W. B. Saunders Co., Philadelphia. pp 64-68.
- Idson, B. (1975).  
Percutaneous absorption.  
*J. Pharmacol. Sci.*, **64**: 901-924.
- Inchley, O. (1921).  
The influence of the electric current on the absorption of drugs.  
*J. Pharm. Exper. Therap.*, **18**: 241-256.
- Jackson, D., McQueen, L., McEwan Jenkinson, D., Nimmo, M., Elder, H. Y. and Montgomery, I. (1983).  
Intercellular passage of lanthanum through the sebaceous gland.  
*Brit. J. Dermatol.*, **109**: 710-711.
- Jacobi, O. K. (1959).  
About the mechanism of moisture regulation in the horny layer of the skin.  
*Proc. Scient. Sect. Text. Goods Ass.*, **31**: 22-24.
- Jacoby, A. and Derbrucke, M. G. (1942).  
Vaginal iontophoresis of a choline compound.  
*Amer. J. Obst. Gynecol.*, **44**: 250-258.



- Jarrett, A. (1973).  
"The Physiology and Pathophysiology of the Skin". Academic Press, London. Vol. 1 - The Epidermis.
- Jarrett, A. (1977).  
"The Physiology and Pathophysiology of the Skin". Academic Press, London. Vol. 4 - The Hair Follicle.
- Jeol Limited. (1983).  
Table of standards supplied with the SEM by Jeol Ltd, Japan.
- Jersild, O. and Plesner, M. (1940).  
Treatment of epidermophytia on the extremities with iontophoresis of copper.  
*Acta Dermato-venereol. (Stockh.)*, 21: 268-279.
- Johnson, E. (1977).  
Cycles and patterns of hair growth. In "The Physiology and Pathophysiology of the Skin", (ed.: Jarrett, A.). Academic Press, London. Vol. 4, The Hair Follicle. pp 1237-1254.
- Juhlin, L. (1961a).  
The fate of iontophoretically introduced epinephrine and norepinephrine in patients with atopic dermatitis and in normal skin.  
*J. Invest. Dermatol.*, 37: 257-261.
- Juhlin, L. (1961b).  
Skin reactions to iontophoretically administered epinephrine and norepinephrine in atopic dermatitis.  
*J. Invest. Dermatol.*, 37: 201-205.
- Kaidbey, K. H., Kligman, A. M. and Yoshida, H. (1975).  
Effects of intensive application of retinoic acid on human skin.  
*Brit. J. Dermatol.*, 92: 693-701.
- Kawamura, Y. and Takata, M. (1960).  
Studies on the permeability of the oral mucosa. I. Permeability of inorganic ions.  
*J. Dental Res.*, 39: 517-524.
- Kawamura, Y. and Takata, M. (1961).  
Permeability of the oral mucous membrane. III. Permeability to amino acids and propylene glycol and biophysiological characteristics of the oral mucous membrane.  
*J. Dental Res.*, 40: 228.
- King, B. F. (1983).  
The permeability of human amniotic epithelium: Studies using lanthanum as a tracer.  
*Anat. Rec.*, 207: 557-561.
- King, C. S., Barton, S. P., Nicholls, S. and Marks, R. (1979)  
The change in properties of the stratum corneum as a function of depth.  
*Brit. J. Dermatol.*, 100: 165-172.

- Kitson, N. and Van Lennep, E. W. (1984).  
Intercellular junctions and the permeability barrier in human sebaceous glands.  
*Brit. J. Dermatol.*, **110**: 601-606.
- Kitson, N., Van Lennep, E. W. and Young, J. A. (1978).  
Gap junctions in human sebaceous glands.  
*Cell Tiss. Res.*, **190**: 115-121.
- Kligman, A. M. (1964).  
The biology of the stratum corneum. In "The Epidermis", (eds: Montagna, W. and Lobitz, W. C.). Academic Press, New York.  
pp 387-433.
- Kligman, A. M. (1965a).  
Topical pharmacology and toxicology of dimethyl sulfoxide, Part I.  
*J. Amer. Med. Ass.*, **193**: 140-148.
- Kligman, A. M. (1965b).  
Topical pharmacology and toxicology of dimethyl sulfoxide, Part II.  
*J. Amer. Med. Ass.*, **193**: 796-804.
- Kligman, A. M. (1979).  
Perspectives and problems in cutaneous gerontology.  
*J. Invest. Dermatol.*, **73**: 39-46.
- Kligman, A. M. and Shelley, W. B. (1958).  
An investigation of the biology of the human sebaceous gland.  
*J. Invest. Dermatol.*, **30**: 99-125.
- Knox, S. C. (1943).  
An improvised field method of management of fungus infections on the feet.  
*U. S. Nav. Med. Bullt.*, **41**: 1746-1747.
- Komatsu, H. and Suzuki, M. (1982).  
Studies on the regeneration of the skin barrier and the changes in P<sup>32</sup> incorporation into the epidermis after stripping.  
*Brit. J. Dermatol.*, **106**: 551-560.
- Kovacs, R. (1937).  
Ionic Medication.  
*Physiotherap. Rev.*, **16**: 89-99.
- Kramer, D. W. (1937).  
The use of acetyl- -methylcholine chloride by iontophoresis in peripheral vascular diseases.  
*Amer. J. Med. Sci.*, **193**: 405-413.
- Krawczyk, W. S. (1976).  
Ultrastructural studies on the external surface coat of epidermal cells: Alcian blue-Lanthanum nitrate staining during wound healing.  
*Arch. Dermatol. Res.*, **225**: 157-162.

- Lavker, R. M. and Sun, T. (1982).  
Heterogeneity in epidermal basal keratinocytes: Morphological and functional correlations.  
*Science*, **215**: 1239-1241.
- Laden, K. (1965).  
A comparative chemical study of dandruff flakes, skin scrapings and callus.  
*J. Soc. Cosmet. Chem.*, **16**: 491-497.
- Laden, K. and Spitzer, R. (1967).  
Identification of a natural moisturizing agent in skin.  
*J. Soc. Cosmet. Chem.*, **18**: 351-360.
- Lampe, M. A., Williams, M. L. and Elias, P. M. (1983).  
Human epidermal lipids: Characterization and modulations during differentiation.  
*J. Lipid Res.*, **24**: 131-139.
- Lansdown, A. and Grasso, P. (1972).  
Physico-chemical factors influencing epidermal damage by surface active agents.  
*Brit. J. Dermatol.*, **86**: 361-373.
- Laug, E. P., Aughey, E. and Umberger, E. J. (1944).  
Factors influencing the absorption of mercury from calomel ointments applied to the skin.  
*Feder. Proceed.*, **3**: 78.
- Laug, E. P., Vas, E. A., Umberger, E. J. and Kunze, F. M. (1947).  
A method for the determination of cutaneous penetration of mercury.  
*J. Pharm. Exper. Therap.*, **89**: 42-51.
- Lavker, R. M. (1976).  
Membrane coating granules: The fate of the discharged lamellae.  
*J. Ultrastruct. Res.*, **55**: 79-86.
- Leach, D. and Oliphant, L. (1983).  
Annular gap junctions of the equine hoof wall.  
*Acta Anat.*, **116**: 1-9.
- Lee, L. D. and Baden, H. P. (1975).  
Chemistry and competition of the keratins.  
*Int. J. Dermatol.*, **14**: 161-171.
- Leeson, T. S. and Leeson, C. R. (1982).  
The use of lanthanum as a marker for intercellular junctions in rat exocrine pancreas.  
*Stain Tech.*, **57**: 245-248.
- Lillie, R. D. (1969).  
"Biological Stains. A Handbook on the Nature and Uses of the Dyes Employed in the Biological Laboratory". Williams and Wilkins, Baltimore. 8th ed.

- Lison, L. (1936).  
 "Histochemie Animale". Gautier Villars, Paris. Cited in  
 "Histochemistry, Theoretical and Applied", (ed.: Pearse, A. G.  
 E.). 2nd edn. J. and A. Churchill Ltd, London. p 711.
- Lison, L. (1953).  
 "Histochemie et Cytochemie Animales". Gautier Villars, Paris.  
 Cited as above.
- Liventsev, N. M. (1964).  
 "Electromedical Apparatus; Principles of Operation,  
 Installation, and Use". Translation of "Elektromeditsinskaya  
 apparatura; printsip deystiviya ustroystvo, ekspluatatiya",  
 Meditsina Press, Moscow. Translated by National Aeronautics and  
 Space Administration (NASA), Clearinghouse for Federal  
 Scientific and Technical Information, Springfield, Virginia.
- Loeffler, R. K. and Thomas, V.  
 A quantitative study of percutaneous absorption. I. Absorption  
 of radiostrontium chloride in minute quantities through intact  
 and mechanically damaged rat skin.  
*Nuc. Sci. Abst.*, 5: 48.
- Luft, J. H. (1961).  
 Improvements in epoxy resin embedding methods.  
*J. Biophys. Biochem. Cytol.*, 9: 409-414.
- Luft, J. H. (1964).  
 Electron microscopy of cell extraneous coats as revealed by  
 ruthenium red staining.  
*J. Cell Biol.*, 23: 54A-55A.
- Luft, J. H. (1971a).  
 Ruthenium red and violet. I. Chemistry, purification, methods  
 of use for electron microscopy and mechanism of action.  
*Anat. Rec.*, 171: 347-368.
- Luft, J. H. (1971b).  
 Ruthenium red and violet. II. Fine structural localization in  
 animal tissues.  
*Anat. Rec.*, 171: 369-416.
- Lundgren, H. P. and Ward, W. H. (1963).  
 The keratins. In "Ultrastructure of Protein Fibres", (ed.;  
 Borasky, R.). Academic Press, New York and London. pp 39-122.
- MacGregor, W. S. (1967).  
 The chemical and physical properties of DMSO.  
*Anal. N. Y. Acad. Sci.*, 141: 3-12.
- MacKee, G. M., Sulzberger, H. H., Hermann, F. and Baer, R. L. (1945).  
 Histologic studies on penetration with special reference to the  
 effect of vehicles.  
*J. Invest. Dermatol.*, 6: 43-61.
- MacKenzie, I. C. (1969).  
 Ordered structure of the stratum corneum of mammalian skin.  
*Nature, (Lond.)*, 222: 881-882.

- Mackenzie, I. C. (1970).  
Relationship between mitosis and the ordered structure of the stratum corneum in mouse epidermis.  
*Nature (Lond.)*, **226**: 653-655.
- Maibach, H. I. and Feldmann, R. J. (1969).  
Effect of applied concentration on percutaneous absorption in man.  
*J. Invest. Dermatol.*, **52**: 382.
- Malkinson, F. D. (1958).  
Studies on the percutaneous absorption of C<sup>14</sup> labelled steroids by use of the gas-flow cell.  
*J. Invest. Dermatol.*, **31**: 19-28.
- Malkinson, F. D. (1960).  
Percutaneous absorption of adrenal steroids.  
*J. Soc. Cosmet. Chem.*, **11**: 146-159.
- Malkinson, F. D. (1964).  
Permeability of the stratum corneum. In "The Epidermis", (eds: Montagna, W. and Lobitz, W. C.). Academic Press, New York. pp 435-452.
- Malkinson, F. D. (1965).  
Industrial problems relating to the stratum corneum.  
*Arch. Environ. Health*, **11**: 538-545.
- Malkinson, F. D. and Ferguson, E. H. (1955).  
Preliminary and short report, Percutaneous absorption of hydrocortisone-4-C<sup>14</sup> in two human subjects.  
*J. Invest. Dermatol.*, **25**: 281-283.
- Mallory, F. B. (1938).  
"Pathological Technique". W. B. Saunders Co., Philadelphia. p 139.
- Mallory, F. B. and Parker, F. (1939).  
Fixing and staining methods for lead and copper in tissues.  
*Amer. J. Pathol.*, **16**: 517-522.
- Marcus, Y. (1985).  
"Ion Solvation". John Wiley and Sons Ltd, Chichester.
- Marks, R., Abell, E. and Nishikawa, T. (1975).  
The junctional zone beneath migrating epidermis.  
*Brit. J. Dermatol.*, **92**: 311-319.
- Martin, L., Eaton, G. O., Ruland, H. and Ruland, L. (1937).  
Effects of acetyl beta-methylcholine iontophoresis in arthritis.  
*Arch. Fur. Phys. Therap.*, **18**: 226-232.
- Martin, R. B. and Richardson, F. S. (1979).  
Lanthanides as probes for calcium in biological systems.  
*Quart. Rev. Biophys.*, **12**: 181-209.
- Martinez, R. and Peters, A. (1971).  
Membrane-coating granules and membrane modifications in

- keratinizing epithelia.  
*Amer. J. Anat.*, **130**: 93-120.
- Martinez-Palomo, A., Benitez, D. and Manis, J. (1973).  
Selective deposition of lanthanum in mammalian cardiac cell membranes. Ultrastructural and electrophysiological evidence.  
*J. Cell Biol.*, **58**: 1-10.
- Marzulli, F. N. (1962).  
Barrier to skin penetration.  
*J. Invest. Dermatol.*, **39**: 387-393.
- Marzulli, F. N., Brown, D. W. C. and Maibach, H. I. (1969).  
Techniques for studying skin penetration.  
*Toxicol. Appl. Pharmacol.*, Suppl. 3, 76-83.
- Marzulli, F. N., Callahan, J. F. and Brown, D. W. C. (1965).  
Chemical structure and skin penetrating capacity of a short series of organic phosphates and phosphoric acid.  
*J. Invest. Dermatol.*, **44**: 339-344.
- Matoltsy, A. G. (1961).  
The envelope of epidermal horny cells.  
*Congress on Invest. Dermatol.*, **13**: 1014-1015.
- Matoltsy, A. G. (1966).  
Membrane-coating granules of the epidermis.  
*J. Ultrastruct. Res.*, **15**: 510-515.
- Matoltsy, A. G. (1976).  
Keratinization.  
*J. Invest. Dermatol.*, **67**: 20-25.
- Matoltsy, A. G. and Parakkal, P. F. (1965).  
Membrane-coating granules of keratinizing epithelia.  
*J. Cell Biol.*, **24**: 297-307.
- Matoltsy, A. G., Downes, A. M. and Sweeney, T. M. (1968).  
Studies of the epidermal water barrier. II. Investigation of the chemical nature of the water barrier.  
*J. Invest. Dermatol.*, **50**: 19-26.
- Matoltsy, A. G., Matoltsy, M. and Schragger, A. (1962).  
Observations on regeneration of the skin barrier.  
*J. Invest. Dermatol.*, **38**: 251-253.
- Matoltsy, A. G. and Parakkal, P. F. (1967).  
Keratinization. In "Ultrastructure of Normal and Pathologic Skin", (ed., Zelickson, A. S.). Lea and Febiger, Philadelphia. pp 76-104.
- McEwan Jenkinson, D., McLean, J. A. and Walton, G. S. (1974).  
The potential use of iontophoresis in the treatment of skin disorders.  
*Vet. Rec.*, **94**: 8-12.



- McKenzie, A. W. (1962).  
Percutaneous absorption of steroids.  
*Arch. Dermatol.*, **86**: 611-614.
- McKenzie, A. W. and Stoughton, R. B. (1962).  
Methods for comparing percutaneous absorption of steroids.  
*Arch. Dermatol.*, **86**: 608-610.
- McNutt, N. S. (1973).  
Freeze-etch study of plasma membrane differentiation and junctions in a keratinized stratified squamous epithelium.  
*J. Cell. Biol.*, **59**: 210.
- Meek, G. A. (1980).  
"Practical Electron Microscopy for Biologists". John Wiley and Sons, Chichester. 2nd edn.
- Menton, D. N. and Elsen, A. Z. (1971).  
Structure and organization of mammalian stratum corneum.  
*J. Ultrastruct. Res.*, **35**: 247-264.
- Mercer, E. H. (1962).  
"Keratin and Keratinization". Pergamon Press, Oxford.
- Merck Index. (1976).  
"An Encyclopaedia of Chemicals and Drugs". Merck and Co. Inc., U. S. A.
- Middleton, J. D. (1968).  
The mechanism of water binding in stratum corneum.  
*Brit. J. Dermatol.*, **80**: 437-450.
- Midtgaard, K. (1986).  
A new device for the treatment of hyperhidrosis by iontophoresis.  
*Brit. J. Dermatol.*, **114**: 485-488.
- Millington, P. F. and Wilkinson, R. (1983).  
"Skin, Biological Structure and Function", (eds: Harrison, R. J. and McMinn, R. M. H.). Cambridge University Press, Cambridge. pp 1-82.
- Moeller, T. (1963).  
"The Chemistry of Lanthanides". Rheinhold, New York.
- Molitor, H. and Fernandez, I. (1930).  
Studies on iontophoresis. I. Experimental studies on the causes and prevention of iontophoretic burns.  
*Amer. J. Med. Sci.*, **198**: 778-785.
- Monash, S. (1957).  
Location of the superficial barrier to skin penetration.  
*J. Invest. Dermatol.*, **29**: 367-376.
- Monash, S. and Blank, H. (1958).  
Location and reformation of the epithelial barrier to water vapour.  
*Arch. Dermatol.*, **78**: 710-714.

- Montagna, W. (1954).  
Penetration and local effect of vitamin A on the skin of the guinea pig.  
*Exp. Biol. Med.*, **86**: 668-672.
- Montagna, W. and Noback, C. R. (1947).  
Histochemical observations on the sebaceous glands of the rat.  
*Amer. J. Anat.*, **81**, 39-62.
- Montagna, W. and Parakkal, P. F. (1974).  
"The structure and Function of Skin". Academic Press, New York and London. 3rd edn.
- Moreton, R. B. (1981).  
Electron-probe-X-ray microanalysis: Techniques and recent applications in biology.  
*Biol. Rev.*, **56**: 409-461.
- Morgan, A. J. (1985).  
"X-ray Microanalysis in Electron Microscopy for Biologists". Royal Microscopical Society, Microscopy Handbooks. Oxford University Press, Oxford.
- Morris, J. G. (1971).  
"A Biologist's Physical Chemistry". Edward Arnold Pub. Ltd, London. Chap. 6, pp 129-164.
- Nachman, R. L. and Esterly, N. B. (1971).  
Increased skin permeability in preterm infants.  
*J. Ped.*, **79**: 628-632.
- Nemanic, M. K. and Elias, P. M. (1980).  
A novel cytochemical technique for visualization of permeability pathways in mammalian stratum corneum.  
*J. Histochem. Cytochem.*, **28**: 273-278.
- Nicolaides, N. (1963).  
Human skin surface lipids - origin, composition and possible function. In "Advances in Biology of the Skin", (eds: Montagna, W., Ellis, R. A. and Silver, A. F.). Pergamon Press, Oxford. Vol. 4 (The sebaceous glands). pp 167-187.
- O'Malley, E. P. and Oester, Y. T. (1955).  
Influence of some physical chemical factors on iontophoresis using radio-isotopes.  
*Arch. Phys. Med.*, **36**: 310-316.
- O'Malley, E. P., Oester, Y. T. and Warnick, E. G. (1954).  
Experimental iontophoresis: Studies with radio-isotopes.  
*Arch. Phys. Med.*, **35**: 500-507.
- Odland, G. F. (1960).  
A submicroscopic granular component in human epidermis.  
*J. Invest. Dermatol.*, **34**: 11-15.

- Odland, G. F. (1983).  
Structure of the skin. In "Biochemistry and Physiology of the Skin", (ed.: Goldsmith, L. A.). Oxford University Press, Oxford. Vol. 1, pp 3-63.
- Olson, R. L., Nordquist, J. and Everett, M. A. (1969).  
Small granules of the superficial epidermis.  
*Arch. Klin. Exper. Derm.*, 234: 15-24.
- Onken, H. D. and Moyer, C. A. (1963).  
The water barrier in human epidermis.  
*Arch. Dermatol.*, 87: 584-590.
- Palade, G. E. (1952).  
A study of fixation for electron microscopy.  
*J. Exper. Med.*, 95: 285-298.
- Pearse, A. G. E. (1961).  
"Histochemistry, Theoretical and Applied". J. A. Churchill Ltd, London. 2nd edn. pp 709-712.
- Pearse, A. G. E. (1972).  
"Histochemistry, Theoretical and Applied". Churchill Livingstone, Edinburgh and London. Vol. 2, 2nd ed.
- Pearse, D. C. (1964).  
"Histological Techniques for Electron Microscopy". Academic Press, New York and London. 2nd edn.
- Pereyra, A. J. (1945).  
Penetration of surface tissues with copper by iontophoresis, penetration with organic and inorganic copper salts and the use of detergents in iontophoresis.  
*Arch. Dermatol. Syphil.*, 52: 96-105.
- Pinkus, H. (1951).  
Examination of the epidermis by the strip method of removing horny layers.  
*J. Invest. Dermatol.*, 16: 383-386.
- Pinson, E. A. (1952).  
Water exchanges and barriers as studied by the use of hydrogen isotopes.  
*Physiol. Rev.*, 32: 123-134.
- Pohla, H., Simonsberger, P. and Adam, H. (1983).  
X-ray microanalysis of rainbow trout (*Salmo gairdneri* RICH) melanosomes with special reference to analytical methods.  
*Microskopie (Wien)*, 40: 273-284.
- Polano, M. K. (1984).  
Model trials for the evaluation of topical drugs. In "Topical Skin Therapeutics", (ed.: Polano, M. K.). Churchill Livingstone, Edinburgh and London. pp 145-160.
- Possick, P. A. (1969).  
Cement dermatitis.  
*Cutis*, 5: 167-170.

- Prottey, C., Hartrop, P. J., Black J. G. and McCromack, J. I. (1976).  
The repair of impaired epidermal barrier function in rats by the  
cutaneous application of linoleic acid.  
*Brit. J. Dermatol.*, **94**: 13-21.
- Reifenrath, W. G., Chellquist, E. M., Stipwash, E. A., Jederberg, W.  
W. and Krueger, G. G. (1984).  
Percutaneous absorption in the hairless dog, weanling pig and  
grafted athymic nude mouse: evaluation of models for predicting  
skin penetration in man.  
*Brit. J. Dermatol.*, **111**: 123-135.
- Rein, H. (1924).  
Experimentelle studien uber Elektronendosmose an uberlebender  
menschlicher Haut.  
*Ztschr. f. Biol.*, **81**: 125-140. Cited by Calvery *et al.* (1946).
- Rein, H. (1925).  
Percutane elektrosmose oder iontophorese.  
*Klin. Wchnschr.*, **4**: 1601-1604. Cited by Calvery *et al.* (1946).
- Rein, H. (1926).  
Zur elektrophysiologie der menschlichen haut.  
*Ztschr. f. Biol.*, **84**: 118-142. Cited by Calvery *et al.* (1946).
- Rein, H. (1929).  
Die elektrophysiologie der haut. In "JADASSOHN, Handb. d. Haut-  
u". Geschlechtskr., **1**: 43-91. Cited in "Physiology and  
Biochemistry of the Skin", (ed.: Rothman, S.). The University  
of Chicago Press, Chicago. 1954. Chapt. 3, p 26-59.
- Revel, J. P. and Karnovsky, M. J. (1967).  
Hexagonal array of subunits in intercellular junctions of the  
mouse heart and liver.  
*J. Cell Biol.*, **33**: C7-C12.
- Reynolds, E. S. (1963).  
The use of lead citrate at high pH as an electron-opaque stain  
in electron microscopy.  
*J. Cell Biol.*, **17**: 208-212.
- Rogers, G. E. (1964).  
Structural and biochemical features of the hair follicle. In  
"The Epidermis", (eds: Montagna, W. and Lobitz, W. C.).  
Academic Press, New York and London. pp 179-236.
- Rogers, S. C. F., Burrows, D. and Neill, D. (1978).  
Percutaneous absorption of phenol and methyl alcohol in Magenta  
paint B. P. C.  
*Brit. J. Dermatol.*, **98**: 559-560.
- Rook, A. J. (1970).  
Hair. In "An Introduction to the Biology of the Skin", (eds:  
Champion, R. H., Gillman, T., Rook, A. J. and Sims, R. T.).  
Blackwell Sci. Pub., Oxford. pp 164-174.

- Rook, A., Wilkinson, D. S. and Ebling, F. J. G. (1975).  
 "Textbook of Dermatology". Blackwell Sci. Pub., Oxford. Vol. 2. 2nd edn, 2nd print. p 175.
- Roomans, G. M. (1979).  
 Standards for X-ray microanalysis of biological specimens.  
*Scan. Elect. Microscop.*, 11: 649-657.
- Rothman, S. (1943).  
 The principles of percutaneous absorption.  
*J. Lab. Clin. Med.*, 28: 1305-1321.
- Rothman, S. (1954).  
 "Physiology and Biochemistry of the Skin". The University of Chicago Press, Chicago.
- Rothman, S. (1955).  
 The mechanism of percutaneous penetration and absorption.  
*J. Soc. Cosmet. Chem.*, 6: 193-200.
- Schatzki, P. F. and Newsome, A. (1975).  
 Neutralized lanthanum solution: A largely non-colloidal ultrastructural tracer.  
*Stain Technol.*, 50: 171-178.
- Scheuplein, R. J. (1965).  
 Mechanism of percutaneous absorption. I. Routes of penetration and the influence of solubility.  
*J. Invest. Dermatol.*, 45: 334-346.
- Scheuplein, R. J. (1966).  
 Analysis of permeability data for the case of parallel diffusion pathways.  
*Biophys. J.*, 6: 1-7.
- Scheuplein, R. J. (1967).  
 Mechanism of percutaneous absorption. II. Transient diffusion and the relative importance of various routes of skin penetration.  
*J. Invest. Dermatol.*, 48: 79-88.
- Scheuplein, R.J. (1978).  
 The skin as a barrier. In "The Physiology and Pathophysiology of the Skin", (ed.: Jarrett, A.). Academic Press, London. Vol. 5, pp 1669-1692.
- Scheuplein, R. J. and Blank, I. H. (1971).  
 Permeability of the skin.  
*Physiol. Rev.*, 51: 702-747.
- Scheuplein, R. J., Blank, I. H., Brauner, G. J. and MacFarlane, D. J. (1969).  
 Percutaneous absorption of steroids.  
*J. Invest. Dermatol.*, 52: 63-70.

- Scheuplein, R. J. and Bronaugh, R. L. (1983).  
Percutaneous absorption. In "Biochemistry and Physiology of the Skin", (ed.: Goldsmith, L. A.). Oxford University Press, New York and Oxford. Vol. 2. pp 1255-1295.
- Scheuplein, R. J. and Morgan, L. J. (1967).  
"Bound-water" in keratin membranes measured by a microbalance technique.  
*Nature (Lond.)*, **214**: 456-458.
- Scheuplein, R. J. and Ross, L. (1970).  
Effects of surfactants and solvents on the permeability of the epidermis.  
*J. Soc. Cosmet. Chem.*, **21**: 853-873.
- Schreiner, E. and Wolff, K. (1969).  
Die Permeabilität des epidermalen intercellularraumes für Kleinmolekulares Prokin.  
*Arch. Klin. Exper. Derm.*, **235**: 78-88.
- Scott, A. (1957).  
The behaviour of radioactive sulphur after its external application to the skin.  
*Brit. J. Dermatol.*, **69**: 39-49.
- Scott, A. and Kalz, F. (1956).  
The penetration and distribution of C<sup>14</sup>-hydrocortisone in human skin after its topical application.  
*J. Invest. Dermatol.*, **26**: 149-158.
- Sekura, D. L. and Scala, J. (1969).  
The percutaneous absorption of alkyl methyl sulfoxides. In "Advances in Biology of Skin - Pharmacology and the Skin", (eds: Montagna, W., Van Scott, E. J. and Stoughton, R. B.). Vol. 12. Appleton Century Crofts, New York. pp 257-269.
- Selby, C. C. (1957).  
An electron microscope study of thin sections of human skin. II. Superficial cell layers of footpad epidermis.  
*J. Invest. Dermatol.*, **29**: 131-149.
- Serri, F. and Montagna, W. (1961).  
The structure and function of the epidermis.  
*The Pedic. Clin. North Amer.*, **8**: 917-941.
- Shaffer, L. W. and Zackheim, H. S. (1947).  
Sporotrichosis.  
*Arch. Fuer. Dermatol. Syph.*, **56**: 244-247.
- Shaklai, M. and Tavassoli, M. (1982).  
Lanthanum as an electron microscopic stain.  
*J. Histochem. Cytochem.*, **30**: 1325-1330.
- Sharov, V. G. (1981).  
Use of colloidal lanthanum as an electron-microscopic tracer.  
*Bull. Exper. Biol. Med.*, **92**: 1748-1750.



- Shelley, W. B. and Melton, F. M. (1949).  
Factors accelerating the penetration of histamine through normal intact human skin.  
*J. Invest. Dermatol.*, **13**: 61-71.
- Shimono, M. and Clementi, F. (1976).  
Intercellular junctions of oral epithelium. I. Studies with freeze-fracture and tracing methods of normal rat keratinized oral epithelium.  
*J. Ultrastruct. Res.*, **56**: 121-136.
- Shrivastava, S. N. and Singh, G. (1977).  
Tap water iontophoresis in palmo-plantar hyperhidrosis.  
*Brit. J. Dermatol.*, **96**: 189-195.
- Sims, R. T. (1970a).  
The epidermis. In "An Introduction to the Biology of the Skin", (eds: Champion, R. H., Gillman, T., Rook, A. J. and Sims, R. T.). Blackwell Sci. Pub., Oxford. pp 61-75.
- Sims, R. T. (1970b).  
Hair as an indicator of incipient and developed malnutrition and response to therapy - principles and practice. *Ibid.*, pp 387-407.
- Skog, E. and Wahlberg, J. E. (1964).  
A comparative investigation of the percutaneous absorption of metal compounds in the guinea pig by means of the radioactive isotopes: Cr<sup>51</sup>, Co<sup>58</sup>, Zn<sup>65</sup>, Ag<sup>130m</sup>, Cd<sup>115m</sup>, Hg<sup>203</sup>.  
*J. Invest. Dermatol.*, **43**: 187-192.
- Smeenk, G. (1969).  
The influence of detergents on the skin (A clinical and biochemical study).  
*Arch. Klin. Exper. Derm.*, **235**: 180-191.
- Smit, H. M. (1936).  
Tissue changes in iontophoresis.  
*Ann. Otol. Rhynolog. Laryngolog.*, **45**: 138-147.
- Smith, J. G., Fischer, R. W. and Blank, H. (1961).  
The epidermal barrier. A comparison between scrotal and abdominal skin.  
*J. Invest. Dermatol.*, **36**: 337-343.
- Smith, J. W. and Stuart, R. J. (1971).  
Silver staining of ribosomal proteins.  
*J. Cell Sci.*, **9**: 253-269.
- Solomon, A. E. and Lowe, N. J. (1979).  
Percutaneous absorption in experimental epidermal disease.  
*Brit. J. Dermatol.*, **100**: 717-722.
- Spearman, R. I. C. (1977).  
The structure and function of the fully developed follicle. In "The Physiology and Pathophysiology of the Skin", (ed.: Jarrett, A.). Academic Press, London. Vol. 4, The hair follicle. pp 1293-1349.

- Squier, C. A. (1973).  
The permeability of keratinized and non-keratinized oral epithelium to horseradish peroxidase.  
*J. Ultrastruct. Res.*, **43**: 160-177.
- Squier, C. A. (1984).  
Effect of enzyme digestion on the permeability barrier in keratinizing and non-keratinizing epithelia.  
*Brit. J. Dermatol.*, **111**: 253-264.
- Squier, C. A. and Edie, J. (1983).  
Localization of lanthanum tracer in oral epithelium using transmission electron microscopy and the electron microprobe.  
*Histochem. J.*, **15**: 1123-1130.
- Squier, C. A. and Hall, B. K. (1985).  
The permeability of skin and oral mucosa to water and horseradish peroxidase as related to the thickness of the permeability barrier.  
*J. Invest. Dermatol.*, **84**: 176-179.
- Squier, C. A. and Rooney, L. (1976).  
The permeability of keratinized and non-keratinized oral epithelium to lanthanum *in vivo*.  
*J. Ultrastruct. Res.*, **54**: 286-295.
- Staehelein, L. A. (1974).  
Structure and function of intercellular junctions.  
*Inter. Rev. Cytol.*, **39**: 191-283.
- Sterling, C. (1970).  
Crystal structure of ruthenium red and stereochemistry of its pectic stain.  
*Amer. J. Botany*, **57**: 172-175.
- Stillwell, G. K. (1983).  
"Therapeutic Electricity and Ultraviolet Radiation". Williams and Wilkins, Baltimore and London. 3rd ed.
- Stoughton, R. B. (1959).  
Relation of the anatomy of normal and abnormal skin to its protective function. In "The Human Integument: Normal and Abnormal", (ed.: Rothman, S.). American Association for the Advancement of Science, Washington D. C. pp 3-24.
- Stoughton, R. B. (1964).  
Some *in vivo* and *in vitro* methods for measuring percutaneous absorption. In "Progress in the Biological Sciences in Relation to Dermatology - 2", (eds: Rook, A. and Champion, R. H.). The University Press, Cambridge. pp 263-274.
- Stoughton, R. B. and Fritsch, W. (1964).  
Influence of dimethyl sulfoxide on human percutaneous absorption.  
*Arch. Dermatol.*, **90**: 512-517.

- Stoughton, R. B., Clendenning, W. E. and Kruse, D. (1960).  
 Percutaneous absorption of nicotinic acid and derivatives.  
*J. Invest. Dermatol.*, **35**: 337-341.
- Sulzberger, M. B. (1960).  
 Special lecture on the biology and functions of the skin surface.  
*Jap. J. Dermatol.*, **70**: 105-122.
- Suzuki, H. and Kakimi, S. (1985).  
 A study of ultrathin frozen sections of epidermal keratinocytes in human skin.  
*J. Invest. Dermatol.*, **84**: 297.
- Suzuki, M. (1956).  
 "Modern Electrotherapy - The Third Effect of Polarizing Electrodes and Low Frequency Current Treatment". Japan society for the promotion of science, Tokyo.
- Swanbeck, G. (1959a).  
 On the keratin fibrils of the skin. An X-ray small angle scattering study of the horny layer.  
*J. Ultrastruct. Res.*, **3**: 51-57.
- Swanbeck, G. (1959b).  
 Macromolecular organisation of epidermal keratin. An X-ray diffraction study of the horny layer from normal, ichthyotic and psoriatic skin.  
*Acta Dermvener. (Stockh.)*, **39**: (Suppl. 43): 1-37.
- Swanbeck, G. and Thyresson, N. (1962).  
 A study of the state of aggregation of the lipids in normal and psoriatic horny layers.  
*Acta Dermvener. (Stockh.)*, **42**: 445-457.
- Switzer, M. E. (1978).  
 The lanthanide ions as probes of calcium ion binding sites in biological systems.  
*Sci. Prog. Oxf.*, **65**: 19-30.
- Szabo, G. (1958).  
 The regional frequency and distribution of hair follicles in human skin. In "The Biology of Hair Growth", (eds: Montagna, W. and Ellis, R. A.). Academic Press, New York. pp 33-38.
- Szakall, A. (1955).  
 Die H-ionenkonzentration bestimmenden Wirkstoffe in der Epidermis.  
*Arch. Klin. Exp. Derm.*, **201**: 331-360. Cited in "Physical Functions of Skin", (ed.: Tregear, R. T.). Academic Press, London. (1966). p 34.
- Szubinska, B. and Luft, J. H. (1971).  
 Ruthenium red and violet. III. Fine structure of the plasma membrane and extraneous coats in amoebae.  
*Anat. Rec.*, **171**: 417-442.

- Tagami, H., Ohi, M., Iwatsuki, K., Kanamaru, Y., Yamada, M. and Ichijo, S. (1980).  
Evaluation of the skin surface hydration *in vivo* by electrical measurement.  
*J. Invest. Dermatol.*, **75**: 500-507.
- Tas, J. and Feige, Y. (1958).  
Penetration of radioiodide ( $I^{131}$ ) through human skin.  
*J. Invest. Dermatol.*, **30**: 193-196.
- Tregear, R. T. (1960).  
Epidermis as a thick membrane.  
*J. Physiol.*, **153**: 54-55.
- Tregear, R. T. (1961).  
Relative penetrability of hair follicles and epidermis.  
*J. Physiol.*, **156**: 303-313.
- Tregear, R. T. (1962).  
The structures which limit the permeability of the skin.  
*J. Soc. Cosmet. Chem.*, **13**: 145-151.
- Tregear, R. T. (1964).  
The permeability of skin to molecules of widely differing properties. In "Progress in the Biological Sciences in Relation to Dermatology - 2", (ed.: Rook, A.). Cambridge University Press, London. pp 275-281.
- Tregear, R. T. (1966).  
"Physical Functions of Skin". Academic Press, London. pp 1-52.
- Treherne, J. E. (1956).  
The permeability of skin to some non-electrolytes.  
*J. Physiol.*, **133**: 171-180.
- Turchini, J. (1930).  
*Bull. Acad. Sci. Letters, Montpellier*, **60**: 29. Cited in "Histochemistry, Theoretical and Applied", (ed.: Pearse, A. G. E.). 2nd edn. J. and A. Churchill Ltd, London. p 711.
- Vickers, C. F. H. (1963).  
Existence of reservoir in the stratum corneum.  
*Arch. Dermatol.*, **88**: 20-23.
- Vinson, L. J. and Choman, B. R. (1960).  
Percutaneous absorption and surface-active agents.  
*J. Soc. Cosmet. Chem.*, **11**: 127-137.
- Wahlberg, J. E. (1968).  
Effect of anionic, cationic and non-ionic detergents on the percutaneous absorption of sodium chromate  $Cr^{VI}$  in the guinea pig.  
*Acta Dermato-venereol.*, **48**: 549-555.
- Wahlberg, J. E. and Skog, E. (1962).  
Percutaneous absorption of mercuric chloride in guinea pigs.  
*Acta Dermatovener.*, **42**: 418-425.

- Wahlberg, J. E., Skog, E. and Friberg, L. (1961).  
Absorption of mercuric chloride and methyl mercury dicyandiamide  
in guinea pigs through normal and pretreated skin.  
*Acta Dermovener.*, 41: 40-52.
- Warner, R. R., Myers, M. C. and Taylor, D. A. (1985).  
Localization of diffusible elements and water in skin.  
*J. Invest. Dermatol.*, 84: 301.
- Watkins, A. L. (1962).  
"A Manual of Electrotherapy". Henry Kimpton, London. 2nd ed.
- Watson, M. L. (1958).  
Staining of tissue sections for electron microscopy with heavy  
metals. II. Application of solutions containing lead and  
barium.  
*J. Biophys. Biochem. CytoI.*, 4: 727-730.
- Weast, R. C. and Astle, M. J. (1980).  
"CRC Handbook of Chemistry and Physics 1980-1981". CRC Press  
Inc., Florida. 61st ed.
- Weigand, D. A. and Gaylor, J. R. (1974).  
Irritant reaction in negro and caucasian skin.  
*South Med. J.*, 67: 548-551.
- Weinstock, M. and Wilgram, G. F. (1970).  
Fine structural observations on the formation and enzymatic  
activity of keratinosomes in mouse filiform papillae.  
*J. Ultrastruct. Res.*, 30: 262-274.
- Welton, J. E. (1984).  
"SEM Petrology Atlas". The American Association of Petroleum  
Geologists, Tulsa, Oklahoma.
- Wester, R. C., Noonan, P. K. and Maibach, H. I. (1980).  
Variations in percutaneous absorption of testosterone in the  
rhesus monkey due to anatomic site of application and frequency  
of application.  
*Arch. Dermatol. Res.*, 267: 229-235.
- Wheatley, V. R. (1963).  
Problems in the analysis of sebum. In "Advances in Biology of  
the Skin", (eds: Montagna, W., Ellis, R. A. and Silver, A. F.).  
Pergamon Press, Oxford. Vol. 4 (The sebaceous glands). pp 135-  
147.
- Wheatley, V. R. and Flesch, P. (1967).  
Horny layer lipids. II. Further studies on the overall  
chemical composition of lipids from normal and pathological  
human stratum corneum.  
*J. Invest. Dermatol.*, 49: 198-205.


- Wills, J. H. (1969).  
 Percutaneous absorption. In "Advances in Biology of Skin - Pharmacology and the Skin", (eds: Montagna, W., Van Scott, E. J. and Stoughton, R. B.). Vol. 12. Appleton Century Crofts, New York. Vol. 12. pp 169-176.
- Winkelmann, R. K. (1969).  
 The relationship of the structure of the epidermis to percutaneous absorption.  
*Brit. J. Dermatol.*, **81**: 11-22.
- Winsor, T. and Burch, G. E. (1944).  
 Differential roles of layers of human epigastric skin on diffusion rate of water.  
*Arch. Intern. Med.*, **74**: 428-436.
- Witten, V. H., Ross, M. S., Oshry, E. and Holmstrom, V. (1953).  
 Studies of thorium X applied to human skin. II. Comparative findings of the penetration and localization of thorium X when applied in alcoholic solution, in ointment and in laquer vehicles.  
*J. Invest. Dermatol.*, **20**: 93-103.
- Witten, V. H., Ross, M. S., Oshry, E. and Hyman, A. B. (1951).  
 Studies of thorium X applied to human skin. I. Routes and degree of penetration and sites of deposition of thorium X applied in selected vehicles.  
*J. Invest. Dermatol.*, **17**: 311-322.
- Wolff, K and Schreiner, E. (1968).  
 An electron microscopic study on the extraneous coat of keratinocytes and the intercellular space of the epidermis.  
*J. Invest. Dermatol.*, **51**: 418-430.
- Wolff, K. and Honigsmann, H. (1971).  
 The permeability of the epidermis and the phagocytic activity of the keratinocytes.  
*J. Ultrastruct. Res.*, **36**: 176-190.
- Woo-Sam, P. C. (1978).  
 A quantitative study of membrane coating granules in follicles undergoing experimental comedo formation.  
*Brit. J. Dermatol.*, **99**: 387-394.
- Yamamoto, T. and Yamamoto, Y. (1976).  
 Electrical properties of the epidermal stratum corneum.  
*Med. Biol. Eng. Comput.*, **14**: 151-158.
- Yankell, S. L. (1969).  
 The effects of various vehicles on absorption rates in skin. In "Advances in Biology of Skin - Pharmacology and the Skin", (eds: Montagna, W., Van Scott, E. J. and Stoughton, R. B.). Vol. 12. Appleton Century Crofts, New York. Vol. 12. pp 511-522.
- Zelickson, A. S. (1967).  
 "Ultrastructure of Normal and Abnormal Skin". Henry Kimpton, London.



# *APPENDICES*

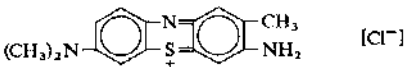
Appendix A

Methylene blue

Colour index Name	Basic blue 9	
Colour index number	52015	
Synonyms	Swiss blue; Solvent blue 8; Tetramethylthionine chloride; Methylthionine chloride; Urolene blue; Methylene blue chloride; Methylene blue BX, B, B6, or BB	
Chemical name	3,7-Bis(dimethylamino)-phenothiazin-5-ium Chloride	
Chemical group	Thiazine	
Empirical formula	C <sub>16</sub> H <sub>18</sub> N <sub>3</sub> S Cl	
Molecular weight (A.M.U.)	319.85	
Cationic weight (A.M.U.)	285	
Structural formula		
Physical properties	Dark green odourless fine crystals with bronze luster.	
Type	Technical, BDH Chemicals Ltd. England.	
Approximate percentage solubility (grams per 100mls.) at 15 C	Water	: 9.5
	Absolute alcohol	: 6.0

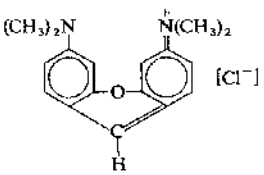
A.M.U. = Atomic Mass Units

Toluidine blue

Colour index Name	Basic blue 17	
Colour index number	52040	
Synonyms	Toluidine blue D; Tolonium chloride; Blutene chloride; Tolazol; Methylene blue T50; Dimethyltoluthionine chloride; Methylene blue T extra.	
Chemical name	3-amino-7-(dimethylamino)-2-methyl-phenothiazin-5-ium chloride.	
Chemical group	Thiazine.	
Empirical formula	$C_{15} H_{14} N_3 S Cl$	
Molecular weight (A.M.U.)	305.84	
Cationic weight (A.M.U.)	269	
Structural formula		
Physical properties	Dark green odourless powder	
Type	Gurr, George T. Gurr Ltd., England.	
Approximate percentage solubility (grams per 100mls.) at 15° C	Water	: 3.25
	Absolute alcohol	: 1.75

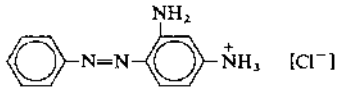
A.M.U. = Atomic Mass Units

### Pyronin Y

Colour index Name	Pyronin Y
Colour index number	45005
Synonyms	Pyronin G; 3,6-Bis(dimethylamino)xanthylium chloride
Chemical name	N-[6-(Dimethylamino)-3H-xanthen-3-ylidene]-N-methylmethan-aminium chloride
Chemical group	Xanthene.
Empirical formula	C <sub>17</sub> H <sub>19</sub> N <sub>2</sub> O Cl
Molecular weight (A.M.U.)	302.81
Cationic weight (A.M.U.)	268
Structural formula	 <p>The structural formula shows a xanthene ring system. At the 6-position, there is a dimethylamino group, <math>(\text{CH}_3)_2\text{N}</math>. At the 3-position, there is a ylidene group, <math>=\text{N}^+(\text{CH}_3)_2</math>. The counterion is a chloride ion, <math>[\text{Cl}^-]</math>.</p>
Physical properties	Dark brownish powder
Type	Microscopical stain, BDH Chemicals, England
Approximate percentage solubility (grams per 100mls.) at 15 °C	Water : 10 Absolute alcohol : 0.5

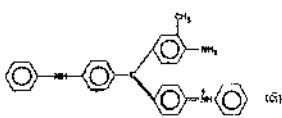
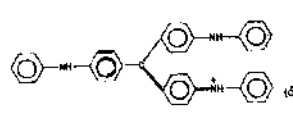
A.M.U. = Atomic Mass Units

### Chrysoidin

Colour index Name	Basic orange 2	
Colour index number	11270	
Synonyms	Chrysoidin Y; Chrysoidin orange; Acid yellow 9; Fast yellow FY, G, S, or BG; Brown salt R; Chrysoidin G and A	
Chemical name	4-(phenylazo)-1,3-benzenediamine monohydrochloride	
Chemical group	Mono-azo	
Empirical formula	C <sub>12</sub> H <sub>13</sub> N <sub>4</sub> Cl	
Molecular weight (A.M.U.)	248.73	
Cationic weight (A.M.U.)	213.20	
Structural formula		
Physical properties	Reddish-brown powder	
Type	Gurr microscopical stain, BDH Chemicals Ltd.	
Approximate percentage solubility (grams per 100mls.) at 15°C	Water	: 5.50
	Absolute alcohol	: 4.75

A.M.U. = Atomic Mass Units

Aniline blue alcohol-soluble

Colour index Name	Solvent blue 3	
Colour index number	42775	
Synonyms	Spirit blue; Gentiana blue 6B; Light blue; Lyon blue; Paris blue	
Chemical group	A mixture of diphenyl iosaniline chloride and triphenyl pararosanilin chloride	
Empirical formula	$C_{32} H_{28} N_3 Cl$	$C_{37} H_{30} N_3 Cl$
Molecular weight (A.M.U.)	490.06	552.13
Cationic weight (A.M.U.)	454.56	516.63
Structural formula	 <p>(a)</p>	 <p>(b)</p>
Physical properties	Dark blue powder	
Type	Gurr microscopical stain, BDH Chemicals, Ltd	
Approximate percentage solubility (grams per 100mls.) at 15°C	Water	: 0.00
	Absolute alcohol	: 1.90

A.M.U. = Atomic Mass Units

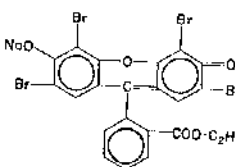


Eosine water soluble

Colour index Name	Acid red 87	
Colour index number	45380	
Synonyms	Eosin Yellowish (YS); Eosin Y; Eosin G, WG; Eosin water-soluble yellowish; Bromo acid J, IS, XL, or XX; Bronze bromo ES; Pigment red 90; Bromofluorescein; Bromofluoresceic acid	
Chemical name	2-(2,4,5,7-tetrabromo-6-hydroxy-3-oxo-3H-xanthen-9-yl) benzoic acid, disodium salt	
Chemical group	Xanthene	
Empirical formula	C <sub>20</sub> H <sub>4</sub> O <sub>5</sub> Br <sub>4</sub> Na <sub>2</sub>	
Molecular weight (A.M.U.)	691.91	
Anionic weight (A.M.U.)	645.91	
Structural formula		
Physical properties	Brownish-red powder	
Type	Gurr microscopical stain, BDH Chemicals Ltd.	
Approximate percentage solubility (grams per 100mls.) at 15° C	Water	: 44.0
	Absolute alcohol	: 2.0

A.M.U. = Atomic Mass Units

Eosin alcohol-soluble

Colour index Name	Solvent red 45
Colour index number	45386
Synonyms	Ethyl eosin; Eosin S.
Chemical group	Xanthene
Empirical formula	$C_{22} H_{11} O_6 Br_4 .Na$
Molecular weight (A.M.U.)	697.99
Anionic weight (A.M.U.)	674.99
Structural formula	
Physical properties	Brownish-red powder
Type	George I. Gurr Ltd., England.
Approximate percentage solubility (grams per 100mls.) at 15 <sup>o</sup> C	Water : 0.0 Absolute alcohol : 1.0

A.M.U. = Atomic Mass Units

Eosin water- and alcohol- soluble

Colour index Name	Acid red 91	
Colour index number	45400	
Synonyms	Eosin I bluish; Eosin bluish; Eosin scarlet; Eosin BA, BN, BS, BW, B or DHV; Nopalin B; Saffrosin; Eosin scarlet B; Scarlet J, JJ or V, Imperial red;.	
Chemical name	2-(4,5-dibromo-2,7-dinitro-6-hydroxy-3-oxo-3H-xanthene-9-yl) benzoic acid, disodium salt.	
Chemical group	Xanthene	
Empirical formula	$C_{20} H_4 Na_2 O_4 Br_2 Na_2$	
Molecular weight (A.M.U.)	624.10	
Anionic weight (A.M.U.)	578.10	
Structural formula		
Physical properties	Red powder	
Type	Merk eosin bluish for microscopical staining, BDH Chemicals Ltd., England.	
Approximate percentage solubility (grams per 100mls.) at 15°C	Water	: 10.0
	Absolute alcohol	: 3.0

A.M.U. = Atomic Mass Units

Aniline blue water-soluble

Colour index Name	Acid blue 22				
Colour index number	42755				
Synonyms	Water blue I; China blue; Soluble blue 3M, 2R; Marine blue V; Cotton blue; Water blue;				
Chemical group	Triphenylmethane				
Empirical formula	C <sub>22</sub> H <sub>16</sub> N <sub>2</sub> O <sub>4</sub> S <sub>2</sub> Na <sub>2</sub>				
Molecular weight (A.M.U.)	737.77				
Anionic weight (A.M.U.)	691.77				
Structural formula					
Physical properties	Blue powder				
Type	Burr for microscopical stain; BDH Chemicals Ltd., England.				
Approximate percentage solubility (grams per 100mls.) at 15 <sup>o</sup> C	<table border="1"> <tr> <td>Water</td> <td>: 50.0</td> </tr> <tr> <td>Absolute alcohol</td> <td>: 0.0</td> </tr> </table>	Water	: 50.0	Absolute alcohol	: 0.0
Water	: 50.0				
Absolute alcohol	: 0.0				

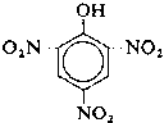
A.M.U. = Atomic Mass Units

Alizarin red S

Colour index Name	Mordant red 3	
Colour index number	59005	
synonyms	Alizarin red water soluble; Alizarin carmine; Alizarin S; Alizarin sodium sulfonate salt	
Chemical name	9,10-Dihydro-3,4-dihydroxy-9,10-dioxo-2-anthracenesulfonic acid monosodium salt	
Chemical group	Anthraquinone	
Empirical formula	C <sub>14</sub> H <sub>7</sub> O <sub>7</sub> S Na	
Molecular weight (A.M.U.)	342.27	
Anionic weight (A.M.U.)	319.27	
Structural formula		
Physical properties	Orange-yellow powder	
Type	Alizarin sodium sulfonate salt, Sigma Chemical Co.	
Approximate percentage solubility (grams per 100mls.) at 15 <sup>o</sup> C	Water	: 6.5
	Absolute alcohol	: 0.1

A.M.U. = Atomic Mass Units

Picric acid

Colour index Name	
Colour index number	10305
Synonyms	2,4,6-Trinitrophenol
Chemical group	Nitro
Empirical formula	$C_6H_3N_3O_7$
Molecular weight (A.M.U.)	229.11
Anionic weight (A.M.U.)	228.11
Structural formula	
Physical properties	As received, a yellow solution. Picric acid is moistened with water (50 percent by weight)
Type	Laboratory reagent, BDH Chemicals Ltd Product number: 29554
Approximate percentage solubility (grams per 100mls.) at 15°C	Water : 1.2 Absolute alcohol : 9.0

A.M.U. = Atomic Mass Units

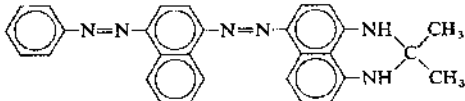
### Trypan blue

Colour index Name	Direct blue 14	
Colour index number	23850	
Synonyms	Chlorazol blue 3B; Benzo blue 3B; Dianil blue H3G; Congo blue 3B; Naphthamine blue 3BX; Benzamine blue 3B; Azidine blue 3B; Niagra blue 3B; Diamine blue	
Chemical name	3,3'-[3,3'-Dimethyl[1,1'-biphenyl]-4,4'-diyl]bis(azo) bis[5-amino-4-hydroxy-2,7-naphthalene disulfonic acid] tetrasodium salt	
Chemical group	Diazo	
Empirical formula	C <sub>34</sub> H <sub>24</sub> N <sub>6</sub> O <sub>14</sub> S <sub>4</sub> Na <sub>4</sub>	
Molecular weight (A.M.U.)	960.85	
Anionic weight (A.M.U.)	868.85	
Structural formula		
Physical properties	Bluish-grey powder	
Type	Microscopical stains, BDH Chemicals Ltd.	
Approximate percentage solubility (grams per 100mls.) at 15 C	Water	: 1.00
	Absolute alcohol	: 0.02

A.M.U. = Atomic Mass Units



**Sudan black B**

Colour index Name	Solvent black 3	
Colour index number	26150	
Synonyms	Sudan black B	
Chemical group	Diazo	
Empirical formula	$C_{29} H_{24} N_6$	
Molecular weight (A.M.U.)	456.56	
Structural formula		
Physical properties	Bluish-black powder	
Type	Revector microscopical stain Hopkin and Williams Ltd., England.	
Approximate percentage solubility (grams per 100mls.) at 15 C	Water	: 0.00
	Absolute alcohol	: 0.25

A.M.U. = Atomic Mass Units

Appendix B

Lanthanum

Salt	Lanthanum nitrate hexahydrate
Physical property	Colourless deliquescent crystals
Chemical structure	$\text{La}(\text{NO}_3)_3 \cdot 6\text{H}_2\text{O}$
Molecular weight (Atomic Mass Units)	433.04
Type	Laboratory agent, BDH Chemicals Ltd
Solubility (grams per 100mls)	151 in cold water; very soluble in hot water; very soluble in alcohol.

Silver

Salt	Silver nitrate
Physical property	Colourless crystals
Chemical structure	$\text{AgNO}_3$
Molecular weight (Atomic Mass Units)	169.87
Type	General Purpose Reagent, BDH Chemicals Ltd., England
Solubility (grams per 100mls)	122 in cold water; 952 in hot water; 3.33 in alcohol

### Ruthenium

Salt	Ruthenium red chloride
Physical property	Brown-red powder
Chemical structure	$\text{Ru}_2(\text{OH})_2\text{Cl}_4 \cdot 7\text{NH}_3 \cdot 3\text{H}_2\text{O}$
Molecular weight (Atomic Mass Units)	551.3
Type	Gurr microscopy material, BDH Chemicals Ltd., England.
Solubility (grams per 100mls)	Soluble in water

### Copper

Salt	Copper sulphate anhydrous
Physical property	Greenish-white fine granules
Chemical structure	$\text{CuSO}_4$
Molecular weight (Atomic Mass Units)	159.61
Type	Hopkin and Williams Ltd., England
Solubility (grams per 100mls)	14.3 in cold water; 75.4 in hot water; insoluble in alcohol

### Iron

Salt	Ferric chloride (hydrated)
Physical property	Brown crystals
Chemical structure	$\text{FeCl}_3 \cdot 6\text{H}_2\text{O}$
Molecular weight (Atomic Mass Units)	270.32
Type	Analar analytical reagent, BDH Chemicals Ltd., England.
Solubility alcohol (grams per 100mls)	Readily soluble in water and

### Iodine

Salt	Potassium iodide
Physical property	White fine granules
Chemical structure	KI
Molecular weight (Atomic Mass Units)	166.02
Type	Laboratory reagent, BDH Chemicals Ltd., England
Solubility (grams per 100mls)	142 in cold water; 200 in hot water; 4.55 in alcohol; 12.5 in hot alcohol

**Appendix CI**

**Table of characteristic X-ray transitions (EDX)**

Element	Symbol	Atomic Mass	Atomic Number	Energy values for characteristic X-ray transitions (Welton, 1984)				
				K		L		M $\alpha$
				$\alpha$	$\beta$	$\alpha$	$\beta$	
Lanthanum	La	138.9	57			4.650	5.041	
Silver	Ag	107.9	47			2.984		
Ruthenium	Ru	101.1	44			2.558*	2.633*	
Copper	Cu	63.5	29	8.046	8.904			
Iron	Fe	55.8	26	6.403				
Iodine	I	126.9	53			3.937		

Some elements that may appear in the X-ray spectra

Chlorine	Cl	35.5	17	2.622*				
Sulphur	S	32.1	16	2.307				
Silicon	Si	28.1	14	1.740				
Sodium	Na	23	11	1.041				
Calcium	Ca	40.1	20	3.691				
Magnesium	Mg	24.3	12	1.253				
Potassium	K	39.1	19	3.310				
Aluminium	Al	26.9	13	1.486				
Osmium	Os	190.2	76			8.910		1.978

\* = very close values

Appendix CII

X-ray emission wavelengths

Pentaaerythritol tetrakis (PET) crystal, first reflection  
order (from Jeol, 1983).

Element	$L\alpha 1$	$L\beta 1$	$K\alpha 1$
Ruthenium	153.21 <sup>0</sup>	147.99 <sup>0</sup>	
Chlorine			151.45 <sup>0</sup>

## Corrigendum

Page	Line	Error	Correction
24	19	Kumatsu	Komatsu
27	26	Scheuplein and Black	Scheuplein and Blank
43	1	whch	which
104	21	ultramicrotome and excess...	ultramicrotome chuck and excess
161	22	Positive iontophoresis of a 2% aqueous chrysoidin Y solution for 15 minutes.	Positive iontophoresis of a 2% aqueous chrysoidin Y solution at 30mA for 15 minutes
177	7	Martinez, Palomo <i>et al.</i> , 1973	Martinez-Palomo <i>et al.</i> , 1973
	17	(Elias and Friend, 1975; Wolff and Schreiner, 1968)	(Wolff and Schreiner, 1968; Elias and Friend, 1975)
	20	Squier and Rooney, 1975	Squier and Rooney, 1976
293	16	Jenkinson <i>et al.</i> (1974)	McEwan Jenkinson <i>et al.</i> (1974)
324	8	O'Malley and Oestler	O'Malley and Oester
345	19	Kawamura and Takala	Kawamura and Takata
350	3	Scheuplein and Black	Scheuplein and Blank
363	6	Tables 4.1 and 4.2 (Page 314)	Tables 4.17 and 4.18 (page 355)
365	3	see Table 4.2, page	see Table 4.2, page 314
366	10	see Appendix II	see Appendix CI
371	5	(Rothman, 1944, 1955)	(Rothman, 1943, 1955)
415	6	positive iontophoresis.	positive iontophoresis, while anionic dyes are introduced by negative iontophoresis.
420	24	Boden	Baden
422	12	Burch, G.E. and Winsor, T. (1944). Rate of...	Burch, G.E. and Winsor, T. (1946). Rate of....
433	1	Alphabetical order	Lavker and Sun (1982) should be positioned between Lavker (1976) and Leech and Oliphant (1983)
434	15	Loeffler, R.K. and Thomas, V.	Loeffler, R.K. and Thomas, V. (1951)
436	26	Alphabetical order	Matoltsy and Parakkal (1965) should be positioned between Matoltsy <i>et al.</i> (1962) and Matoltsy and Parakkal (1967)
437	35	Molitor, H. and Fernandez, I. (1930).	Molitor, H. and Fernandez, I. (1939).
445	43	Szubinska	Szubinski